

AD-A067 838

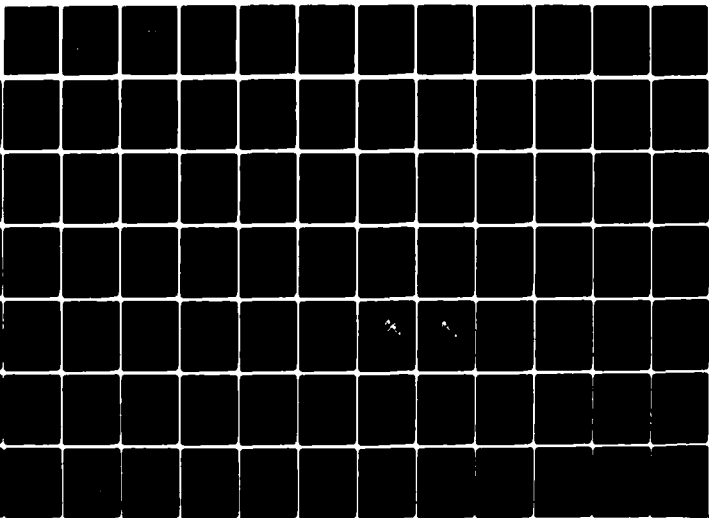
AIRESEARCH MF6 CO OF ARIZONA PHOENIX F/G 10/2  
ADVANCED TECHNOLOGY COMPONENTS FOR MODEL 6TP305-2 AIRCRAFT AUXI--ETC(U)  
FEB 80 J R KIDWELL, G D LARGE F33615-75-C-2016

UNCLASSIFIED

AFAPL-TR-79-2106

ML

1 of 2  
A067 838



1 (2)  
4  
LEVEL  
AFAPL-TR-79-2106

ADA 087838

**ADVANCED TECHNOLOGY COMPONENTS  
FOR MODEL GTP305-2  
AIRCRAFT AUXILIARY POWER SYSTEM**

AIRESEARCH MANUFACTURING COMPANY OF ARIZONA  
A DIVISION OF THE GARRETT CORPORATION  
402 S. 36 STREET  
PHOENIX, ARIZONA 85010

FEBRUARY 1980

TECHNICAL REPORT AFAPL-TR-79-2106  
FINAL REPORT FOR PERIOD 6 MAY 1975 - 15 JULY 1979

THIS DOCUMENT IS BEST QUALITY PRACTICABLE.  
THE COPY FURNISHED TO DDC CONTAINED A  
SIGNIFICANT NUMBER OF PAGES WHICH DO NOT  
REPRODUCE LEGIBLY.

APPROVED FOR PUBLIC RELEASE;  
DISTRIBUTION UNLIMITED

DTIC  
JUN 6 1980

A

80 6 6 031  
AERO PROPULSION LABORATORY  
AIR FORCE WRIGHT AERONAUTICAL LABORATORIES  
AIR FORCE SYSTEMS COMMAND  
WRIGHT-PATTERSON AIR FORCE BASE, OHIO 45433

FILE COPY  
DDC

NOTICE

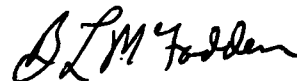
When Government drawings, specifications, or other data are used for any purpose other than in connection with a definitely related Government procurement operation, the United States Government thereby incurs no responsibility nor any obligation whatsoever; and the fact that the government may have formulated, furnished, or in any way supplied the said drawings, specifications, or other data, is not to be regarded by implication or otherwise as in any manner licensing the holder or any other person or corporation, or conveying any rights or permission to manufacture, use, or sell any patented invention that may in any way be related thereto.

This report has been reviewed by the Information Office (OI) and is releasable to the National Technical Information Service (NTIS). At NTIS, it will be available to the general public, including foreign nations.

This technical report has been reviewed and is approved for publication.



DANIEL J. GURECKI, Capt, USAF  
Power Systems Branch  
Aerospace Power Division  
Aero Propulsion Laboratory



B. L. MCFADDEN, Acting Chief  
Power Systems Branch  
Aerospace Power Division  
Aero Propulsion Laboratory

FOR THE COMMANDER



JAMES D. REAMS  
Chief, Aerospace Power Division  
Aero Propulsion Laboratory

"If your address has changed, if you wish to be removed from our mailing list, or if the addressee is no longer employed by your organization please notify AFHAF/POOS, W-PAFB, OH 45433 to help us maintain a current mailing list".

Copies of this report should not be returned unless return is required by security considerations, contractual obligations, or notice on a specific document.

## **DISCLAIMER NOTICE**

**THIS DOCUMENT IS BEST QUALITY PRACTICABLE. THE COPY FURNISHED TO DTIC CONTAINED A SIGNIFICANT NUMBER OF PAGES WHICH DO NOT REPRODUCE LEGIBLY.**



62203F

SECURITY CLASSIFICATION OF THIS PAGE (When Data Entered)

19 REPORT DOCUMENTATION PAGE		READ INSTRUCTIONS BEFORE COMPLETING FORM
1. REPORT NUMBER (18) AFAPL-TR-79-2106	2. GOVT ACCESSION NO. AD-A087838	3. RECIPIENT'S CATALOG NUMBER
4. TITLE (and Subtitle) (6) Advanced Technology Components for Model GTP305-2 Aircraft Auxiliary Power System	5. TYPE OF REPORT & PERIOD COVERED (9) Final Report, 6 May 1975 15 July 1979	6. PERFORMING ORG. REPORT NUMBER
7. AUTHOR(s) (10) James R. Kidwell Gerold D. Large	8. CONTRACT OR GRANT NUMBER(s) (15) F33615-75-C-2016	
9. PERFORMING ORGANIZATION NAME AND ADDRESS AiResearch Manufacturing Co. of Arizona A Division of The Garrett Corporation Phoenix, Arizona 85010	10. PROGRAM ELEMENT, PROJECT, TASK AREA & WORK UNIT NUMBERS (13) 3145-01-03	
11. CONTROLLING OFFICE NAME AND ADDRESS Air Force Aeropulsion Laboratory Air Force System Command Wright-Patterson AFB, Ohio 45433	12. REPORT DATE (11) February 1980	13. NUMBER OF PAGES
14. MONITORING AGENCY NAME & ADDRESS (if different from Controlling Office) (12) 541	15. SECURITY CLASS. (of this report) Unclassified	15a. DECLASSIFICATION/DOWNGRADING SCHEDULE
16. DISTRIBUTION STATEMENT (of this Report)  Approved for public release; distribution unlimited.		
17. DISTRIBUTION STATEMENT (of the abstract entered in Block 20, if different from Report)		
18. SUPPLEMENTARY NOTES		
19. KEY WORDS (Continue on reverse side if necessary and identify by block number)		
20. ABSTRACT (Continue on reverse side if necessary and identify by block number) The GTP305-2 Advanced APU is a single shaft, all shaft power engine incorporating an axial-centrifugal compressor, a reverse flow annular combustor and a radial-axial turbine. Cycle analyses indicated a 10-percent high pressure compressor flow increase improved matching characteristics with the low pressure compressor. The combustion system is a reverse flow annular combustor with an air-assist/airblast fuel injection system.		

DD FORM 1473

EDITION OF 1 NOV 65 IS OBSOLETE

SECURITY CLASSIFICATION OF THIS PAGE (When Data Entered)

404776

The radial-axial turbine stage is characterized by an integrally cast turbine rotor and a cast exhaust duct assembly. The Integrated Components Assembly (ICA) rig consists of the combustor and turbines with a dummy mass on the shaft to simulate the compressor. ICA testing was conducted to establish component performance at design operating conditions. ICA and cold air aerodynamic testing of the turbine stage and cooling flow effects, indicates design efficiency goals were exceeded. ICA test results, cold-air testing and combustion system parameters were input to the cycle model. Room temperature strain-control LCF tests were performed and results analyzed on a Weibull distribution. Data analysis indicated LCF life improvement was obtained through HIP and heat treatment.

Accession For	
NTIS	<input checked="" type="checkbox"/>
DDC	<input type="checkbox"/>
Unclassified	<input type="checkbox"/>
JAN 1981	
<i>Little on file</i>	
By	
PLANNING	
ACQUISITION	
Dist	Available for
A	Special
	23
	CD

## TABLE OF CONTENTS

SECTION		PAGE
I	INTRODUCTION	1
II	SUMMARY	2
III	APU DESIGN	5
	3.1 Cycle Analysis and Matching Studies	5
	3.1.1 Preliminary Design Point Selection	5
	3.1.2 Final Design Point Selection	15
	3.1.3 Off-Design Performance Analysis	24
	3.2 Compressor	32
	3.3 Combustion System	34
	3.3.1 Combustor	36
	3.3.2 Fuel Injection System	43
	3.4 Turbine	49
	3.4.1 Radial Turbine Nozzle	49
	3.4.2 Aerodynamic Design	49
	3.4.3 Cooling Flow Analysis	55
	3.4.4 Radial Nozzle Vane	59
	3.4.5 Aft Sidewall, Shroud Combustion Chamber Ramp	61
	3.4.6 Forward Sidewall, Support Cylinder, Combustor Shroud	65
	3.4.7 Stress Analysis	69
	3.4.8 Radial Turbine Rotor	83
	3.4.9 Axial Turbine Aero/Mech Optimization	106
	3.4.10 Axial Turbine Stator	111
	3.4.11 Axial Turbine Rotor	124
	3.4.12 Turbine Exhaust Diffuser	133
	3.5 Rotor Dynamics	145
IV	COMPONENT DEVELOPMENT TESTING	159
	4.1 Combustion System Development Testing	159
	4.1.1 Test Rig	159
	4.1.2 Instrumentation	162
	4.1.3 Test Procedure	163
	4.1.4 Test Results	163

## TABLE OF CONTENTS (Contd)

SECTION	PAGE
4.2 Turbine Cold Air Testing	184
4.2.1 Radial Turbine Test Rig	187
4.2.2 Radial/Axial Turbine Test Rig	187
4.2.3 Instrumentation	187
4.2.4 Test Procedure	191
4.2.5 Test Results	195
V INTEGRATED COMPONENTS ASSEMBLY	259
5.1 Test Rig Description	259
5.2 Hardware Fabrication	273
5.2.1 Radial Turbine Rotor	273
5.2.2 Radial Turbine Nozzle	279
5.2.3 Axial Turbine Stator	285
5.2.4 Axial Turbine Rotor	285
5.2.5 Exhaust Duct Assembly	294
5.2.6 Combustor Liner	294
5.3 Instrumentation	294
5.4 Build and Installation Procedure	299
5.5 Test Procedure	299
VI INTEGRATED COMPONENTS ASSEMBLY TEST RESULTS	319
6.1 Turbine Aerodynamic Performance	319
6.1.1 Performance Analysis	319
6.1.2 GTP305-2	339
6.2 Combustion System Performance	340
6.3 Mechanical Test Results	344
6.3.1 Radial Turbine Rotor	344
6.3.2 Radial Nozzle	351
6.3.3 Axial Turbine Nozzle	351
6.3.4 Axial Turbine Rotor	355
VII CONCLUSIONS	358
APPENDIX A	361
APPENDIX B	392
APPENDIX C	451
APPENDIX D	464
APPENDIX E	510

# LIST OF ILLUSTRATIONS

FIGURE	TITLE	PAGE
1	Axial compressor stage performance	6
2	Centrifugal compressor stage performance	7
3	GTP305-2 match point preliminary analysis	10
4	GTP305-2 preliminary match point cycle analysis	11
5	GTP305-2 design point analysis	14
6	GTP305-2 preliminary turbine configuration 92.5-percent speed	16
7	GTP305-2 turbine optimization for 2050°F T.I.T. cycle	18
8	GTP305-2 final design point cycle analysis	20
9	GTP305-2 all cast configuration	23
10	IGV test data correlation	25
11	GTP305-2 off-design performance	26
12	GTP305-2 off-design performance	27
13	GTP305-2 off-design performance	28
14	Estimated off-design performance of GTP305-2 APU	29
15	Estimated off-design performance of GTP305-2 APU	30
16	Estimated off-design performance of GTP305-2 APU	31
17	GTP305-2 hp compressor 10 percent flow increase recontour	33
18	Principal features of GTP305-2 combustion system	35
19	GTP305-2 inner annulus $P_g$ distribution	40
20	Radial turbine nozzle cooling flow schematic	42
21	Prototype air-assist/airblast fuel nozzle with outer shroud installed	44
22	Prototype air-assist/airblast fuel nozzle with outer shroud removed	45
23	Schematic of typical air-assist/airblast fuel atomizer	46
24	GTP305-2 flow divider	47
25	GTP305 fuel system characteristics (5) air-assist/airblast, (5) pure airblast	48
26	Radial turbine stage	50
27	GTP305-2 radial turbine meridional flow path	52
28	One-dimensional radial turbine vector diagram	53
29	GTP305-2 stator nozzle ring with final vane profile	54
30	GTP305-2 radial nozzle cooling flow circuits	57
31	GTP305-2 radial turbine nozzle vane cross section	58
32	Radial turbine nozzle fore and aft cooling fins	62
33	GTP305-2 radial turbine nozzle hub shroud boundary conditions	64

# LIST OF ILLUSTRATIONS (Contd)

FIGURE	TITLE	PAGE
34	Forward sidewall cooling circuit	67
35	GTP305-2 radial turbine nozzle outer shroud boundary conditions	68
36	GTP305-2 turbine nozzle (Inconel 738) finite element model	70
37	GTP305-2 turbine nozzle cooling fin thickness (204 fins) and tangential vane thicknesses for an equivalent solid vane	71
38	GTP305-2 turbine nozzle nodal numbering system	72
39	GTP305-2 turbine nozzle finite element model pressures (psia)	73
40	GTP305-2 turbine nozzle average steady state temperatures calculated from heat transfer analysis	74
41	GTP305-2 turbine nozzle temperature and pressure	76
42	GTP305-2 turbine nozzle temperature and pressure axial bending stress (ksi)	77
43	GTP305-2 turbine nozzle temperature and pressure radial bending stress (ksi)	78
44	GTP305-2 turbine nozzle temperature and pressure hoop stress (ksi)	79
45	GTP305-2 turbine nozzle temperature and pressure equivalent stress (ksi)	80
46	GTP305-2 turbine nozzle temperature and pressure principal stress (ksi)	81
47	GTP305-2 turbine nozzle temperature and pressure principal stress (ksi)	82
48	Variation of optimum tip speed with turbine stage work	84
49	GTP305-2 radial rotor final flow path	88
50	Area of wheel which exceeds one percent creep for an uncooled bore	90
51	Radial turbine nozzle bore cooling flow path	91
52	GTP305-2 interturbine seal clearance flow rate vs buffer	95
53	Area of wheel which exceeds one percent creep for a cooled bore	97
54	GTP305-2 radial turbine steady state temperature distribution bore flow = 0.023 lb/sec, front face flow = 0.01 lb/sec	98
55	GTP305-2 temperature distribution program to hub line film coefficient bore cooling flow 0.023 lb/sec front face flow 0.06 lb/sec	100
56	GTP305-2 radial turbine displacements program 700 film coefficients bore cooling flow 0.023 lb/sec front face flow 0.060 lb/sec	101

# LIST OF ILLUSTRATIONS (Contd)

FIGURE	TITLE	PAGE
57	GTP305-2 radial turbine tangential stress distribution program 700 hub line film coefficients bore cooling flow 0.023 lb/sec front face flow 0.060 lb/sec	102
58	GTP305-2 equivalent stress distribution program 700 film coefficients bore cooling flow 0.023 lb/sec front face flow 0.060 lb/sec	103
59	GTP305-2 radial turbine radial stress distribution program 700 hub line film coefficients bore cooling flow 0.023 lb/sec front face flow 0.060 lb/sec	104
60	Annular diffuser design chart for interturbine duct	105
61	GTP305-2 final interturbine duct contour	107
62	GTP305-2 axial turbine radial efficiency distribution	110
63	GTP305-2 axial turbine flowpath	112
64	Radial trailing edge thickness and wedge angle distributions	113
65	Stacked stator vane	116
66	Meridional view of stacked stator vane	117
67	GTP305-2 estimated steady state temperature distribution and assumed steady state pressures	118
68	GTP305-2 interturbine duct structure, finite element model	119
69	GTP305-2 preliminary interturbine duct steady state deflections	121
70	GTP305-2 interturbine duct structure, reference locations for primary stresses	122
71	GTP305-2 estimated transient temperature distribution during start condition	123
72	Axial rotor blade stack about center of gravity	128
73	Axial turbine flow path with final design sections	129
74	GTP305-2 axial blade untwist calculated at engine operating conditions	130
75	Steady state metal temperatures - °F	132
76	Steady state radial stresses - ksi	134
77	Steady state tangential stresses - ksi	135
78	Steady state equivalent stresses - ksi	136
79	Performance effect due to diffuser recovery	137
80	Correlation for annular diffuser geometry	138
81	Exhaust diffuser meridional view	140
82	Circumferential location of exhaust diffuser struts and oil lines	144

# LIST OF ILLUSTRATIONS (Contd)

FIGURE	TITLE	PAGE
83	Exhaust diffuser meridional view	146
84	Exhaust diffuser area distribution	147
85	Exhaust diffuser static pressure distribution	148
86	Exhaust diffuser velocity distribution	149
87	GTP305-2 final layout rotating group and wheel property information	151
88	GTP305-2 final design rotating group mass and stiffness critical speed model	152
89	GTP305-2 final design rotating group critical speeds versus bearing stiffness	153
90	GTP305-2 final design rotating group first critical speed mode shape	155
91	GTP305-2 final design rotating group second critical speed mode shape	156
92	GTP305-2 final design rotating group third critical speed mode shape	157
93	Combustion system development test rig P/N 3605880	161
94	Sketch of top view of combustor showing atomizer back angle	167
95	Thermosensitive paint (test 2)	168
96	Titanium dioxide traces - test 4	170
97	Therminex paint - test 6	171
98	Primary air jet fuel entrainment test 7	173
99	Test 8 therminex paint	175
100	S/N 1 combustor features for test 10	176
101	Dome cooling skirt attachment	178
102	Locations of dome cooling skirt	179
103	Pretest inspection of test no. 11 combustor S/N 1	181
104	Test no. 11 therminex paint	182
105	Combustor life versus temperature gradient for hastelloy X	183
106	Radial turbine cold test rig	188
107	Turbine flow path secondary flows	189
108	Radial/axial cold turbine test rig	190
109	Rig radial turbine rotor	192
110	Rig axial nozzle	193
111	Rig axial rotor	194
112	Digital data acquisition schematic	196
113	Effects of rotor backface clearance on peak efficiency GTP305-2 data	200
114	Variation of radial turbine efficiency with backface clearance with a constant scallop depth	201
115	Nomenclature for cooled radial turbine efficiency	204



# LIST OF ILLUSTRATIONS (Contd)

FIGURE	TITLE	PAGE
116	Effects of rotor backface cooling on turbine performance	205
117	GTP305-2 radial turbine test no. 1	209
118	GTP305-2 radial turbine test no. 1	210
119	GTP305-2 radial turbine test no. 1	211
120	GTP305-2 radial turbine test no. 1	212
121	GTP305-1 radial turbine test no. 1	213
122	GTP305-2 radial turbine test no. 1	214
123	GTP305-2 radial turbine exit flow conditions	215
124	GTP305-2, comparison of duct exit total pressures	219
125	GTP305-2 interturbine duct loss analysis	220
126	Axial stator inlet angle distribution	222
127	NASA calculations for radial turbines	224
128	GTP305-2, two-stage test, test no. 3	227
129	GTP305-2, two-stage test, test no. 3	228
130	GTP305-2, two-stage test, test no. 3	229
131	GTP305-2, two-stage test, test no. 3	230
132	GTP305-2, two-stage test, test no. 3	231
133	GTP305-2, two-stage test axial turbine correction	233
134	GTP305-2, test no. 3 and 4 radial-axial stage test	234
135	GTP305-2, two-stage data test no. 3 and no. 4	239
136	GTP305-2 2-stage test air angle distribution	240
137	GTP305-2 2-stage test radial rotor exit	241
138	GTP305-2 2-stage test radial rotor exit pressure ratio	242
139	GTP305-2 2-stage test absolute mach number distribution	243
140	GTP305-2 2-stage test axial stator inlet air angle distribution	245
141	GTP305-2 2-stage test axial stator inlet pressure ratio	246
142	GTP305-2 2-stage test axial stator inlet absolute mach number distribution	247
143	GTP305-2 2-stage test axial rotor exit pressure ratio distribution	248
144	GTP305-2 2-stage test axial rotor exit air angle distribution	249
145	GTP305-2 2-stage test axial rotor exit absolute mach number distribution	250
146	Relative air angle distribution	251
147	GTP305-2 2 stage test axial rotor exit pressure ratio	252
148	GTP305-2 2-stage test axial rotor exit efficiency	253
149	GTP305-2, two-stage test diffuser	255

# LIST OF ILLUSTRATIONS (Contd)

FIGURE	TITLE	PAGE
150	GTP305-2, two-stage test, test nos. 3 and 4	256
151	GTP305-2, two-stage test, test no. 3	258
152	Integrated components assembly test rig	260
153	GTP305-2 final design rotating group with modified quill shaft first critical speed mode shape	262
154	GTP305-2 final design rotating group with modified quill shaft second critical speed mode shape	263
155	GTP305-2 final design rotating group with modified quill shaft third critical speed mode shape	264
156	GTP305-2 integrated rig with quill shaft and pinion gear	265
157	GTP305-2 integrated components rig with quill shaft and pinion gear	266
158	GTP305-2 integrated components rig with quill shaft and pinion gear	267
159	GTP305-2 water brake-bull gear	268
160	GTP305-2 water brake-bull gear	269
161	GTP305-2 water brake-bull gear	270
162	Simulated ICA radial turbine bore cooling flowpath	271
163	Integrated components assembly test gearbox	272
164	Cast AF2-1DA alloy GTP305-2 radial turbine wheel	274
165	Macroscopic grain structure produced in cast AF2-1DA alloy radial turbine rotor	275
166	Small cracks produced by rapid gas quenching during heat treatment	277
167	Cast radial turbine rotor (looking forward) P/N 3605248	283
168	P/N 3605601 wax patterns	284
169	Cast radial nozzle wax pattern with ceramic cores in place	286
170	Cast radial nozzle mold	287
171	GTP305-2 partially machined nozzle	288
172	GTP305-2 partially machined nozzle	289
173	Cast radial nozzle (looking aft) P/N 3605601	290
174	Cast radial nozzle (looking forward) P/N 3605601	291
175	Axial turbine stator (looking aft) P/N 3606194	292
176	Machined axial turbine rotor (looking aft) P/N 3605601	293
177	Exhaust duct (looking aft) P/N 3606195	295

# LIST OF ILLUSTRATIONS (Contd)

FIGURE	TITLE	PAGE
178	GTP305-2 combustor liner (P/N 3605621-1)	296
179		297
180		298
181	GTP305-2, ICA rotating group assembly P/N 3606189	300
182	ICA partial assembly P/N 3606180	301
183	ICA partial assembly P/N 3606180	302
184	ICA partial assembly	303
185	ICA test rig	304
186	ICA test rig (looking aft)	305
187	ICA test rig (looking forward)	306
188	ICA installation prior to instrumentation hookup	307
189	ICA installation-instrumentation hookup	308
190	ICA installation showing waterbrake, gearbox, ICA and exhaust ducting	309
191	Model GTP305-2 forward roller bearing information	318
192	GTP305-2 radial turbine pressure ratio correlation	325
193	GTP305-2 cast radial nozzle flow calibration	326
194	Stations for data reduction model	329
195	GTP305-2 turbine comparison of cold rig and ICA rig performance	334
196	Comparison of hot rig and cold rig axial rotor exit total pressure distributions at design point conditions	335
197	Comparison of hot rig and cold rig turbine exit temperature distributions at design point conditions	336
198	KAHN 3000 hp water brake dyno dead weight calibration	338
199	Model GTP305-2 combustor auxiliary power unit advanced technology components	345
200	Model GTP305-2 combustor auxiliary power unit advanced technology components	346
201	Model GTP305-2 auxiliary power unit advanced technology components ICA radial turbine after test	347
202	Radial turbine (radial crack) model GTP305-2 auxiliary power unit advanced technology components	348
203	Radial turbine (2 tangential cracks) model GTP305-2 auxiliary power unit advanced technology components	349
204	Radial turbine nozzle thermindex paint results model GTP305-2 auxiliary power unit advanced technology components	352

# LIST OF ILLUSTRATIONS (Contd)

FIGURE	TITLE	PAGE
205	Radial turbine nozzle combustor ramp therminindex paint results model GTP305-2 auxiliary power unit advanced technology components	353
206	Axial turbine nozzle therminindex paint results model GTP305-2 auxiliary power unit advanced technology components	354
207	Axial turbine (forward side) model GTP305-2 auxiliary power unit advanced technology components	356
208	Axial turbine (aft side) model GTP305-2 auxiliary power unit advanced technology components	357
B-1	Drawing 3606180 (Instrumentation Schematic Sheet 4)	396
B-2	Drawing 3606180 (Instrumentation Schematic Sheet 5)	397
B-3	Percent corrected speed $\% N/\sqrt{\theta}$	405
B-4	GTP305-2 Fuel system characteristics (5) air-assist/airblast, (5) pure airblast	411
B-5	Predicted waterbrake torque/percent Engine speed	412
D-1	SEM micrographs of as-cast and heat-treated microstructure of the hub region of the GTP305-2 turbine casting	472
D-2	SEM micrographs of as-cast and heat-treated microstructure of the hub region of the GTP305-2 turbine casting	473
D-3	SEM micrographs of as-cast and heat-treated microstructure showing grain boundary areas (arrows)	474
D-4	Location of test specimen for mechanical property testing	476
D-5	SEM micrographs (500X) showing microporosity (arrows) one fracture surfaces at room temperature tensile tested bars from base- line as-cast and heat-treated GTP305-2 turbine wheel casting	478
D-6	Average stress-rupture test results of heat- treated (un-HIPped) cast AF2-1DA alloy turbine wheels compared to specification minimums	480
D-7	Microstructure of as-cast AF2-1DA showing typical shrinkage porosity Mag: 400X Etch: electrolytic oxalic acid	482
D-8	Microstructure of HIPped AF2-1DA alloy Mag: 400X Etch: electrolytic oxalic acid	492

# LIST OF ILLUSTRATIONS (Contd)

FIGURE	TITLE	PAGE
D-9	Microstructure of HIPped AF2-1DA alloy note void formations form incipient melting after 2250°F HIP Mag: 400X Etch: electrolytic oxalic acid	493
D-10	Microstructure of HIPped AF2-1DA showing effects of solution heat treatment temperature in void formation Mag: 400X Etch: electrolytic oxalic acid	494
D-11	Uniform section LCF test specimen	496
D-12	As-cast plus 2175°F solution, 2200°F/15 ksi/ 3 hrs plus 2175°F solution	499
D-13	As-cast plus 2175°F solution, 2200°F/15 ksi/ 3 hrs plus 2225°F solution	500
D-14	As-cast plus 2175°F solution, 2225°F/15 ksi/ 3 hrs plus 2175°F solution	501
D-15	As-cast plus 2175°F solution, 2225°F/15 ksi/ 3 hrs plus 2210°F solution	502
D-16	As-cast plus 2175°F solution, all HIPped results	504
D-17	SEM micrographs showing specimen numbered 82-2 LCF test bar fracture surface exhibiting inclusion type defect (enclosed area) (A) area of high HF, (B) area of high Hf, Ta and Ti and (C) area of fracture origin. This was the only inclusion found on LCF test bar fracture surfaces	505
D-18	As-cast and HIP stress-rupture test results AF2-1DA alloy compared with AiResearch specifications	508

# LIST OF TABLES

TABLE	TITLE	PAGE
1	GTP305-2 PRELIMINARY DESIGN POINT CYCLE ASSUMPTIONS	9
2	SELECTED CANDIDATE TURBINE CONFIGURATIONS FROM PRELIMINARY WORK SPLIT ANALYSIS	13
3	GTP305-2 FINAL DESIGN POINT CYCLE ASSUMPTIONS	21
4	GTP305-2 TURBINE FINAL DESIGN POINT CONDITIONS	22
5	GTP305-2 COMBUSTION SYSTEM DESIGN POINT OPERATING CONDITIONS	37
6	COMPARISON OF GTP305-2 AND GTP305-2 COMBUSTION SYSTEM DESIGN PARAMETERS	38
7	RADIAL NOZZLE DESIGN PARAMETERS	56
8	DESIGN DATA FOR NON-FREE VORTEX TURBINES	109
9	STATOR VANE DESIGN PARAMETERS	114
10	MAXIMUM STRESSES DURING STEADY STATE OPERATING CONDITIONS	120
11	MAXIMUM STRESSES DURING THE RAPID START TRANSIENT CONDITION	125
12	GTP305-2 AXIAL ROTOR DESIGN PARAMETERS N = 75,682 RPM	127
13	GTP305-2 AXIAL TURBINE ROTOR TOOLING LAYOUT PRETWIST	131
14	GTP305-2 TURBINE EXHAUST DIFFUSER BASIC STRUT COORDINATES FOR CONSTANT CROSS SECTION 5 STRUTS TOTAL	141
15	GTP305-2 EXHAUST DIFFUSER OIL IN AIRFOIL DEFINITION	142
16	GTP305-2 EXHAUST DIFFUSER OIL OUT AIRFOIL DEFINITION	143
17	COMBUSTION SYSTEM PERFORMANCE GOALS	160
18	COMBUSTION SYSTEM OPERATING CONDITIONS	164
19	COMBUSTION SYSTEM DEVELOPMENT TEST SUMMARY	165
20	CTP305-2 TURBINE COLD AIR TESTING	185
21	SUMMARY OF GTP305-2 COLD TURBINE TESTING	186
22	GTP305-2 COLD AIR TEST NO. 2 ROTOR BACKFACE CLEARANCE TEST PARAMETER MATRIX (WITHOUT BACKFACE COOLING FLOW)	198
23	GTP305-2 COLD AIR TEST NO. 2 BACKFACE COOLING FLOW TEST PARAMETER MATRIX	199
24	GTP305-2 COLD AIR TEST NO. 1 MAP MATRIX (NO ROTOR BACKFACE COOLING FLOW)	208
25	GTP305-2 RADIAL TURBINE RIG TEST 2A INTERTURBINE DUCT TEST MATRIX	217
26	RADIAL-AXIAL TURBINE BASELINE PERFORMANCE MAP MATRIX (NO COOLING GLOW)	225
27	GTP305-2 RADIAL-AXIAL TURBINE STAGE CLEARANCE COMPARISON 100 PERCENT CORRECTED SPEED	232

# LIST OF TABLES (Contd)

TABLE	TITLE	PAGE
28	RADIAL-AXIAL TURBINE PERFORMANCE MAP MATRIX (WITH COOLING FLOW*)	235
29	COOLING RATE STUDY RESULTS ON CAST AF2-1DA	278
30	ROOM AND ELEVATED TEMPERATURE TENSILE PROPERTIES OF HEAT-TREATED*	280
31	ELEVATED TEMPERATURE STRESS RUPTURE PROPERTIES OF HEAT-TREATED*	281
32	ROOM TEMPERATURE LOW-CYCLE FATIGUE (LCF) PROPERTIES OF HEAT-TREATED*	282
33	INTEGRATED COMPONENTS ASSEMBLY PERFORMANCE DEMONSTRATION TEST POINTS	312
34	TEST MATRIX	313
35		314
36	BALANCE INSPECTION DATA	317
37	RIG RADIAL ROTOR DIMENSIONAL INSPECTION	320
38	RIG RADIAL NOZZLE DIMENSIONAL INSPECTION	321
39	RIG AXIAL NOZZLE DIMENSIONAL INSPECTION	322
40	RIG AXIAL ROTOR DIMENSIONAL INSPECTION	323
41	DESIGN POINT PARAMETERS MEASURED OR DERIVED FROM RIG CORRELATIONS (DATA SCAN 12:12:22.55)	328
42	COMPUTER MATCH OF DESIGN POINT ICA DATA SCAN	332
43	GTP305-2 DESIGN POINT CYCLE DATA	341
44	COMPARISON BETWEEN ORIGINAL GTP305-2 ENGINE CYCLE AND NEW CYCLE BASED ON ICA TEST RESULTS	342
45	GTP305-2 ICA TEST RESULTS AT DESIGN POINT CONDITIONS	343
B-1	INSTRUMENTATION DATA ASSIGNMENT SHEET	398
B-2	INSTRUMENTATION DATA ASSIGNMENT SHEET	399
B-3	INSTRUMENTATION DATA ASSIGNMENT SHEET	400
B-4	STATE POINT DATA	409
B-5	COMBUSTION SYSTEM OPERATING CONDITIONS	410
B-6	HORSEPOWER/TORQUE VALUES	414
B-7	INTEGRATED COMPONENTS ASSEMBLY PERFORMANCE DEMONSTRATION TEST POINTS	416
B-8	GTP305-2 FINAL DESIGN POINT CYCLE ANALYSIS	418
D-1	SERIAL NUMBER MASTER HEAT NUMBER AND CAST AF2-1DA ALLOY CHEMISTRY	469
D-2	2200°F TENSILE PROPERTIES OF AS-CAST AF2-1DA ALLOY MEASURED ON TEST BARS MACHINED FROM A TURBINE WHEEL	470
D-3	ROOM AND ELEVATED TEMPERATURE TENSILE PROPERTIES OF HEAT-TREATED (UN-HIPped) CAST AF2-1DA ALLOY TURBINE WHEELS	477
D-4	ELEVATED TEMPERATURE STRESS RUPTURE PROPERTIES OF HEAT-TREATED (UN-HIPped) CAST AF2-1DA ALLOY TURBINE WHEELS	479

# LIST OF TABLES (Contd)

TABLE	TITLE	PAGE
D-5	ROOM TEMPERATURE LOW-CYCLE FATIGUE (LCF) PROPERTIES OF HEAT-TREATED (UN-HIPped) CAST AF-21DA ALLOY TURBINE WHEELS	483
D-6	HIP/HEAT TREATMENT COMBINATION	485
D-7	ROOM TEMPERATURE TENSILE PROPERTIES OF HIPped AND HEAT-TREATED CAST AF2-1DA TURBINE WHEELS	486
D-8	1400°F TENSILE PROPERTIES OF HIPped AND HEAT TREATED CAST AF2-1DA TURBINE WHEELS	487
D-9	1400°F CREEP-RUPTURE PROPERTIES OF HIPped AND HEAT-TREATED CAST AF2-1DA TURBINE WHEELS	488
D-10	1600°F CREEP-RUPTURE PROPERTIES OF HIPped AND HEAT-TREATED CAST AF2-1DA TURBINE WHEELS	489
D-11	1800°F CREEP-RUPTURE PROPERTIES OF HIPped AND HEAT-TREATED CAST AF2-1DA TURBINE WHEELS	490
D-12	ROOM TEMPERATURE LOW-CYCLE-FATIGUE (LCF) PROPERTIES OF HIPped AND HEAT-TREATED CAST AF2-1DA ALLOY TURBINE WHEELS	497
D-13	ROOM TEMPERATURE LOW-CYCLE-FATIGUE PROPERTIES OF HIPped AND HEAT-TREATED CAST AF2-1DA ALLOY TURBINE WHEELS	498
D-14	TENSILE TEST RESULTS OF HIP/HEAT TREATMENT COMBINATIONS WITHIN ACCEPTABLE PROCESSING RANGES (ALL VALUES ARE AVERAGE)	507



ADVANCED TECHNOLOGY COMPONENTS FOR  
MODEL GTP305-2 AIRCRAFT AUXILIARY POWER SYSTEM

SECTION I

INTRODUCTION

This document is submitted by AiResearch Manufacturing Company of Arizona, a Division of the Garrett Corporation, in compliance with data from A009 of Air Force Systems Command Contract F33615-75-C-2016. The contractual effort entitled "Advanced Technology Components for Aircraft Auxiliary Power System" encompassed two primary phases; Phase I-APU Design, and Phase II-Component Development.

Specific guidelines adhered to during APU design included maintaining compressor performance as defined from previous contracts, use of cast AF2-1DA alloy for the radial turbine, and component life requirements of 2500 hours based on a 5 hour duty cycle. Turbine and combustion system components were tested separately and then collectively at design operating conditions of temperature, pressure and speed.

During the course of the contract, an additional task was negotiated. This effort, AF2-1DA HIP/heat treatment study, was included to improve the as cast AF2-1DA fatigue life through the use of hot isostatic pressing (HIP) to close casting micro-shrinkage and eliminate crack initiation sites. The results of this effort are reported herein and are included as Appendix D.

## SECTION II

### SUMMARY

The Advanced Technology Components for the Model GTP305-2 Aircraft Auxiliary Power Unit Program performed under Contract F33615-75-2016, was a four-year contract aimed at developing turbine-end components culminating in an integrated component assembly test at design speed, temperature and pressure ratio. The program was divided into two phases: Phase I - APU Design, and Phase II - Component Development. This report presents the results of the effort conducted during this program.

The Model GTP305-2 Advanced APU is a single shaft, all shaft power engine incorporating an axial-centrifugal compressor, a reverse flow annular combustor and a radial-axial turbine. At a design speed of 76,585 rpm and an average turbine rotor inlet temperature of 2050°F, the APU was designed to be capable of 186.3 shaft horsepower, 171.0 horsepower/ft<sup>3</sup> and 1.86 horsepower/lb at 130°F sea level ambient conditions.

Cycle analyses indicated a 10-percent high pressure compressor flow increase improved matching characteristics with the low pressure compressor. This was accomplished by increasing the impeller inducer blade and impeller exit blade height. The deswirl vane configuration was also adjusted to accommodate a 25 degree exit swirl angle as required for the combustion system.

The combustion system for the Model GTP305-2 Advanced APU consists of a reverse flow annular combustor with an air-assist/airblast fuel injection system. Two principal features of the combustion system are:

- o Improved combustor durability and lower cost through a ceramic coated sheet metal design

- o Effective utilization of turbine nozzle sidewall coolant air, via introduction of airflow into the combustor, prior to entry into the turbine which increases cycle efficiency

Primary combustion system goals were to achieve an average combustor discharge temperature of 2067°F (equivalent to 2050°F turbine rotor inlet temperature with cooling flow), a temperature spread factor of 0.15, and a combustor liner pressure drop of 5.0 percent. At design point conditions, the combustor demonstrated a temperature spread factor of 0.163 and a combustor liner pressure drop of 4.1 percent during combustion system rig testing. Thermal paint test results indicated liner temperatures of 1700°F at ten discrete locations. Primary zone outer wall temperatures were 1500°F or lower which demonstrates ceramic thermal barrier coating effectiveness.

The radial-axial turbine stage is characterized by an integrally cast radial turbine nozzle with internally cooled vanes, a cast AF2-1DA radial turbine rotor and a cast exhaust duct assembly. Vane internal, chordwise, integrally cast fins enhance the internal vane cooling effects of the radial nozzle. External, fore and aft, radially oriented ribs augment cooling of the nozzle sidewalls. The cast radial turbine rotor is a bore cooled design, twenty blades (ten full blades and ten splitter blades), with a tip speed limitation of 1880 ft/sec, and optimized for a radial-to-axial turbine work split of 64.7-35.3 percent. The radial-axial turbine stage is designed for an 87-percent total-to-diffuser exit static efficiency level.

Cold air turbine testing including cooling flow effects, indicate design efficiency goals were exceeded. The turbine achieved a total-to-diffuser exit static efficiency of 0.884 at design corrected speed and pressure ratio.

Combustion system and turbine components were installed in the integrated components assembly (ICA) hot test rig. ICA testing was conducted to establish component performance at design operating conditions of, temperature, pressure and speed. ICA testing results confirmed cold air test results at the rated design point conditions.

ICA test results, cold air testing and combustion system parameters were input to the cycle model. All other model parameters were unchanged. The Model GTP305-2 Advanced APU is capable of 225.3 shaft horsepower, 206.8 horsepower/ft<sup>3</sup> and 2.25 horsepower/lb at 130°F sea level ambient day.

AF2-1DA radial turbine rotor castings were x-ray inspected, as-cast elevated temperature tensile strength measured, and as-cast/heat treated room temperature tensile and stress-rupture properties determined. The rotors were HIPped in four combinations with temperatures varying from 2150 to 2250°F, pressures of 15 or 29 ksi and a constant 3 hour time period. Evaluations were performed using four HIP conditions in combination with eight heat treatments. Four HIP/heat treatment combinations were selected for LCF testing on the basis of acceptable microstructures and mechanical properties. Room temperature strain-control LCF tests were performed and results analyzed on a Weibull distribution. Data analysis indicated that LCF life improvement was obtained through HIP and heat treatment. Specifically, a 3X LCF life improvement was achieved for as-cast wheels predicted to fail in less than 1000 cycles.

## SECTION III

### APU DESIGN

The Model GTP305-2 Advanced APU is a single shaft, all shaft power engine incorporating an axial-centrifugal compressor, a reverse flow annular combustor and a radial-axial turbine. At a design speed of 76,685 rpm and an average turbine inlet temperature of 2050°F, the APU design intent was an engine capable of 186.3 shaft horsepower, 171.0 horsepower/ft<sup>3</sup> and 1.86 horsepower/pound at 130°F sea level ambient day. A 2500 hour life based on a 5 hour duty cycle was established for design considerations along with production design methodology where applicable.

The following sections describe the cycle matching studies, combustor design and turbine design including aerodynamic and stress.

#### 3.1 Cycle Analysis and Matching Studies

##### 3.1.1 Preliminary Design Point Selection

A preliminary design point cycle analysis was conducted to define an engine cycle that meets the program performance goals. The analysis was conducted for sea level static, 130°F ambient conditions. The baseline compressor configuration for this analysis consisted of components developed under Contract F33615-72-C-1936 [Reference (1)]. The axial and centrifugal compressor stage performance data are presented in Figures 1 and 2, respectively. The axial stage data was used without modification, while the centrifugal stage data was scaled on flow. This scaling is to be accomplished in the engine by means of a minor shroud recontour. The 100 percent shaft speed shown in the above

(1) Humble, C.E. Swenski, D.F., et al, "Advanced Auxiliary Power Unit", Technical Report AFAPL-TR-75-22, July 1975.

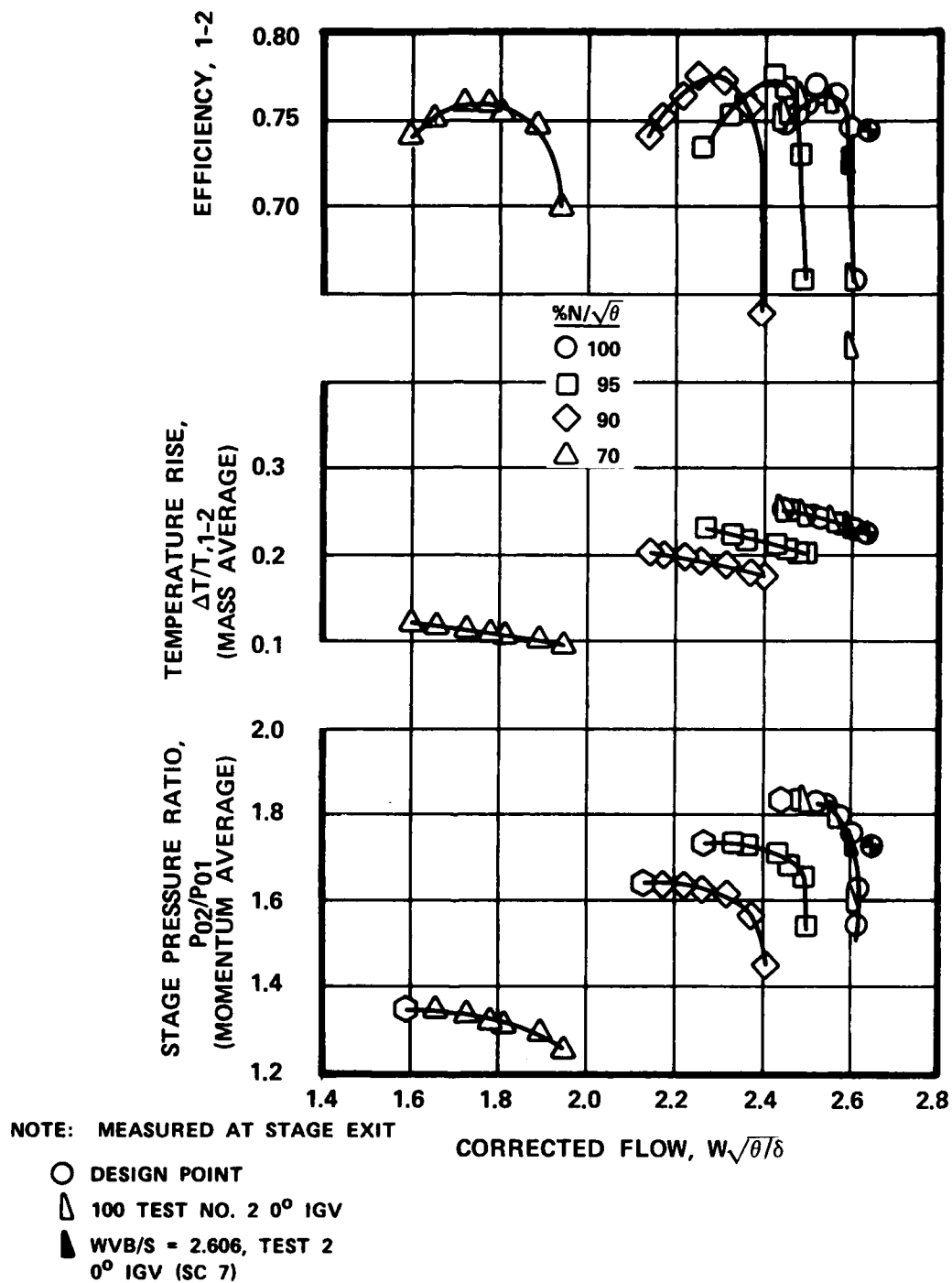


Figure 1. Axial compressor stage performance

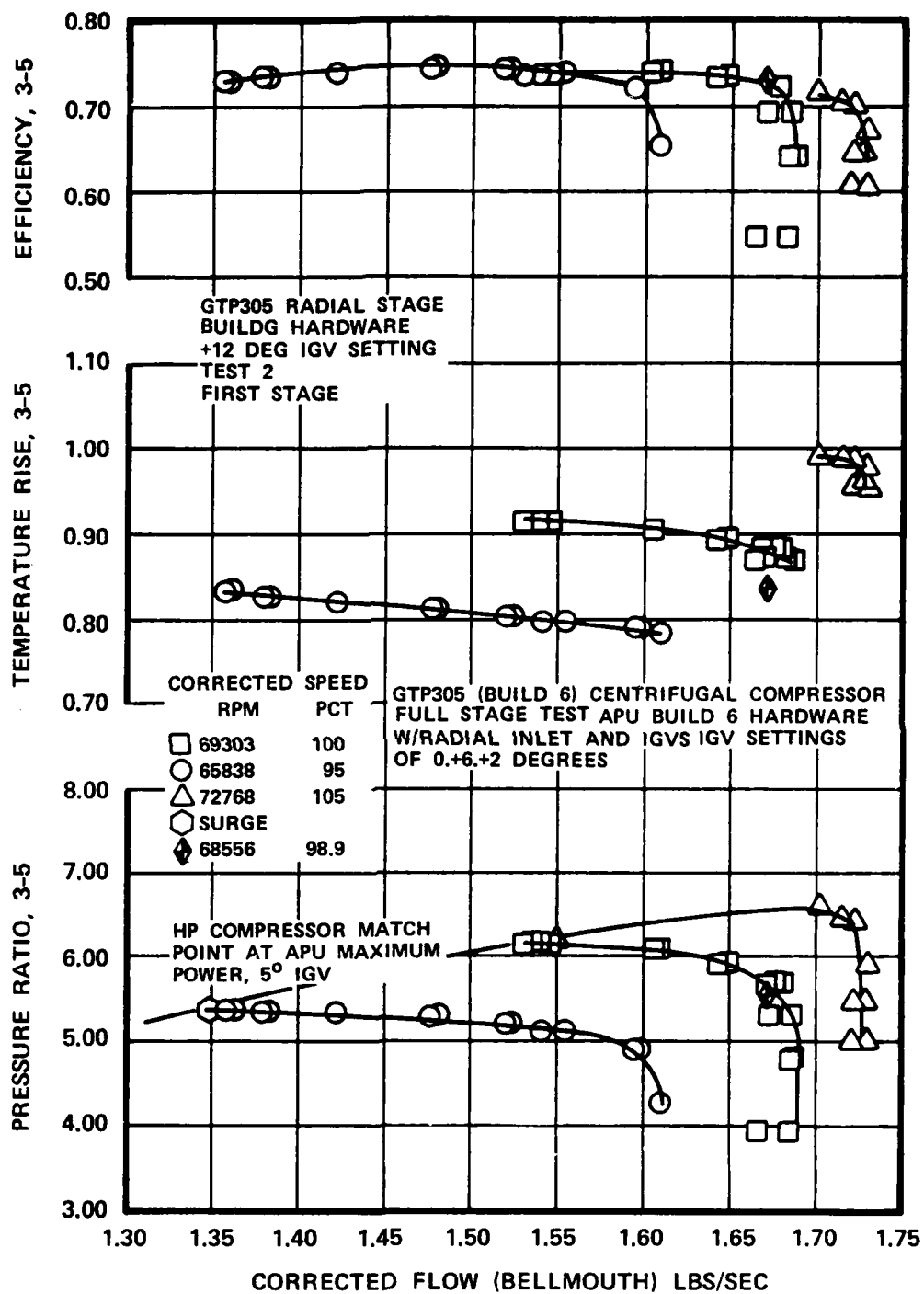


Figure 2. Centrifugal compressor stage performance

figures is 81,822 rpm. The turbine in this cycle analysis was assumed to have an overall efficiency (inlet total to diffuser exit static) of 86 percent, and a turbine rotor inlet temperature of 2100°F. Additional assumptions used in this analysis are listed in Table 1.

Results of this preliminary cycle analysis are presented in Figure 3. Specific power, specific fuel consumption and output shaft horsepower are plotted as a function of percent engine shaft speed. The preliminary match point was selected at 92.5 percent shaft speed, since Figure 3 shows that this results in:

- o A high specific power
- o Near minimum specific fuel consumption
- o Near maximum output shaft horsepower

Detailed cycle analysis data for this preliminary match point are presented in Figure 4. It should be noted that an approximate 9.0 percent flow increase of the centrifugal compressor stage is required to match both compressor stages at maximum efficiency.

The overall turbine performance requisite for the preliminary match point was identified in this cycle analysis. An additional analysis was conducted to optimize the work split between the radial and axial turbine stages at this match point. In addition to aerodynamic performance considerations, this work split optimization analysis also included preliminary stress and life estimates. In these stress and life analyses, the radial wheel was considered to be constructed of cast AF2-1DA material, while two candidate materials, forged Astroloy and cast AF2-1DA, were considered for use in the axial wheel. IN713LC, the axial turbine material used in the previous F33615-72-C-1936 program, has insufficient properties for use in this current program.



TABLE 1. GTP305-2 PRELIMINARY DESIGN POINT  
CYCLE ASSUMPTIONS.

SEA LEVEL, 130°F AMBIENT	
Compressor	
Inlet plenum total pressure loss, $\Delta P/P$	2.0%
First Stage Axial Performance	Figure 3-1
Interstage Total Pressure Loss, $\Delta P/P$	2.0%
Second Stage Centrifugal Performance	Derived from Figure 3-2
Compressor Exit Diffuser Total Pressure Dump Loss, $\Delta P/P$	1.0%
Leakage Flow	2.0%
Cooling Flow (bypasses turbine and does no work)	2.5%
Combustor	
Efficiency	99.5%
Total Pressure Loss, $\Delta P/P$	5.0%
Turbine Nozzle Inlet Total Pressure Loss, $\Delta P/P$	1.0%
Turbine	
Efficiency (inlet total to diffuser exit static)	86%*
Rotor Inlet Total Temperature	2100°F
Accessory Horsepower	13.5
Gear Efficiency	98%

\*Derated by 1-efficiency point due to rotor backface cooling  
flow pumping work.

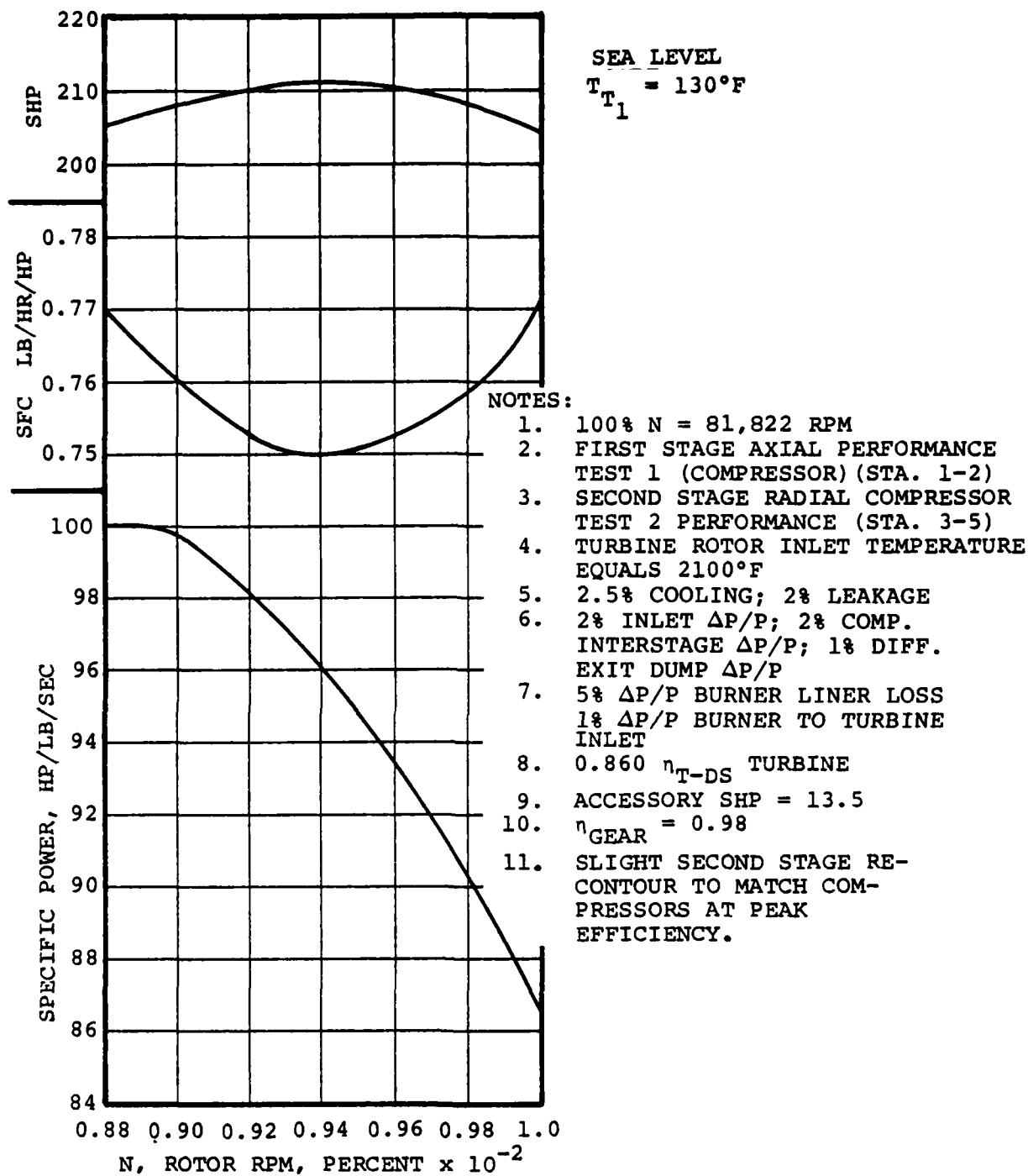


Figure 3. GTP305-2 match point preliminary analysis

## ENGINE

LHV	H/C	ALTITUDE	FPS
18400.0	.16786	0.0	0.000

DRIVING TURBINE		COMPRESSIONS			TURBINE			BEFORE MIXING	
	HP	ENERGY CORR.	WATER	SHAFT HP	ACC HP	HP REQUIRED	MECHANICAL EFFICIENCY	ENTHALPY	TEMP
1	86.92	0.000	0.000	210.2	13.5	723.5	.980	639.14	1724.0
1	408.23	0.000	0.000						

BURNER	WATER	FUEL FLOW
	0.000	157.95

CR FLOW	PRESSURE	TEMP	DELTA	THETA	H	ENTHALPY	GAMMA	F/A	W/A	EFF	P/P	DEL P	LEAKAGE	COOLING
AMBIENT	2.303	15.606	569.7	1.000	1.137	53.349	141.03	1.399	0.0000					
INLET	2.150	15.402	589.7	.980	1.137	53.349	141.03	1.399	0.0000	1.000	1.000	.020	0.000	AMBIENT
COMPRESS	1.531	23.907	707.6	1.627	1.364	53.349	169.47	1.396	0.0000	.775	1.660	0.000	0.000	INLET
DIFFUSER	1.531	23.429	707.6	1.594	1.364	53.349	169.47	1.396	0.0000			0.000	0.000	COMPRESS
COMPRESS	.496	118.781	1245.8	8.083	2.462	53.349	303.06	1.366	0.0000	.747	5.076	0.000	.020	DIFFUSER
DIFFUSER	.400	117.599	1245.8	8.002	2.462	53.349	303.06	1.366	0.0000			.010	0.000	COMPRESS
BURNER	.610	111.714	2559.7	4.935	4.935	53.385	681.87	1.398	.0213	.995	1.000	.050	0.000	BURNER
DIFFUSER	.622	110.602	2559.7	7.526	4.935	53.385	681.87	1.398	.0213			.010	0.000	DIFFUSER
TURBINE	3.026	171.27	1.000	7.302	53.384	435.14	1.325	.0207	0.0000	.860	7.526	0.000	0.000	TURBINE

FUEL FLOW	TOTAL	CONNECTED	SFC	POWER	NET	CORRECTED	SPECIFIC
	15d.0	151.2	.751		210.2	201.2	97.34

**Figure 4. GTP305-2 preliminary match point cycle analysis**

Results of the work split optimization studies indicated that:

- o The obtainable overall turbine efficiency is higher with forged Astroloy axial wheels than with cast AF2-1DA axial wheels.
- o The obtainable overall turbine efficiency increases as the turbine speed decreases.
- o For given stress levels, the turbine exit velocity level decreases (exit tip radius increases) as turbine speed decreases.

Using these general trends, one candidate turbine configuration was selected for each shaft speed considered. Selections were made at a work split that maximized overall turbine life, while simultaneously attempting to maximize turbine performance. Forged Astroloy axial rotors were selected for 92.5- and 95-percent speeds and a cast AF2-1DA rotor for 90-percent speed. Table 2 summarizes the important parameters associated with each candidate configuration. These three candidate configurations are compared on the cycle analysis data in Figure 5. Note that the 92.5 percent speed candidate has maximum output power, is close to the minimum specific fuel consumption, and maintains a high level of specific power.

Based on the above analyses, the GTP305-2 engine preliminary match point was selected at 92.5-percent engine speed. The turbine configuration selected had a:

- o Cast AF2-1DA radial turbine wheel producing 63 percent of the overall turbine work output.
- o Forged Astroloy axial turbine wheel producing 37 percent of the overall turbine work output.

TABLE 2. SELECTED CANDIDATE TURBINE CONFIGURATIONS FROM  
PRELIMINARY WORK SPLIT ANALYSIS.

T.I.T. = 2100°F									
Parameters	90.0% Speed			92.5% Speed			95.0% Speed		
	Radial	Axial Astroloy	Axial AF2	Radial	Axial Astroloy	Axial AF2	Radial	Axial Astroloy	Axial AF2
Work Split	67.2		32.8	63.0	37.0		66.0	34.0	
Overall $\eta_{T-DE}$		0.874	0.874		0.874			0.868	
Life, Hours	400		400	280	260		360	400	
$R_T$ Axial, Inches			2.960		2.98			2.91	
$\beta$ Axial, Degrees			56.5		58.0			56	
H/T Axial			0.518		0.547			0.53	
$V_{acr}$ Exit	0.3876		0.353	0.346	0.37		0.374	0.400	
Exit, Degrees	-14.2		0	-14.0	0		-22.10	0	
Hub Cooling Req'd			200°F		170°F			130°F	
Burst Margin	25%		25%	25%	25%		23.7%	25%	

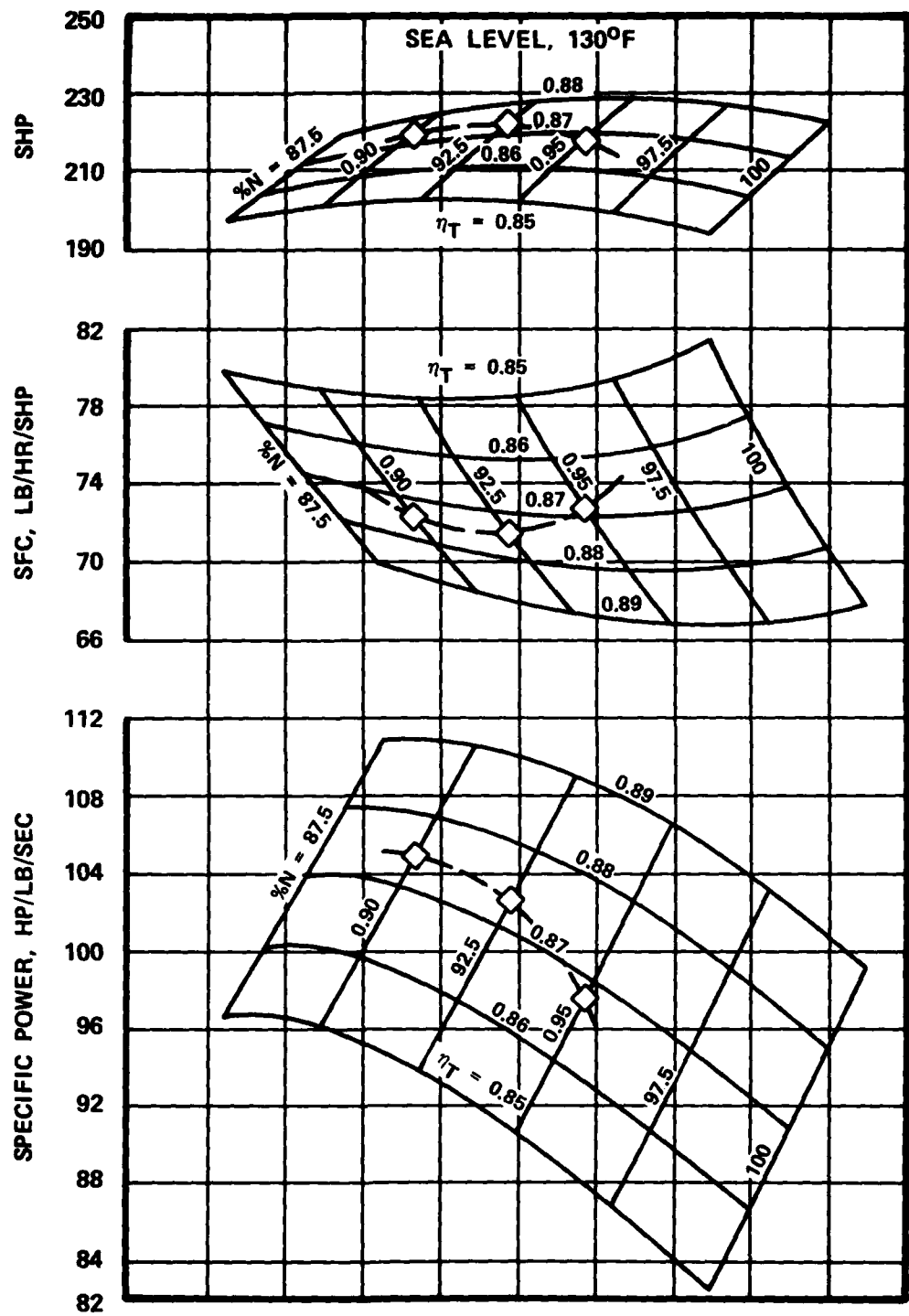


Figure 5. GTP305-2 design point analysis

Figure 6 presents the flowpath for the selected turbine configuration. This flowpath contains one minor perturbation that was accomplished to increase available combustor liner height (i.e., the axial wheel exit tip radius was intentionally reduced by 0.050 inch, 2.98 to 2.93 inch. The axial turbine exit critical velocity ratio was thereby increased from 0.370 to 0.390, and predicted overall turbine efficiency decreased from 0.874 to 0.8715.

An Air Force/AiResearch Technical Coordination Meeting was held on September 2, 1975 to review the preliminary engine design point selection. Since the calculated engine output shaft horsepower at the preliminary design point was well above the program goal, the existing contract objectives were assigned priorities to best achieve overall USAF contract goals. The design point selection was to be reviewed, to consider an engine performance trade-off analysis on turbine inlet temperature and turbine efficiency, and to maximize turbine life and minimize turbine cost while using a cast axial turbine rotor design.

### 3.1.2 Final Design Point Selection

Cycle analysis studies evaluating the effects of variations of:

- o Turbine rotor inlet temperature
- o Turbine efficiency
- o Engine rotor speed;

on engine output shaft horsepower, specific fuel consumption, and specific power were conducted. Results of these studies indicated that at or near 92.5-percent engine speed, any combination of turbine efficiency and turbine inlet temperature results in:

$$\eta_{T-DE} / \eta_{OA} = 87.15$$

$$b_S = 0.310$$

$$b_R = 0.34 \text{ (TO ROTOR SHROUD)}$$

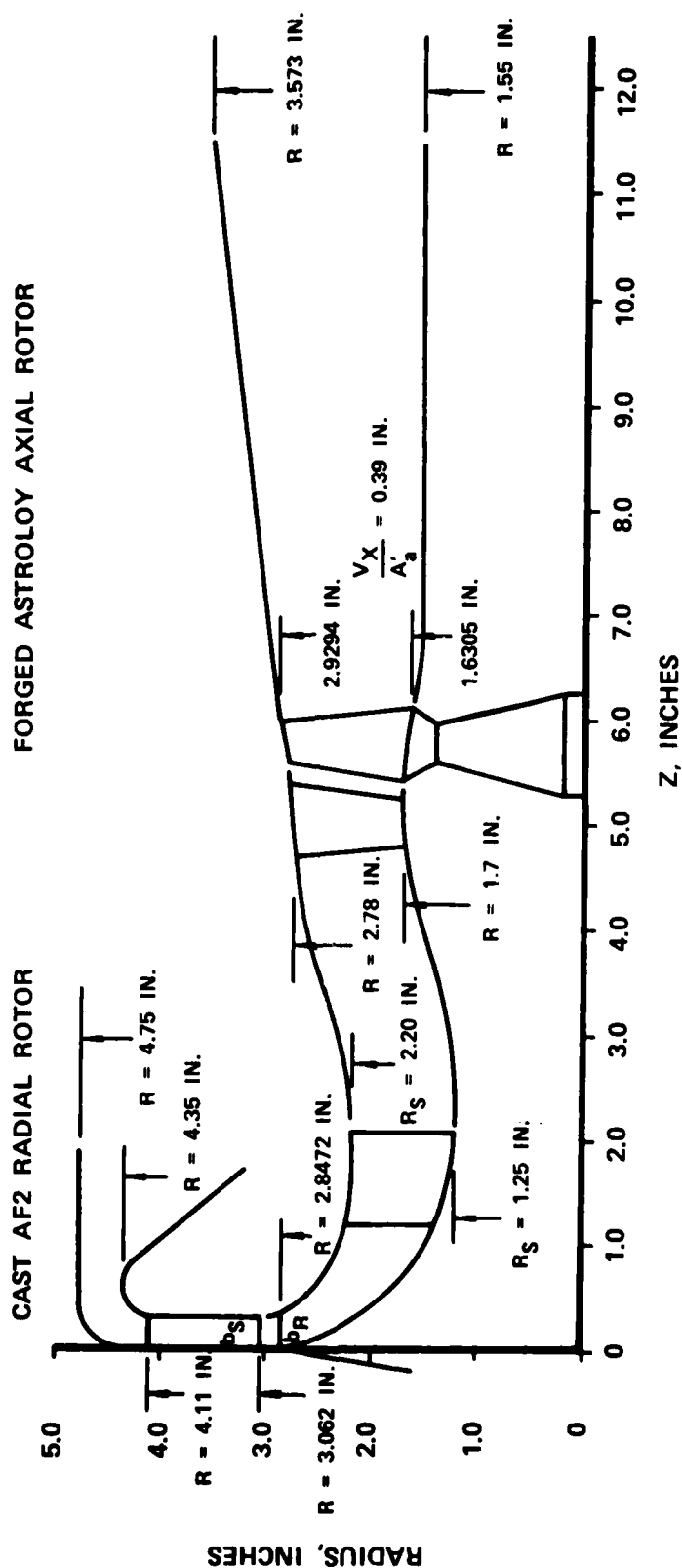


Figure 6. GTP305-2 preliminary turbine configuration 92.5-percent speed



- o Near maximum output shaft horsepower
- o Near minimum specific fuel consumption
- o A high specific power

In addition these studies indicated that a turbine rotor inlet temperature of 2050°F still produces engine output shaft horsepower levels above the contract goal. A revised engine match point, of 92.5-percent speed and a turbine rotor inlet temperature of 2050°F, was therefore selected for a turbine work split analysis.

The turbine considered in the work split analysis was to have both the radial and axial stages constructed of cast AF2-1DA material. Figure 7 presents the results of the turbine work split analysis at the revised engine match point. This figure shows that for a work split range of approximately 28 to 35 percent, the original 86-percent engine overall turbine efficiency goal can still be achieved (because of the reduced turbine work requirement at the revised match point). Examining Figure 7 further, it would appear that the obvious choice of work split, based on turbine wheel lives, is at approximately 31 percent. But the axial turbine configuration dictated by this work split involves additional problems not addressed in this work split analysis. These problems involve excessively high peak local blade stresses. For this reason, a preliminary stress analysis was conducted to investigate the relative change in peak blade stresses between the axial wheel configurations required to accomplish:

- o 31-percent axial stage work output
- o 35-percent axial stage work output

The blade hub-to-tip radius (H/T) ratios for these axial wheels are approximately 0.50 and 0.55, respectively. The preliminary three-dimensional stress analysis results for these two axial wheels showed that the 0.50 H/T ratio blade increased the peak

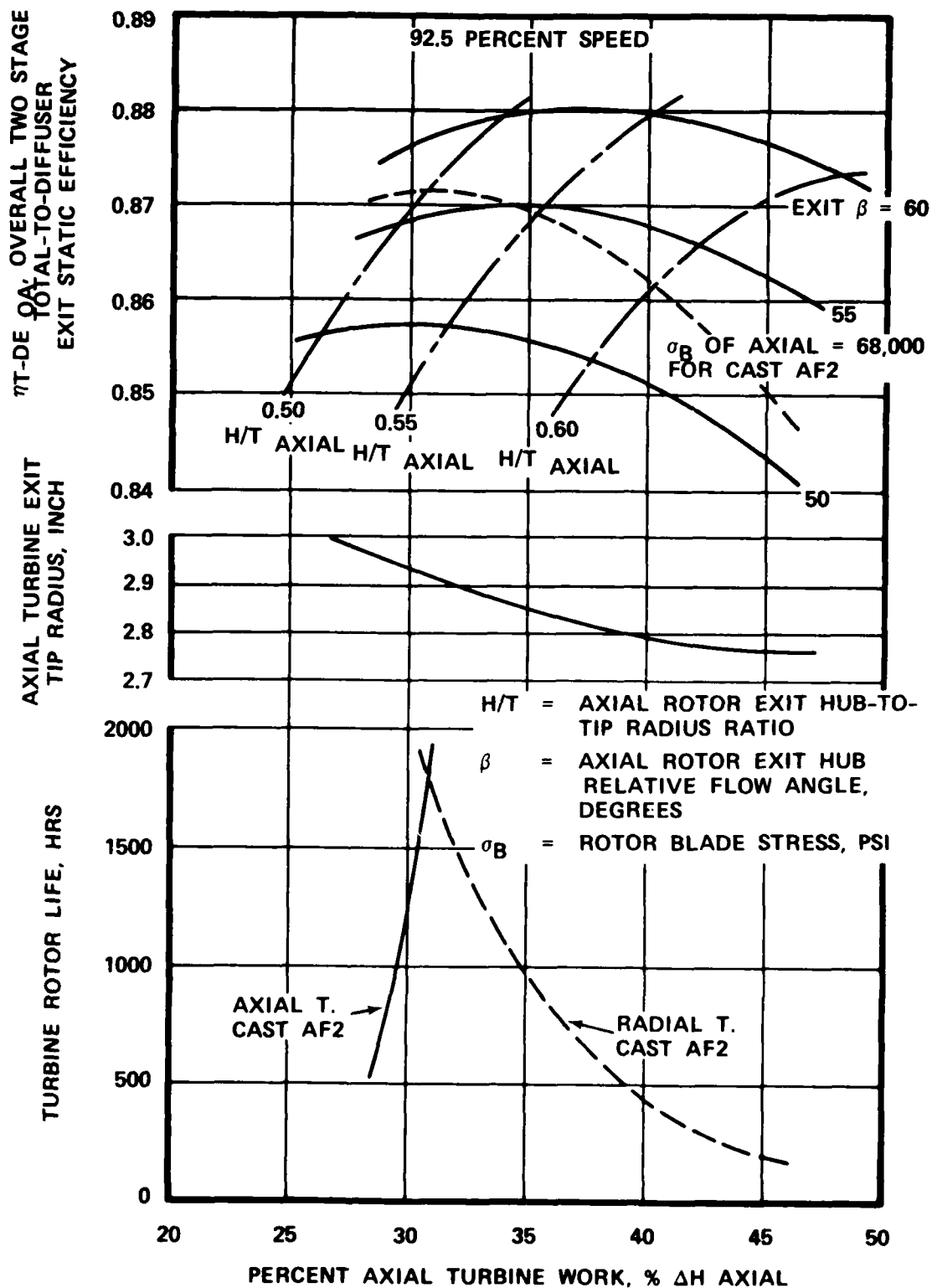


Figure 7. GTP305-2 turbine optimization for 2050°F T.I.T. cycle

local blade stress by 15 to 20 percent over that of the 0.55 H/T ratio blade. This increase is unacceptable.

Based on results of the above cycle analysis, turbine work split analysis, and preliminary stress analysis, the GTP305-2 final match point was selected at:

- o 92.5-percent speed
- o 2050°F turbine-rotor inlet temperature,

with a turbine configuration having a:

- o Cast AF2-1DA radial turbine wheel producing 64.7 percent of the overall turbine work output
- o Cast AF2-1DA axial turbine wheel producing 35.3 percent of the overall turbine work output

For this final design point, the preliminary life estimates indicate that radial, and axial turbine lives are increased by a factor of 2.5 to 3.0, when compared with preliminary match point 2100°F turbines.

The final design point cycle analysis, showing the engine output power reduced to 186 horsepower, is presented in Figure 8. A full listing of the cycle assumptions used in this cycle analysis is presented in Table 3. The final turbine design point conditions are presented in Table 4, and the turbine conceptual flow path is presented in Figure 9.

Another Air Force/AiResearch Technical Coordination Meeting was held on October 2, 1975 to review the final engine design point selection. The Air Force concurred with the final design point selection.

305 ENGINE - (1100) FCLL BEARINGS										ENGINE	
DRIVING TURBINE		COMPRESSION HEADS		ENERGY CORR.		TURBINE		THERMAL		BEFORE MIXING	
	MP	COOLING AIR	WATER	SHAFT HP	ACC HP	MECHANICAL EFFICIENCY	ENTHALPY				TEMP
1	86.42	0.000	0.000	186.0	13.5	.990	431.17				1696.9
1	404.13	0.000	0.000								
BURNER		WATER		FUEL FLOW		NET		CORRECTED		SPECIFIC	
FUEL FLOW		TOTAL		CORRECTED		SFC		POWER		NET	
		151.1		144.6		.813				186.0	
										178.0	
										86.10	

Figure 8. GTP305-2 final design point cycle analysis

TABLE 3. GTP305-2 FINAL DESIGN POINT CYCLE ASSUMPTIONS.

SEA LEVEL, 130°F AMBIENT	
Rotor Physical Speed, rpm	75,685
Compressor	
Inlet plenum total pressure loss, $\Delta P/P$	2.0%
First Stage Axial Performance	Figure 3-1
Interstage Total Pressure Loss, $\Delta P/P$	2.0%
Second Stage Centrifugal Performance	Derived from Figure 3-2
Second Stage Compressor Flow Multiplier	1.10
Compressor Exit Diffuser Total Pressure Dump Loss, $\Delta P/P$	1.0%
Leakage Flow	2.0%
Cooling Flow (bypasses turbine and does no work)	2.5%
Combustor	
Efficiency	99.5%
Total Pressure Loss, $\Delta P/P$	5.0%
Turbine Nozzle Inlet Total Pressure Loss, $\Delta P/P$	1.0%
Turbine	
Efficiency (inlet total to diffuser exit)	85%*
Rotor Inlet Total Temperature	2050°F
Radial Turbine Stator Vane Cooling Flow	2.5%
Accessory Horsepower	13.5
Gear Efficiency	98%

\*Derated to allow for rotor backface cooling flow pumping work

TABLE 4. GTP305-2 TURBINE FINAL DESIGN  
POINT CONDITIONS.

Parameter	Radial	Axial	Overall
$T_{in}$ , °R	2509.70*	1983.811	-
$\Delta H$ , Btu/lb	152.045	82.955	235.00
$P/P)_{T-T}$	3.2415	2.1597	
$P/P)_{T-X}$	3.2566	2.1597	
$P/P)_{T-DE}$	-	-	7.529
$W\sqrt{\theta/\delta})_{in}$ , lbs/sec	0.615	1.735	
N, RPM	75685.0	75685.0	
$N/\sqrt{\theta}$ , RPM	34407.8	38700.6	
$\Delta P/P$ , Interturbine duct percent		1.69	
Diffuser Recovery, $T_D$	-	-	0.400
$\eta_{T-T}$ Stage, Total-to-Total Efficiency	0.8847**	0.8909**	
$\eta_{T-DE}$ , Predicted Overall Total- to-Diffuser Exit Static	-	-	0.871**
$\eta_{T-DE}'$ Predicted With 1.5 Percent Radial Rotor Cooling and 0.5 Percent Axial Rotor Disk Cooling			0.866
$\eta_{T-DE}'$ Cycle, With Cooling Flow			0.850

\*Based on Rotor Inlet

\*\*Predicted Values With No Radial or  
Axial Rotor Cooling Flows and  
0.015 Inch Rotor Shroud Clearances.

2050°F TIT CYCLE  
 92.5 PERCENT SPEED  
 PERCENT AXIAL TURBINE WORK = 35.3  
 AXIAL TURBINE - CAST AF2-1DA

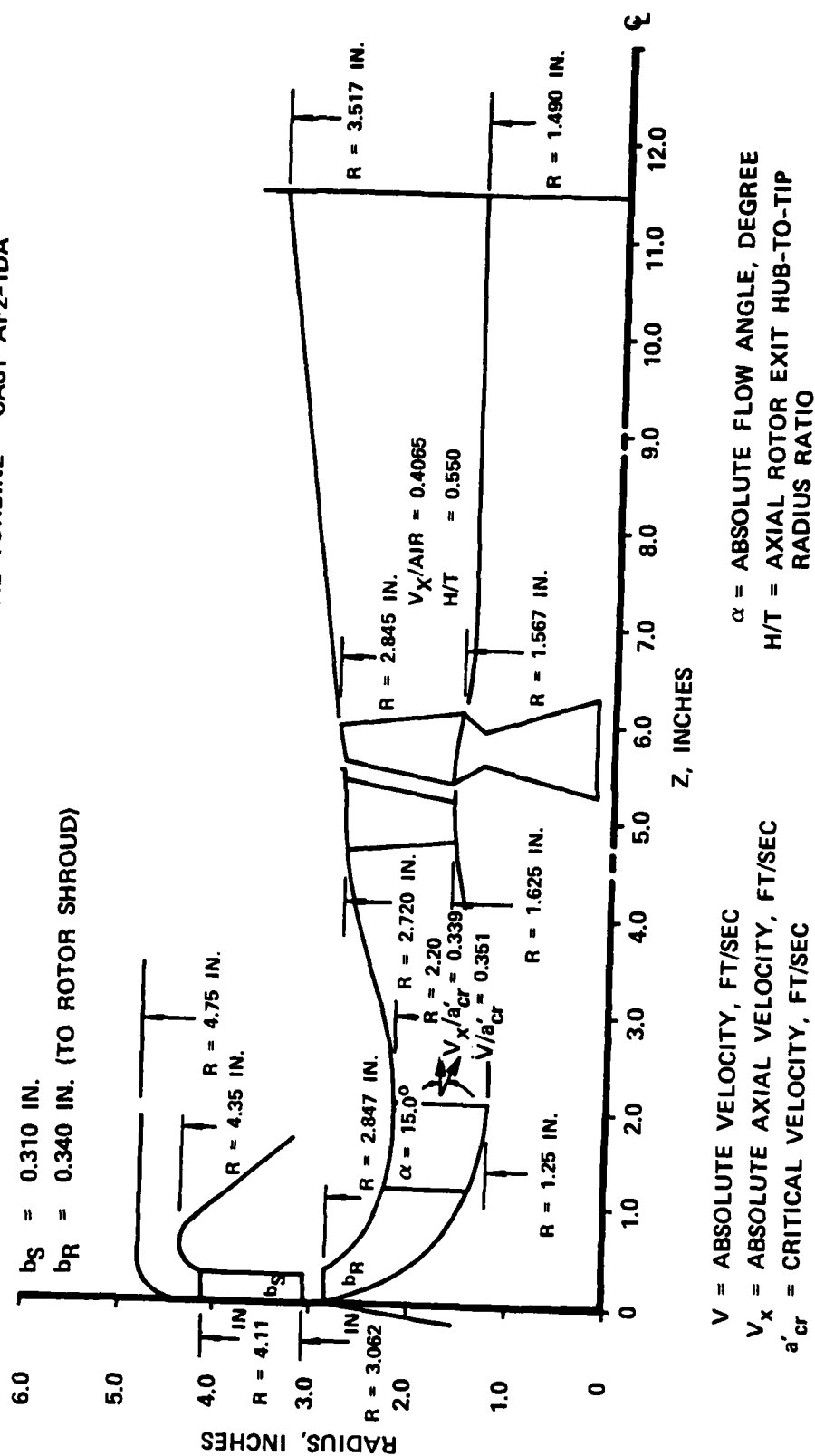


Figure 9. GTP305-2 all cast configuration

### 3.1.3 Off-Design Performance Analysis

Off-design performance was calculated for the GTP305-2 engine. The basic cycle assumptions used in this analysis are the same as, or scaled from, those used in the final design point cycle analysis (Figure 8). The compressor inlet guide vane (IGV) performance used in the off-design analysis is presented in Figure 10. The compressor performance is the same as that presented in Section 3.1. Off-design turbine maps were estimated using the turbine geometry and the design point parameters.

Estimated performances for unit inlet sea level ambient temperatures of 130, 59, and  $-65^{\circ}\text{F}$  were calculated for three different IGV settings, and are presented in Figures 11 through 13 respectively. These figures present the variation of:

- o Radial turbine inlet temperature
- o Unit inlet airflow
- o Overall compressor pressure ratio
- o Fuel flow
- o Unit exhaust temperature

as a function of engine output shaft horsepower with IGV settings as a parameter. These figures show that the engine horsepower output at any given turbine inlet temperature, is highest with an IGV setting of one degree.

The thermodynamic state points through the engine for unit inlet sea level ambient temperatures of 130, 59 and  $-65^{\circ}\text{F}$ , and a turbine inlet temperature of  $2050^{\circ}\text{F}$ , are presented in Figures 14 through 16, respectively.



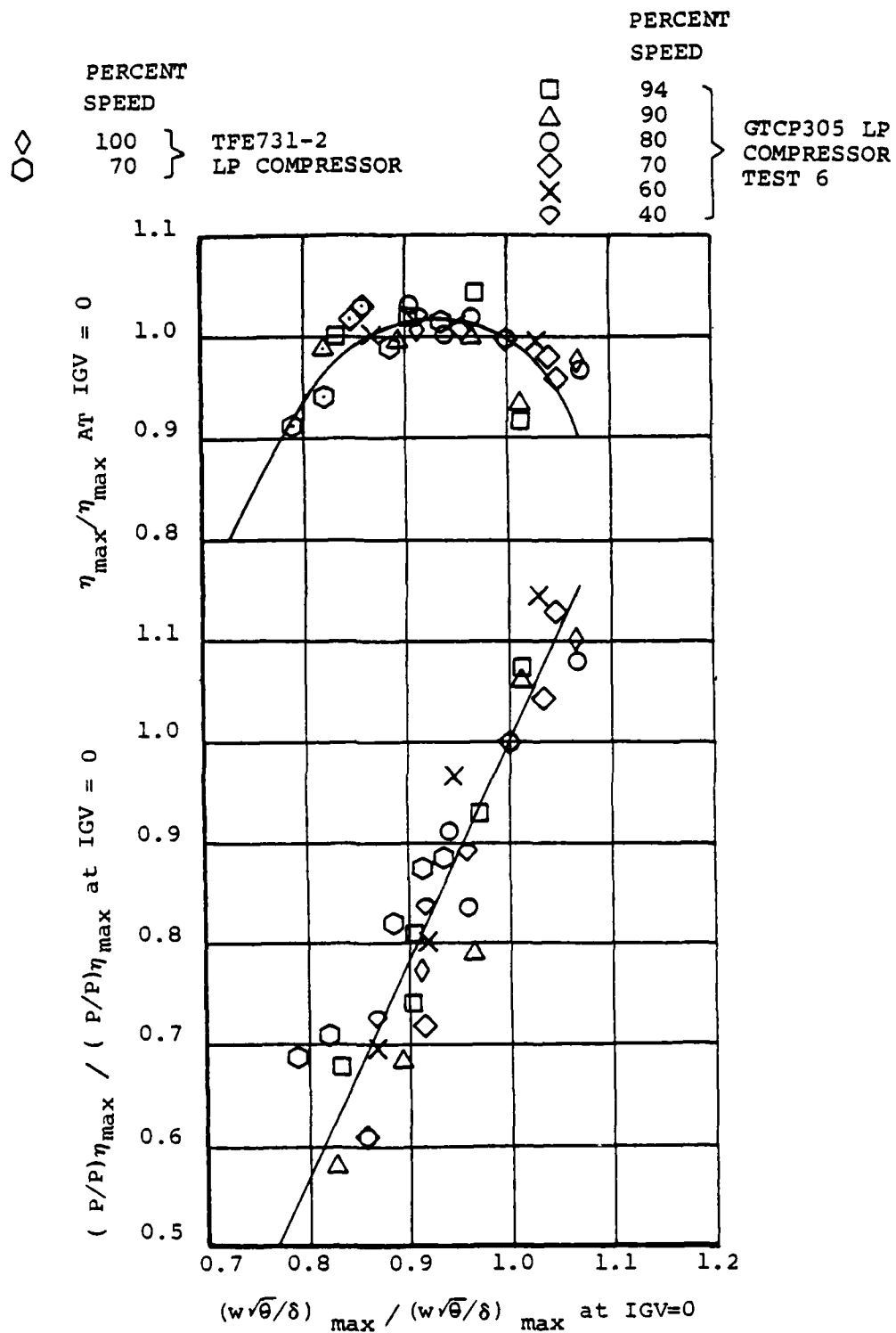


Figure 10. IGV test data correlation

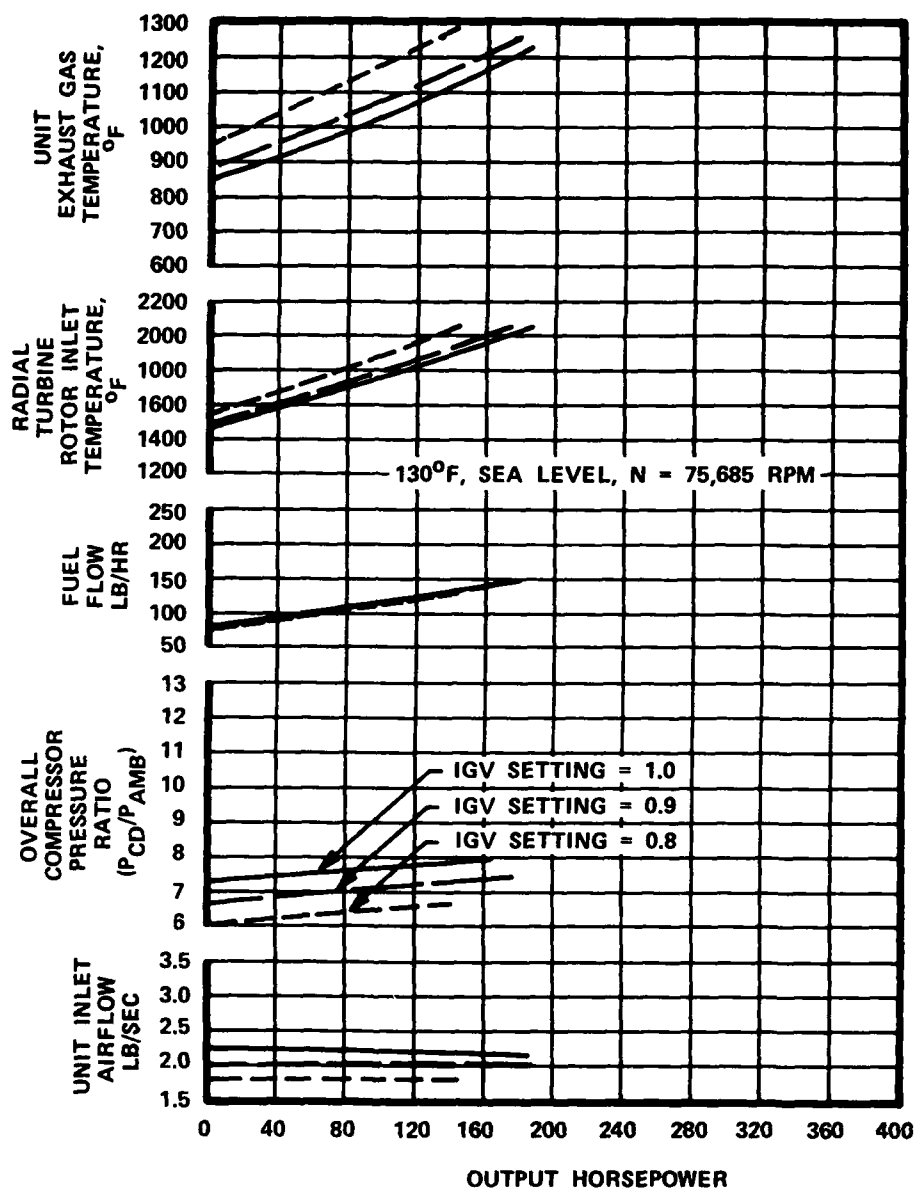


Figure 11. GTP305-2 off-design performance

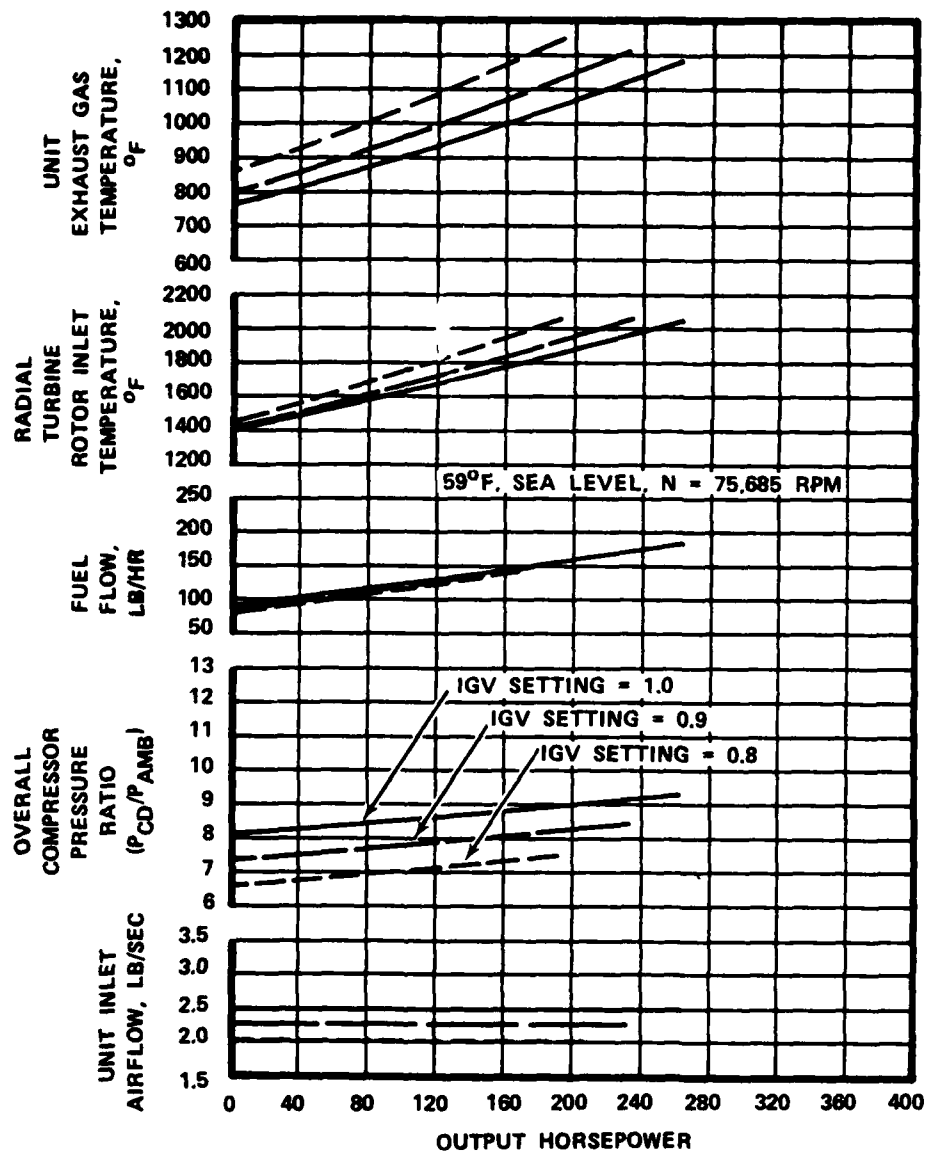


Figure 12. GTP305-2 off-design performance

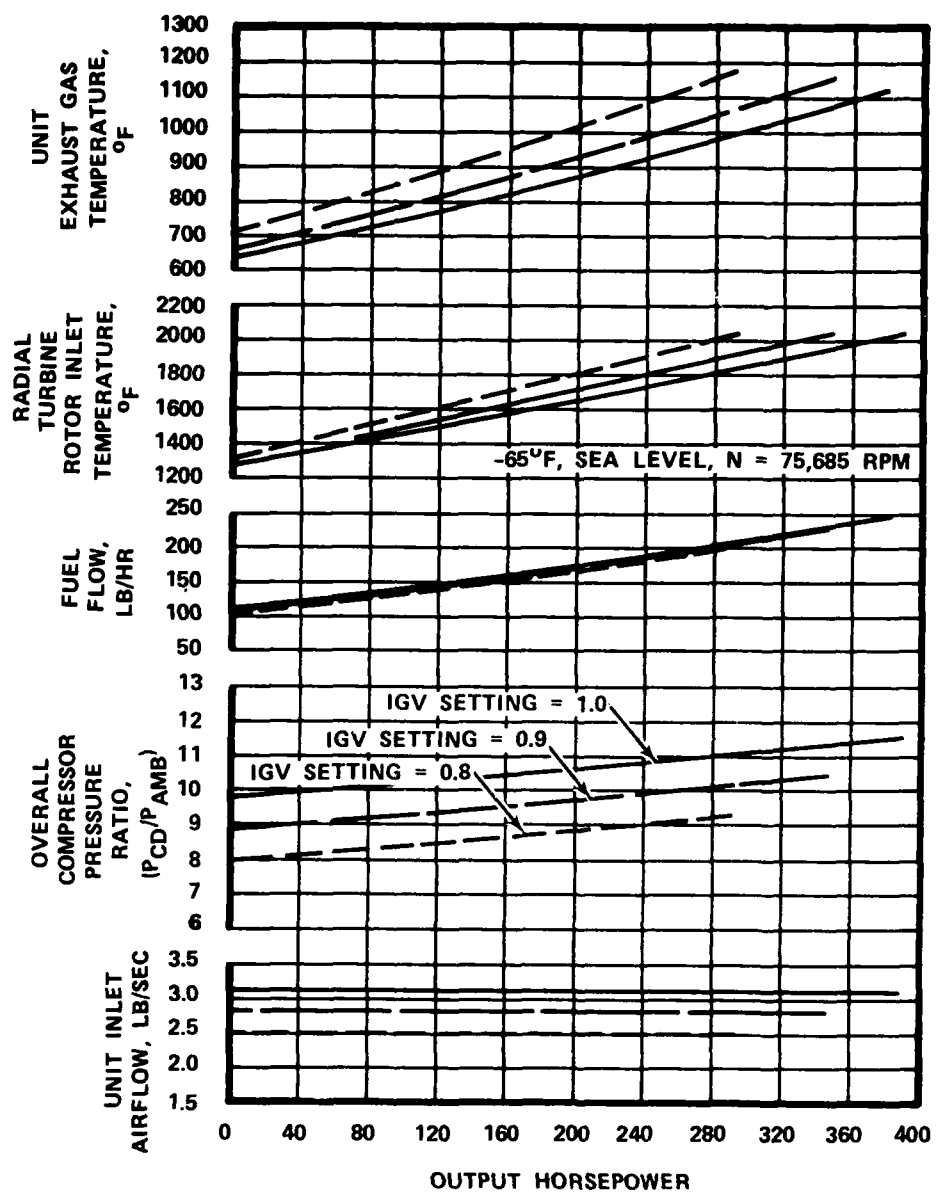


Figure 13. GTP305-2 off-design performance

NOTE:

1. Ambient Conditions : 130°F,  
14.696 PSIA

2. Miscellaneous Data:  
Accessory Horsepower - 13.5  
Shaft Horsepower - 186.3  
Leakage Flow - 2%  
Cooling Flow - 2.5%  
IGV Setting,  $C_1$  - 1.0

3. Nomenclature:

P - Total Pressure PSIA  
P/P - Pressure Ratio  
T - Total Temperature, °F  
 $W_C$  - Corrected Flow, Lb/Sec  
 $W_A$  - Actual Throughflow, Lb/Sec  
 $\eta$  - Efficiency  
J - Ratio of Station to Ambient Pressure

$W_A = 2.16$   
 $W_C = 2.35$   $W_C = 1.55$   $W_C = 1.58$   $W_C = 0.40$   $W_C = 0.61$   $W_C = 0.61$   $W_C = 3.89$   
J = 0.98 J = 1.63 J = 1.59 J = 8.01 J = 7.53 J = 7.61 J = 1.00

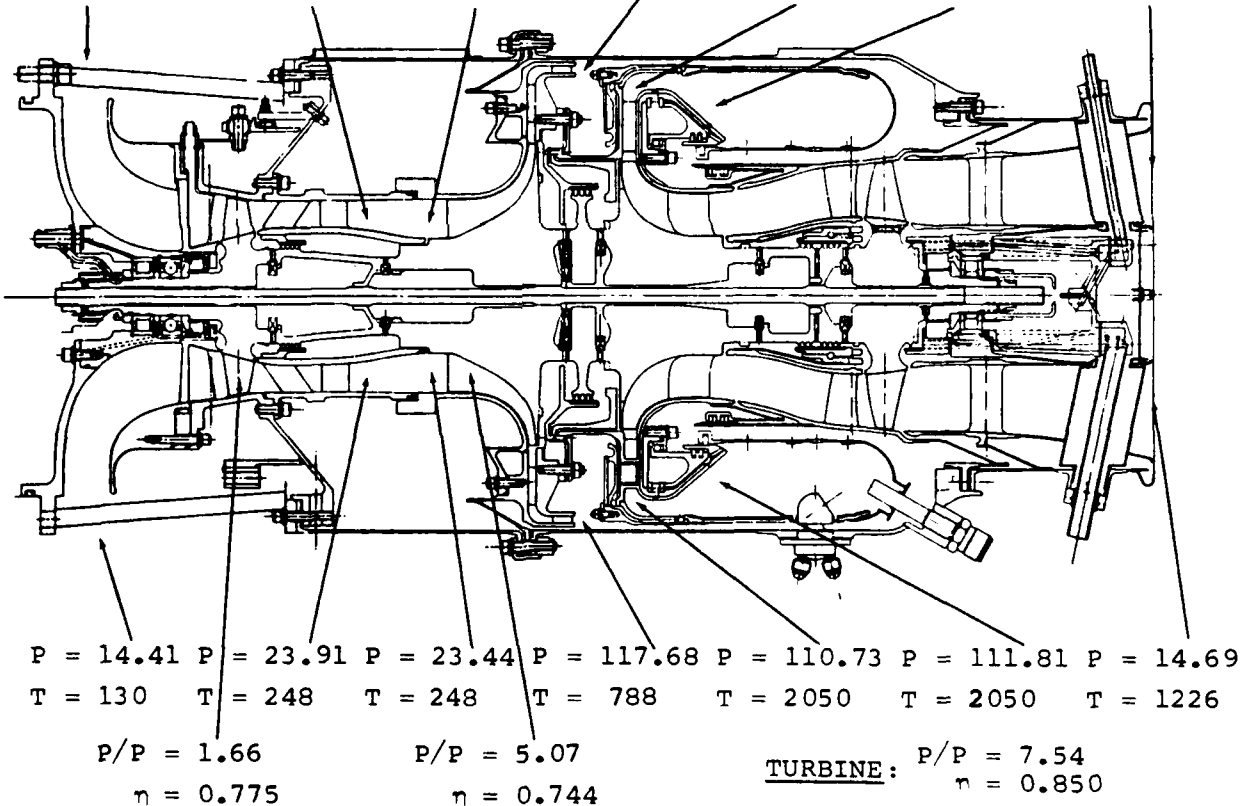


Figure 14. Estimated off-design performance of GTP305-2 APU

NOTES:

1. Ambient Conditions: 59°F,  
14.696 PSIA

2. Miscellaneous Data:

Accessory Horsepower - 13.5  
Shaft Horsepower - 262.6  
Leakage Flow - 2%  
Cooling Flow - 2.5%  
IGV Setting,  $C_1$  - 1.0

3. Nomenclature:

P - Total Pressure, PSIA  
P/P - Pressure Ratio  
T - Total Temperature, °F  
 $W_C$  - Corrected Flow,  
Lb/Sec  
 $W_A$  - Actual Throughflow,  
Lb/Sec  
 $\eta$  - Efficiency  
J - Ratio of Station to  
Ambient Pressure

$W_A = 2.52$   
 $W_C = 2.58$   $W_C = 1.70$   $W_C = 1.75$   $W_C = 0.39$   $W_C = 0.61$   $W_C = 0.61$   $W_C = 4.49$   
J = 0.98 J = 1.63 J = 1.59 J = 9.33 J = 8.79 J = 8.88 J = 1.00

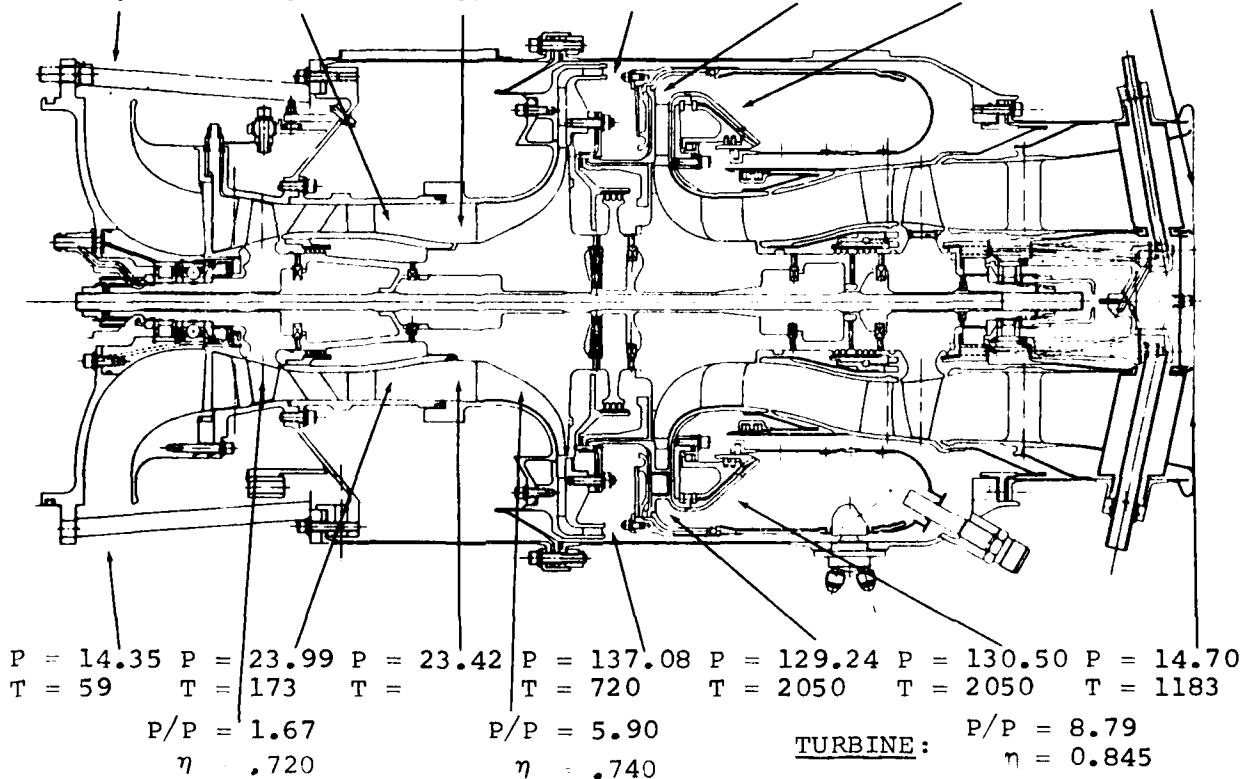


Figure 15. Estimated off-design performance of GTP305-2 APU

NOTES:

1. Ambient Conditions: -65°F,  
14.696 PSIA

2. Miscellaneous Data:

Accessory Horsepower - 13.5  
Shaft Horsepower - 388.5  
Leaking Flow - 2%  
Cooling Flow - 2.5%  
IGV Setting,  $C_1$  - 1.0

3. Nomenclature:

P - Total Pressure, PSIA  
P/P - Pressure Ratio  
T - Total Temperature, °F  
 $W_C$  - Corrected Flow,  
Lb/Sec  
 $W_A$  - Actual Throughflow,  
Lb/Sec  
 $\eta$  - Efficiency  
J - Ratio of Station to  
Ambient Pressure

$W_A = 3.13$

$W_C = 2.73$   $W_C = 1.87$   $W_C = 1.92$   $W_C = 0.37$   $W_C = 0.61$   $W_C = 0.61$   $W_C = 5.50$

J = 0.97 J = 1.65 J = 1.61 J = 11.57 J = 10.95 J = 11.05 J = 1.00

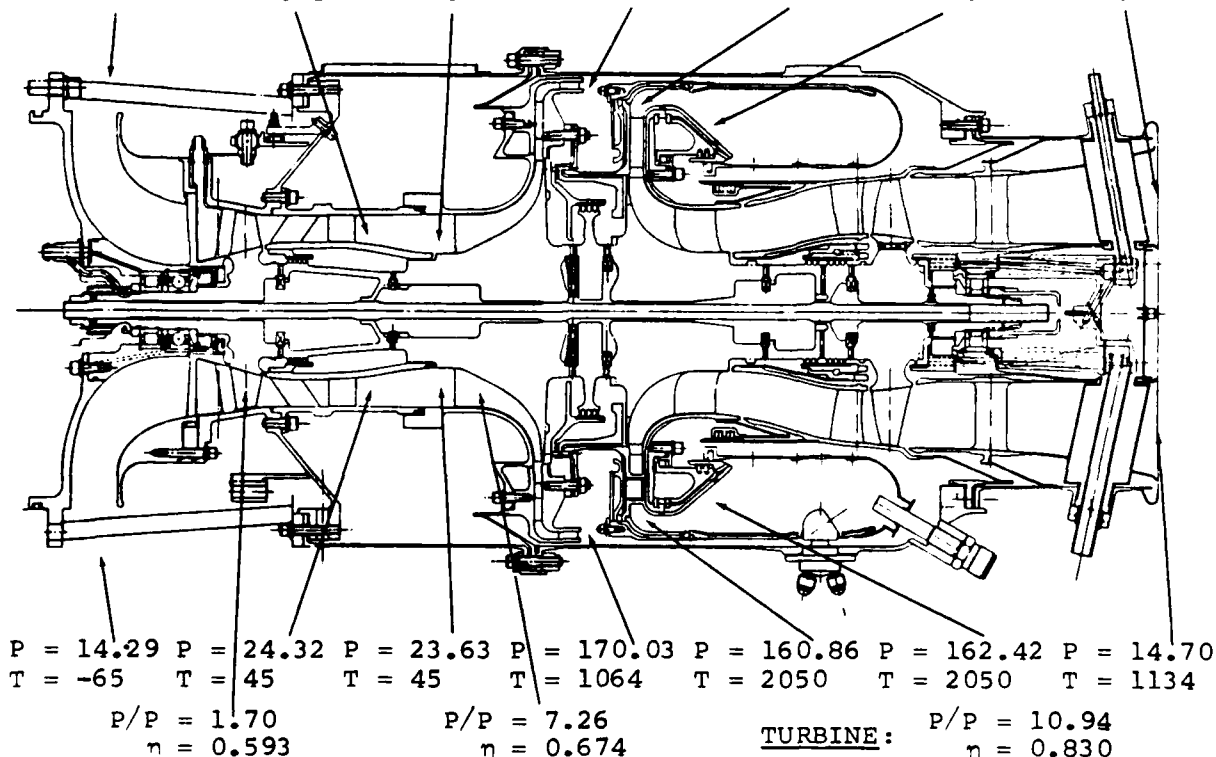


Figure 16. Estimated off-design performance of GTP305-2 APU

### 3.2 Compressor

As previously discussed, cycle analyses indicates that a 10-percent high pressure (HP) compressor flow increase would improve matching characteristics with the low pressure (LP) compressor stage. Based on selected design point conditions, the following procedures were utilized during the rematching calculation:

- o HP blade geometry and hub contour were maintained
- o Flow analysis station lines were extrapolated to 110 percent flow streamline
- o Interstage duct recontoured to join axial stage second stator exit shroud line and recontoured HP compressor inducer shroud line
- o Interstage duct wall velocity distribution and impeller blade loadings from existing design reviewed and compared with values calculated from flow analysis program for the new contour.
- o Diffuser vane height, 90-degree radius bend, and deswirl vane height adjusted to be consistent with recontour
- o Deswirl vane stagger and meridional flow path redefined for exit swirl angle of 25 degrees, based on combustion input requirement

Figure 17 depicts the contouring change required on the HP compressor stage for cycle matching. Flow analysis station lines shown on the figure were used to accurately extrapolate to the 110 percent flow streamline. The impeller inducer blade height



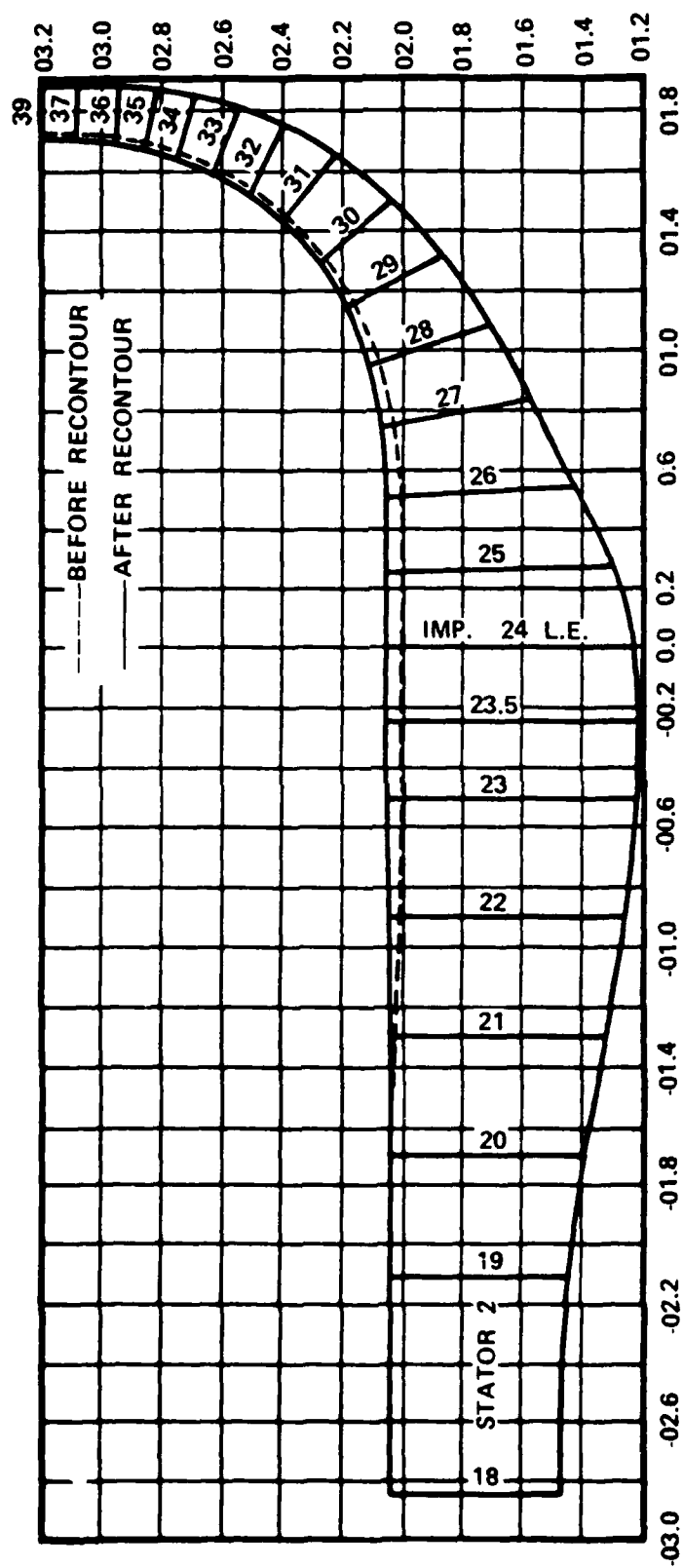


Figure 17. GTP305-2 hp compressor 10 percent flow increase recontour

was increased by 0.050 inch, and impeller exit blade height (b-width) by 0.0156 inch.

### 3.3 Combustion System

The combustion system for the Model GTP305-2 APU consists of a reverse-flow annular combustor with an air-assist/airblast fuel injection system. Airflow is delivered to the combustor from the centrifugal compressor stage. Primary combustion system goals were an average combustor discharge temperature of 2067°F\*, a temperature spread factor (TSF) of 0.15, and a combustor liner pressure drop of 5 percent.

Principal features characterizing the GTP305-2 combustion system shown in Figure 18 include:

- o Reduction in the number of fuel injection points from 12 to 10 (Model GTP305-1 to Model GTP305-2) with no degradation of TSF, which was accomplished by incorporating air blast fuel injectors and increased primary zone channel height
- o Improved combustor durability and lower cost through upgrading of original Model GTP305-1 ceramic coating (Rockide-2) to current state-of-the-art thermal barrier ceramic coating (Zirconia stabilized with Yttria). This eliminates the need for sintered sheet metal (Regimesh) to provide a good mechanical bond

\*Combustor discharge temperature of 2067°F is equivalent to turbine rotor inlet temperature of 2050°F when vane internal cooling flow mixes with mainstream flow.

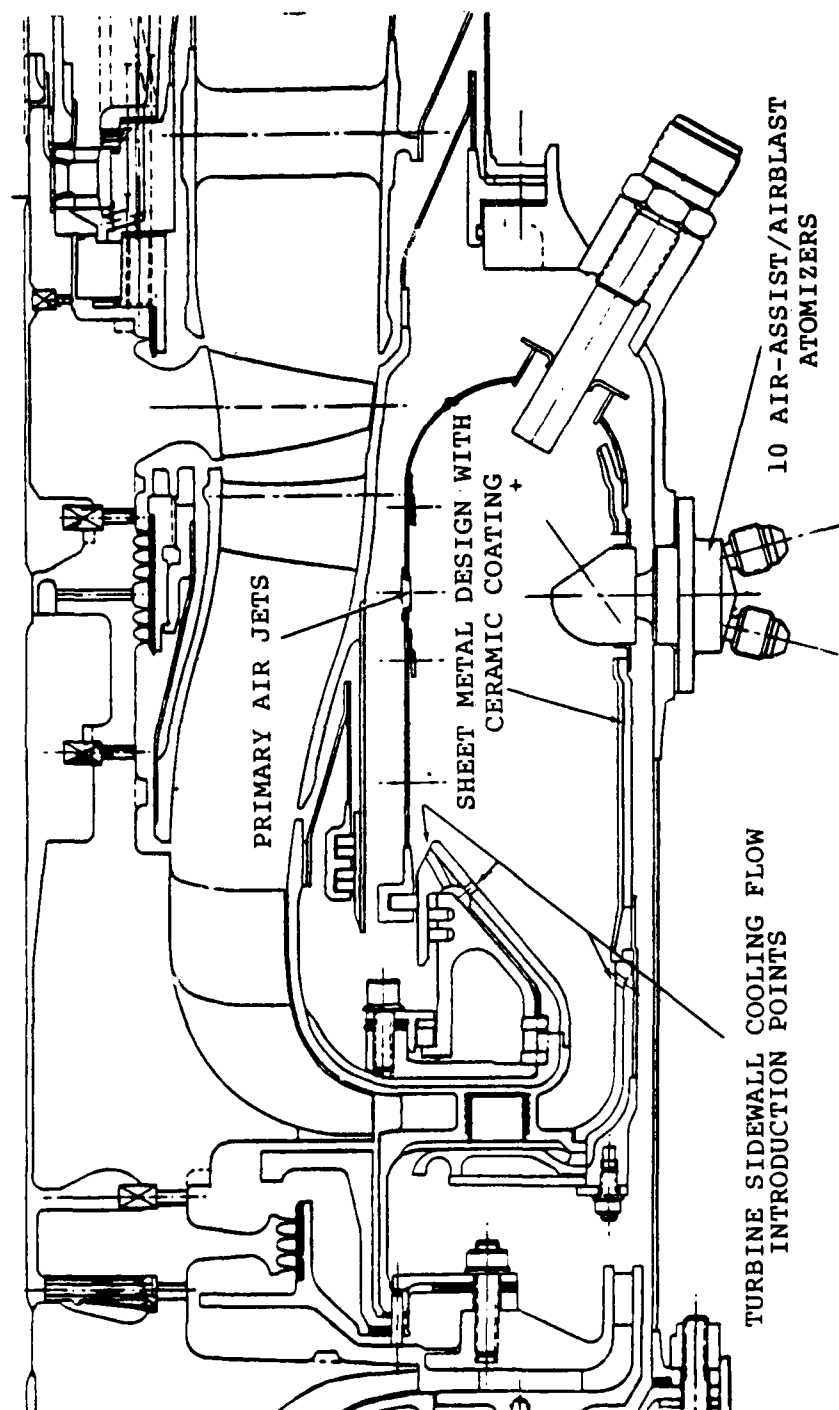


Figure 18. Principal features of GTP305-2 combustion system

- o Effective utilization of turbine side wall coolant air-flow via introducing flow into combustor where mixing with the bulk gas flow is accomplished prior to entry into the turbine, thus increasing cycle efficiency

Design point operating conditions for the GTP305-2 combustion system are listed in Table 5. A comparison of the Models GTP305-2 and GTP305-1 combustion system design parameters is provided in Table 6.

### 3.3.1 Combustor

Previous experience with the Model GTP305-1 APU indicated that combustion system performance is strongly influenced by control of the combustor primary zone aerodynamics. To better control primary zone aerodynamics in the Model GTP305-2 APU and provide for single-sided recirculation in the primary zone, all primary and dilution air is introduced through the inner combustor wall. This manner of air insertion into the combustor also maximizes the outer plenum annulus air velocity, and provides increased external convective cooling to the combustor outer wall. The inside surface of the outer wall is coated with a thermal barrier ceramic coating and requires no internal film cooling. The inner combustor wall is film cooled. Air is introduced at three locations, one at the edge of the dome, and two others further downstream on the inner combustor wall.

A flow analysis was conducted on the annular passage surrounding the combustor. Results indicate that the static pressure in the vicinity of the primary jets (see Figure 18) was too low (velocity head too high) for adequate penetration into the combustor. While the velocity in general was too high, the swirl component in particular was excessively high. Two approaches were investigated to reduce the localized high velocities near the primary ports:

TABLE 5. GTP305-2 COMBUSTION SYSTEM DESIGN  
POINT OPERATING CONDITIONS.

Combustor Airflow	2.07 lb/sec
Combustor Inlet pressure	117.6 psia
Combustor Inlet Temperature	786°F
Combustor Outlet Temperature	2067°F
Fuel Flow	150.5 lb/hr
Fuel/Air Ratio	0.0202
Temperature Spread Factor	0.15

TABLE 6. COMPARISON OF GTP305-1 AND GTP305-2  
COMBUSTION SYSTEM DESIGN PARAMETERS.

	<u>GTP305-1</u>	<u>GTP305-2</u>
Reference Velocity (ft/sec)	25	29
Heat Load (Btu/Hr Ft <sup>3</sup> ATM)	3.3 X 10 <sup>6</sup>	3.01 X 10 <sup>6</sup>
Combustor Pressure Loss (%)	3.6	3.5
Combustor Channel Height (inch)	1.18	1.64
Combustor Length (inch)	4.98	5.0
L/H	3.86	3.05
Combustor Volume (Ft <sup>3</sup> )	0.075	0.121
Number and Type of Injectors	12 Simplex	10 AA/AB
Injector Spacing Ratio	1.84	1.50

- o Increase local flow area
- o Decrease the flow swirl angle

An increased flow area could be accomplished by shortening the combustor and/or reducing channel height. The required 25- to 30-percent length reduction was considered impractical due to a significant reduction in available mixing length. The possibility of reducing channel height was also eliminated because of the critical influence on mixing and spreading of fuel and air in the primary zone.

The principal mechanism available for decreasing swirl velocity near the inner wall primary jets is to reduce the combustion system inlet swirl angle. As shown in Figure 19, a reduction from 35 to 25 degrees inlet swirl angle could effect a 2.7-percent increase in the static pressure level along the inner annulus, thereby allowing adequate air penetration at the primary air jets. This inlet swirl angle change was accomplished by restaggering the centrifugal compressor stage deswirl vanes, as discussed in Section 4.0. This vane restaggering was accomplished with minimum impact on the centrifugal compressor stage and resulted in significant benefits to the combustion system.

The inadequate penetration problem was further alleviated by incorporation of the STAGG turbine backface configuration which allowed the combustor to move axially forward approximately 3/8 inch. Although the inner annulus area was not significantly increased by this shift, placement of the primary combustor holes was more favorable.

Detail information related to turbine sidewall cooling flow introduction into the mainstream flow, method of combustor attachment to mating engine structure, and ceramic coating on the combustor outer wall are discussed below.

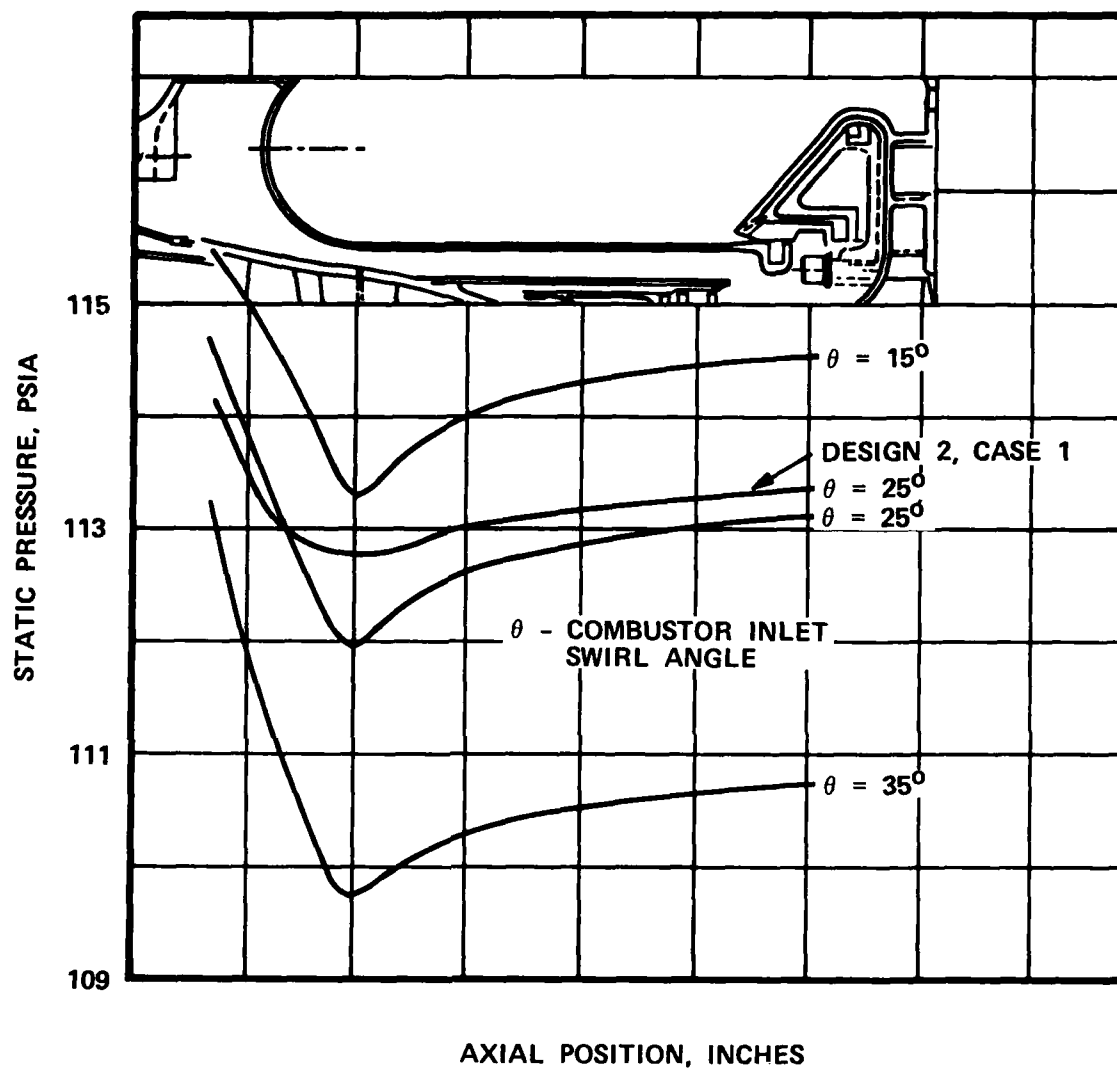


Figure 19. GTP305-2 inner annulus  $P_s$  distribution



As shown in Figure 20, radial nozzle coolant flow is directed along the forward and aft nozzle sidewalls. To maintain a high overall engine cycle efficiency, the nozzle coolant flows are returned to the mainstream flow in the combustor, rather than being diverted around the combustor. The forward cooling air discharge orifices are positioned to allow adequate coolant flow penetration into the combustor bulk flow, followed by a sufficient mixing length. The orifices are also positioned to prevent scrubbing of the liner ceramic coating edge. The aft nozzle sidewall cooling air is introduced into the combustor at two closely spaced positions near the dilution zone, again providing an adequate mixing length with the combustor bulk flow.

The combustor is attached to the mating engine structure at the outer bolt circle. As shown in Figure 20, a floating machined forging forms a flow path for the forward nozzle sidewall cooling flow. The floating machined forging effects a butt-type seal near the combustor ceramic coating. A 100-pound spring force is transmitted through the combustor outer wall, solid ring, machined forging and reacted against the forging-nozzle interface, closing the flow path and maintaining the mechanical seal.

The Model GTP305-2 combustor outer wall, unlike the Model GTP305-1, is a sheet metal design, ceramically coated with a Zirconia base ceramic stabilized with Yttria. The Model GTP305-1 utilized sintered sheet metal (Regimesh), a porous material used for bonding Rockide-Z. The current state-of-the-art coating is applied through a series of plasma spray passes with varying degrees of Zirconia composition. This method of ceramic-to-metal bonding has been proven [Reference (2)] and is considered to have better structural integrity than the Model GTP305-1 design. In

(2) Liebert, C.H. and Stepka, F.S., "Ceramic Thermal-Barrier Coatings For Cooled Turbines:", AIAA Paper No. 76-729, July 1976.

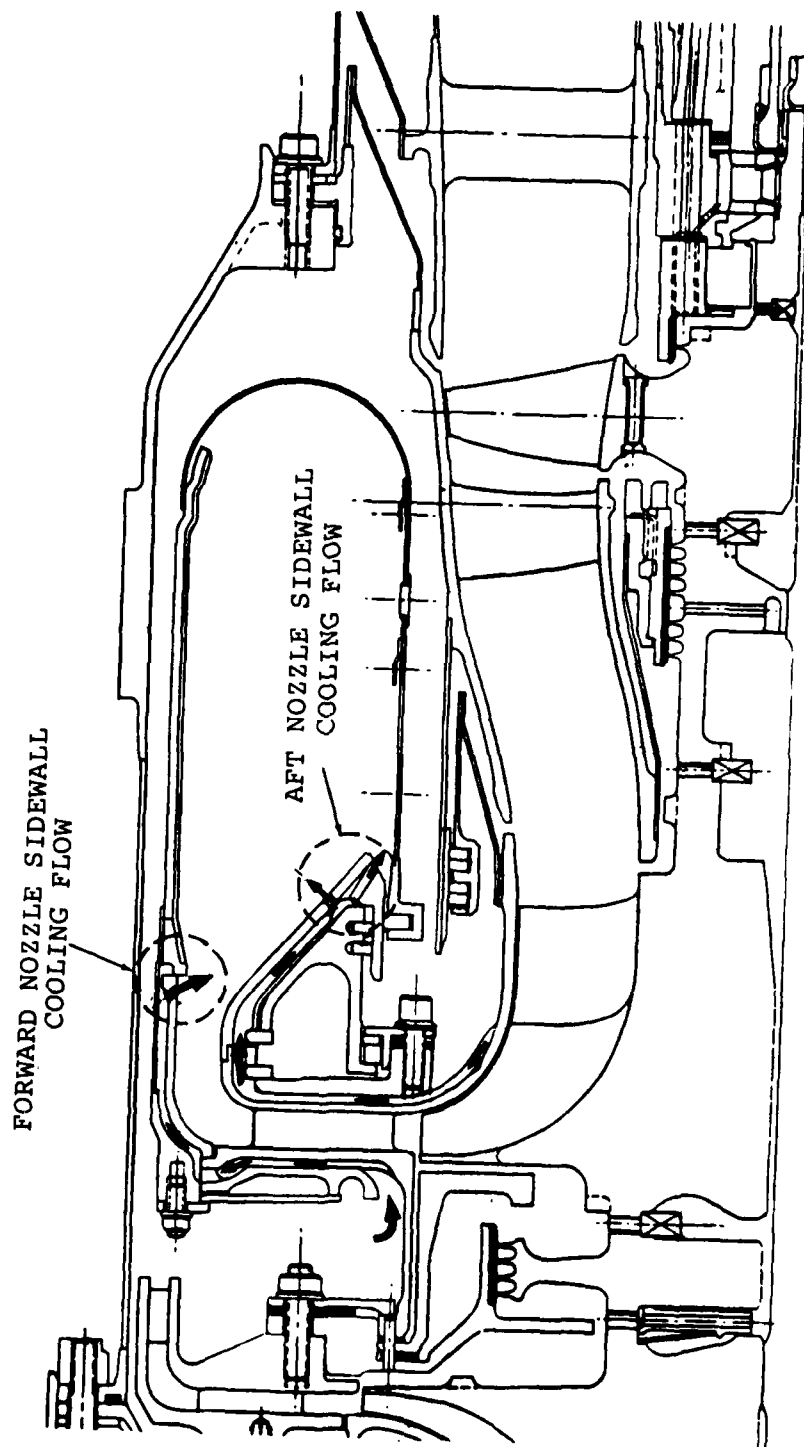


Figure 20. Radial turbine nozzle cooling flow schematic

addition, analytical cost studies indicate a 25-percent reduction in production cost can be realized using the sheet metal design.

### 3.3.2 Fuel Injection System

The Model GTP305-2 fuel injection system consists of 5-airassist/airblast atomizers and 5-pure airblast atomizers. The 10-fuel injection points were established, based on an atomizer spacing ratio of 1.5 (distance between atomizers/combustor channel height). Five start air-assist/airblast atomizers are used to assure a rapid and stable light-around of the combustion system. Figures 21 and 22 show a prototype air-assist/airblast atomizer with and without the shroud, respectively. Figure 23 is a typical cross section of this atomizer. All 10 Model GTP305-2 atomizers have identical fuel passage sizes to reduce injection system complexity and cost. Fuel passages were sized at the ignition condition where fuel flow is a minimum and only the air-assist/airblast atomizers are utilized. Since assist air is used to break up the fuel, the only required fuel pressure drop is that needed to overcome flow variations around the fuel manifold due to head effects. A 4.5-percent flow variation was selected as the design criterion, and resulted in fuel passages having a flow number of 3.0 ( $\text{Flow No.} = W_F / \sqrt{\Delta P_F}$ ).

An existing Model GTCP85 Series APU flow divider was utilized to determine the total fuel system flow characteristics. Figure 24 illustrates this flow divider. Since this divider normally operates with a high pressure atomizing fuel system, orifices will be placed downstream of the primary and secondary outlets to compensate for the reduced pressure drop of the airblast type atomizers used in the Model GTP305-2 APU. Figure 25 shows the resulting system flow characteristics. As indicated in this figure, the flow divider would crack at a fuel flow of 30 pounds per hour. This flow corresponds to an estimated 50 percent engine speed. The air-assist will be shut off at a



Figure 21. Prototype air-assist/airblast fuel nozzle  
with outer shroud installed



Figure 22. Prototype air-assist/airblast fuel nozzle  
with outer shroud removed

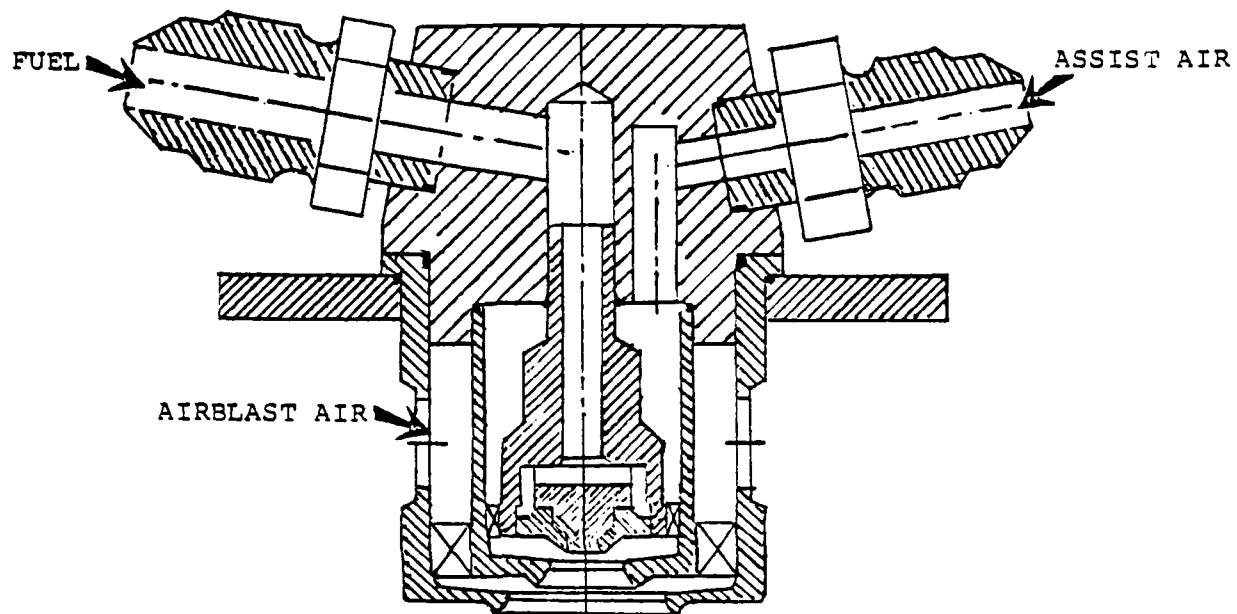


Figure 23. Schematic of typical air-assist/airblast fuel atomizer

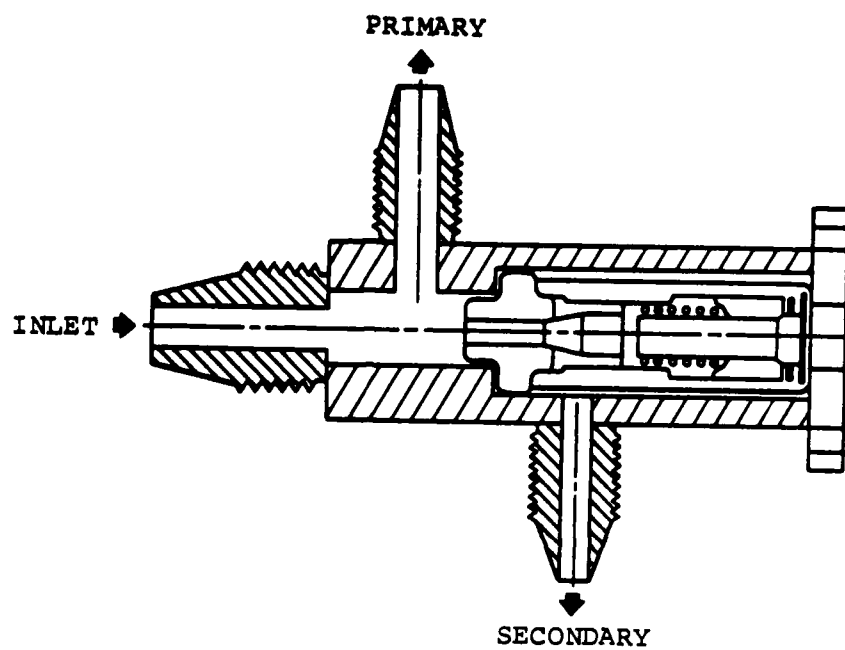


Figure 24. GTP305-2 flow divider

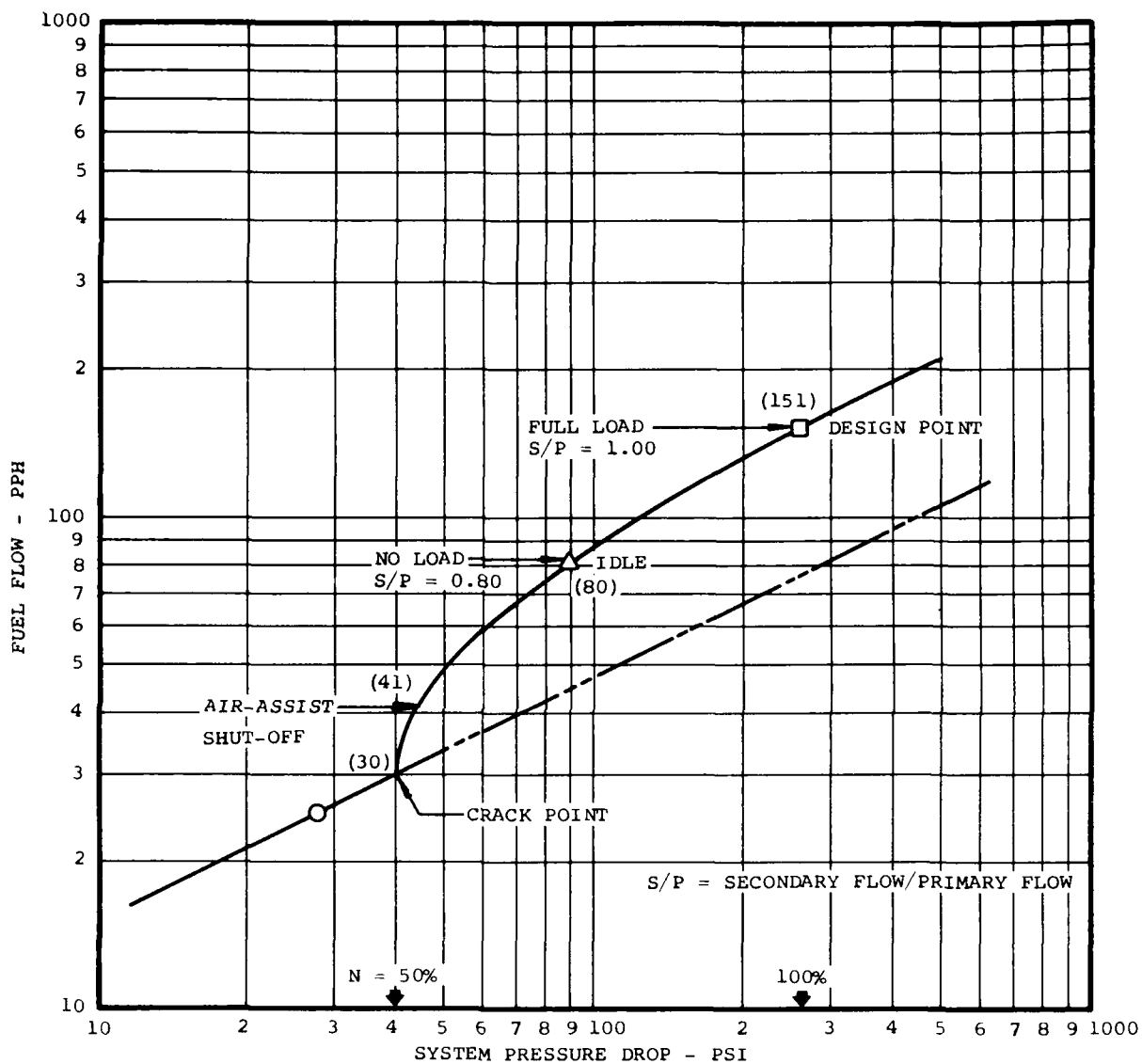


Figure 25. GTP305-2 fuel system characteristics  
 (5) air-assist/airblast,  
 (5) pure airblast



weight flow of 41 pounds per hour. Utilization of this scheduling procedure insures that the primary air-assist/airblast atomizers maintain stable combustion until the secondary airblast atomizers have initiated burning. An added advantage of this type of injection system is that an airblast to air-assist/airblast fuel flow split of approximate unity can be maintained throughout the sea level operating envelope. This equal flow split translates into a uniform fuel distribution at all operating conditions, which benefits the pattern factor.

### 3.4 Turbine

#### 3.4.1 Radial Turbine Nozzle

The radial turbine stage meridional view is presented in Figure 26. Principal features of the radial nozzle include:

- o Integrally cast, Inconel 738, material, incorporating vanes, sidewalls, radial shroud and support cylinder
- o Vane internal, chordwise, integrally cast fins to enhance internal vane cooling flow effectiveness
- o External sidewall radially oriented ribs, 204 constant passage width, fore and aft
- o Vane height (B-width) 0.300-inch with 0.040-inch fillet radii

#### 3.4.2 Aerodynamic Design

Radial turbine design is based on a one-dimensional optimization procedure which maximizes radial turbine efficiency for tip speed limited designs. Optimization established the basic turbine flow path dimensions and vector diagram. A detailed

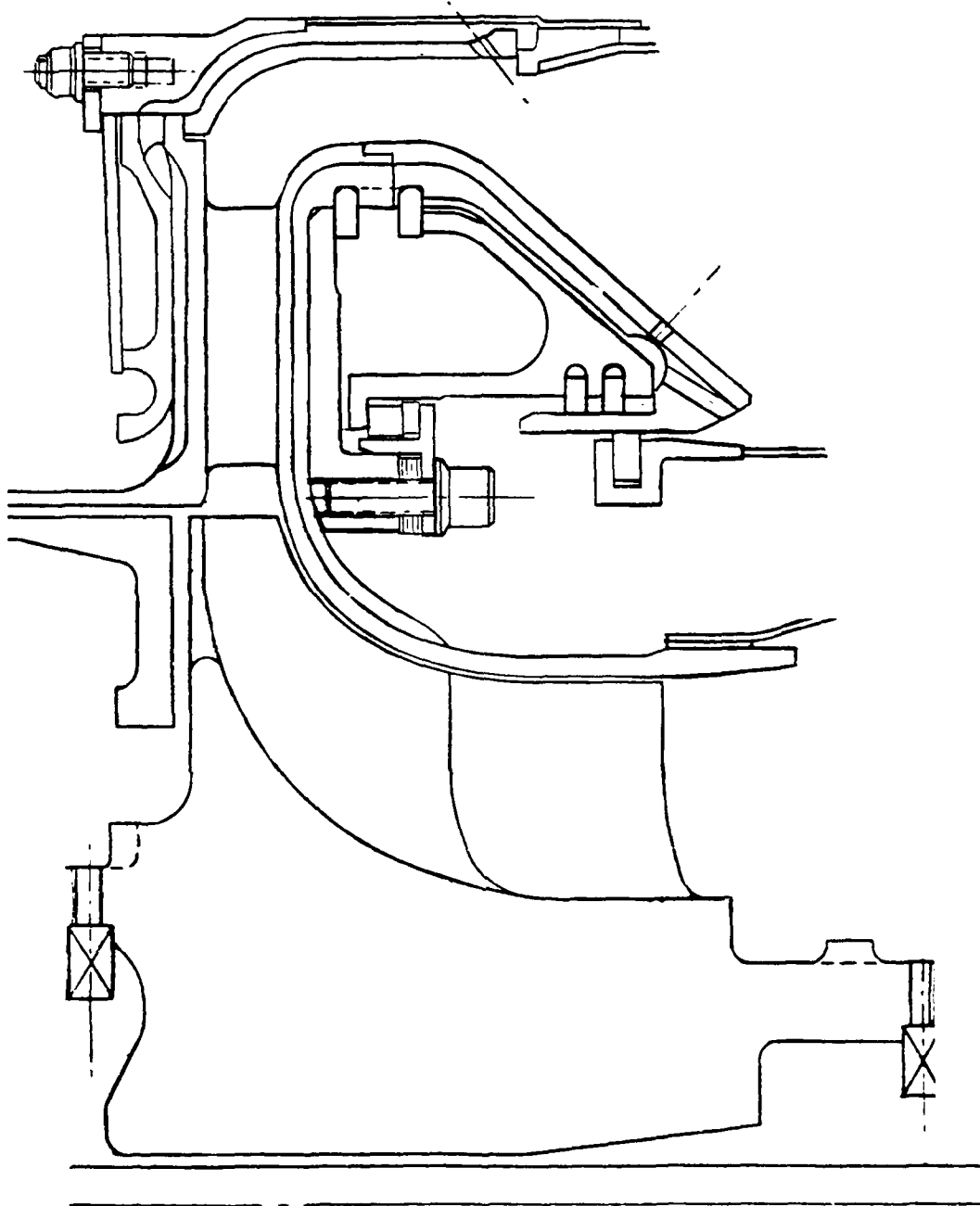


Figure 26. Radial turbine stage

design of the radial turbine inlet section, stator and rotor were then analyzed with multi-dimensional flow analysis techniques. In most cases the design features and geometries of the Model GTP305-1 turbine were retained although local blade shapes and thicknesses were modified to reflect the new vector diagram and maximize turbine mechanical integrity.

The nozzle inlet section (combustor exit to nozzle inlet) is a 90 degree radius bend. Design intent was to minimize the span-wise velocity gradient at the nozzle vane inlet. This was accomplished by maintaining a constant bend radius of 0.275 inch for the inner (shroud) contour and varying the outer (hub) contour radius until a smooth velocity distribution was achieved. A velocity gradient of less than 90 ft/sec was achieved across the nozzle inlet.

The radial nozzle chord, "b"-width, and number of blades (Figure 27), were established from the vector diagram optimization based on a trailing edge thickness of 0.040 inch. The one-dimension vector diagram is presented in Figure 28. The detailed vane shape was then optimized with a blade-to-blade flow solution consistent with the local thickness required for internal cooling flow passages. The aerodynamic design procedure is to first design a vane profile in the axial plane. This profile is then transformed to the radial plane by a modified conformal transformation technique that maintains the desired throat dimension. The vane suction and pressure surface velocity distributions are then evaluated. This process is repeated with local vane modifications until acceptable velocity distributions are acknowledged.

The final stator nozzle ring (Z-section) with the final stator vane profile is presented in Figure 29. Continuous flow acceleration was achieved on both surfaces except for a small diffusion region near the suction surface throat region. The

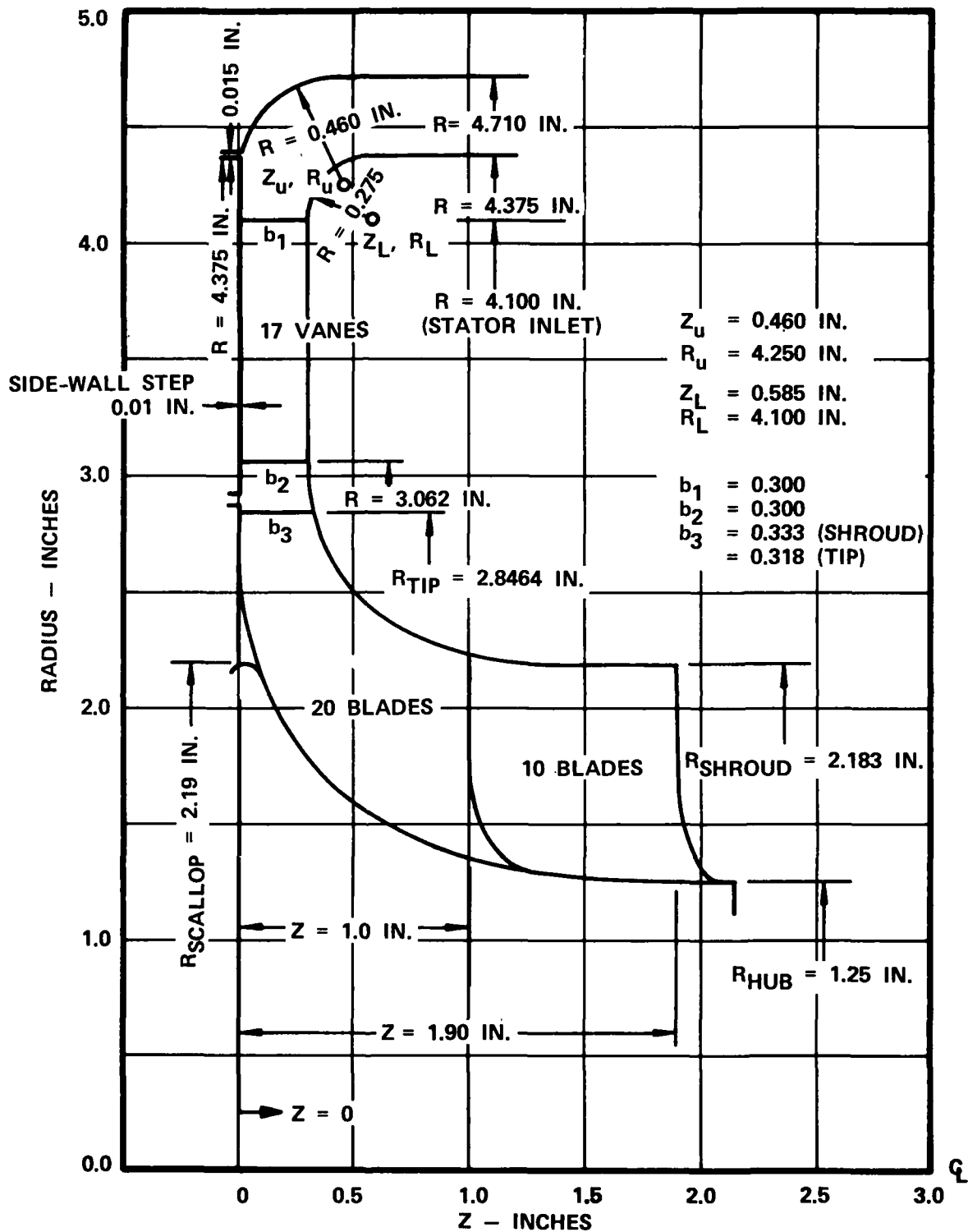


Figure 27. GTP305-2 radial turbine meridional flow path

# STATOR INLET

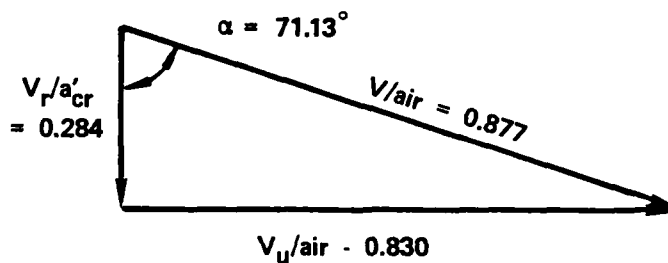
$R = 4.100''$

$V_r/air = 0.148$

# STATOR EXIT

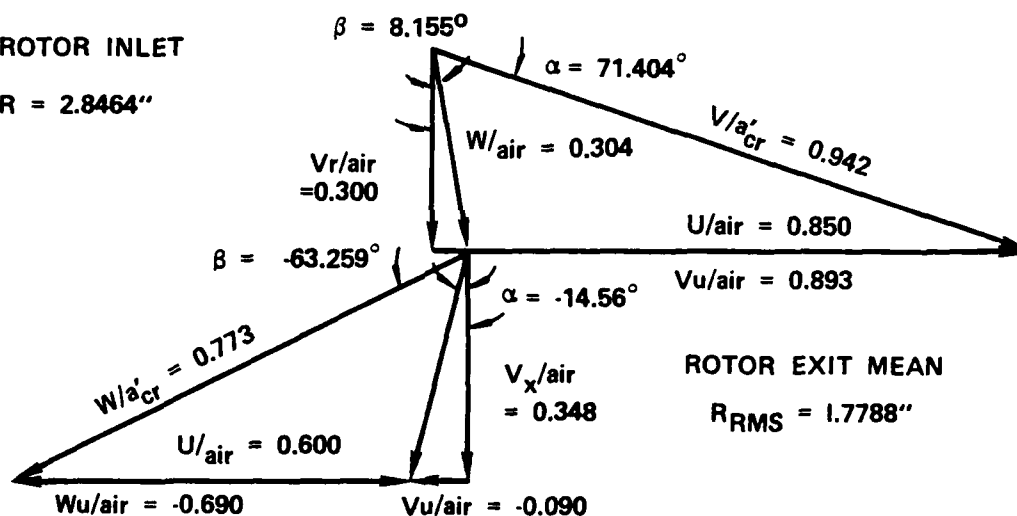
Without Trailing  
Edge Cooling  
Flow

$R = 3.062''$



# ROTOR INLET

$R = 2.8464''$



# ROTOR EXIT MEAN

$R_{RMS} = 1.7788''$

# ROTOR INLET

$T'_{in} = 2509.7 \text{ R}$

$T''_{in} = 2240.8 \text{ R}$

$A'_{ir} = 2211.5 \text{ FT/SEC}$

# ROTOR EXIT MEAN

$T'_{exit} = 1968.0 \text{ R}$

$T''_{exit} = 2092.1 \text{ R}$

$A'_{ir} = 1958.4 \text{ FT/SEC}$

Figure 28. One-dimensional radial turbine Vector diagram

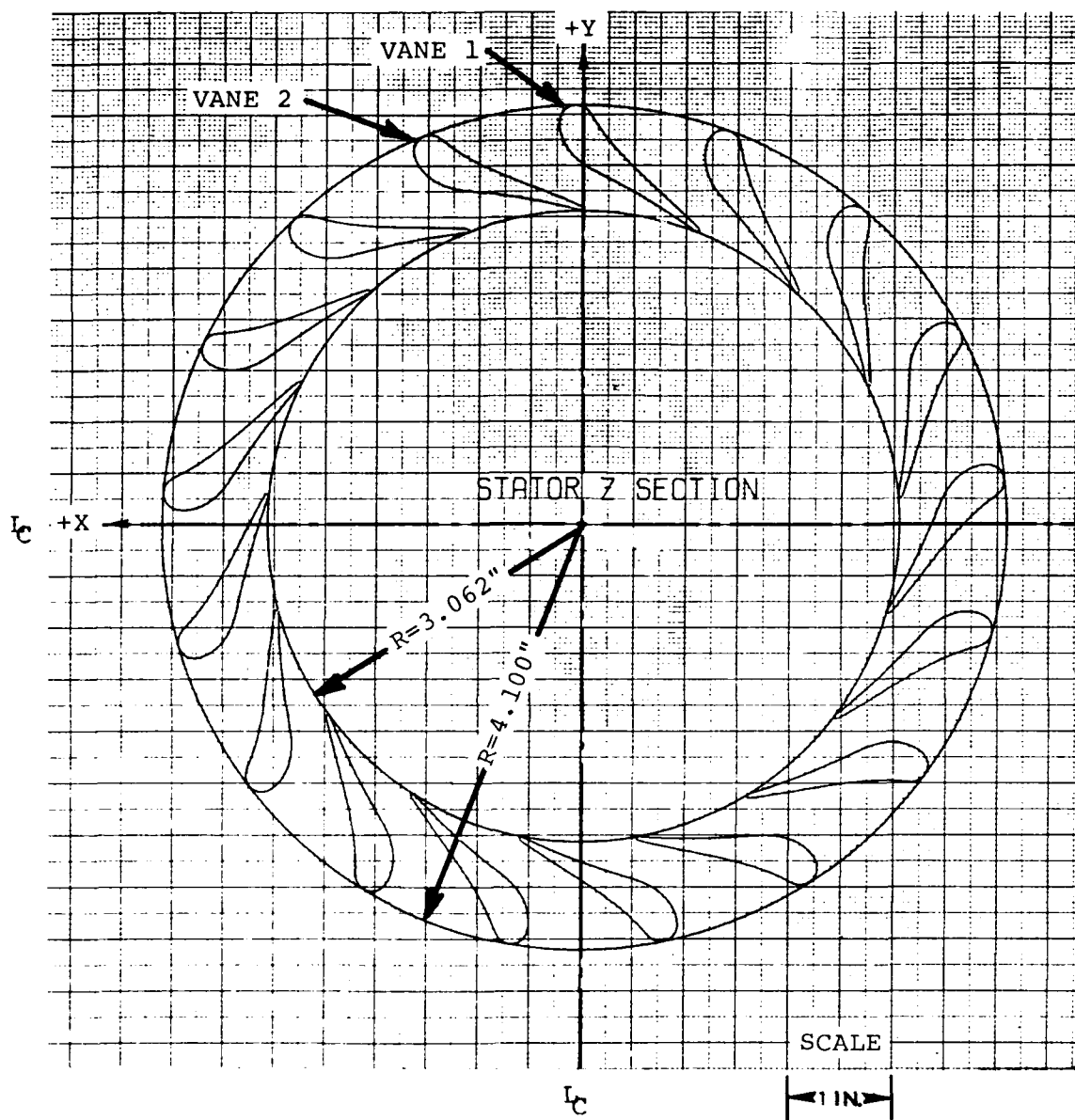


Figure 29. GTP305-2 stator nozzle ring with final vane profile

design parameters for the radial nozzle are summarized in Table 7.

### 3.4.3 Cooling Flow Analysis

A thermal analysis of the Model GTP305-2 radial nozzle was conducted to define the required cooling flow scheme to maintain required acceptable metal temperature. Although the basic design of the cooling scheme is similar with that demonstrated on STAGG, the Model GTP305-2 APU application is more severe. Refinements were required because of higher turbine inlet gas temperature and increased compressor discharge air temperature available for cooling. A peak metal temperature of 1950°F was considered acceptable.

Figure 30 depicts the radial nozzle cooling flow circuits for the Model GTP305-2. As shown, principal flow paths are up the nozzle forward and aft sidewalls. A portion of the forward sidewall flow branches and provides vane internal cooling flow. After cooling the vane, the internal cooling flow is returned to the cycle ahead of the radial turbine rotor. The remaining forward sidewall cooling flow continues radially outward along the sidewall, passing through the combustor transition liner, and is returned to the cycle near the combustor exit. Aft sidewall cooling flow travels along the radial shroud prior to entering the sidewall cavity. The flow continues up the sidewall and down through mating fin passages on the combustor ramp before being returned to the cycle near the combustor dilution zone.

As shown in Figure 31, the Model GTP305-2 APU nozzle vane has 5-integrally cast chordwise cooling fins on the inner cavity walls. These fins enhance the effectiveness of the cooling flow.

Prior to initiating the cooling flow analysis, the potential peak temperature "hot-streak" obtainable at the radial nozzle inlet was determined using the following considerations:

TABLE 7. RADIAL NOZZLE DESIGN PARAMETERS

<u>Axial Section Parameters</u>	
Section radius, inch	3.062
Inlet flow angle, degrees	10.0
Exit flow angle, degrees	-71.133
Inlet flow critical Mach no	0.198
Exit flow critical Mach no	0.87746
Exit blade angle, degrees	-68.984
Exit blade critical Mach no	0.9012
L.E. thickness, inch	0.260
T.E. thickness, inch	0.040
Downstream turning, degrees	4.0
Suction surface involute angle, degrees	30.0
Axial loading coefficient	0.770
<u>Transformed Radial Section Parameters</u>	
Inlet radius, inch	4.100
Exit radius, inch	3.062
Radial chord ( $\Delta R$ ), inch	1.0380
Inlet flow angle, degrees	0.0
Exit flow angle, degrees	-71.133
Inlet blade angle, degrees	0.000
Exit blade angle, degrees	-68.984
Inlet flow critical Mach no	0.148
Exit flow critical Mach no	0.87746
Leading edge thickness, in.	0.000
Trailing edge thickness, inch	0.040
Vane passage ("b") width	0.300
Aspect ratio $b/\Delta R$	0.289
Radial loading coefficient	0.468



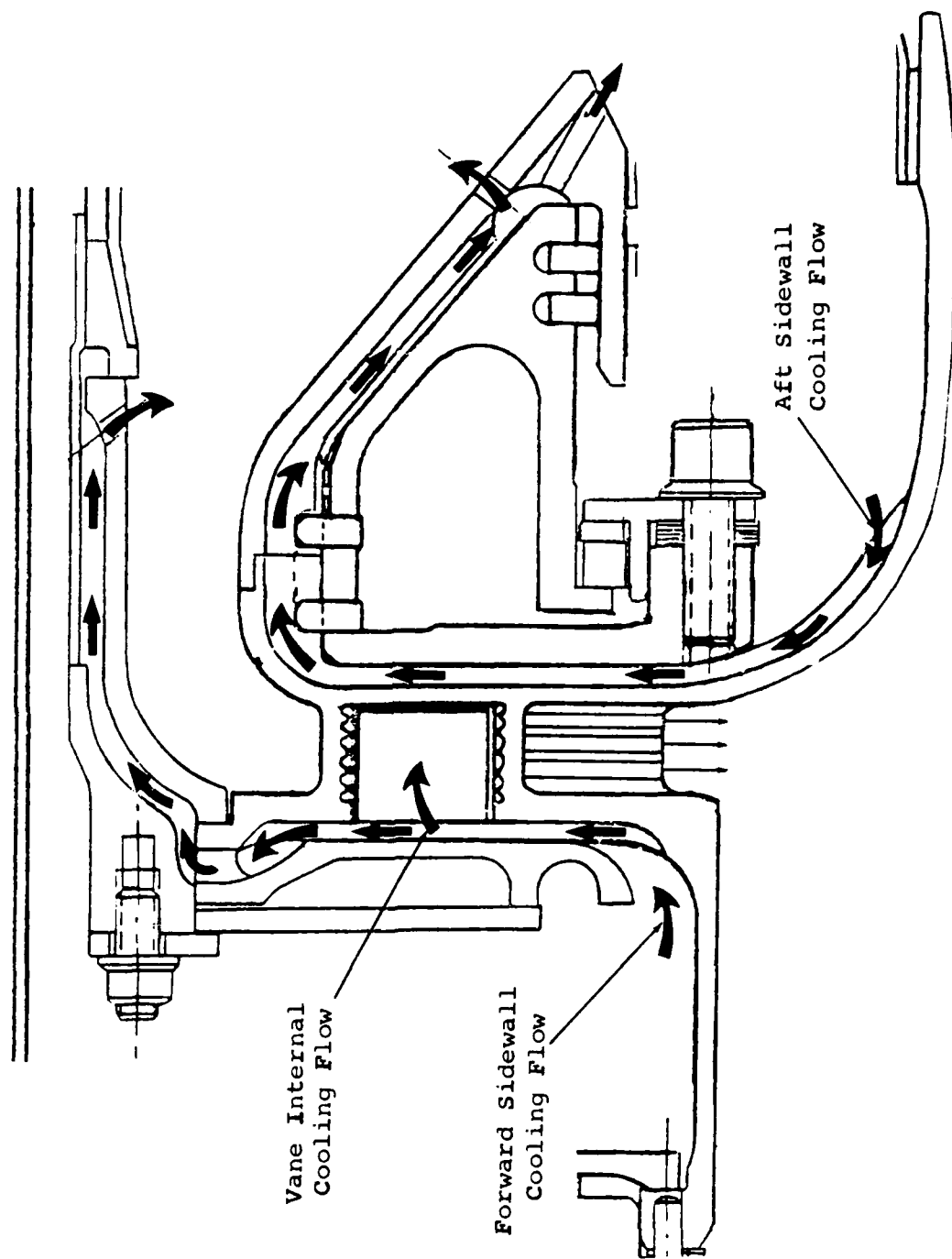


Figure 30. GTP305-2 radial nozzle cooling flow circuits

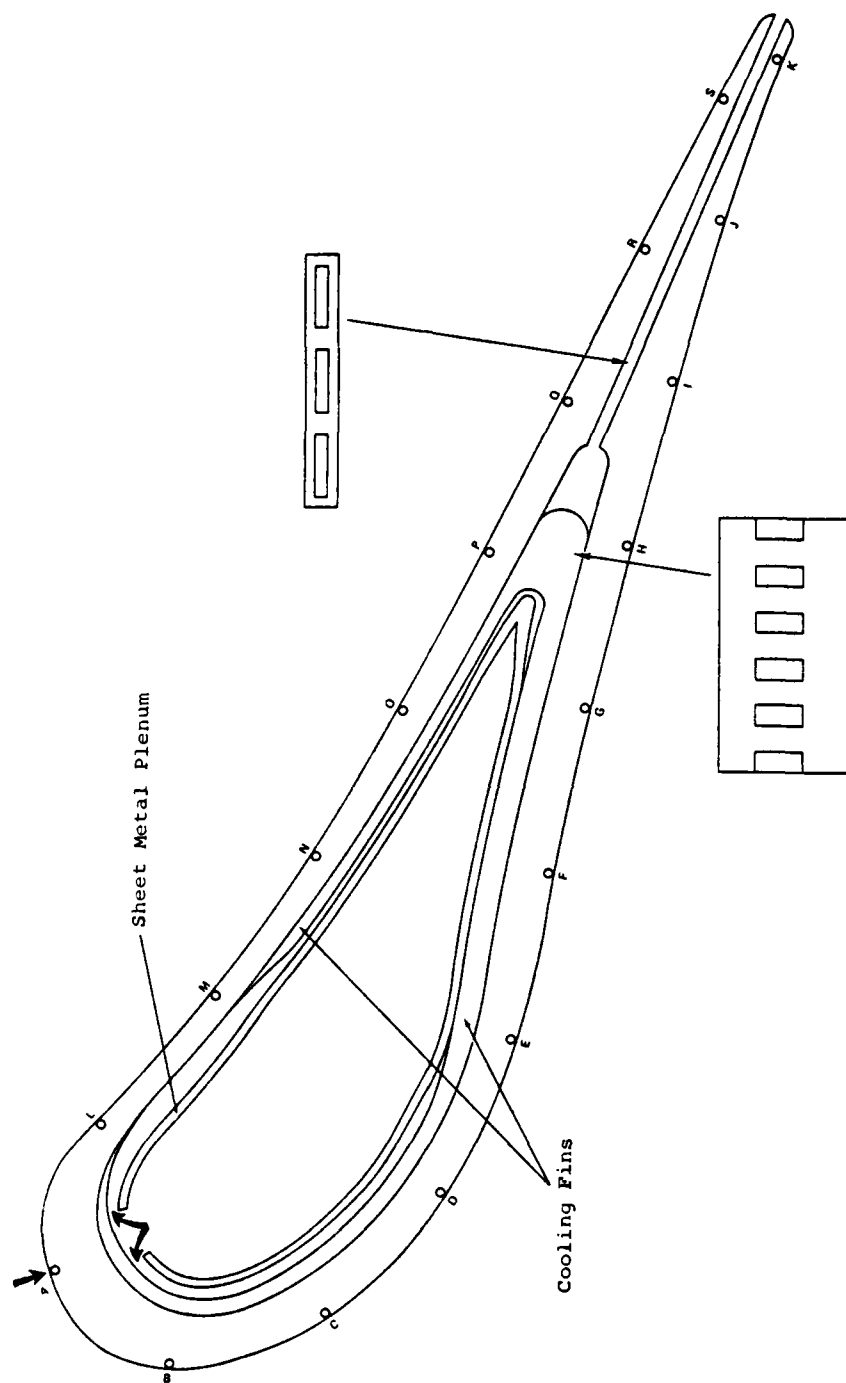


Figure 31. GTP305-2 radial turbine nozzle vane cross section

- o Turbine rotor average inlet temperature is 2050°F. This is the mixed-out temperature with internal vane cooling flow included. Nozzle inlet temperature excluding internal vane cooling flow is 2067°F (see Section 5.0)
- o Combustion system pattern factor goal is 0.15. To achieve a margin of safety, a nozzle thermal analysis was conducted with a pattern factor of 0.215

$$\text{Pattern Factor} = \frac{T_{HS} - T_{avg}}{T_{avg} - T_{CDT}}$$

Where:

$T_{HS}$  = vane inlet hot-spot absolute temperature (°F) due to circumferential and axial symmetry of the combustor profile

$T_{avg}$  = average absolute total inlet temperature to the nozzle vane (°F)

$T_{CDT}$  = compressor discharge temperature (°F)

Assuming a pattern factor of 0.215, a compressor discharge temperature of 800°F, and an average turbine nozzle inlet temperature of 2067°F, the predicted "hot-streak" total temperature is 2338°F. Using the 2338°F "hot-streak" temperature, a calculated vane internal cooling flow of 2.14 percent of engine inlet flow is required to maintain metal temperatures below 1950°F. This equates to a total internal flow of 0.0502 lb/sec for the 17 vanes or 0.00295 lb/sec/vane.

#### 3.4.4 Radial Nozzle Vane

Due to the severity of operating conditions imposed on the Model GTP305-2 APU, particular emphasis was placed on accurate

prediction of thermal boundary conditions. A combination of current analytical tools was used to calculate the nozzle vane external film heat transfer coefficients. Specific assumptions and/or considerations accounted for in the calculation were:

- o Flow symmetry across the vane B-width (the developing boundary layer on the vane was considered two-dimensional and spanwise constant)
- o Laminar flow coefficients were adjusted for free stream turbulence intensity levels
- o Stimulation of occurrence of boundary layer transition from laminar to turbulent flow as a result of existing free-stream turbulence level
- o Potential for formation of Taylor-Goertler vortices on vane pressure surface, and resultant adjustment of film coefficient

Internal vane cooling flow is supplied from forward sideband cooling flow. Cooling flow travels up the forward sidewall and enters the vane inlet plenum (Reference Figure 30). The plenum is piloted by a flange at the nozzle forward sidewall and brazed in place. This flange is contoured, thereby forcing the inlet plenum walls to a specified shape. This results in cooling flow passages (outside plenum wall, internal vane wall) of desired height and predetermined width. Flow is then introduced into these passages through holes in the forward end of the plenum, opposite the external stagnation point (Point "A", Figure 31). A pressure side/suction side flow split at "A" is determined by the metering characteristics of the respective cooling flow passages. By controlling the passage height (0.017 inch) between Points "O" and "P" (Figure 31), a sufficient pressure drop is established to allow 64 percent of the total vane flow to cool the suction side, with the remainder washing the pressure side.

The vane internal cooling flow is returned to the mainstream gas flow through slots in the vane trailing edge. Three machined slots (0.015 inch by 0.075 inch, nominal) in the vane trailing edge (Figure 31) meter the total cooling flow for each vane by virtue of flow choking through these slots. Approximately 90 percent of the total 48 psi pressure drop potential available for vane cooling results from flow through these slots.

#### 3.4.5 Aft Sidewall, Shroud Combustion Chamber Ramp

The radial nozzle aft and forward sidewalls utilize counter-flow cooling air passages similar to the STAGG (Figure 32) incorporating integral cooling fins to augment the heat transfer. Specific problems encountered during design of the aft sidewall cooling flow circuit (turbine shroud, nozzle sidewall and combustion chamber ramp) primarily evolved from the long cooling flow path, and the wide variation in available flow area as the flow expands radially outward along the sidewall.

The cooling flow circuit (Figure 30) is characterized by:

- o A cooling flow rate of 0.1373 lb/sec at engine design point
- o Flow metering is effected by orifices in the combustion chamber ramp. These orifices also serve as return ports for delivering used cooling flow to the mainstream gas flow
- o 204 integrally machined fins in the cooling flow passages, originating on the shroud and terminating at the foot of this combustion chamber ramp

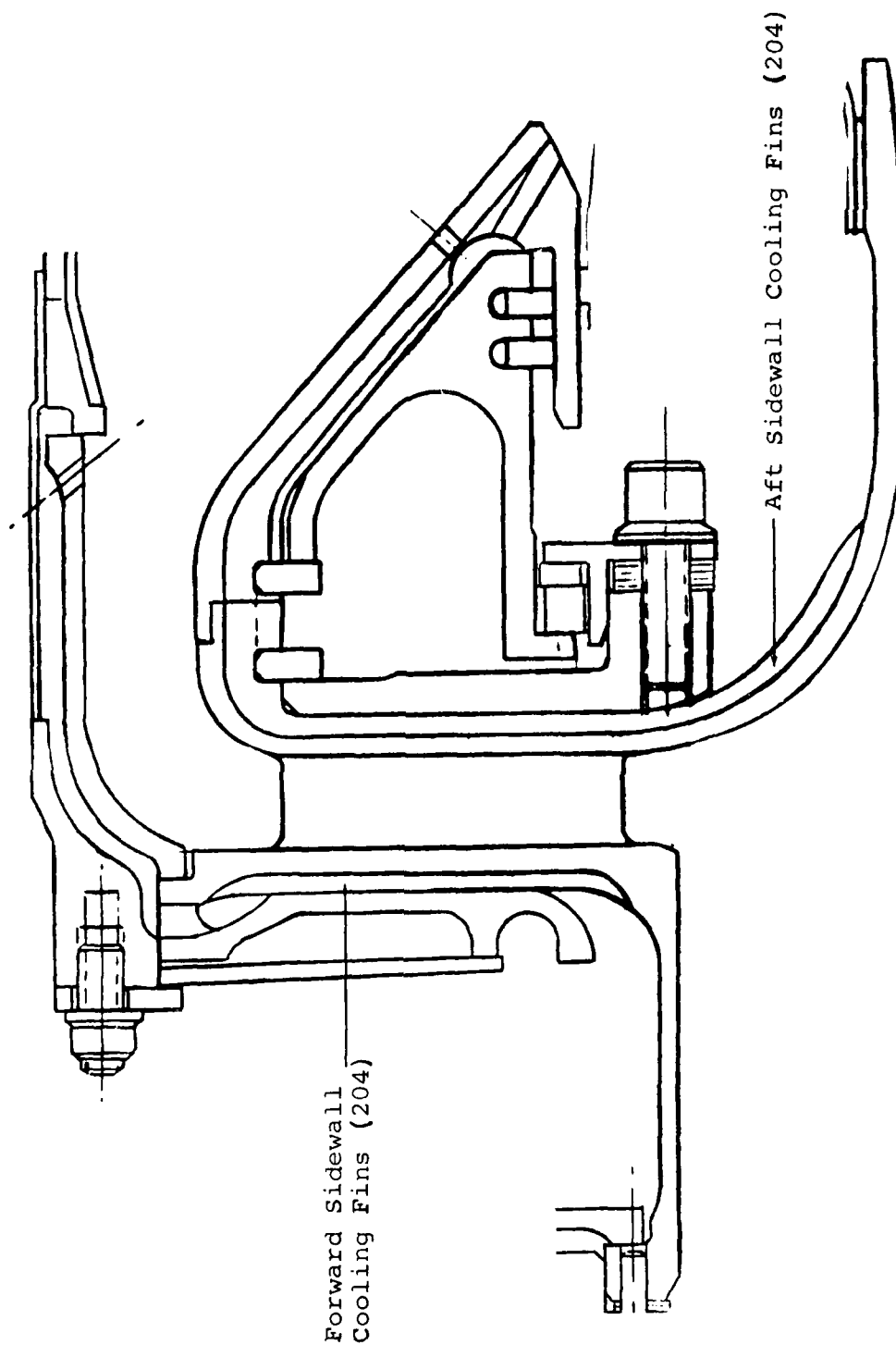


Figure 32. Radial turbine nozzle fore and aft cooling fins

- o Constant interfin passage width (0.052 inch), with fin thicknesses varying from 0.032 inch minimum, to 0.080 inch maximum at the combustion chamber ramp apex
- o Constant fin height of 0.063 inch throughout the cooling flow passageway

External heat transfer to the combustion chamber ramp results from convection of the mainstream "hot-streak" gas, and combustor primary zone luminous radiation and nonluminous radiation to portions having no "view" of the primary zone. Radiation effects are superimposed on the convection effects, with a radiation reference temperature of 2338°F. The primary zone gas temperature was estimated to be 4978°F. Luminous radiation effects were accounted for on the inclined portions of the combustion chamber ramp (Stations 0.0 to 1.8, Figure 33). The apex of the ramp has no direct view of the primary zone gas, and therefore, receives only nonluminous radiation from the "hot-streak" gas.

Due to strongly accelerating mainstream flow, a newly developed boundary layer is assumed to originate at the base of the combustion chamber ramp and persists up the ramp to Station 2.2, (Figure 33). External ramp film coefficients were adjusted to account for the free stream turbulence intensity levels.

The sidewall boundary layer in the region of the vane is a well-developed turbulent boundary layer. Therefore, boundary conditions applied to the sidewalls were not adjusted to account for sidewall area due to the presence of the vanes.

Along the shroud (sidewall) at the turbine rotor inlet, it was assumed that a new boundary layer was initiated. This was due to the "wiping away" by the rotating rotor inducer of the existing fully-developed turbulent boundary layer. A nominal blade-to-shroud clearance of 0.015 inch was assumed as the maximum thickness boundary layer formed on the turbine shroud. The

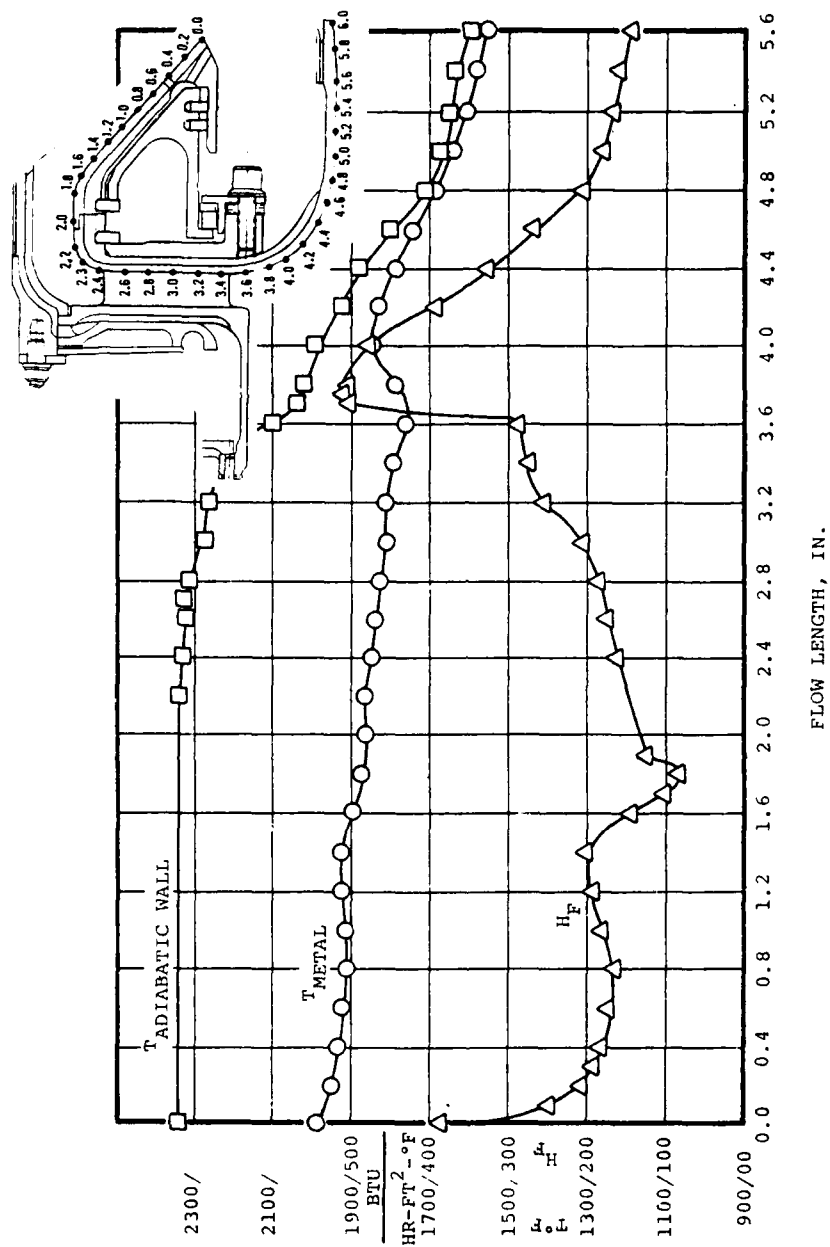


Figure 33. GTP305-2 radial turbine nozzle hub shroud boundary conditions



aerodynamic flow solution defines the rotor inlet gas properties and the calculated shroud line gas properties through the rotor. Local film coefficients were then determined using existing correlations.

Calculation of the internal film coefficients in the cooling air passageways employed either a laminar or turbulent tube flow correlation depending upon the local hydraulic diameter Reynolds number. Cooling flows in the transition regime were handled through an interpolation between the appropriate laminar or turbulent correlations as a function of the transition Reynolds number. No thermal entry length effects were included, because the hydraulic diameter of each flow passage is sufficiently small to cause thermal and hydraulic entry effects to dampen in relatively short flow lengths.

The calculated external adiabatic wall temperature, effective film coefficients and resultant metal temperatures for the combustion chamber ramp, aft nozzle sidewall, and turbine shroud are presented in Figure 33. As can be seen, a 1900 to 1950°F metal temperature region in the initial length of the combustion chamber ramp is predicted. Metal temperatures below 1900°F are shown for the remainder of the cooling flowpath.

#### 3.4.6 Forward Sidewall, Support Cylinder, Combustor Shroud

Similarly, the forward sidewall cooling flow circuit is characterized by the following features:

- o A gross entering cooling flow rate of 0.186 lb/sec at engine design point, from which approximately 0.0501 lb/sec branches to provide vane internal cooling flow

- o Metering of the forward sidewall flow (exclusive of vane internal cooling flow) is effected by orifices in the combustor transition liner. These orifices also serve as return ports for delivering used cooling flow to the mainstream gas flow
- o 204 integrally machined fins in the cooling flow passages, mirroring those on the aft sidewall. Constant interfin passage width (0.052 inch) and fin height (0.063 inch)

Figure 34 depicts the forward sidewall cooling flow circuit.

External convection film coefficients for the combustor outer shroud and nozzle forward sidewall were calculated in the same manner as those for the combustion chamber ramp and nozzle aft sidewall. Similar to the combustion chamber ramp, the combustor outer shroud experiences heat transfer due to luminous and nonluminous radiation, in addition to convection from the mainstream gas flow. Radiation to the outer shroud is primarily confined to the region between Stations 0.0 and 1.3 in Figure 35. Nonluminous radiation occurs between Stations 0.0 and 0.6, while Stations 0.7 through 1.3 sustain a restricted view of the primary zone (view factor 0.1). The calculated laminar film coefficients were adjusted to account for the free-stream turbulence intensity levels, similar to aft sidewall methodology.

The internal film coefficients in the cooling air passages on the forward sidewall and combustor outer shroud were calculated in the same manner as those for the aft sidewall cooling air circuit.

Detailed analysis of the nozzle cylinder thermal boundary condition involved consideration of several factors (Stations 2.6 to 3.8, Figure 35). The outer diameter of the support cylinder

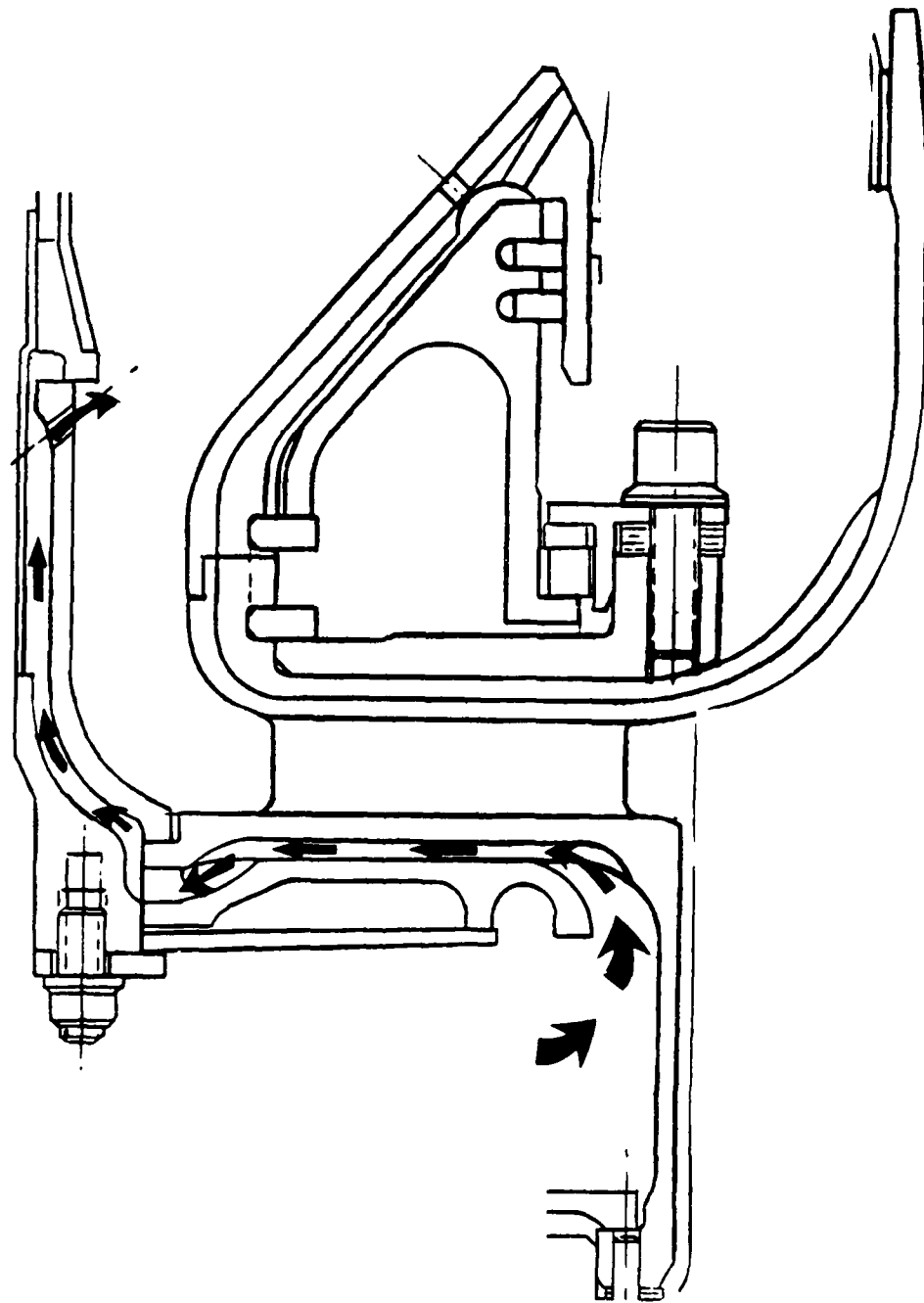


Figure 34. Forward sidewall cooling circuit

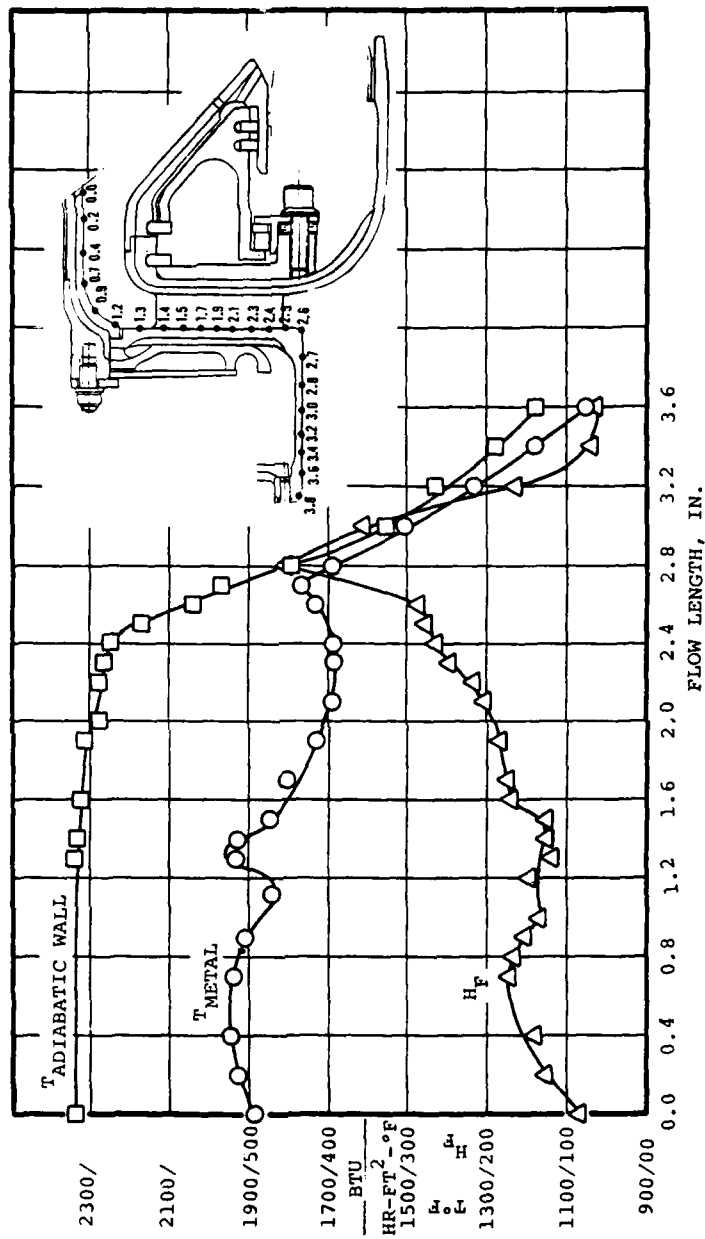


Figure 35. GTP305-2 radial turbine nozzle outer shroud boundary conditions

is partially scrubbed by entering forward sidewall cooling flow. Influencing the inner diameter of the cylinder are the turbine backshroud support cylinder and the propagation of effects of the mainstream gas within the intercylinder gap axially forward of the radial turbine rotor inducer. The intercylinder gas tangential velocity was assumed to decay exponentially with axial length into the gap from the inlet. A finite element hand calculation of the local gas temperature and film coefficient was performed to establish the gap boundary condition of the inner surface of the nozzle support cylinder.

The calculated external adiabatic wall temperature, effective film coefficient, and resultant metal temperatures for the nozzle support cylinder, forward sidewall, and outer combustor shroud are presented in Figure 35. The resultant metal temperatures and thermal gradients are within satisfactory limits.

#### 3.4.7 Stress Analysis

Utilizing temperature data generated from the cooling flow analysis, a steady-state two-dimensional finite element stress model was prepared. The finite element model is shown in Figure 36. The one-piece Inconel 738 casting is supported axially and piloted radially at the forward end of the support cylinder. Analytically, the 17-hollow vanes were simulated using 17-solid vanes having a tangential vane thickness of equivalent stiffness. Figure 37 depicts the assumed equivalent tangential vane thickness and the assumed cooling fin thickness. Nodal system modeling is shown in Figure 38. Average steady-state pressures and temperatures subjected to the model are shown in Figures 39 and 40, respectively. Temperature distribution was assumed to be uniform circumferentially.

Resultant displacement of the nozzle structure due to temperature and pressure loads during steady-state operation is

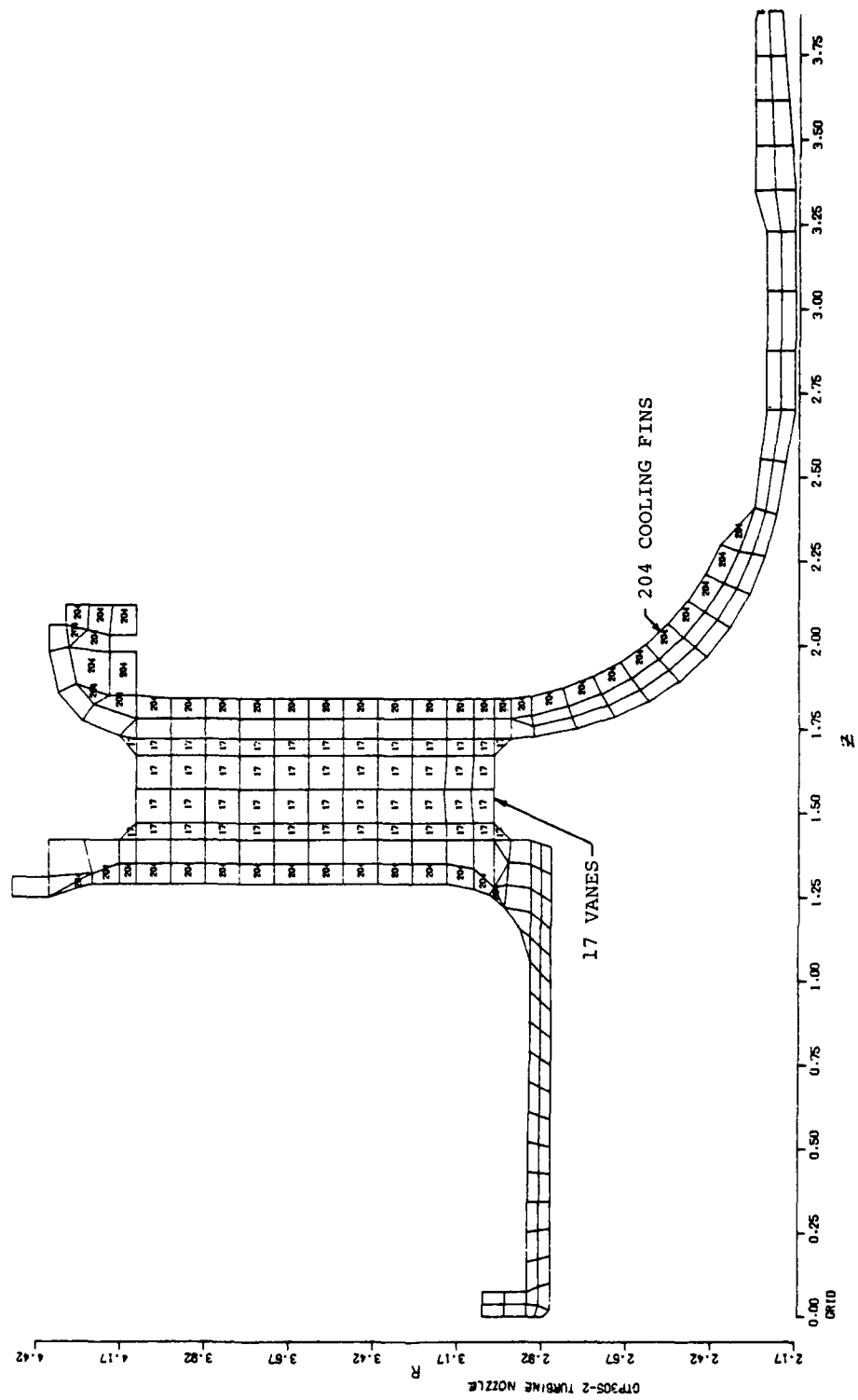


Figure 36. GTP305-2 turbine nozzle (Inconel 738) finite element model







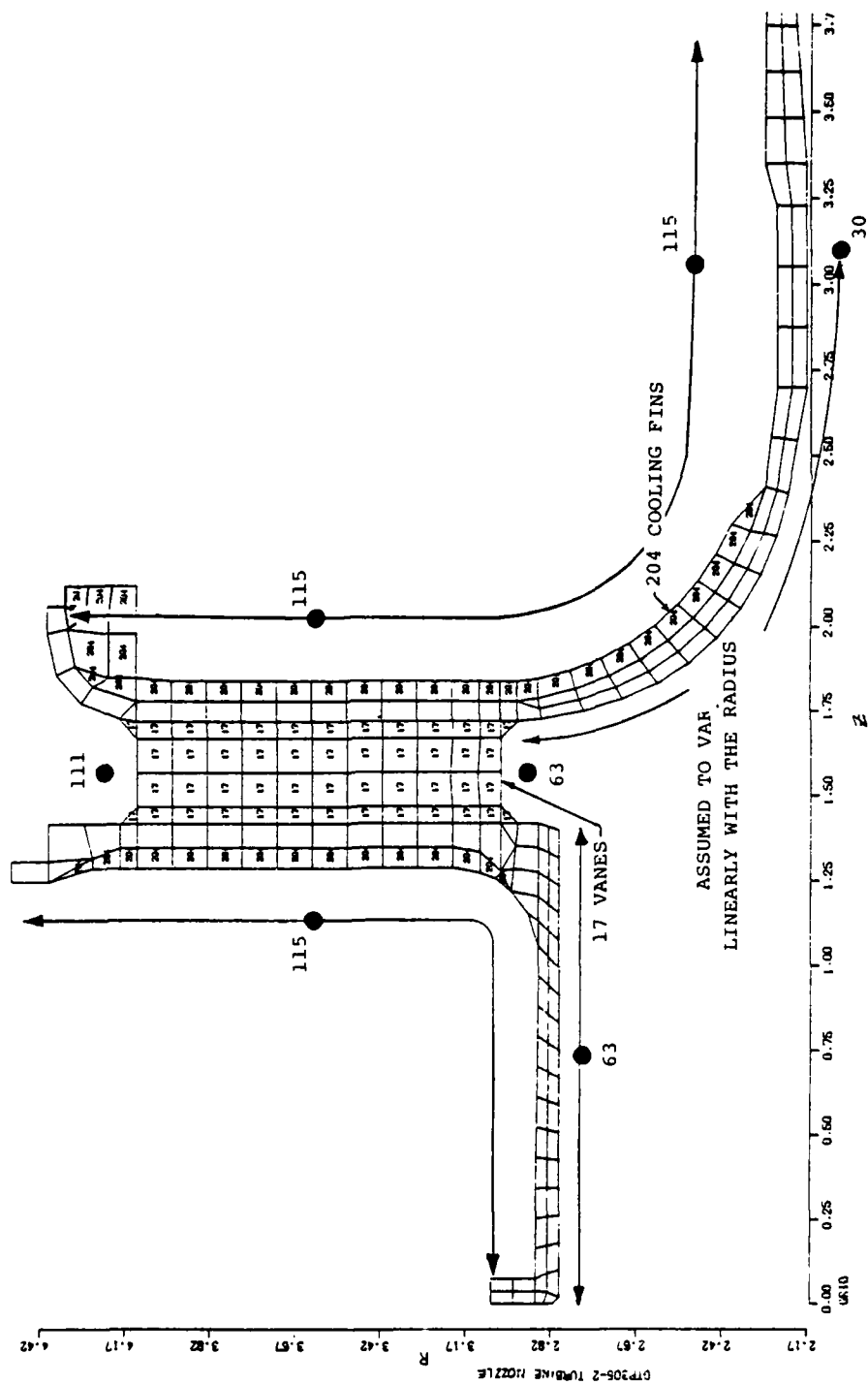


Figure 39. GTP305-2 turbine nozzle finite element model pressures (psia)

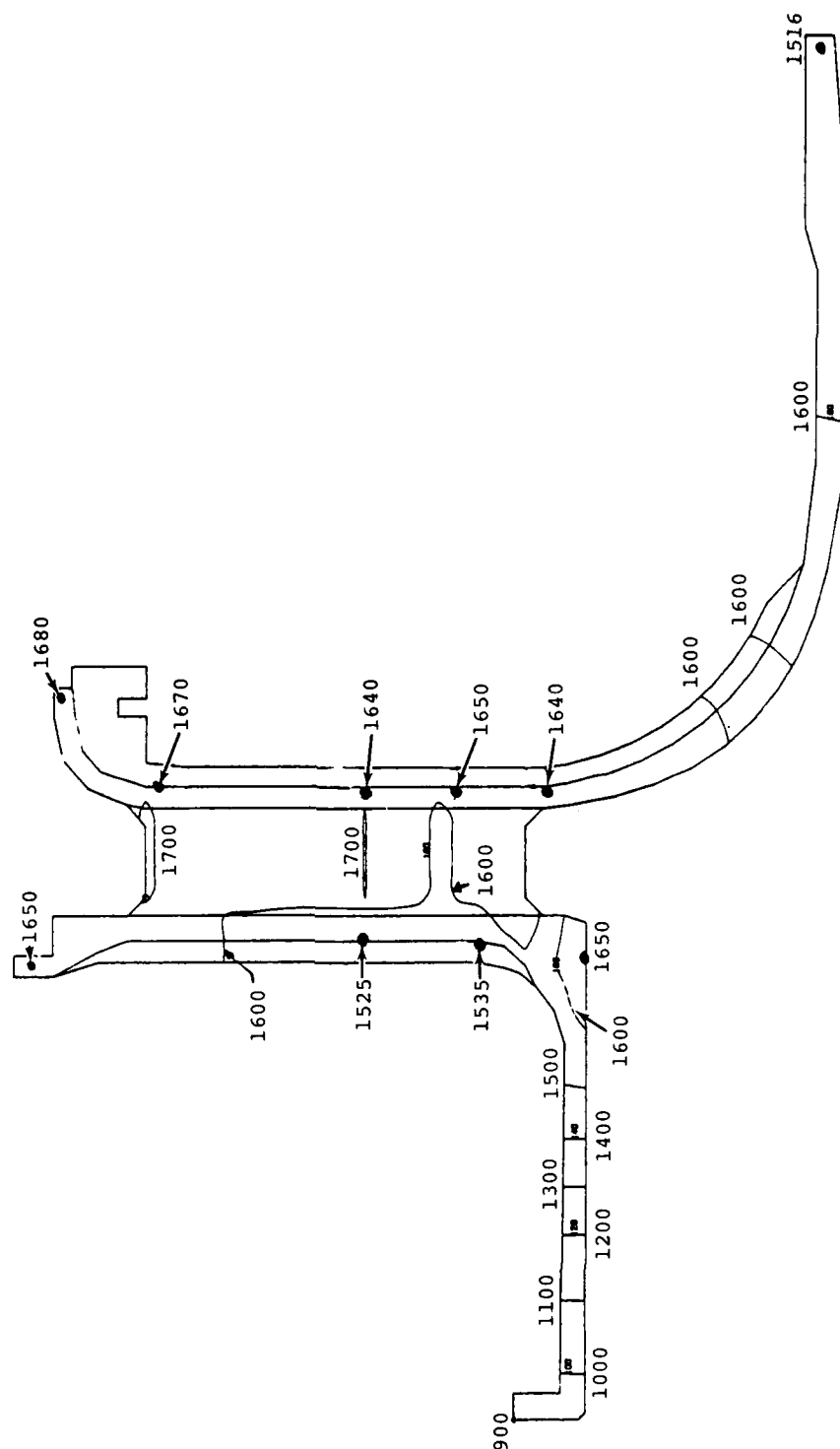


Figure 40. GTP305-2 turbine nozzle average steady state temperatures calculated from heat transfer analysis

shown in Figure 41. The predicted distribution of stresses is shown in Figures 42 through 47. Axial and radial bending stress are given in Figures 42 and 43, respectively, with hoop stress predictions shown in Figure 44. The minimum margin of safety\* occurs at Point A, wherein the hoop stress is 32,100 psi in compression and equals +0.90. The equivalent stress distribution is shown in Figure 45 with principal stresses given in Figures 46 and 47. Predicted vane minimum margin of safety occurs at Point B, Figure 45 and is calculated to be +0.42.

All regions of the cast nozzle, with the exception of the hollow cooled vanes, were analytically determined to be structurally adequate for steady-state operating conditons. Inasmuch as the hollow cooled vanes were simulated in this analysis as being solid, predicted solid vane stresses do not account for the cooling flow. Therefore, additional information was assimilated and reviewed relative to past experience on the STAGG nozzle, from which the Model GTP305-2 nozzle design was derived.

A detailed three-dimensional finite element and heat transfer analysis was conducted on the STAGG nozzle vanes, the critical region of the vane was predicted to be the trailing edge. Due to ere thermal transient conditions after light-off, an estimated LCF life as low as 300 cycles could be expected. As stated in AiResearch Report SA-9359-MR, several methods of LCF estimating were researched with predictions ranging from 300 to 3000 cycles. In reviewing the analysis, it was noted that the effect of surface temperature gradients on local heat transfer rates was not considered. This effect reduces the rate of change in metal temperatures in the trailing edge region, thus reducing the thermal stress range and increasing LCF life.

---

\*Minimum margin of safety  $\frac{\text{Yield Strength (typ)}}{\text{Predicted Stress}}$  -1

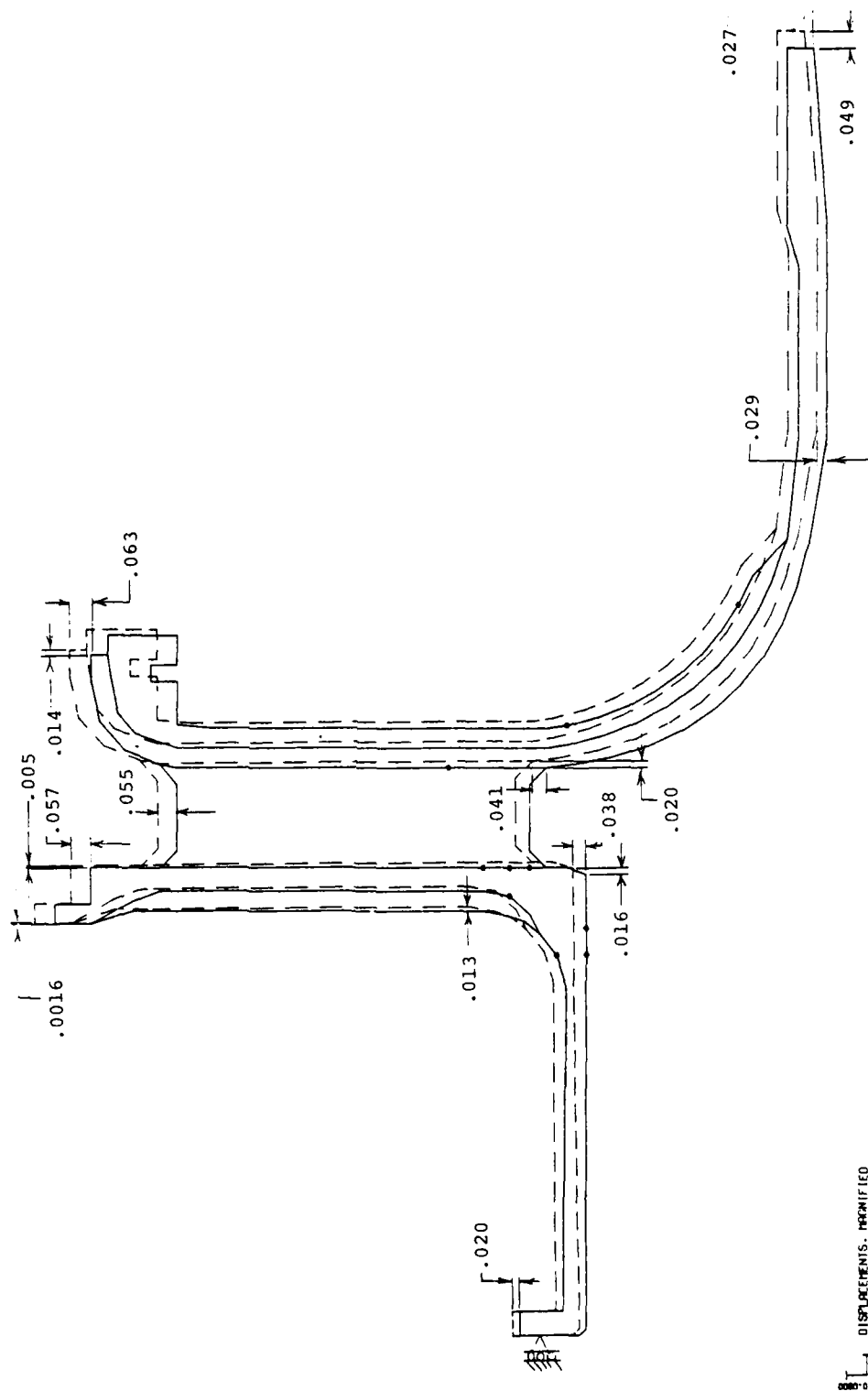


Figure 41. GTP305-2 turbine nozzle temperature and pressure

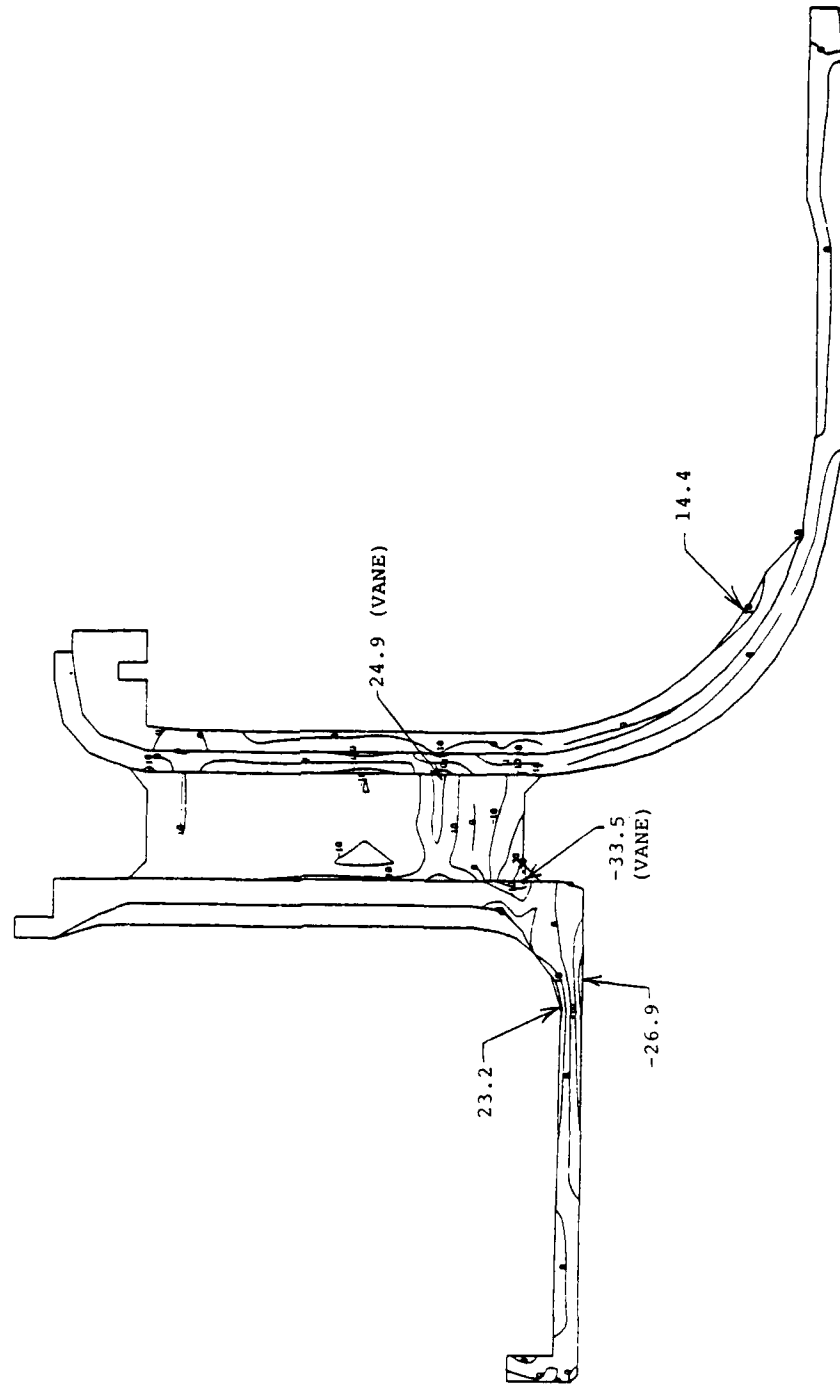


Figure 42. GTP105-2 turbine nozzle temperature and pressure axial bending stress (ksi)

AD-A087 838

AIRESEARCH MFG CO OF ARIZONA PHOENIX

F/G 10/2

ADVANCED TECHNOLOGY COMPONENTS FOR MODEL 6TP305-2 AIRCRAFT AUXI--ETC(U)

FEB 80 J R KIDWELL, G D LARGE

F33615-75-C-2016

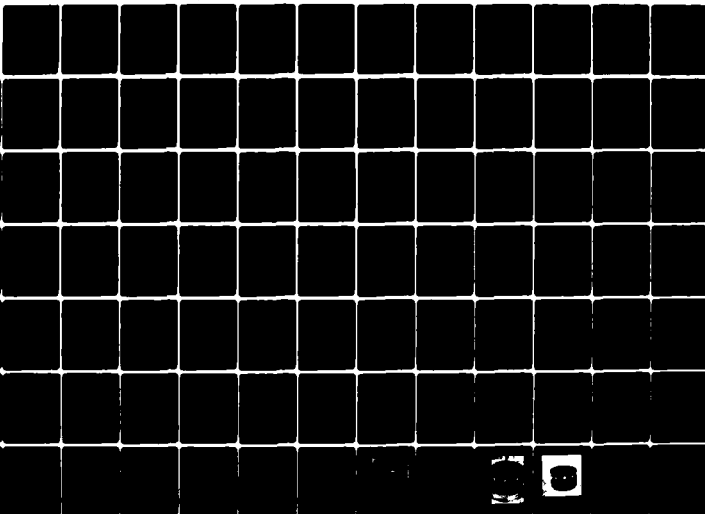
UNCLASSIFIED

AFAPL-TR-79-2106

NL

2 OF 6

4 00838



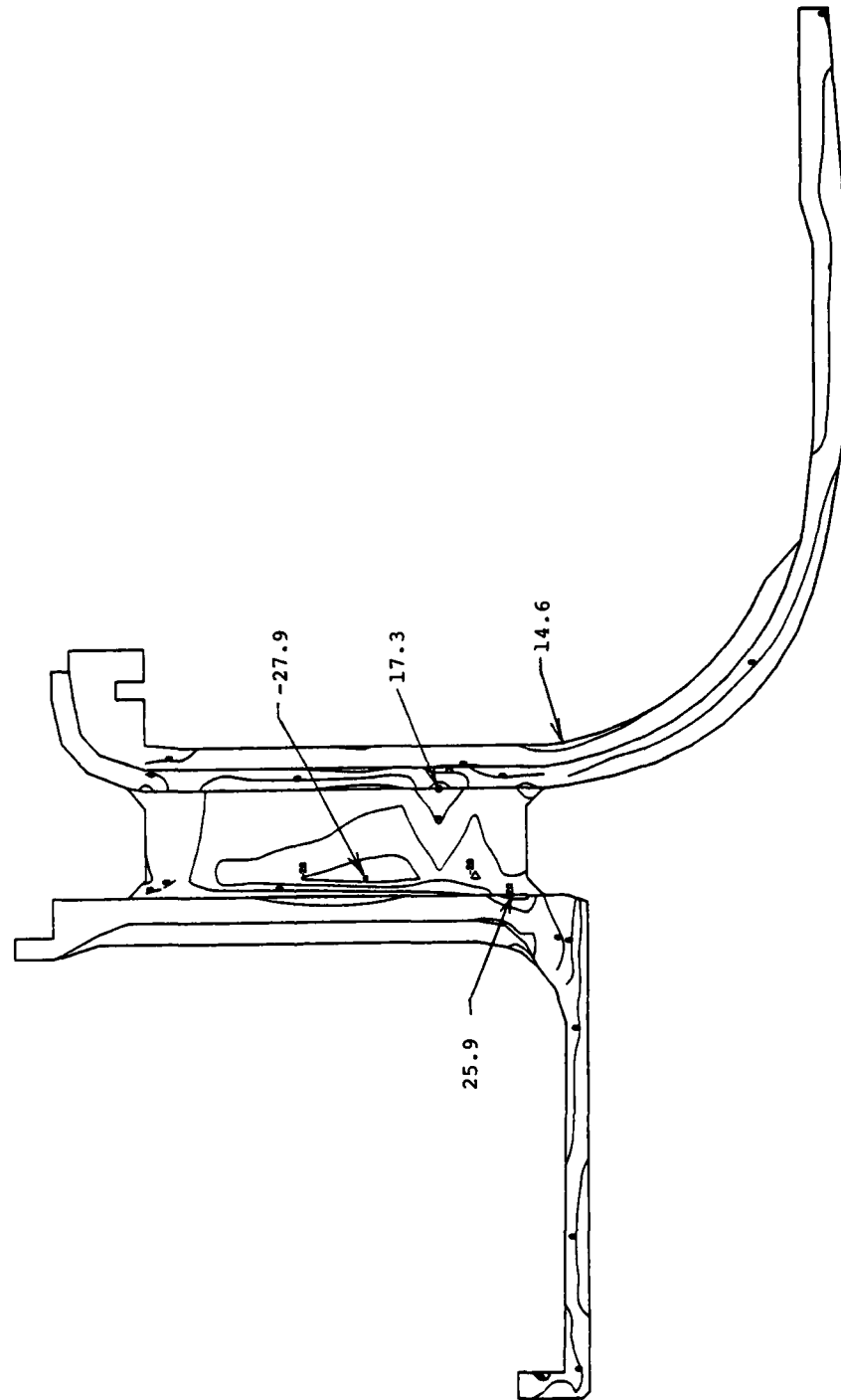


Figure 43. GTP305-2 turbine nozzle temperature and pressure radial bending stress (ksi)

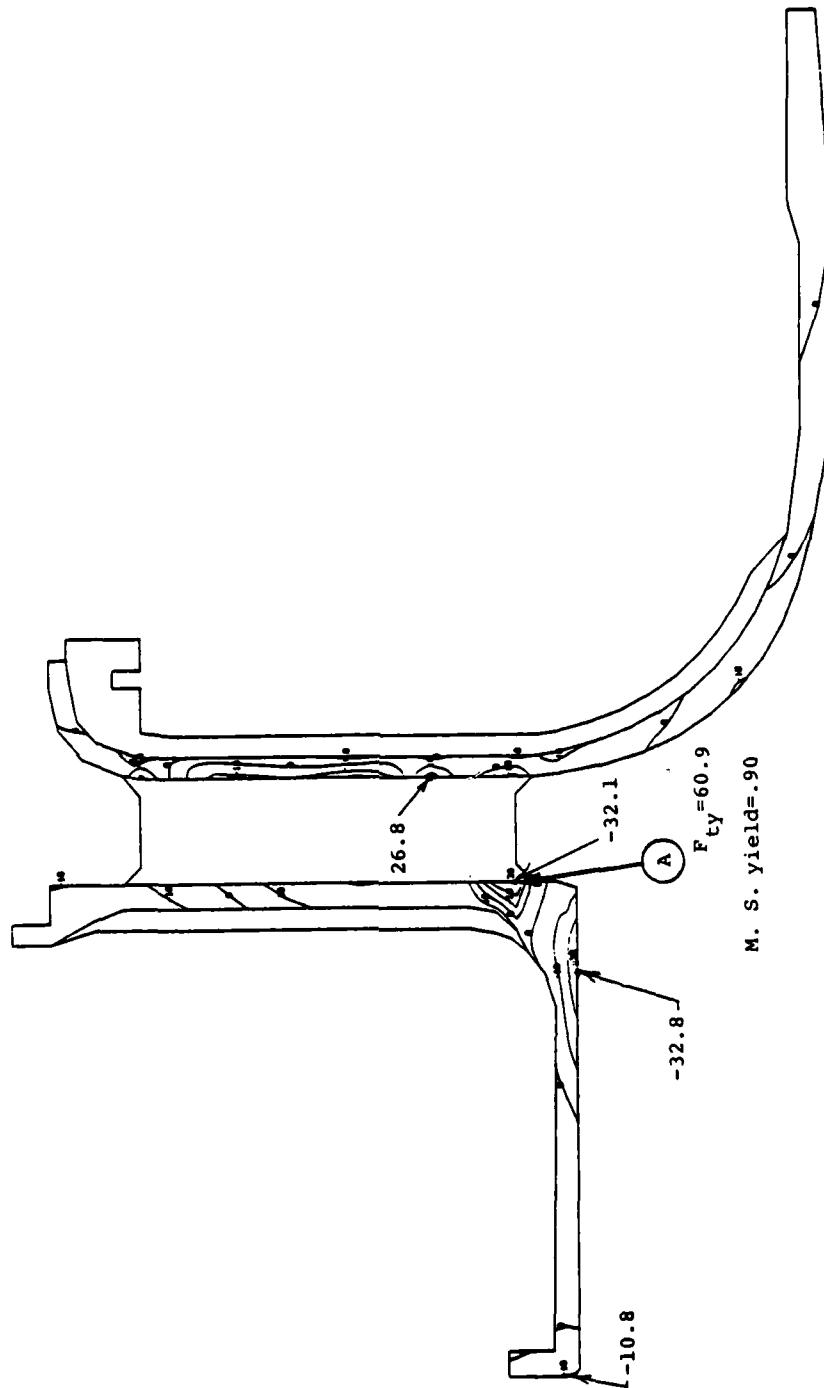


Figure 44. GTP305-2 turbine nozzle temperature and pressure hoop stress (ksi)



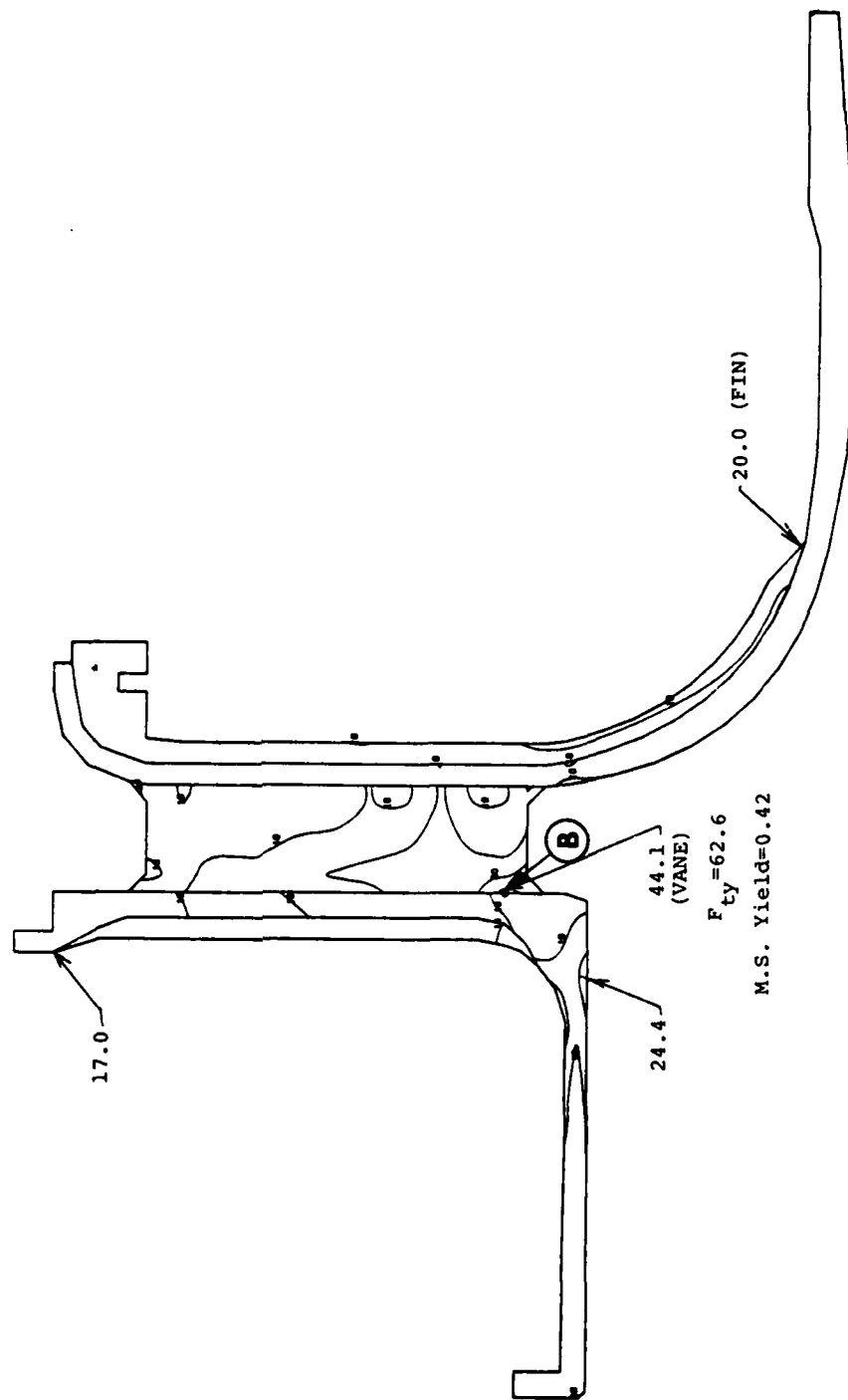


Figure 45. GTP305-2 turbine nozzle temperature and pressure equivalent stress (ksi)

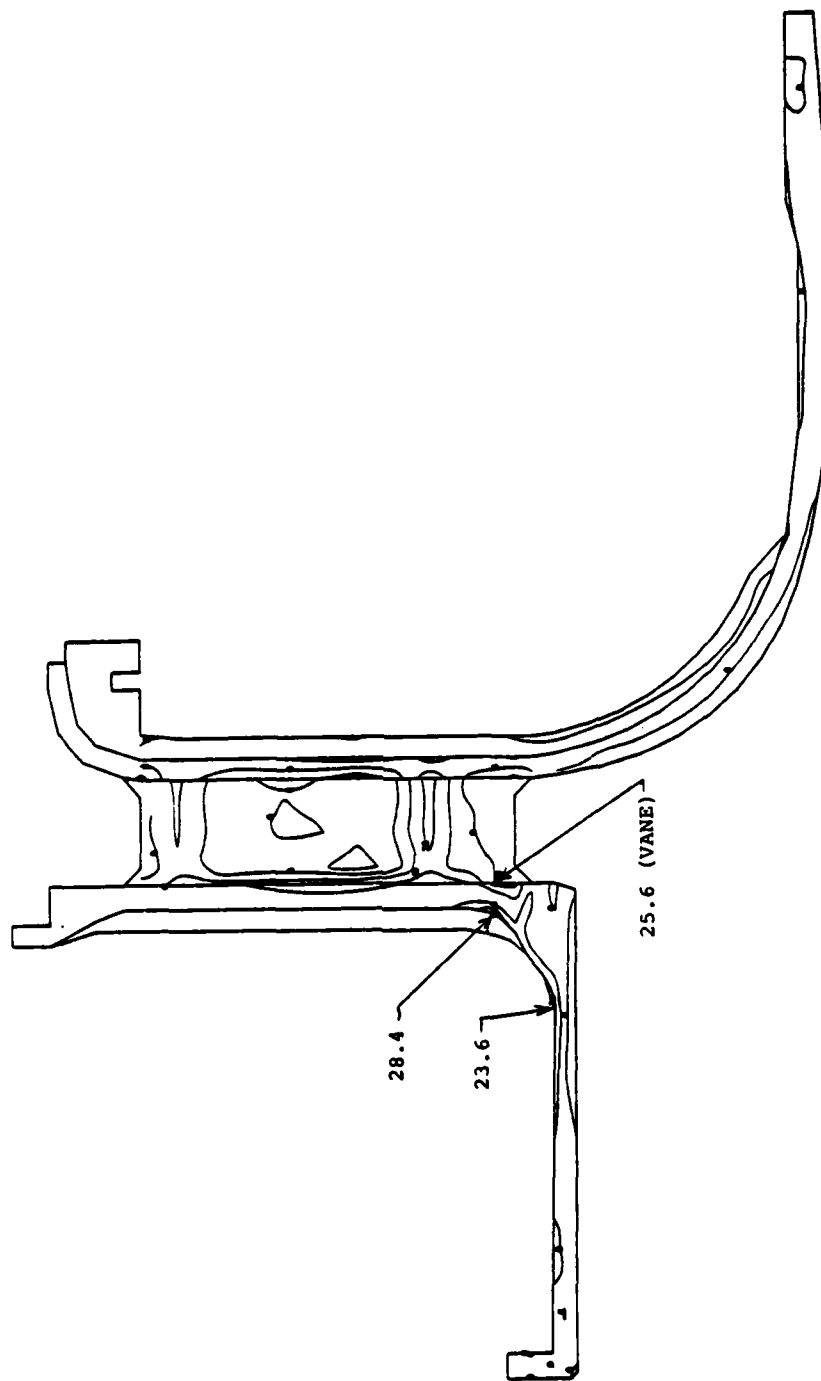
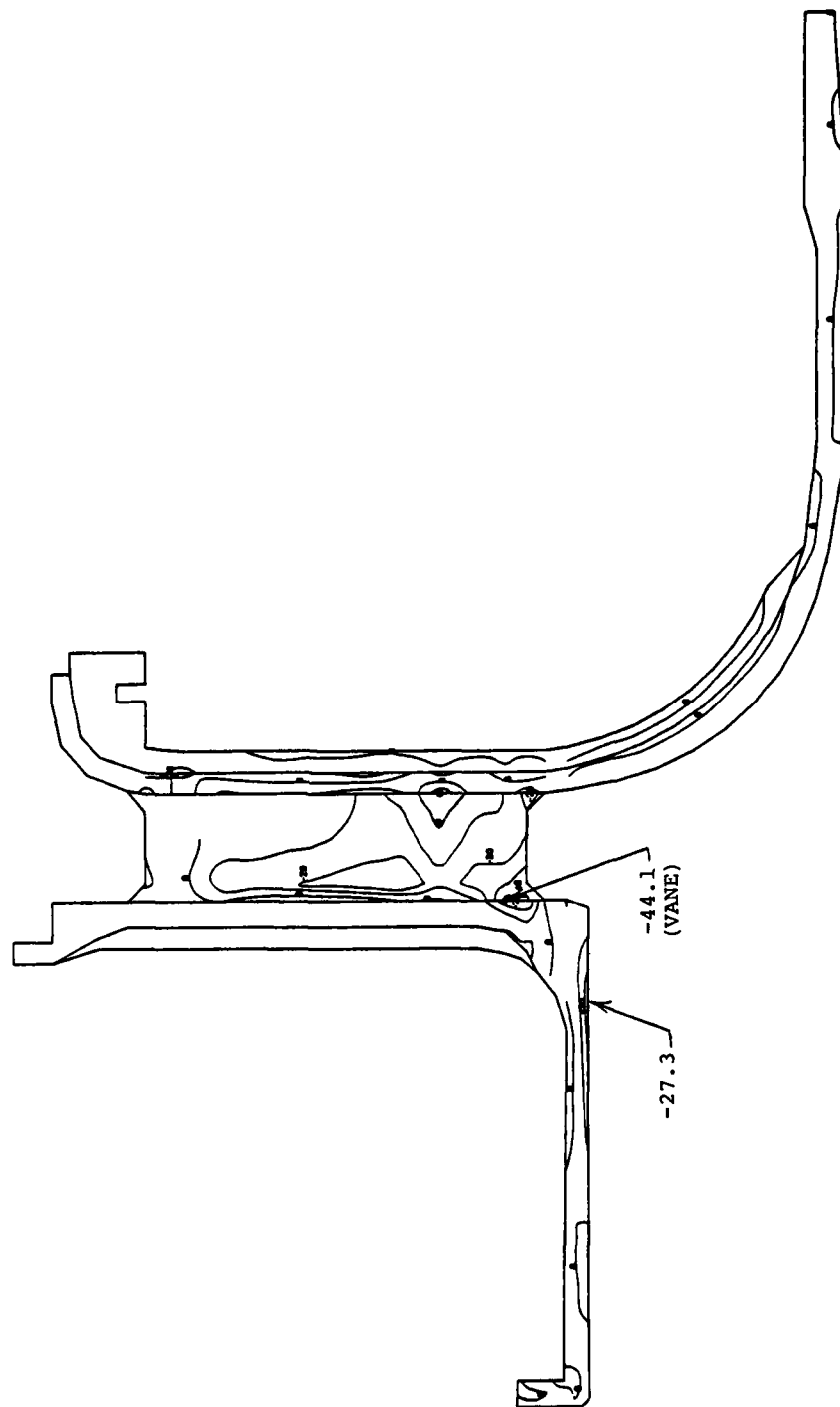


Figure 46. GTP305-2 turbine nozzle temperature and pressure principal stress (ksi)



SI (MPa)  $\times 10^3$

Figure 47. GTP305-2 turbine nozzle temperature and pressure principal stress (ksi)

Based on the conservatism stated above, and AiResearch gas turbine experience, it is not unreasonable to expect an LCF failure mode for the STAGG or Model GTP305-2 to occur in approximately 600 to 800 cycles. This mode would certainly not be present in 100-percent of the vanes for any one nozzle and it would definitely not be manifested in 100-percent of the engines.

Detailed three-dimensional finite element modeling such as described above requires several man months of effort and usually results in statements presented herein. Therefore, utilizing STAGG and other related program experience, the cast nozzle design for the Model GTP305-2 application is judged structurally adequate over the duty cycle and satisfies program life requirements as stated in Section 3.0.

#### 3.4.8 Radial Turbine Rotor

##### 3.4.8.1 Aerodynamic Design

The initial step in analyzing the radial turbine rotor was to determine the optimum rotor inlet and exit velocity diagram at the selected rotor-to-axial turbine work split of 64.7 to 35.3 percent.

For a specified work level, the optimum rotor inlet condition (corresponding to peak efficiency) for radial turbines is based on the "slip" factor criteria. The slip factor relates stator exit tangential velocity ( $v_u$ ) to inducer blade speed ( $U$ ) for a specified rotor blade number ( $N_b$ ) in the following manner:

$$\lambda_{2, \text{ opt}} = \frac{v_u}{U} \quad \text{opt} = 1 - \frac{2}{N_b} \left[ \text{OPTIMUM ROTOR INLET WORK COEFFICIENT} \right]$$

For high work levels and zero exit swirl, it is generally not possible to satisfy this criteria due to inlet blade speed limitations imposed by the material properties. Figure 48 shows

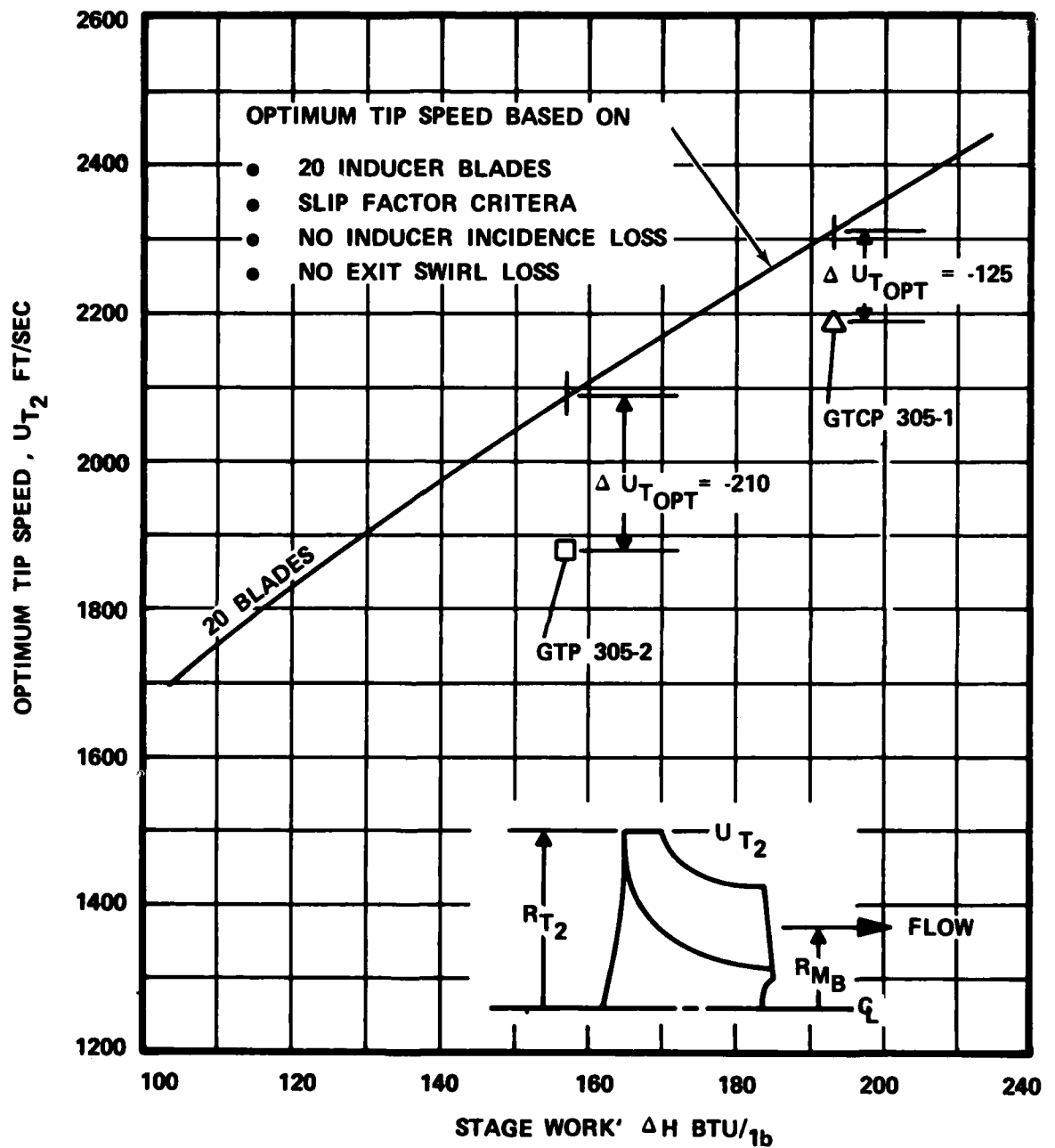


Figure 48. Variation of optimum tip speed with turbine stage work

the variation of optimum tip speed as a function of radial stage work for a 20-inducer blade rotor. As shown in Figure 48, the Model GTP305-2 radial stage, with a tip speed limitation of 1880 ft/sec, has a 205 ft/sec tip speed deficiency, compared to 125 ft/sec deficiency for the Model GTCP305-1 radial stage. For non-optimum inlet conditions, a performance penalty is therefore imposed due to an increase in inducer loading. A recent analytical study at AiResearch indicates that this performance penalty can be minimized by redistributing the total work between the rotor inlet and exit. This analysis shows that total losses with exit swirl (assuming the rotor exit tangential component is not recoverable) are less than inducer losses with no exit swirl and that an optimum rotor exit swirl exists for maximum efficiency. The Model GTP305-2 radial turbine, when applying this analysis, showed that maximum stage efficiency occurs at an inlet work coefficient ( $V_u/U$ ) of 1.0507 and a meanline exit work coefficient of -0.1507 (which corresponds to -14.5 degrees meanline exit swirl).

Having established the optimum vector diagram, an internal aerodynamic analysis of the radial rotor was conducted. The analysis was based on a computer program that solves the radial equilibrium equation along an arbitrary line in the rotor meridional plane between hub and shroud contours. Flow conditions are established at specified rotor upstream and downstream stations and on a mean flow basis between blades in the rotor. Entropy and enthalpy gradients in the meridional plane are recognized. Blade-to-blade velocities are then calculated based on the conditions of zero absolute circulation and a linear variation of suction to pressure surface velocity. The analysis objective was to obtain smooth accelerating flows and avoid severe local diffusions with the following constraints:

- o Rotor inducer tip speed was limited to 1880 ft/sec for cast AF2-1DA

- o The 10-full blade and 10-splitter blade configuration of the Model GTP305-1 radial rotor was retained. However, to minimize exit blade root low cycle fatigue, the splitter and exducer axial length were reduced by 0.200 inch, and a curved trailing edge configuration was incorporated at both the splitter and full blade trailing edges
- o Achieve maximum possible scallop depth without severely deteriorating aerodynamic performance. Previous AiResearch test results indicate that rotor scallop effects can be minimized by limiting scallop depth to the exducer tip radius and by minimizing hub meridional turning from the inducer inlet to the scallop location. If turning is too great, the hub flow will impact on the bottom of the scallop, resulting in mainstream flow distortions. More specifically, Hiett and Johnston [Reference (3)] test results show that reducing the scallop depth significantly below the exducer tip radius could result in efficiency decrements of 2.0 to 4.0 points
- o A blade thickness distribution that would minimize uncooled rotor blade stress was selected. This thickness distribution is similar to that used for the STAGG uncooled rotor
- o The Model GTP305-1 rotor exducer hub and shroud radii were maintained

(3) Hiett, G.F., Johnston, I.H. "Experiments Concerning The Aerodynamic Performance of Inward Flow Radial Turbines."

Inst. Mechanical Engineers, Thermodynamics and Fluid Mechanics Convention, April 1964, Paper No. 13

- o Rotor radial loss distribution and exit blade deviation data were based on correlations from previous AiResearch radial turbine tests

For a rotor inlet work coefficient of 1.0507, and rotor constraints listed above, a number of internal rotor flow solutions were examined by varying hub and shroud contours and rotor blade angle distribution. Since scallop depth was reduced to the exducer shroud radius, a major change in the rotor hub line was necessary to minimize scallop effects. A comparison of the Model GTP305-2 flow path with the Model GTCP305-1 is shown in Figure 49. The inducer region for all three streamlines shows the expected high loading as a result of the non-optimum tip speed inherent in the reduced-radius cast design. These analyses showed that rotor blading could be improved slightly by extending the splitter blades. However, due to the increased blade thickness required to maximize the uncooled rotor life, extending the splitter blades downstream resulted in significant mainstream diffusion beyond the splitter blade ends. Higher mainstream diffusion also resulted from the higher splitter turning required at the extended length. Conversely, reducing the splitter length would be mechanically favorable but analysis showed that reducing the splitter blade length by a significant amount would result in large local diffusion on the full blade pressure surface downstream of the splitter blades.

#### 3.4.8.2 Radial Rotor Stress Analysis

In concert with the aerodynamic design of the radial turbine rotor, a steady-state thermal/stress analysis was conducted. As stated in Paragraph 3.4.8.1, a blade thickness distribution similar to that of the uncooled STAGG rotor was utilized, and the Model GTP305-1 exducer hub and shroud radii were maintained. Axial blade lengths for the full and splitter blades was reduced by 0.200 inch to incorporate a trailing edge configuration that



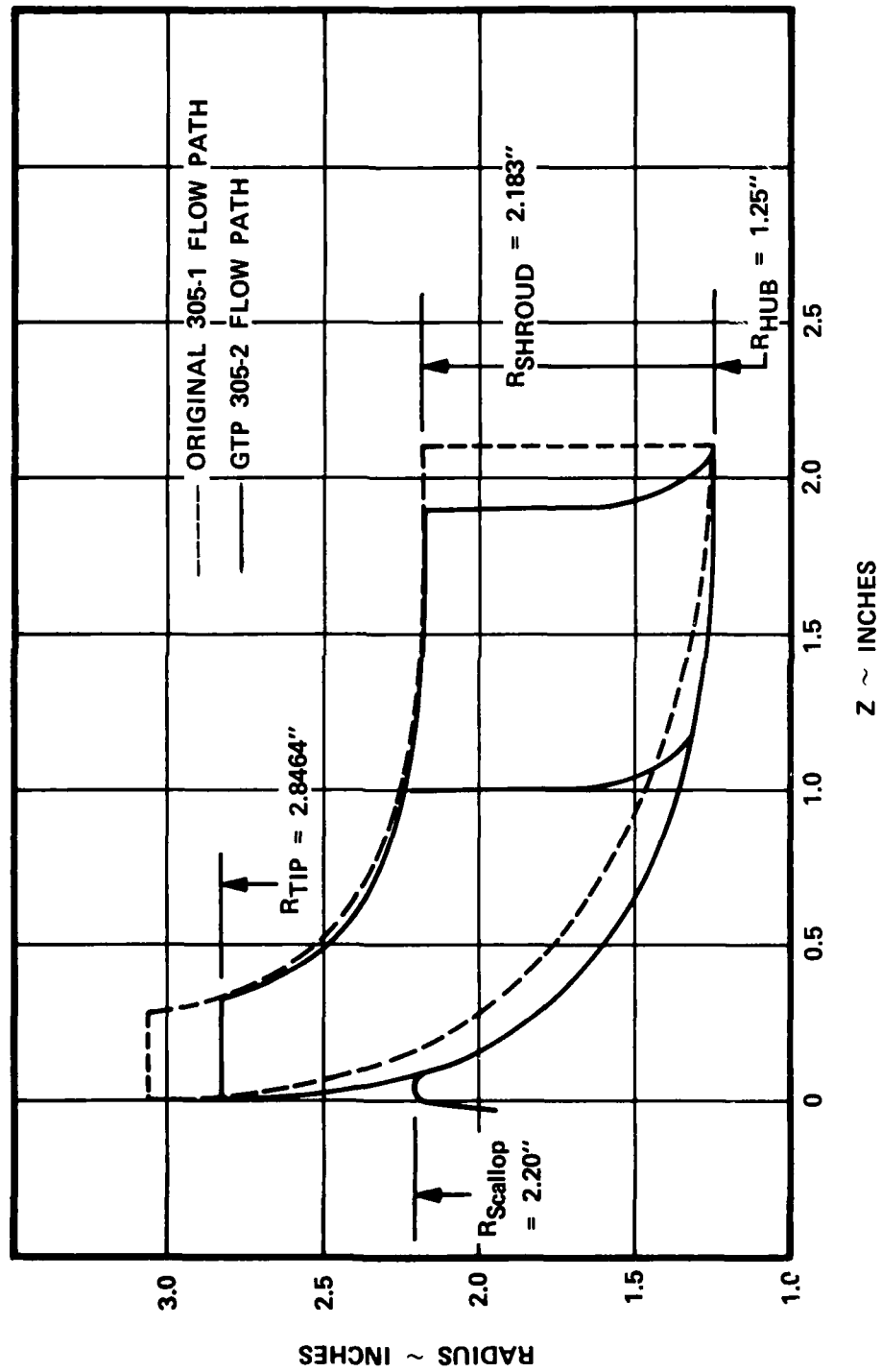


Figure 49. GTP305-2 radial rotor final flow path

will reduce low cycle fatigue (LCF) effects at the exit blade roots. The rotor meridional flow path is shown in Figure 49. The Model GTP305-1 configuration is also shown for comparison.

Preliminary finite element stress analyses indicated a large region of creep in the rotor bore. Discussion of the analysis is included in Paragraph 3.4.8.4.

#### 3.4.8.3 Bore Cooling Flow Analysis

As shown in Figure 50, preliminary stress analysis indicated a large region of the bore would exceed 1-percent creep. The introduction of bore cooling air was investigated to reduce this area within acceptable limits. Introduction of air from the compressor backface via the compressor/seal curvic to cool the turbine bore and buffer the interstage seal between the radial and axial turbines provided a desirable flow path while minimizing cycle losses and complex flow metering hardware.

Figure 51 depicts the selected flow path. The static pressure of the main flow gas exiting the radial turbine is 31.5 psia. For this reason the buffer pressure of the cooling air being supplied between the knives of the interstage turbine seal should exceed 31.5 psia. A redesign of the intercompressor/turbine seal was accomplished for the purpose of reducing seal leakage. Bore cooling air is supplied from the relatively low (50 psia) compressor backface. It was desirable that primary metering of the total flow occur as a result of the interturbine seal knives. The nominal interturbine seal leakage rate is approximately 1 percent of engine mainflow, 0.023 lb/sec. Achieving this flow rate at a pressure level sufficient to buffer the interturbine seal was complicated by pressure losses characteristic of the chosen bore cooling flow path. Primary pressure loss mechanisms included:

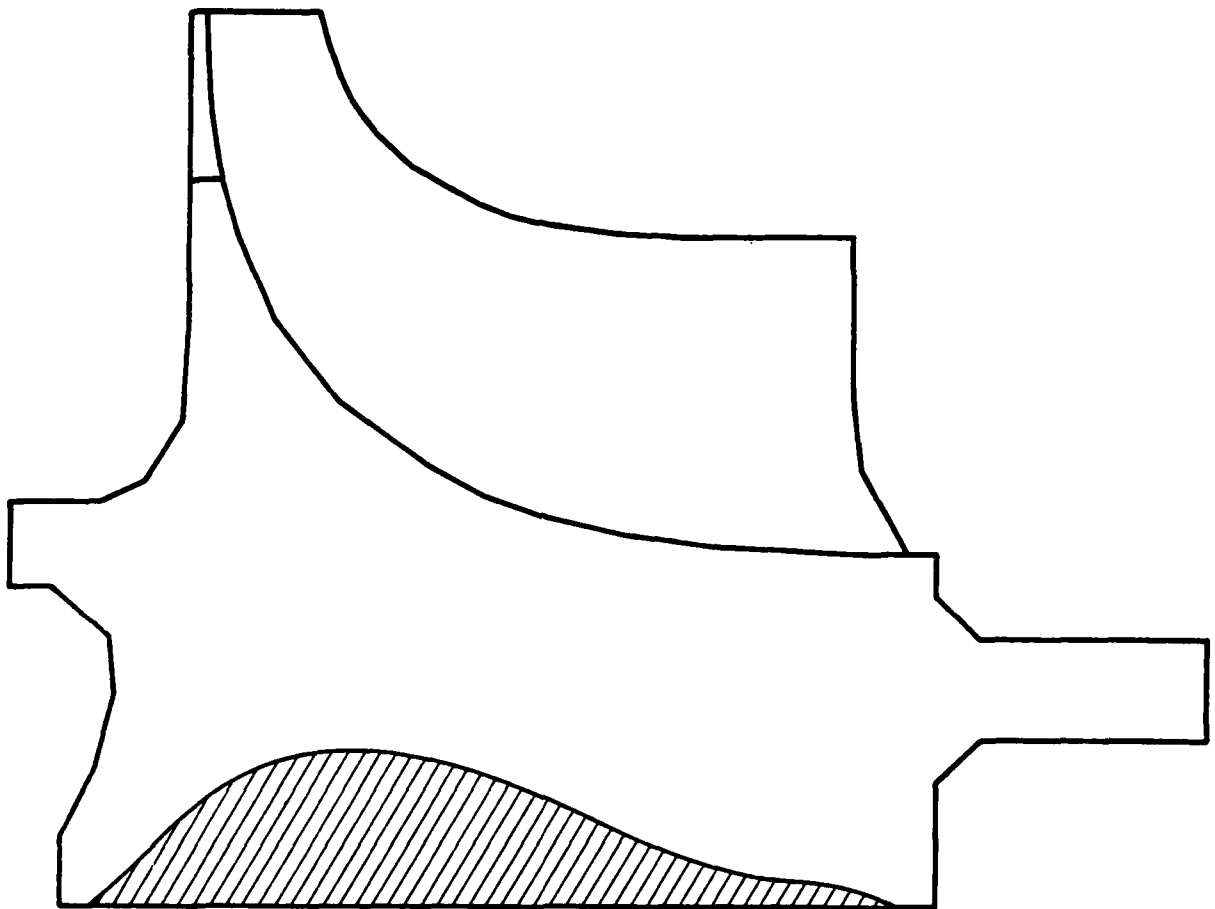


Figure 50. Area of wheel which exceeds one percent creep for an uncooled bore

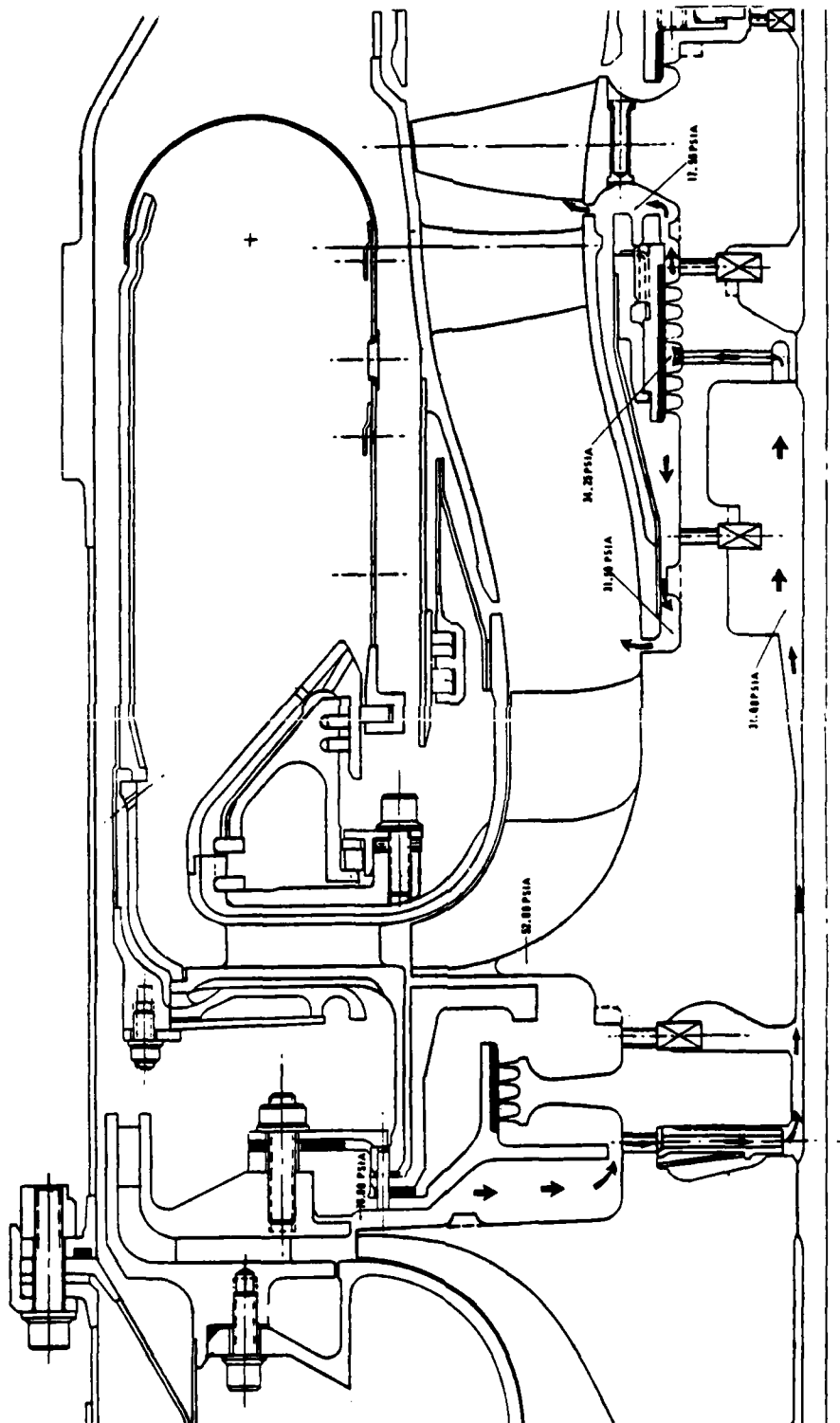


Figure 51. Radial turbine nozzle bore cooling flow path

- o Swirl-down of radial inward flow to the curvics
- o Flow choking, due to heating, in the turbine bore
- o Swirl-up of radial outward flow to the interturbine seal

Addressing each loss inducing item above, the bore cooling flow path includes such features as a radial inflow deswirl vane, contoured corners at each duct entry point along the flow path, a conical diffuser cone on the aft portion of the radial turbine, and a radial outflow swirl-up vane to pump cooling air out to the interturbine seal. Of particular importance were the tiebolt and radial turbine bore machine tolerances, since these clearance areas directly effect the choked flow rate for cooling.

Figure 51 also shows the intercompressor/turbine seal design. System pressures shown are for design point operation and nominal seal clearance dimensions. At the intercompressor/turbine seal, a 0.009 inch radial clearance was assumed. The compressor backshroud extending to the curvic outer radius inhibits the tangential acceleration of the cooling flow moving radially inward on the compressor backface. Drag caused by this shroud brings the gas tangential velocity down to a level very near wheel speed at the curvic inlet and provides a reduced static pressure drop as required for pumping the cooling flow to the turbine bore. The total power loss due to drag induced by the cooling flow on the static shroud and the adjacent rotating structure is 6.2 horsepower.

A detailed calculation of the available flow area through the compressor seal curvics was performed. The difference between the gas tangential velocity and the wheel speed at the inlet to the curvics reduces the effective discharge coefficient through the rotating orifices formed by the curvics. Extension

of the compressor backshroud to the radius of the curvic inlet causes this velocity differential to be approximately 130 ft/sec. Reference (4) indicates that no tangential velocity component is recovered as pressure. By using inlet static pressure and a detailed calculation of the required pressure drop across the orifice, Reference (5), the static pressure leaving the curvics was conservatively predicted.

For gas flows induced radially inward against the natural outward pumping action of rotating disks, conservation of angular momentum tends to increase the gas tangential velocity. High shearing forces between the rotating gas and both the neighboring static structure and/or the more slowly rotating disc cause losses that are manifested by a lack of pressure recovery in the gas. Rotational energy is traded for irreversible heat generation on the shroud and disc surfaces. A deswirl vane extending radially from near the tie-bolt to the ID of the curvic has the effect of reducing the tangential shear losses of the inlet cooling flow by forcing the gas tangential velocity to conform to that of the wheel at each radial location. A disc with sixteen radial holes of 0.090 inch diameter was designed. The outside diameter of the disc has a circumferential "trough" acting as a plenum in which to collect gas emanating from the curvics. A calculated Mach No. of 0.18 at the ID represents a fairly large dynamic pressure head which is not recovered in the 90 degree bend required for the gas to pass beneath the seal hub.

To facilitate a reduced cooling flow restriction, the inner radius of the seal hub has been increased to 0.24 inch. A contoured radius on the cooling flow inlet and exit at the bore of the seal hub effectively reduces sharp-edged flow losses.

(4) Amman, C.A., Nordenson, G.E. and Raxinsky, E.H. "The Turbine Interstage Duct" SAE Paper No. 710553, June 1971.

Flow pressure losses through the turbine bore were reduced by:

- o Contouring the inlet
- o Increasing the radius of the bore to 0.21 inch (from 0.19 inch)
- o Introducing a diffuser cone on the aft end of the turbine bore
- o By maintenance of minimum tolerance variation on the machined tiebolt and turbine bore surfaces

As the cooling flow is heated passing through the turbine bore, it approaches a choked condition. Flow choking occurs at Mach 1 where a high velocity head exists. If this cooling flow is exhausted at  $M = 1$  into the cavity aft of the radial turbine, practically no pressure recovery results. However, a diffuser with a gradual one-to-four area increase extending over the last 1-inch of the radial turbine bore theoretically produces an approximately 78-percent dynamic pressure recovery. This diffuser feature was included in the radial turbine design with no significant amplification of bore stresses. Figure 52 is a plot of the bore cooling flow versus resultant seal buffering pressure. The horizontal portion of the operating line shows choked bore flow due to Rayleigh heating there. The three data points shown in Figure 52 correspond with the following choked flows for clearance areas that correspond to; a minimum area produced by the maximum tiebolt and minimum turbine bore dimensions, a nominal area produced by nominal dimensions, and a maximum area produced by minimum tiebolt and maximum turbine bore tolerances.

- (5) "Radial - Inflow Turbine Performance with Exit Diffusers Designed for Linear Static Pressure Variation," NASA TMX-2357, August 1971.

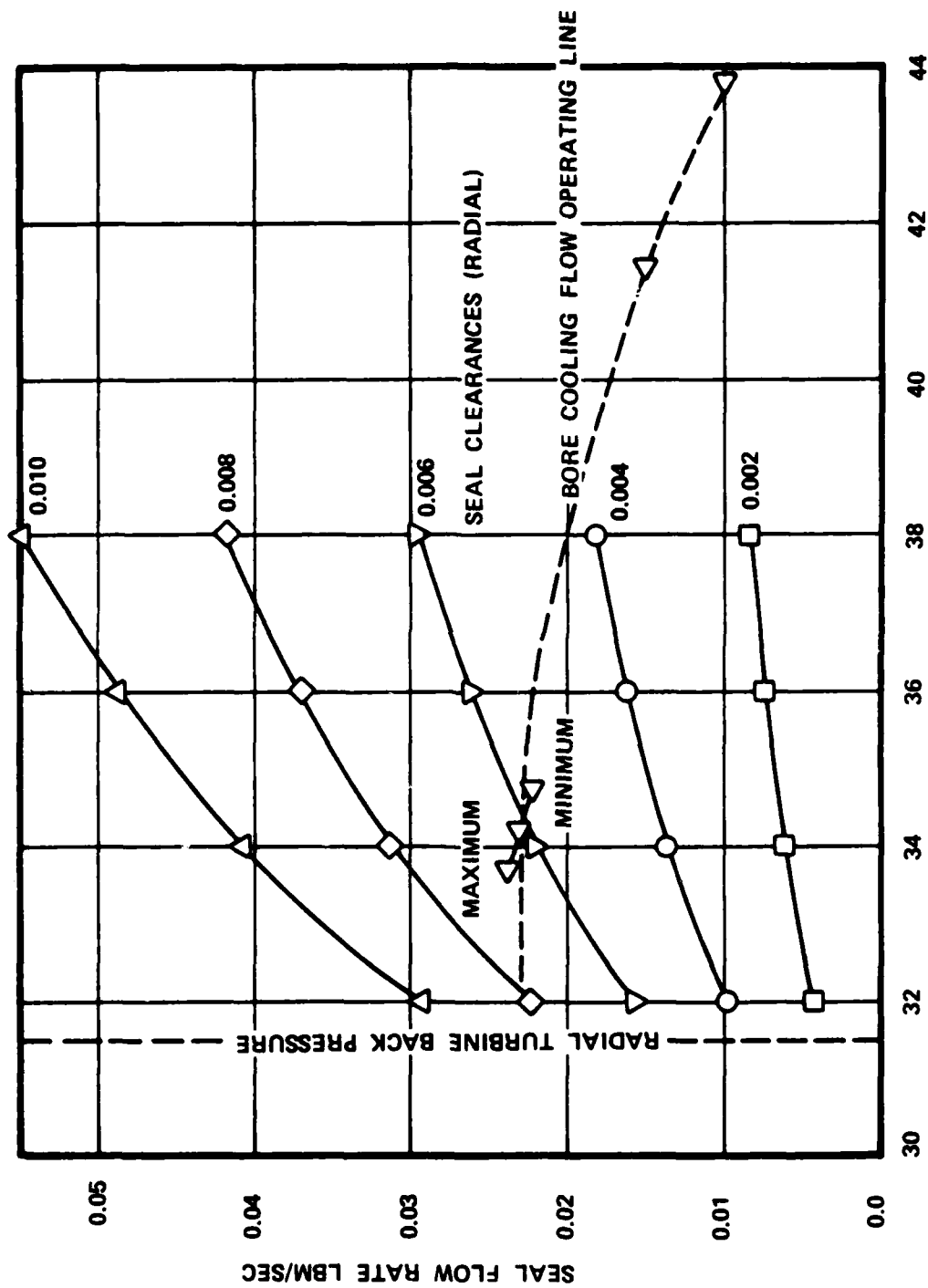


Figure 52. GTP305-2 interturbine seal clearance flow rate vs buffer



<u>Flow Area</u>	<u>Tiebolt Radius</u>	<u>Turbine Radius</u>
Minimum 0.5460 inch <sup>2</sup>	0.1625 inch	0.20925 inch
Nominal 0.5635 inch <sup>2</sup>	0.16175 inch	0.2100 inch
Maximum 0.05810 inch <sup>2</sup>	0.1610 inch	0.21075 inch

As in the case of the previously discussed deswirl vane which is used for reducing rotational shearing losses for radially inward flowing gas, the swirl vane is used to pump the low radius cooling gas from the turbine bore out to the buffered seal. Shearing losses, characteristic of disc pumping, were reduced with the swirl disc containing twenty 0.10-inch diameter radially drilled holes.

Figure 53 illustrates the region of the bore exceeding one percent creep. As compared to Figure 50, this region has been greatly reduced due to the incorporation of bore cooling flow.

#### 3.4.8.4 Thermal/Stress Analysis

Figure 54 shows the radial turbine rotor temperature distribution with bore cooling and forward face cooling. While the uncooled bore temperatures average approximately 1400°F, the cooled-bore reaches a steady-stage average temperature near 1275°F.

Heat transfer film coefficients were calculated during the radial rotor thermal/stress analysis. During this analysis, several methods of calculation were investigated. Current test data from other programs indicated the method of calculation employed was overly conservative. Thus, the thermal/stress analysis was repeated based on updated analytical tools.

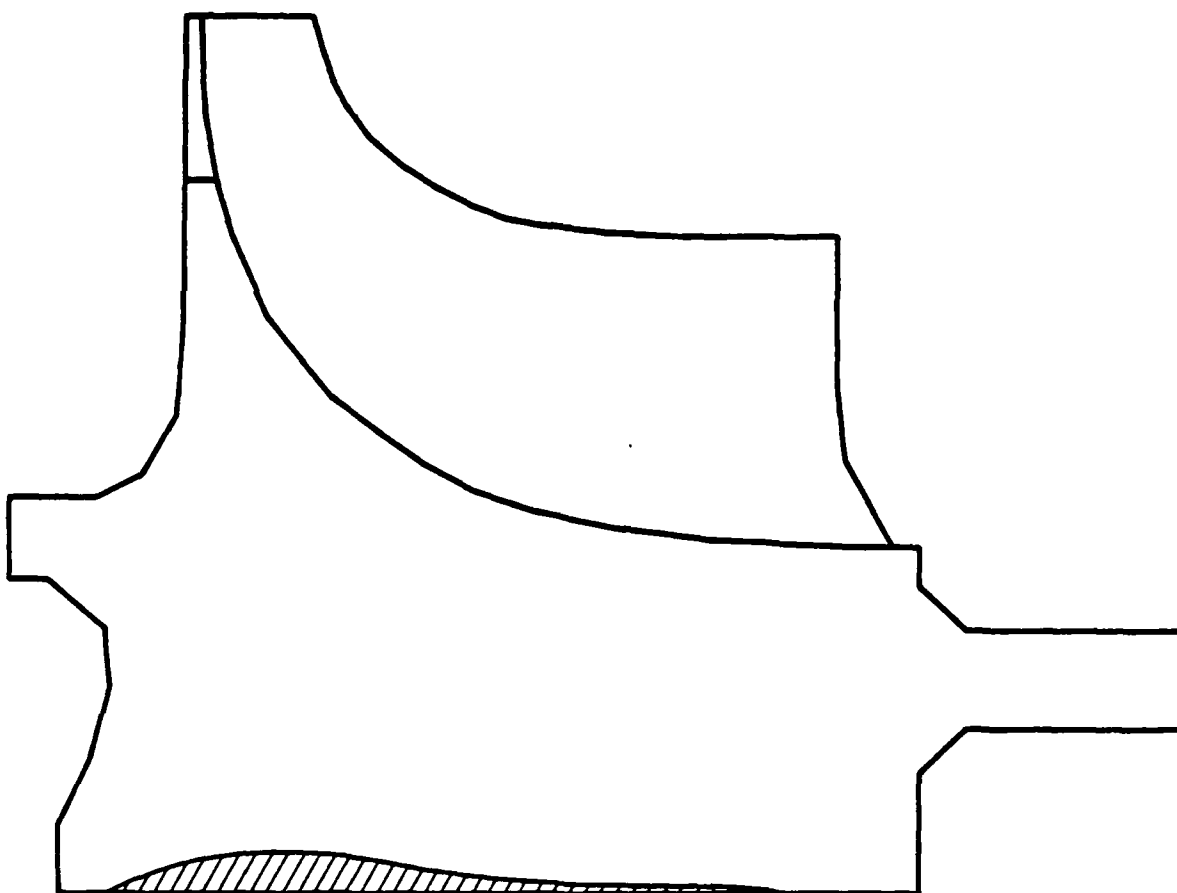


Figure 53. Area of wheel which exceeds one percent creep for a cooled bore

GTP305-2 TURBINE WHEEL TEMPERATURES WITH  
BORE COOLING AND LOW FLOW FACE

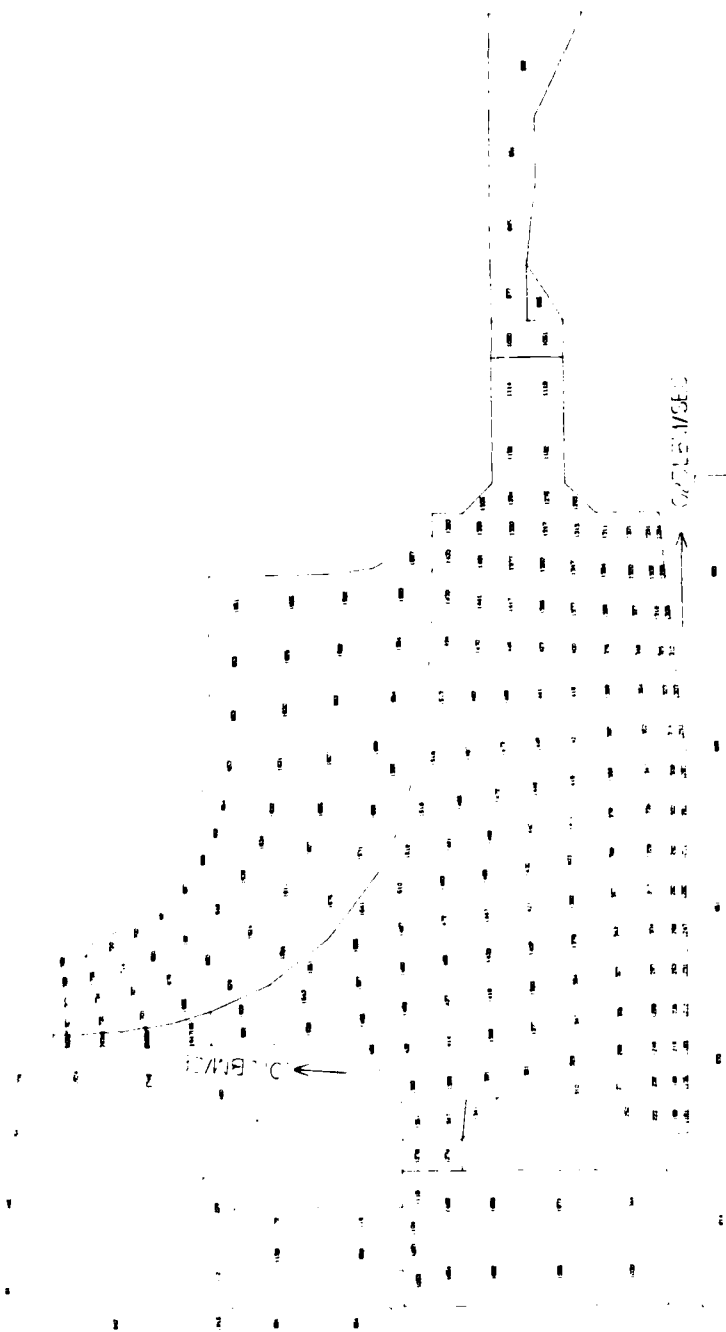


Figure 54. GTP305-2 radial turbine steady state temperature distribution  
bore flow = 0.023 lb/sec, front face flow = 0.01 lb/sec

Figure 55 shows the thermal profile of the radial rotor utilizing the updated analytical tools. As can be seen, the hubline temperatures drop by approximately 30°F when compared to Figure 54. However, the hubline-to-bore gradient does not change appreciably. Figures 56 through 59 show the displacements, tangential, equivalent, and radial stress, respectively.

Bore cooling reduces the steady-state bore temperature level by 200°F while allowing sufficient flow to buffer the interturbine seal. In spite of the attendant rise in steady-state thermal stress, bore cooling improves the creep life of the radial turbine (see Figures 50 and 53). With the high potential stress range in the bore, in excess of 200 ksi, LCF is the significant failure mode. Sufficient test data has not been compiled on the AF2-1DA material to accurately access LCF characteristics. However, part of the Model GTP305-2 program is to obtain room temperature strain-controlled LCF property data. Final evaluation of the radial rotor will be assessed upon completion of the LCF property data file (see Appendix D).

#### 3.4.8.5 Interturbine Duct

The interturbine duct provides a smooth aerodynamic transition from the radial turbine exit, to the power turbine inlet. Exit velocity should be as low as possible to maximize the reaction across the power turbine stator. An annular diffuser design for the interstage duct, is required to achieve a relatively high radial turbine exit velocity. Optimization of the radial and axial turbines, result in an area ratio, between stages, of 1.47. The optimum length for a given area ratio is correlated along the  $Cp^{**}$  line, as reflected in Figure 60. Test results from Sovran and Klomp (Reference 1, Paragraph 3.4.12), shows that the  $Cp^{**}$  line results in minimum pressure loss for a given diffuser area ratio. Figure 60 shows that the nondimensional duct length ( $L/\Delta R$ ) is short of optimum duct length, when compared with the

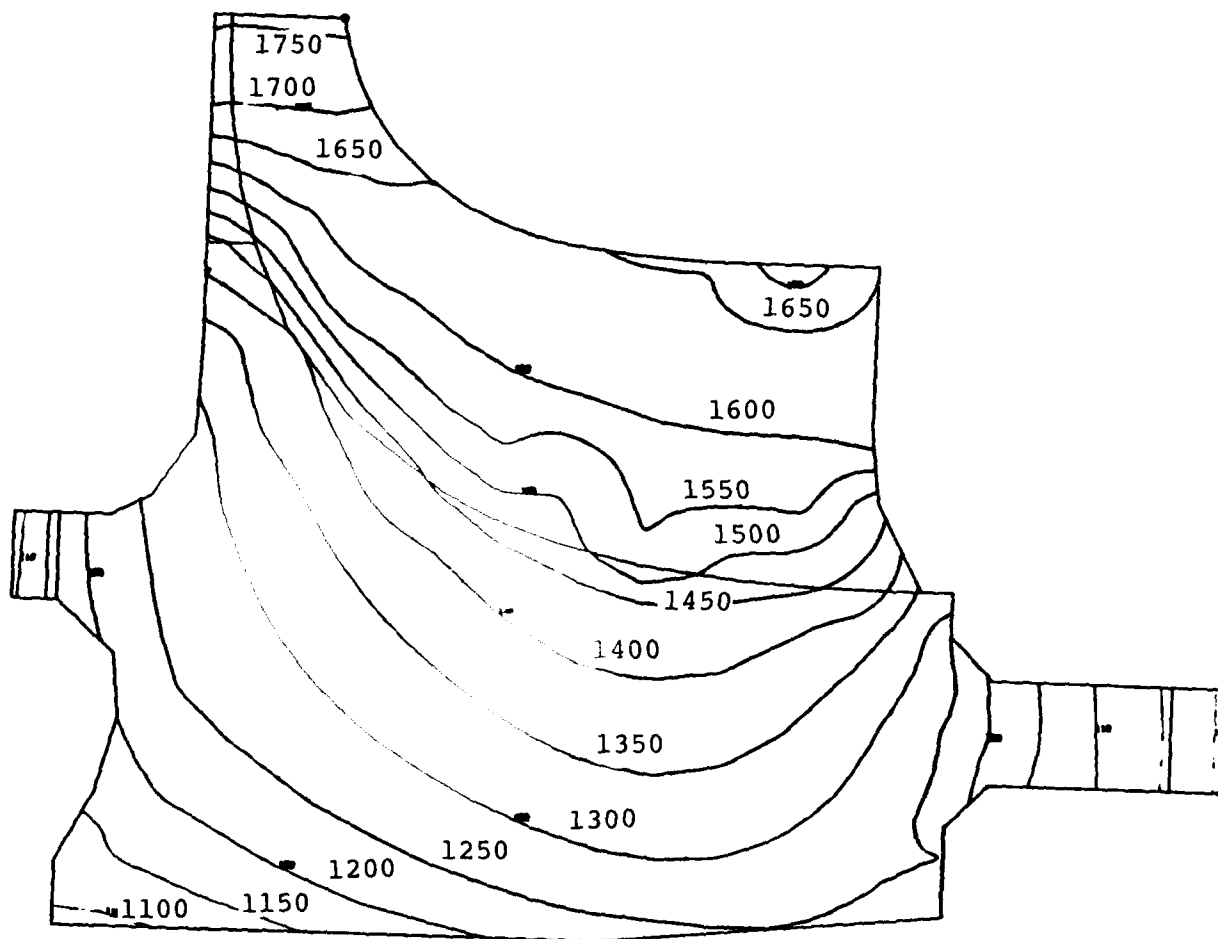


Figure 55. GTP305-2 temperature distribution program to hub line  
 film coefficient bore cooling flow 0.023 lb/sec  
 front face flow 0.06 lb/sec

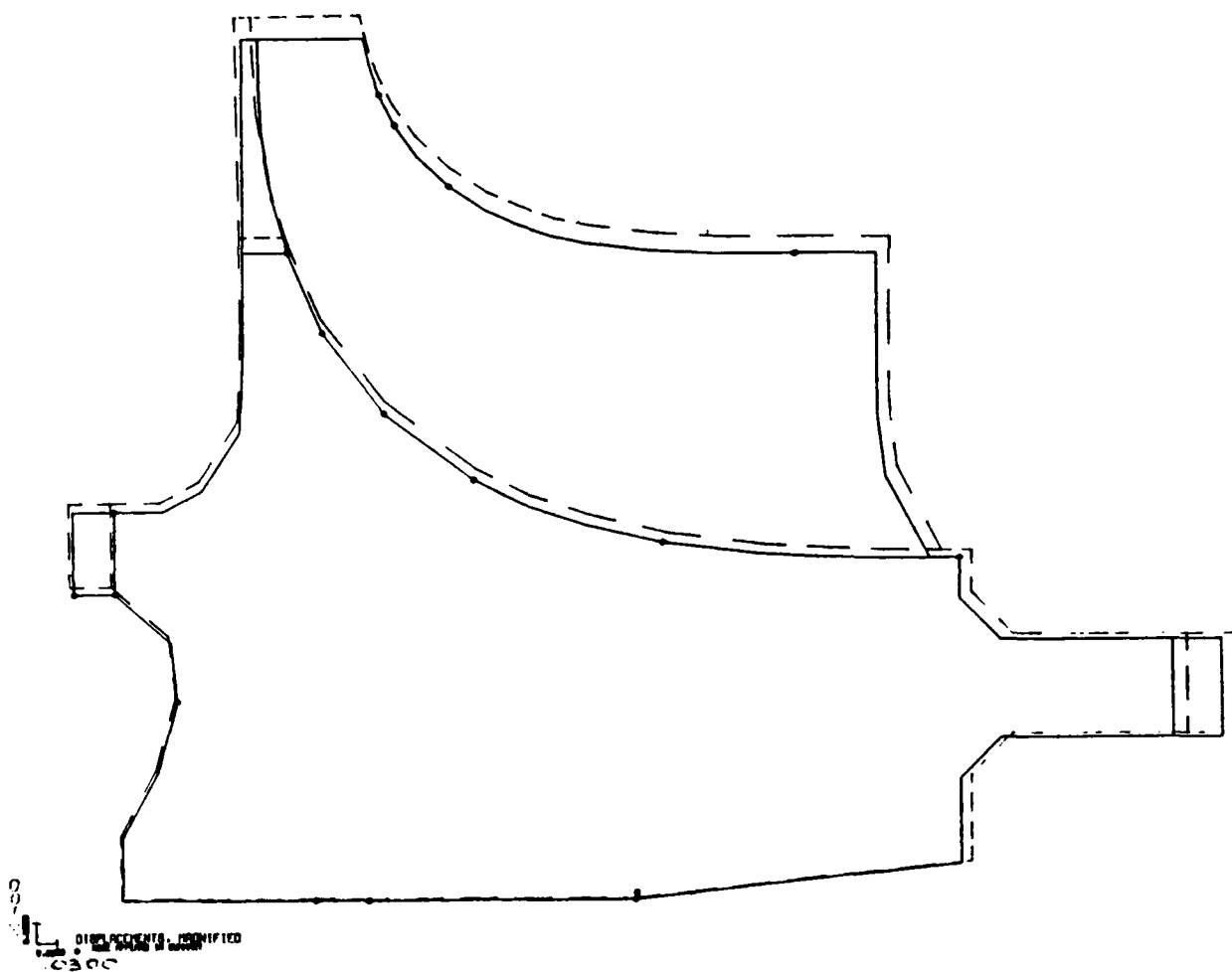


Figure 56. GTP305-2 radial turbine displacements  
program 700 film coefficients  
bore cooling flow 0.023 lb/sec  
front face flow 0.060 lb/sec

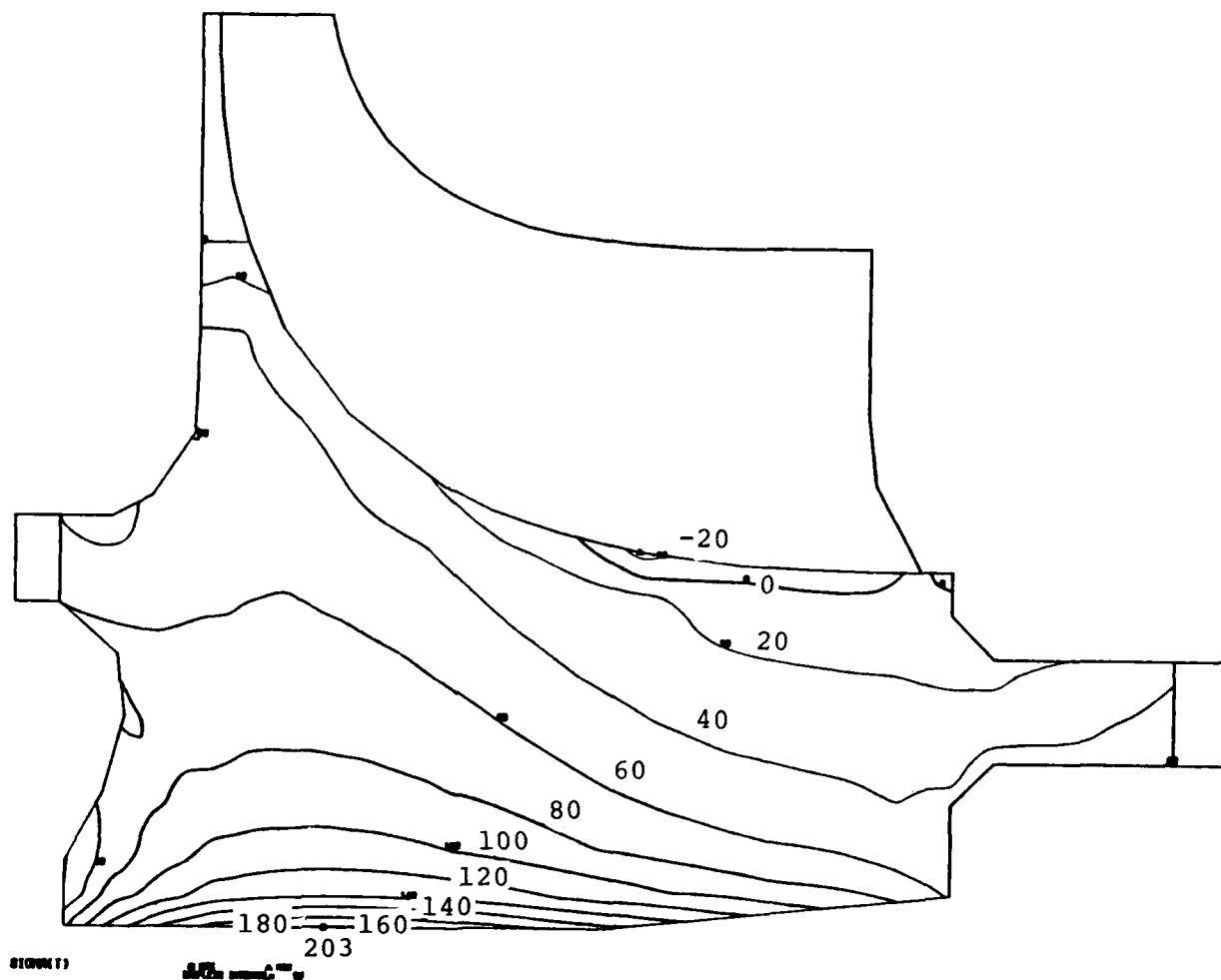


Figure 57. GTP305-2 radial turbine tangential  
stress distribution program 700  
hub line film coefficients  
bore cooling flow 0.023 lb/sec  
front face flow 0.060 lb/sec

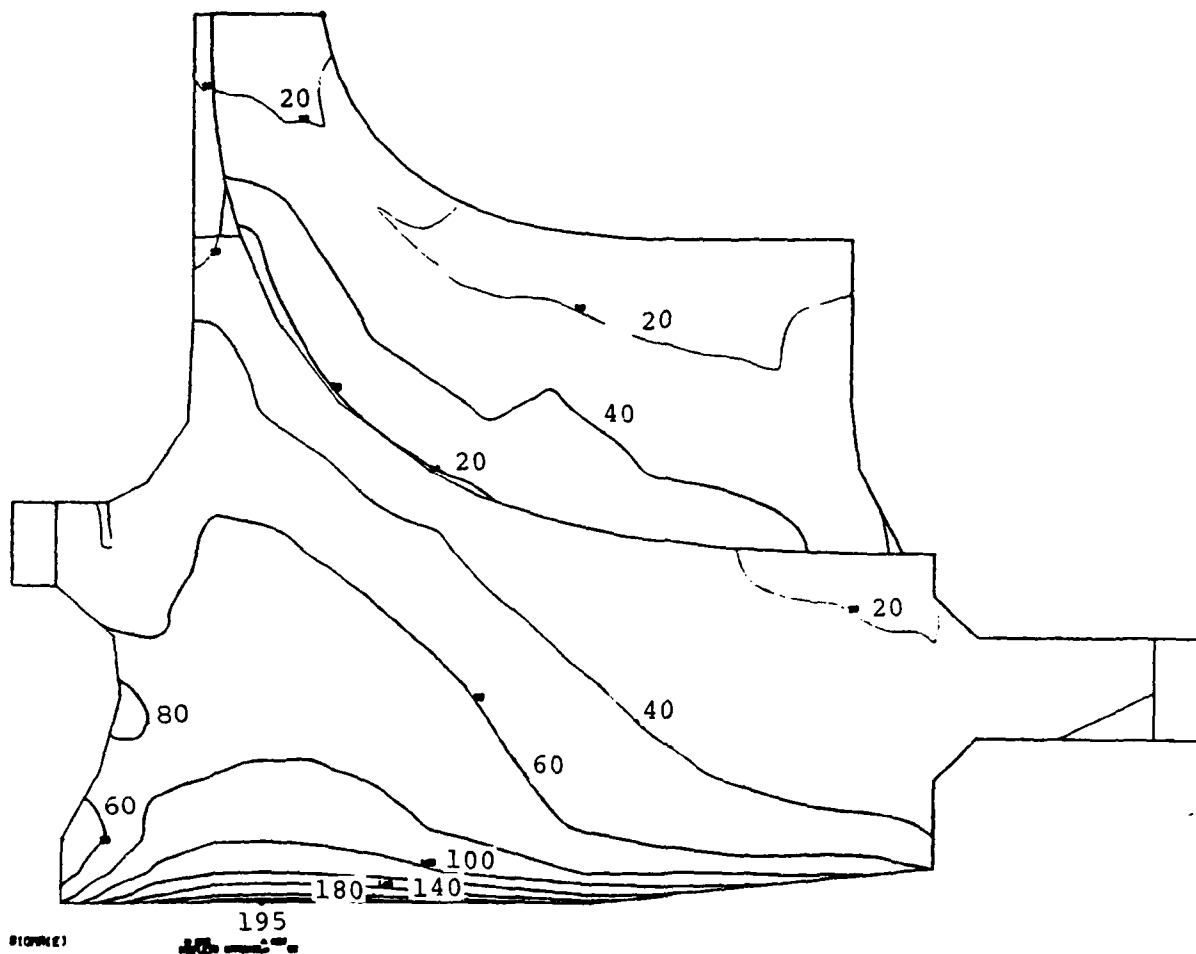


Figure 58. GTP305-2 equivalent stress distribution  
 program 700 film coefficients  
 bore cooling flow 0.023 lb/sec  
 front face flow 0.060 lb/sec



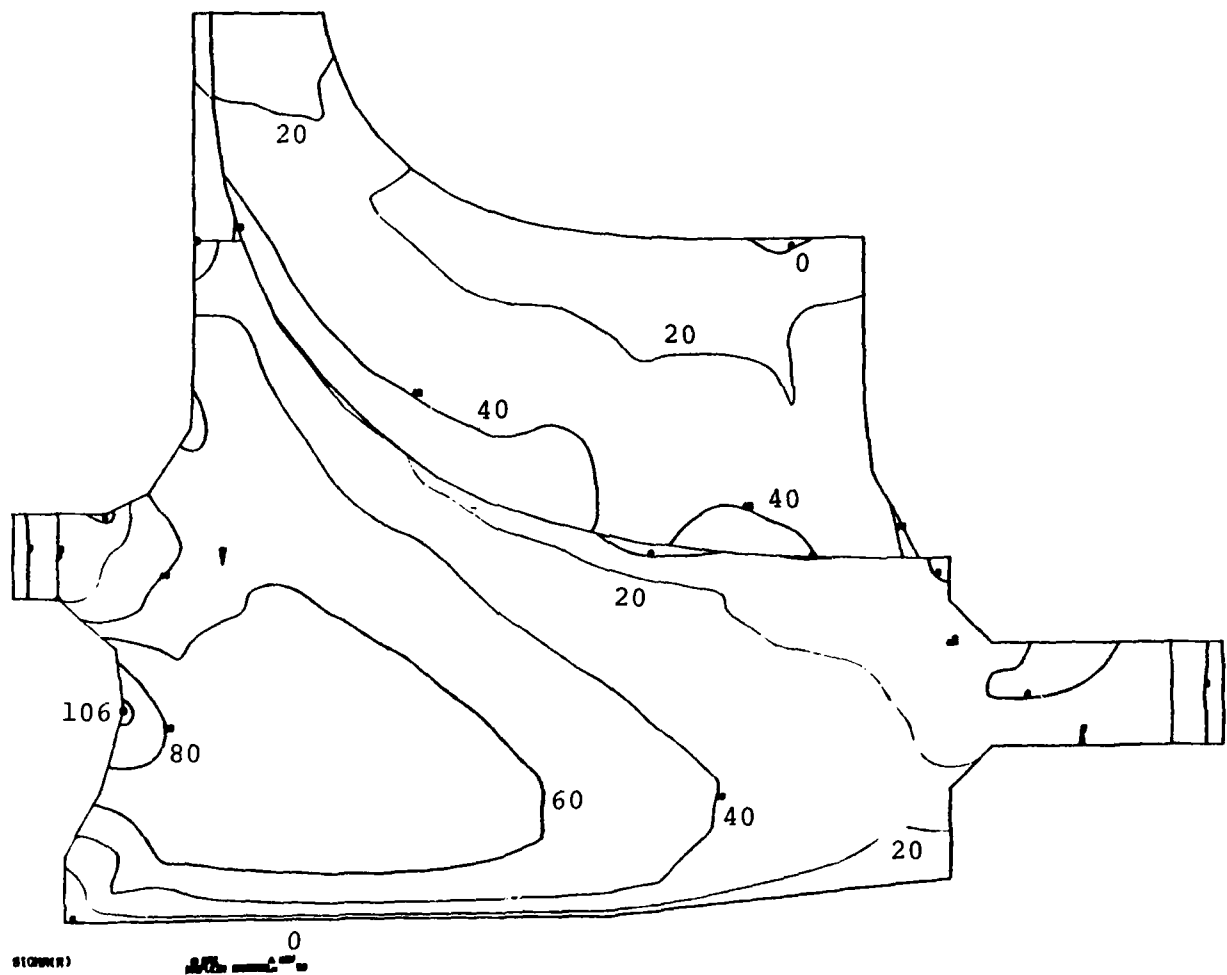


Figure 59. GTP305-2 radial turbine radial stress distribution program 700  
 hub line film coefficients  
 bore cooling flow 0.023 lb/sec  
 front face flow 0.060 lb/sec

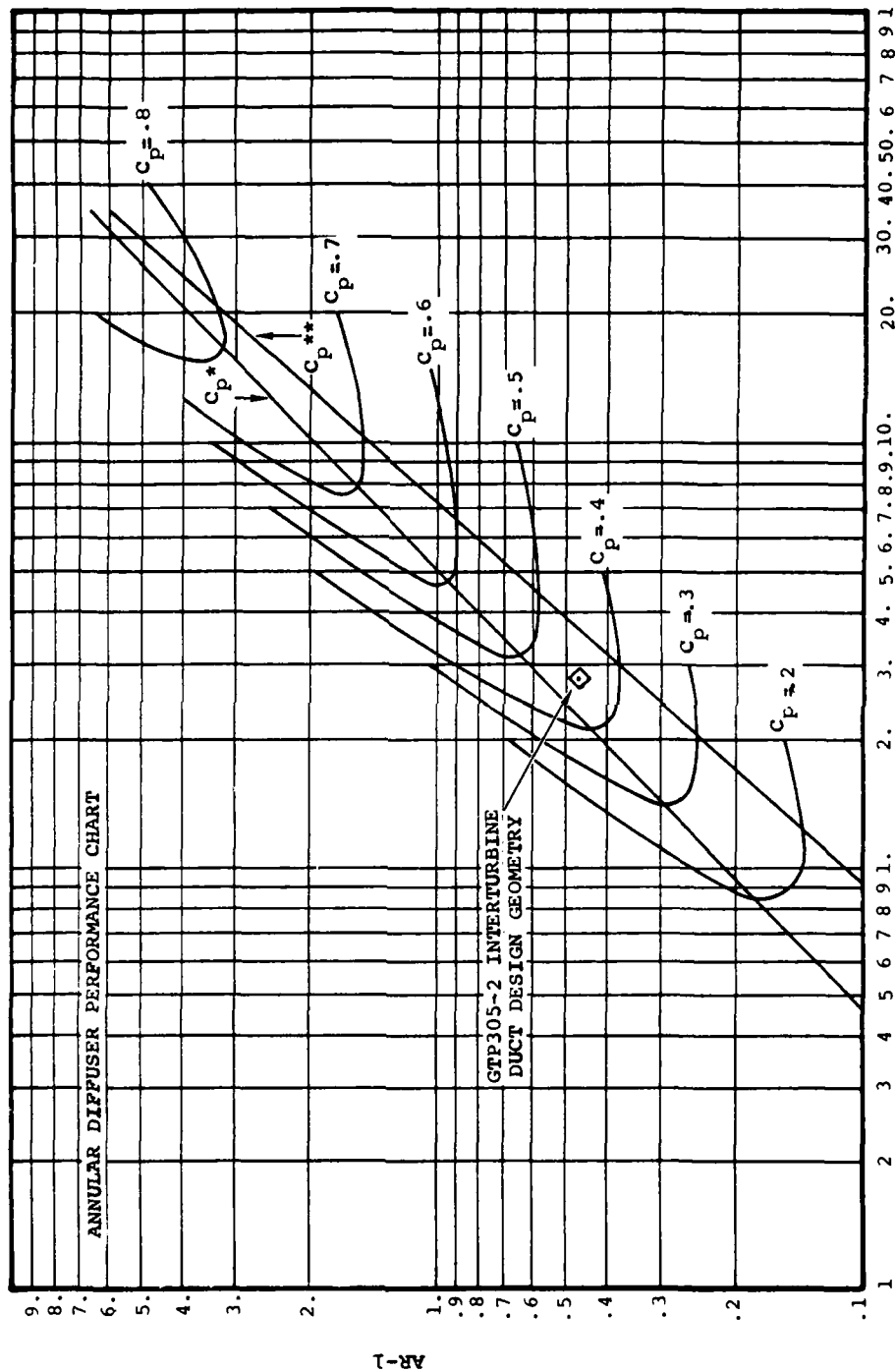


Figure 60. Annular diffuser design chart for interturbine duct

original Model GTP305-2 bearing span. However Amann's test results (Reference 6) indicate increased duct loss under these conditions is not significant. Predicted pressure loss ( $\Delta P/P$ ) for the Model GTP305-2 interturbine duct is based on a pressure loss coefficient ( $\bar{w}$ ) of 0.25. This is based on a previously tested AiResearch interturbine duct of similar geometry. Thus, the calculated pressure loss for the Model GTP305-2 interturbine duct is 0.169.

Design objective of the interturbine duct was to achieve a hub and shroud contour which would attain non-separated flow and minimize radial velocity gradients at the stator inlet. Figure 61 reflects predicted streamline distribution from the hub to the shroud, for final duct contour. Radial velocity gradients are unavoidable due to endwall curvatures. The hub stator inlet angle of 30 degrees, results from upstream radial turbine exit swirl and will require a high turning blade section at the axial stator hub.

Structurally, the interturbine duct is part of the integrally cast axial stator assembly. The material is INCO-713LC. A detailed discussion of the interturbine duct stress and deflection analysis is contained in Section 3.4.10.

#### 3.4.9 Axial Turbine Aero/Mech Optimization

Preliminary geometry and work requirements for the power turbine were established during the optimization study presented in Section 3.1. Free vortex design methods resulted in a constant radial work distribution. However, test results indicate significant performance improvement relative to free vortex

(6) Amman, C. A., Nordenson, G. E. and Raxinsky, E. H. "The Turbine Interstage Duct," SAE Paper No. 710553, June 1971.

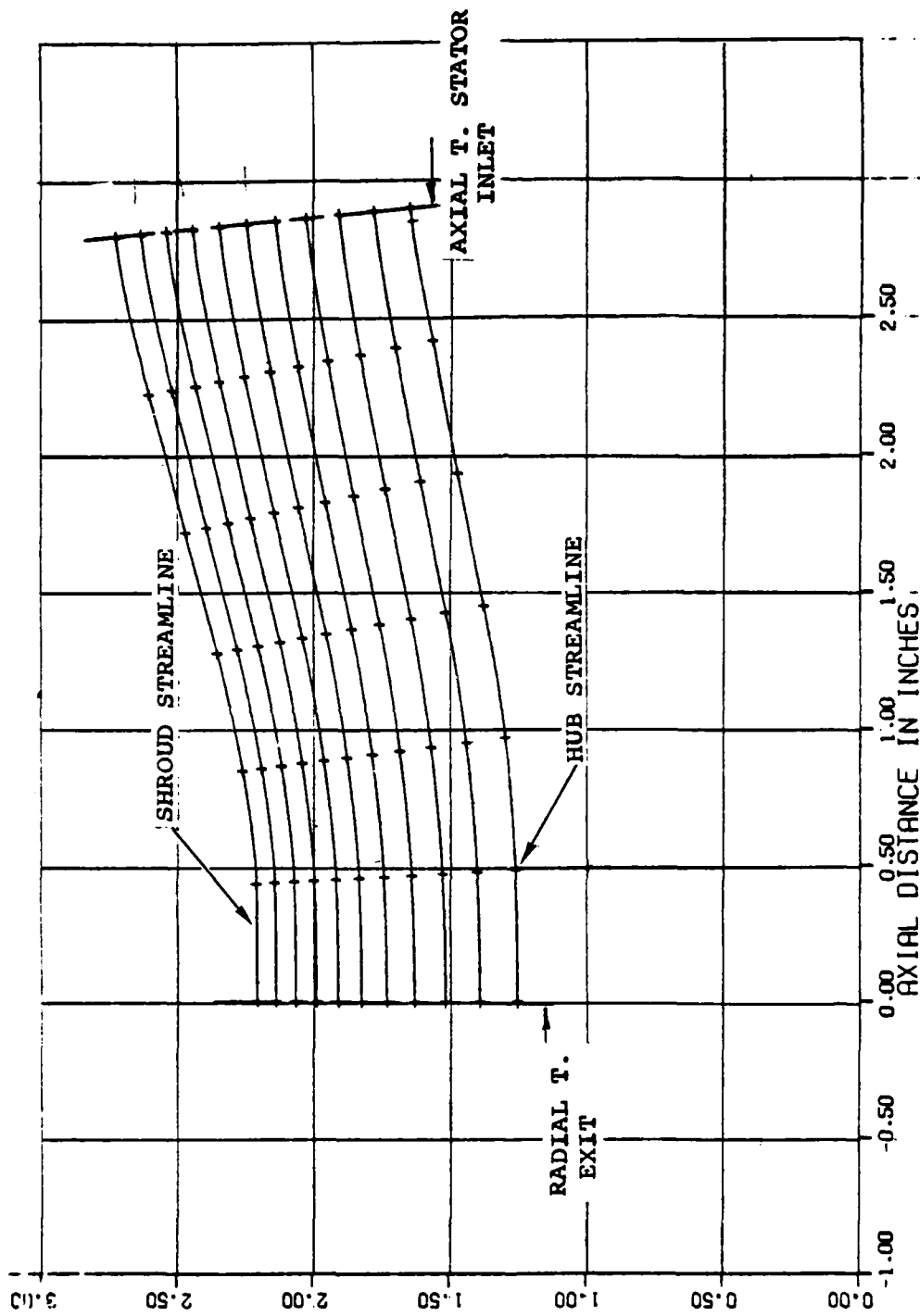


Figure 61. GTP305-2 final interturbine duct contour

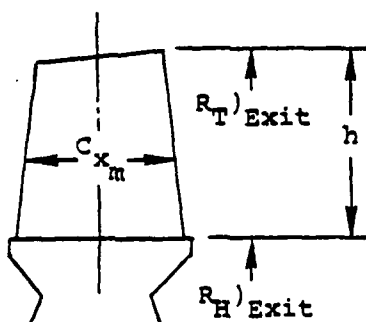
design, can be achieved with non-free (forced) vortex design techniques. Physically, non-free vortex methods relieve the requirements for constant radial work distribution which permits work reduction in the high loss end wall region. Uniform blade row exit flow conditions and a reduction in losses, result.

The non-free vortex optimization studies began with the free vortex flow path established from the overall turbine optimization study. This also established rotor exit dimensions that satisfied maximum allowable average stress levels for cast AF2-1DA. Since the non-free vortex solution allowed arbitrary distributions of stator and rotor exit angles, a number of linear and non-linear distributions were investigated, based on the two-dimensional loss distributions obtained from the efficiency prediction program. The objective for the Model GTP305-2 axial turbine was to minimize rotor radial twist, hub relative temperature, exit axial velocity gradients and exit swirl while simultaneously maximizing rotor hub reaction. After extensive analysis, it was apparent that a parabolic stator exit angle, and near linear rotor exit angle, distribution would best achieve these objectives. At this point, previous AiResearch non-free vortex designs were reviewed to determine the final loss distribution.

Table 8 compares design point data for three previous AiResearch non-free vortex designs with the Model GTP305-2 design. Test data for two tip clearance values were available from the TFE731 Model Turbofan Engine high pressure (HP) turbine and were used to extrapolate to zero clearance. Rotor exit survey data for the designs shown in Table 8 are plotted in Figure 62 in terms of exit radius ratio and total-to-total efficiency. Figure 62 shows the final radial efficiency distribution predicted for the Model GTP305-2 axial turbine for zero clearance. The loss level and radial loss distribution were adjusted in the non-free vortex vector diagram to achieve this efficiency distribution and satisfy the required pressure ratio. The loss

TABLE 8. DESIGN DATA FOR NON-FREE VORTEX TURBINES

Parameters	305-2 PT	TFE731 HP	XJ-401-GA-400 Harpoon	JFS190 GGT
Design Point Pressure Ratio $P/P_{T-T}$	2.1597	1.889	2.179	2.072
Inlet Corrected Flow, $\frac{W\sqrt{\theta}}{\delta}$	1.735	4.424	4.503	1.273
$R_H$ Exit, Inches	1.567	4.242	3.26	1.92
$R_T$ Exit, Inches	2.845	5.573	4.8	2.775
$R_H/R_T$	0.550	0.761	0.679	0.692
Blade Height (h), Inches	1.278	1.331	1.54	0.855
Aspect Ratio $h/C_{x_m}$	2.04	1.85	2.18	1.426
Measured Clearance, Inches	0.015	0.0235 0.0066	0.017	0.013



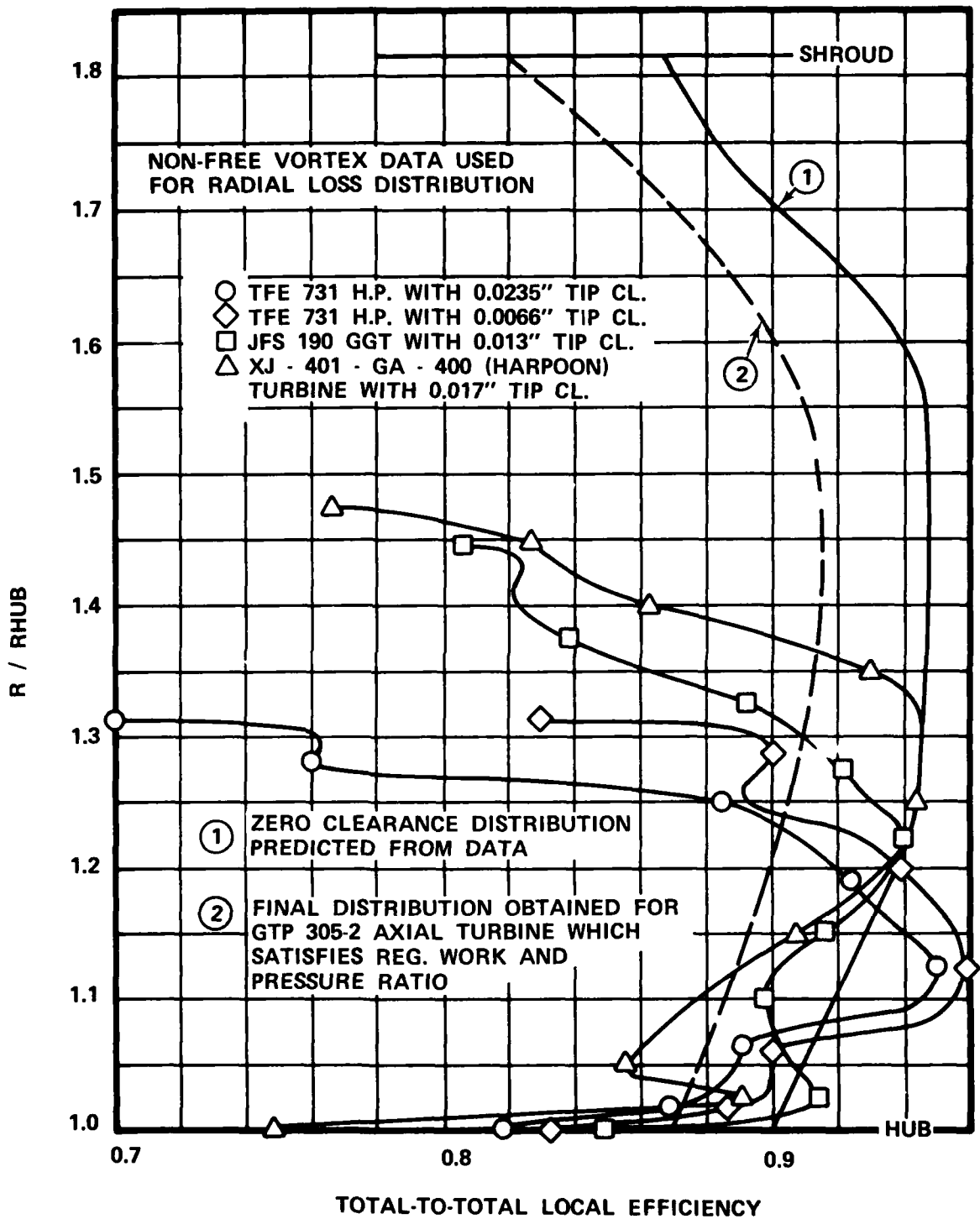


Figure 62. GTP305-2 axial turbine radial efficiency distribution

split between the stator and rotor was based on results of the efficiency prediction program. Figure 63 shows the final flow path for the non-free vortex solution. The final non-free vortex solution resulted in an acceptable rotor hub reaction (21 percent) without excessive rotor exit swirl (8 degrees at the hub compared with zero for the preliminary free vortex design), and a reduction in rotor twist.

#### 3.4.10 Axial Turbine Stator

##### 3.4.10.1 Axial Stator Aerodynamic Design

The integrally-cast axial stator utilizes a 25-vane configuration with no cooling flow. Several combinations of trailing edge thickness and wedge angles were evaluated. As shown in Figure 64, a 0.015 inch trailing edge and relatively large wedge angle were selected. The larger wedge angle provides vane trailing edge thermal cracking resistance.

Due to the non-linear stator inlet angle and parabolic stator exit angle distribution, vane geometry at five-radial station was required for definition. The five sections were required to ensure that a proper throat area and a smooth three-dimensional fairing were achieved. Table 9 summarizes stator vane design parameters for these radii. Two methods were used to evaluate the stator suction and pressure surface velocity distribution. The velocity gradient method is incorporated in the blade design program and is based on satisfying continuity and momentum along suction-to-pressure lines emanating from the suction surface involute spiral. The stream function solution is based on the Katsanis method [Reference (7)]. Predicted characteristics are similar, however, the velocity gradient method over

(7) Katsanis, Theodore; and McNally, William D.:

Revised Fortran Program for calculating velocities and streamlines on a blade-to-blade surface of a turbomachine. NASA TM X 1764, 1969.



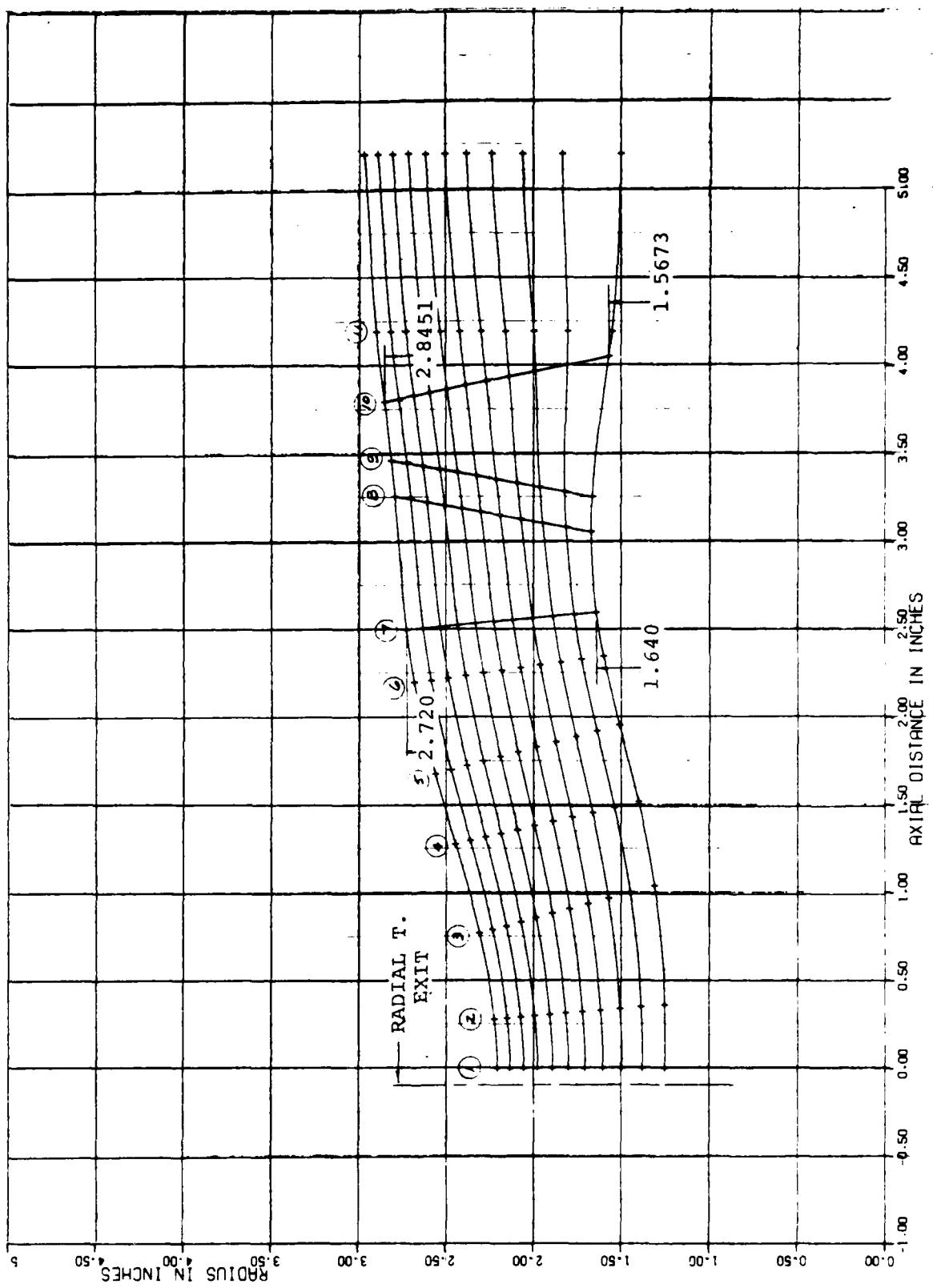


Figure 63. GTP305-2 axial turbine flowpath.

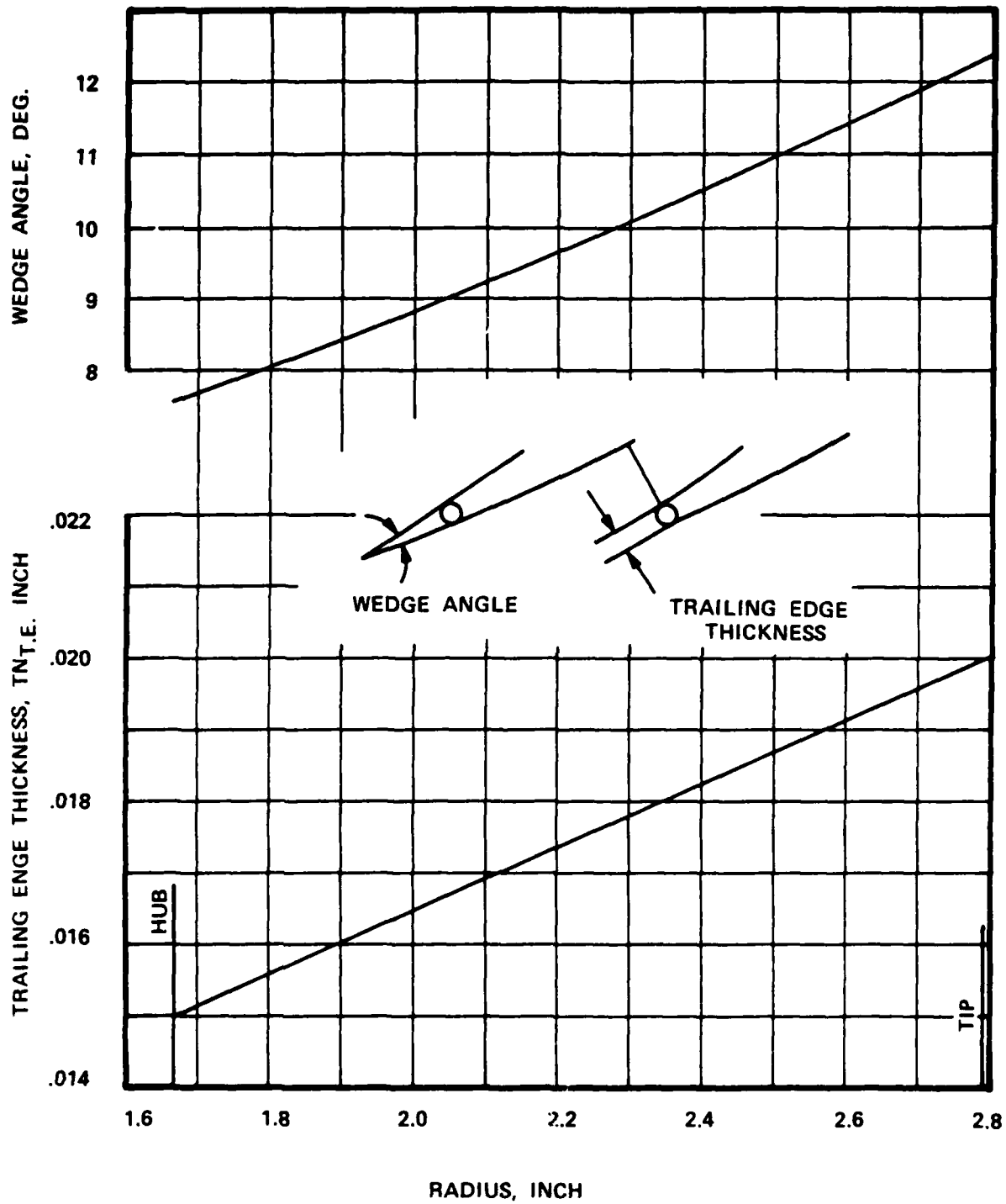


Figure 64. Radial trailing edge thickness and wedge angle distributions

TABLE 9. STATOR VANE DESIGN PARAMETERS.

% of total flow streamline at stator exit	10	30	50	70	90
Radius (in.)	1.791	2.035	2.281	2.506	2.70
Chord, C (in.)	0.72	0.839	0.94	1.011	1.048
Axial chord, $C_x$ (in.)	0.5375	0.580	0.630	0.680	0.725
Pitch, S (in.)	0.45013	0.5120	0.5733	0.6298	0.6786
Solidity, $C_x/S$	1.194	1.1328	1.099	1.0797	1.068
Inlet flow angle (deg)	-29.95	-25.6	-10.75	-3.25	-0.025
Exit flow angle (deg)	66.753	69.175	69.991	68.358	65.174
Inlet freestream critical Mach No.	0.2692	0.2555	0.2400	0.2253	0.2164
Exit freestream critical Mach No.	0.9289	0.8274	0.7552	0.6885	0.6353
Zweifel coefficient of loading	0.7578	0.6936	0.6254	0.6493	0.7138
L.E. thickness (in.)	0.04	0.048	0.056	0.0635	0.07
T.E. thickness (in.)	0.0155	0.0166	0.0177	0.0187	0.0196
Max. thickness	0.086	0.101	0.112	0.114	0.119
Max. thickness/chord	0.1194	0.1200	0.1192	0.1130	0.1139
Angle of downstream turning (deg)	4.0	4.5	5.0	5.5	6.0
Trailing edge wedge angle (deg)	8	9	10	11	12
Inlet blade angle (deg)	-29.95	-25.6	-10.75	-3.25	-0.025
Exit blade angle (deg)	64.555	67.171	68.108	66.565	63.459
L.E. blockage	0.1026	0.1039	0.0994	0.1010	0.1032
T.E. blockage	0.0872	0.0912	0.0902	0.0805	0.0688
Inlet total pressure $P'$ , (psia)	33.544	33.544	33.544	33.544	33.544
Inlet total temperature $T'$ , ( $^{\circ}$ R)	1968.04	1968.04	1968.04	1968.04	1968.04

No of vanes = 25

Aspect ratio = 1.95

Mid passage hub/tip ratio = 0.60

predicts the velocity peak near the stator suction surface throat region. Figure 65 presents a 3-dimensional vane profile generated by stacking the five cylindrical sections on a radial line passing through the throat center of each section. Figure 66 shows the meridional view of the stacked stator vane.

#### 3.4.10.2 Axial Stator Stress Analysis

As stated in Paragraph 3.4.9, the interturbine duct and axial stator is an integrally cast structure. Stress analysis of the structure was conducted to substantiate the structural integrity during steady-state operating conditions and rapid start transients.

Steady-state temperature distributions through the Model GTP305-2 interturbine duct structure were estimated from currently available gas path and combustor data and are presented on Figure 67. The data, including static pressure distributions, were introduced into the finite element model shown on Figure 68 to determine stresses throughout the structure. Except for the Inconel 713LC cast duct walls and vanes, the structural members are fabricated entirely from Hastelloy-X as indicated in Figure 68.

Table 10 shows a tabulation of calculated stresses at selected locations throughout the structure for the steady-state condition. The steady-state deflections are shown in Figure 69. Locations of the tabulated stresses are illustrated on Figure 70. The highest stresses calculated at steady-state conditions occur at Locations E, G, and T, the corners of the vanes, and the minimum margins of safety on yield (Table 10) are shown to be 1.41, 1.30, and 1.30 respectively.

Figure 71 shows the estimated temperature distribution for the rapid-start transient condition where maximum thermal

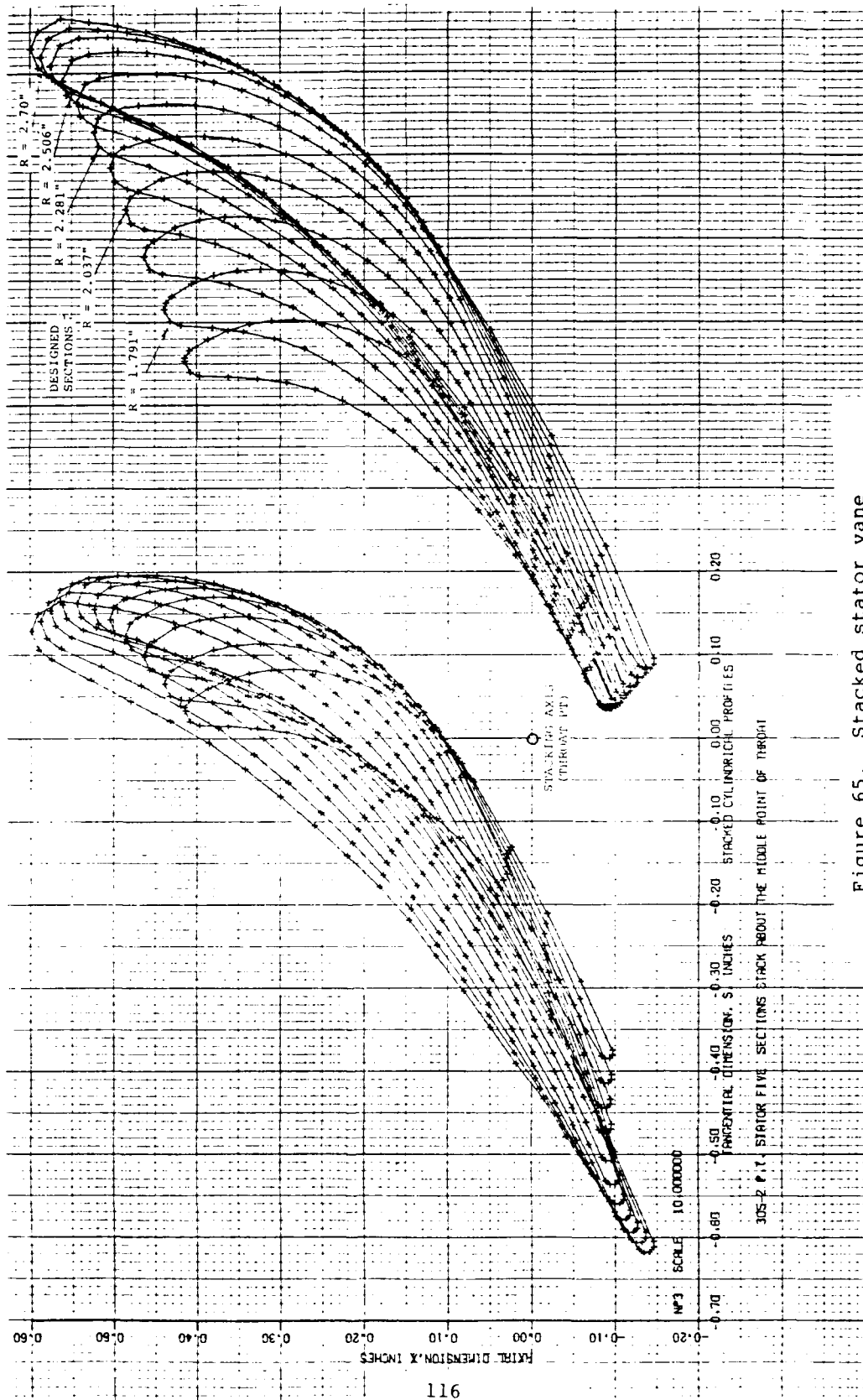
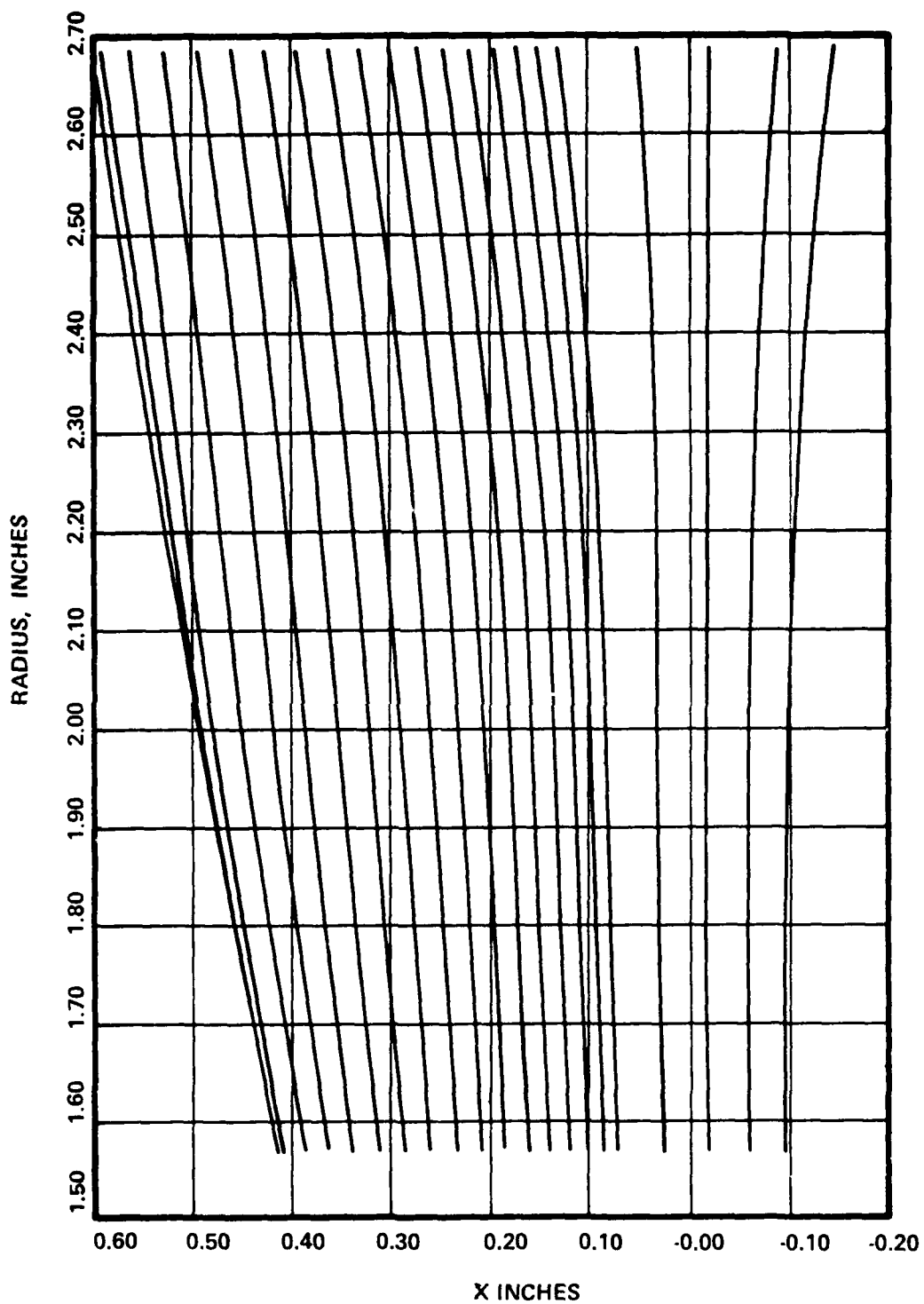


Figure 65. Stacked stator vane



305-2 P.T. STATOR FIVE SECTIONS STACK ABOUT THE MIDDLE POINT OF THROAT

Figure 66. Meridional view of stacked stator vane

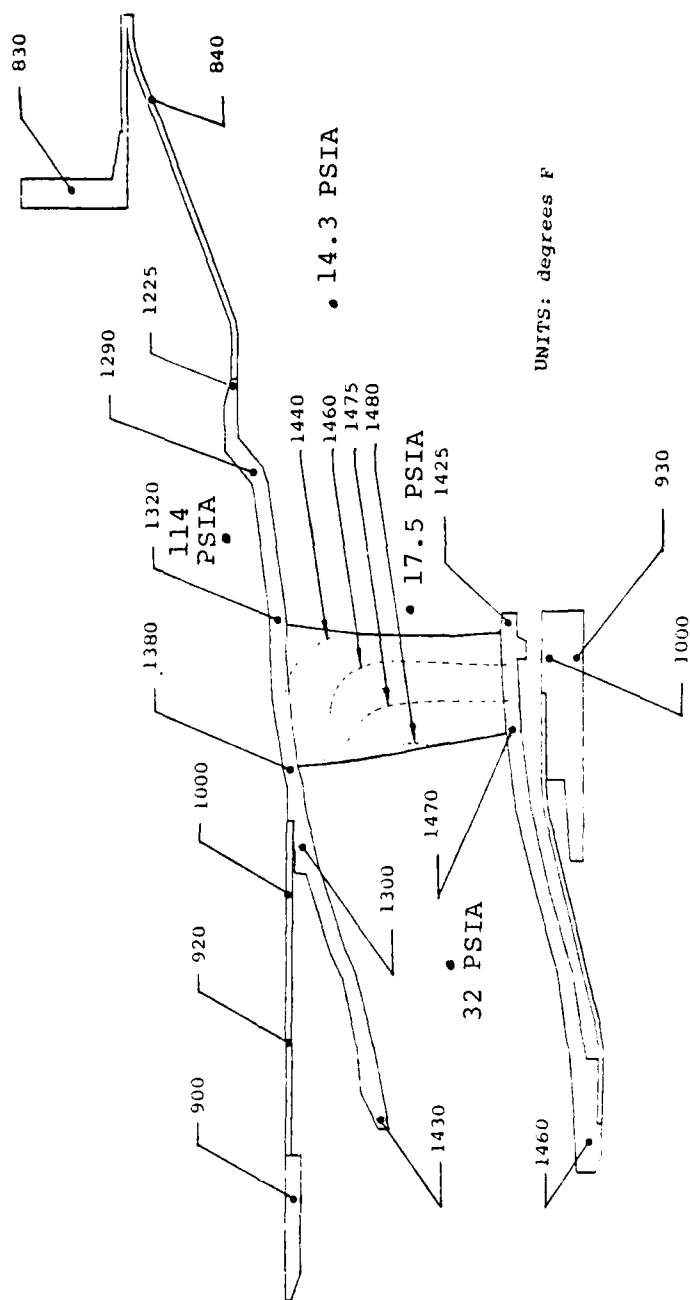


Figure 67. GTP305-2 estimated steady state temperature distribution and assumed steady state pressures

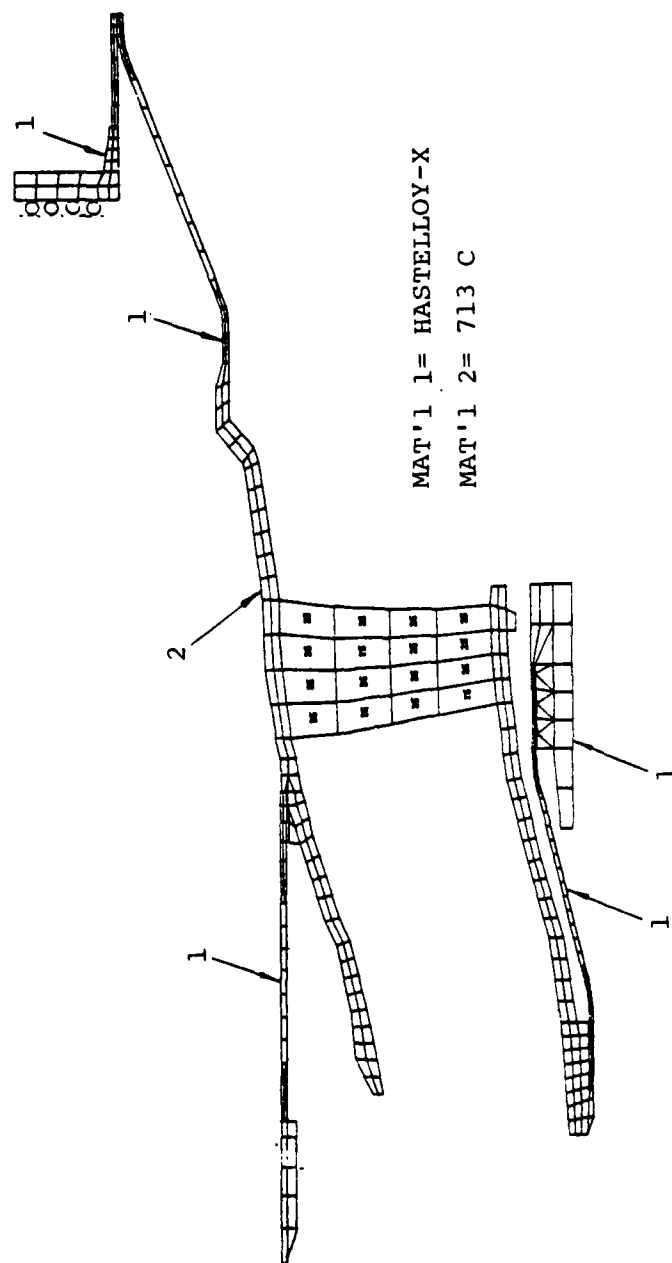


Figure 68. GTP305-2 interturbine duct structure, finite element model



TABLE 10. MAXIMUM STRESSES DURING STEADY STATE OPERATING CONDITIONS.

Location	Material	Temp (°F)	Stress (ksi)	Type Of Stress	MS Yield
A	Hastelloy X	1060	- 7.1	hoop	4.85
B	"	1300	29.0	bending	.36
C	713 C	1410	- 0.7	hoop	high
D	"	1370	13.4	equivalent	high
E	"	1460	44.1	equivalent	1.41
F	"	1350	-18.7	bending	4.96
G	"	1470	46.1	equivalent	1.30
H	"	1230	13.6	equivalent	high
I	Hastelloy X	1230	32.6	hoop	0.23
J	"	1200	-20.4	hoop	0.96
K	"	1100	-13.4	hoop	2.06
L	"	870	-11.4	bending	2.82
M	"	830	6.8	hoop	high
N	"	830	6.4	hoop	high
O	"	830	5.0	bending	high
P	713 C	1460	16.0	bending	high
Q	Hastelloy X	1460	-25.2	hoop	0.40
R	713 C	1470	1.5	bending	high
S	"	1470	-28.6	hoop	2.71
T	"	1470	46.1	equivalent	1.30
U	"	1440	-24.1	hoop	3.46
V	"	1460	22.1	equivalent	3.82
W	Hastelloy X	1320	- 1.0	bending	high
X	"	1010	27.0	equivalent	0.56
Y	713 C	960	7.2	equivalent	high
Z	"	980	- 7.9	hoop	high

$$MS_{\text{yield}} = \frac{\text{Yield Strength}}{\text{Calculated Stress}} - 1$$

Margins of Safety greater than 5.00 have been designated "high"

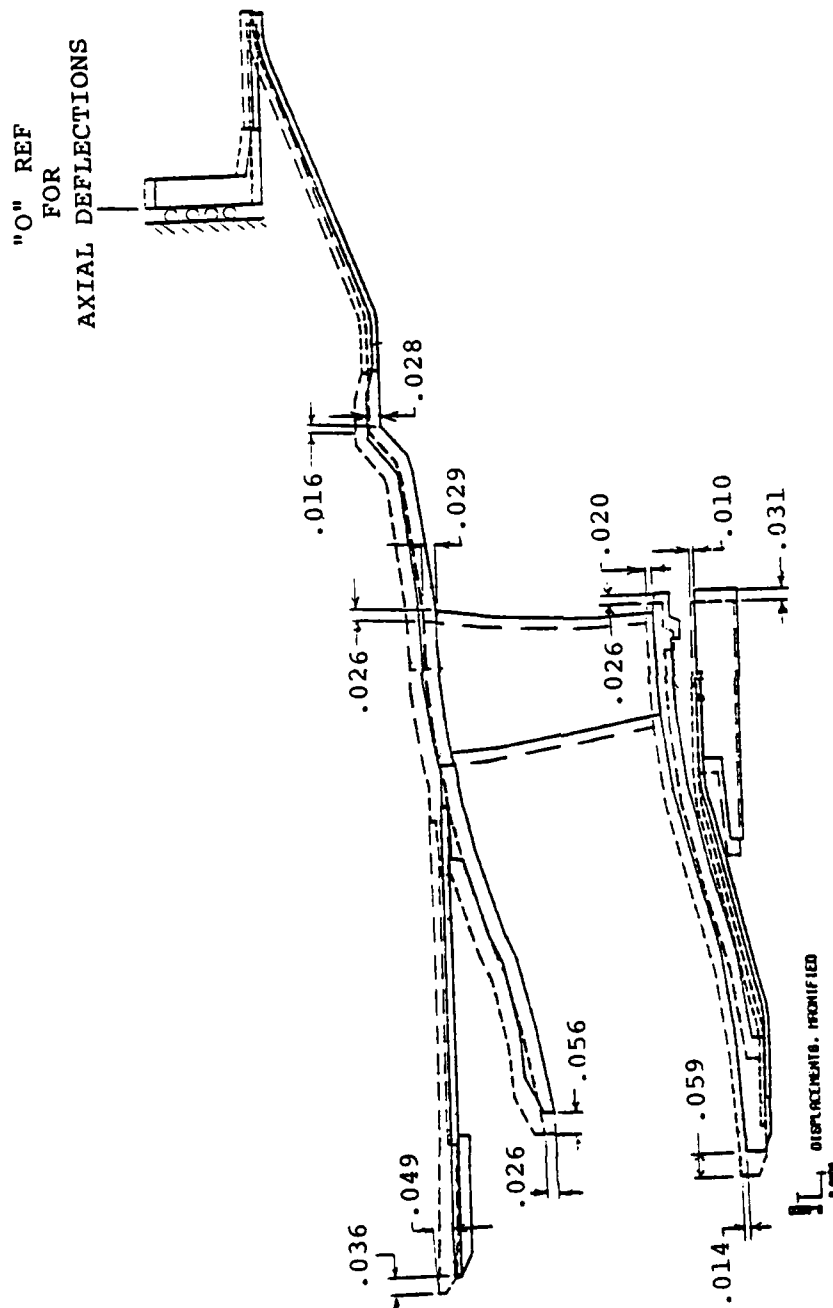


Figure 69. GTP305-2 preliminary interturbine duct steady state deflections

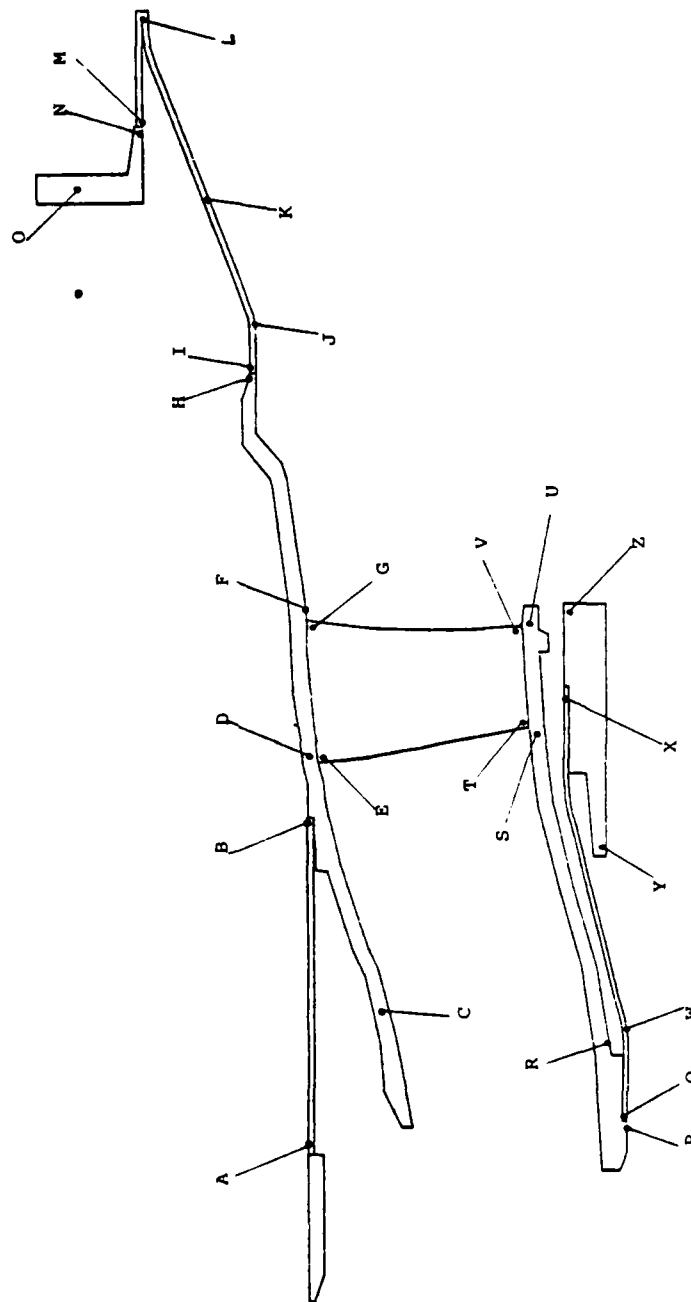


Figure 70. GTP305-2 interturbine duct structure, reference locations for primary stresses

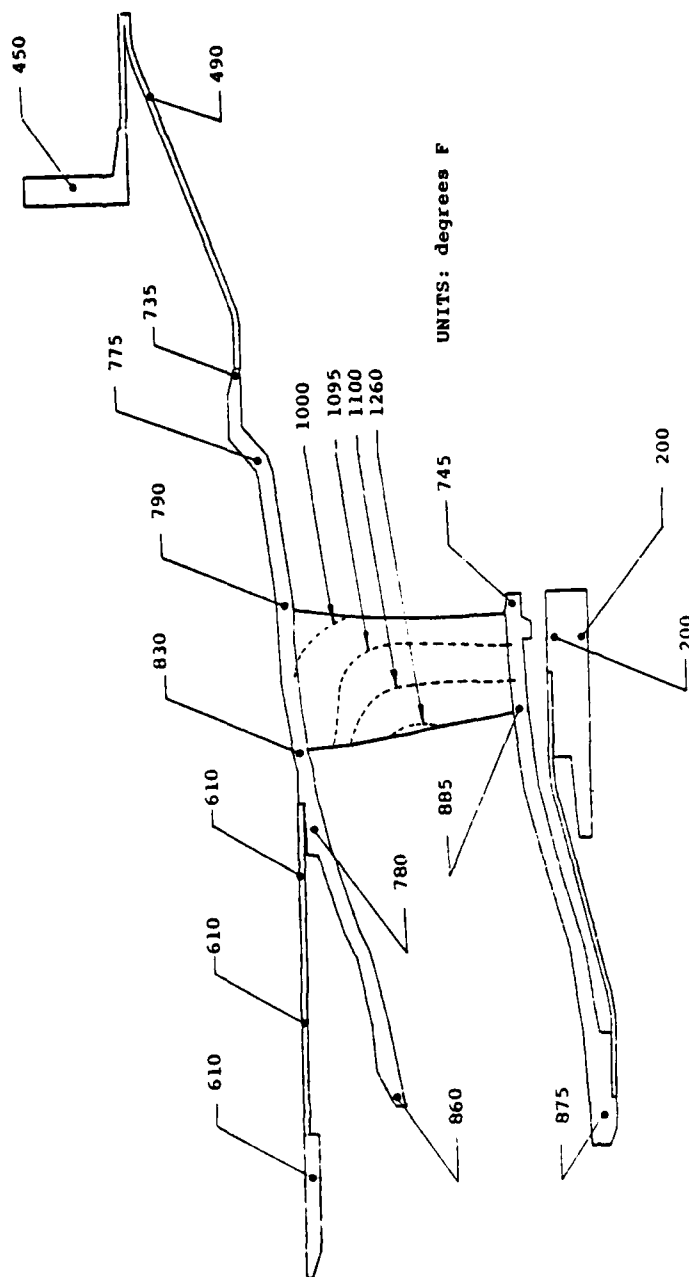


Figure 71. GTP305-2 estimated transient temperature distribution during start condition

gradients exist throughout the structure. Pressure loads for the start transient were unchanged; that is, pressures were retained at steady-state values for the start condition stress calculations.

Calculated stresses for the start transient are presented on Table 11. As before, the calculated stresses at the corners of the vanes were much higher than at other locations. However, the yield strength is slightly higher since the vane has not yet reached maximum temperature. The maximum stress developed at the vane root occurs at Location E, and is 80.3 ksi, which results in a minimum margin of safety on yield of 0.40.

A maximum stress of -29.4 ksi is developed in the 0.025 inch Hastelloy-X shell (see Location Q) while the Inconel 713 vane (see Location E) developed a stress of 81.3 ksi. Since the minimum margins of safety on yield are 1.30 for the steady-state operating condition and a 0.40 during the transient condition, this structure is considered adequate for the design life of the part.

### 3.4.11 Axial Turbine Rotor

#### 3.4.11.1 Axial Turbine Rotor Aerodynamic Design

Detail rotor design objective was to achieve satisfactory blade surface velocity distributions while maintaining and/or improving preliminary blade section area taper ratio. Rotor blade life and stress level predictions were based on a "nominal" area taper ratio utilized in previous AiResearch axial rotor designs.

A minimum 0.025 inch trailing edge thickness for an as-cast AF2-1DA rotor, was selected. Additionally, rotor hub exit blockage of ten (10) percent, established a rotor blade number of 24.

TABLE 11. MAXIMUM STRESSES DURING THE RAPID  
START TRANSIENT CONDITION.

Location	Material	Temp (°F)	Stress (ksi)	Type Of Stress	MS Yield
A	Hastelloy X	610	5.8	hoop	high
B	"	610	20.2	bending	1.28
C	713 C	860	- 0.4	hoop	high
D	"	860	21.9	equivalent	3.91
E	"	1080	80.3	equivalent	0.40
F	"	810	-19.7	bending	4.44
G	"	1160	56.3	equivalent	1.02
H	"	740	11.5	equivalent	high
I	Hastelloy X	730	-28.6	hoop	0.57
J	"	720	-18.7	bending	1.41
K	"	650	-13.1	hoop	2.55
L	"	480	- 8.3	bending	4.73
M	"	450	9.1	hoop	4.27
N	"	450	9.4	hoop	4.11
O	"	450	4.1	bending	high
P	713 C	880	16.2	bending	1.67
Q	Hastelloy X	880	-29.4	hoop	0.47
R	713 C	880	0.4	bending	high
S	"	880	43.9	equivalent	1.43
T	"	1120	77.8	equivalent	0.45
U	"	800	24.3	hoop	3.41
V	"	1050	44.3	equivalent	1.52
W	Hastelloy X	700	- 1.5	bending	high
X	"	220	19.2	equivalent	1.63
Y	713 C	960	7.2	equivalent	high
Z	"	200	0.2	equivalent	high

Margins of Safety greater than 5.00 have been designated "high"

$$MS_{\text{yield}} = \frac{\text{Yield Strength}}{\text{Calculated Stress}} - 1$$

Optimum rotor blade section designs were then achieved by varying axial chord and local blade shapes.

Radial design sections were selected at 1.667, 2.005, 2.2876, 2.5697, and 2.9954 inches radii, respectively. These radii correspond to rotor inlet streamline locations from the Non-free vortex vector diagram. Final rotor blade design parameters are presented in Table 12. Figure 72, shows the final rotor three-dimensional stack of interpolated sections used for tooling layout. Axial turbine meridional flow path with final stator and rotor design sections, is presented in Figure 73. Mechanical analysis indicates that rotor radial blade twist has improved relative to free vortex design. However, Figure 74 shows that significant blade unwrap will still occur at engine rotational speed. To maintain the design rotor throat dimensions under these conditions, the rotor sections were rotated "closed", by the angle indicated in Figure 74. The indicated radii corresponds to the selected tooling layout section used for manufacture. Rotor untwist will also occur with the cold air test rotor as reflected in Figure 74, although rotational speed is only approximately 50 percent of design speed. For this reason, a separate set of tooling layouts were defined for the cold air axial rotor. Distribution of pre-twist and resultant rotor throat dimensions for the engine and cold rig rotor tooling sections are presented in Table 13.

#### 3.4.11.2 Axial Rotor Stress Analysis

A steady-state thermal analysis was calculated for the non-free vortex axial turbine rotor for a 130°F day, 2050°F turbine rotor inlet temperature operating point. Figure 75 presents resultant isotherms. This thermal analysis was included in the axial rotor stress analysis.

TABLE 12. GTP305-2 AXIAL ROTOR DESIGN PARAMETERS  
N = 75,682 RPM.

Section Design Radius, in.	1.667	2.005	2.2876	2.569	2.795
Axial Chord, $C_x$ (in.)	0.8101	0.6625	0.5618	0.4483	0.3604
Pitch, S (in.)	0.4364	0.5251	0.5989	0.6728	0.7318
Solidity i $C_x/S$	1.8560	1.2617	0.9380	0.6663	0.4924
Inlet Flow Angle (deg)	40.427	20.920	-13.135	-42.543	-55.656
Exit Flow Angle (deg)	-58.758	-62.750	-65.241	-67.136	-68.472
Inlet Freestream Critical Mach No.	0.5626	0.3404	0.2833	0.3668	0.4642
Exit Freestream Critical Mach No.	0.7523	0.8475	0.9190	0.9849	1.025
Zweifel Loading Coefficient	0.8028	0.7730	0.766	0.6590	0.5860
L.E. Thickness (in.)	0.050	0.039	0.032	0.032	0.303
T.E. Thickness (in.)	0.025	0.0250	0.025	0.025	0.025
Downstream Turning Angle (deg)	6.0	5.0	4.0	3.0	2.0
Trailing Edge Wedge Angle (deg)	12.0	10.0	8.0	6.0	4.0
Inlet Blade Angle (deg)	40.427	20.920	-13.135	-42.543	-55.656
Exit Blade Angle (deg)	-55.271	-59.783	-62.593	-64.723	-66.242
T.E. Blockage	0.1005	0.0946	0.0907	0.0870	0.0848
Inlet Relative Total Pressure (psia)	21.286	22.532	24.188	26.764	29.597
Inlet Relative Total Temperature ( $^{\circ}$ R)	1780.95	1805.15	1835.78	1818.39	1925.81
Throat Dimension, (in.)	0.2236	0.2392	0.2507	0.2623	0.2692

Number of Blades = 24

Aspect Ratio = 3.853

Hub/Tip Exit Radius Ratio = 0.550



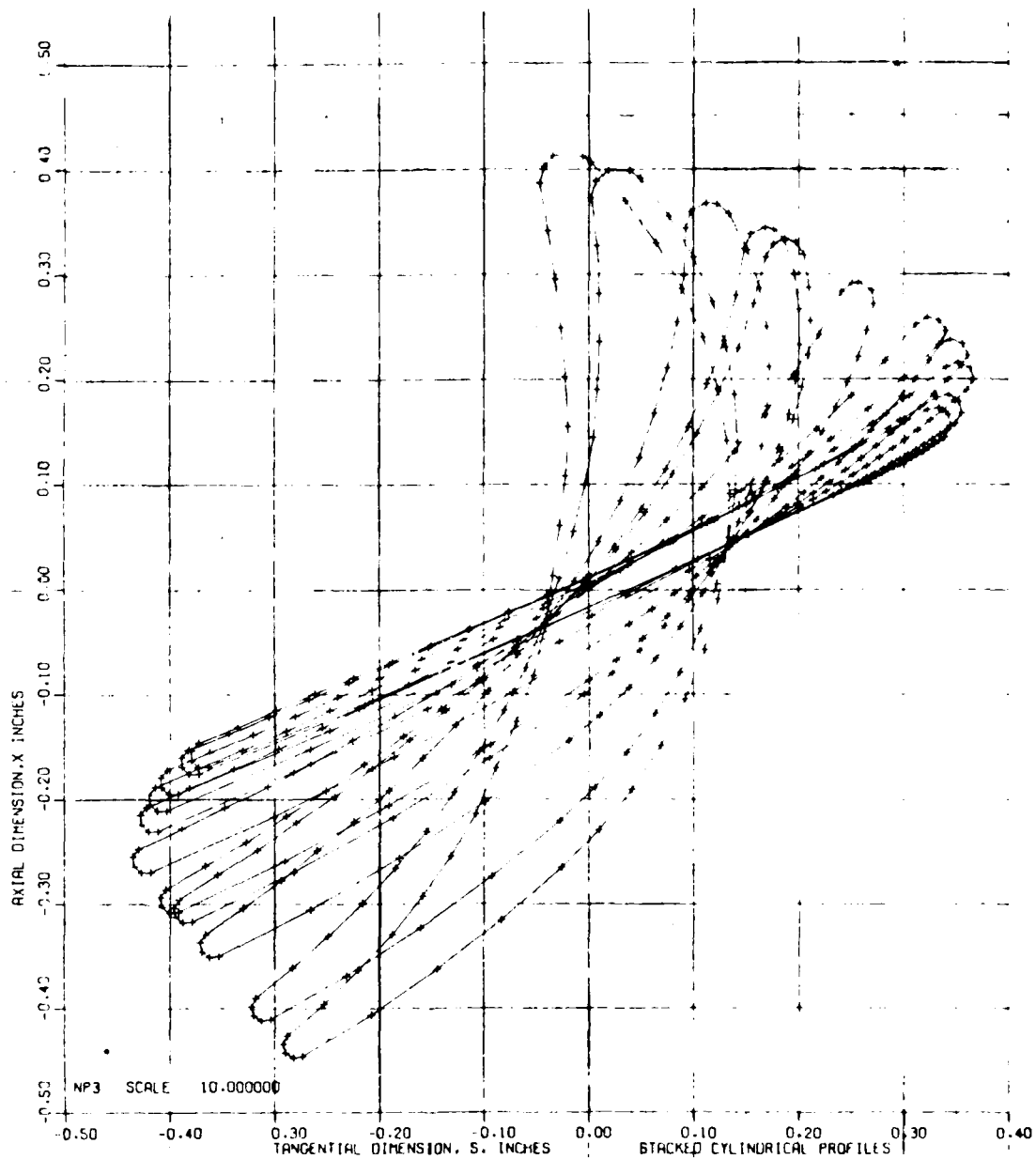


Figure 72. Axial rotor blade stack about center of gravity

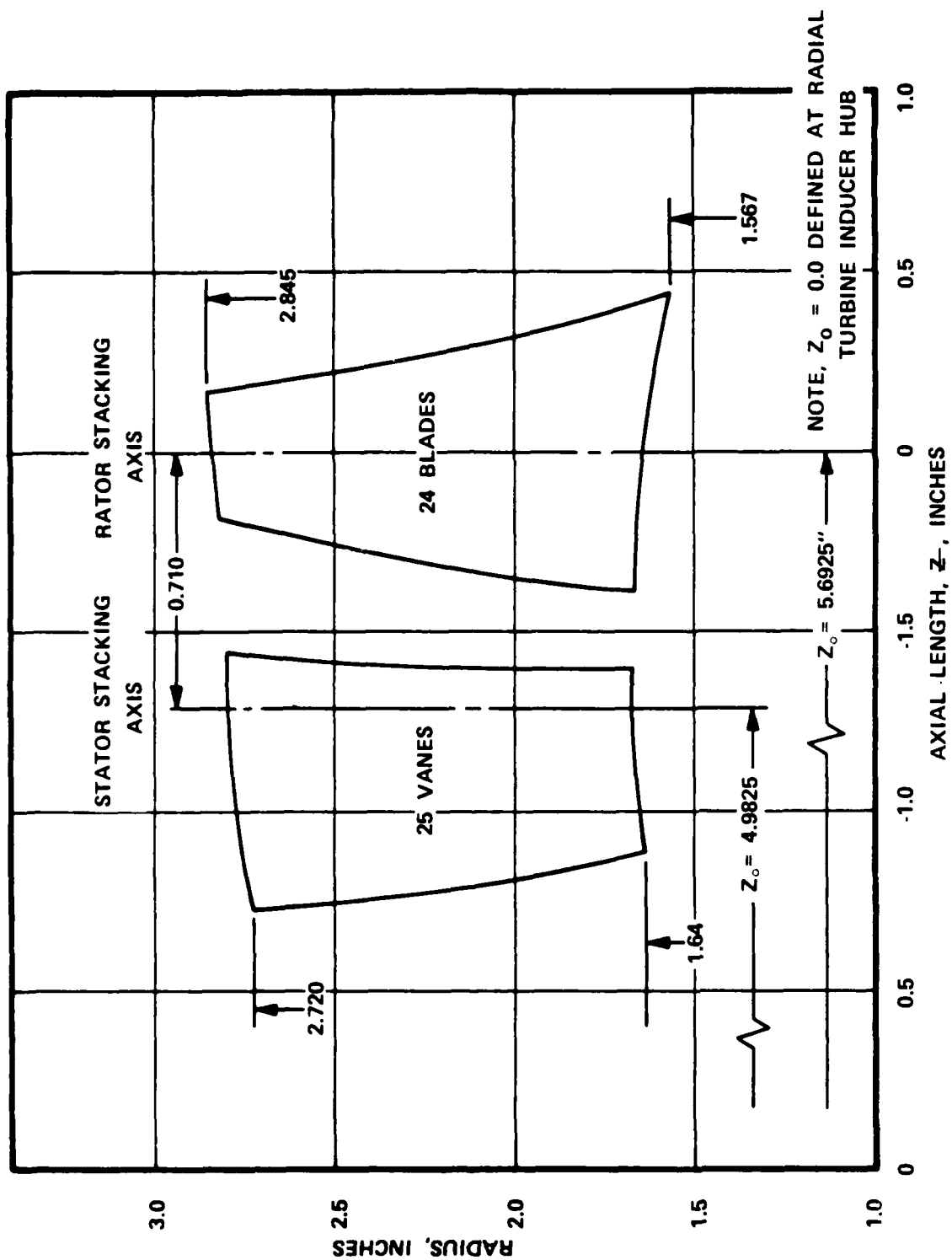


Figure 73. Axial turbine flow path with final design sections

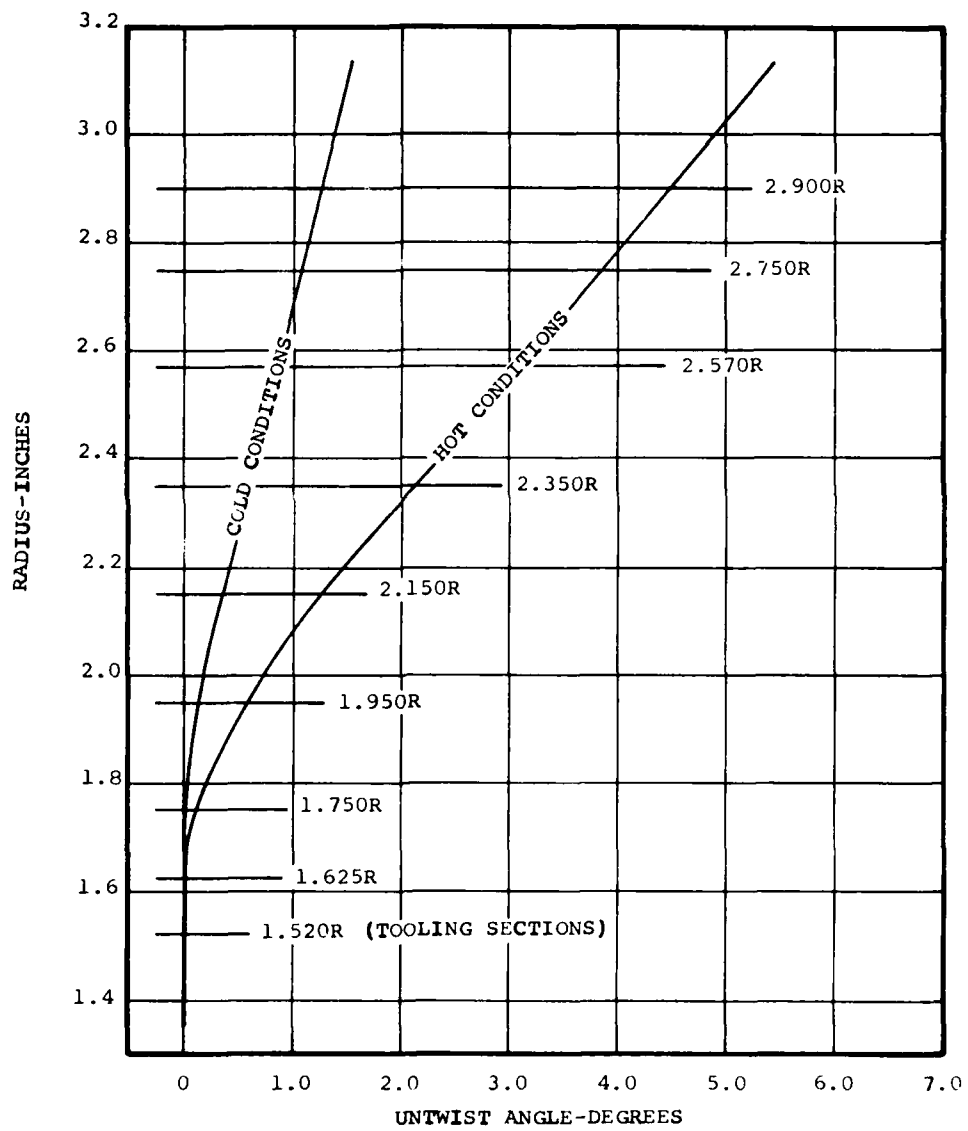
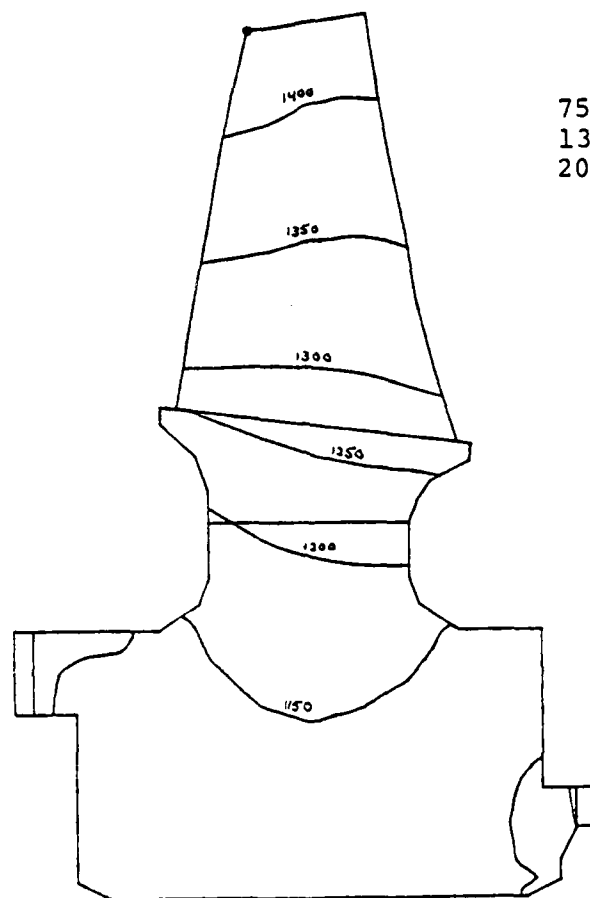


Figure 74. GTP305-2 axial blade untwist calculated at engine operating conditions

TABLE 13. GTP305-2 AXIAL TURBINE ROTOR  
TOOLING LAYOUT PRETWIST.

Radius (Inches)	Engine Rotor Tooling Sections		Cold Rig Rotor Tooling Sections	
	Pretwist (Degrees)	Throat Dimension (Inches)	Pretwist (Degree)	Throat Dimension (Inches)
1.520	0.000	0.2164	0.000	0.2164
1.625	0.000	0.2216	0.000	0.2216
1.750	0.100	0.2270	0.025	0.2275
1.950	0.585	0.2326	0.155	0.2356
2.150	1.270	0.2345	0.360	0.2420
2.350	2.140	0.2338	0.600	0.2479
2.570	3.125	0.2301	0.860	0.2534
2.750	3.875	0.2245	1.080	0.2558
2.900	4.500	0.2178	1.250	0.2567



75685 RPM  
 130°F DAY  
 2050°F TURBINE ROTOR  
 INLET TEMPERATURE

TEMP DEG F

© 1988 AEP  
 1200/1200 1200/1200 50

Figure 75. Steady state metal temperatures - °F

Steady-state stresses were calculated for the axial turbine rotor for a 130°F day, 2050°F turbine rotor inlet temperature operating point. Figures 76 through 78 present the resultant stress isopleths and identify locations of peak steady-state stresses.

#### 3.4.12 Turbine Exhaust Diffuser

The turbine exhaust diffuser function is to convert relatively high rotor exit kinetic energy to an increase in static pressure. Since residual rotor exit kinetic energy is charged to the turbine system, ultimate efficiency potential will be a function of exhaust diffuser performance. Figure 79 shows that total change in overall turbine efficiency, from zero to 100-percent diffuser recovery, is over 3 points.

Sovran and Klomp [Reference (8)] have extensively investigated performance potential for annular diffusers. Results of this study are presented in Figure 80, in terms of area ratio ( $AR-1$ ) and diffuser length divided by diffuser inlet height ( $\bar{L}/\Delta R$ ). Maximum pressure recovery is represented by the  $C_p^*$  line for a prescribed length and is the desired characteristic for the exhaust diffuser. This correlation shows that for a fixed non-dimensional length ( $\bar{L}/\Delta R$ ), both area ratio and potential diffuser recovery ( $C_p$ ), are specified. The Model GTP305-2 envelope length and rotor exit dimensions result in a diffuser area ratio of 1.794 and an indicated recovery of 0.550 based on a 2.0-percent diffuser inlet blockage. However, test results have shown that 75 percent of the indicated recovery from Figure 80, is achieved when non-uniform rotor discharge conditions are imposed on the diffuser inlet. Therefore predicted diffuser recovery for

(8) Sovran, G., and Klomp, E.D., "Experimentally Determined Optimum Geometries for Rectangular, Conical or Annular Cross Sections," General Motors Research Publication GMR-511, November 1965.

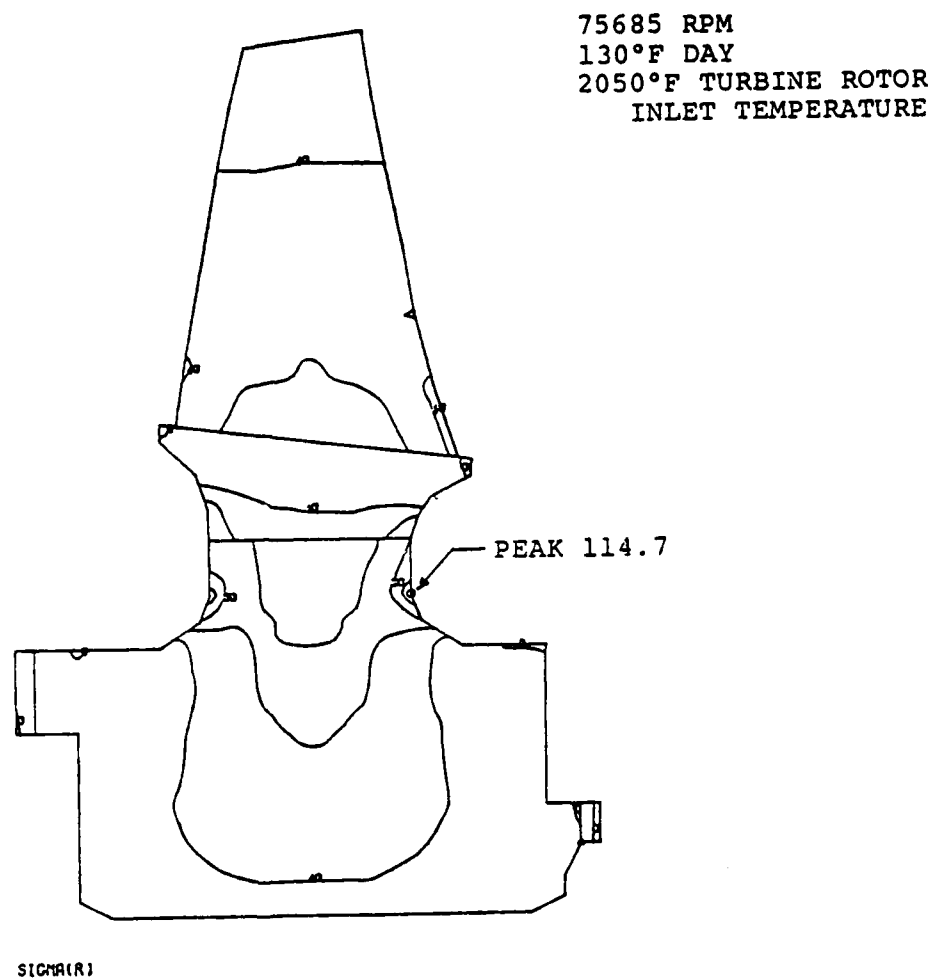


Figure 76. Steady state radial stresses - ksi

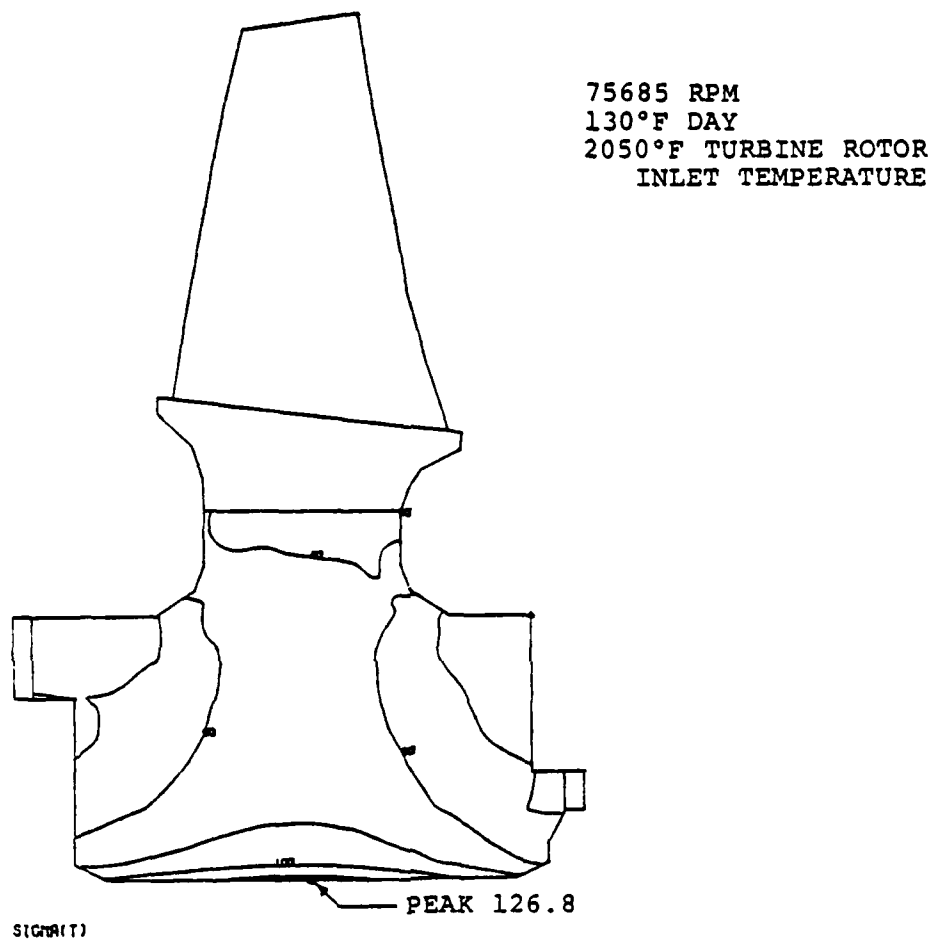


Figure 77. Steady state tangential stresses - ksi



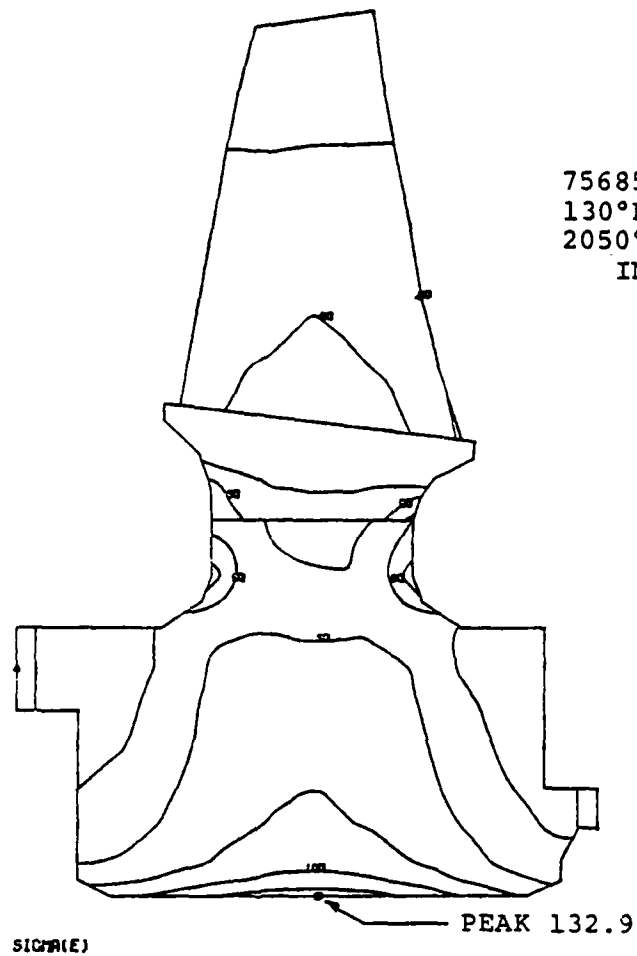


Figure 78. Steady state equivalent stresses - ksi

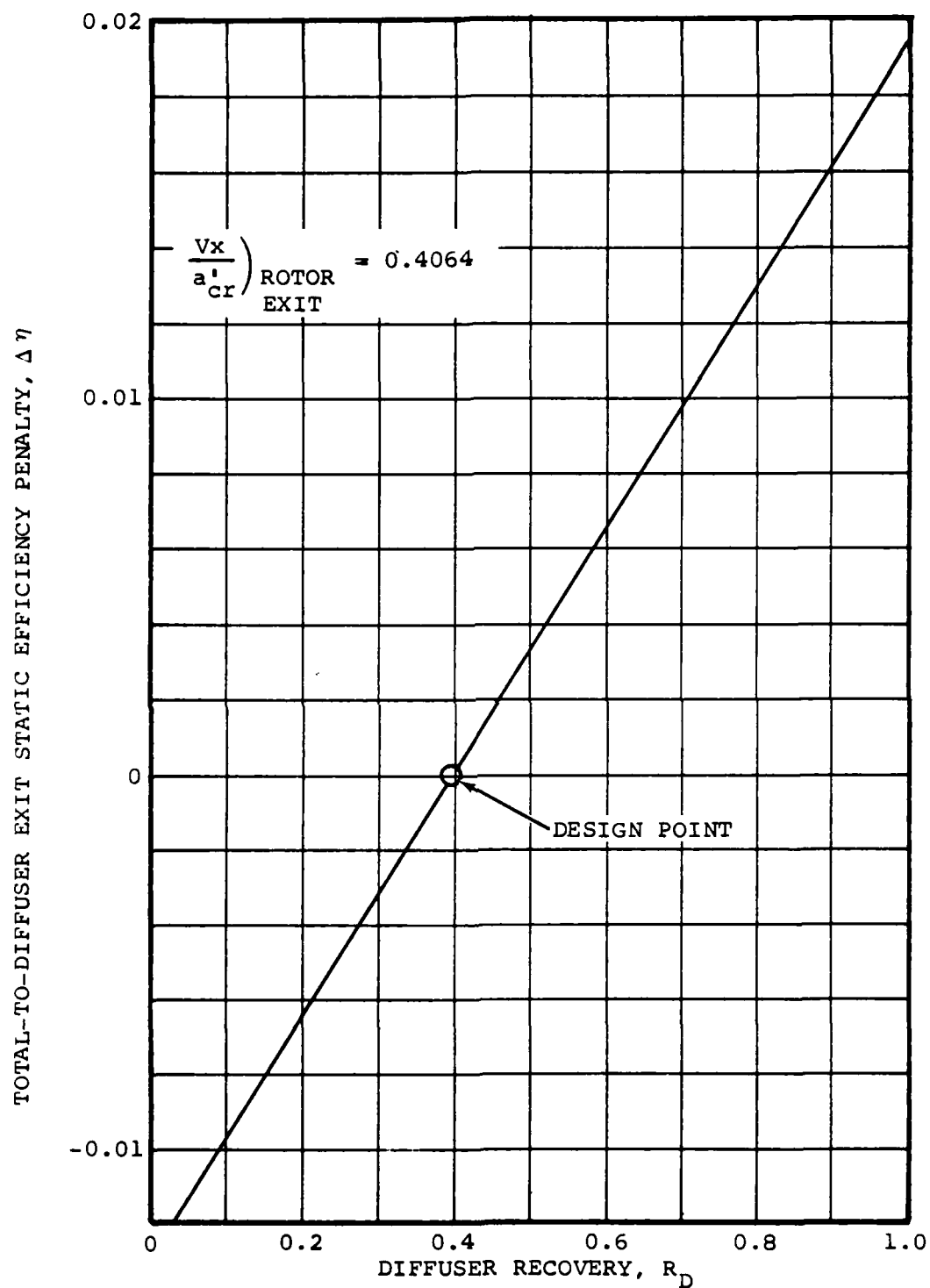


Figure 79. Performance effect due to diffuser recovery

$C_p^*$  = MAXIMUM PRESSURE RECOVERY FOR A PRESCRIBED LENGTH  
 $C_p^{**}$  = MINIMUM PRESSURE LOSS FOR A PRESCRIBED AREA RATIO

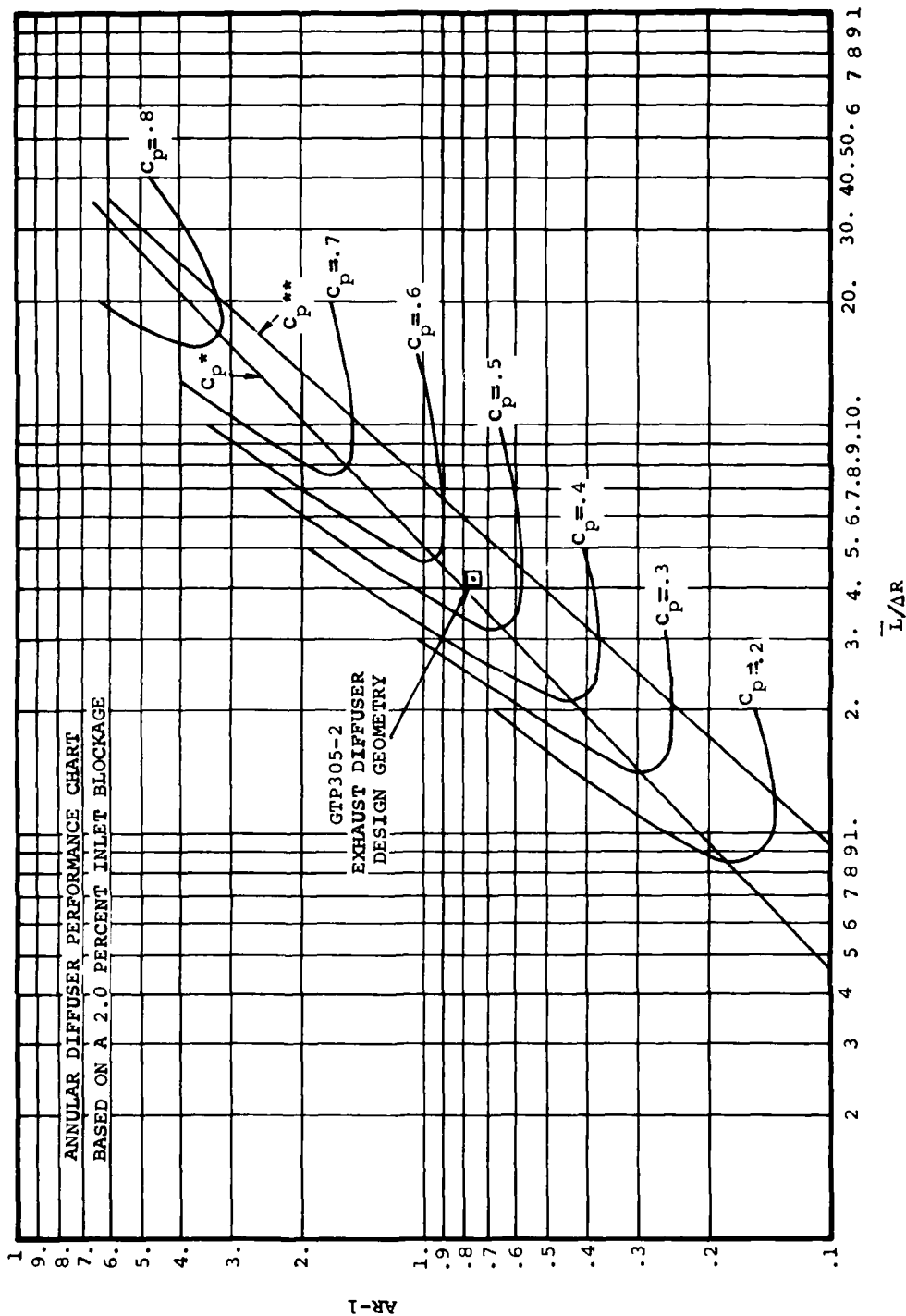


Figure 80. Correlation for annular diffuser geometry

the Model GTP305-2 is 0.40. Diffuser configurations presented in Figure 81 for the Models GTCP305-1 and GTCP305-2 illustrate that with the same envelope, area ratios and non-dimensional diffuser lengths are essentially identical. However, detailed mechanical and aerodynamic analyses indicate refinements could be achieved within this envelope, which would enhance, integrity of the aft bearing support and allow diffuser recovery to increase from 0.34 (Model GTCP305-1) to 0.40.

Bearing support stiffness was significantly increased by mechanically relocating the diffuser struts over the rear bearing housing and increasing the number of struts to five. Analysis of strut losses with a NACA 16-021 profile, indicates that strut relocation is aerodynamically acceptable, though located in a higher velocity region compared with the Model GTCP305-1. Uniform surface velocity acceleration is maintained by the 16-021 profile up to 70 percent of strut cord and will minimize trailing edge wake. Table 14 illustrates strut cross section and lists coordinates for strut construction.

Analysis also indicates that aerodynamic contouring of the rear bearing oil lines would improve the diffuser design. Tables 15 and 16 illustrate selected oil line profiles and lists profile coordinates. Profiles are based on scaling maximum thickness of the NACA 16-021 profile to the required oil tube diameters. Strut and oil line circumferential location is presented in Figure 82. The objective was to minimize influence of the upstream strut wakes on the downstream oil line profiles.

The aerodynamic design approach was to modify the diffuser area distribution from linear to parabolic. Based on NASA test results, predicted diffuser performance is significantly increased by use of a parabolic area distribution resulting in a linear static pressure distribution. Physically, a linear static pressure distribution results in a small area change for the

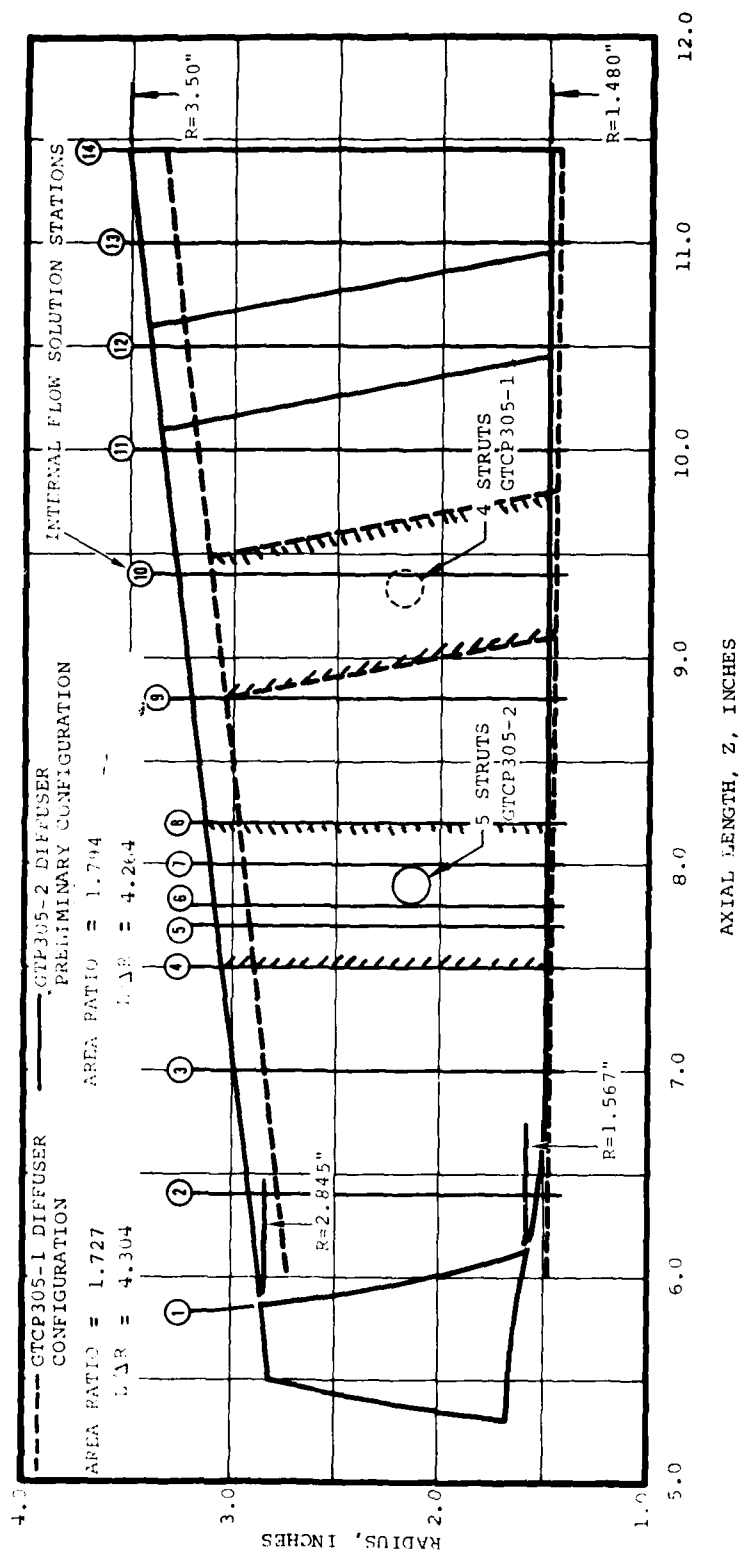
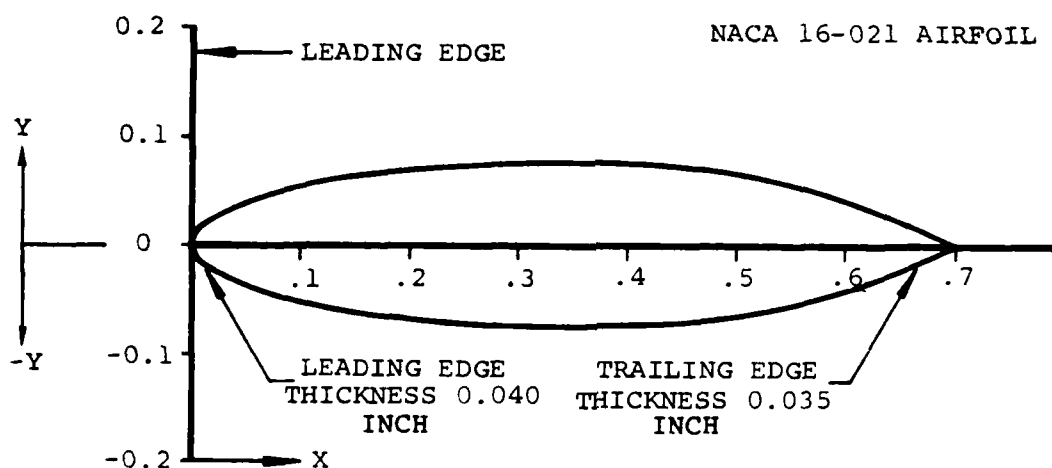


Figure 81. Exhaust diffuser meridional view

TABLE 14. GTP305-2 TURBINE EXHAUST DIFFUSER  
BASIC STRUT COORDINATES FOR  
CONSTANT CROSS SECTION  
5 STRUTS TOTAL.

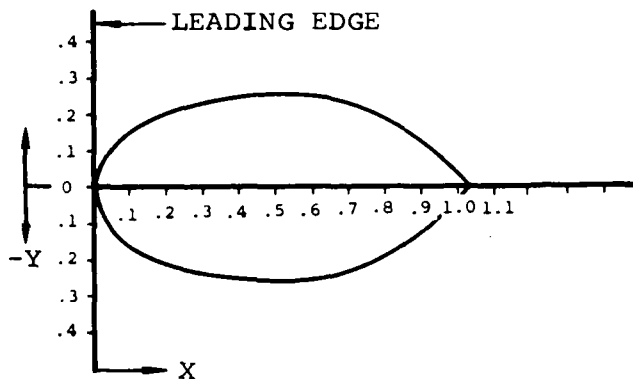


X (CHORD) - INCH

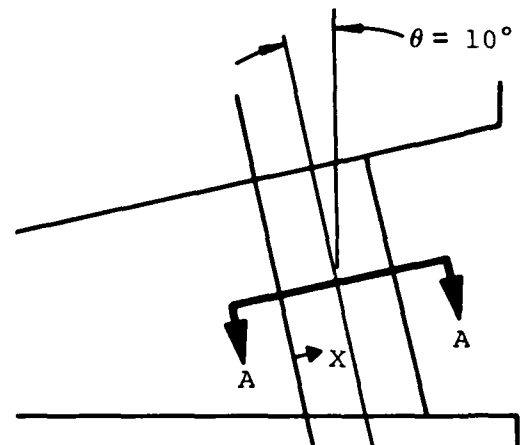
Y (THICKNESS) - INCH

0.0000	0.0000
0.0080	0.0158
0.0170	0.0221
0.0350	0.0307
0.0520	0.0371
0.0700	0.0423
0.1050	0.0506
0.1400	0.0571
0.2100	0.0663
0.2800	0.0717
0.3500	0.0735
0.4200	0.0714
0.4900	0.0645
0.5600	0.0514
0.6300	0.0308
0.6650	0.0173
0.7000	0.0000

TABLE 15. GTP305-2 EXHAUST DIFFUSER OIL  
IN AIRFOIL DEFINITION.



STRUT PROFILE (SECTION A-A)



X ( CHORD ) - INCH

Y ( THICKNESS ) - INCH

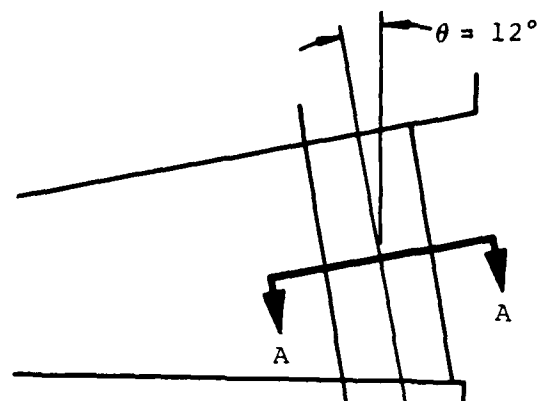
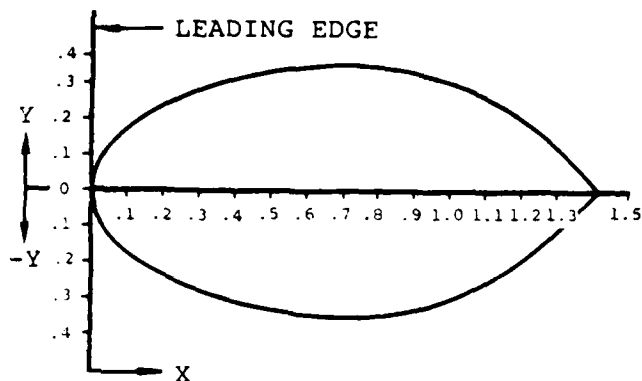
0.0000  
0.01285  
0.02570  
0.0514  
0.0771  
0.1028  
0.1542  
0.2056  
0.3084  
0.4112  
0.5140  
0.6168  
0.7196  
0.8224  
0.9252  
0.9766  
1.0000  
1.0400

0.0000  
0.0553  
0.0773  
0.1074  
0.1298  
0.1480  
0.1771  
0.1997  
0.2320  
0.2507  
0.2570  
0.2499  
0.2256  
0.1798  
0.1078  
0.0606  
0.0230  
0.0000



AIRESARCH MANUFACTURING COMPANY OF ARIZONA  
A DIVISION OF THE BARRETT CORPORATION  
PHOENIX, ARIZONA

TABLE 16. GTP305-2 EXHAUST DIFFUSER OIL  
OUT AIRFOIL DEFINITION.



STRUT PROFILE (SECTION A-A)

X (CHORD) - INCH

$\pm Y$  (THICKNESS) - INCH

0.0000	0.0000
0.0176	0.0758
0.0352	0.1059
0.0704	0.1472
0.1056	0.1778
0.1408	0.2028
0.2112	0.2425
0.2816	0.2736
0.4224	0.3178
0.5632	0.3434
0.7040	0.3520
0.8448	0.3423
0.9856	0.3091
0.1264	0.2463
0.2672	0.1476
1.3376	0.0830
1.3650	0.0400
1.3725	0.0000



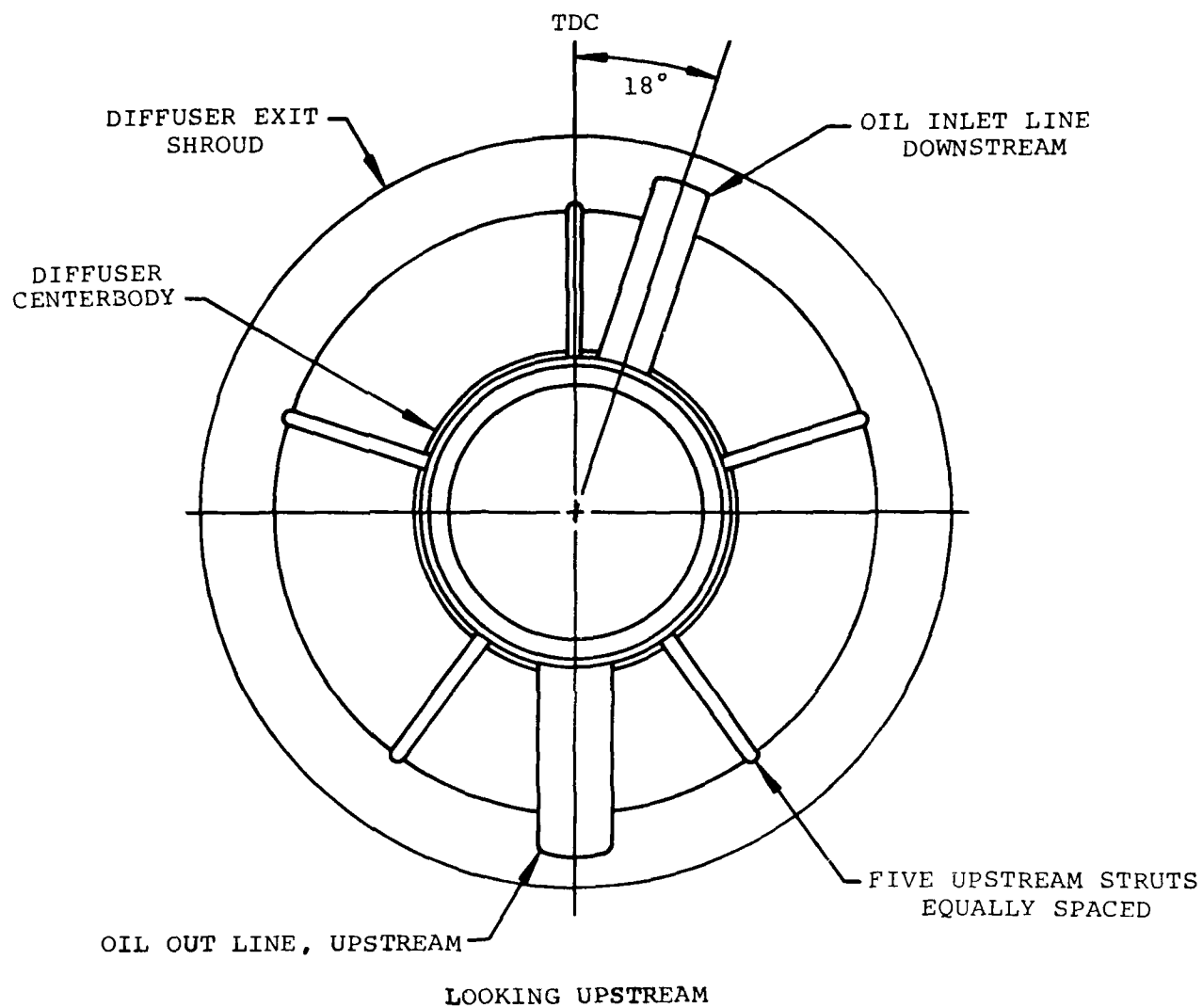


Figure 82. Circumferential location of exhaust diffuser struts and oil lines

first 25 to 30 percent of diffuser length, (which allows rotor exit gradients to mix and stabilize). Resultant static pressure rises during the mixing process and provides a stable flow for rapid downstream diffusion. Final diffuser shroud contour, based on this concept, is presented in Figure 83 and is compared with the straight conical shroud contour normally utilized. Variation of local area, static pressure, and velocity as a function of diffuser axial length is presented in Figures 84, through 86 respectively. Figure 85 indicates that ideal linear static pressure distribution was not achieved. However, significant improvement relative to the Model GTCP305-1 APU configuration has occurred.

Major design changes relative to the Model GTCP305-1 APU, are listed below:

- o A diffuser recovery goal of 0.40 compared with cold air test results of 0.34 for the Model GTCP305-1
- o Five struts in a relative upstream location compared with four-downstream struts
- o Oil line airfoil profiles compared with cylindrical oil lines
- o Linear static pressure distribution compared with linear area distribution

### 3.5' Rotor Dynamics

An analytical model was developed to assess rotating group dynamic response and identify critical speeds encountered throughout the operating range.

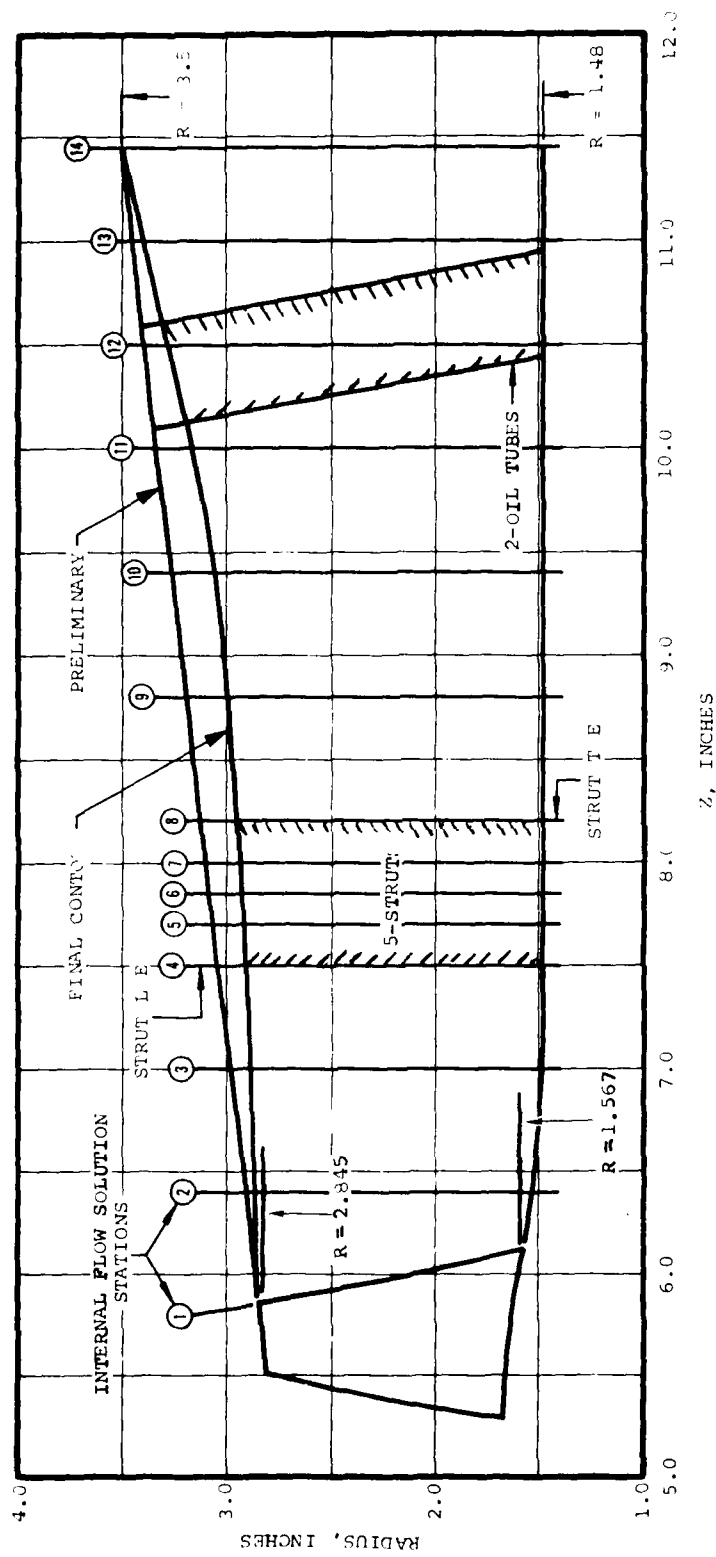


Figure 83. Exhaust diffuser meridional view

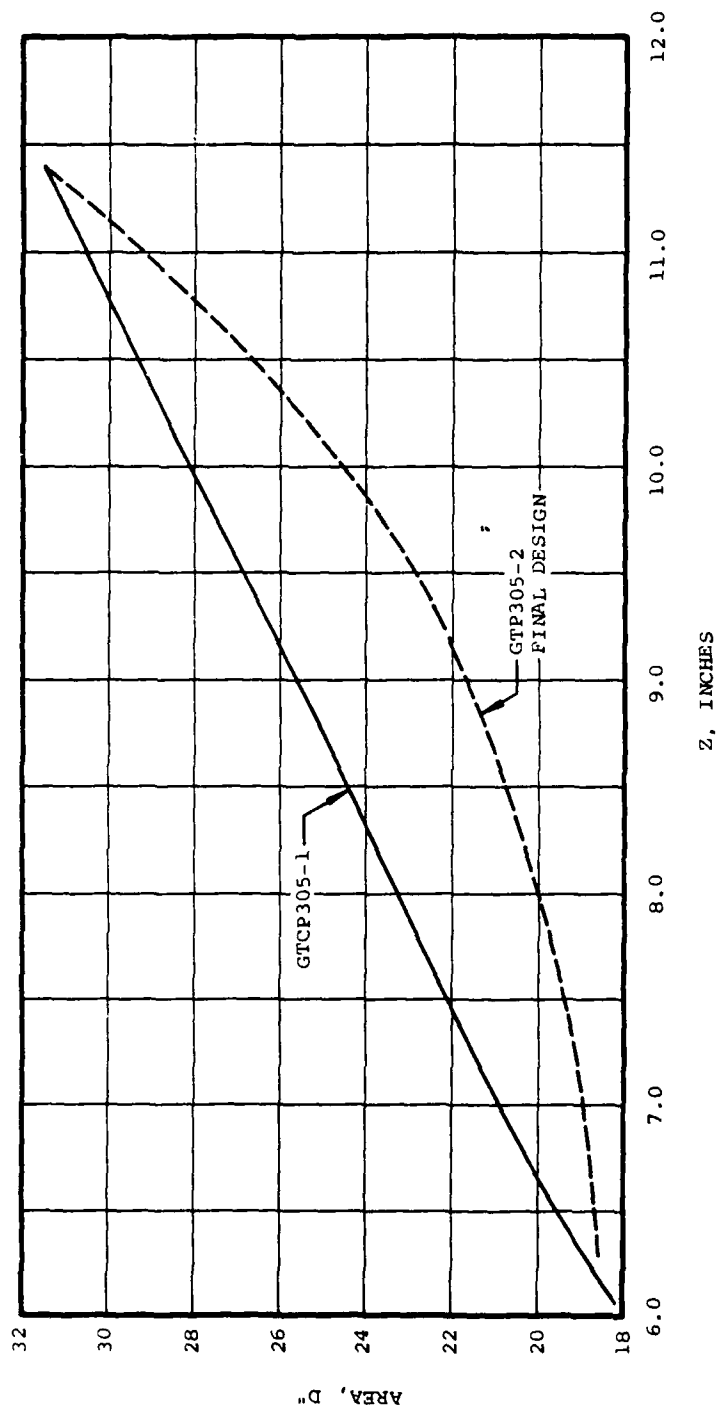


Figure 84. Exhaust diffuser area distribution

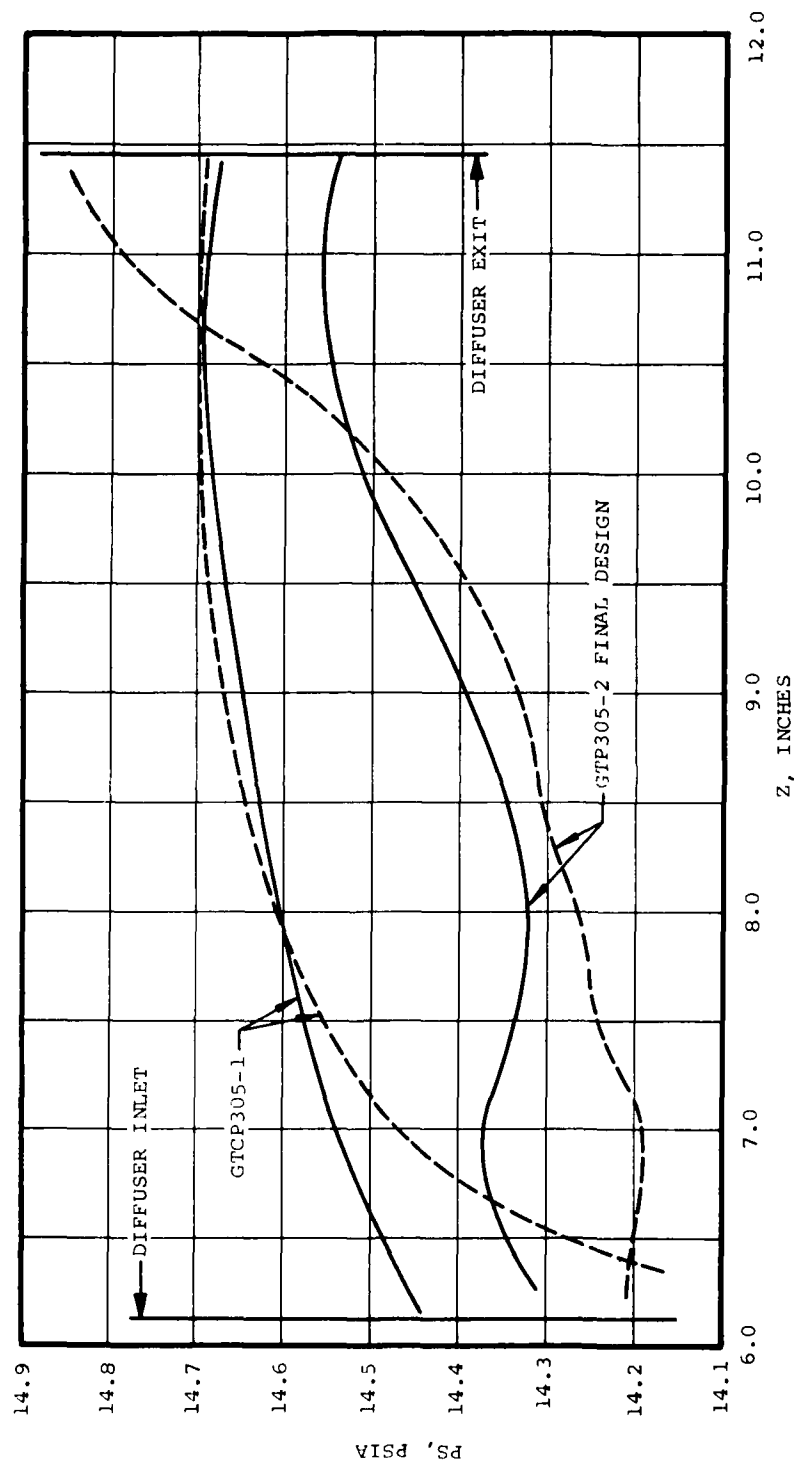


Figure 85. Exhaust diffuser static pressure distribution

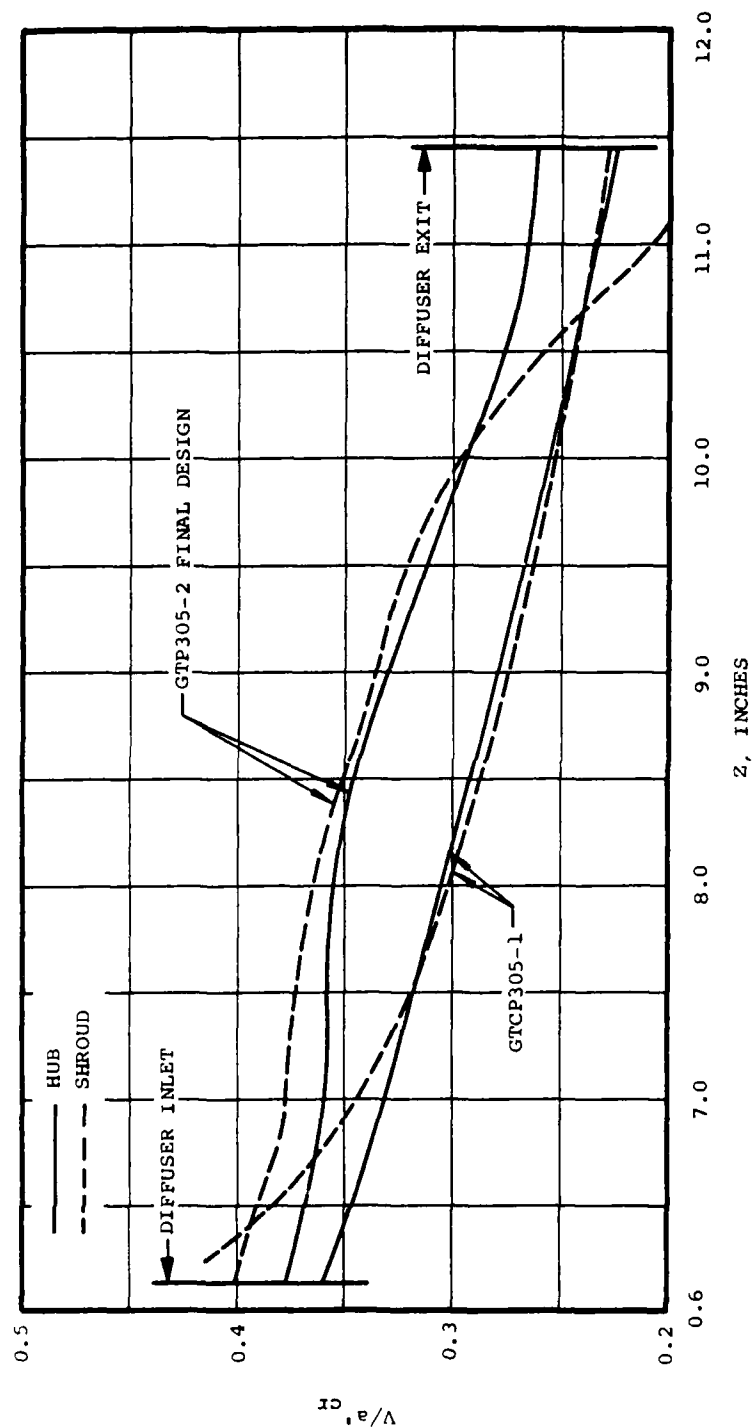


Figure 86. Exhaust diffuser velocity distribution

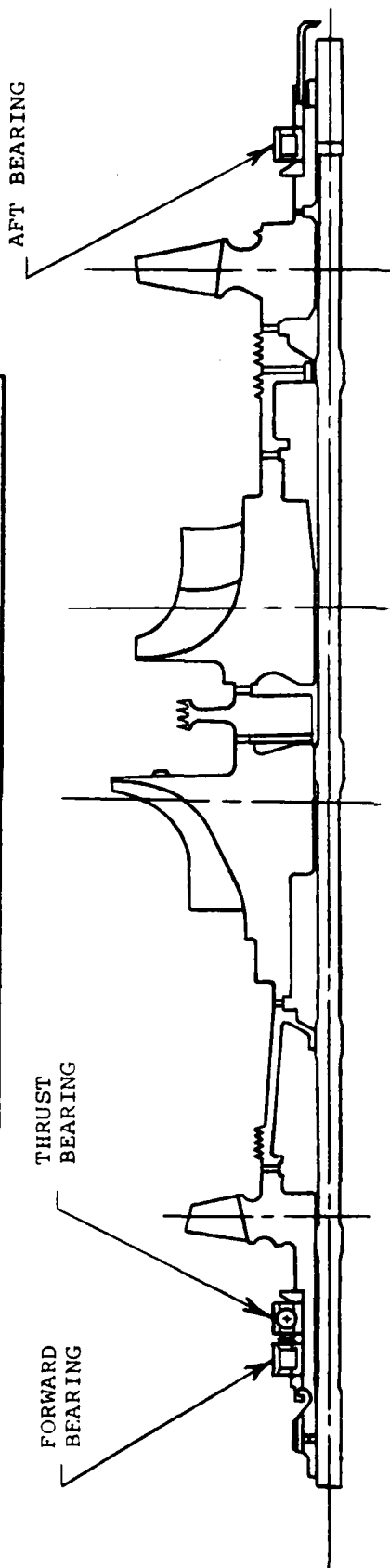
Figure 87 illustrates the Model GTP305-2 APU rotating group as modeled in this analysis. The wheel properties used to model the bladed rotating components, as well as total rotating group properties, are also given in the tables on Figure 87.

The engine rotating group is supported at both ends by hydrodynamically mounted rolling element bearings. Support for these bearings largely consists of strut-mounted static structures, and was not considered to be rigid in this analysis. Engine output is delivered through a quill shaft attached to the engine using an internal/external spline arrangement.

The mass model shown in Figure 88 indicates representation of the four-bladed components by equivalent lumped masses. The stiffness model primarily pertains to incorporation of components which would directly contribute to rotor stiffening. While blades do stiffen the rotor, it is difficult to assess the exactly extent. Therefore, the blades were not included in this analysis and, the stiffness model is conservative in this respect. All values of elastic modulus were input as a function of temperature calculated in the rotating group thermal analysis; thus the model more accurately predicts the critical speed locations at steady state-operating conditions (but the model will underpredict the critical speeds for a cold rotor, such as in cold starts).

Utilizing these mass and stiffness representations, a parametric study of the critical speeds as a function of bearing stiffness is given in Figure 89. Analytical critical speeds generated in Figure 89 represents a range of bearing stiffness from 50,000 to 250,000 lbf/inch, with the stiffness of the front and rear bearings equal. The affect of the ball thrust bearing has been neglected, as it is designed to carry little, if any, radial load and does not support a diametral bending moment. The engine incorporates a radial load bearing system composed of a roller bearing supported by a squeeze-film mount.

TOTAL ROTATING GROUP PROPERTIES		
MASS (lbf-sec <sup>2</sup> /in)	POLAR INERTIA (in-lbf-sec <sup>2</sup> )	DIAMETRAL INERTIA (in-lbf-sec <sup>2</sup> )
0.05073	0.07664	0.8707



COMPONENT	MASS (lbf-sec <sup>2</sup> /in)	POLAR INERTIA (in-lbf-sec <sup>2</sup> )	DIAMETRAL INERTIA (in-lbf-sec <sup>2</sup> )
AXIAL COMPRESSOR	0.00246	0.0027	0.0027
RADIAL COMPRESSOR	0.0113	0.0224	0.0234
RADIAL TURBINE	0.0167	0.0270	0.0192
AXIAL TURBINE	0.0073	0.0115	0.0065

NOTE: CENTERLINES INDICATE APPROXIMATE CENTER OF MASS

Figure 87. GTP305-2 final layout rotating group and wheel property information



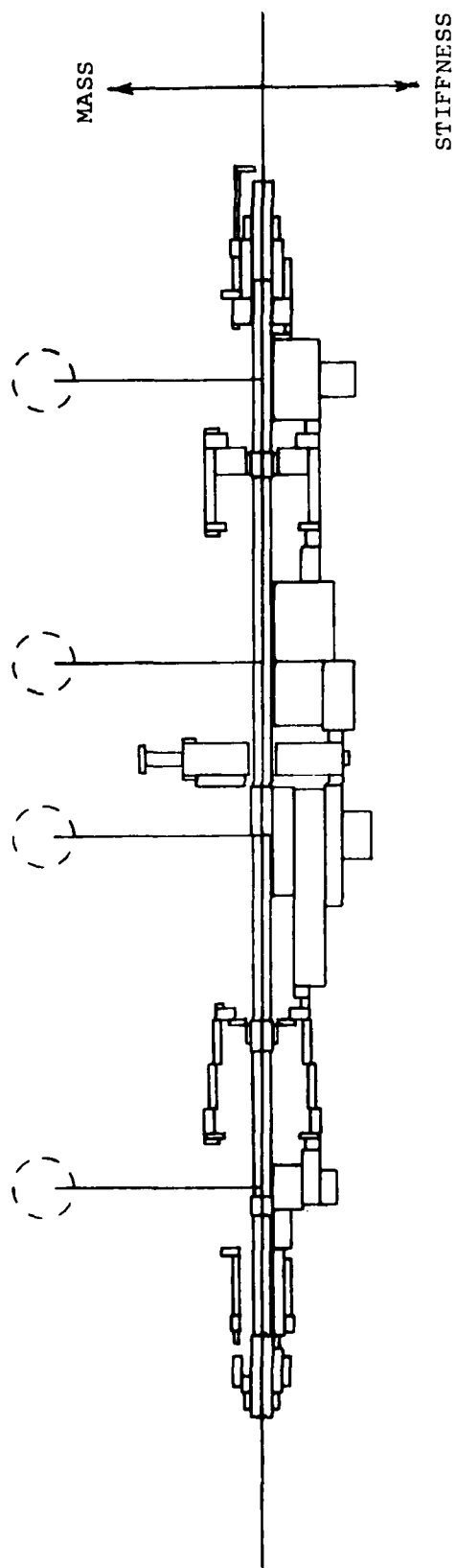


Figure 88. GTP305-2 final design rotating group mass and stiffness critical speed model

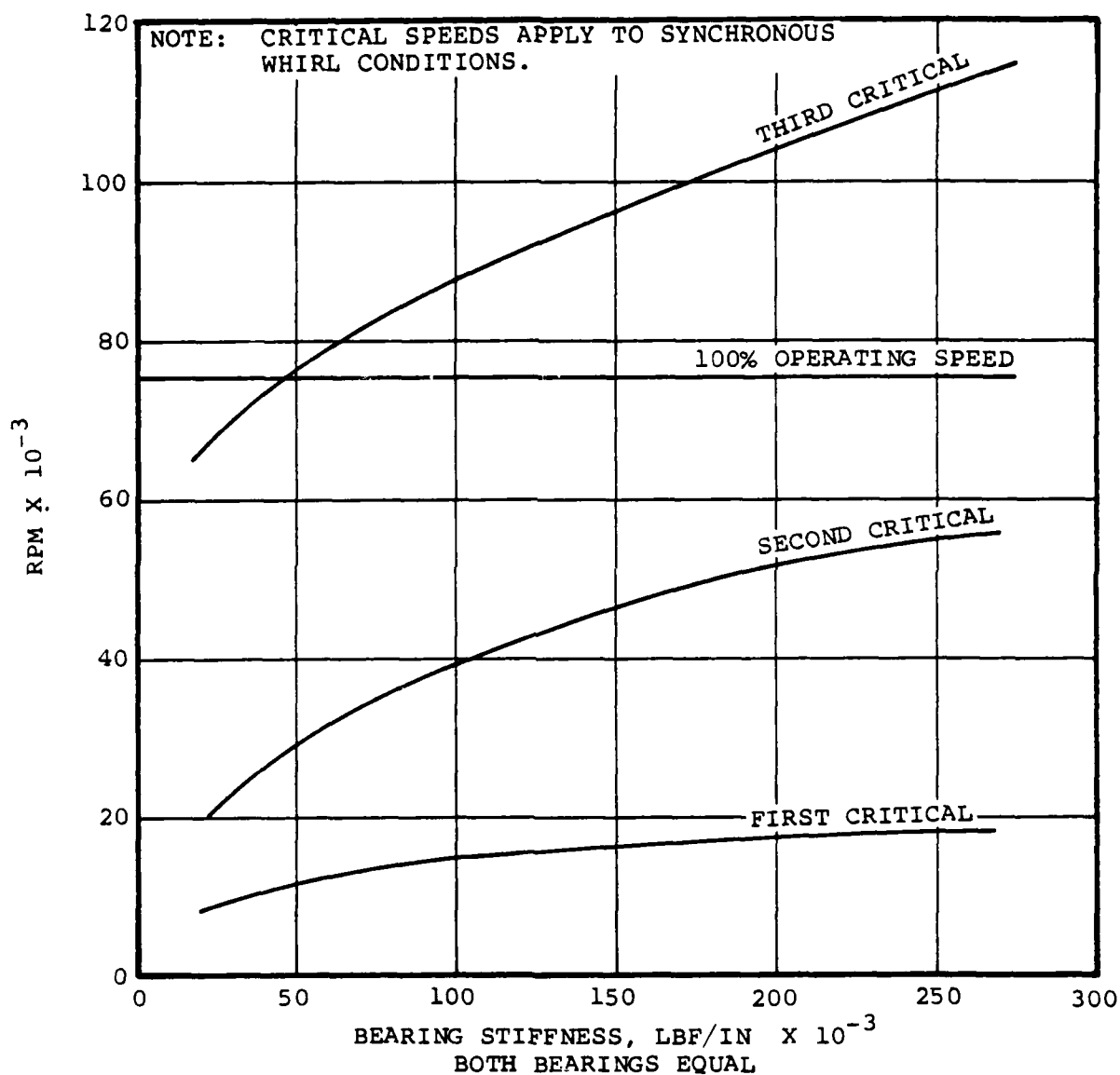


Figure 89. GTP305-2 final design rotating group critical speeds versus bearing stiffness

Figure 89 illustrates the first three criticals. Modes above the third were not considered as the 100-percent operating speed of the engine roughly falls between the second and third criticals. As noted, this figure, as well as the following three figures, apply to synchronous whirl conditions only (whirl ratio equal to one).

Figures 90 through 92 illustrate the first critical speed mode shapes. Bearing locations are indicated by perpendicular arrow-headed lines extending from the axial distance axis. As shown on these figures, a nominal bearing stiffness of 150,000 lbf/inch. was used to calculate these modes. This value was chosen as a reasonable estimate of the stiffness due to the combined three component series representation of the bearing system. The first critical, shown in Figure 90, occurs at 16,000 rpm and is a cylindrical mode involving a large excursion near the rotor midspan. From Figure 89 it is noted that this mode occurs at approximately 16,000 rpm to 18,000 rpm for a range of bearing stiffness from 125,000 to 250,000 lbf/inch, which leads to the conclusion that this mode is largely a function of bearing geometry rather than bearing stiffness. Figure 91 illustrates the second critical, a conical mode occurring at 46,000 rpm. This mode depicts a relatively large amount of bearing activity, and from Figure 89 it is shown to be strongly influenced by bearing stiffness. With proper application of the squeeze-film mount, this mode should be effectively damped. The third mode is shown in Figure 92, which is a bending critical occurring at 96,000 rpm. This mode again shows a fair amount of bearing activity, and is influenced the most by bearing stiffness changes, which implies that a properly designed squeeze-film bearing should enable engine operation extremely close to this critical. This mode has a 26.6-percent margin over 100-percent operating speed using nominal values of bearing stiffness which is less than the accepted standard of 40 percent. However, it is felt that the demonstrated operation of the Model GTP305-1 and

NOTES. ( ) BEARING STIFFNESS 100 000 LBF/IN., BOTH BEARINGS  
 ( ) OPTIMAL SPEED CALCULATED FOR SYNCHRONOUS WHIRL  
 CONDITIONS

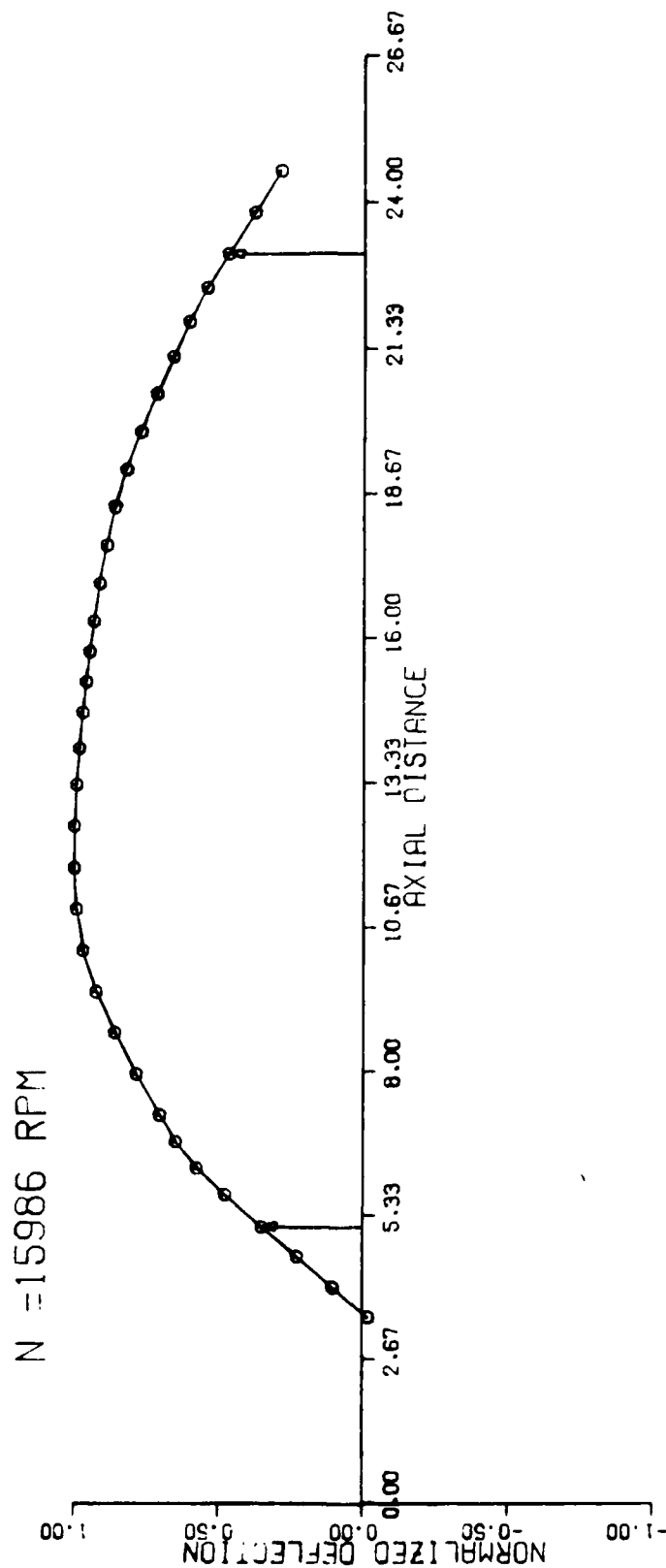


Figure 90. GTP305-2 final design rotating group  
 first critical speed mode shape

NOTES: (1) BEARING STIFFNESS 150,000 LBF/IN., BOTH BEARINGS  
 (2) CRITICAL SPEED CALCULATED FOR SYNCHRONOUS WHIRL  
 CONDITIONS

N = 45743 RPM

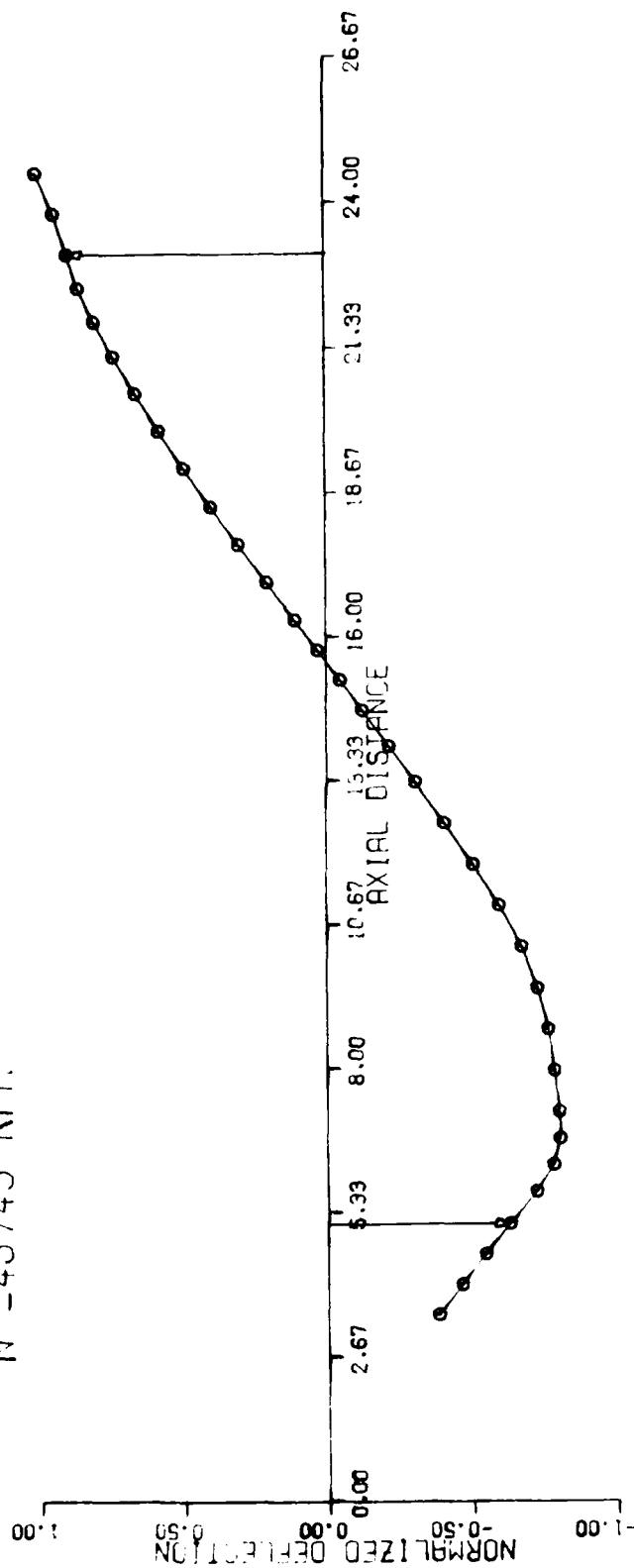


Figure 91. GTP305-2 final design rotating group  
 second critical speed mode shape

NOTES: (1) BEARING STIFFNESS 150,000 LBF/IN., BOTH BEARINGS  
 (2) CRITICAL SPEED CALCULATED FOR SYNCHRONOUS WHIRL  
 CONDITIONS

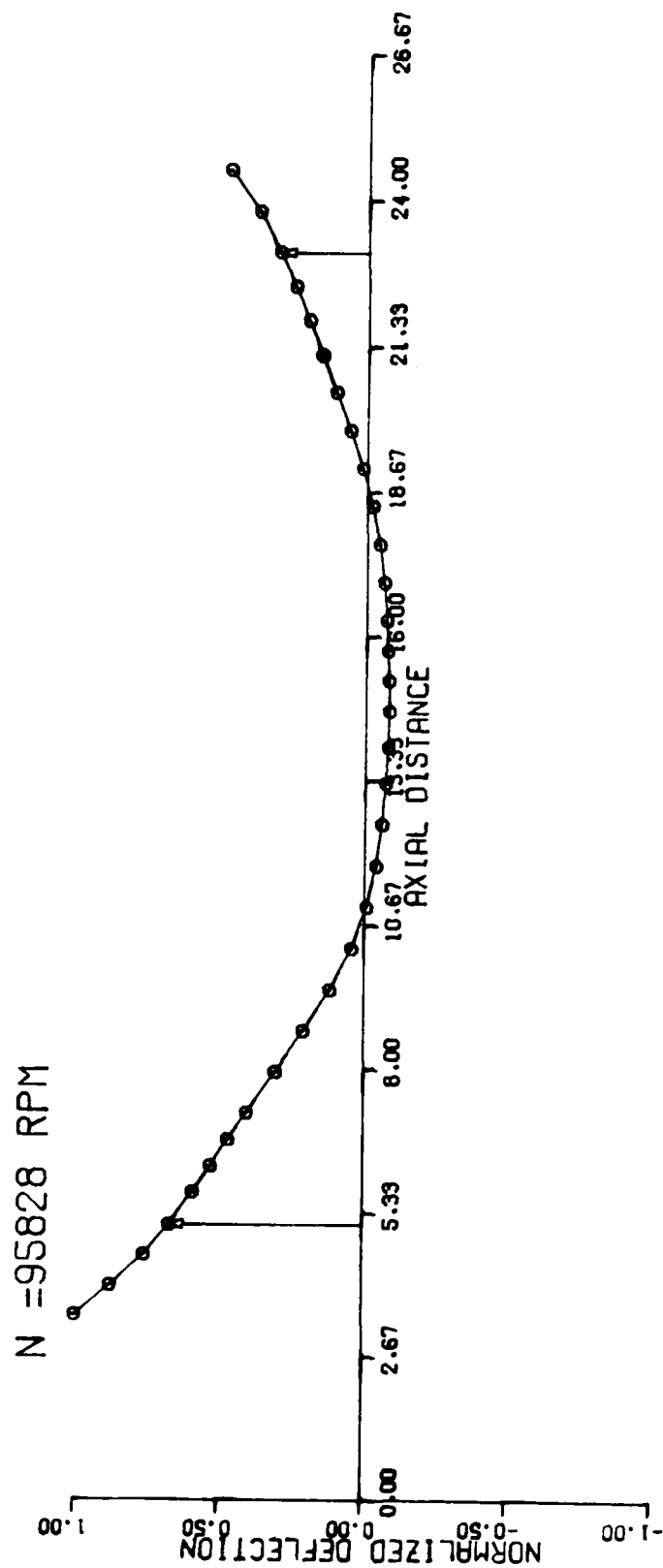


Figure 92. GTP305-2 final design rotating group  
 third critical speed mode shape

the influence on rotor response from the squeeze-film mounts will ensure acceptable operation at such a margin.

To pass cooling air under the radial turbine, certain devices and geometrical changes were incorporated to the rotating group, as compared with the case without any modifications (i.e., Model GTP305-1), it was found that virtually no affect on the critical speeds would result from these changes. For instance, moving a tiebolt pilot from underneath the compressor-turbine interstage seal to underneath the aft end of the radial compressor increased the third mode critical by 0.13 rpm.

## SECTION IV

### COMPONENT DEVELOPMENT TESTING

The turbine stage and combustion system were tested separately using test rigs designed and fabricated to facilitate developmental testing. The following sections describe the development testing of the combustion system, radial turbine stage and radial/axial turbine stage. This effort was previously reported in AiResearch Document 31-2918, and is summarized herein.

#### 4.1 Combustion System Development Testing

##### 4.1.1 Test Rig

Combustion system rig testing was conducted to evaluate and define combustor performance (i.e., temperature spread factor, wall temperature, stability, pressure loss, ignition capability, and combustion efficiency) at design, and off-design, conditions. Salient design features of the combustion system were discussed in Section 3.3. Table 17 summarizes specific combustion system performance goals, and lists performance levels.

The combustion system test rig (Figure 93) was designed to duplicate the geometries of engine components adjacent to the combustor. Since combustion system performance is affected by the airflow pattern into the combustor, this duplication was required to ensure that the engine and rig airflow patterns were the same.

A toroidal plenum, incorporating preswirl vanes at the plenum exit, was designed for the combustion system rig. These vanes turn the flow, thereby duplicating the 25 degree combustion system inlet swirl angle. The plenum was also used on the Integrated Components Assembly (ICA) Test Rig. The rig radial nozzle



TABLE 17. COMBUSTION SYSTEM PERFORMANCE GOALS.

Parameter	Goal	Allowable
Temperature Spread Factor (TSF) = $\frac{T_{MAX} - T_{AVG}}{T_{AVG} - T_{IN}}$	0.15	0.216
Wall Temperature (Maximum)	1500°F	1700°F
Lean Blowout Fuel-Air Ratio (Combustor Stability)		
Design Point	0.005	0.008
Idle	0.005	0.008
Combustor Pressure Loss	4%	4%
Sea Level Ignition Fuel-Air Ratio	0.02	0.03
Combustor Efficiency ( $\eta_b$ ) at Design Point	99.8%	99%
Carbon Deposits	No Deposits	Soft Deposits

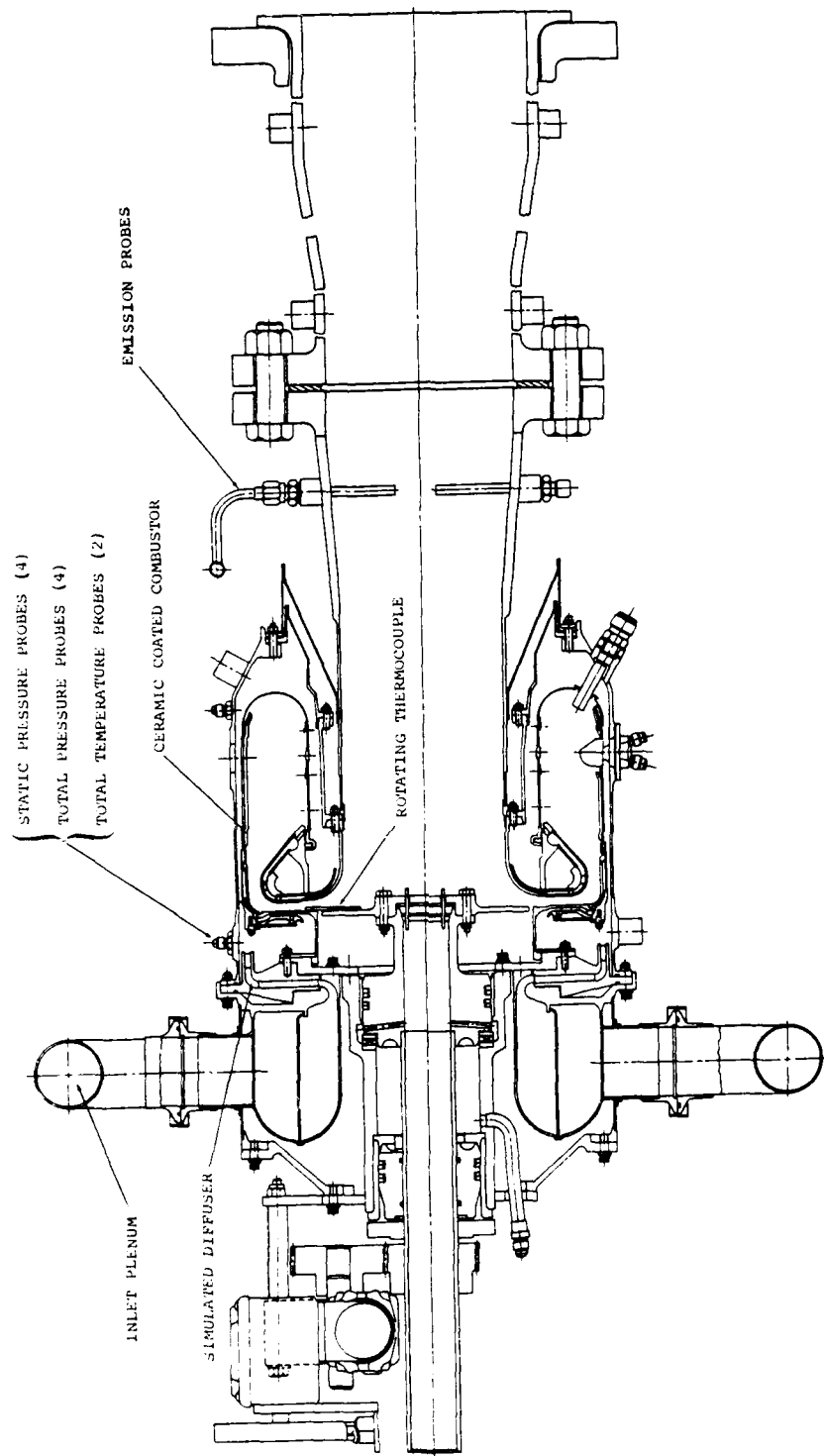


Figure 93. Combustion system development test rig  
P/N 3605880

was a vaneless design to allow installation of the rotating combustor exit total temperature/pressure probe. However, the fore and aft nozzle sidewall cooling flow passage configurations accurately simulated the dilution zone airflow, introduced into the combustor from these areas.

#### 4.1.2 Instrumentation

- o Combustion system inlet airflow was measured by test facility orifice measuring equipment and fuel flow was determined by a rotameter
- o Pressure, temperature, and emission probes were located at various stations in the rig to evaluate combustor performance (see Figure 93)
- o Inlet total and static pressures were measured at four-circumferential locations at the preswirl vane exit. Inlet total temperature was measured in the same axial plane at two-circumferential locations at 180-degrees apart
- o Combustion discharge gas total temperature was measured by ten thermocouples at five-axial positions in two-circumferential groups at the axial station simulating the turbine nozzle inlet
- o Discharge total pressures were measured at two-circumferential positions at the axial station simulating the turbine nozzle midstream
- o Total temperature and total pressure probes rotated through 360 degrees and automatically recorded data at 15-degree intervals

- o Gaseous emission samples were obtained from a manifold of four-stationary, three-element probes located 90 degrees apart in the exhaust duct
- o Metal temperatures were determined by using Thermindex temperature-sensitive paint. This paint test indicates full load temperature levels, including gradients and hot spots

#### 4.1.3 Test Procedure

During the test phase, atomizer and combustor tests were conducted. Atomizers were individually tested in a flow fixture to assure that adequate atomization characteristics were obtained over the GTP305-2 operating range (see Table 18). Initial combustor tests concentrated on design point airflow conditions (Table 18) with gradual increments in fuel flow so the maximum peak temperature could be monitored as the design point turbine inlet temperature was approached. This technique of limiting maximum peak temperature prevented serious damage to instrumentation and test hardware. During each test series, overall combustor performance was evaluated. If results were not within design specifications, combustor modifications were made and the test sequence repeated. Once a satisfactory temperature spread factor (TSF) was attained, performance mapping was conducted on the combustion system. Mapping involved a check of TSF, liner skin temperature, lean stability, ignition, and gaseous emissions at off-design conditions.

#### 4.1.4 Test Results

Eleven tests were conducted during the development program. Each succeeding test utilized information from the preceding test in an effort to correct associated problems and improve demonstrated test results, where applicable. Table 19 contains a

TABLE 18.. COMBUSTION SYSTEM OPERATING CONDITIONS

Atomizer Fuel Flow	Idle Full power Ignition	80 lb/hr 151 lb/hr 20 lb/hr
Combustor Airflow	Idle Full power Ignition	2.08 lb/sec 2.01 lb/sec 0.16 lb/sec
Combustor Inlet Temperature	Idle Full power	770°F 788°F
Combustor Inlet Pressure	Idle Full power	109.6 psia 118.8 psia
Average Combustor Discharge Temperature	Idle Full power	1480°F 2085°F

## NOTES:

1. Operating parameters are for a 130°F sea level day.
2. For test purposes, these parameters will be held within  $\pm 1$  percent of stated values.

TABLE 19. COMBUSTION SYSTEM DEVELOPMENT TEST SUMMARY.

Date	Goal	Require- ment	Test Number											Final Configuration Combustor
			1	2	3	4	5	6	7	8	9	10	11	
Combustor S/N			8/17/77	8/24/77	8/27/77	9/13/77	9/20/77	9/26/77	10/10/77	10/21/77	11/9/77	2/15/78	3/9/78	
T <sub>4</sub> (°F)			1	1	1	1	1	1	2	2	1	2	1	
Patten Factor	2066	2066	1900	2004	2004	---	1986	2041	2005	2011	1954	2043	2015	
Mix. Metal Temp. (°F)	0.150	0.216	0.279	0.180	0.180	---	0.257	0.158	0.188	0.167	0.297	0.223	0.163	
Lean Blowout*	1500	1700	1650	1650	1650	---	1700	1900	1900	1700	1500	1650	1700	
	0.005	0.007	0.005	0.005	0.005	---	0.005	0.0012	0.0014	0.004	---	---	---	
Atomizer Angle (Degrees)			30	30	25	25	25	20	20	25	25	25	25	25
Combustor Configuration														
0.25 In OD, SS, ID Seal			X	X	X	X	X	X	X	X	X	X	X	X
Design Seal Configuration														
Dome Cooling Skirt-Dome ID														
Dome Cooling Skirt-Dome ID														
Flush Primary Holes														
Coating Thickness (In)			0.012	0.012	0.012	0.012	0.012	0.012	0.012	0.012	0.012	0.030	0.012	0.012
Coating-Dome ID														
I.D. Cooling Skirt Short														
Combustor Configuration Anomalies														
Warpage-OD														
Warpage-Dome Contour														

\*Lean Blowout based on 10 atomizers.

\*\*Minimum Dioxide flow check only.

$$* \text{ Pattern Factor } \frac{T_{\text{MAX}} - T_{\text{AVE}}}{T_{\text{RISE}}}$$

summary of test results and the combustor configuration details for the eleven tests conducted.

Testing was initiated on August 17, 1977 with P/N 3605621-2, S/N 1 Combustor and an atomizer back angle setting of 30 degrees as illustrated in Figure 94. After ignition, a 1200°F combustor discharge temperature was maintained and a rig mechanical check-out was performed. Post test inspection of the Thermindex paint on the combustion liner indicated a uniform temperature distribution of approximately 1100°F. No hot spots were noted.

Following modifications to the rig rotating instrumentation shaft, Test 2 was completed. The fuel nozzles were again set at a 30 degree back angle. A 1900°F maximum average discharge temperature limit was imposed at design inlet conditions, to assure that excessive metal temperatures were not encountered.

Temperature discharge measurements, recorded at 1900°F, indicated a 0.282 pattern factor. Inspection of the Thermindex temperature sensitive paint identified ten 10-hot spots on the combustor dome as shown in Figure 95, and a maximum temperature of 1650°F. Analysis indicates that these hot spots were caused by unburned fuel from the nozzle spray cone impinging on the dome. The uncooled outer wall showed an average metal temperature of 1500°F between fuel nozzles.

To eliminate fuel impingement, Test 3 utilized the same combustor configuration and reduced the back angle setting of the atomizers from 30 to 25 degrees. A pattern factor of 0.180 was obtained at the design inlet condition and an average discharge temperature of 2000°F. Post test inspection of the thermindex paint showed three 1700°F areas located on the combustor dome. Outer wall temperatures near the primary zone increased from 1500°F, witnessed after Test 2, to 1650°F. This increase was largely due to the increased discharge temperature of Test 3. An

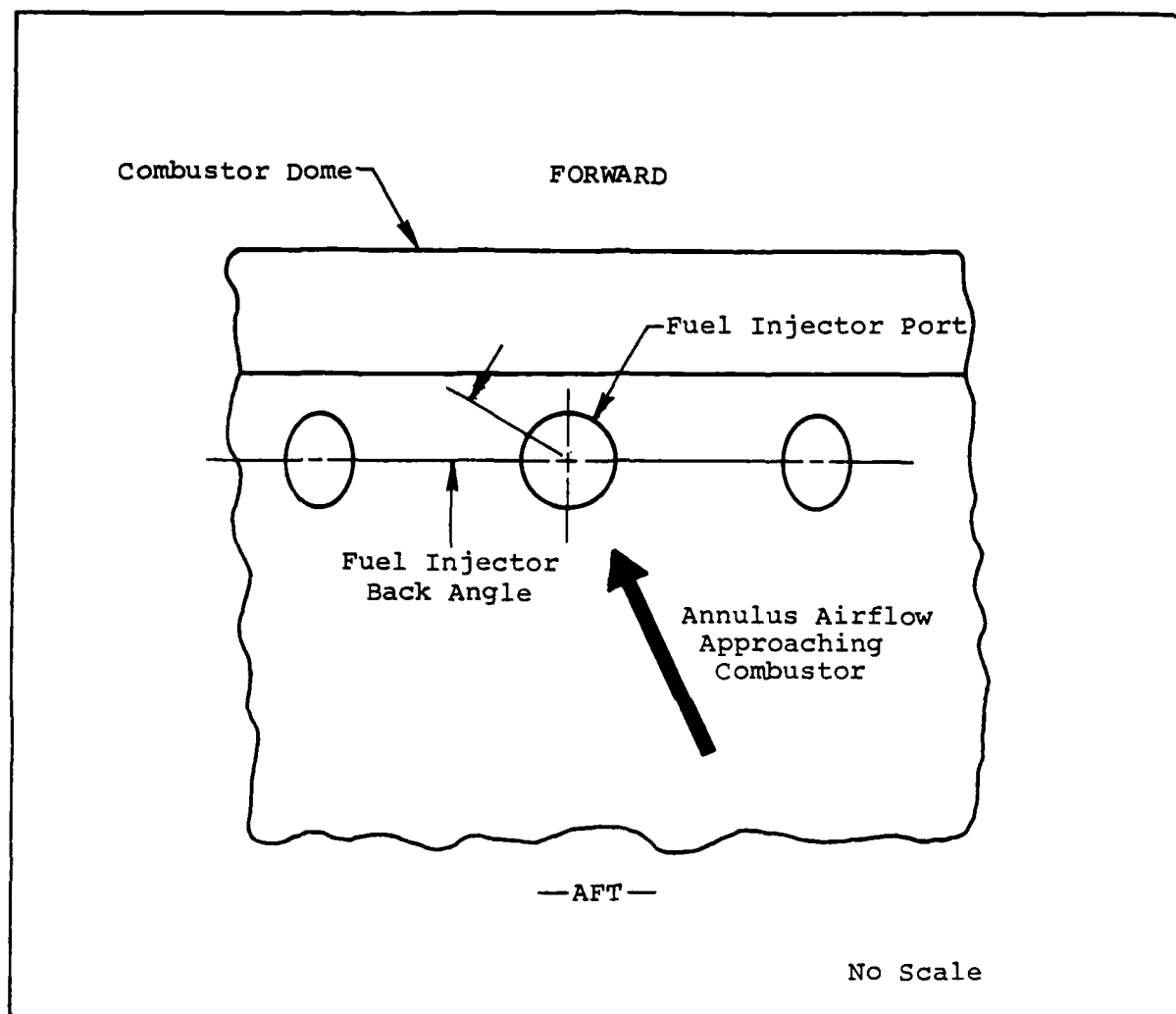


Figure 94. Sketch of top view of combustor showing atomizer back angle



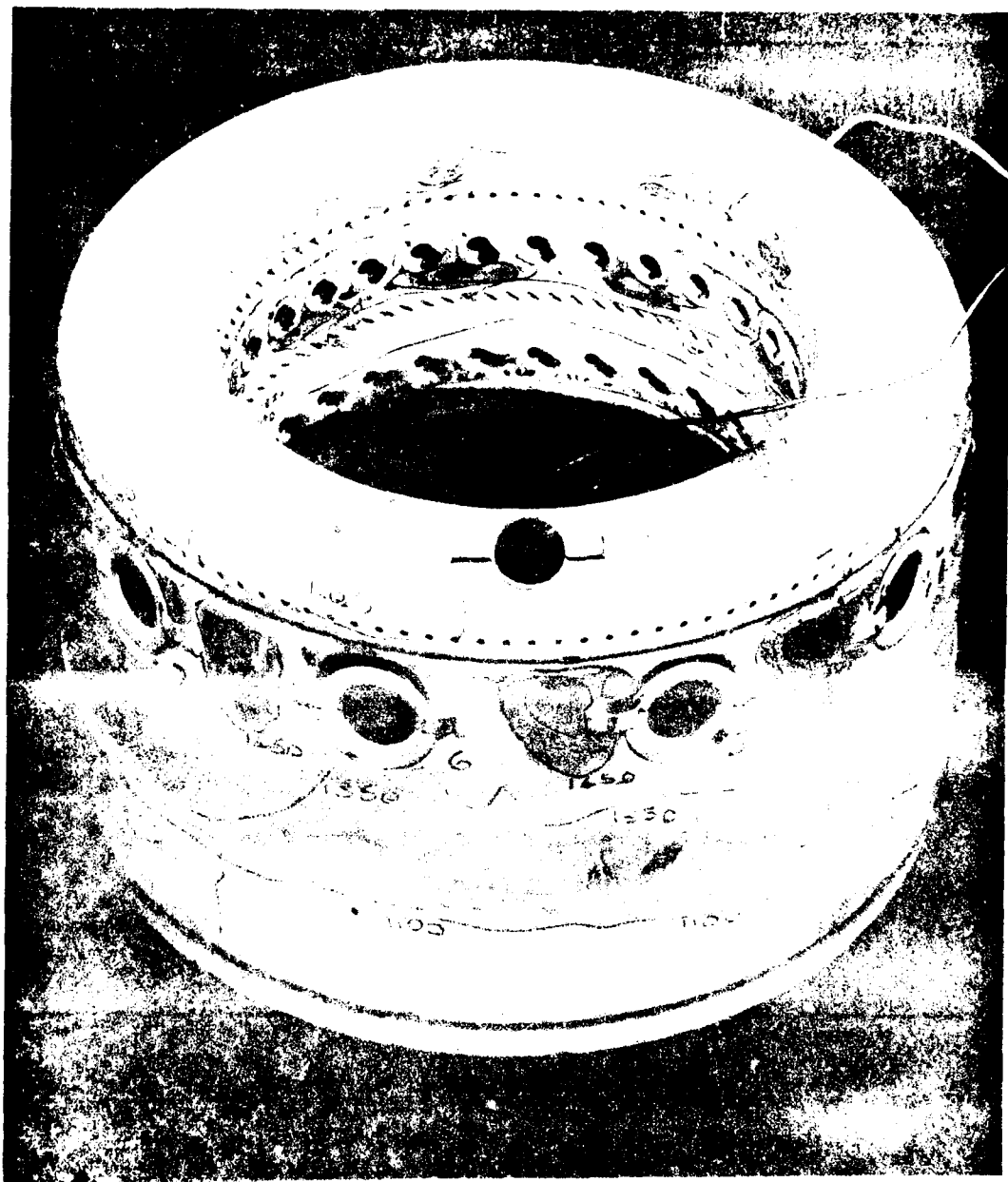


Figure 11. Thermosensitive paint (test 2)

internal inspection of the combustor showed no visible ceramic coating cracking or flaking on the inside of the outer liner. Light carbon build-up was noted in three areas near the fuel injector ports and inline with the fuel nozzle spray cone. This type of buildup is indicative of fuel being sprayed too close to the outer wall.

Prior to rotating the atomizers to the next shallower back angle, Test 4 was run to determine the aerodynamic flow patterns around the annulus. The liner was coated with a composition of titanium dioxide blended in a silicon oil binder. Design point inlet conditions were setup. Airflow patterns were produced by high velocity air scrubbing the titanium dioxide away, exposing bare metal. As indicated in Figure 96, the airflow distribution was uniform. A 25 degree inlet air swirl angle was measured.

Test 5 was initiated as a repeatable test but was not completed due to fuel flow distribution problems.

The atomizers were rotated to a 20-degree back angle to further reduce dome fuel impingement for Test 6. The maximum average discharge temperature attained during testing was 2041°F. At this condition, the measured pattern factor was 0.158. A lean blowout was recorded at 8.7-pounds per hour at design inlet conditions. This value yields a 0.0012 lean blowout fuel-air ratio. Figure 97 shows the Thermindex paint test results. The previously observed 1600°F areas on the linear outer diameter were still present. These areas appear to be due to a combination of close proximity of the fuel spray to the outer wall, and excessive penetration of the primary jets. This tends to force the combustion process towards the outer wall. On the combustor dome, ten discrete hot spots were noted. On the inner diameter, the area aft of the primary holes showed elevated temperature levels. Results indicate that the shallower 20-degree angle facilitated recirculation of fuel back into the primary zone where it can burn in a quiescent zone near the dome.

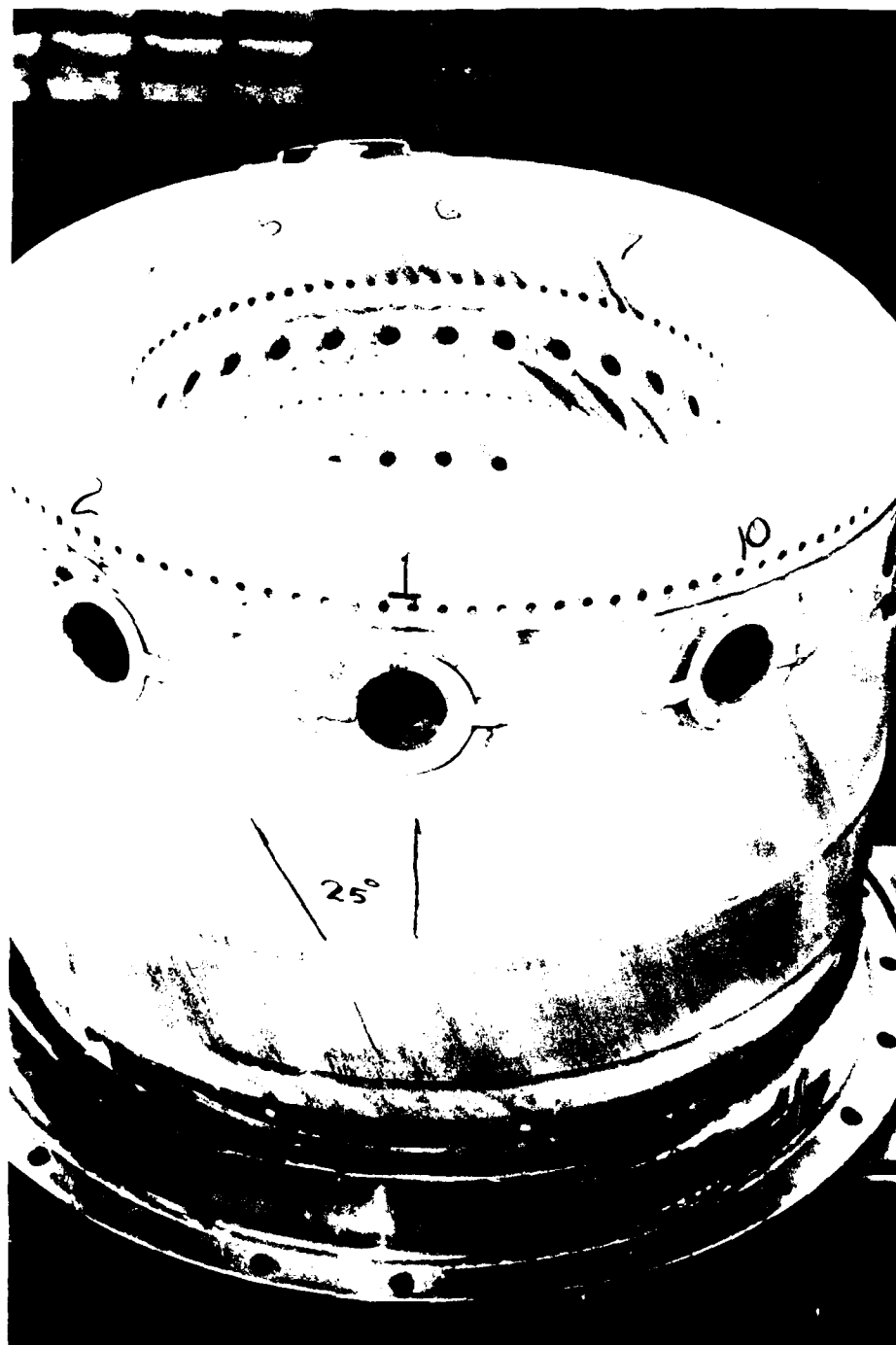


Figure 96. Titanium dioxide traces - test 4



Figure 97. Therminindex paint - test 6

Based on Test 6 results, modifications to incorporate an additional cooling skirt into the dome centerline were made on the S/N 2 combustor. This cooling flow was minimized to reduce the possibility of quenching the reactions occurring in the primary zone. With the addition of the cooling skirt, a slight reduction in pressure loss across the liner was anticipated, thereby potentially reducing the penetration of the primary jets.

Test 7 utilized S/N 2 combustor with the fuel nozzles set at a 20-degree back angle. At design inlet conditions, the maximum average discharge temperature recorded was 2005°F, with a measured pattern factor of 0.188. The lean blowout fuel-air ratio utilizing ten nozzles was 0.0014 at design inlet conditions. Combustor inspection at the conclusion of the test revealed ten discrete hot spots of approximately 1900°F on the dome inner diameter. In addition, skin temperatures of approximately 1600°F were in evidence on the outer liner. Analysis indicates that these same hot spots are probably caused by primary jet entrainment of fuel and recirculation of this composition back into the primary zone as portrayed in Figure 98. The combination of additional airflow from the dome centerline cooling skirt and the 20-degree fuel nozzle back angle setting appeared to reinforce, rather than attenuate the primary zone recirculation pockets. The ceramic coating showed two areas of internal cracking and flaking near the fuel nozzles. Cracks in the coating appear to initiate on the short radius ridge in the sheet metal. Since Thermindex paint on the sheet metal showed no severe temperature gradients, it is considered that the coating separation is due to a weakness in initial bonding. This conclusion was confirmed when S/N 1 combustor failed to crack after six severe temperature gradient tests were completed.

Modifications to effect a shift in the combustion zone away from the outer wall were made by replacing the plunged primary holes with flush holes of the same equivalent flow area. This

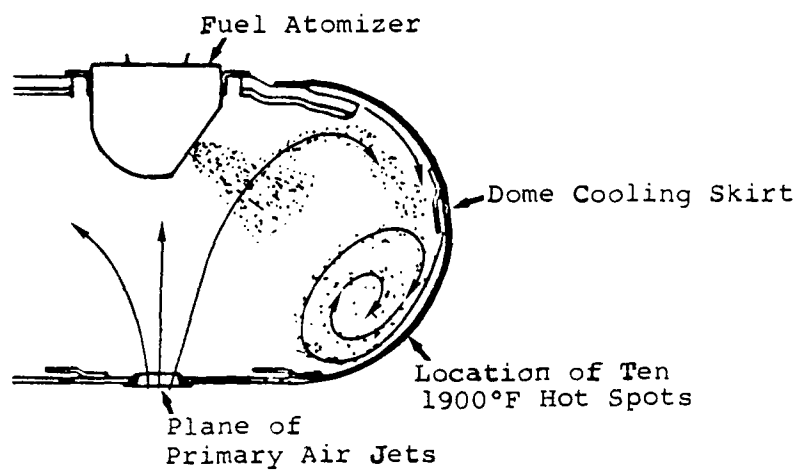


Figure 98. Primary air jet fuel entrainment test 7

AD-A087 838

AIRESEARCH WFG CO OF ARIZONA PHOENIX F/G 10/2  
ADVANCED TECHNOLOGY COMPONENTS FOR MODEL 6TP305-2 AIRCRAFT AUXILIARY--ETC(U)  
FEB 80 J R KIDWELL, G D LARGE F33615-75-C-2016

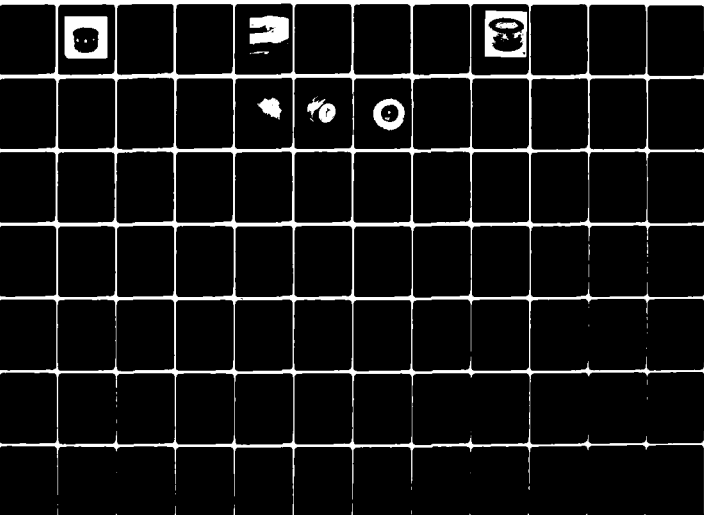
UNCLASSIFIED

AFAPL-TR-79-2106

NL

3 of 6

A 857432



approach evaluated in Test 8, was intended to reduce primary jet penetration. The atomizer back angle was readjusted to 25-degrees, prior to the test. This setting was selected to minimize the amount of fuel being recirculated next to the dome inner wall.

The maximum average discharge temperature for Test 8, was recorded at 2015°F at design inlet conditions, with a 0.167 measured pattern factor. The lean blowout fuel-air ratio, utilizing ten fuel nozzles, was 0.004 at design inlet conditions. Results of the combustor Thermindex Paint Test are shown in Figure 99. Four distinct areas of 1700°F are noted on the inner diameter of the dome. Examination of the combustor internal surfaces indicated that the inner diameter cooling skirt leading edge had pulled away from the liner in areas at high metal temperatures and then formed an aerodynamic pocket for circulation and combustion.

Although combustion results at this point were considered acceptable for integrated components rig testing, additional modifications were initiated to further reduce liner metal temperatures. These modifications included:

- o Dome cooling skirt relocation from the dome centerline to a point nearer the dome inner diameter.
- o Utilizing the Test 8 combustor and increasing the ceramic coating to a thickness of 0.020 - 0.030 inch, (from 0.012 inch). In addition, a layer of ceramic coating was applied to the dome in the area illustrated in Figure 100.

S/N 1 combustor was modified to evaluate any effects from relocating the dome cooling skirt toward the inner diameter. S/N 2 combustor was disassembled to permit application of the





Figure 99. Test 8 thermindex paint

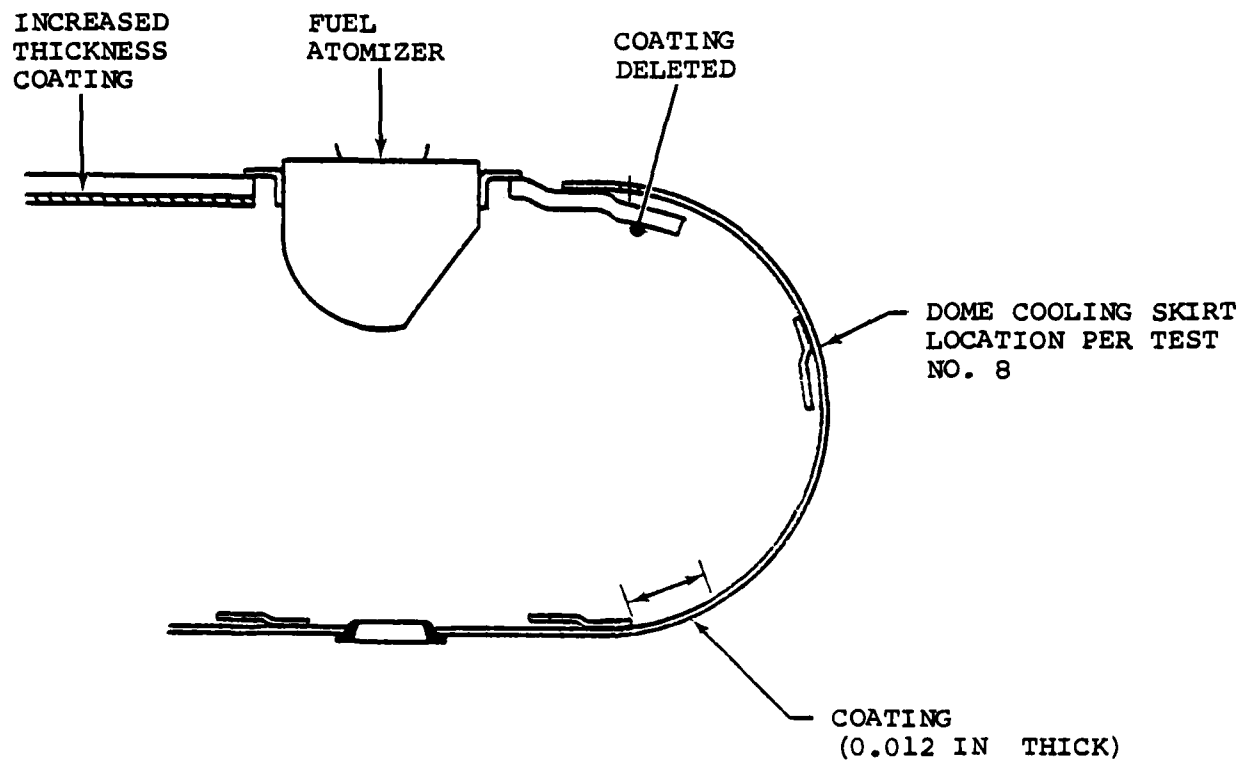


Figure 100. S/N 1 combustor features for test 10

increased thickness ceramic coating on the dome and outer liner. The disassembly permitted close examination of the inner diameter cooling skirt (Figure 101), which was noted to be a problem area during Test 8. The skirt leading edge was determined to be excessively long, extending over the dome radius. The weld bead was located approximately 0.200 inch behind the leading edge. This allows the unsupported leading edge to pull away from the dome during operation, producing the problems evidenced in Test 8. The skirt leading edge was shortened, during final assembly.

Test 9 was conducted to evaluate relocation of the dome cooling skirt nearer the dome inner diameter and Figure 102 illustrates this relocation, as compared with the Test 8 configuration. This modification was intended to reduce the dome hot spots, resulting from fuel recirculation. At combustor design inlet conditions, the average discharge temperature recorded was 1950°F, with a measured pattern factor of 0.297. The sharp increase noted in pattern factor is attributable to excessive fuel quenching and entrainment by the dome cooling air film. Fuel is apparently carried out of the primary combustion zone, by the cooling flow, and burns in the wake of the primary jets. In addition, close proximity of the relocated cooling skirt to the inner wall appears to hamper fuel recirculation back into the combustion zone. Combustor Thermindex paint test results indicated maximum temperature level on the dome was 1400°F, which is an approximate 300°F reduction, when compared with Test 8.

Test 10 was conducted to evaluate the ceramic coating increased thickness. Prior to the test, combustor inspection revealed considerable sheet metal distortion on the outer liner, produced during the welding operation joining the outer liner to the remainder of the combustor. Based on these findings, the major test emphasis was focused on evaluating the effects of manufacturing tolerances. The measured pattern factor was 0.223 at design inlet conditions, with an attendant average discharge

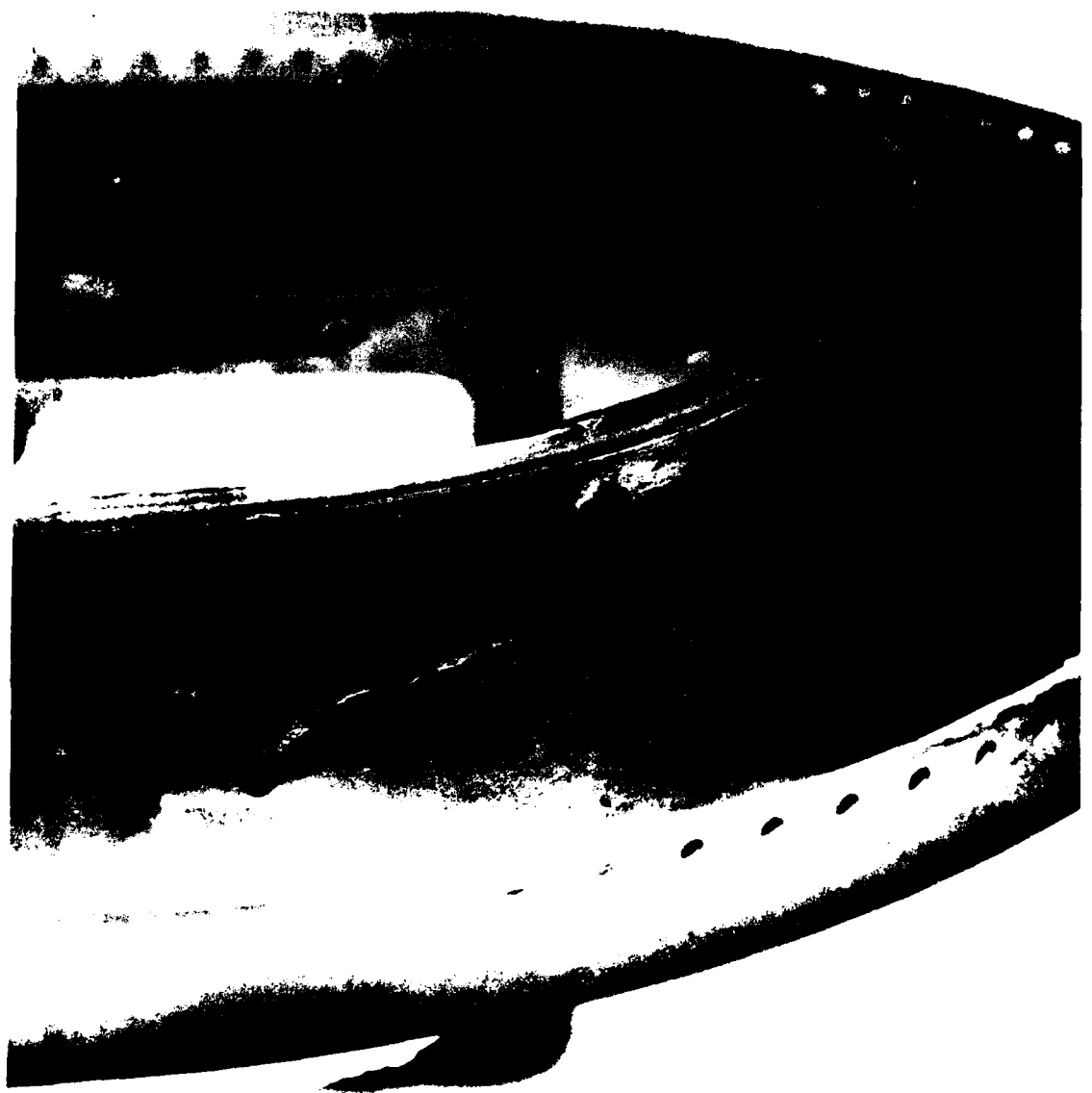


Figure 101. Dome cooling skirt attachment

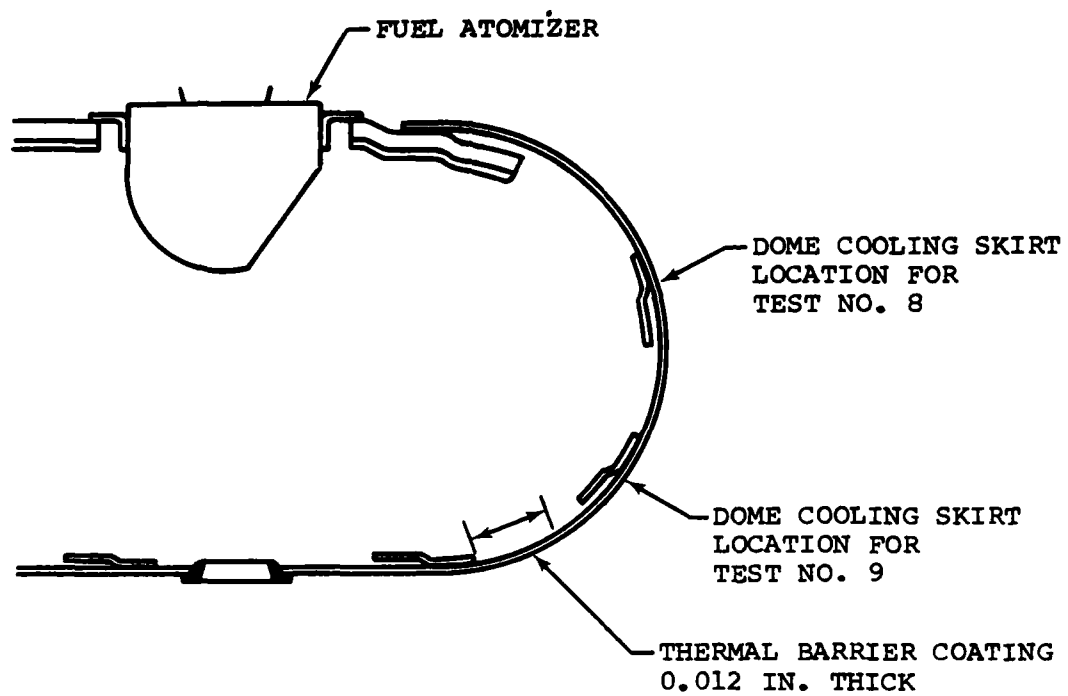


Figure 102. Locations of dome cooling skirt

temperature of 2043°F. Thermindex paint results indicated skin temperatures were approximately 100°F hotter on the outer liner in the vicinity of the outer diameter weld, than with the Test 8 combustor. Hot spots located on the dome did not change appreciably from the Test 8 configuration. During rig disassembly it was noted that bolts had worked loose allowing the combustor to sag. In addition to causing an improper airflow distribution, the loose bolts resulted in a probable leak path for combustor air. Considering the discrepancies involved in testing, no conclusive results were drawn relative to the thicker ceramic coating.

S/N 1 combustor was modified, to the acceptable Test 8 configuration, for future testing. This rework involved dome cooling skirt relocation back to the dome centerline. Combustor inspection after rework disclosed that the dome contour had been drawn flat by repeated modifications (Figure 103). Internally, the inner diameter cooling skirt was shortened only in the areas where previous burning had occurred. Since earlier testing indicated that manufacturing tolerances can affect performance, the combustor was installed in the combustion rig to verify that performance had not changed. Previous rig problems were corrected. At design inlet conditions and an average discharge temperature of 2015°F, the pattern factor was 0.162. Metal temperatures on the inner and outer liner (Figure 104) were similar to the Test 8 configuration.

The predicted combustor life exceeds the 2500 hr program goal, as shown in Figure 105. This prediction is based on previous AiResearch experience with a wide range of combustors.

Based on Tests 8 and 11 results, combustion system development testing was concluded and, as noted on Table 19, required combustion system performance levels were demonstrated. Further, the demonstrated pattern factor of 0.162 was a significant

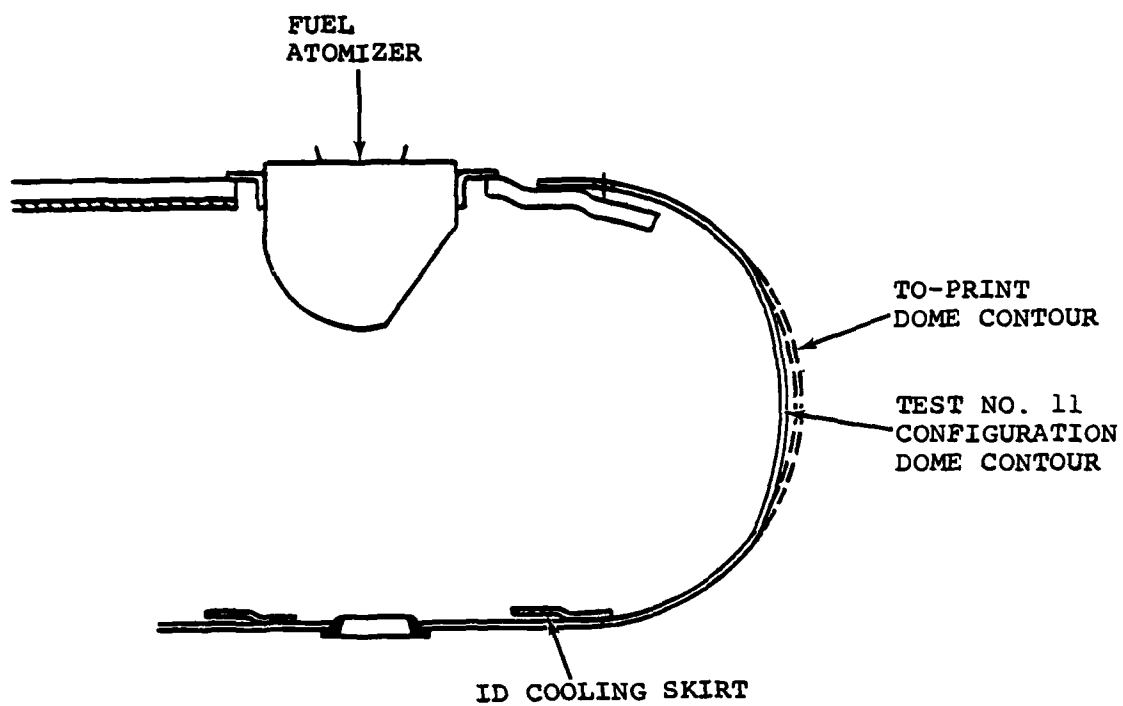


Figure 103. Pretest inspection of test no. 11  
combustor S/N 1



Figure 104. Test no. 11 Thermindex paint



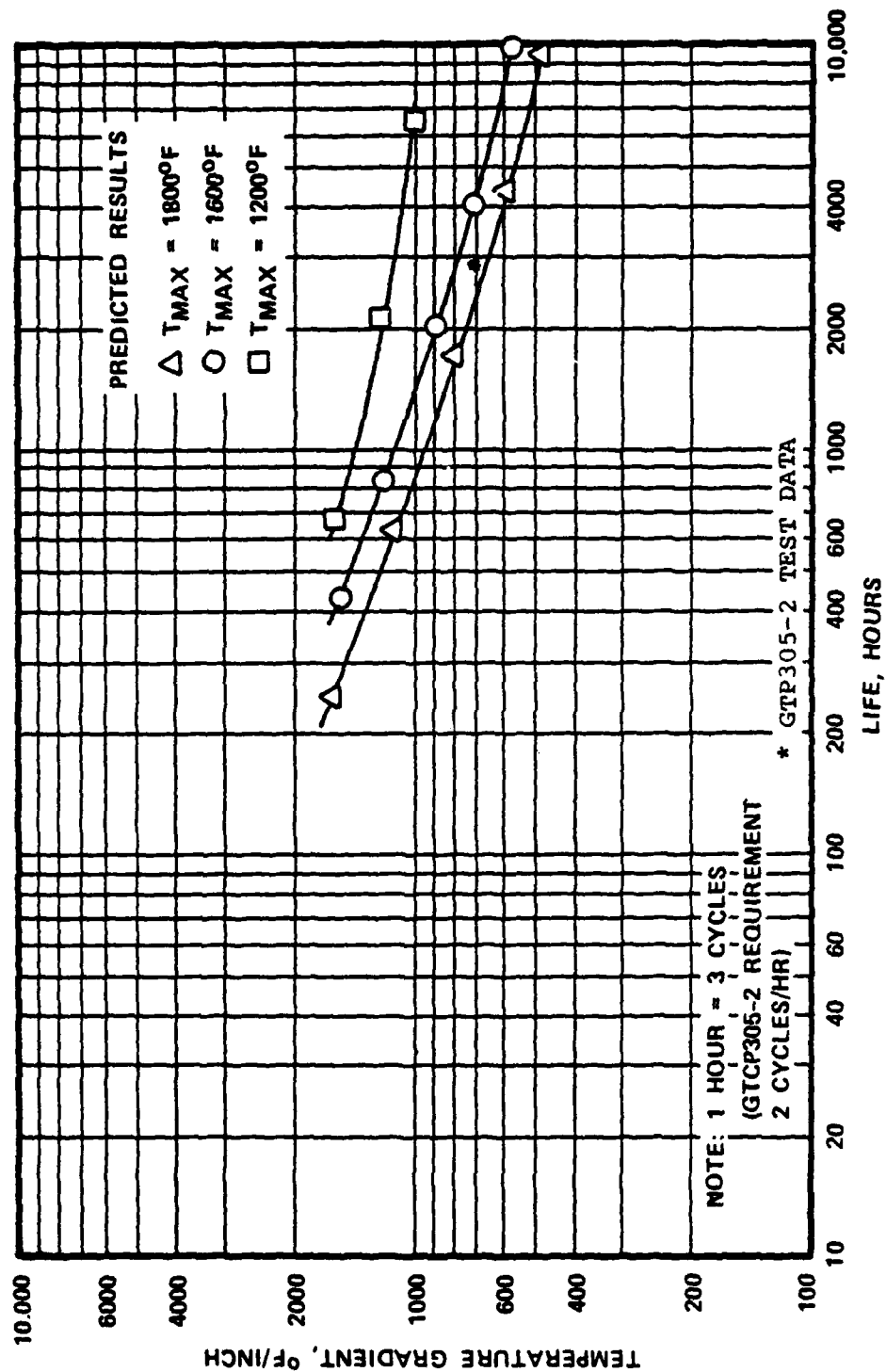


Figure 105. Combustor life versus temperature gradient for hastelloy-X

improvement over the allowable 0.216. Although further development could be conducted in an effort to achieve program goals, the Test 8 configuration is hereby recommended for use in the ICA Test Rig.

#### 4.2 Turbine Cold Air Testing

Turbine cold air testing was conducted for the GTP305-2 two-stage turbine. A complete final turbine design description was presented in Section 3.4. The turbine test program consisted of a radial nozzle flow calibration and the turbine tests described in Table 20. Table 21 contains the results of those tests.

Cold air test hardware aerodynamically duplicated engine geometry from the radial nozzle inlet to exhaust diffuser exit. Two specific aerodynamic design changes were incorporated, during rig testing, to compensate for cold operation. First, the rig radial nozzle B-width was increased to duplicate engine design corrected flow through the turbine rotors. This change was required because engine radial nozzle vane trailing edge cooling flow discharge holes were not incorporated for rig testing. The second change pertains to the axial turbine rotor. Although the cold rigs operated at the same corrected speed as the engine, cold rig physical speeds were considerably less. Since axial rotor blades tend to untwist with centrifugal force, cold rig axial rotor blades were subjected to less untwist due to a lower operating speed. Therefore, the cold rig axial rotor was fabricated with less blade twist, so that the throat areas at corrected design speed (i.e., engine and rig) were equal.

Two turbine test rigs (radial and radial/axial) were utilized during cold air turbine testing. Each rig is separately discussed below. In addition to testing, the radial turbine rig was used to statically flow the rig radial nozzle to obtain a

TABLE 20. GTP305-2 TURBINE COLD AIR TESTING

Test Number	Rig Configuration	Test Purpose	Test Conditions	
			Pressure Ratio (Total-Total)	Corrected Speed (Percent)
1	Radial only - design turbine clearances, no cooling flow	Determine radial turbine baseline performance	2:1 - 5:1	80 - 120
2	Radial only - 4 different backface clearances, 3 different backface cooling flows	Assess effect of back-face clearance and cooling flow rate on radial turbine performance	3:1 - 4:1	80 - 110
2A	Radial only plus axial turbine stator design turbine clearances	Determine interturbine duct performance and assess effect of inter-turbine seal buffering airflow	2:5 - 3:505	100
3	Full radial/axial- design turbine clearances, no cooling flow	Determine full stage turbine performance	5:1 - 10:1	80 - 120
4	Full radial/axial - design turbine clearances, design cooling flows	Assess the effect of secondary flows on full stage turbine performance	7:1 - 9:1	90 - 110

TABLE 21. SUMMARY OF GTP305-2 COLD TURBINE TESTING

PARAMETER	RADIAL TURBINE				RADIAL/AXIAL TURBINE			
	DESIGN GOAL	TEST 2 ①	TEST 1 ①	TEST 2A ①	TEST 3 ②	TEST 3 ③	TEST 4 ②	TEST 4 ③
TIN-OR (ROTOR INLET)	2509.7	740.66	740.8	725.94	895.49	-	896.99	-
W <sub>0</sub> /δ - LBS/SEC (ROTOR INLET)	0.615	0.625	0.625	0.625	0.622	-	0.621	-
N <sub>A</sub> θ - RPM	34407.8	34868.07④	34868.07	34837.63	34883.07④	-	34853.93	-
N - RPM	75,685	41665.7	41669.7	41213.6	45833.9	-	45833.9	-
P/PIT-T (RADIAL STAGE)	3.2415	3.505④	3.505	3.505	3.343	-	3.305	-
P/PIT-T (AXIAL STAGE)	2.1597	-	-	-	2.397	-	2.3908	-
P/PIT-T (OVERALL)	7.00	-	-	-	8.0	-	8.0	-
P/PIT-DE (OVERALL)	7.529	-	-	-	8.506④	-	8.506	-
T-T (RADIAL STAGE)	0.8847	0.8862	0.8857	0.8864	0.878	0.892	0.8825	0.894
T-T (AXIAL STAGE)	0.8909	-	-	-	0.891	0.8865	0.8917	0.8896
T-T (OVERALL)	0.896	-	-	-	0.895	0.894	0.904	0.902
T-DE (OVERALL)	0.871	-	-	-	0.876	0.876	0.886	0.884
INTERSTAGE DUCT LOSS ΔP/P	0.169	-	-	0.0145	0.011	-	0.0123	-
INTERSTAGE DUCT LOSS ΔP/P (1.0% BACKFACE + 1.5% INTERSTAGE COOLING FLOW)	-	-	-	0.0170	-	-	-	-
DIFFUSER RECOVERY R <sub>D</sub>	0.40	-	-	-	0.447	-	0.467	-
REYNOLDS NUMBER (RADIAL)	2.63X10 <sup>5</sup>	3.237X10 <sup>5</sup>	3.22X10 <sup>5</sup>	4.749X10 <sup>5</sup>	3.35X10 <sup>5</sup>	-	4.44X10 <sup>5</sup>	-
REYNOLDS NUMBER (AXIAL)	2.843X10 <sup>5</sup>	-	-	-	5.24X10 <sup>5</sup>	-	6.97X10 <sup>5</sup>	-
T-T CORRECTED TO DESIGN	-	0.885	0.885	0.885	0.893	-	0.901	-
REYNOLDS NUMBER (OVERALL)	-	-	-	-	-	-	-	-

① MEASURED CLEARANCES: RADIAL BACKFACE - 0.028 IN., RADIAL ROTOR RADIAL - 0.015 IN., RADIAL FRONTFACE - 0.013 IN.

② MEASURED CLEARANCE: RADIAL BACKFACE - 0.036 IN., RADIAL ROTOR RADIAL - 0.015 IN., RADIAL FRONTFACE - 0.025 IN., AXIAL ROTOR RADIAL - 0.011 IN.

③ CORRECTED CLEARANCE: RADIAL BACKFACE - 0.030 IN., RADIAL ROTOR RADIAL - 0.015 IN., RADIAL FRONTFACE - 0.025 IN., AXIAL ROTOR RADIAL - 0.015 IN.

④ TURBINE PRESSURE RATIO AND CORRECTED SPEED HAVE BEEN ADJUSTED TO SIMULATE DESIGN AERODYNAMIC CONDITIONS IN COLD AIR TURBINE TESTING DUE TO A CHANGE IN SPECIFIC HEATS RATIO, γ.

flow coefficient. This was accomplished without the rotor or bearing system in position, which allowed the nozzle to choke.

#### 4.2.1 Radial Turbine Test Rig

Radial turbine performance was evaluated by utilizing a modified cold air component test rig, as shown in Figure 106. The radial turbine rotor was overhung on a double spring-loaded, hydrodynamically mounted, ball bearing assembly.

The lower half of Figure 106 shows the radial turbine rig configuration used for radial turbine performance evaluation, Test 1, Table 21. This configuration incorporated air supply and flow control providing backface cooling air introduction (Flow Number 1, Figure 107), Test 2, Table 21. The upper half of Figure 106 shows this rig with the addition of the axial nozzle required for evaluation of interstage duct losses. This configuration also incorporated provisions for simulating inter-turbine seal buffering air (Flow Number 2, Figure 107).

#### 4.2.2 Radial/Axial Turbine Test Rig

The radial/axial turbine test rig, Figure 108 utilized the same inlet plenum, support housing, rig radial nozzle, rig radial rotor, and backshroud as the radial turbine rig configuration. The rotating assembly was a straddle mounted ball/roller bearing configuration. In addition to the radial turbine rig secondary flow provisions, the radial/axial turbine rig incorporated a flow supply and control for simulating axial turbine rotor front face cooling flow (Flow Number 3, Figure 107).

#### 4.2.3 Instrumentation

The turbine drive air flowed through a sonic measuring nozzle prior to entering the inlet plenum where it was straightened,

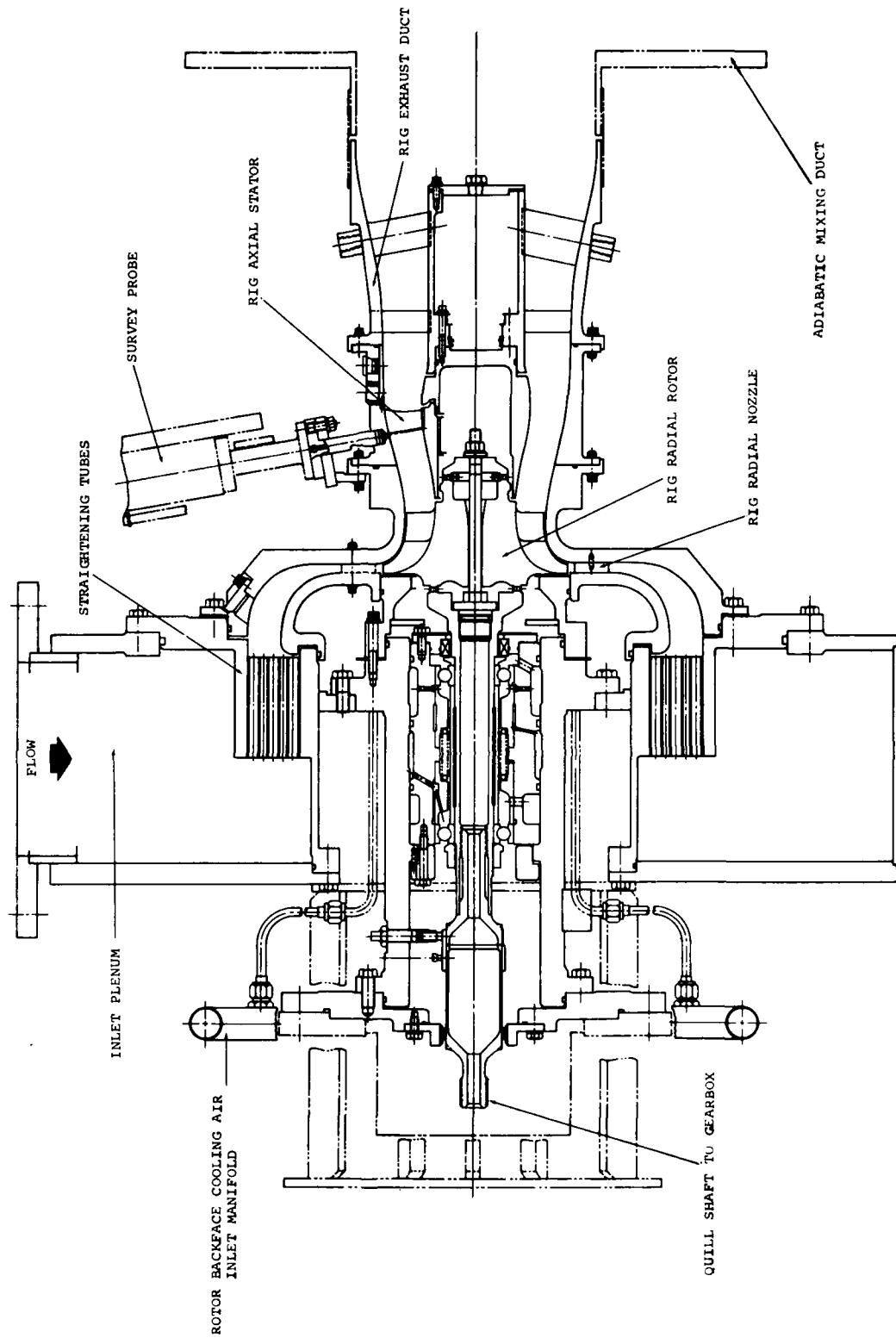


Figure 106. Radial turbine cold test rig

10-1071000-1

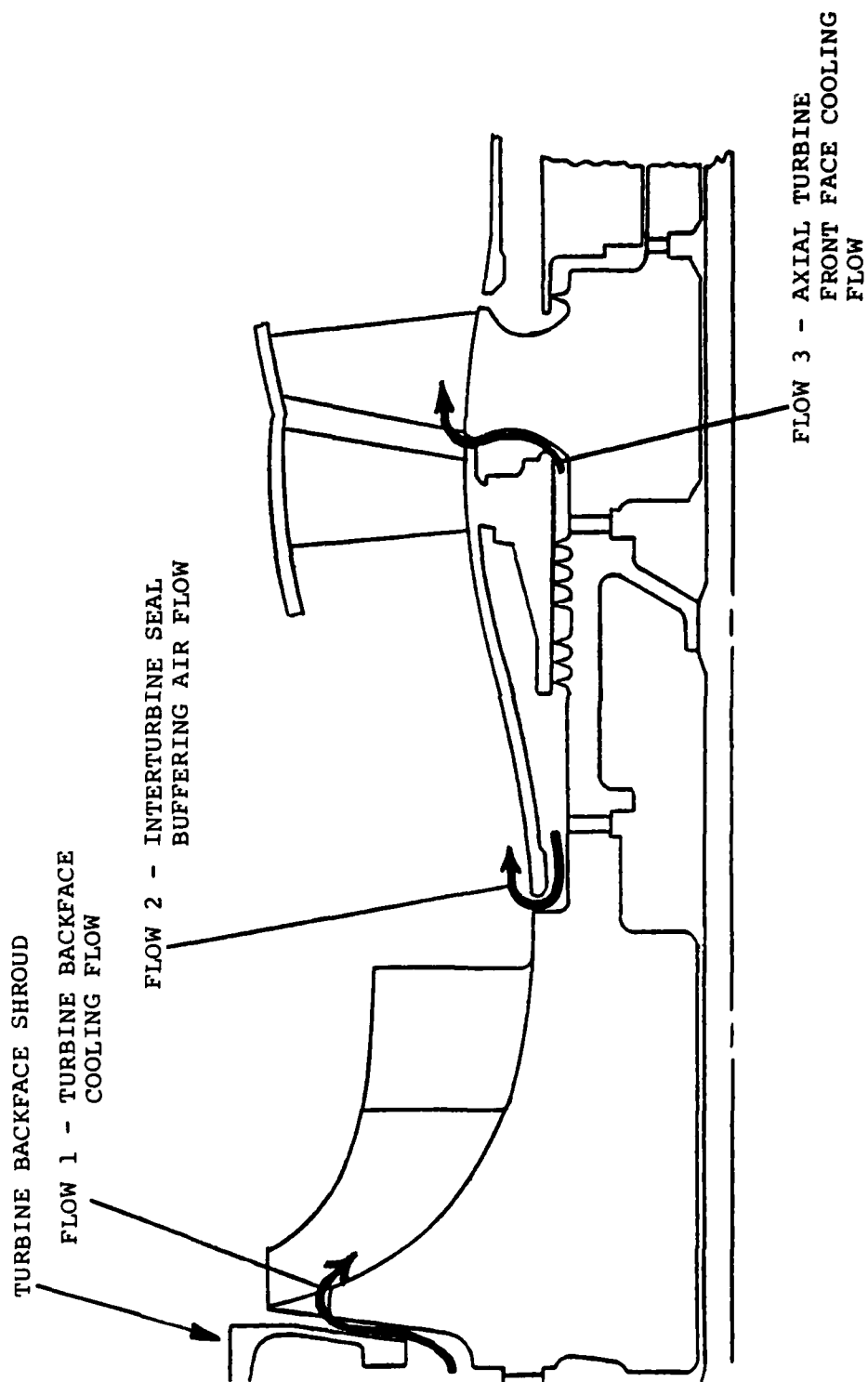


Figure 107. Turbine flow path secondary flows

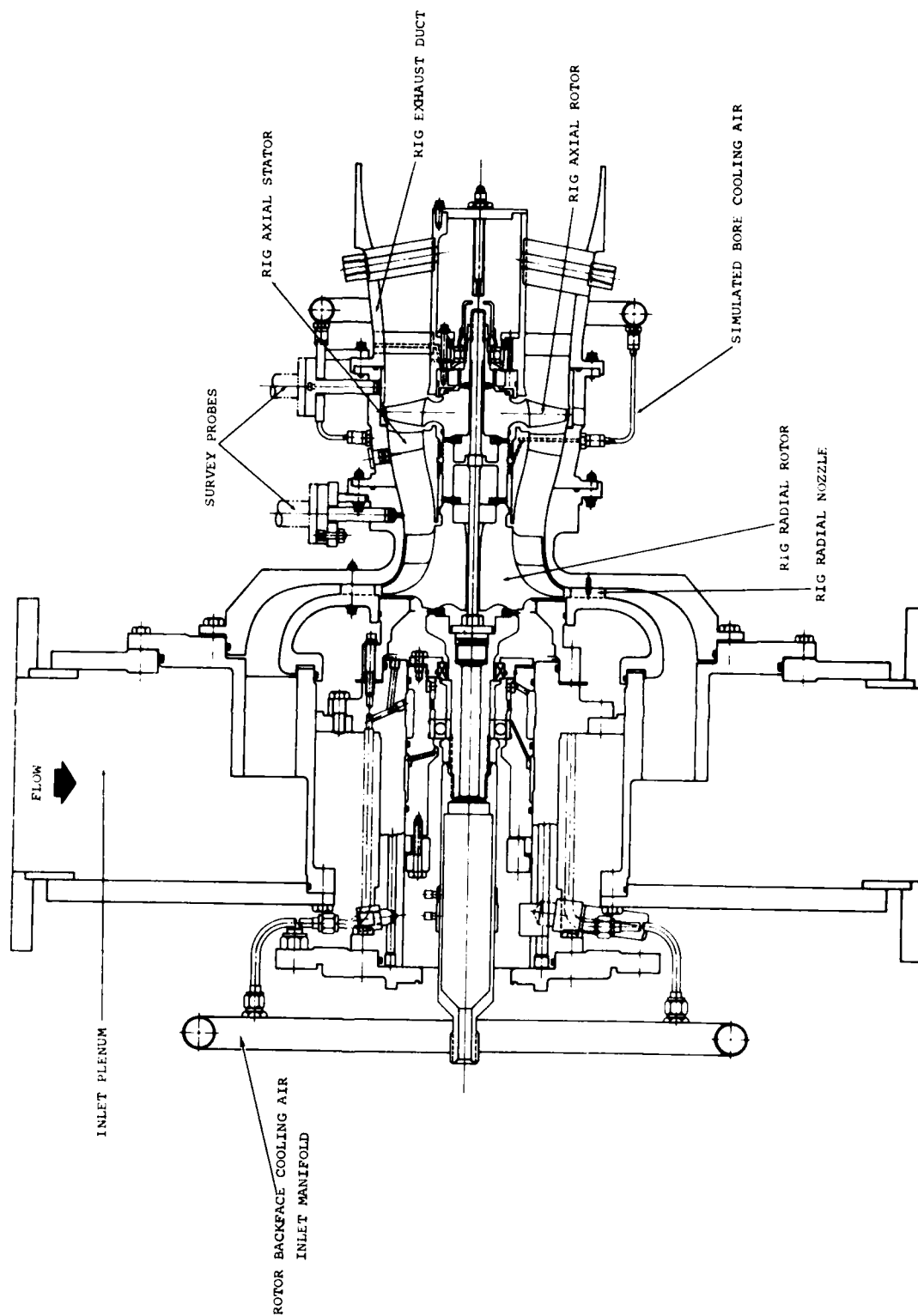


Figure 106. Partial axial cold turbine test rig



thus ensuring uniform delivery to the turbine inlet. Turbine inlet temperature and pressure were measured at the straightening section exit where relatively low velocity and uniform flow minimized error. Static pressure probes were located throughout the stage for comparison with design values. Capacitance probes were located at the radial turbine rotor inlet, exit, and backshroud planes and in the axial turbine rotor tip shroud. Running clearances were monitored throughout testing. Total, and static, pressure probes were located in the interturbine duct at the radial stage exit. Total pressure rakes were used to measure axial stator core flow conditions, which allowed evaluation of interturbine duct losses. Total and static pressure probes were utilized downstream of the axial stage, to determine overall two stage performance. Separate flowmeters were used for simulated backface cooling flow evaluation, Test 2, Table 21 and interturbine seal buffering air. In addition to fixed instrumentation, radial temperature, pressure, and flow angle surveys were obtained at two circumferential positions behind each rotor. An axial nozzle inlet survey was also obtained during Test 2A, Table 21. Exhaust temperature was measured in an adiabatic mixing duct downstream of the axial turbine stage.

To minimize temperature measurement errors due to heat loss to the environment, the test rigs were fully insulated. Turbine inlet temperatures were controlled to obtain an ambient turbine discharge temperature during test.

#### 4.2.4 Test Procedure

Prior to test rig assembly the rig radial nozzle, radial rotor (Figure 109), axial nozzle (Figure 110), and axial rotor (Figure 111) were inspected to determine any deviation from design intent. Deviations from design intent, based on throat area calculation were as follows:

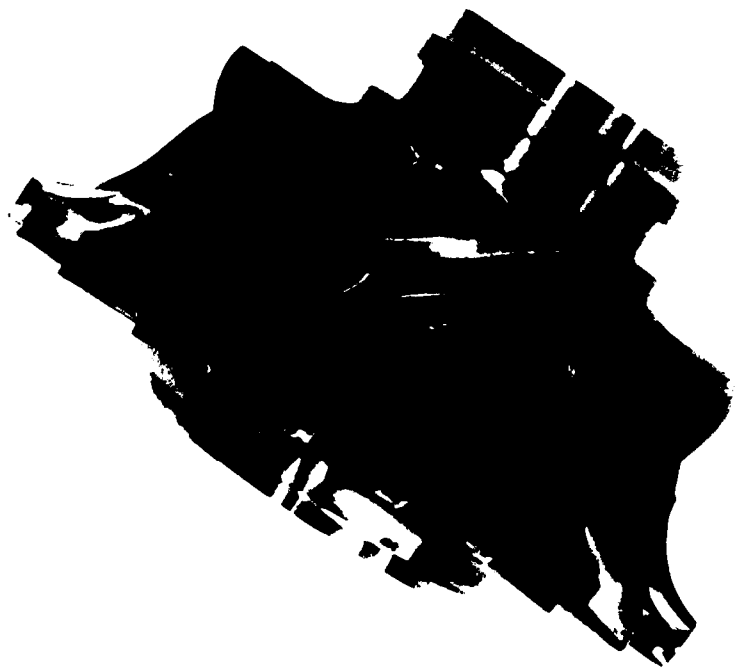


Figure 109. Rig radial turbine rotor



Figure 110. Rig axial nozzle



Figure 111. Rig axial rotor

- o Rig radial nozzle 1.08 percent closed
- o Rig radial rotor 1.25 percent closed
- o Rig axial nozzle 1.40 percent closed
- o Rig axial rotor 0.19 percent closed

Although the above noted hardware was not "nominal" all were considered within acceptable blueprint tolerances.

The turbine rig was mounted on the turbine component test rig dynamometer test stand. The test stand incorporated an inlet air system capable of blending air at desired test inlet temperature and pressure levels, 18.48:1 ratio reduction gearbox to reduce turbine speed consistent with the absorption dynamometers and hold test turbine speed within one-half of one percent of the set test point, and an adiabatic exhaust duct system to obtain an accurate discharge temperature. Airflow was measured by a flat plate orifice and a redundant choked nozzle in accordance with ASME power test codes. Steady state conditions were assured by visually monitoring a continuous recording device to ensure control of inlet and discharge temperatures. Vibration, rotor-shroud clearances, oil temperatures, quill shaft excursion, bearing temperatures and other parameters were continuously monitored during the test from a remote control console. All performance parameters were sampled using a high speed digital data acquisition system. This system, shown schematically in Figure 112, is capable of supplying corrected test data to the control console within thirty seconds after each sample scan.

#### 4.2.5 Test Results

Prior to dynamic rig testing, the machined radial nozzle was flow tested to evaluate maximum flow capacity. The nozzle flow calibration was run in the turbine rig with the rotor and bearing housing removed. A range of imposed inlet total-to-stator exit static pressure ratios was imposed across the nozzle until maximum flow was achieved. At choke conditions the measured stator

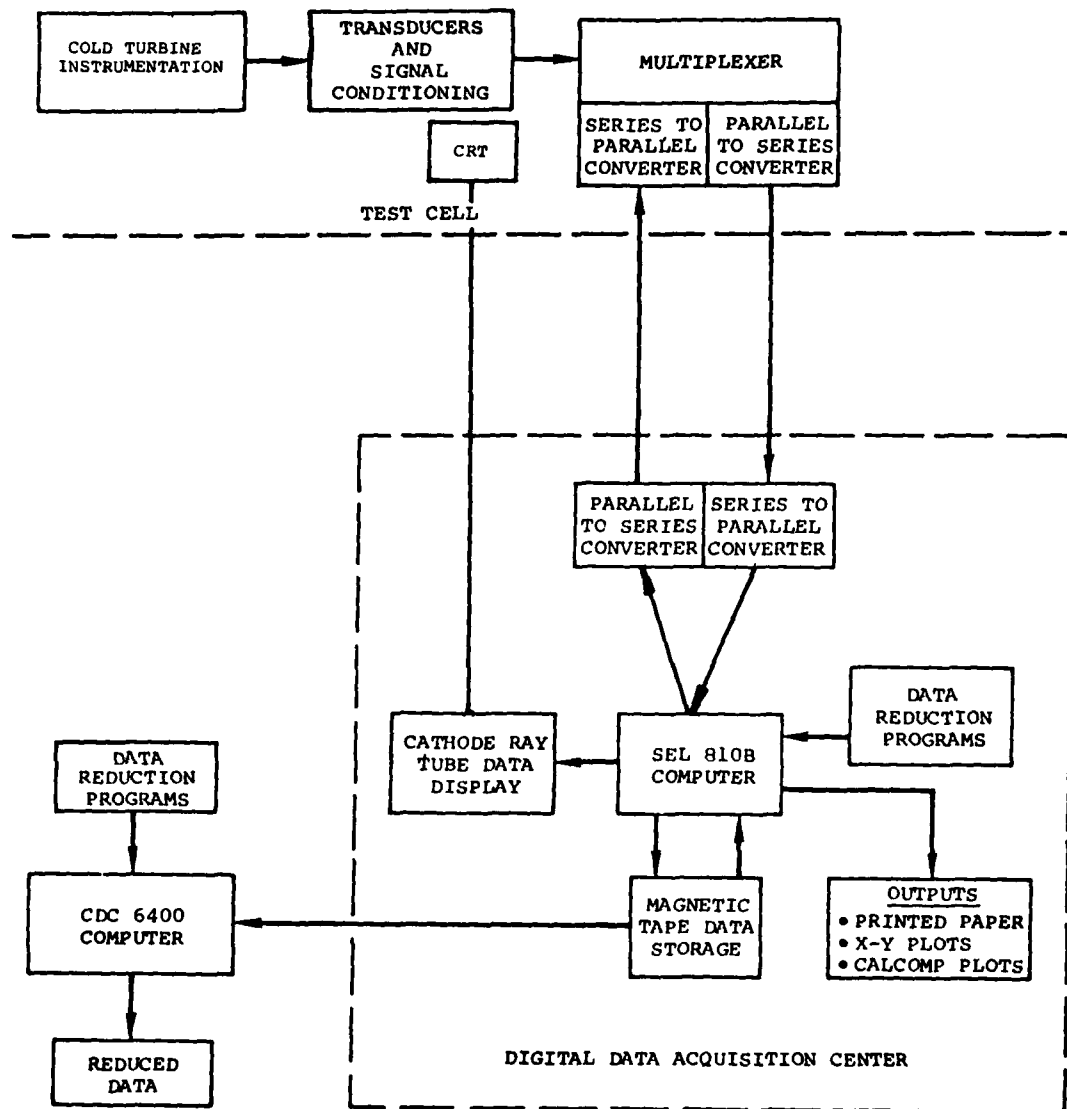


Figure 112. Digital data acquisition schematic

corrected flow was 0.6338 lbs/sec, which results in a nozzle flow coefficient of 0.990. This value is consistent with previous radial turbine nozzle characteristics.

As previously shown in Table 21, five tests were conducted in the following order:

- o Test No. 2
- o Test No. 1
- o Test No. 2A
- o Test No. 3
- o Test No. 4

#### 4.2.5.1 Test No. 2 Radial Only - Rotor Backface

Test No. 2 was conducted to establish the performance effects of rotor backface clearance and cooling flow on radial turbine performance. The matrix of test conditions evaluated are presented in Tables 22 and 23.

##### 4.2.5.1.1 Effects of Rotor Backface Clearance

The characteristics are presented in Figure 113 for the range of backface clearances tested. Figure 113 shows no appreciable change in clearance effects with inducer loading, but rather, the clearance effects appear to be a constant loss for each value of clearance tested. Note that as the clearance value increases, the efficiency characteristic tends to flatten out over the range of pressure ratios, indicating a higher constant loss with increasing clearance. Figure 114 shows turbine efficiency characteristics as a function of backface clearance at design corrected speed and pressure ratio. Figure 114 also shows that a minimum clearance of 0.030 inch is required to achieve the predicted efficiency of 88.5 percent ( $\eta_{T-T}$ ). Mechanical analysis indicate that this clearance level is feasible and a 0.030 inch backface clearance was defined as the design value.

TABLE 22. GTP305-2 COLD AIR TEST NO. 2 ROTOR BACKFACE  
CLEARANCE TEST PARAMETER MATRIX (WITHOUT  
BACKFACE COOLING FLOW)

Percent Corrected Speed		
90	100	110
	3.0 <sup>①</sup>	
3.505	3.505	3.505
	4.0	

① Identifies radial turbine overall total pressure ratio

NOTES:

1. Each test condition run with backface clearance of 0.010, 0.028, 0.039 and 0.082 inches.
2. "Cold Air" radial turbine test rig equivalent design overall total pressure ratio = 3.505.



TABLE 23. GTP305-2 COLD AIR TEST NO. 2 BACKFACE  
COOLING FLOW TEST PARAMETER MATRIX

Percent Corrected Speed		
90	100	110
3.505	3.505 <sup>①</sup>	3.505
3.505	3.505	3.505
3.505	3.505	3.505

① Identifies radial turbine overall total pressure ratio

NOTES:

1. Each test condition run with backface clearance of 0.010, 0.028, 0.039 and 0.082 inch
2. "Cold Air" radial turbine test rig equivalent design overall total pressure ratio = 3.505
3. Each test condition run with backface cooling flow rate of 1.5, 3.0 and 6.0 percent

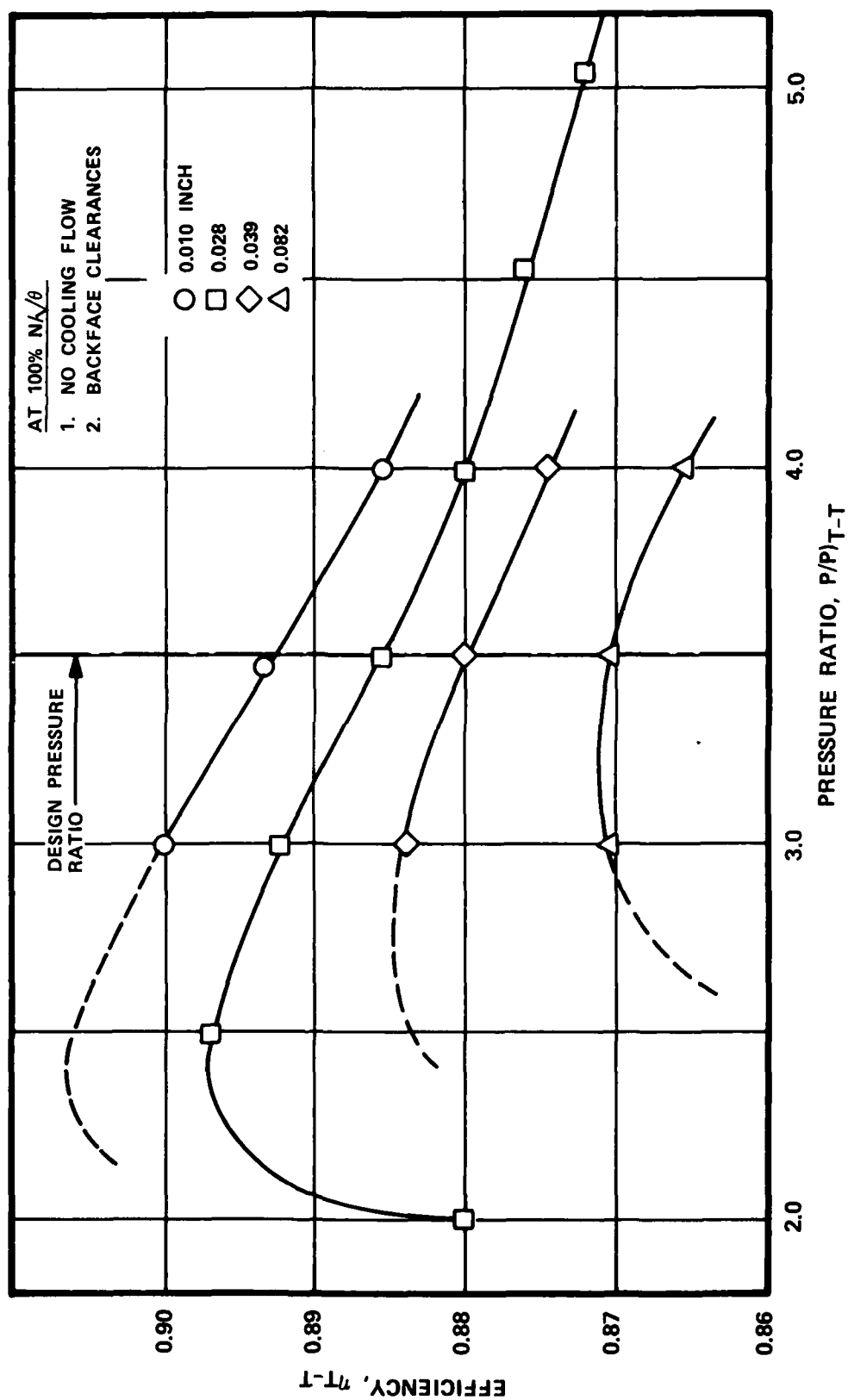


Figure 113. Effects of rotor backface clearance on peak efficiency GTP305-2 data

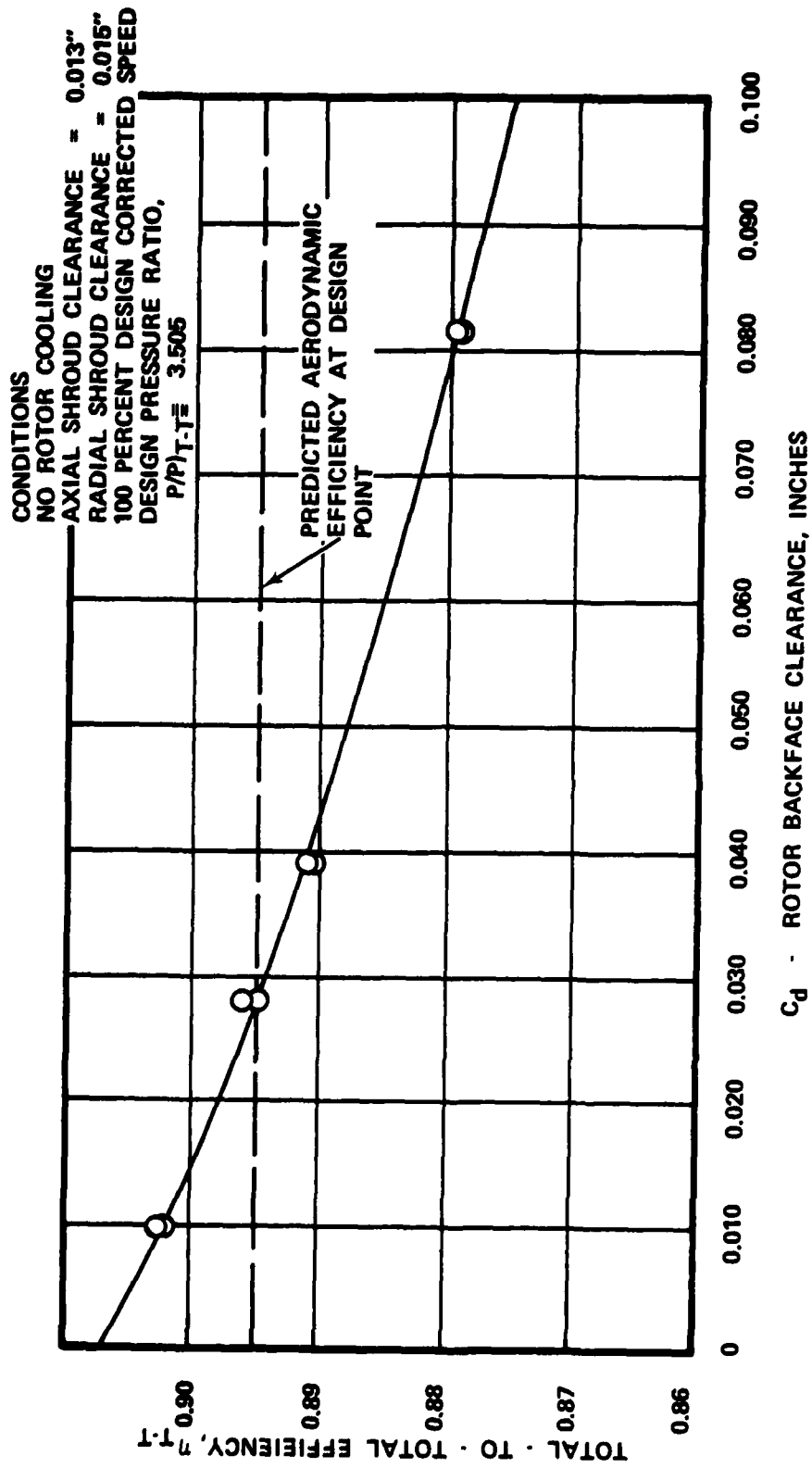


Figure 114. Variation of radial turbine efficiency with backface clearance with a constant scallop depth

#### 4.2.5.1.2 Effects of Rotor Backface Cooling Flow (Design Backface Clearance)

A range of cooling flows was run at design backface clearance to determine the penalty associated with pumping the cooling flow through the rotor. Backface cooling is required to prevent high temperature turbine inlet flow from recirculating on the rotor disk. Magnitude of the cooling flow required to prevent recirculation is based on compressor discharge conditions, backface clearance, and gas properties at the rotor scallop region. The predicted backface cooling flow rate is 1.5 percent. Prior to available data, the cooling flow penalty was based on the assumption that cooling flow entered the rotor scallop region and was entrained in the rotor inducer blade-to-blade secondary flow, exiting the rotor at the exducer tip. On this basis, the pumping penalty consisted of the work required to pump the cooling flow to the exducer tip radius ( $\frac{u_t^2 r_{tc}^2}{gJ}$ ).

Powder traces obtained by introducing Fuller's earth in the cooling flow passages (from a separate program) shows that the cooling flow does migrate to the exducer tip region. However, test data indicates that the cooling flow mixes with the mainstream flow and is not confined to the rotor blade boundary layer. Work done by the cooling flow, due to acceleration through the rotor plus the higher velocity of the mainstream flow in the throat region (due to the increased rotor flow), offsets the required pumping along the rotor backface. This conclusion is based on two methods of calculating turbine efficiency. The first method derives the turbine work based on the thermodynamic mixing of cooling and mainstream flows. The resultant expression is:

Reference (1)

$$\eta_{\text{cooled}} = \frac{(T_{\text{in}} - T_{3, \text{mix}}) + \frac{W_c}{W_p} (T_c - T_{3, \text{mix}})}{T_{\text{in}} \left[ 1 - \left( \frac{1}{Pr} \right) \frac{\gamma - 1}{\gamma} \right]}$$

The second method is based on calculating turbine work from the momentum equation by integrating rotor exit survey data and calculating the rotor inlet tangential velocity from on a constant stator loss coefficient obtained with no cooling. The resultant expression is:

Reference (2)

$$\eta_{\text{cooled}} = \frac{\frac{U_2}{g} \frac{Vu_2}{j_{cp}} + \left( \frac{W_p + W_c}{W_p} \right) \left[ \frac{U_3 Vu_3}{g j_{cp}} \right]}{T_{\text{in}} \left[ 1 - \left( \frac{1}{Pr} \right) \frac{\gamma - 1}{\gamma} \right]}$$

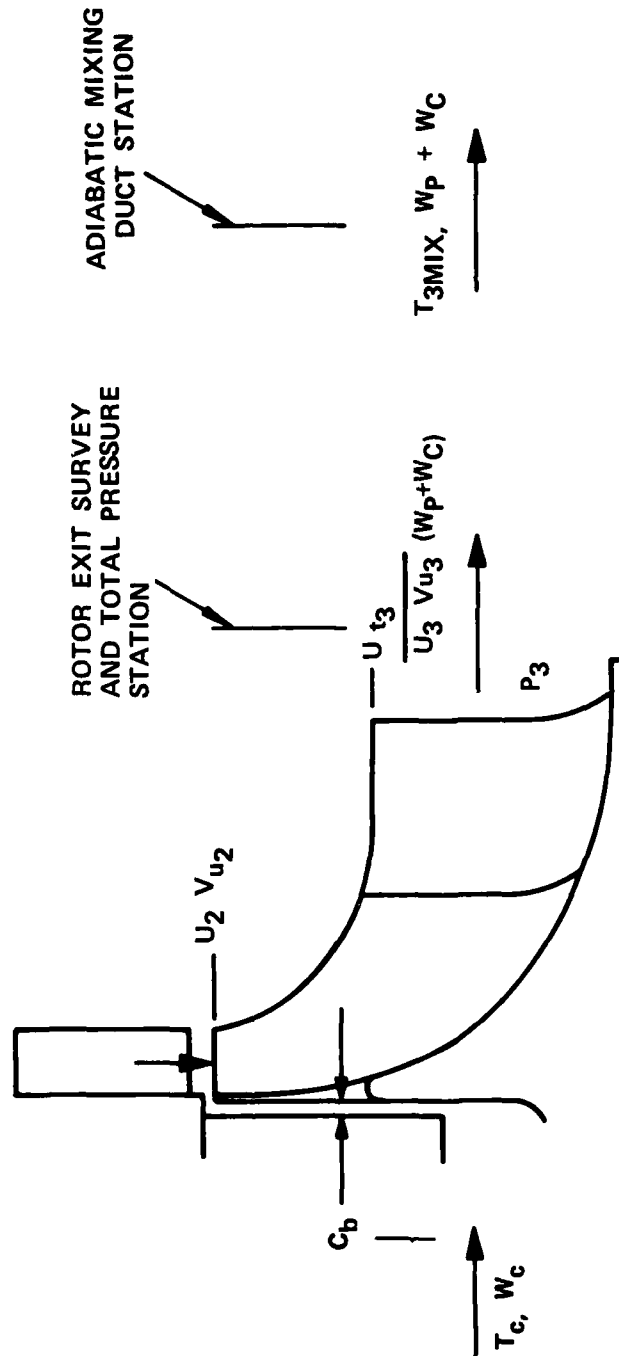
(See Figure 115 for Nomenclature)

Note that both cooled turbine efficiency definitions only consider the isentropic available energy of the primary flow ( $W_p$ ). For this reason the efficiency is not an aerodynamic efficiency but is for cycle purposes only.

Figure 116 shows the result of applying References (1) and (2) equations to a range of cooling flows at design speed and pressure ratio, 0.028 inch backface clearance, 0.013 inch axial face clearance, and 0.015 inch radial clearance.

- (1) Dovzhik, S.A., V.M. Kartavenko, "Measurement of the Effect of Flow Swirl on the Efficiency of Annular Ducts and Exhaust Nozzles of Axial Turbomachines," Fluid Mechanics, Soviet Research, Vol. 4, No. 4, July-August 1975.
- (2) Horlock, J.N., "Axial Flow Turbines," Butterworths London 1966, Figure 3.25, Page 108.

$V_{U2}$  = ROTOR INLET ABSOLUTE TANGENTIAL VELOCITY, T  
 $V_{U2}$  = ROTOR INLET ABSOLUTE TANGENTIAL VELOCITY, FT/SEC.  
 $V_{U3}$  = ROTOR EXIT ABSOLUTE TANGENTIAL VELOCITY, FT/SEC.  
 $T_{MIX}$  = ROTOR EXIT ADIABATIC MIXED TEMP, OR

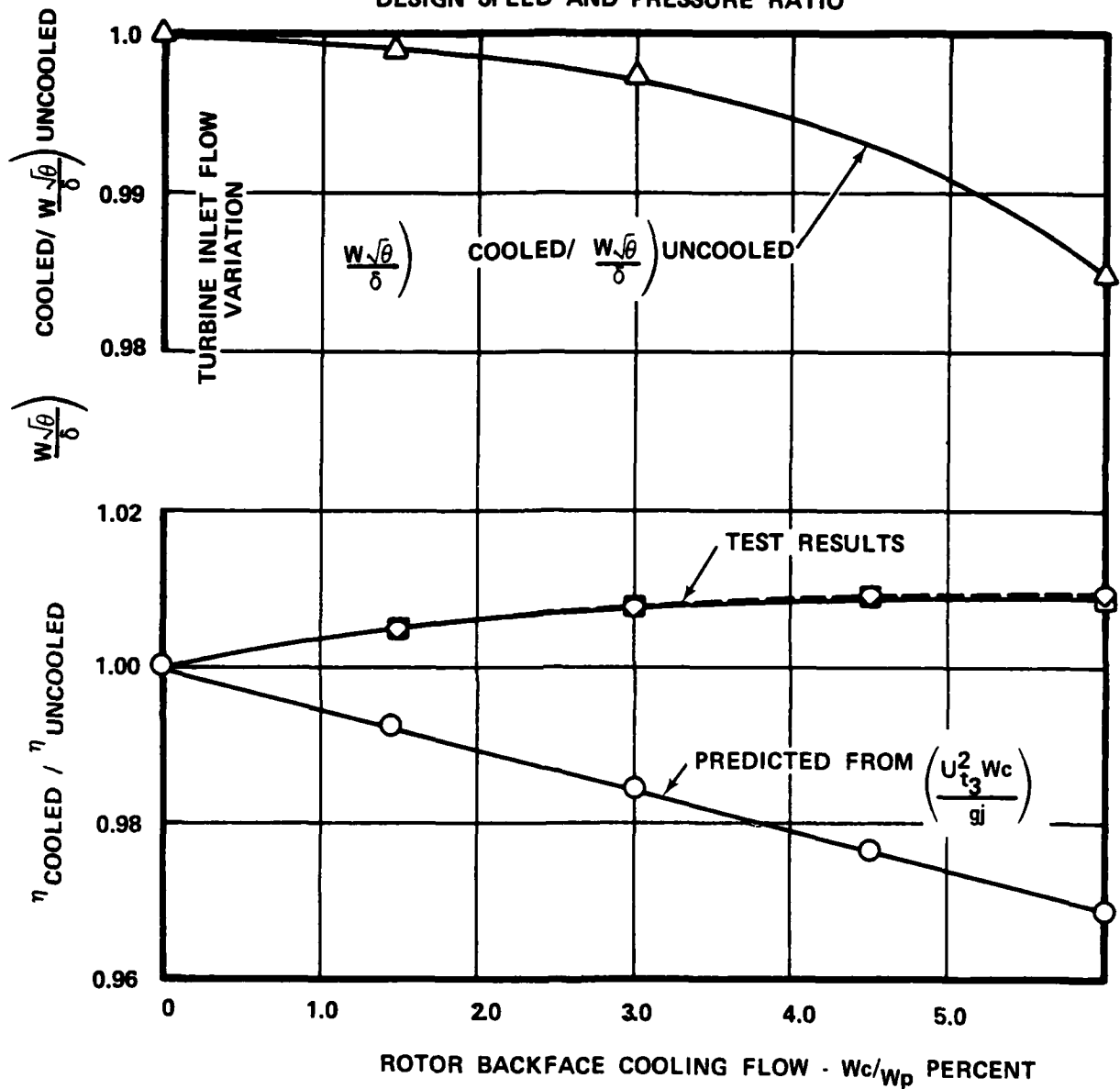


$T_{IN}$  = TURBINE INLET TOTAL TEMP., ° R  
 $W_P$  = TURBINE PRIMARY FLOW' LBS/SEC.  
 $T_C$  = BACKFACE COOLING FLOW INLET TOTAL TEMP., ° R  
 $W_C$  = BACKFACE COOLING FLOW, LBS/SEC  
 $C_b$  = ROTOR BACKFACE CLEARANCE, INCHES  
 $U_2$  = ROTOR INLET WHEEL SPEED, FT/SEC.  
 $U_3$  = ROTOR EXIT WHEEL SPEED, FT/SEC.

$U_3 V_{U3}$  = ROTOR EXIT MASS AVERAGE WORK FROM SURVEY DATA  
 $P_r$  = TURBINE TOTAL PRESSURE RATIO,  $P_{IN}/P_3$

Figure 115. Nomenclature for cooled radial turbine efficiency

GTP 305-2 TURBINE, TEST NO. 2  
DESIGN SPEED AND PRESSURE RATIO



- BASED ON EXDUCER TIP PUMPING
- BASED ON MIXING EQUATION
- ◇ BASED ON ROTOR EXIT SURVEY

Figure 116. Effects of rotor backface cooling on turbine performance

Results show that as the cooling flow rate is increased, there is a corresponding rise in turbine efficiency, compared with the uncooled value, and a corresponding decrease in turbine inlet flow, from back-pressuring the radial nozzle due to the higher flow through the rotor throat. On a first order basis it can be concluded that the increase in turbine efficiency is offset by the decrease in turbine flow. Thus, net turbine horsepower is unchanged.

However, from Figure 116 the significant trend is that no additional performance penalty to pump the cooling flow to the exducer tip speed is required, due to interaction of the cooling flow and mainstream flow in the rotor.

Examination of turbine characteristics at the design cooling flow rate of 1.5 percent indicates:

- o No decrement in turbine efficiency due to rotor back-face cooling flow pumping
- o That turbine inlet corrected flow is reduced by 0.09 percent
- o That total-to-total efficiency increased from 0.885 to 0.8894

The conclusion from Figure 116 is that the turbine aerodynamic performance map, obtained with no rotor backface cooling flow, is applicable with no additional performance decrement. However, since cooling flow bypasses the turbine inlet, the bypass cooling flow must still be accounted for in the cycle.



#### 4.2.5.2 Test No. 1 - Radial Only - Baseline Performance

Test No. 1 established the radial stage baseline aerodynamic performance over a range of speeds and pressure ratios with the following clearances:

- o Rotor axial shroud clearance of 0.013 inch
- o Rotor radial shroud clearance of 0.015 inch
- o Rotor backface clearance of 0.028 inch
- o No rotor backface cooling flow

The matrix of conditions used to establish baseline performance are presented in Table 24.

Measured turbine efficiencies, as a function of imposed pressure ratios, for 80, 90, 100, 110 and 120 percent of turbine design corrected speed, are presented in Figures 117 through 121, respectively. Measured corrected turbine inlet flow, as a function of imposed total-to-total pressure ratio and percent of turbine design corrected speed, is presented in Figure 122. Figure 119 shows measured total-to-total turbine efficiency of 88.5 percent, compared with the predicted efficiency of 88.47 percent, at equivalent design speed and pressure ratio. Figure 122 shows measured corrected turbine inlet flow at 0.625 lb/sec, compared with the design value of 0.615 lb/sec, at equivalent design speed and pressure ratio. Figure 123 compares the measured and predicted exit swirl angle distributions at design equivalent conditions. The comparison shows that the predicted swirl distribution was achieved. Variance near the shroud is attributable to rotor clearance effects.

TABLE 24. GTP305-2 COLD AIR TEST NO. 1 MAP MATRIX  
(NO ROTOR BACKFACE COOLING FLOW).

Percent Corrected Speed					
	80	90	100	110	120
Total-to-Total Pressure Ratio	2.0	2.0	2.0		
	2.5	2.5	2.5	2.5	
	3.0	3.0	3.0	3.0	3.0
	3.505	3.505	3.505	3.505	3.505
	4.0	4.0	4.0	4.0	4.0
		4.5	4.5	4.5	4.5
			5.0	5.0	5.0

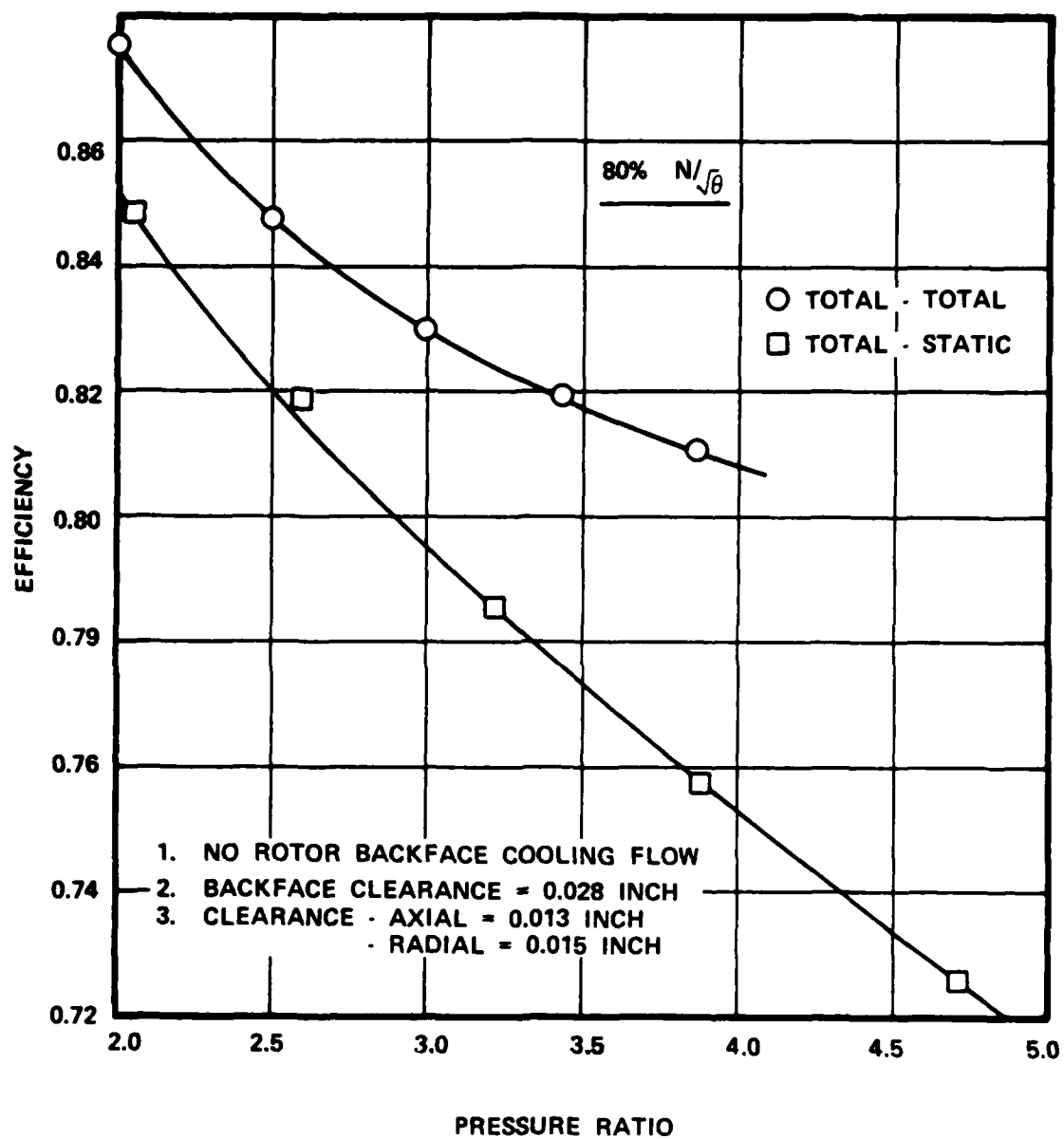


Figure 117. GTP305-2 radial turbine  
test no. 1

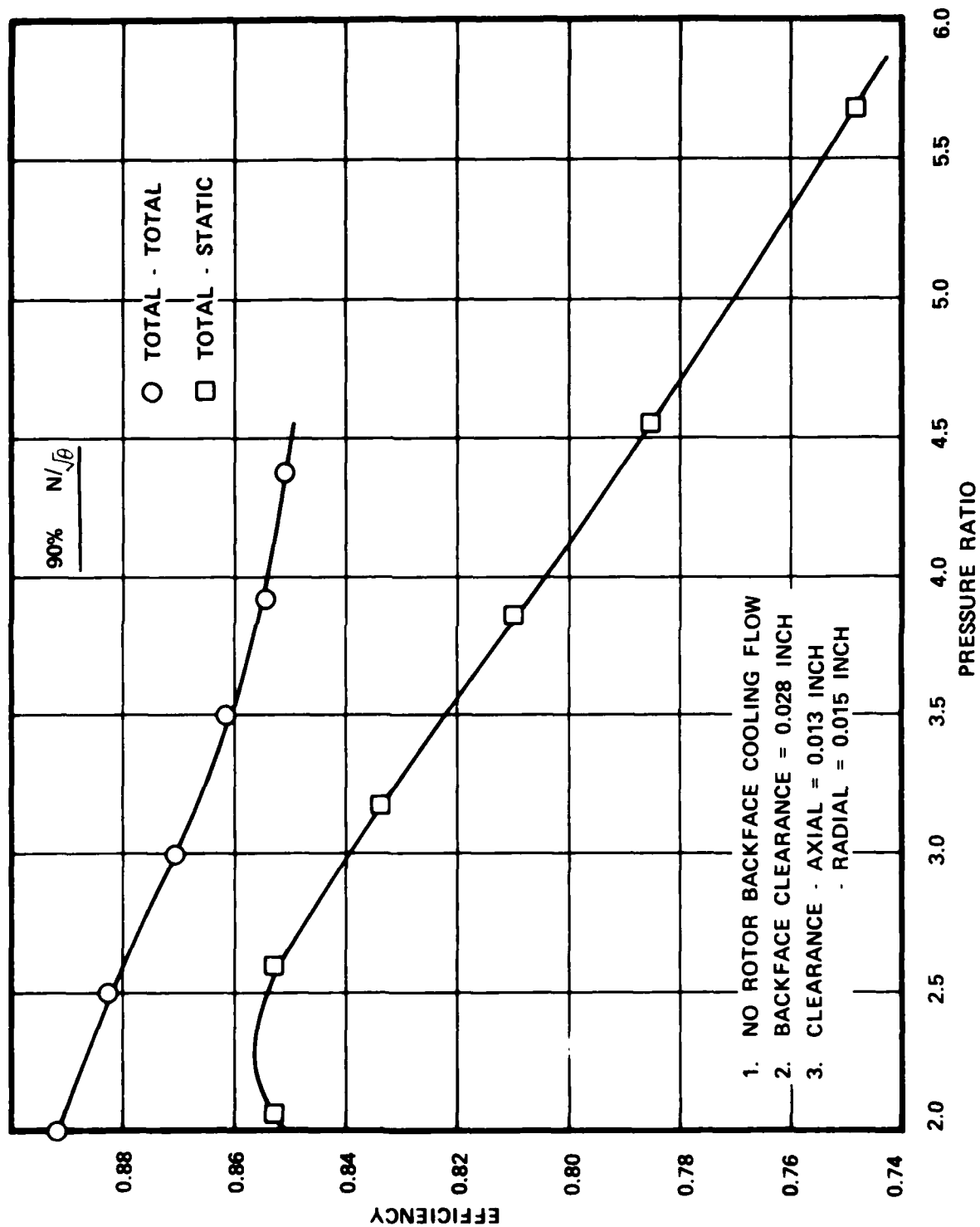


Figure 118. GTP305-2 radial turbine test no. 1

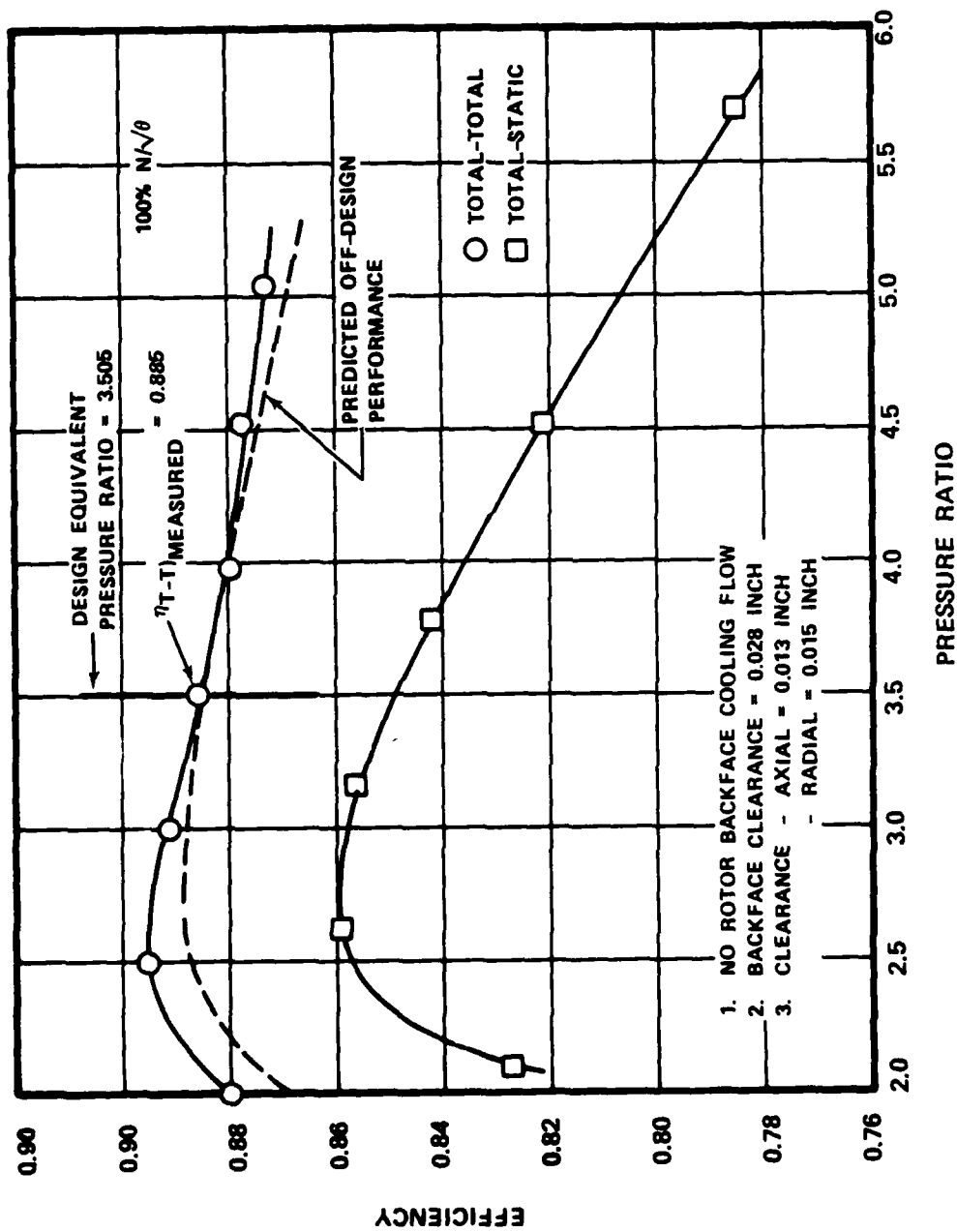


Figure 119. GTP305-2 radial turbine  
test no. 1

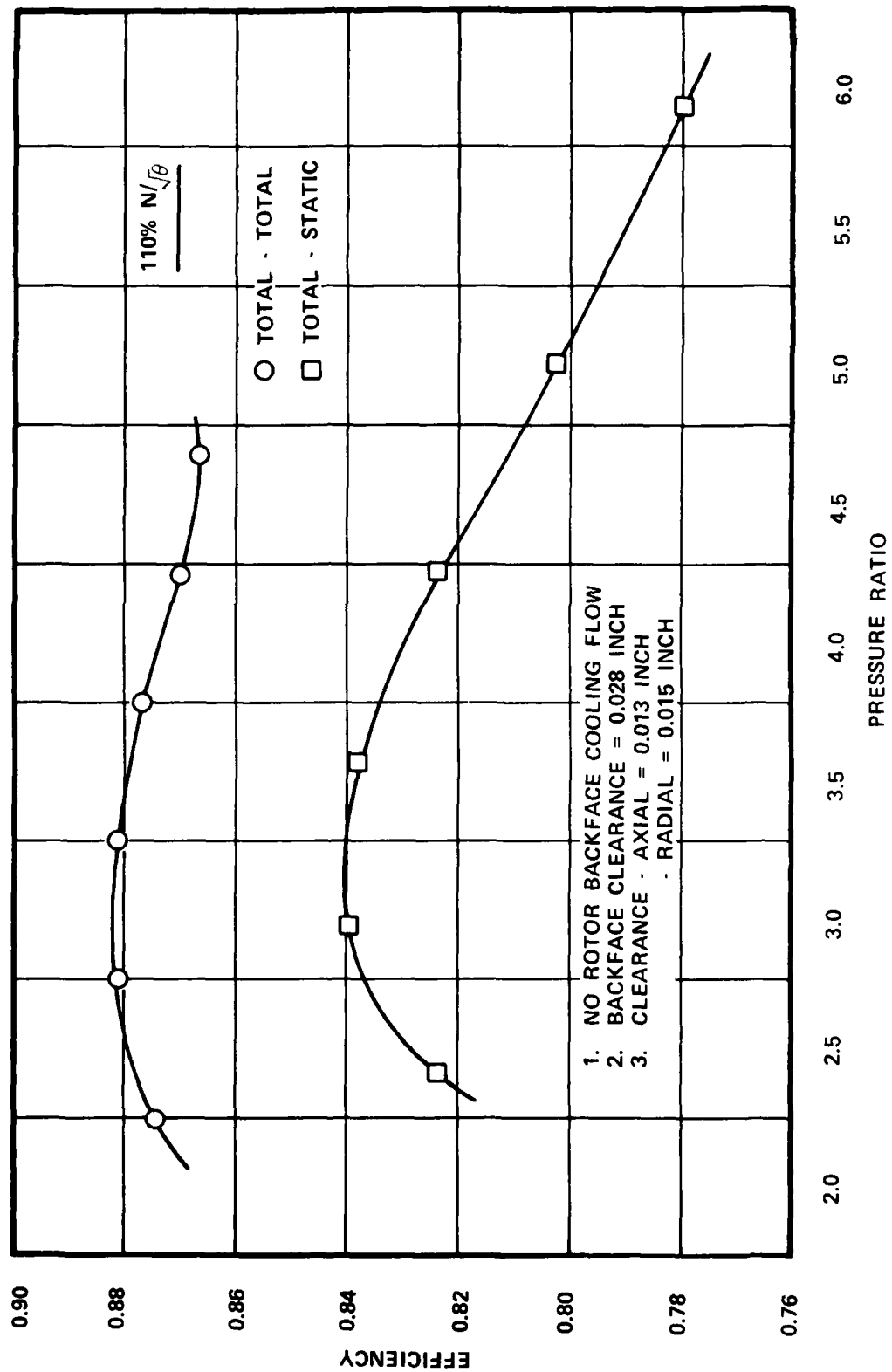


Figure 120. GTP305-2 radial turbine test no. 1

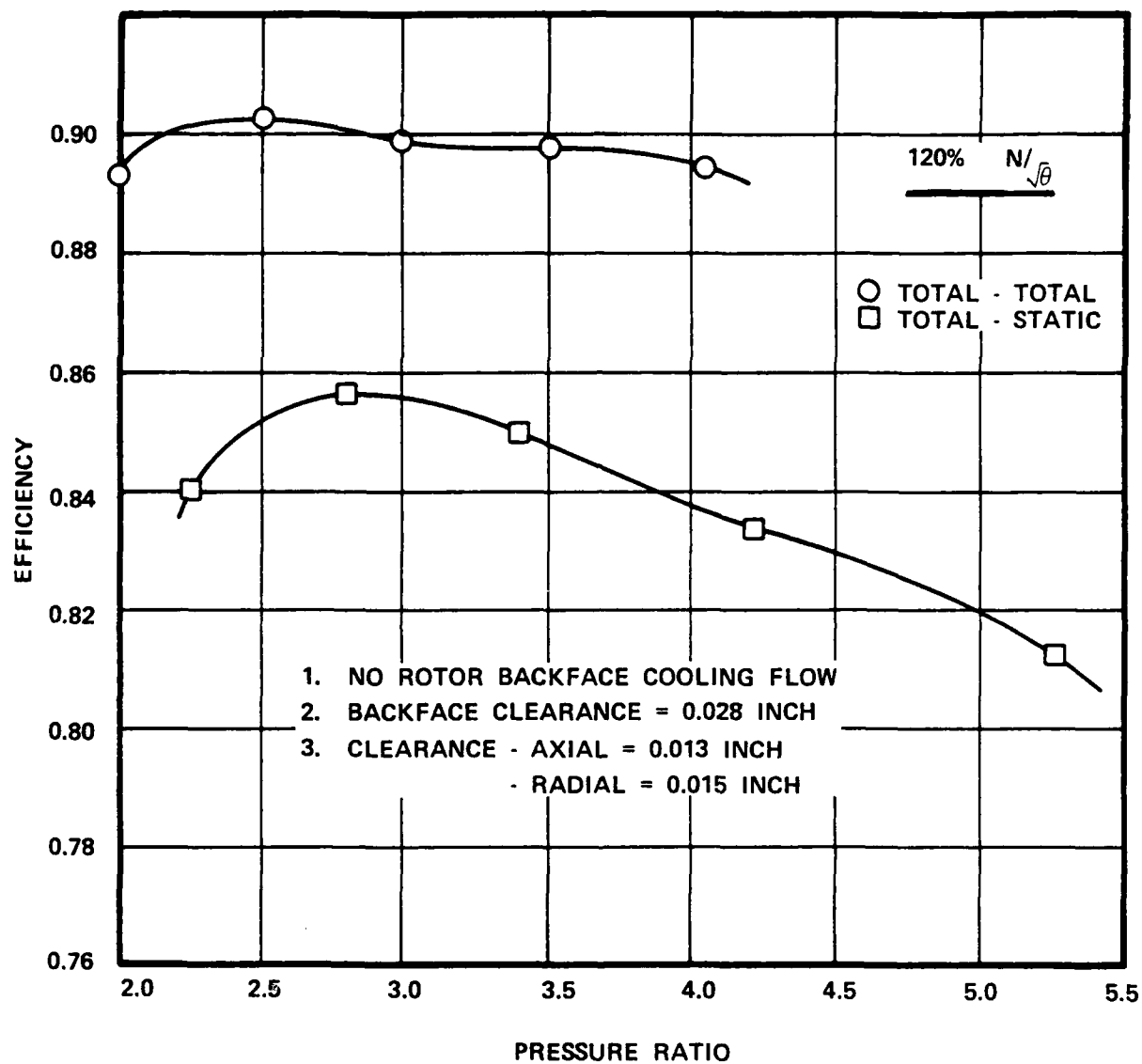


Figure 121. GTP305-1 radial turbine  
test no. 1

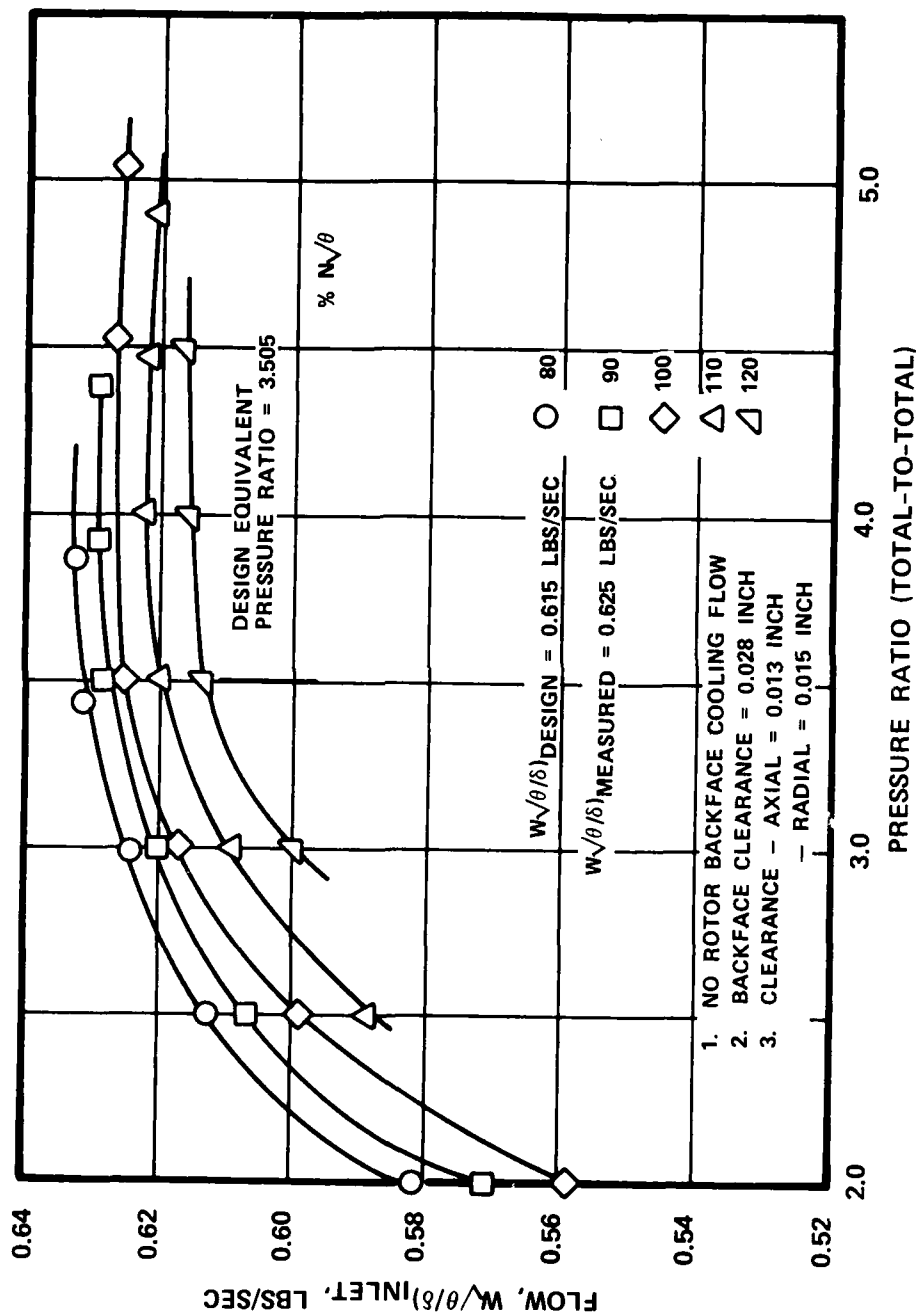


Figure 122. GTP305-2 radial turbine  
test no. 1



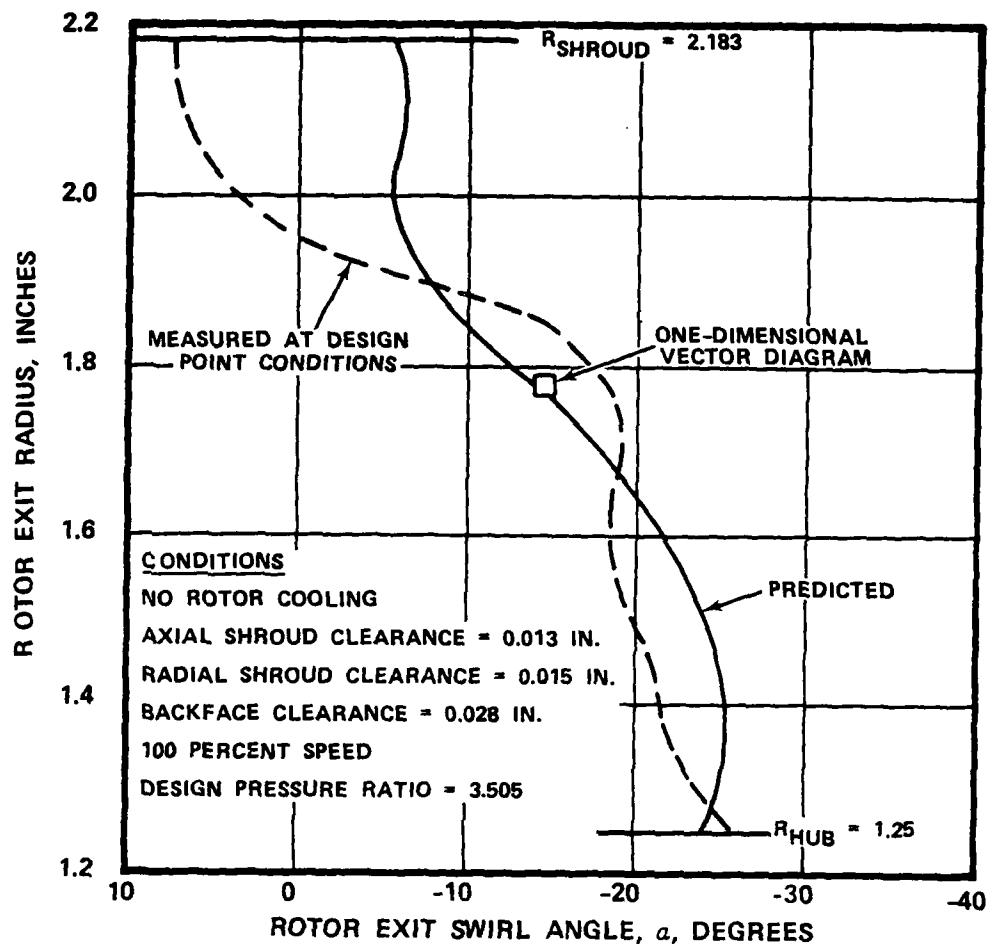


Figure 123. GTP305-2 radial turbine exit flow conditions

#### 4.2.5.3 Test No. 2A - Radial Only Plus Interstage Duct

Test 2A determined the interturbine duct loss at design radial turbine corrected speed over a range of pressure ratios with and without cooling flows (rotor backface cooling flow and simulated bore cooling flow). Test 2A was run with the following clearances:

- o Rotor axial shroud clearance of 0.013 inch
- o Rotor radial shroud clearance 0.015 inch
- o Rotor backface clearance of 0.028 inch

The matrix of conditions used to establish interturbine duct loss is presented in Table 25.

Instrumentation remained the same as that used during Tests 1 and 2, except for addition of the following:

- o Interturbine duct hub and shroud static pressure sensors
- o Interturbine duct (axial stator inlet) survey probe
- o Two - 6-element total pressure rakes located at the axial stator exit

Methodology used for determining interturbine duct loss was based on a comparison of the radial rotor exit total pressure and the axial stator exit total pressure rakes. Stator exit core total pressure was recorded by positioning the axial stator rakes at mid-passage between the stator vanes, which is equivalent to stator inlet total pressure. A redundant measuring system (i.e., stator inlet survey probe), provided verification of rake positioning and data validity.

TABLE 25. GTP305-2 RADIAL TURBINE RIG TEST 2A  
INTERTURBINE DUCT TEST MATRIX.

Test Condition	Percent Corrected Speed	Total-to-Total Pressure Ratio		
No Cooling Flow	100.0	2.5	3.0	3.45
1.0 Percent Rotor Backface Cooling Flow	100.0	2.5	3.0	3.45
1.0 Percent Rotor Backface Cooling Flow Plus 1.5 Percent Interstage Buffer Air Cooling Flow	100.0	2.5	3.0	3.37

Figure 124 presents the total pressure distribution measured from the stator exit rakes, superimposed with the stator inlet survey trace, for no cooling flow. At maximum attainable radial turbine pressure ratio, agreement between these data was less than desired. This lack of agreement was attributable to stator over expansion, which induces stator exit shock waves originating in the hub region that propagate to the shroud, as stator exit pressure is further reduced. In an effort to eliminate this problem, the rakes were reshimmed closer to the trailing edge, and expansion across the stator was controlled to the design exit Mach number. Although these adjustments resulted in a significant improvement, interference with the stator trailing edge region was still observed. For this reason, interturbine duct losses were determined, using the stator inlet survey system, by integrating the measured radial pressure distribution.

Using the survey data, duct loss data for Test 2A is presented, as a function of radial turbine total-to-total pressure ratio, in Figure 125. At radial stage design equivalent total pressure ratio of 3.505, test results indicate the following:

- o Uncooled interturbine duct loss ( $\Delta P/P$ ) is 1.45 percent
- o With 1-percent backface cooling flow, duct loss is 1.5 percent
- o With 1-percent backface cooling flow plus 1.5 percent simulated bore cooling flow, duct pressure loss is 1.70 percent

Note that closing the axial stator throat area 1.4 percent reduces the pressure ratio across the radial stage from 3.508 to approximately 3.45, with no cooling flow, and to 3.37 with both cooling flows. Figure 125 further illustrates that duct losses are relatively insensitive to the introduction of cooling flows.

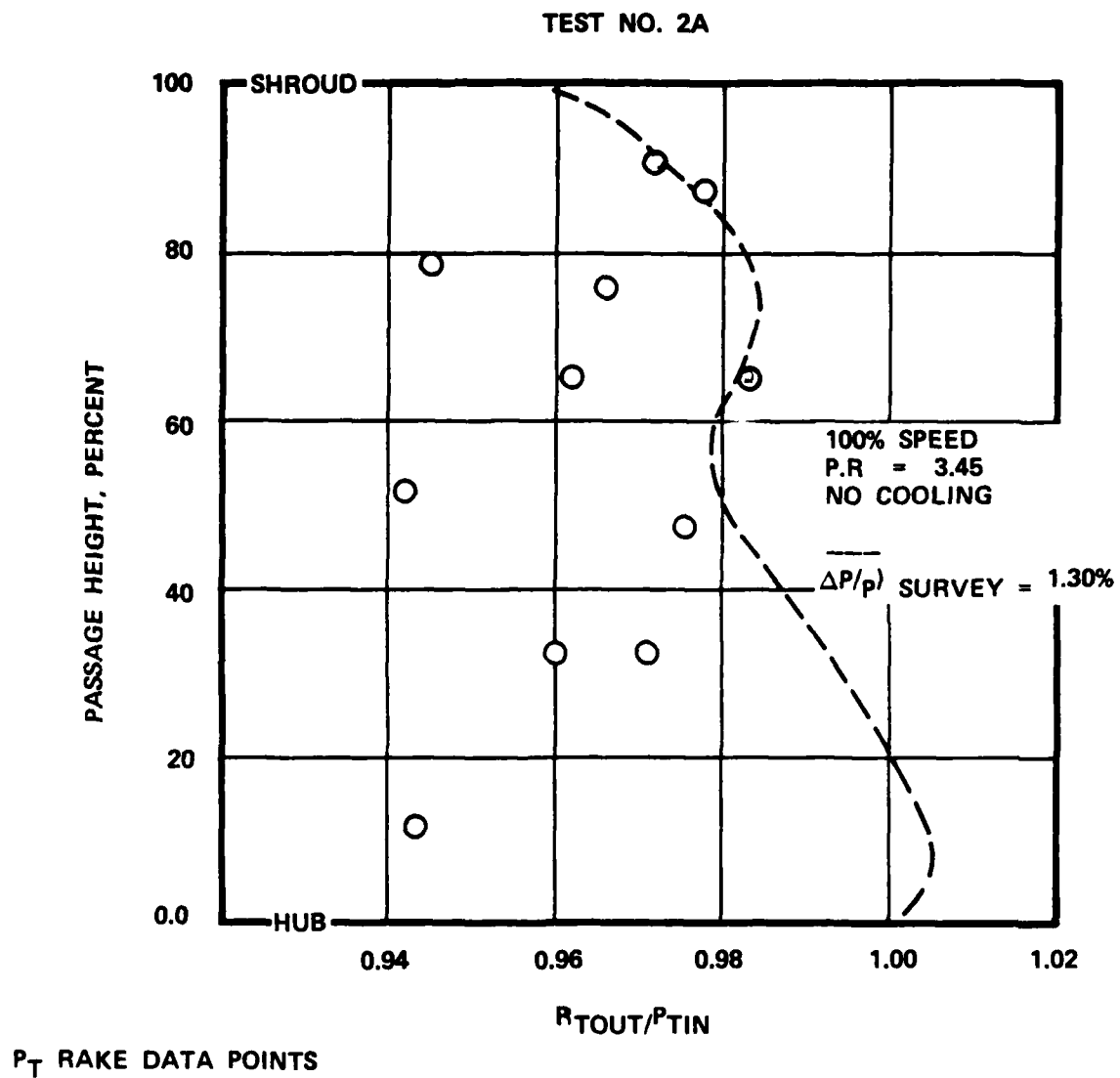


Figure 124. GTP305-2, comparison of duct exit total pressures

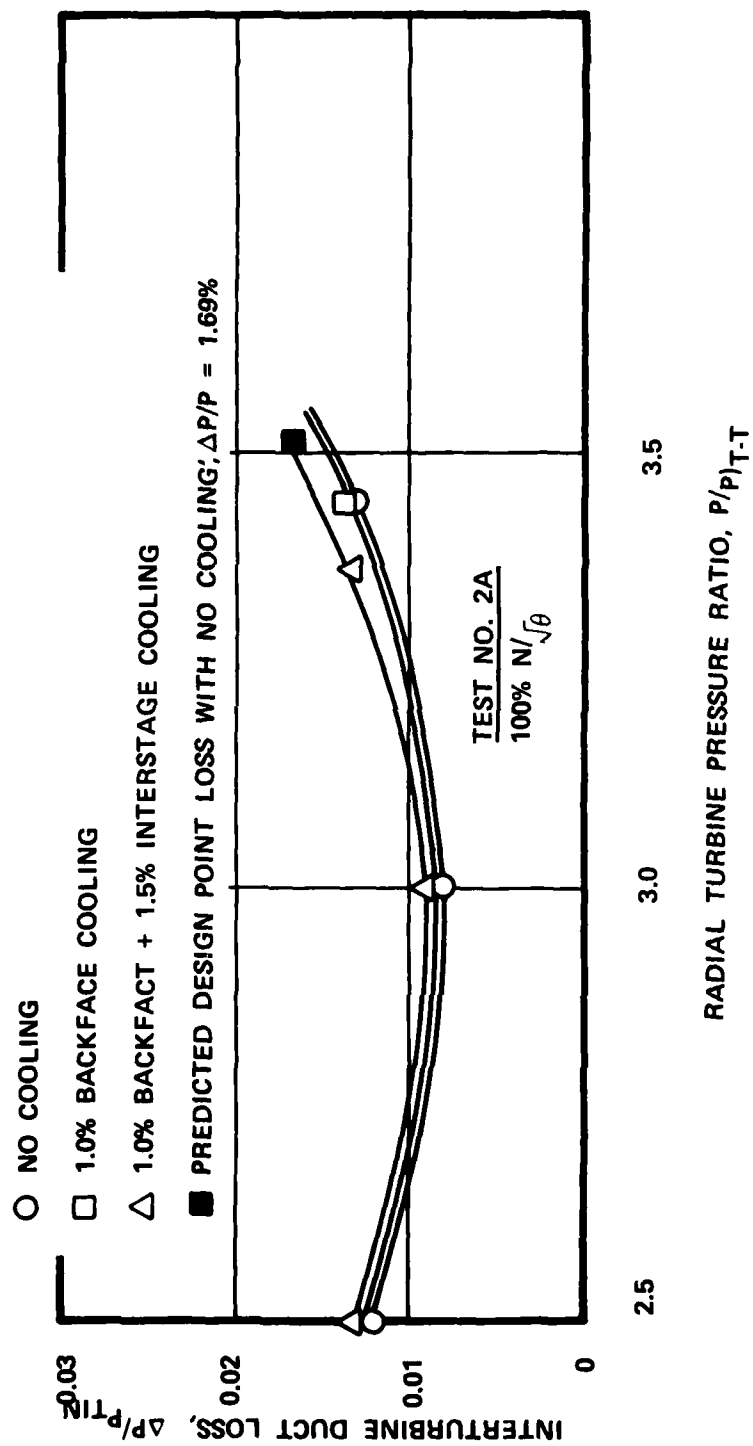


Figure 125. GTP305-2 interturbine duct loss analysis

In Figure 125, note that minimum duct losses occur at a pressure ratio of 3. The increase in duct loss from 3 to higher pressure ratios, is due to higher radial rotor exit velocities, and larger gradients in radial total pressure, which result in higher mixing losses. The increase in duct losses from a pressure ratio of 3 to lower pressure ratios is attributable to another phenomena (i.e., the level of duct inlet, rotor exit swirl). At pressure ratios of 3 and 2.5, duct inlet swirl is approximately 9 and 30 degrees, respectively. Reference (1) shows that the duct loss coefficient is minimum at approximately 11-degrees inlet swirl and increases rapidly above 25 degrees. This is in general agreement with the behavior shown in Figure 125.

Axial stator inlet flow angle radial distribution, at design pressure ratio, is presented in Figure 126. Although good agreement was achieved in mid-channel, the hub and shroud regions depict an approximate 10 degrees negative incidence. However, a condition lower than design swirl (negative incidence) effectively reduces the required stator turning and generally results in slightly reduced stator losses [Reference (2)].

#### 4.2.5.4 Analysis of Reynolds Number Effects of the Radial Turbine Performance

Magnitude of stator and rotor frictional losses is directly related to the Reynolds number of the working fluid passing through the turbine. Since a cold air test implies a drastic change in turbine inlet temperature, the turbine inlet pressure level must be adjusted to achieve similarity between engine and rig turbine Reynolds numbers. For a given turbine pressure ratio, this usually requires an exit pressure adjustment to sub-atmospheric levels. This is accomplished in the rig with a

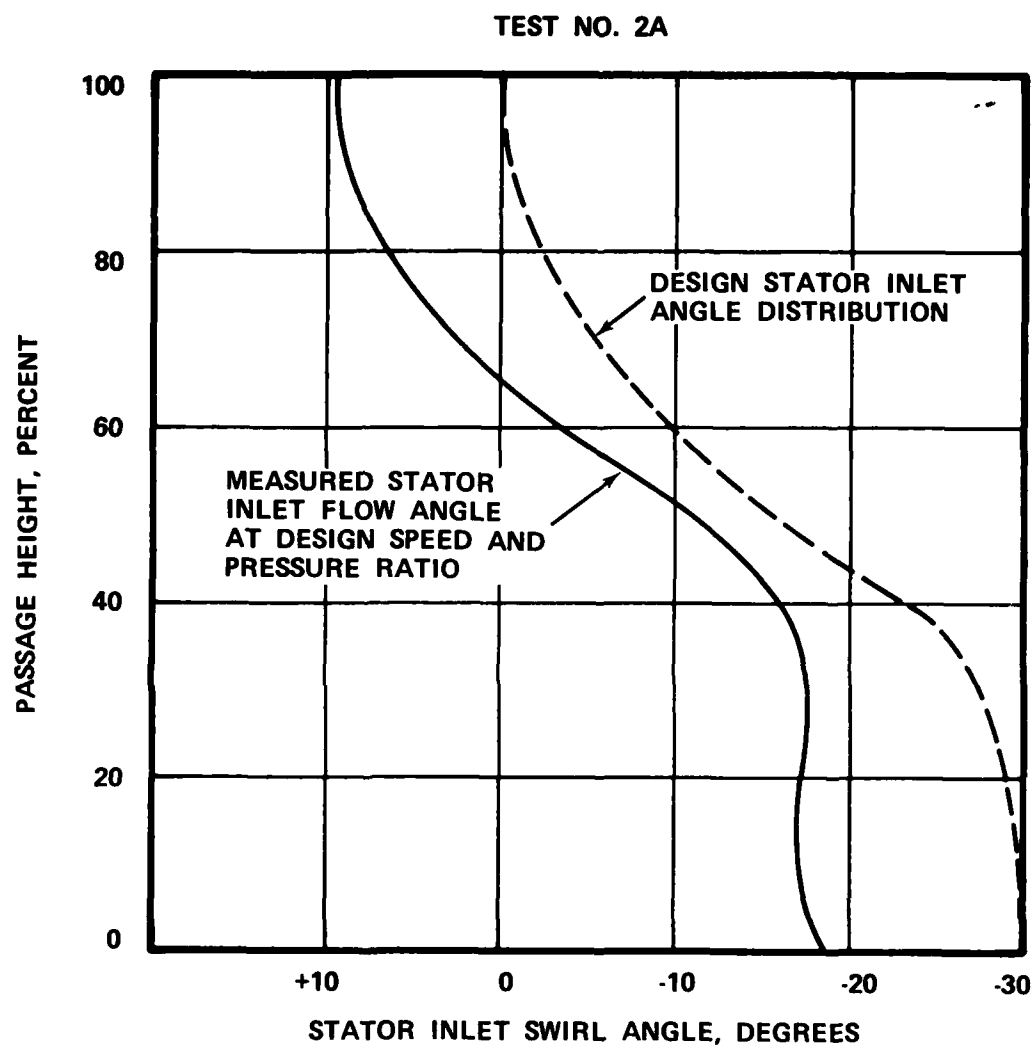


Figure 126. Axial stator inlet angle distribution



vacuum system connected to the turbine exhaust. NASA [Reference (3)] examined the effect of Reynolds number on radial turbine performance. The experimental results are presented in Figure 127. The Reynolds number shown in Figure 127 is defined as:

$$Re = \frac{Wg}{R_t \mu}$$

Where:

$Wg$  = Turbine physical flow, lbs/sec

$R_t$  = Rotor inducer tip radius, ft

$\mu$  = Absolute viscosity, lbs/sec-ft

The calculated Reynolds number for Test 1 at design point condition and no cooling flow is 3.22 times  $10^5$  compared with the engine Reynolds number of 2.625 times  $10^5$ . From Figure 127 the change in turbine efficiency from rig to engine is minus 0.0007 points. The average rig efficiency, based on averaging all data scans at the design point, is 0.8860. Therefore, engine radial turbine efficiency is maintained at the quoted value of 0.885.

#### 4.2.5.5 Test 3 - Aerodynamic Performance Without Cooling Flow

Test 3 established the overall two-stage baseline aerodynamic performance over a range of speeds and pressure ratios. The matrix of conditions used to establish the baseline performance is presented in Table 26.

- (3) Nusbaum, W.J., C.A. Wasserbauer, "Experimental Performance Evaluation of a 4.59-Inch Radial-Inflow Turbine Over a Range of Reynolds Number," NASA TN D-3835.

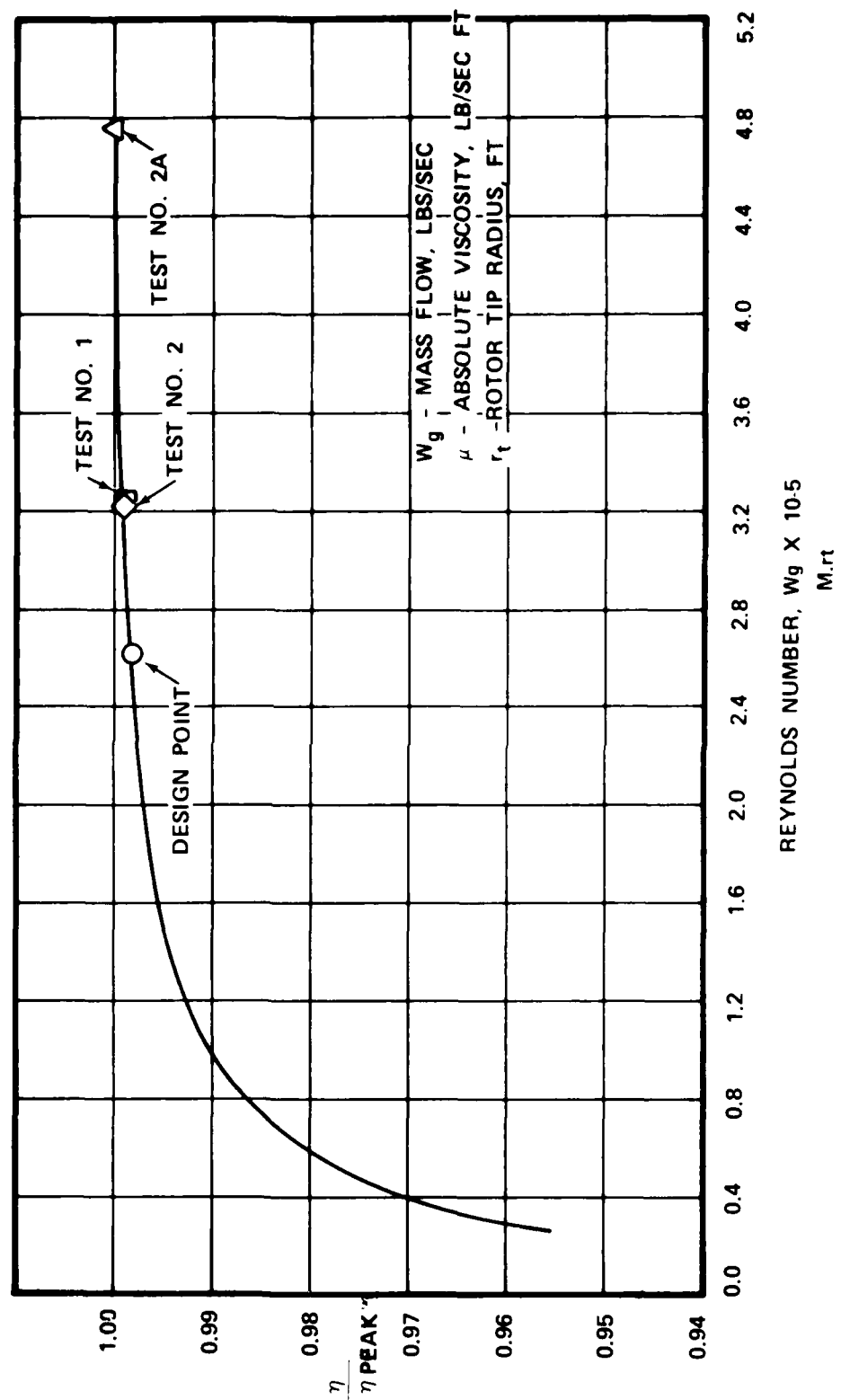


Figure 127. NASA calculations for radial turbines

TABLE 26. RADIAL-AXIAL TURBINE BASELINE  
PERFORMANCE MAP MATRIX  
(NO COOLING FLOW).

TEST NO. 3

Total-To-Total Overall Pressure Ratio	Percent Corrected Speed				
	80	90	100	110	120
	5.0	5.0	5.0	5.0	---
	6.0	6.0	6.0	6.0	---
	7.0	7.0	7.0	7.0	7.0
	8.0	8.0	8.0	8.0	8.0
	9.0	9.0	9.0	9.0	---
	10.0	10.0	10.0	10.0	---

Measured uncooled turbine performance, as a function of imposed pressure ratio, for 80, 90, 100, 110 and 120 percent turbine corrected speeds is presented in Figures 128 through 132, respectively. At design equivalent speed and pressure ratio, the measured total-to-diffuser exit static efficiency is 0.876, compared with the design goal of 0.871 (Figure 130). Correcting the measured performance to design clearance and Reynolds number results in a design point efficiency ( $\eta_{T-DE}$ ) of 0.876. The measured clearances are compared to the design values in Table 27. The variation of performance with Reynolds number is presented in Figure 133 for the axial turbine. The axial turbine correlation shown in Figure 133 is based on a curve match of test data from NASA TMX-9 and shows the tested and design values.

#### 4.2.5.6 Test 4 - Radial Axial With Cooling Flows

At the conclusion of Test 3, the effects of engine secondary cooling flows on turbine performance were investigated. Cooling flow circuits duplicate the engine configuration, and consist of radial rotor backface cooling flow (1.5 percent) and interstage buffer seal cooling flow (1.5 percent). The interaction of these cooling flows with the mainstream flow is shown in Figure 134.

The test matrix for Test 4 is presented in Table 28.

Overall two-stage turbine performance, with cooling flow, was determined from a thermodynamic heat balance between the mainstream and secondary cooling flows. The cooled turbine "efficiency" is based on a value consistent with current cycle methods of bypassing cooling flow and calculating turbine horsepower based on radial rotor inlet flow only (an exception is the radial nozzle vane internal cooling flow, which is not bypassed in cycle calculations). On this basis, any additional mass flow from the rotor backface cooling and interstage buffer air seal, which is available to do work in the downstream axial stage, need

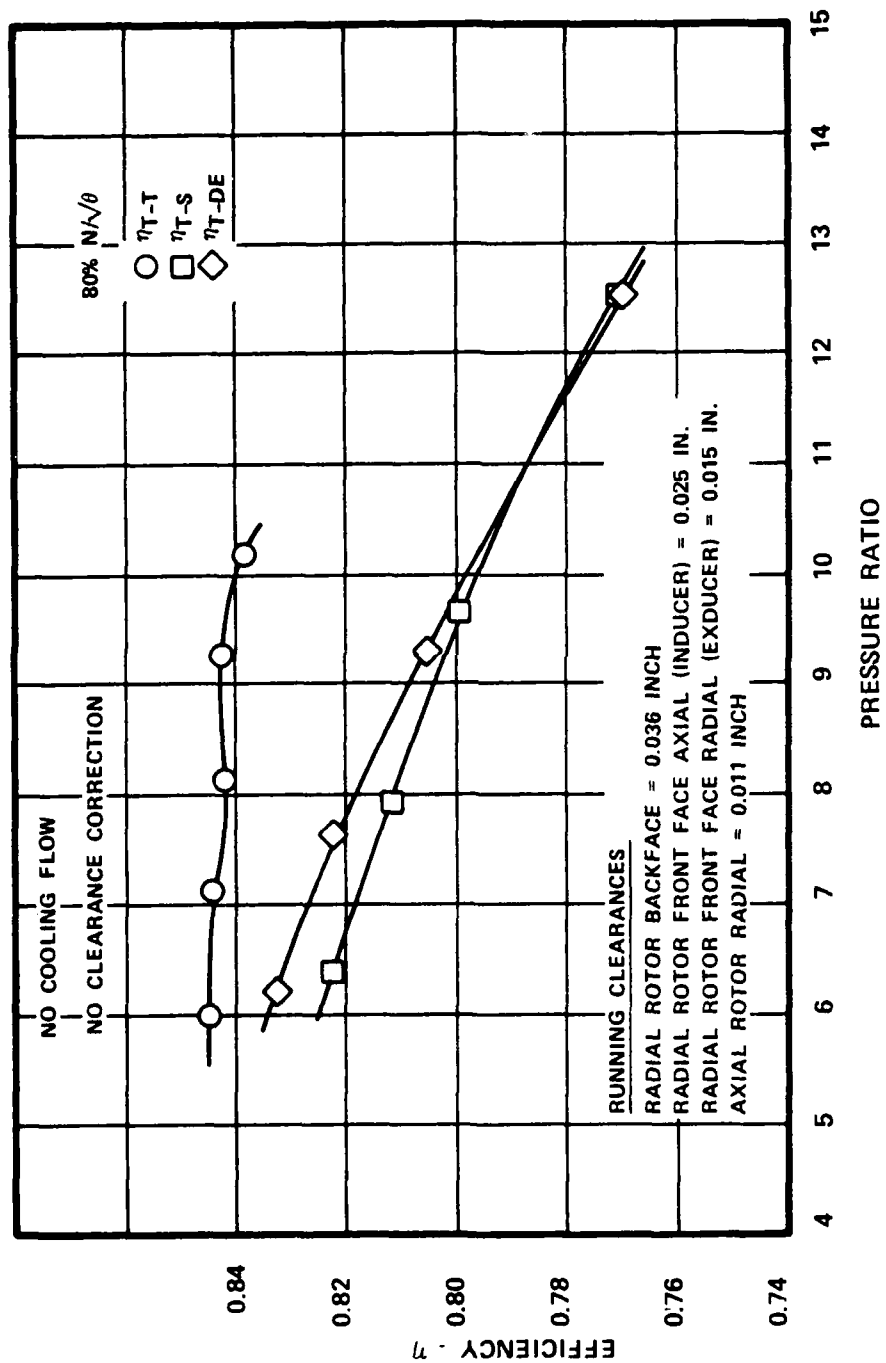


Figure 128. GTP305-2, two-stage test test no. 3

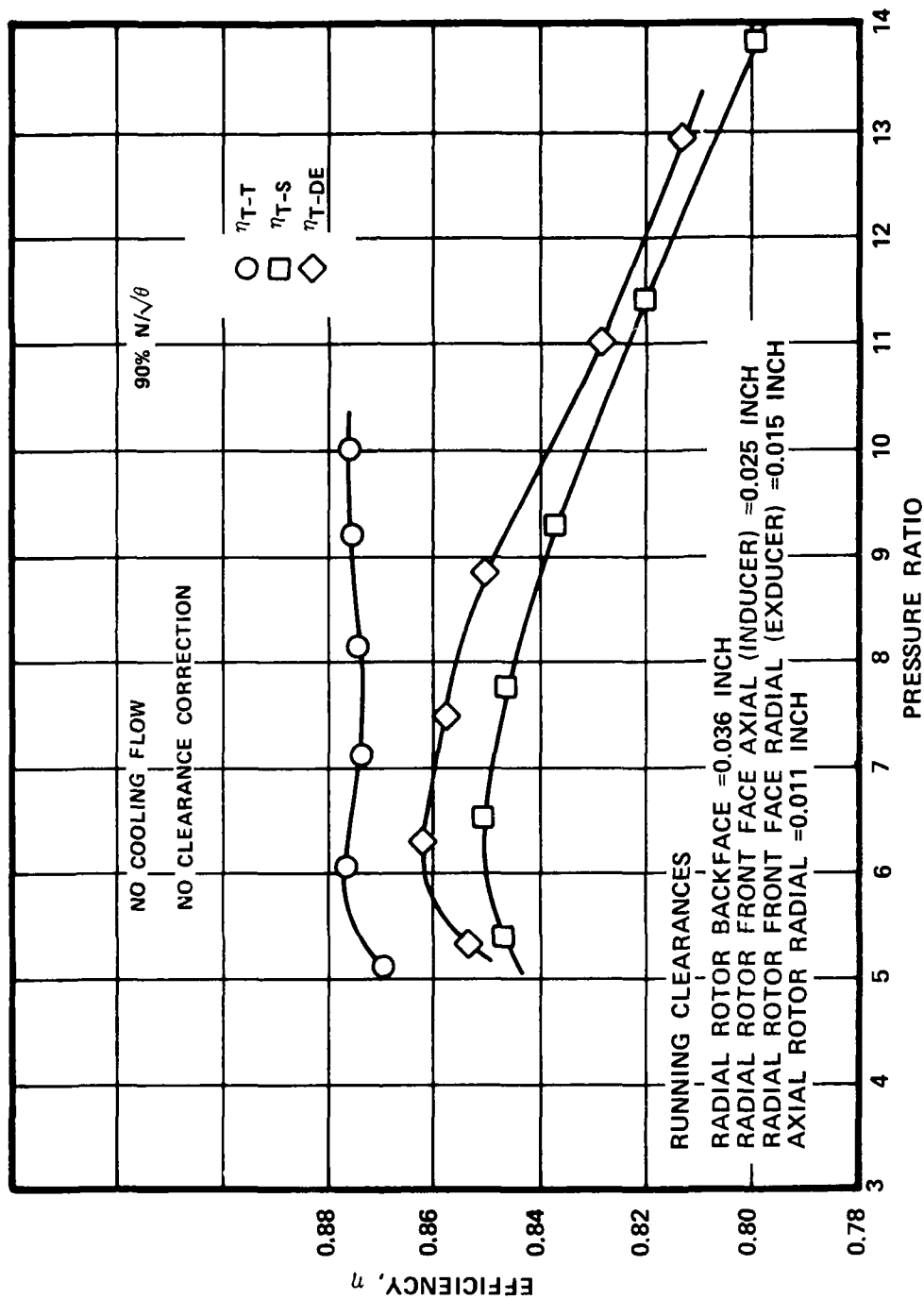


Figure 129. GTP305-2, two-stage test  
test no. 3

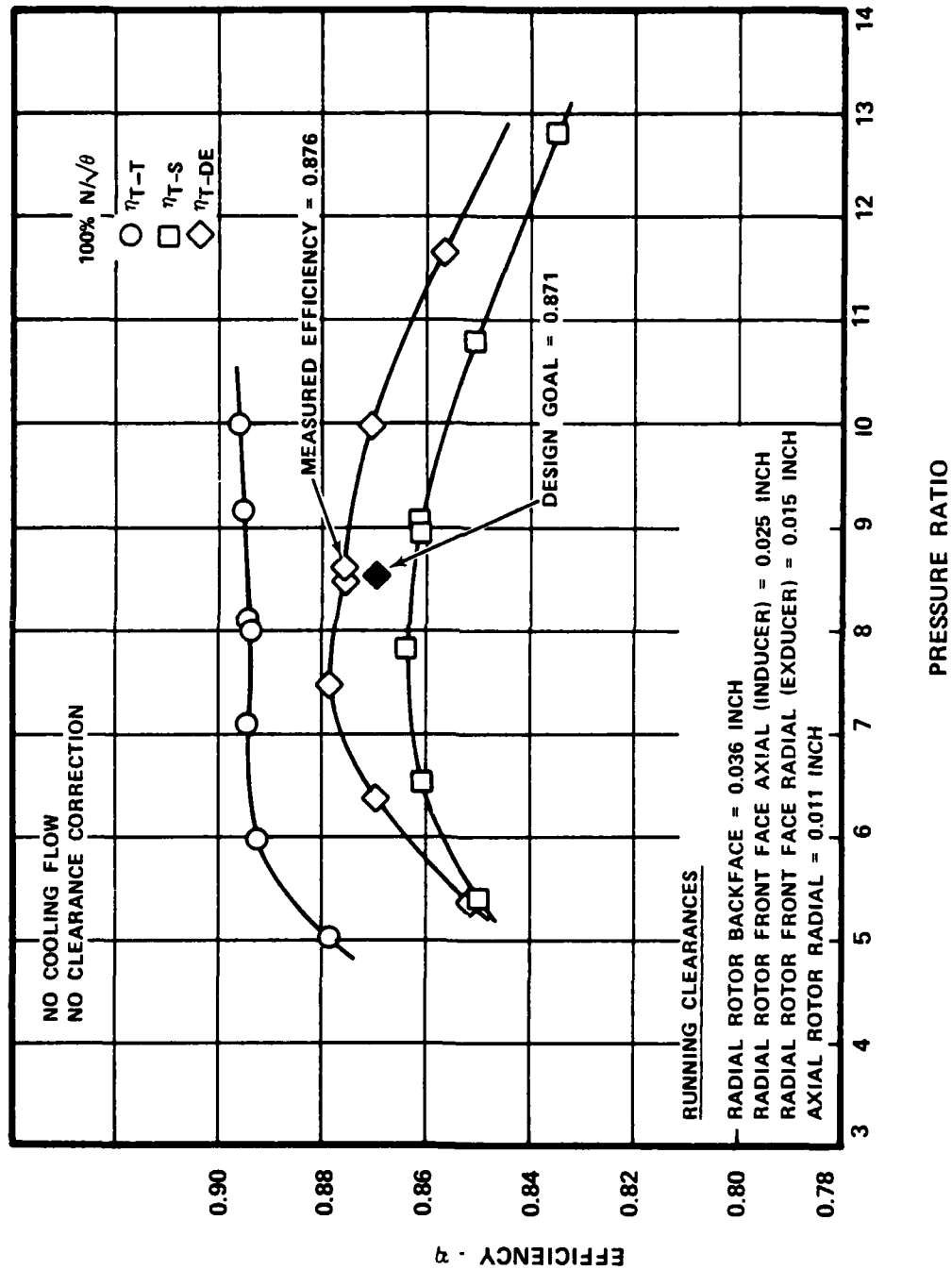


Figure 130. GTP305-2, two-stage test test no. 3

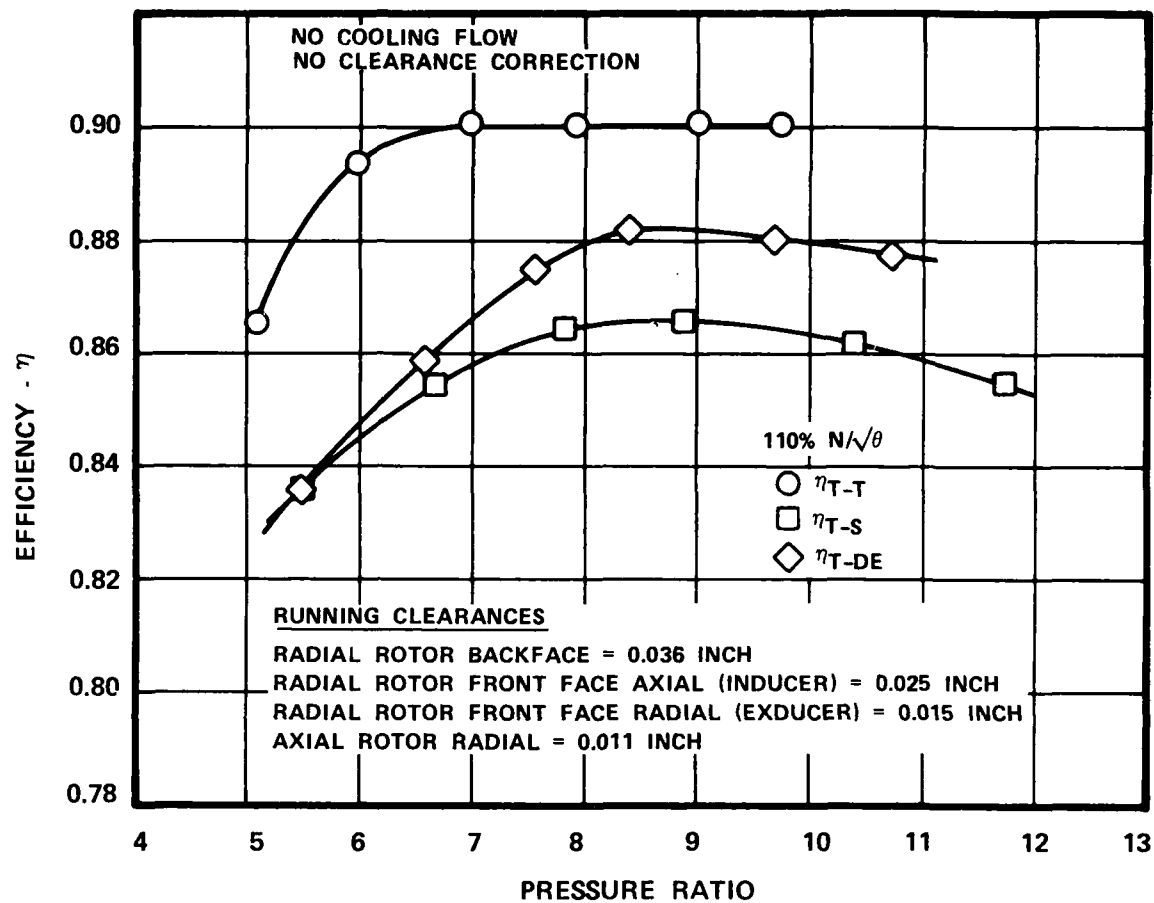


Figure 131. GTP305-2, two-stage test  
test no. 3



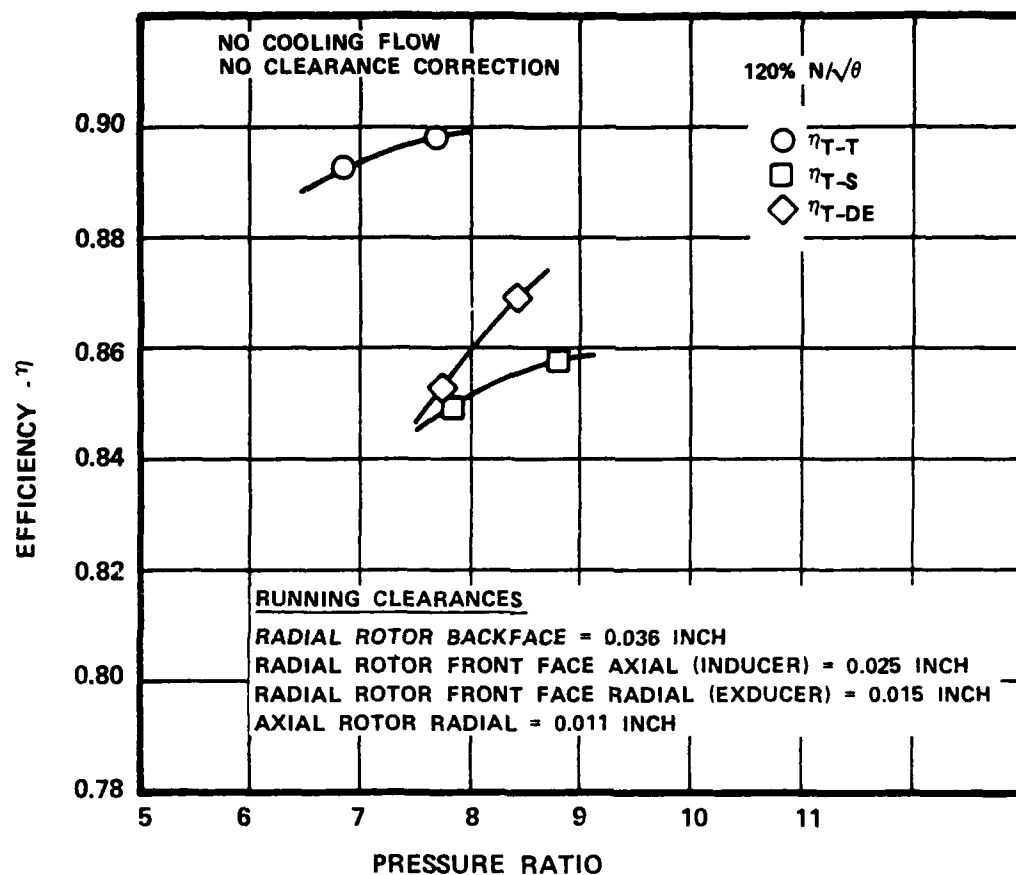


Figure 132. GTP305-2, two-stage test  
test no. 3

TABLE 27. GTP305-2 RADIAL-AXIAL TURBINE  
STAGE CLEARANCE COMPARISON  
100 PERCENT CORRECTED SPEED.

Location	Design Goal (Inch)	Measured Test Values (Inch)
Radial Rotor Backface Clearance, Inch	0.030	0.036
Radial Rotor Axial Clearance, Inch	0.015	0.025
Radial Rotor Radial Clearance, Inch	0.015	0.015
Axial Rotor Radial Clearance, Inch	0.015	0.011

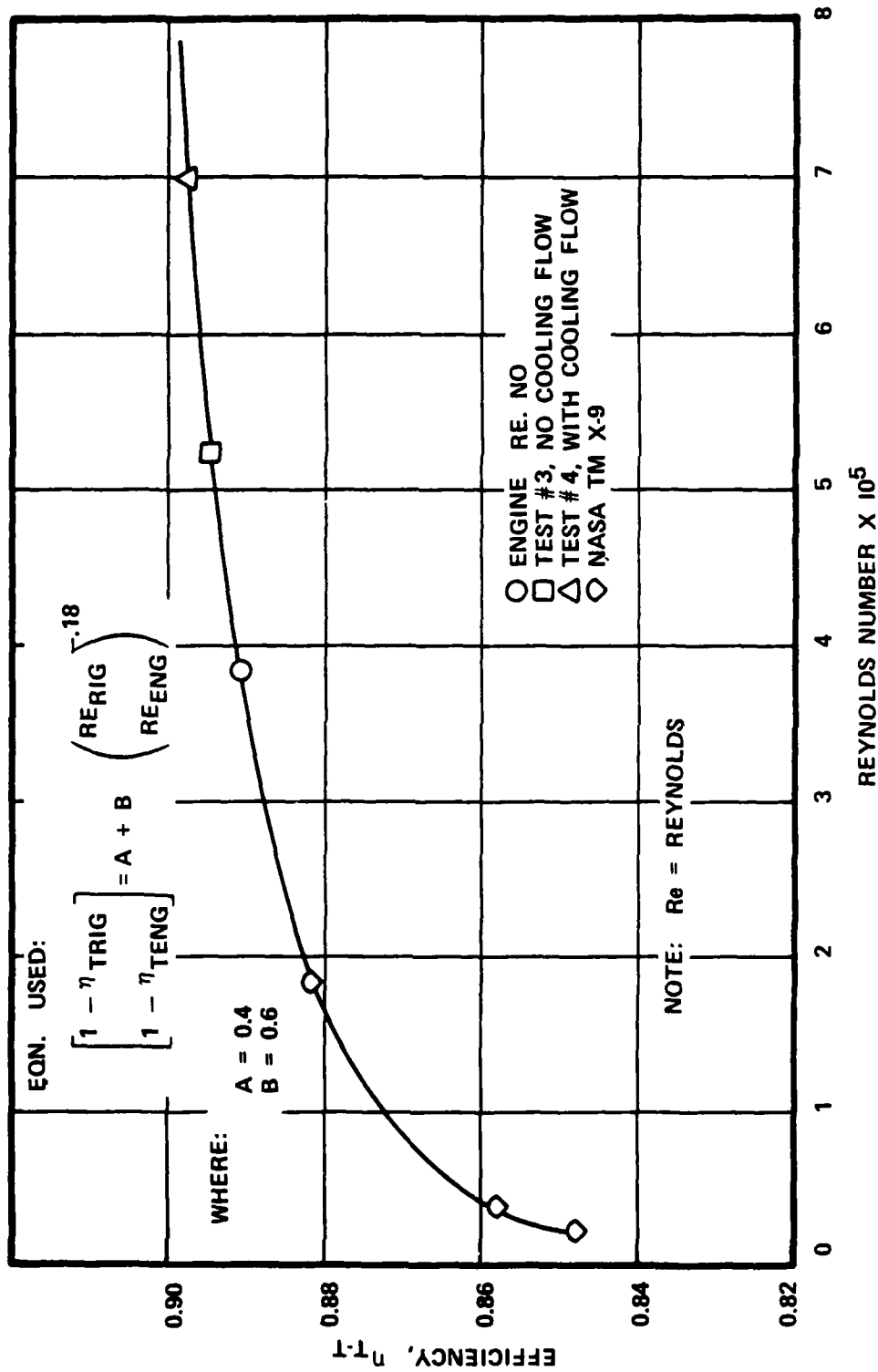
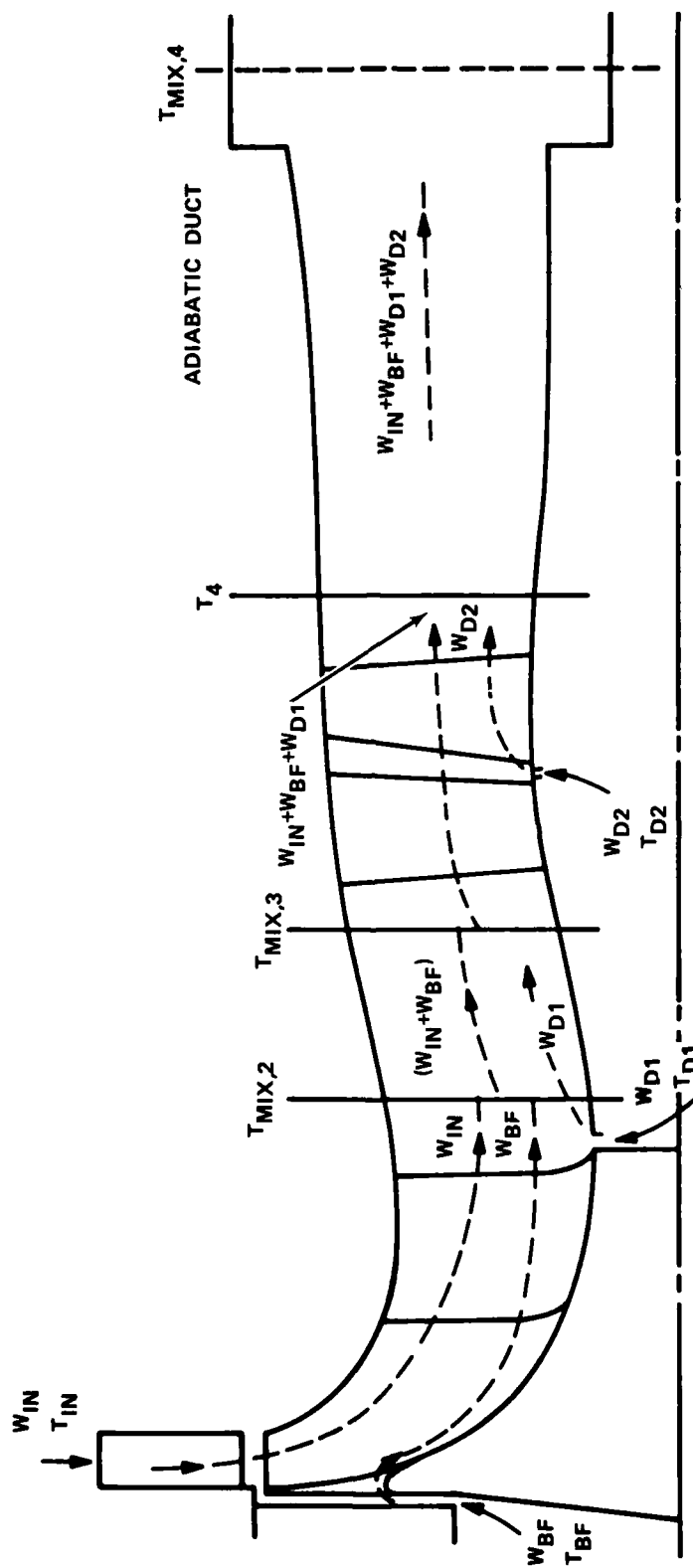


Figure 133. GTP305-2, two-stage test axial turbine correction



$W_{IN}$  = TURBINE INLET FLOW, LBS/SEC

$T_{IN}$  = TURBINE INLET TOTAL TEMPERATURE, °R

$W_{BF}$  = ROTOR BACKFACE COOLING FLOW, LBS/SEC

$T_{BF}$  = BACKFACE COOLING FLOW INLET TOTAL TEMPERATURE, °R

$W_{D1}$  = INTERSTAGE DUCT FLOW CIRCUIT NO. 1, LBS/SEC

$T_{D1}$  = INTERSTAGE DUCT FLOW TOTAL TEMPERATURE, °R

$T_{MIX,2}$  = ROTOR EXIT MIXED TEMPERATURE, °R

$T_{MIX,3}$  = AXIAL STATOR INLET MIXED TEMPERATURE, °R

$W_{D2}$  = INTERSTAGE DUCT FLOW CIRCUIT NO. 2, LBS/SEC

$T_{D2}$  = INTERSTAGE DUCT FLOW TOTAL TEMPERATURE, °R

$T_4$  = AXIAL ROTOR EXIT TOTAL TEMPERATURE, °R

$T_{MIX,4}$  = ADIABATIC DUCT TOTAL TEMPERATURE, °R

Figure 134. GTP305-2, test no. 3 and 4 radial-axial stage test

TABLE 28. RADIAL-AXIAL TURBINE PERFORMANCE  
MAP MATRIX (WITH COOLING FLOW\*).

Total-To-Total Overall Pressure Ratio	Percent Corrected Speed		
	90	100	110
	7.0	7.0	7.0
	8.0	8.0	8.0
	9.0	9.0	9.0

\*Cooling Flow: 1.5-Percent Radial  
Rotor Backface  
Cooling Flow plus  
1.0-Percent  
Interstage Buffer  
Air Cooling Flow

not be considered in turbine cycle calculation. It has already been accounted for in turbine "efficiency."

The procedure used to calculate cooled turbine efficiency is presented below:

- o For an imposed speed and overall two-speed pressure ratio, the measured radial stage pressure ratio, together with the radial turbine characteristics established in Tests 1, 2, and 2A, were used to define the radial turbine exit mixed temperature,  $T_{MIX, 2}$  (Figure 134)
- o From the measured buffer seal cooling flow temperature, and predicted flow split, the axial turbine inlet mixed temperature ( $T_{MIX, 3}$ ) and total flow were calculated
- o The axial turbine inlet total pressure was calculated from the measured radial turbine pressure ratio and the corresponding duct loss established in Test 2A
- o The cooled axial turbine efficiency level was then calculated based on derived inlet conditions and measured exit conditions
- o Cooled radial and axial turbine efficiencies were then combined into an overall cooled "efficiency"

Expressions for individual cooled efficiencies for radial and axial stages are presented below:

$$\eta_{T-T \text{ cooled radial}} = \frac{W_{in} (T_{in} - T_{mix,2}) + W_{BF} (T_{BF} - T_{mix,2})}{W_{in} T_{in} \left[ 1 - \left( \frac{1}{Pr_{T-T}} \right) \frac{\gamma-1}{\gamma} \right]}$$

$$\eta_{T-T} \text{ cooled radial} = \frac{(W_{in} + W_{BF} + W_{D1}) T_{mix,3}}{(W_{in} + W_{BF} + W_{D1}) T_{mix,3} + W_{D2} T_{D2} - T_{mix,4} (W_{in} + W_{BF} + W_{D1} + W_{D2}) \left[ 1 - \left( \frac{1}{PR_{T-T}} \right)^{\frac{\gamma-1}{\gamma}} \right]}$$

See Figure 134 for nomenclature of terms.

Overall stage efficiencies are then defined as the sum of the work of individual stages compared with available energy at the radial turbine inlet. Resultant expressions are:

$$\eta_{T-T} \text{ cooled overall} = \frac{A + B}{W_{in} T_{in} \left[ 1 - \left( \frac{1}{PR_{T-T}} \right)^{\frac{\gamma-1}{\gamma}} \right]}$$

$$\eta_{T-DE} \text{ cooled overall} = \frac{A + B}{W_{in} T_{in} \left[ 1 - \left( \frac{1}{PR_{T-DE}} \right)^{\frac{\gamma-1}{\gamma}} \right]}$$

where:

$$A = \left[ (W_{in} (T_{in} - T_{mix,2}) + W_{BF} (T_{BF} - T_{mix,2})) \right]$$

$$\text{and } B = \left[ (W_{in} + W_{BF} + W_{D1}) T_{mix,3} + W_{D2} T_{D2} - T_{mix,4} (W_{in} + W_{BF} + W_{D1} + W_{D2}) \right]$$

See Figure 134 for nomenclature of terms.

Figure 135 compares the measured aerodynamic efficiency from Test 3 with the calculated cooled "efficiency" from Test 4 for 100 percent corrected speed over a range of pressure ratios. The increase in performance with cooling flow is primarily due to the 2.5 percent cooling flow, which is available to do work in the power turbine. A comparison of inlet corrected flows and diffuser recoveries are also presented in Figure 135.

#### 4.2.5.6.1 Survey Results

Tests 3 and 4 utilized four survey probe systems to examine the flow properties as a function of the radial direction. One survey probe was located at the radial rotor exit one at the interstage duct exit, and two at the axial rotor exit. Results of the survey probe systems are discussed in the following sections.

#### 4.2.5.6.2 Radial Rotor Exit

Radial rotor exit characteristics are presented in Figures 136 through 139. The rotor exit absolute swirl angle, total-to-total efficiency, total-to-total pressure ratio, and absolute Mach number as a function of radius are presented with and without cooling flow. Figure 136 shows that the desired rotor exit swirl, from the optimized one-dimensional vector diagram was achieved. However, significant deviation from the predicted distribution exists below and above the meanline region. Below the meanline (5-50 percent of the passage height), the deviation is attributed to either higher than predicted blade deviation or to flow disturbance in the rotor scallop region (although powder traces didn't indicate any significant accumulation in this area). Above the meanline, the deviation is attributed to both the blade clearance effects and to the influx of



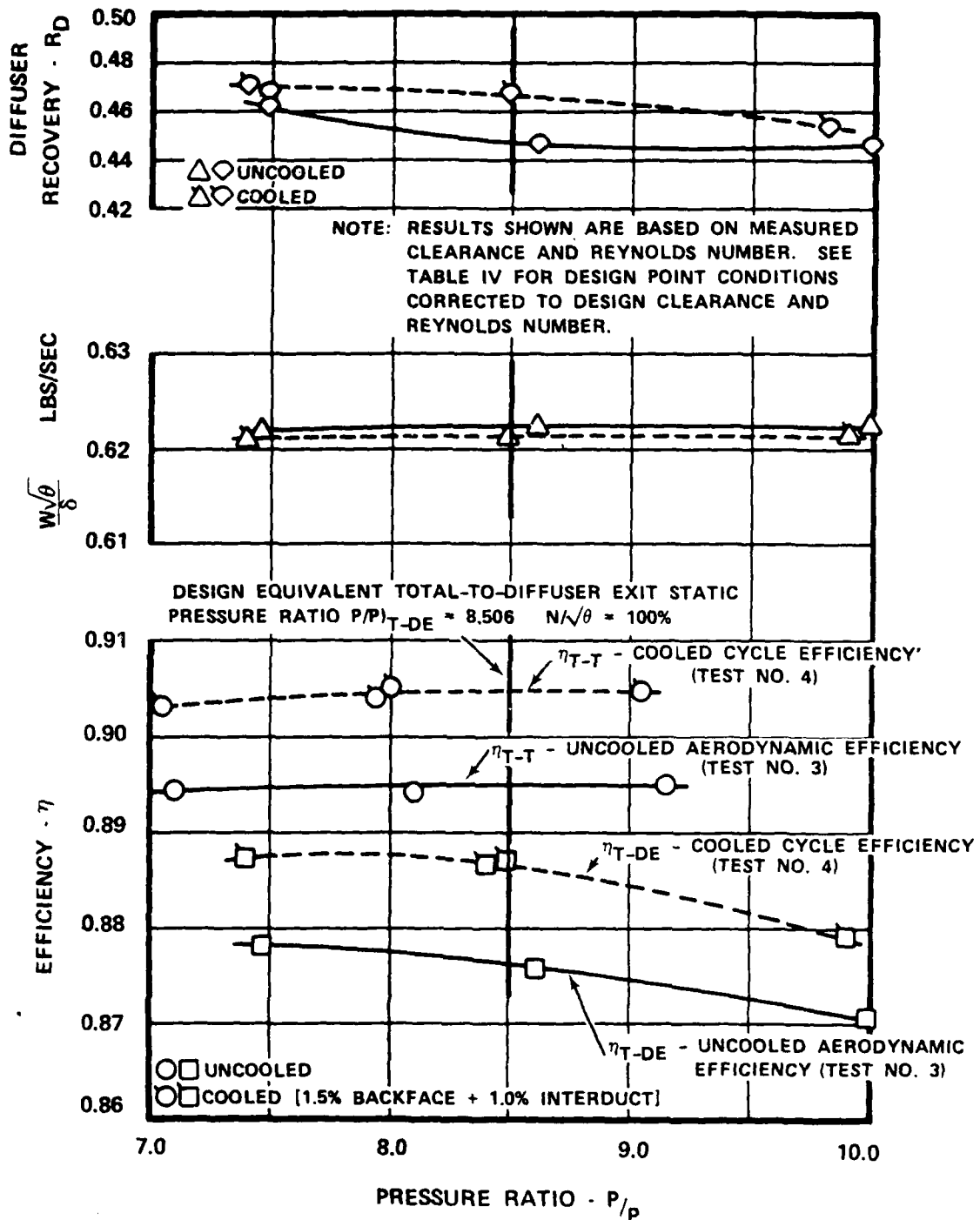


Figure 135. GTP305-2, two-stage data test no. 3 and no. 4

Figure 136. GTP305-2 2-stage test air angle distribution

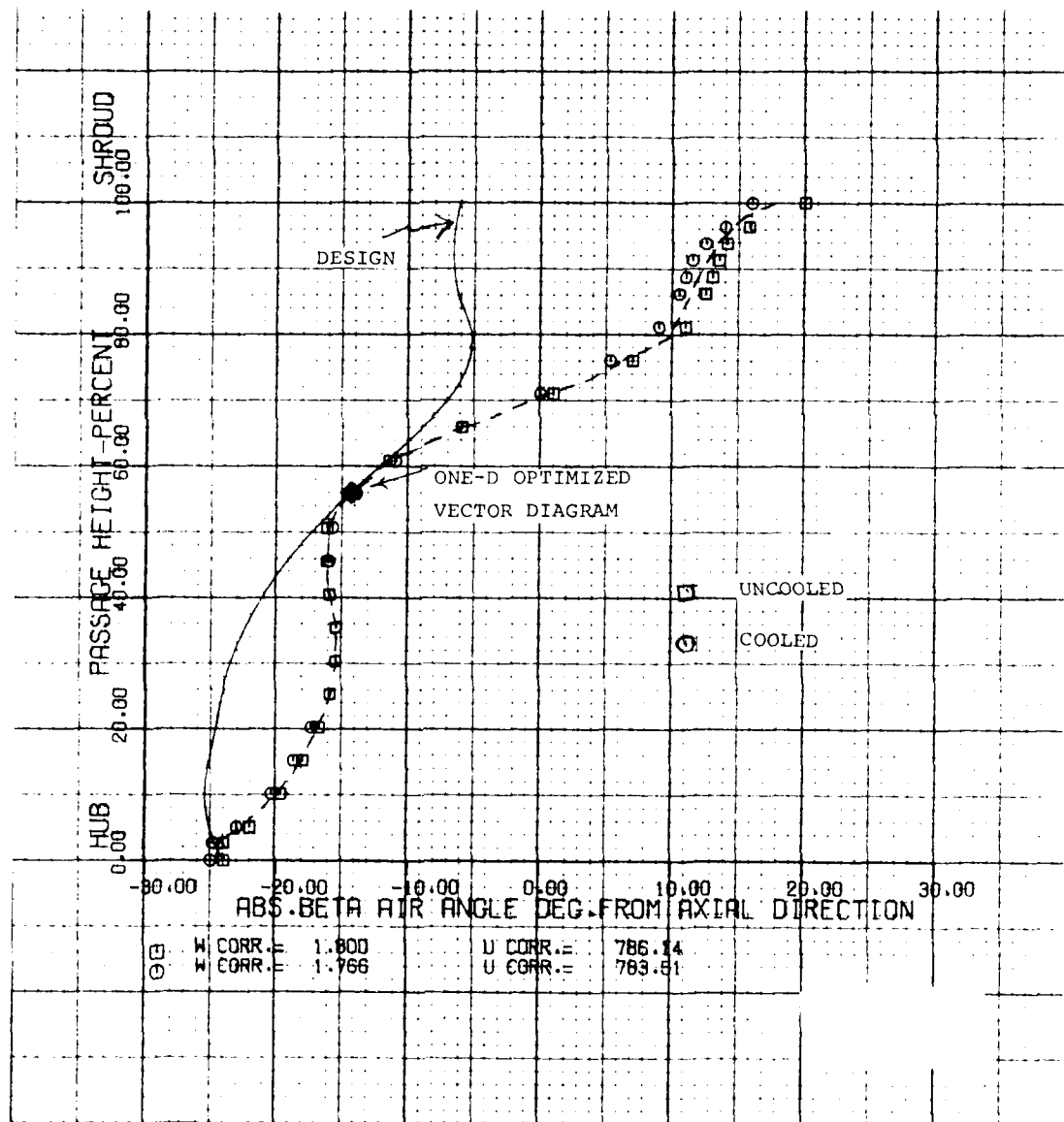


Figure 137. GTP305-2 2-stage test radial rotor exit

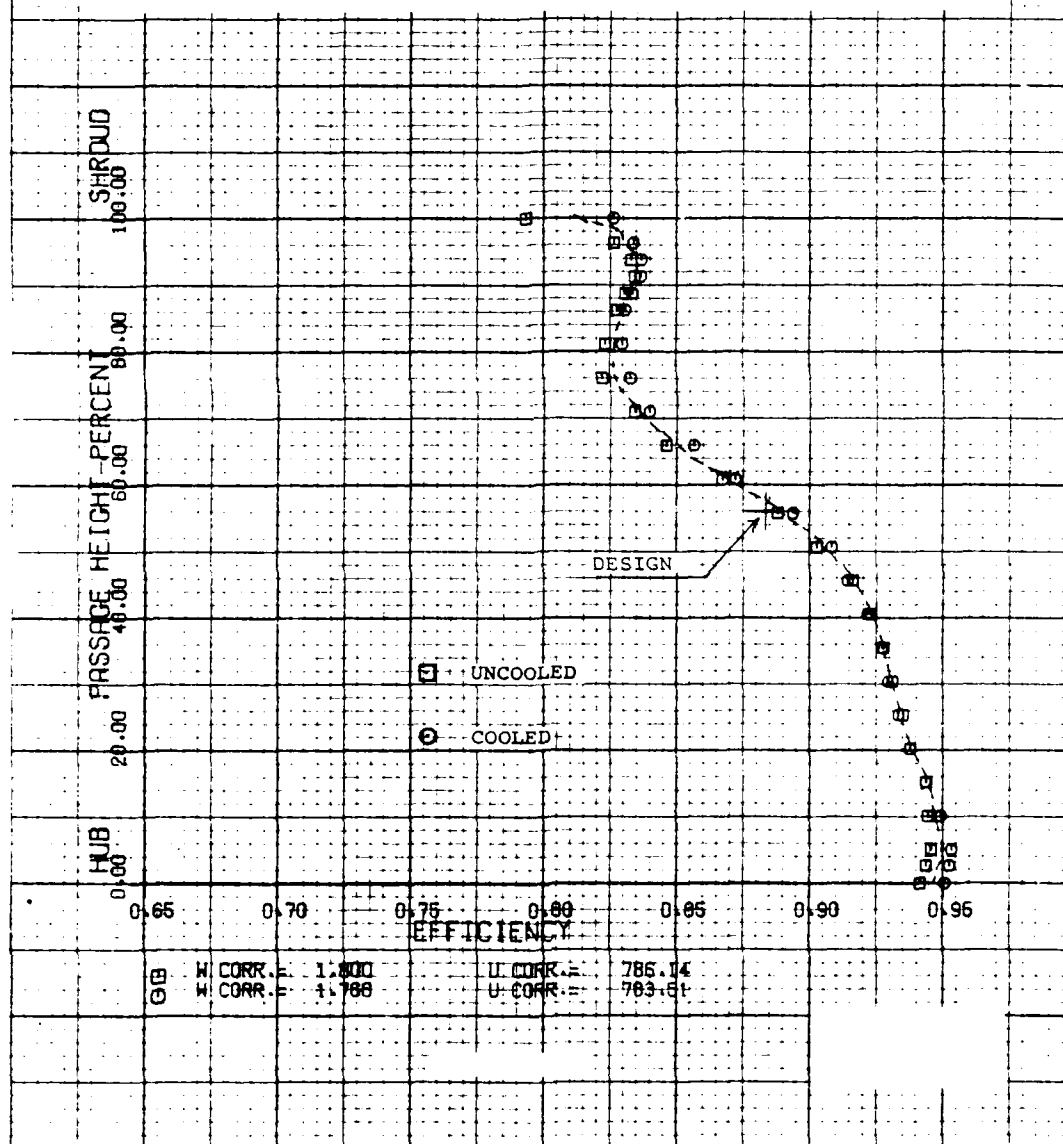


Figure 138. GTP305-2 2-stage test radial rotor  
exit pressure ratio

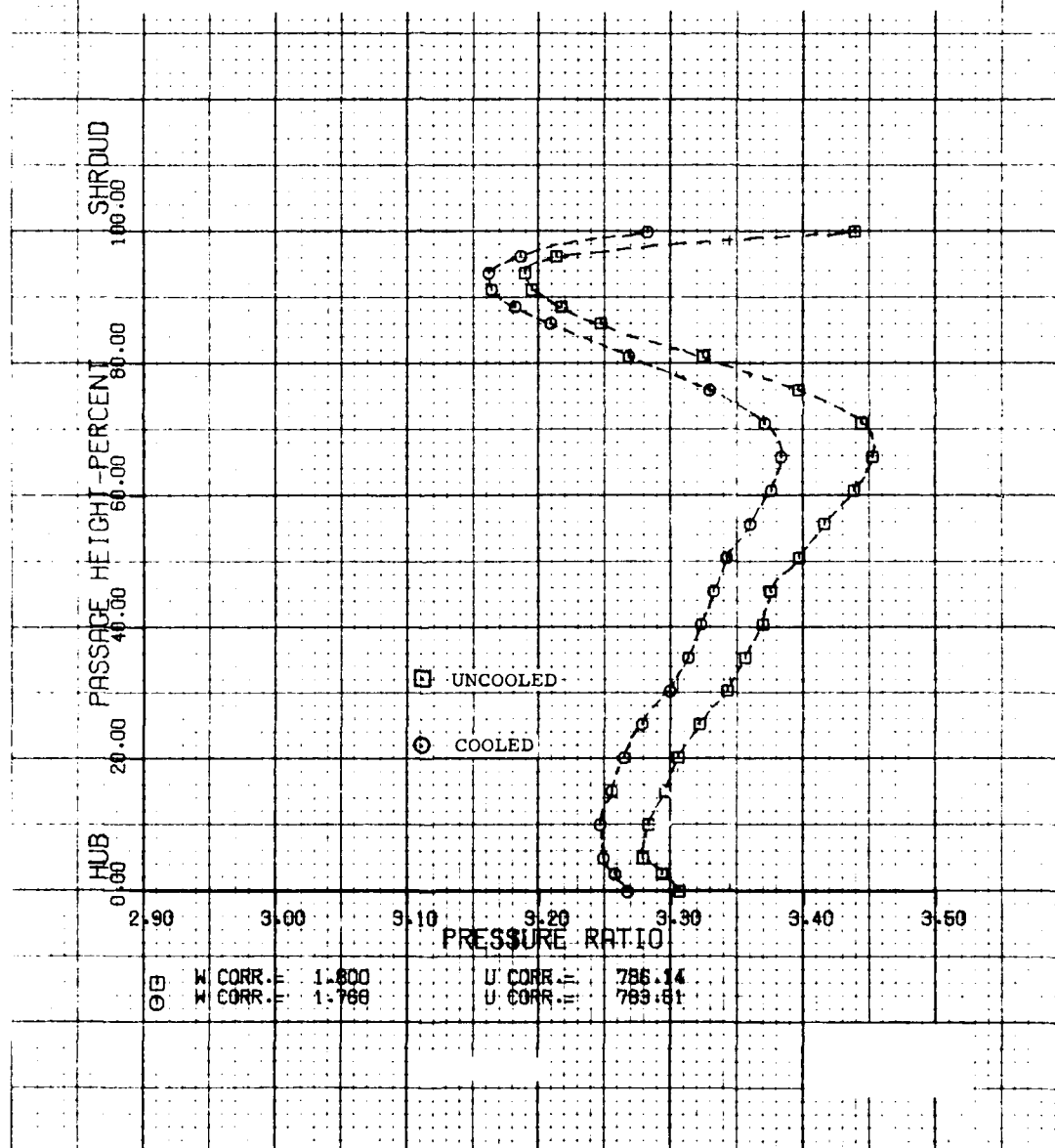
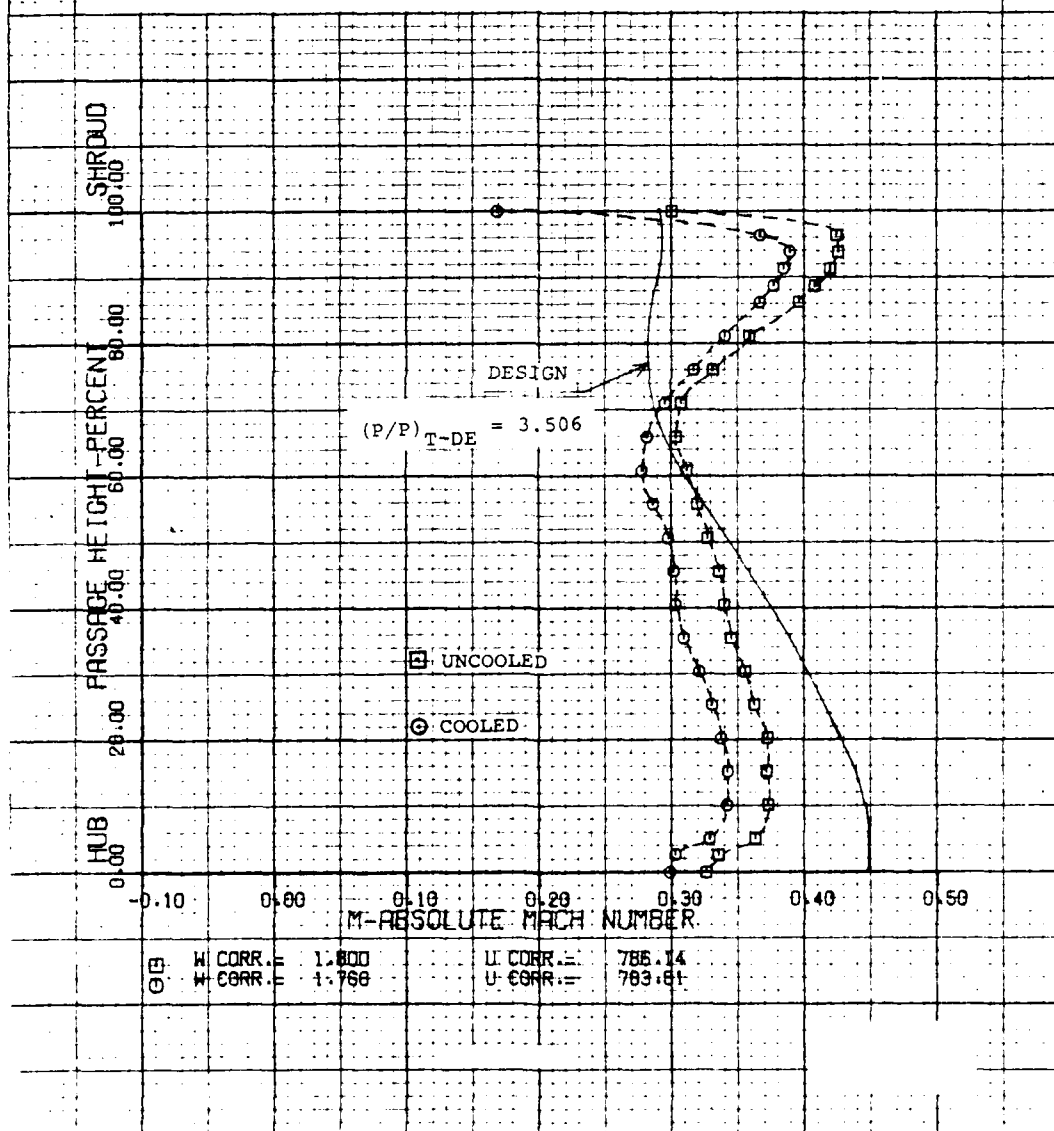


Figure 139. GTP305-2 2-stage test absolute mach number distribution



secondary flow, which propagates to this region from the high inducer loading. This is evident in Figure 137 where the local efficiency distribution shows a decrease from approximately 50-80 percent where the local efficiency distribution shows a decrease from approximately 50-80 percent of the passage height. From Figure 137, it appears that the influx of secondary flow is concentrated at about 70 percent of the blade height. The pressure ratio in Figure 138 shows the same trend and, in addition, shows the effect of cooling flows on the radial turbine attainable pressure ratio. For a fixed radial turbine nozzle area, the radial turbine pressure ratio is primarily a function of the down stream axial turbine stator area. Increasing flow through the axial turbine with cooling flow has the effect of reducing the effective axial power turbine stator area and consequently the radial turbine pressure ratio. Finally, Figure 139 shows the expected decrease in radial turbine exit absolute Mach number with cooling flow due to the reduction in pressure ratio.

#### 4.2.5.6.3 Interstage Duct Exit

Interstage duct exit (power turbine inlet) characteristics are similar with predicted (Figure 140) except that the inlet swirl magnitude has shifted. At the meanline the swirl is lower than the design, indicating a slightly higher than design through-flow velocity. Deviations above and below the meanline are consistent with the radial turbine exit conditions described earlier. The interstage duct exit pressure ratio (Figure 141) and absolute Mach number (Figure 142) are also consistent with the radial turbine with and without cooling flow.

#### 4.2.5.6.4 Axial Turbine Exit

The axial turbine exit radial flow characteristics are presented in Figure 143 through 148. Figure 143 compares the local total pressure distribution obtained from the survey probe

Figure 140. GTP305-2 2-stage test axial  
stator inlet air angle  
distribution

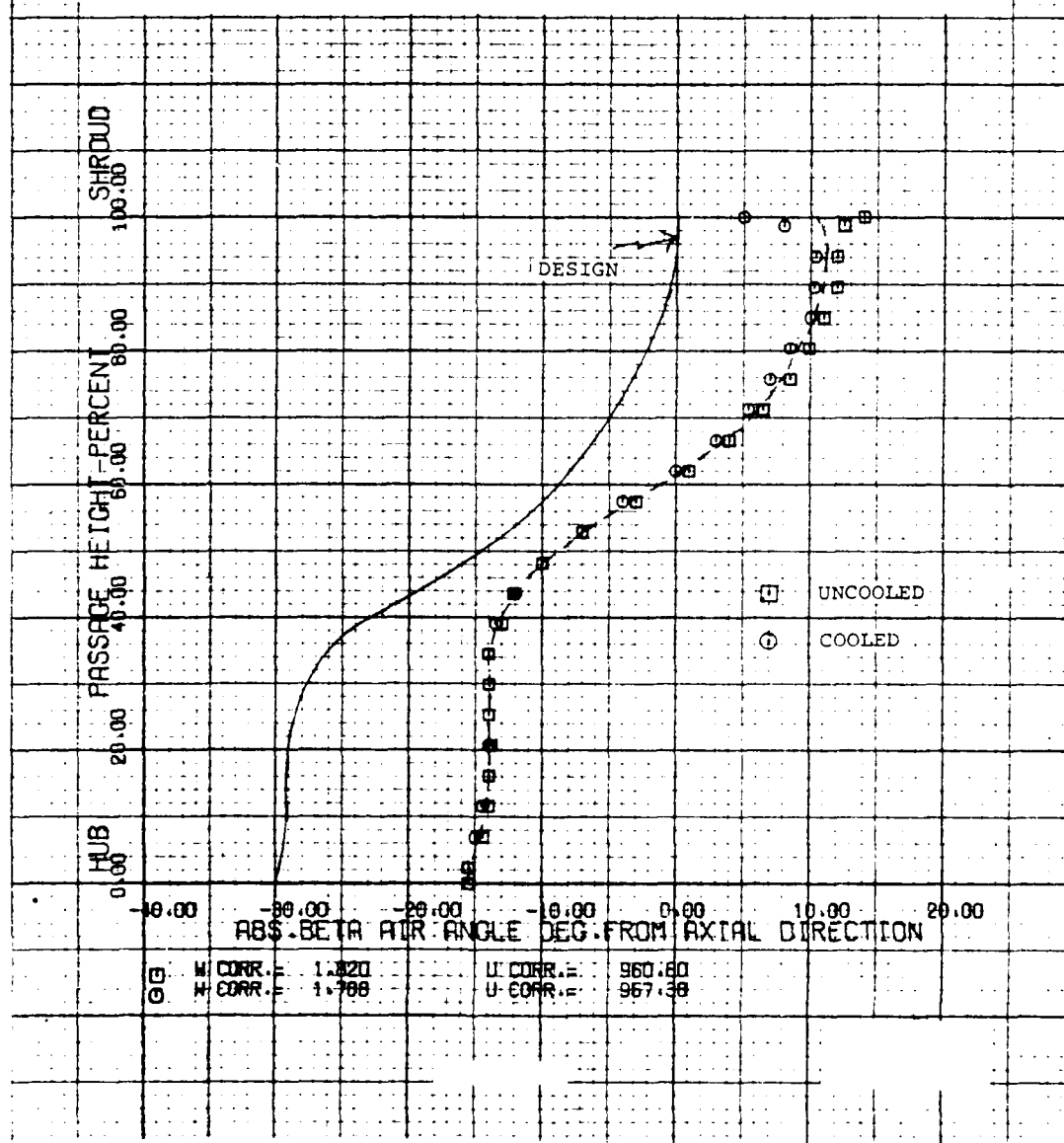


Figure 141. GTP305-2 2-stage test axial stator inlet pressure ratio

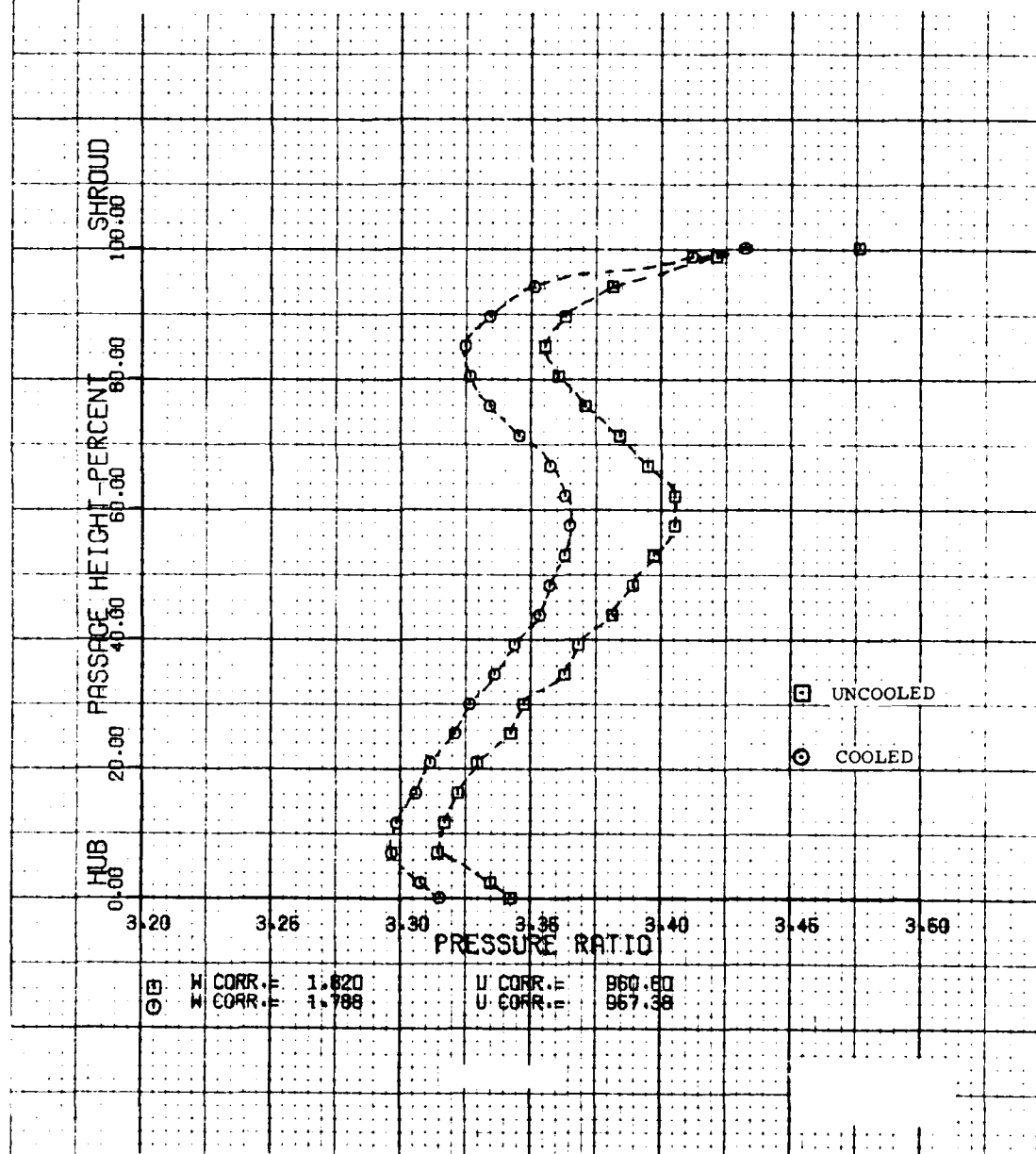




Figure 142. GTP305-2 2-stage test axial stator inlet  
absolute mach number distribution

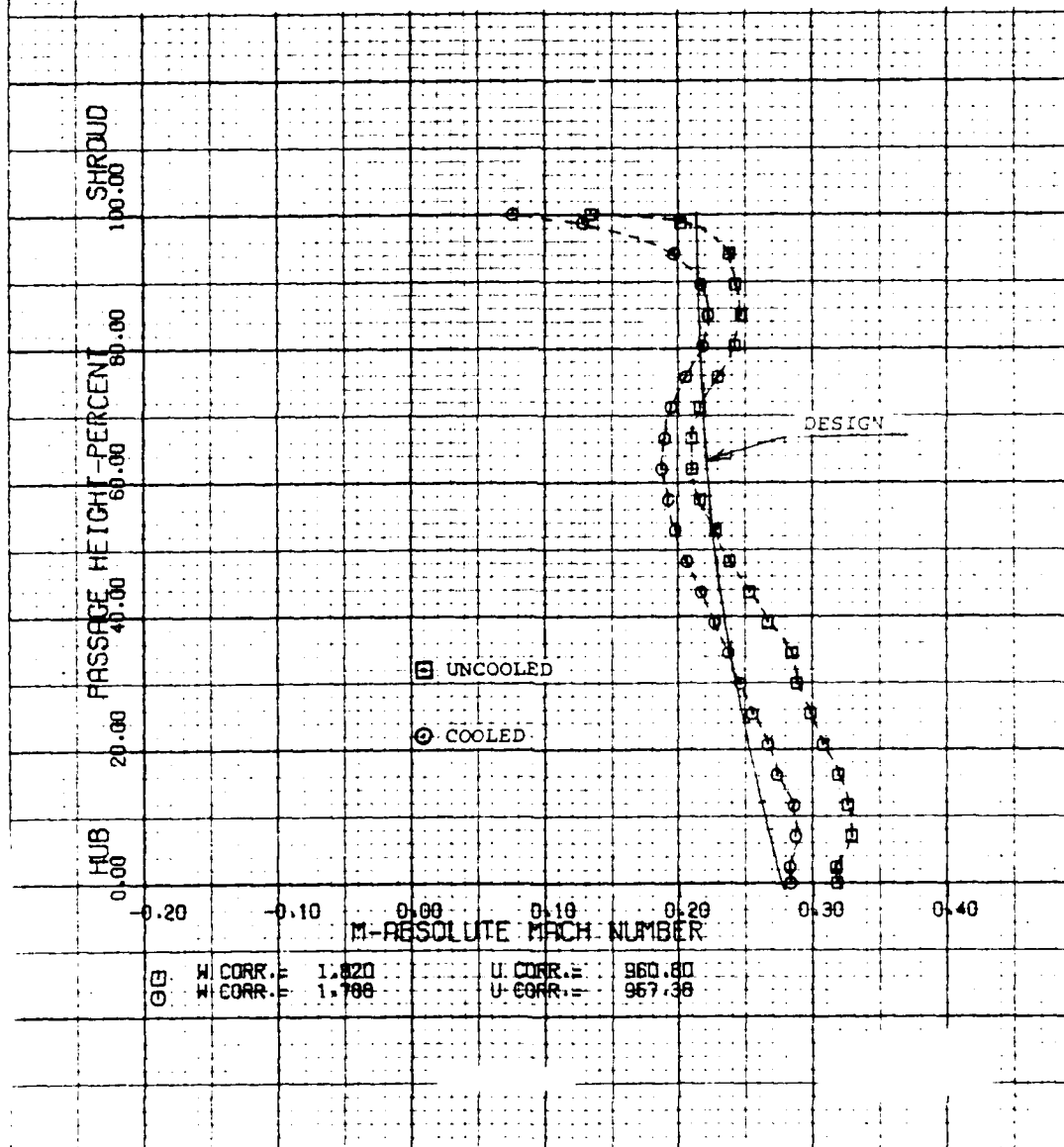


Figure 143. GTP305-2 2-stage test axial rotor exit pressure ratio distribution

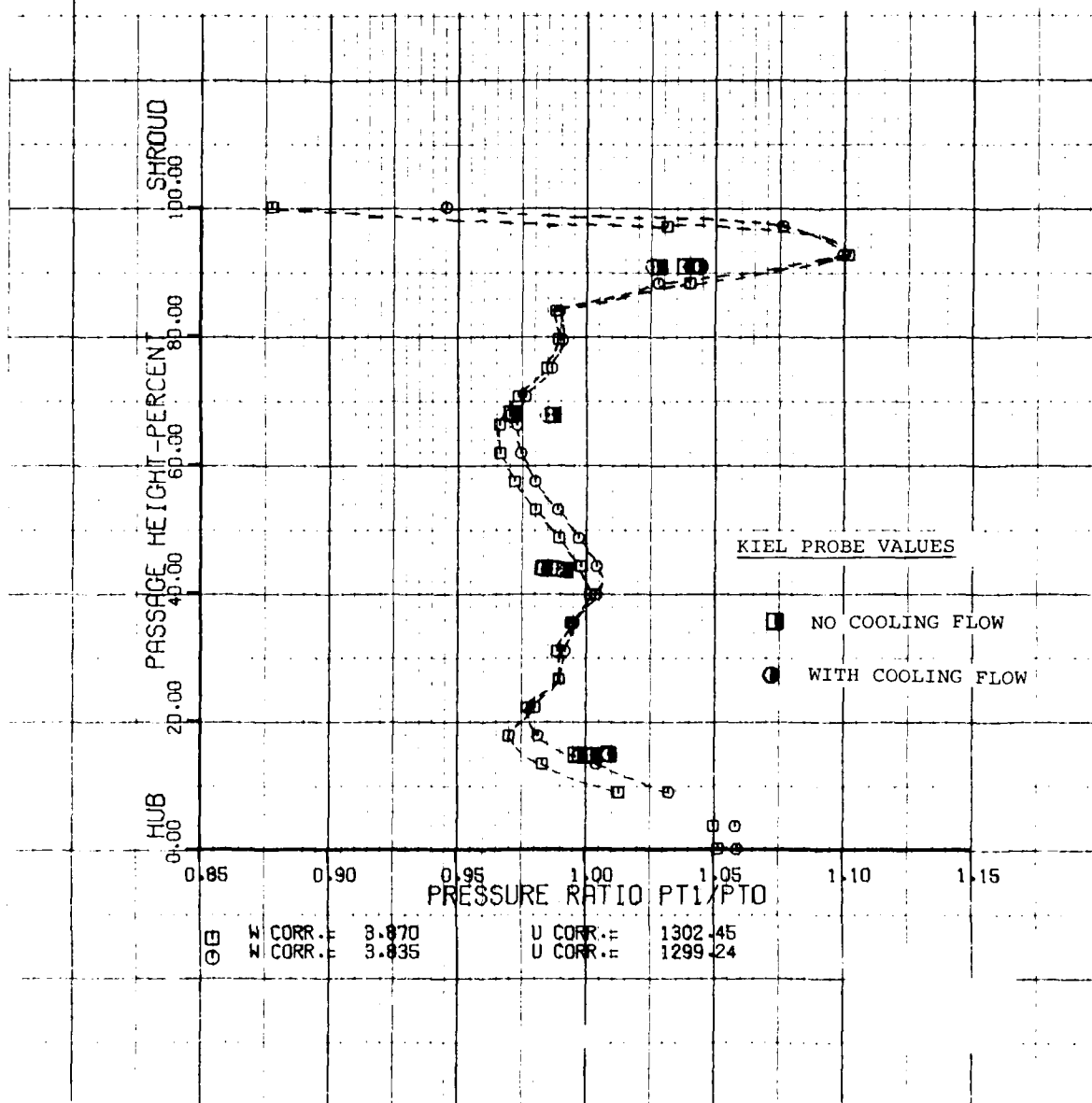


Figure 144. GTP305-2 2-stage test axial rotor exit air angle distribution

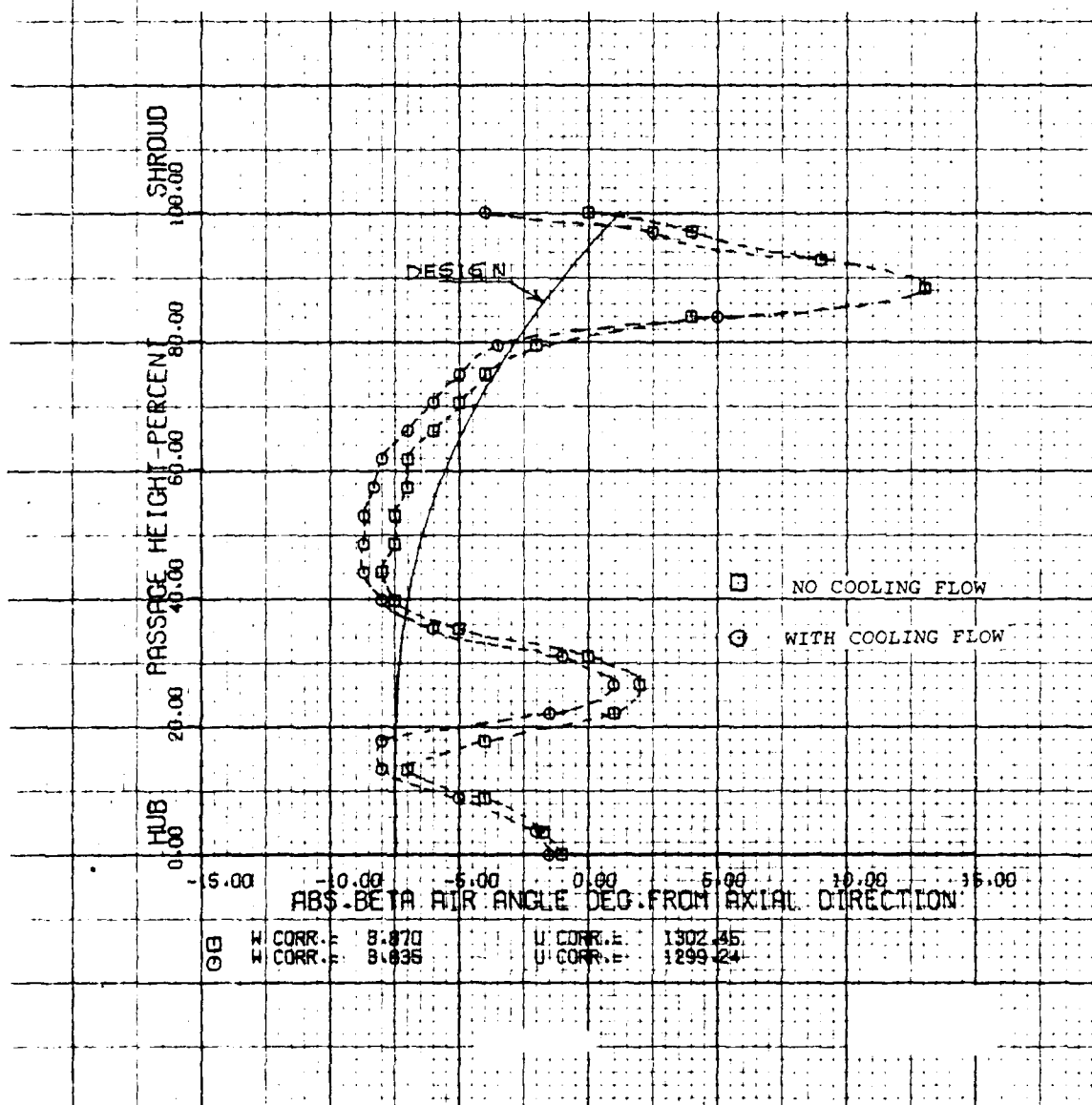


Figure 145. GTP305-2 2-stage test axial rotor exit absolute mach number distribution

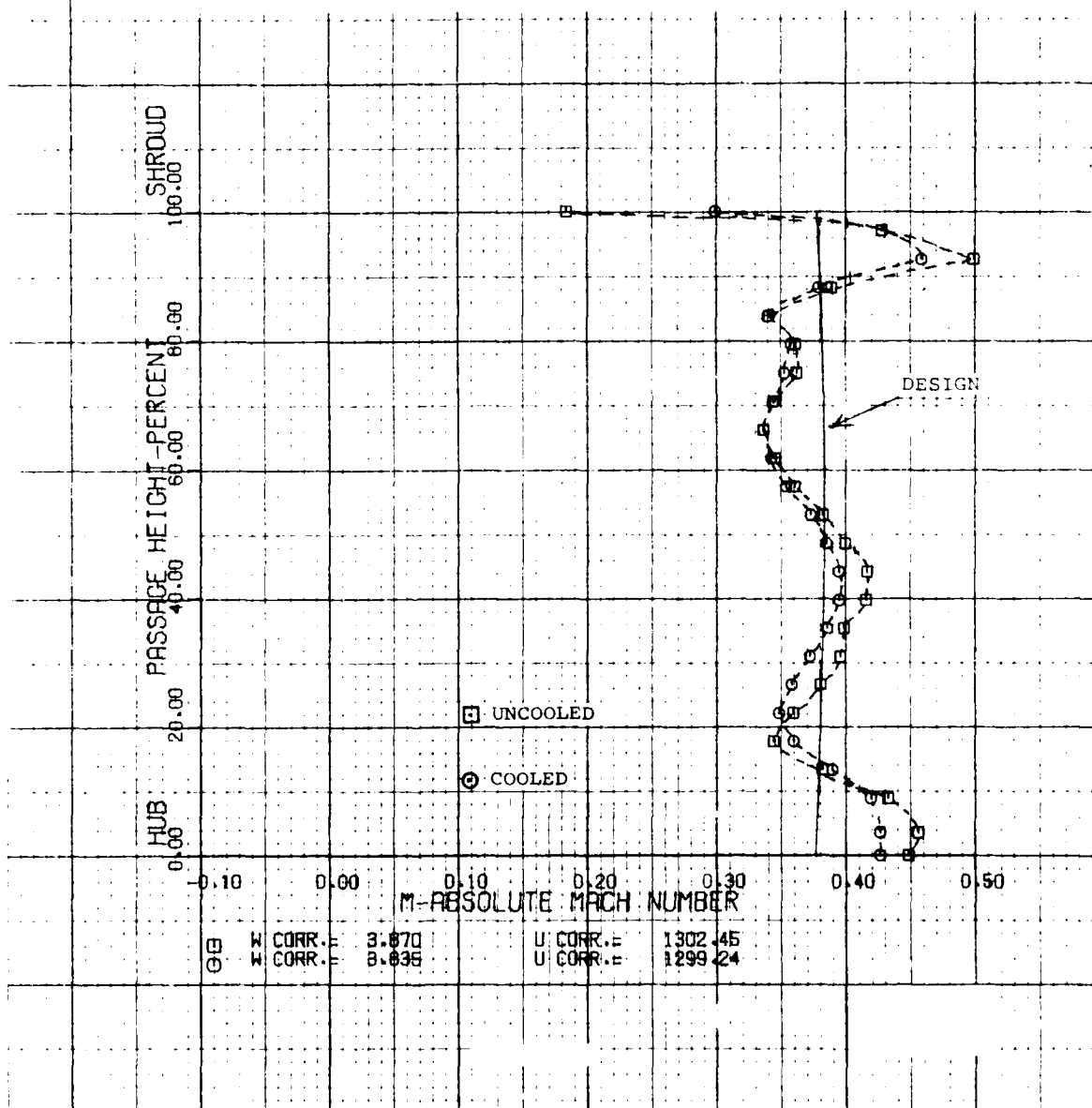


Figure 146. Relative air angle distribution

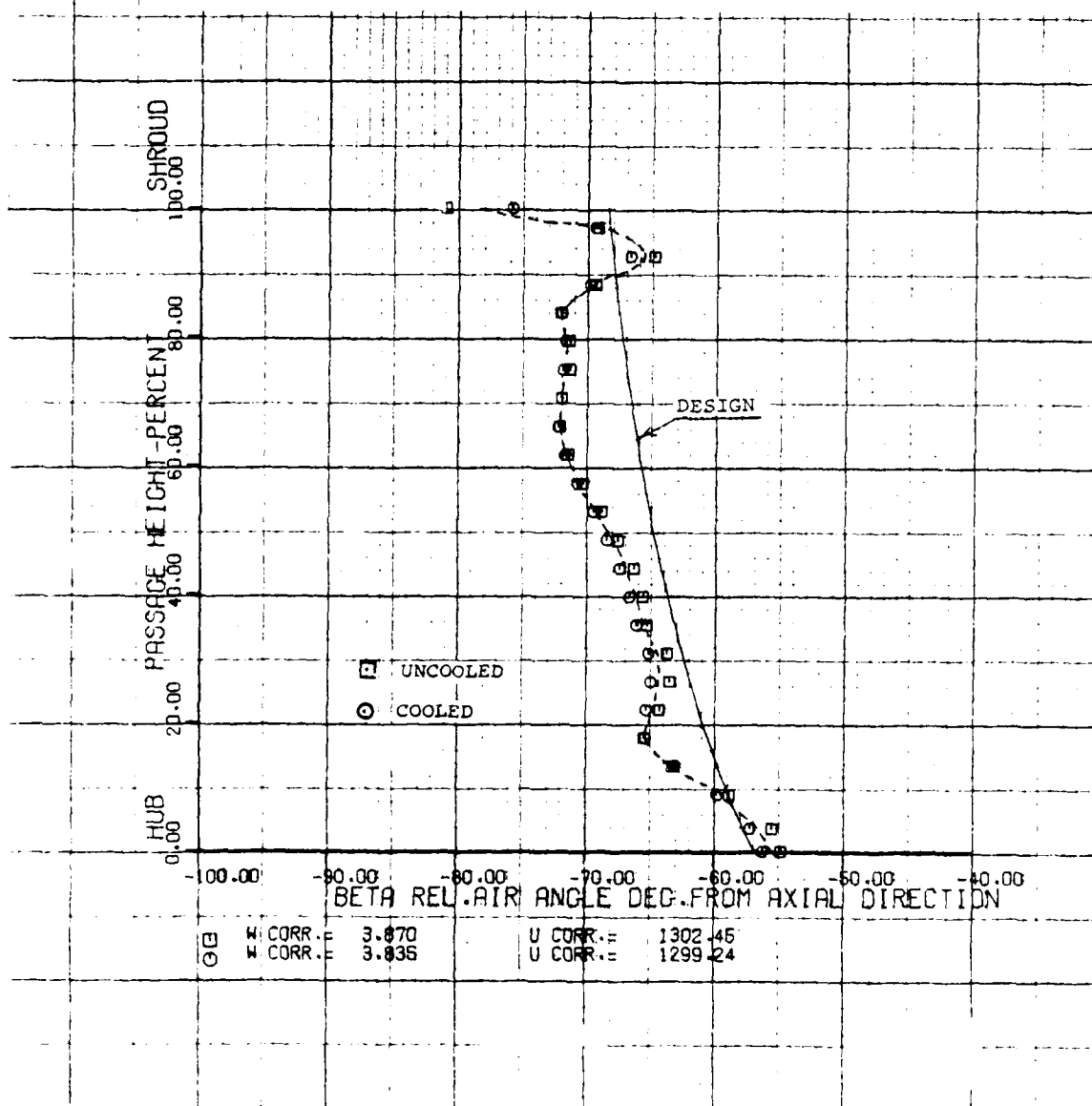


Figure 147. GTP305-2 2-stage test axial rotor exit pressure ratio

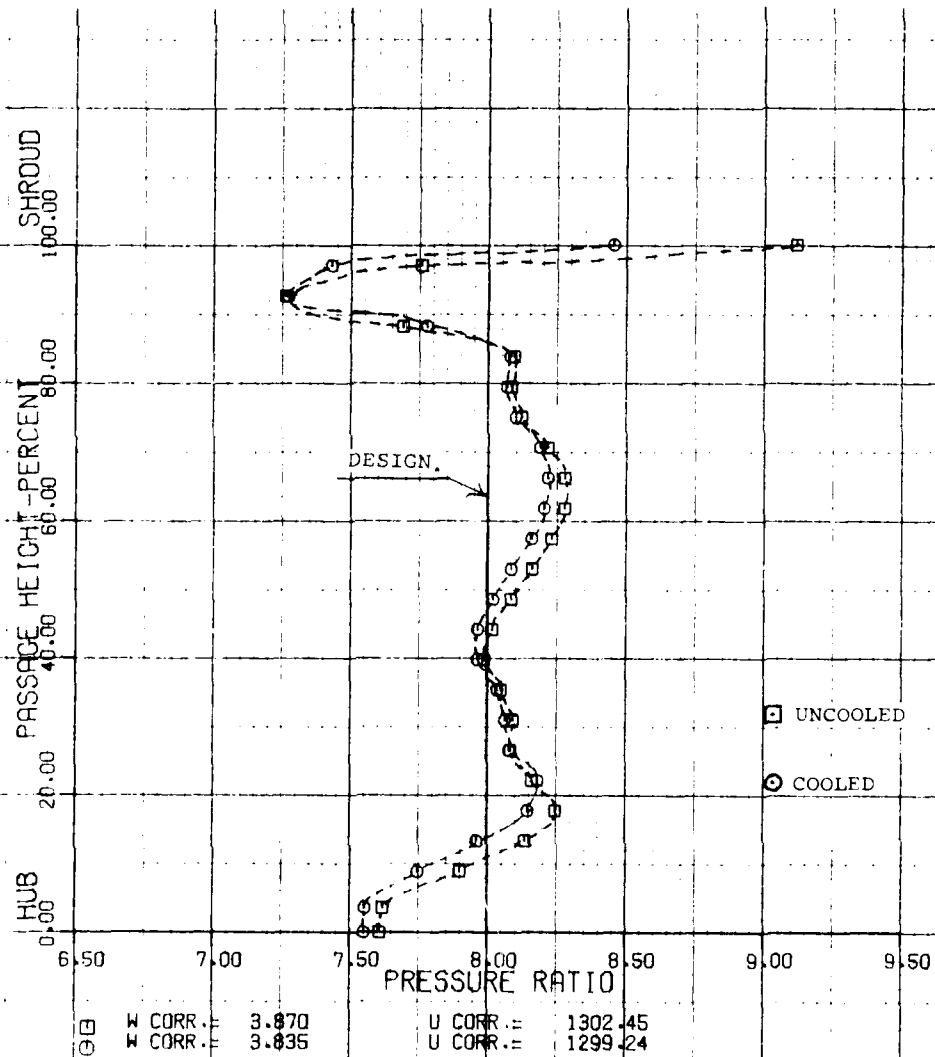
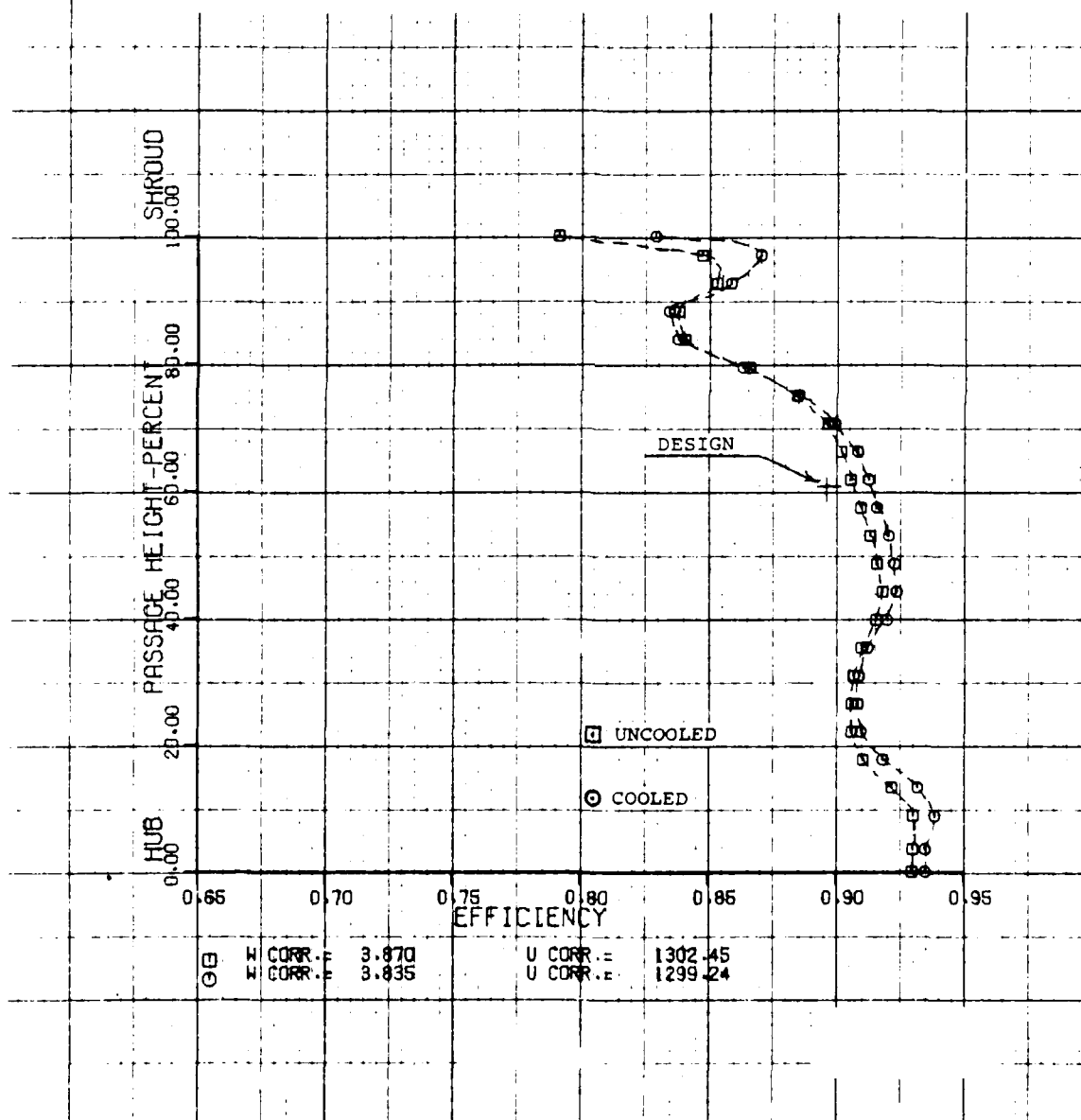


Figure 148. GTP305-2 2-stage test axial rotor exit efficiency



to that measured from the fixed total pressure Kiel probes and shows excellent agreement. Rotor exit swirl distribution is compared with the predicted distribution in Figure 144 and shows good agreement over most of the passage. However, deviations were observed at 26 and 88 percent of the passage height. These deviations are attributed to secondary flow from the stator end wall, which propagates through the rotor. Note that the pressure ratio and total-to-total efficiency distributions shown in Figures 147 and 148 are for overall two-stage conditions.

#### 4.2.5.6.5 Exhaust Diffuser Performance

Since the residual exit kinetic energy is charged to the turbine, maximizing the exhaust diffuser recovery was an integral part of the GTP305-2 turbine system design. The diffuser design was based on a linear static pressure distribution, which from NASA test results indicated significant increases in diffuser recovery, when compared with conventional linear area distribution designs. The predicted diffuser recover was 0.40, based on previous AiResearch diffuser test data with struts. The rig diffuser, which duplicates the engine configuration, is presented in Figure 149, together with the hub and shroud static pressure locations. The turbine system is rated from radial turbine inlet (combustor discharge), to exhaust diffuser exit flange plane.

Additional instrumentation (shroud pressures) were added approximately 1-inch downstream from the diffuser exit, to evaluate the effects of increased area ratio and hub centerbody dump. At the overall design equivalent speed and pressure ratio, the measured diffuser recovery was 0.447, without cooling flow, and 0.467 with cooling flow. The diffuser hub and shroud static pressure distributions for these conditions are presented in Figure 150, together with the predicted distribution.



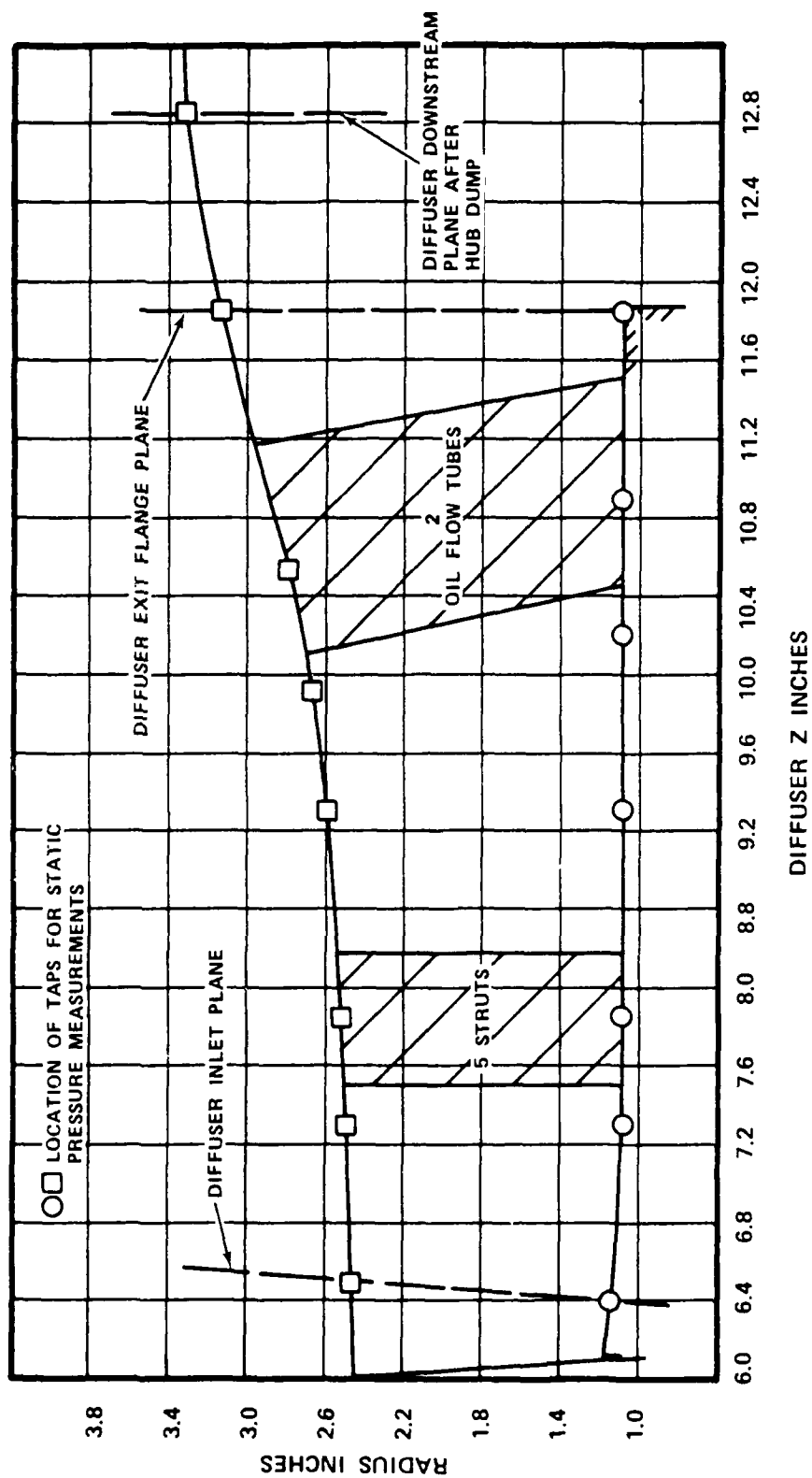


Figure 149. GTP305-2, two-stage test diffuser

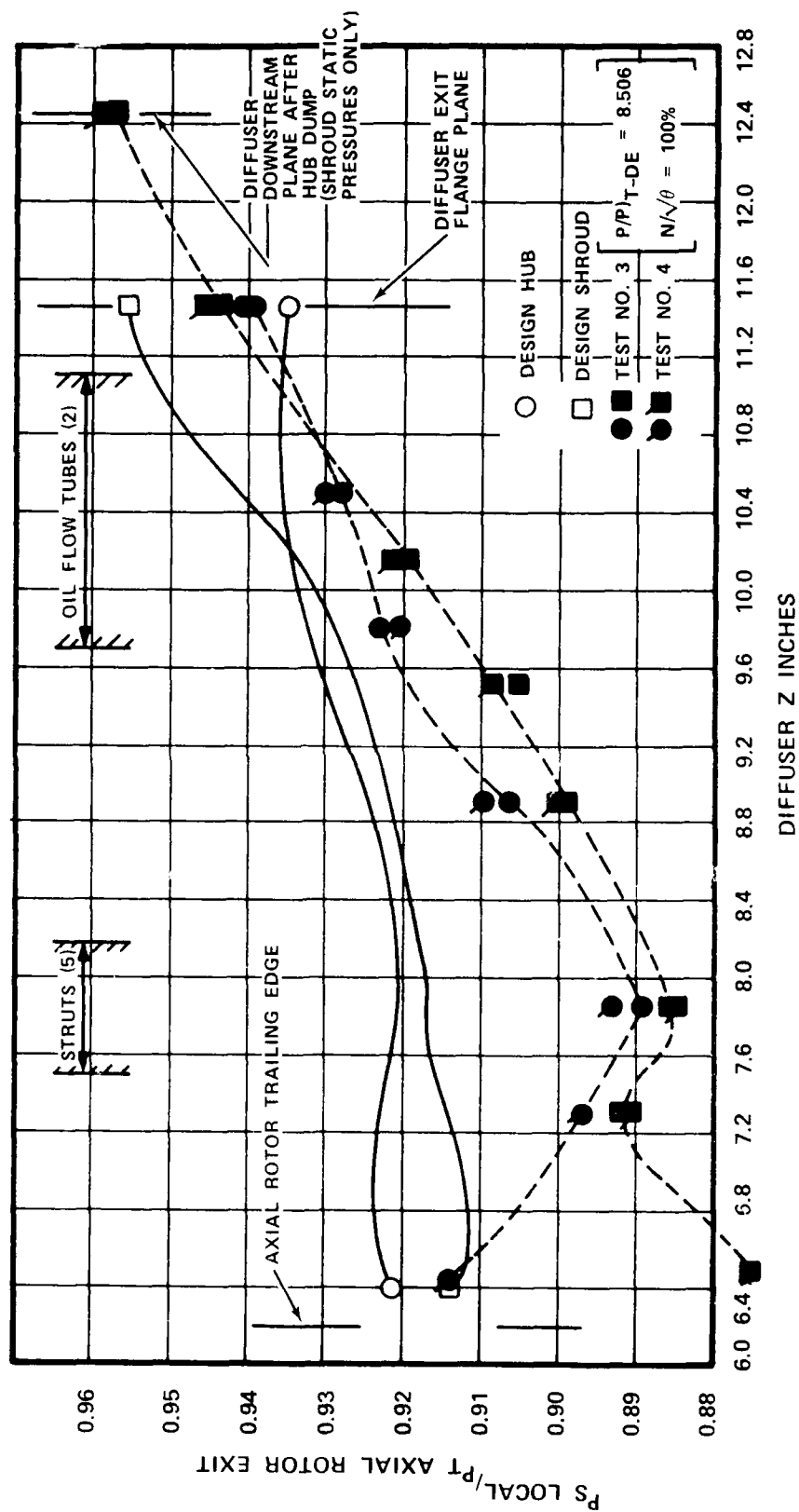


Figure 150. GTP305-2, two-stage test, test nos. 3 and 4

Although the overall predicted diffuser recovery was exceeded, significant deviations from design intent exists throughout the diffuser length. At the diffuser inlet, Figure 150 shows that the rotor exit hub and shroud Mach numbers are higher than design and account for the deviation at the diffuser inlet. At the strut location, Figure 150 shows that locally high incidence at the strut leading edge resulted in increased blockage due to local separation. The diffuser static pressure distribution was then investigated at a lower pressure ratio (reduced inlet velocity and swirl). This result is shown in Figure 151 for an overall pressure ratio of 7.47 and 100 percent speed. Under these conditions, excellent agreement between predicted and measured diffuser static pressure distributions is achieved.

Increasing the diffuser length and area ratio (diffuser down stream plane) increases the diffuser recovery from 0.467 to 0.60 as design speed and pressure ratio (Figure 150). This is equivalent to an increase in efficiency of approximately 0.5 points.

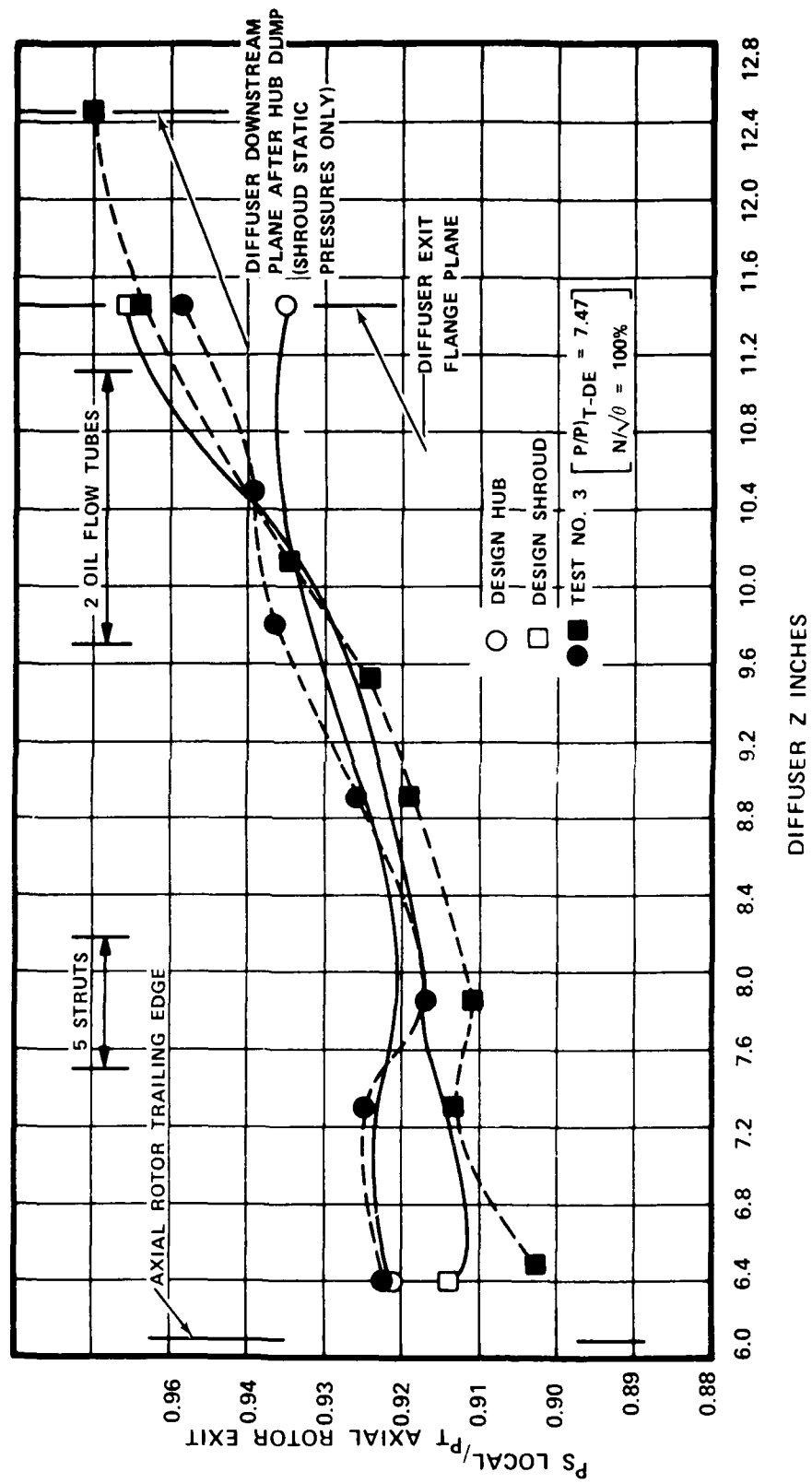


Figure 151. GTP305-2, two-stage test, test no. 3

## SECTION V

### INTEGRATED COMPONENTS ASSEMBLY

The engine combustion system and turbine section components were integrated into a hot turbine test rig to allow for the determination of aerodynamic and mechanical performance under actual operating conditions. The rig utilized the same simulated compressor inlet discharge plenum as the combustion system test rig. Engine rotor dynamics were simulated using dummy compressor masses. Testing consisted of cold (unfired) mechanical checkout, to verify mechanical integrity and critical speeds, and fired mechanical checkout including controls familiarization, performance testing, and Thermindex paint testing to define component operating temperatures.

#### 5.1 Test Rig Description

The test rig, shown in Figure 152, consisted of engine turbine section components (i.e., all components aft of the compressor/diffuser). These components were assembled into the rig to mate with forward structural members, thereby, simulating overall engine length and bearing span.

Dynamically the test rig simulated the engine by substituting dummy rotating masses for the compressors. Rig structure incorporated a toroidal plenum, with inlet pipes at two circumferential locations, for distribution of facility air to the turbine plenum. The inlet plenum was the same as that used during combustion system testing. Preswirl vanes, located at the inlet plenum exit, induce a 25-degree swirl to simulate combustion inlet flow conditions.

As stated above, dummy compressor rotor hardware duplicating rotor mass distribution and stiffness were designed to replicate engine rotor dynamic characteristics in the rig. Figures 153

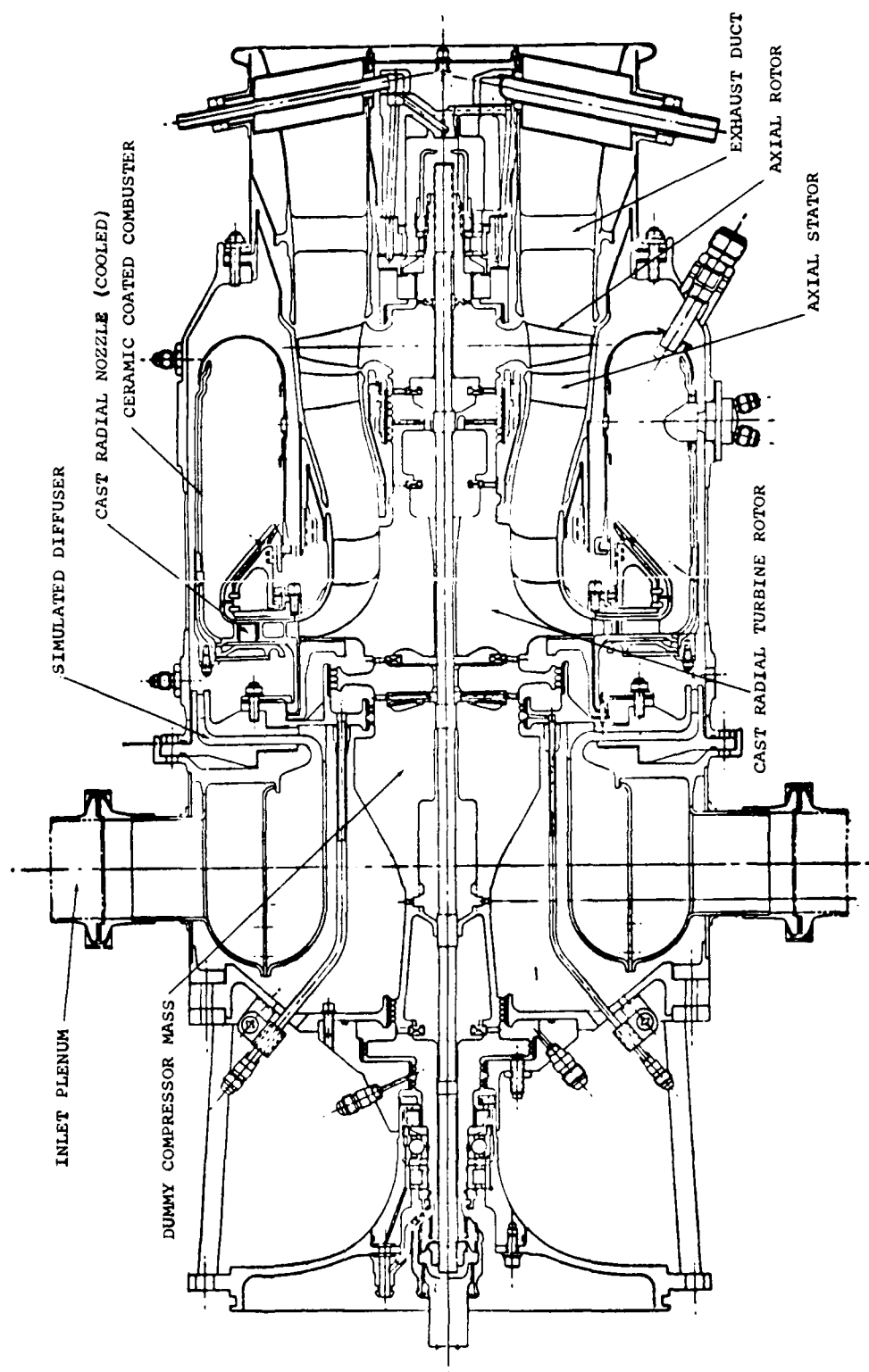


Figure 152. Integrated components assembly test rig

through 155 depict engine rotor dynamic mode shapes. Figures 156 through 157 illustrate predicted rig modal patterns. Note the similarity of shape, approximate speed, and general deflection characteristics at the three predicted critical speeds.

Rotor dynamic modeling was extended to include the gearbox and test facility water brake. Figures 159 through 161 depict the predicted critical speed modes for the gearbox, bull gear, and water brake. An operating speed of 13,000 rpm at the water brake input was determined, based on a gearbox input to output reduction of 5.6. This results from previous analyses and no critical speed problems are anticipated with the test setup.

Provisions were made in the rig to facilitate thrust balance air, as required, in either a forward or rearward thrust mode.

Radial turbine bore cooling air was supplied from the main ICA inlet plenum. Figure 162 illustrates the bore cooling air flow path.

To mate with the test facility water brake the ICA test rig required a reduction gearbox. The gearbox was an industrial quality type designed and fabricated by General Electric, Lynn, Massachusetts. The gearbox employed a single reduction, double helical, speed reduction design. Input speed was 75,685 rpm with an output speed of 13,435 rpm, rated at 1125 hp. As shown in Figure 163, the pinion gear is connected to the turbine by a flexible coupling. The coupling shaft has a shear notch designed to protect the gears from overload. The gear was connected to the water brake by another flexible coupling.

A self contained packaged lubrication oil system was designed and supplied by General Electric. This system also provided ICA bearing lubrication.

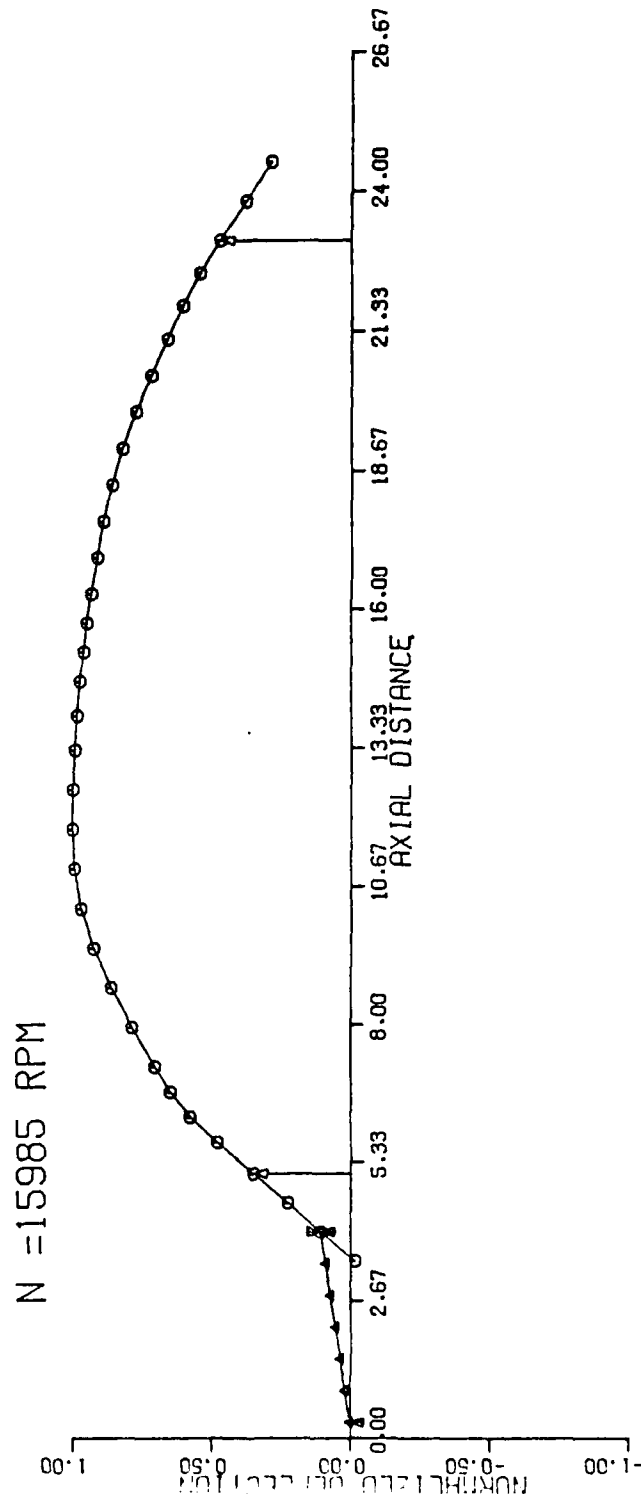


Figure 153. GTP305-2 final design rotating group with modified quill shaft first critical speed mode shape



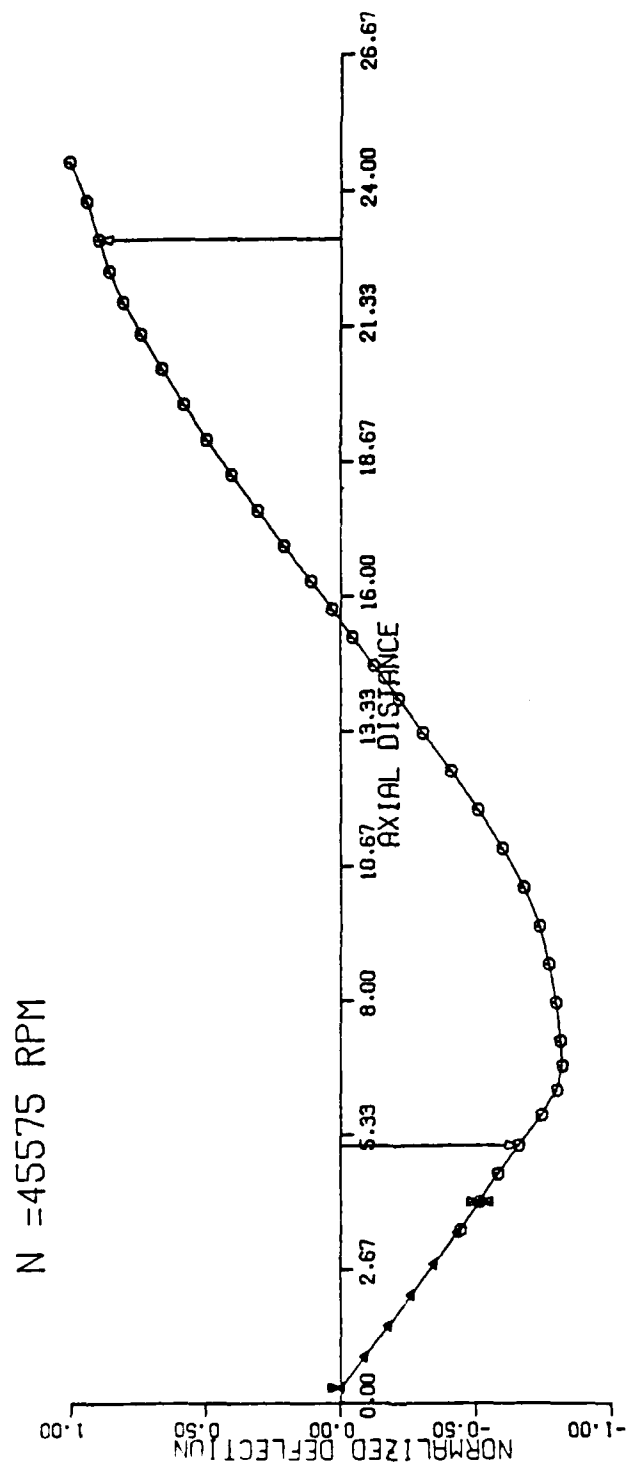


Figure 154. GTP305-2 final design rotating group with modified quill shaft second critical speed mode shape

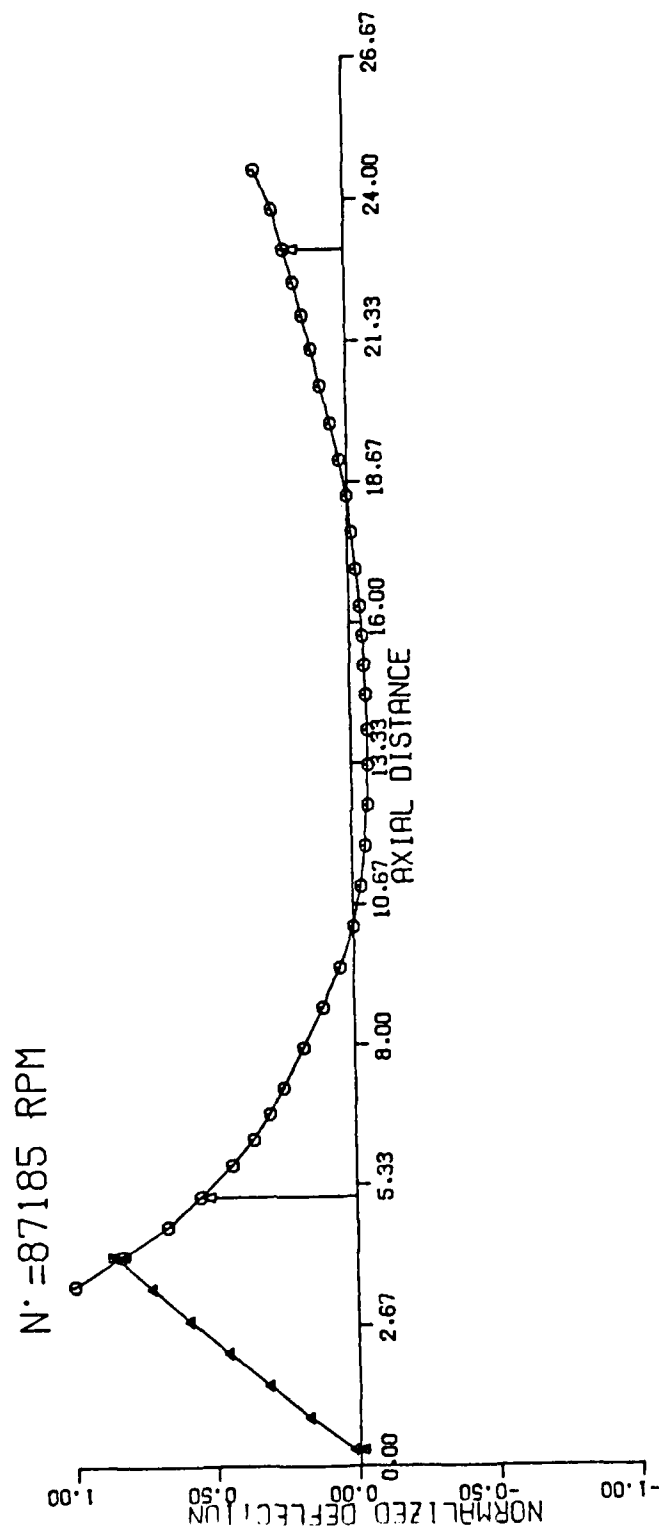


Figure 155. GTP305-2 final design rotating group with modified quill shaft third critical speed mode shape

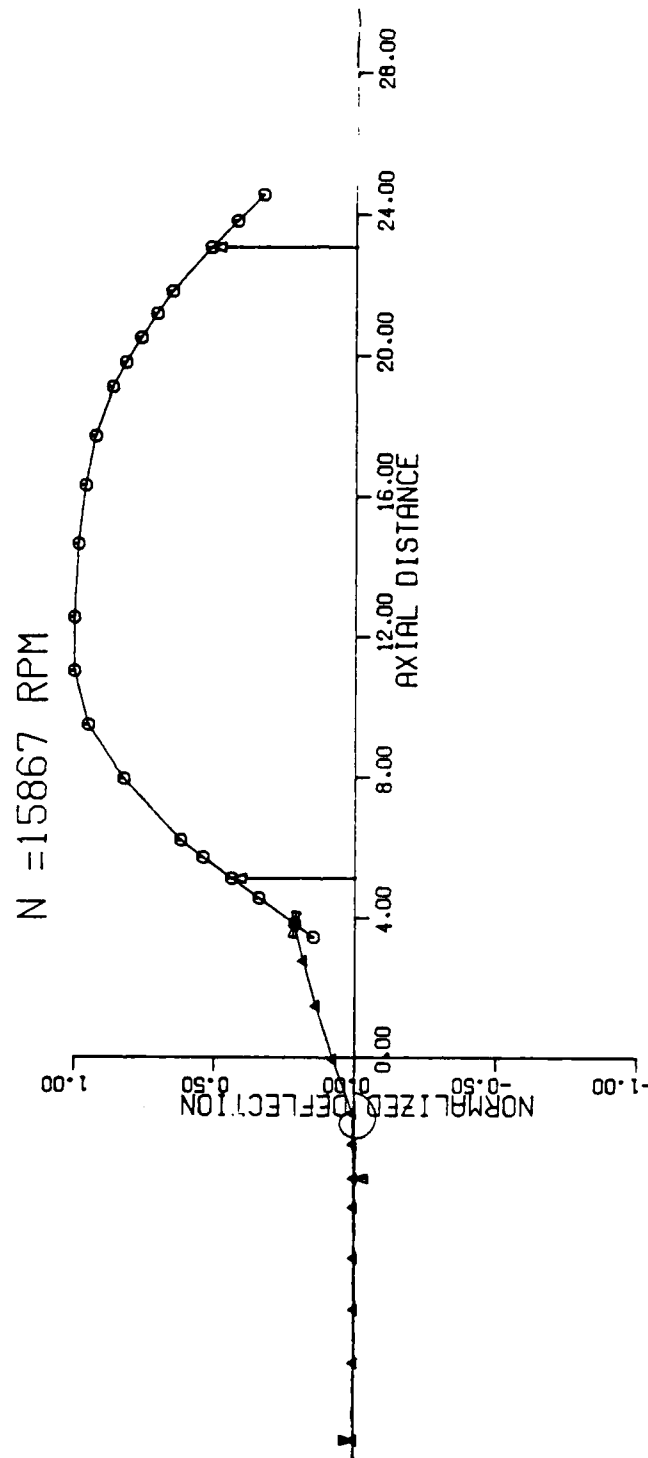


Figure 156. GTP305-2 Integrated rig with quill shaft and pinion gear

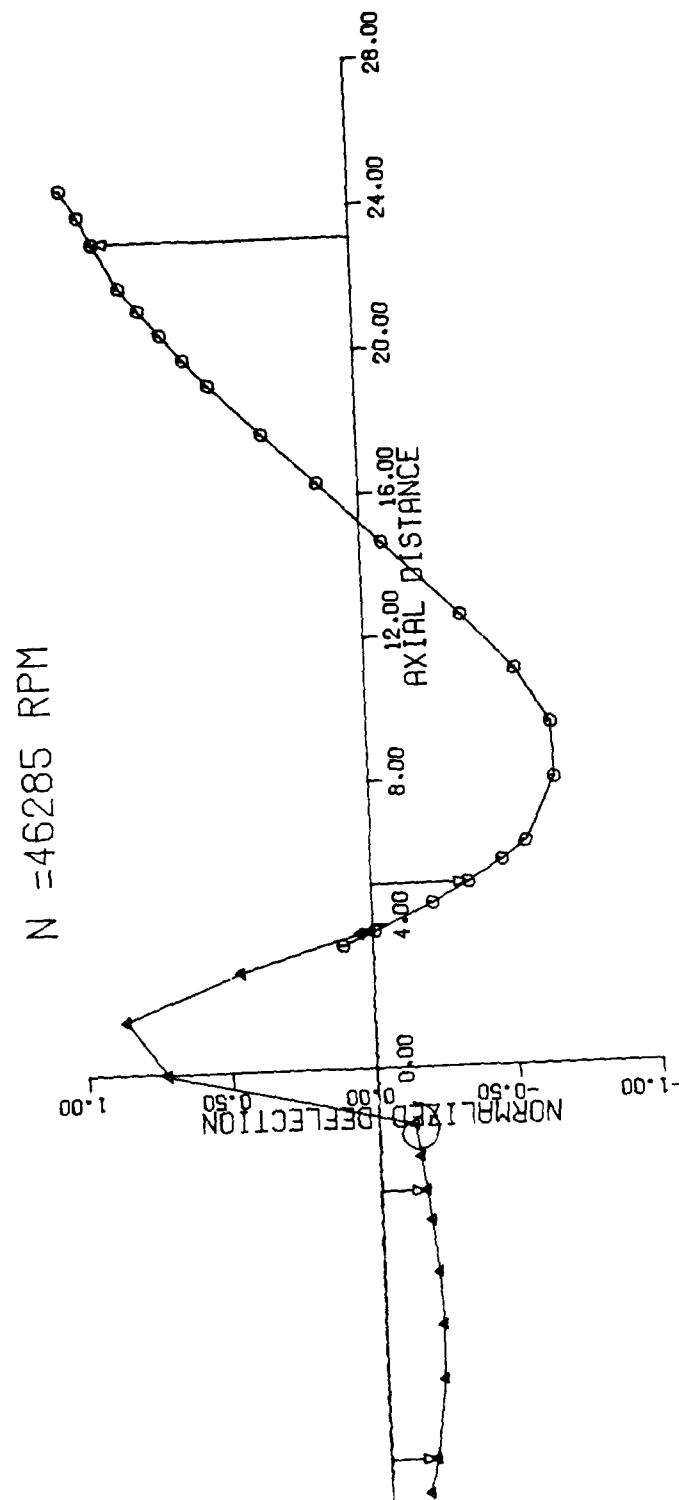


Figure 157. GTP305-2 integrated components rig with quill shaft and pinion gear

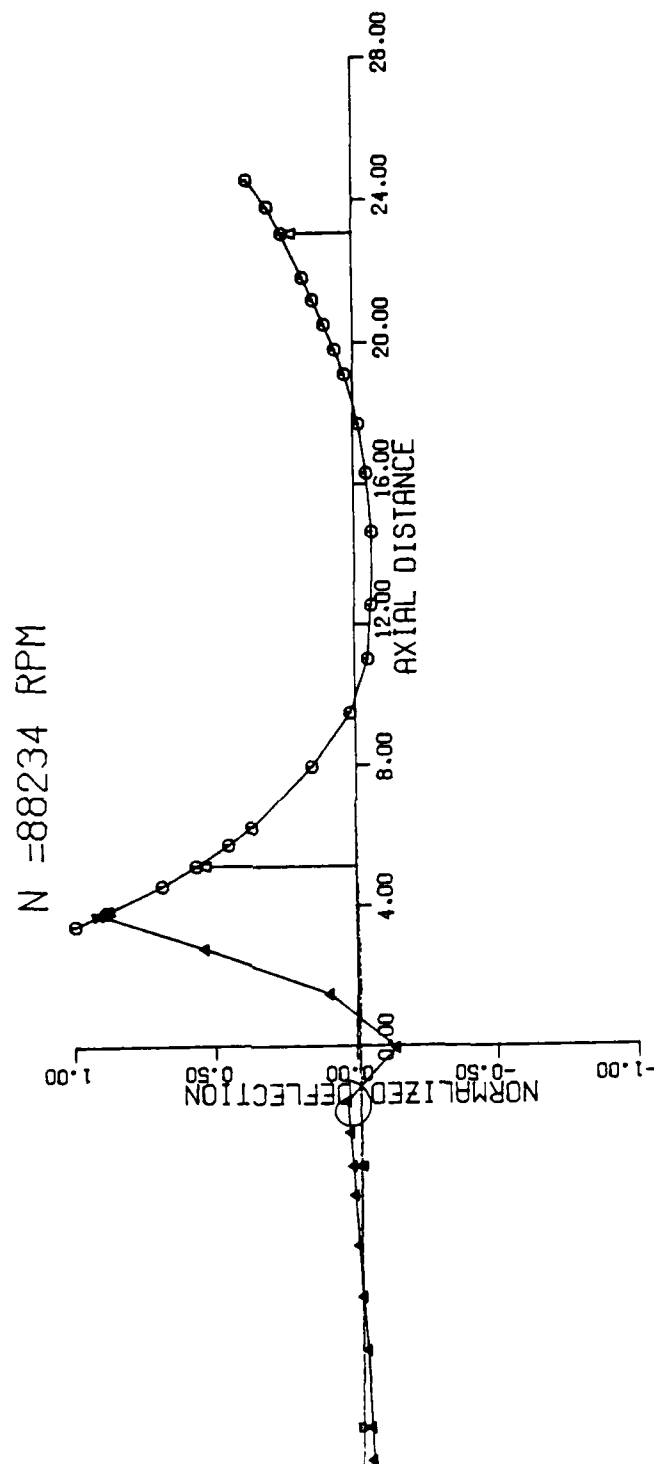


Figure 158. GTP305-2 integrated components rig with quill shaft and pinion gear

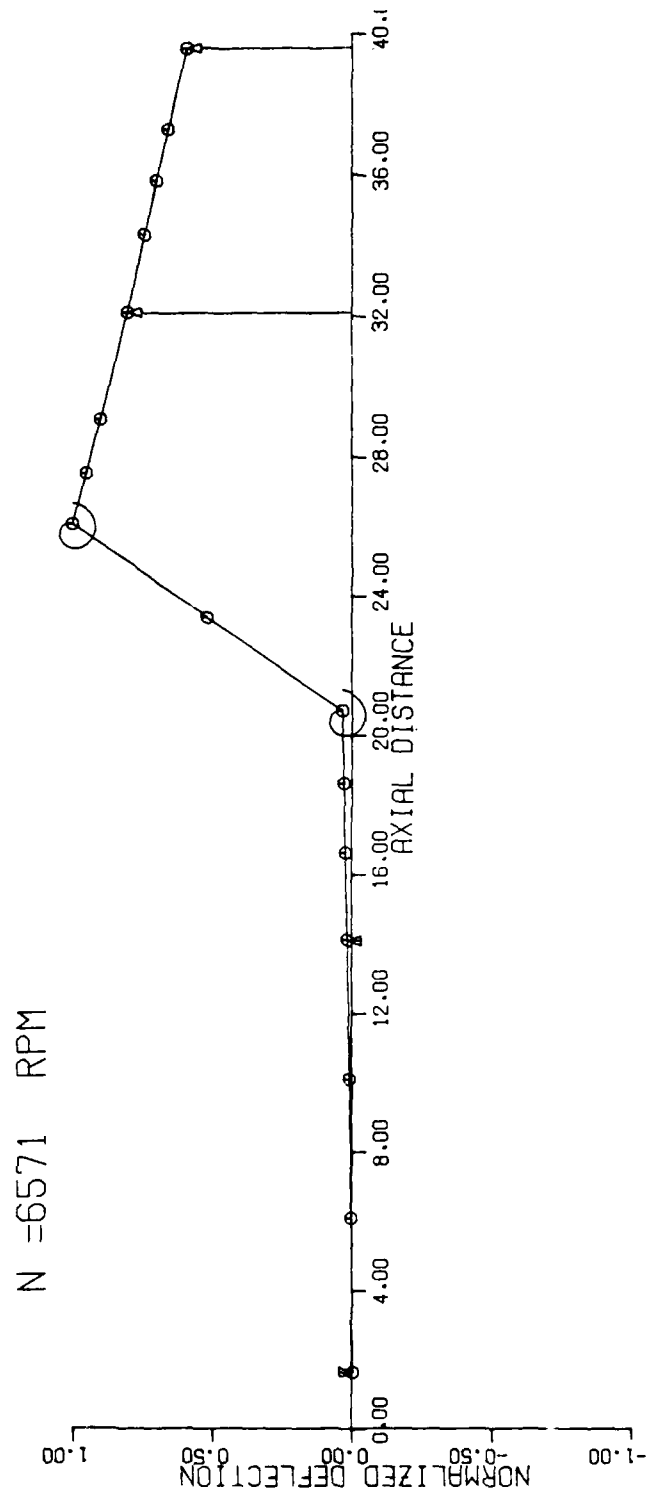


Figure 159. GTP305-2 Water Brake-Bull Gear

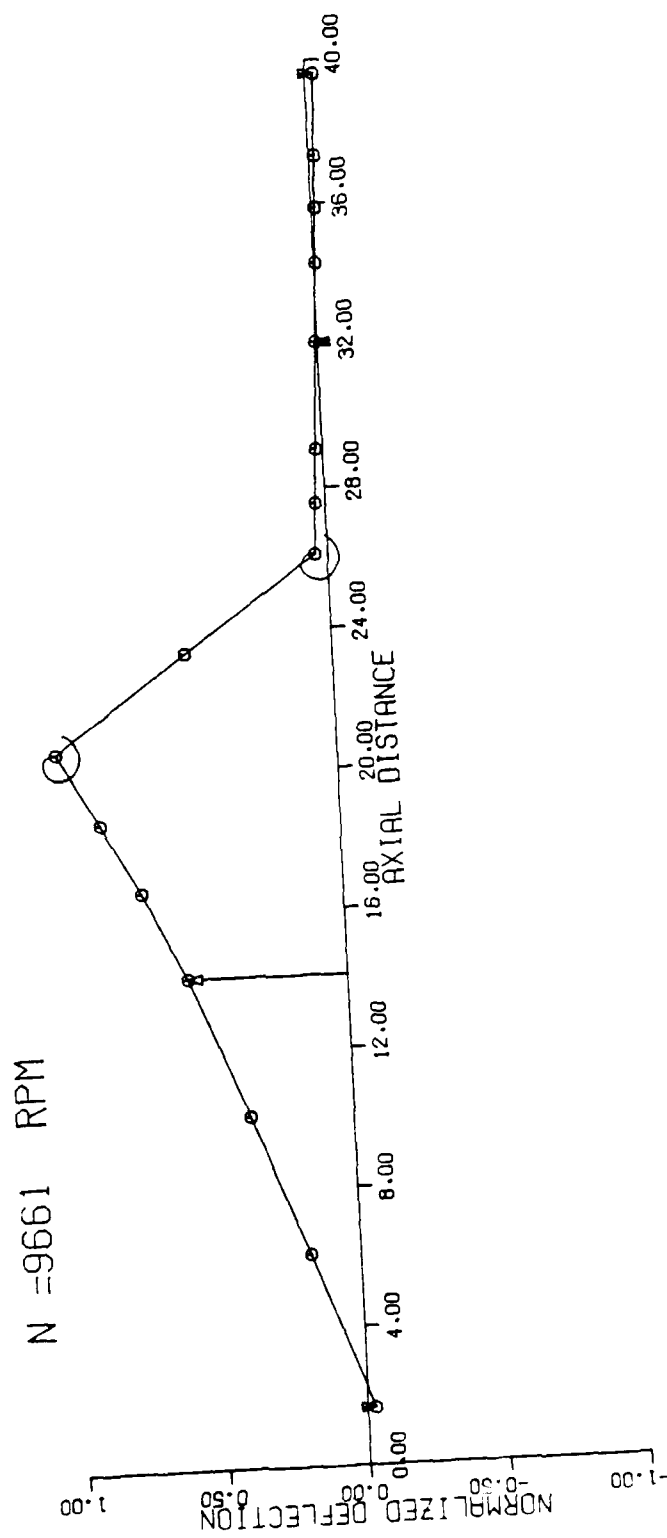


Figure 160. GTP305-2 water brake-bull gear

AD-A087 838

AIRESEARCH MFG CO OF ARIZONA PHOENIX

F/G 10/2

ADVANCED TECHNOLOGY COMPONENTS FOR MODEL 6TP305-2 AIRCRAFT AUXI--ETC(U)

FEB 60 J R KIDWELL, G D LARGE

F33615-75-C-2016

UNCLASSIFIED

AFAPL-TR-79-2106

NL

4 of 6

AD-A087 838

AD-A087 838

AD-A087 838

AD-A087 838

AD-A087 838

AD-A087 838

AD-A087 838

AD-A087 838

AD-A087 838

AD-A087 838

AD-A087 838

AD-A087 838

AD-A087 838

AD-A087 838

AD-A087 838

AD-A087 838

AD-A087 838

AD-A087 838

AD-A087 838

AD-A087 838

AD-A087 838

AD-A087 838

AD-A087 838

AD-A087 838

AD-A087 838

AD-A087 838

AD-A087 838

AD-A087 838

AD-A087 838

AD-A087 838

AD-A087 838

AD-A087 838

AD-A087 838

AD-A087 838

AD-A087 838

AD-A087 838

AD-A087 838

AD-A087 838

AD-A087 838

AD-A087 838

AD-A087 838

AD-A087 838

AD-A087 838

AD-A087 838



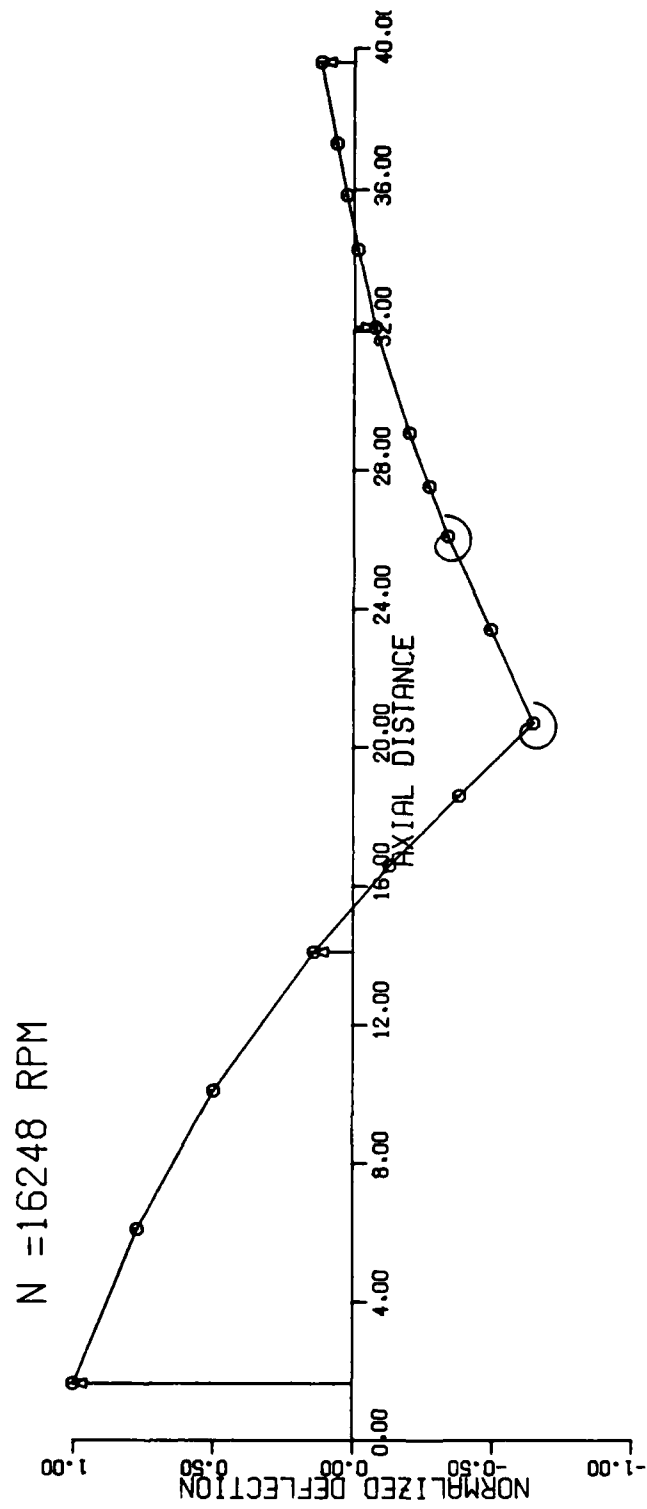


Figure 161. GTP305-2 water brake-bull gear

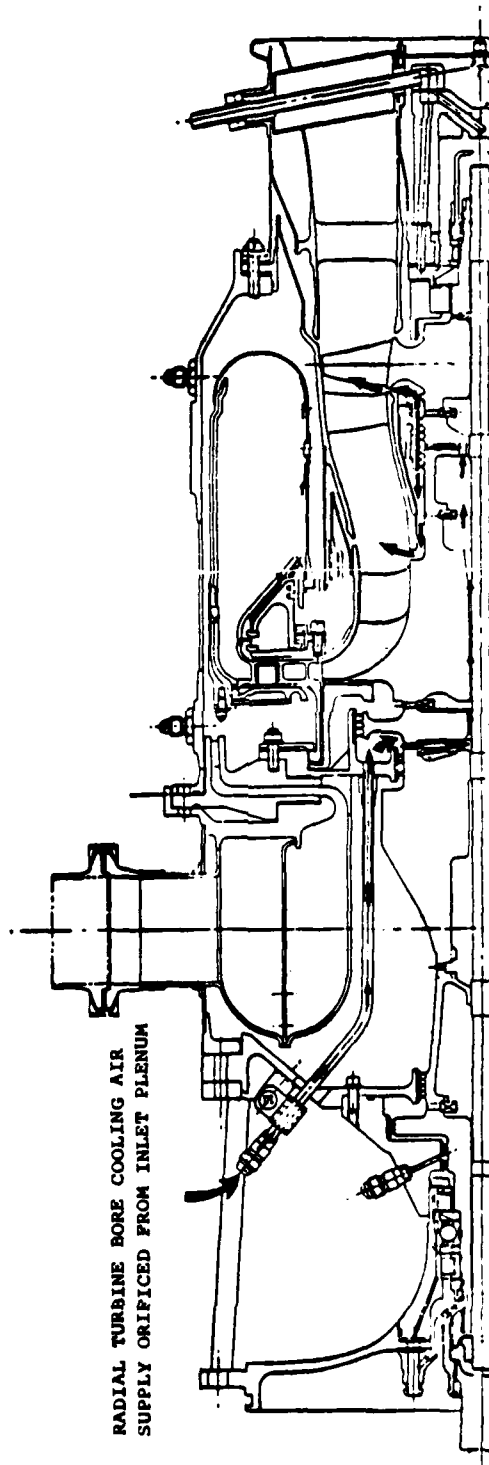
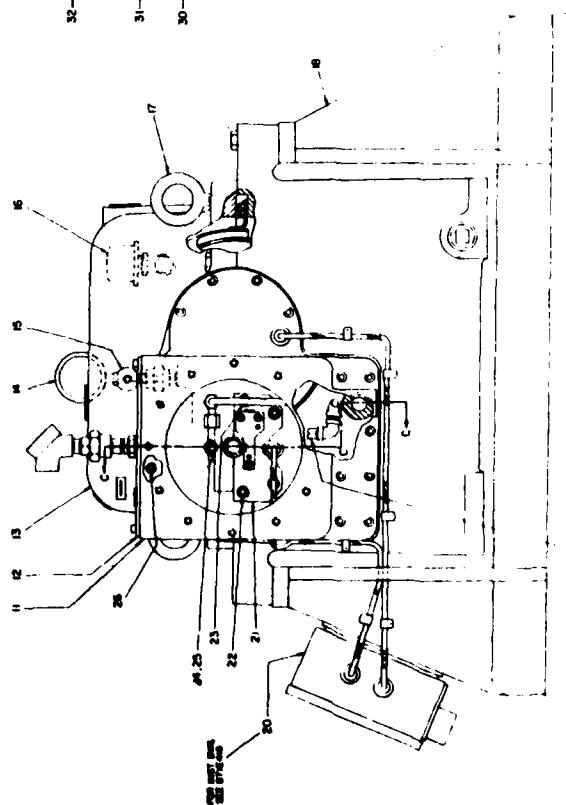
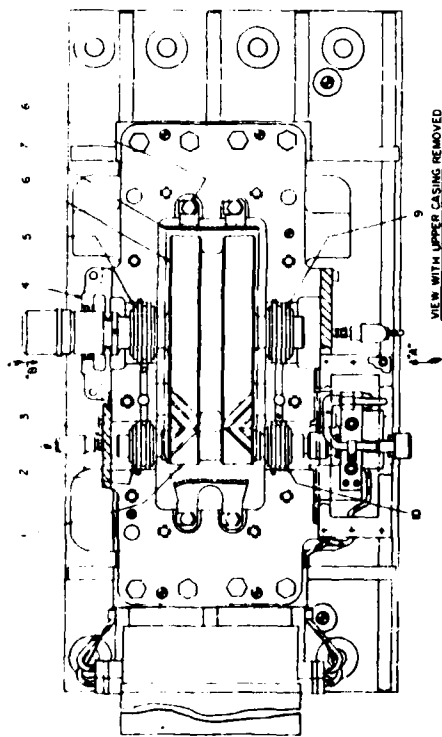


Figure 162. Simulated ICA radial turbine bore cooling flowpath



- 1 Pinion Bearing
- 2 End Cover
- 3 Oil Deflector
- 4 Gear Bearing
- 5 Shaft and Gear
- 6 Oil Shroud
- 7 Lockwasher
- 8 Gear Bearing
- 9 Pinion Bearing
- 10 Turbine Support Adapter
- 11 Cover
- 12 Gearing Assembly
- 13 Pressure Gauge
- 14 Gate Cock
- 15 Vent Assembly
- 16 Pinion Support
- 17 Oil Nozzle
- 18 Instrumentation Assembly
- 19 Limiter Excursion Assembly
- 20 Bolt
- 21 Bolt
- 22 Bolt
- 23 Bolt
- 24 Clip
- 25 Bolt
- 26 Bolt
- 27 Orifice Plug
- 28 "O" Ring
- 29 Coupling Hub (Turbine)
- 30 Coupling Gull Assembly
- 31 Coupling Gull Assembly
- 32 "O" Ring
- 33 "O" Ring

Desg. 871E553 - General Electric Company  
Gear Type S-230  
Photo No. 1230597

- Recommended Maintenance Spares
- Recommended Insurance Spares

PHOTO NO 1230597

GENERAL ELECTRIC COMPANY	
ASSEMBLY	
10-1889	871E553

ENLARGED SECTION "C-C-C"

Figure 163 Integrated Components Assembly Gearbox

## 5.2 Hardware Fabrication

ICA hardware fabrication required deviation from APU design intent in several areas, including the axial turbine rotor, axial turbine stator, exhaust duct, and oil transfer housing. In all cases, these items were initially designed as cast hardware for the APU, however, due to program scope, the items were fabricated using machined forgings or bar stock.

The following paragraphs describe the major aerodynamic hardware fabrication task for the ICA.

### 5.2.1 Radial Turbine Rotor

The radial turbine rotor was fabricated in the as-designed state. The rotor was investment cast using AF2-1DA material. The cast version of AF2-1DA alloy, developed under AFML Contract No. F33615-71-C-1573 (Report AFML-TR-74-227), was selected for use in the radial turbine rotor. Selection was based upon wheel design, ultimate strength, stress rupture and LCF requirements. These criteria eliminated candidate alloys IN100, MM002 and C-101.

#### 5.2.1.1 Casting Process

An investment casting process, producing acceptable internal grain structure and mechanical properties in a 15 pound radial turbine rotor, was developed under the AF2-1DA program. This process required modification for the smaller 9-pound rotor, depicted by Figure 164, used in the GTP305-2 turbine engine. These modifications included mold insulation, superheat temperature modification and six iterations to produce the internal and external grain structure depicted by Figure 165. Three tool modifications were also required to produce correct blade profiles and thicknesses and were incorporated in the six casting iterations.

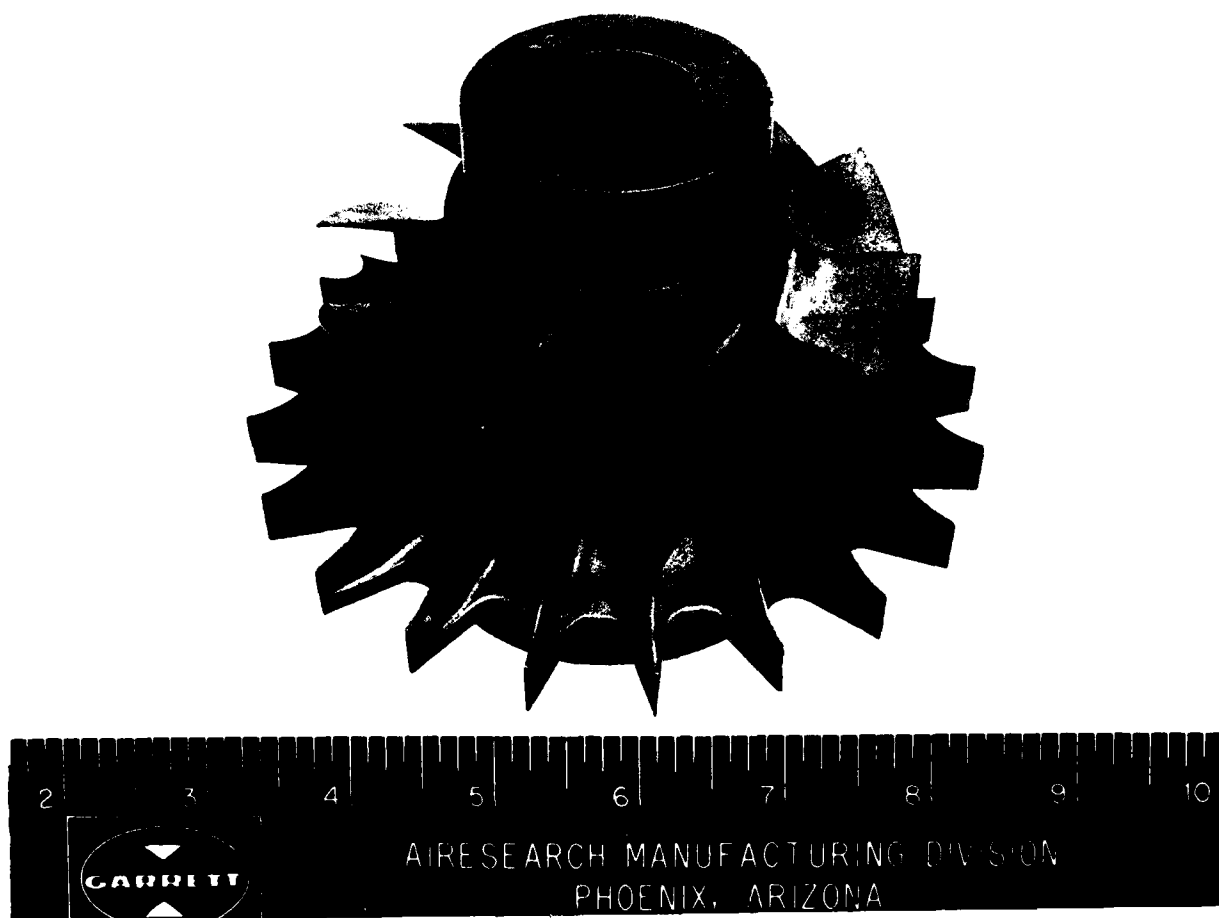
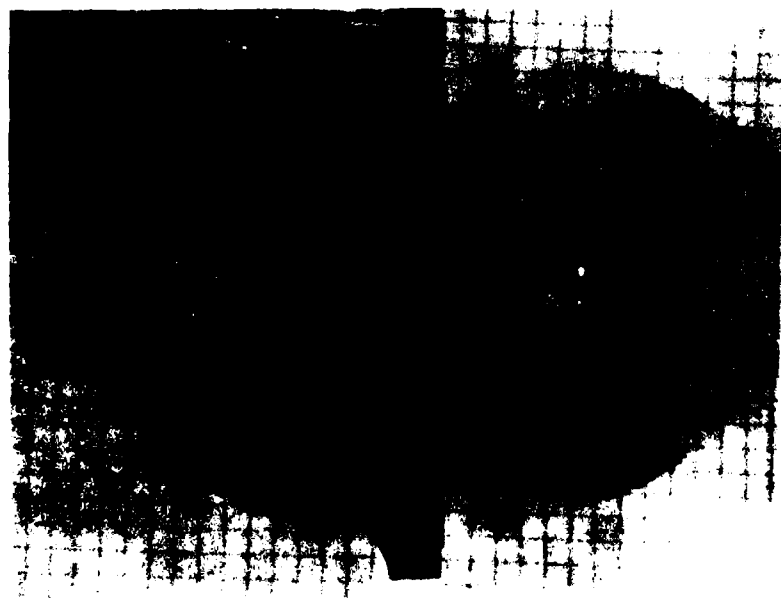
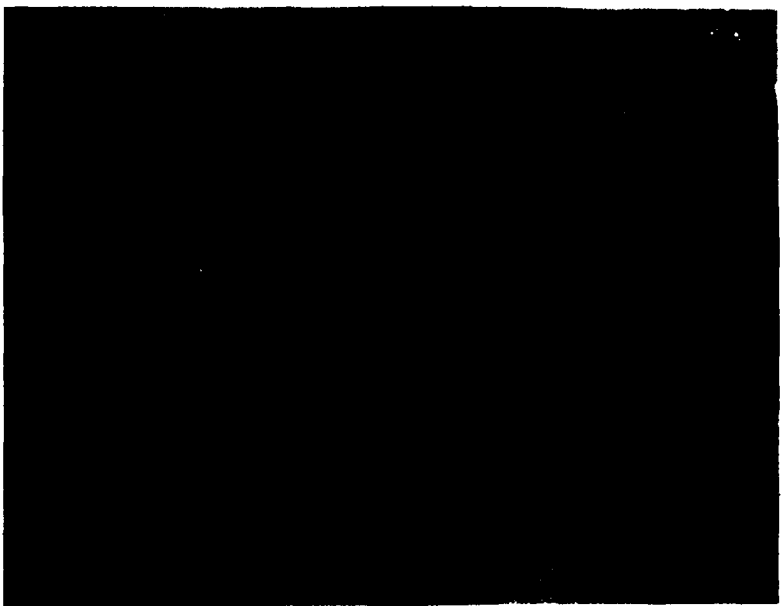


Figure 164. Cast AF2-1DA alloy GTP305-2 radial turbine wheel



EXTERNAL SURFACE  
ETCH:  $\text{HCL-H}_2\text{O}_2$



INTERNAL GRAIN STRUCTURE  
ETCH:  $\text{HCL-H}_2\text{O}_2$

Figure 165. Macroscopic grain structure produced in  
cast AF2-1DA alloy radial turbine rotor

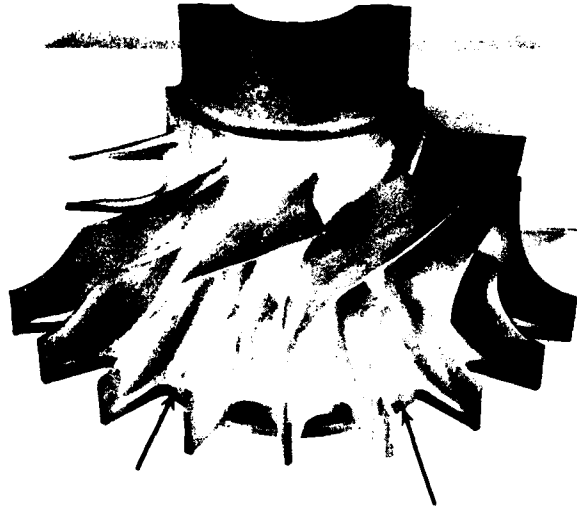
### 5.2.1.2 Heat Treatment Process

Heat treatment developed for cast AF2-1DA alloy, in the AFML Program, produced tensile properties at minimum values shown below and could be achieved with confidence.

	0.2 Percent Yield Strength	Ultimate Tensile Strength	Elongation Percent
Room Temperature	115 ksi	130 ksi	5.0
1400°F	105 ksi	130 ksi	5.0

This process required a solution treatment at 2175°F and two intermediate ages; one at 1950°F and the other at 1400°F. Rapid argon gas quenching was performed after the solution treatment and the first age. Gamma prime size was controlled, resulting in tensile properties above minimum levels. However, saddle cracks occurred between the blades when the developed heat treatment was used on the GTP305-2 radial turbine rotor (see Figure 166). Approximately 50 percent of the wheels heat treated using this method revealed at least one cracked saddle and a number exhibited more than one cracked region.

A study to modify the heat treatment argon quench rate was performed with the objective of maintaining tensile properties above minimum levels. Vacuum furnace cooling modifications, resultant cooling rates measured in the rotor hub center, and the average tensile properties are shown in Table 29. Results indicate argon gas backfill (without the circulating fan) produced acceptable tensile properties without exhibiting saddle cracks.



LOCATION OF CRACKS (ARROWS) MAG: 1/2X



DETAIL OF CRACKS (ARROWS) MAG: 6X

Figure 166. Small cracks produced by rapid gas quenching during heat treatment



TABLE 29. COOLING RATE STUDY RESULTS ON CAST AF2-1DA

Cooling Modification	Cooling (1) Rate, °F/min	Saddle Cracks Detected	Room Temperature Tensile Properties		
			0.2 Percent YS, ksi	UTS ksi	Percent Elongation
Gas Scan Quench	90-100	Yes	131.4	140.0	4.2
Gas Cool	44-50	No	124.2	132.9	5.9
Gas Cool - Insulated Wheel	20-30	No	121.2	126.4	5.5
Vacuum Cool	18	No	121.4	123.2	4.4
Property Specification Minimums			115.0	130.0	5.0

YS = Yield Strength

UTS = Ultimate Tensile Strength

(1) Rate measured in wheel center average value from 2175-1400°F.

The heat treatment process is shown below:

- o Solution: 2175±25°F (2 hours) argon gas cool at a rate of approximately 50°F min \*
- o Intermediate Age: 1950±25°F (2 hours) argon gas cool at a rate of approximately 50°F min \*
- o Age: 1400±25°F (16 hours) air cool

\*Rate measured in wheel center; average to 1400°F.

Tables 30, 31, and 32 show tensile, stress rupture, and low cycle fatigue (LCF) properties produced by the developed casting and heat treatment procedure. These baseline wheel properties were produced as part of the hot isostatic pressure (HIP) study disclosed in Section 7.0. Average tensile properties exceed AiResearch specification minimum values. Stress-rupture properties, although tested at stresses different from AiResearch specifications, exceed minimum values, when analyzed on a Larson-Miller plot.

Following successful casting trials, the rotor was final machined as shown in Figure 167 and delivered to the ICA rig assembly area.

#### 5.2.2 Radial Turbine Nozzle

The radial turbine nozzle was fabricated as designed. Inconel 738 material was used consistent with design analysis. As shown in Figure 168, wax patterns were gated using a five-gate arrangement to fill both forward and aft walls. Inspection of initial castings revealed microporosity and shrinkage in the

TABLE 30.

ROOM AND ELEVATED TEMPERATURE TENSILE  
PROPERTIES OF HEAT-TREATED\*

## CAST AF2-1DA ALLOY TURBINE WHEELS

Specimen Number	Temperature (°F)	0.2% YS (ksi)	UTS (ksi)	EL (%)	RA (%)
72-3	RT	122.4	133.6	3.6	13.7
75-3	RT	120.1	125.7	4.3	10.5
83-5	RT	129.0	144.7	4.8	8.0
72-5	1400	111.7	134.5	5.7	14.8
81-3	1400	112.1	142.5	5.9	13.5
87-3	1400	114.0	134.3	6.3	16.4

Property  
Specifica-  
tion  
Minimums

RT	115.0	130.0	5.0
1400	105.0	130.0	5.0

\*2175°F for 2 hours with Argon gas quench; plus 1950°F for 2 hours with Argon gas quench; plus 1400°F for 16 hours with air cooling.

TABLE 31.

ELEVATED TEMPERATURE STRESS RUPTURE  
PROPERTIES OF HEAT-TREATED\*

## CAST AF2-1DA ALLOY TURBINE WHEELS

Specimen Number	Temperature (°F)	Stress (ksi)	Rupture Time (Hours)	Elongation (%)	Reduction of Area (%)
72-6	1400	90	152.4	4.0	10.6
81-4	1400	90	102.7	4.3	8.0
75-4	1600	55	158.8	7.9	11.2
83-6	1600	55	161.4	6.2	8.9
81-6	1800	27	89.0	7.8	16.2
87-4	1800	27	97.1	8.3	16.7

Property  
Specifi-  
cation  
Minimums

1400	95	23.0	3.0
1800	30	23.0	4.0

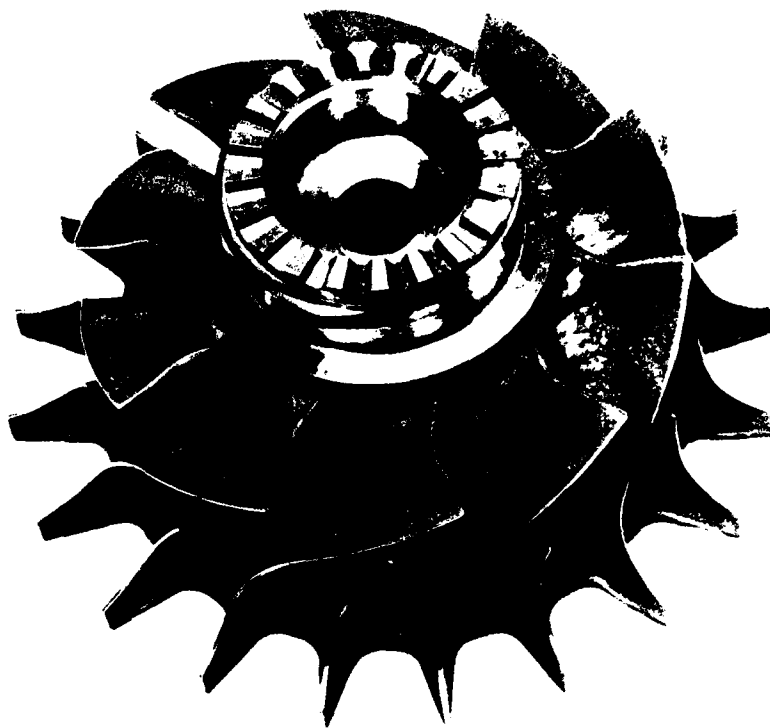
\*2175°F for 2 hours with Argon gas quench; plus 1950°F for 2 hours with Argon gas quench; plus 1400°F for 16 hours with air cooling.

TABLE 32. ROOM TEMPERATURE LOW-CYCLE FATIGUE  
(LCF) PROPERTIES OF HEAT-TREATED\*  
CAST AF2-1DA ALLOY TURBINE WHEELS

Specimen Number	Total Strain Range (%)	Measured Elastic Modulus (E X 10 <sup>6</sup> PSI)	N <sup>f</sup> (Cycles to Failure)
72-1	0.77	26.1	3,957
87-2	0.69	29.0	14,894
75-1	0.66	30.9	7,974
75-2	0.65	31.3	17,722
83-1	0.62	32.9	13,182
83-2	0.60	33.3	8,932
81-1	0.60	33.1	10,111
87-1	0.60	33.8	13,221

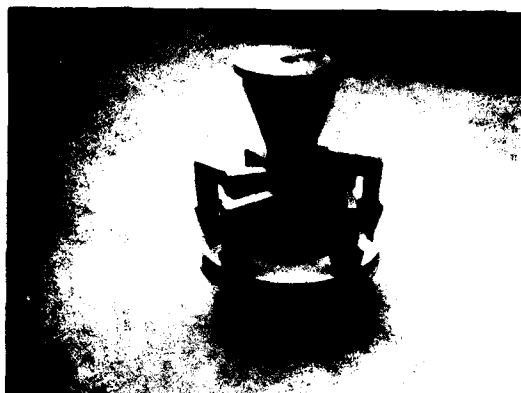
Test Parameters: Axial strain control, A Ratio =  $\infty$   
(As defined in the statement of work) 20 CPM frequency and 200 ksi pseudo-stress

\*2175°F for 2 hours with Argon gas quench; plus  
1950°F for 2 hours with Argon gas quench; plus  
1400°F for 16 hours with air cooling.



Garrett

Figure 167. Cast radial turbine rotor (looking forward)  
P/N 3605248



VIEW A



VIEW B



VIEW C

Figure 168. P/N 3605601 wax patterns

nozzle shroud region. Adjustment was made to the gating arrangement (i.e., an internal spider gate arrangement, rather than external finger gating). In addition, two casting parameters were adjusted to achieve a better material flow condition. These were the material pour temperature, which was lowered 100°F and the mold preheat temperature, which was raised 100°F. These changes resulted in an aerodynamically and metallurgically acceptable part. Figures 169 and 170 show the cast nozzle wax pattern with ceramic cores inserted and the slurry dipped mold ready for preheat. Figures 171 and 172 show an early nozzle that is partially machined to inspect the internal chordwise cooling fins.

Following final machining the nozzle was instrumented as shown in Figures 173 and 174 and delivered to the ICA rig assembly area.

#### 5.2.3 Axial Turbine Stator

The APU design incorporates a cast axial stator assembly. ICA fabrication was accomplished by machining the individual stator vanes and brazing the vanes to the hub and shroud, which were sheet metal formed. The stator was then instrumented and delivered to the ICA rig assembly area. Figure 175 shows a view of the stator assembly after instrumentation.

#### 5.2.4 Axial Turbine Rotor

Detail design of the GTP305-2 APU axial rotor required a cast design using AF2-1DA material. Due to program scope, fabrication of the ICA rotor required machining an AF2-1DA forging. However a material substitution was required because forged AF2-1DA could not be obtained on a timely basis. Astroloy was substituted with no significant impact on integrated components testing. The machined axial rotor is shown in Figure 176.





Figure 169. Cast radial nozzle wax pattern with ceramic cores in place

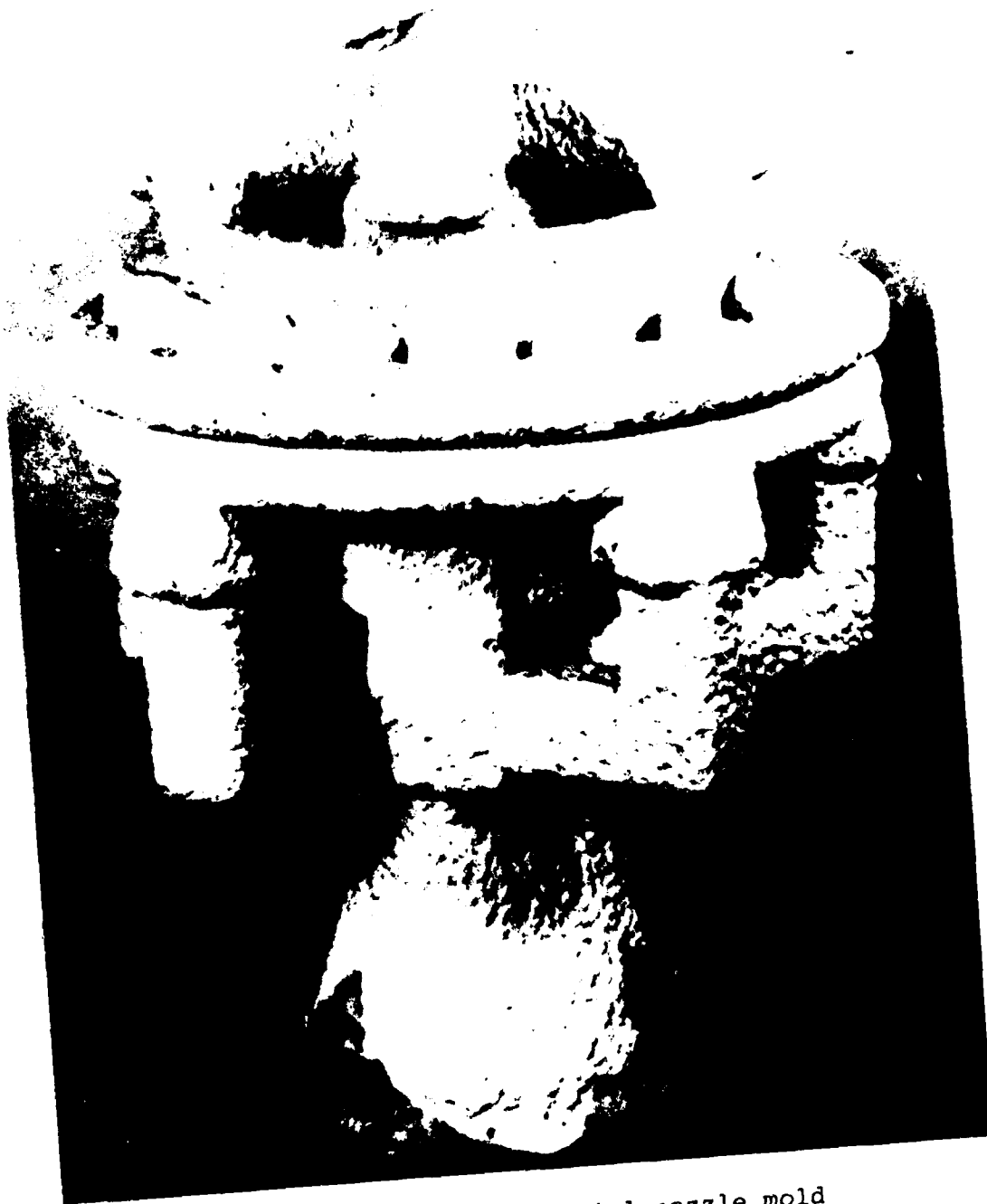


Figure 170. Cast radial nozzle mold

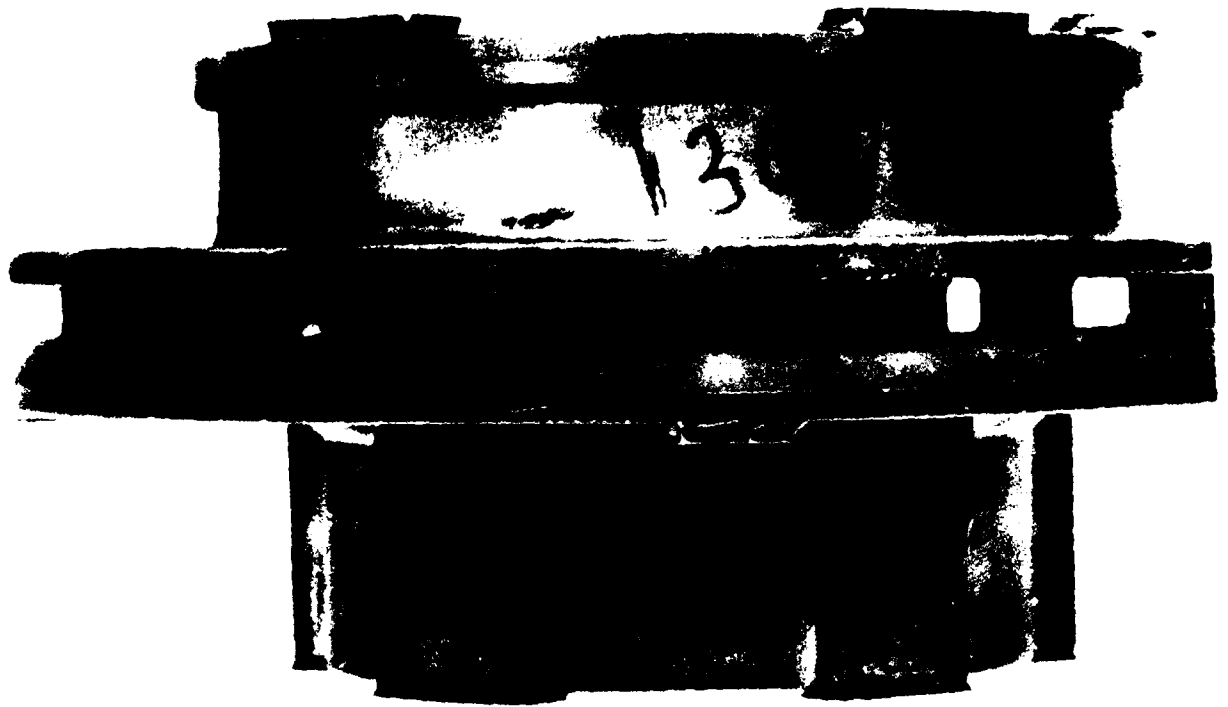


Figure 171. GTP305-2 partially machined nozzle

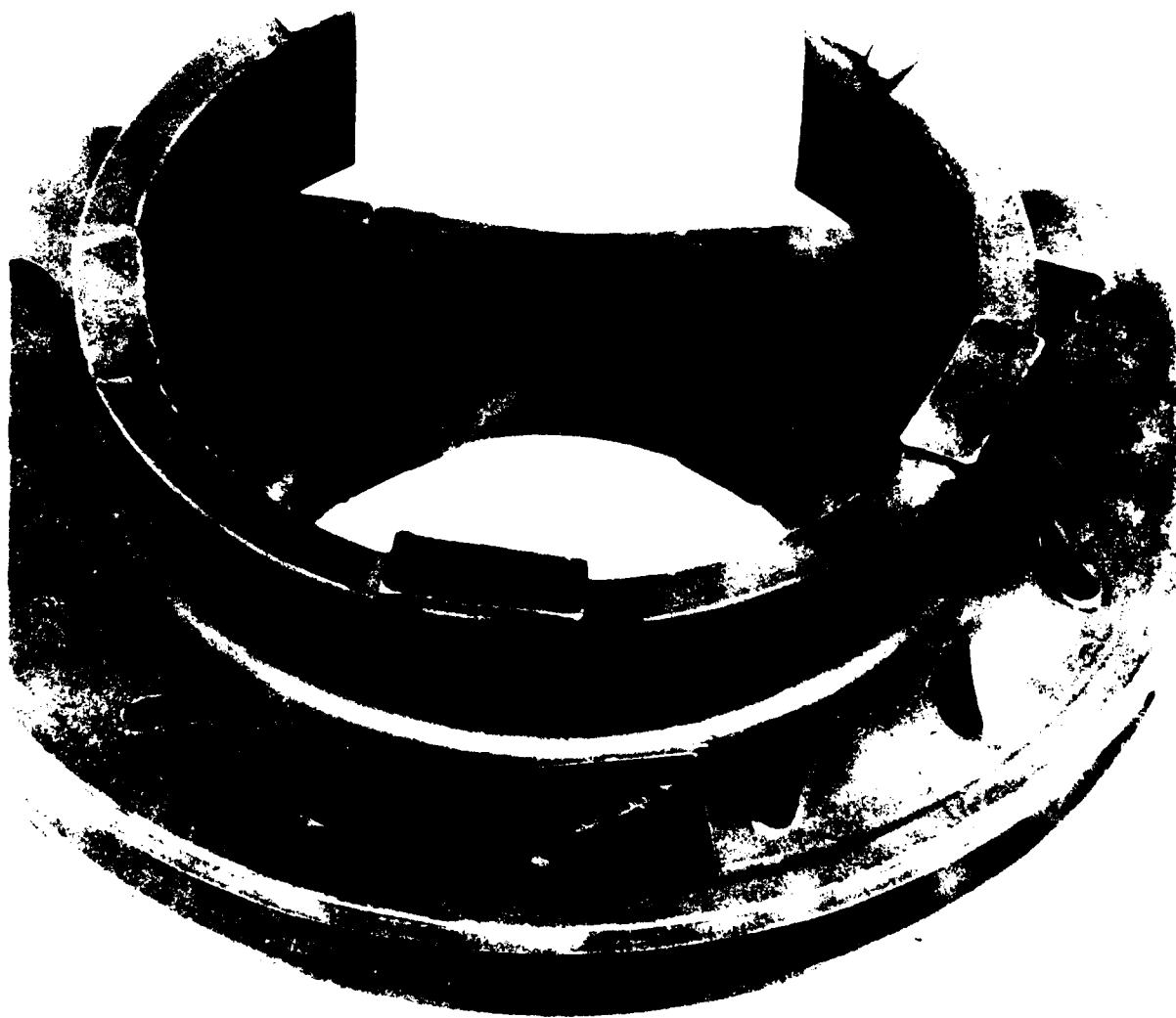


Figure 172. GTP305-2 partially machined nozzle

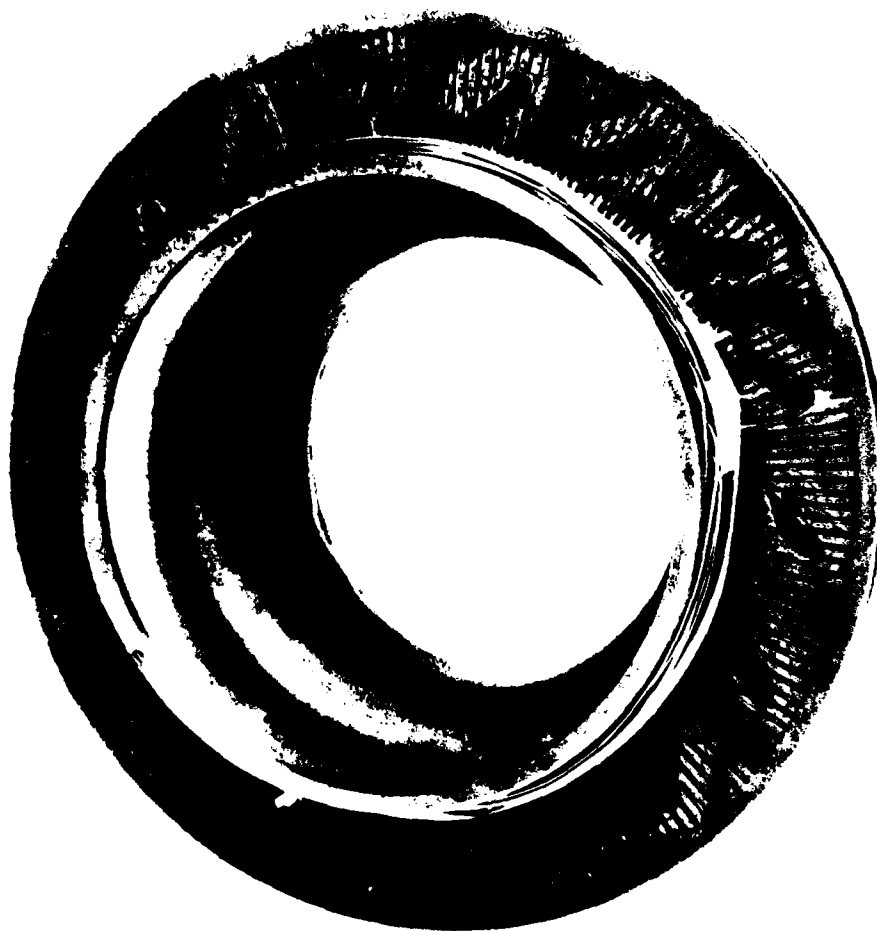


Figure 173. Cast radial nozzle (looking aft)  
P/N 3605601

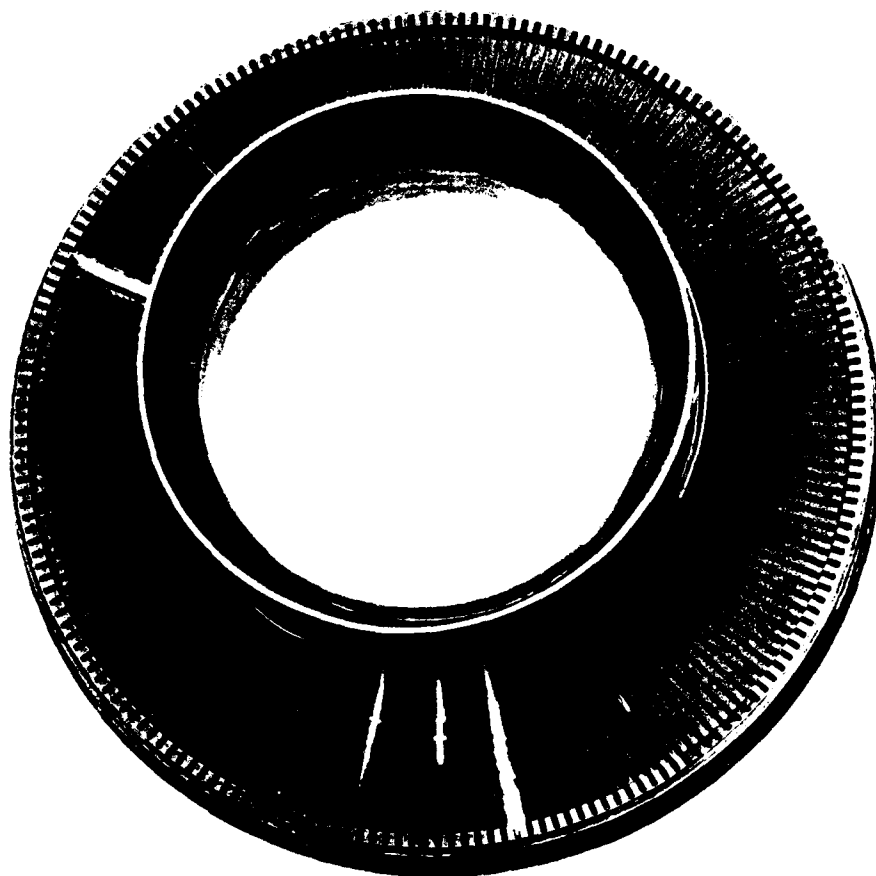


Figure 174. Cast radial nozzle (looking forward)  
P/N 3605601



Figure 175. Axial turbine stator (looking aft)  
P/N 3606194

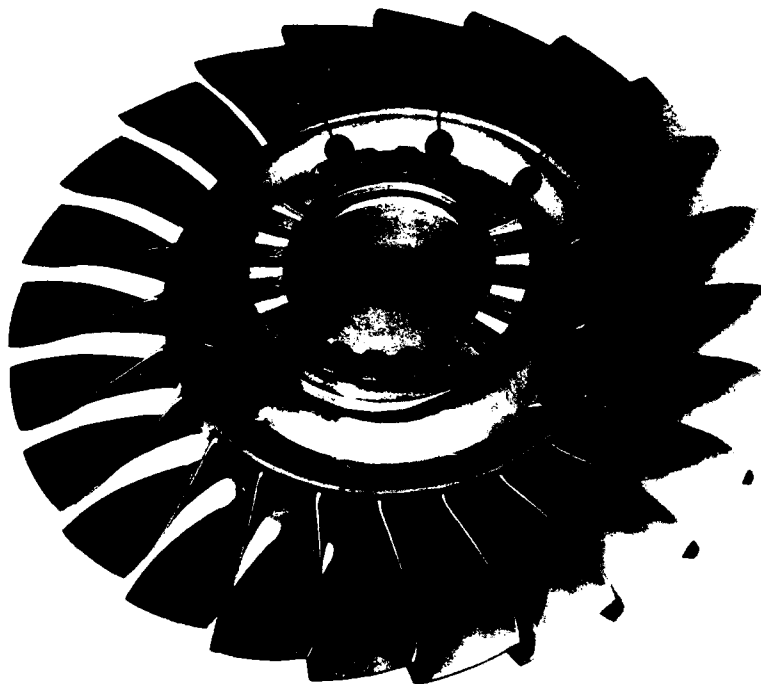


Figure 176. Machined axial turbine rotor  
(looking aft) P/N 3605601



#### 5.2.5 Exhaust Duct Assembly

Fabrication of the turbine exhaust duct assembly deviated from APU design intent in that the radial struts were machined from bar stock rather than cast. Again this method of fabrication was a result of overall program scope. Figure 177 depicts the instrumented exhaust duct prior to ICA assembly.

#### 5.2.6 Combustor Liner

The as designed combustor was fabricated using Hastelloy-X sheet metal coramically coated on the internal wall. Figure 178 depicts the liner ready for ICA assembly.

#### 5.3 Instrumentation

Combustion system inlet flow parameters were measured upstream of the inlet plenum. As inlet flow entered the plenum bore, cooling air was extracted. Static pressure sensors located in the bore cooling supply cavity were used to assure that supply pressure, as designed, was maintained. Flow path instrumentation, which was used to define aerodynamic and mechanical performance, was as shown in Figures 179 and 180. In addition to the instrumentation mentioned above, the following instrumentation was incorporated in the facility portion of the test setup:

- o Turbine exit temperature thermocouples were located downstream of the turbine exhaust diffuser in the insulated facility exhaust duct
- o Emission probes were located in the facility exhaust duct

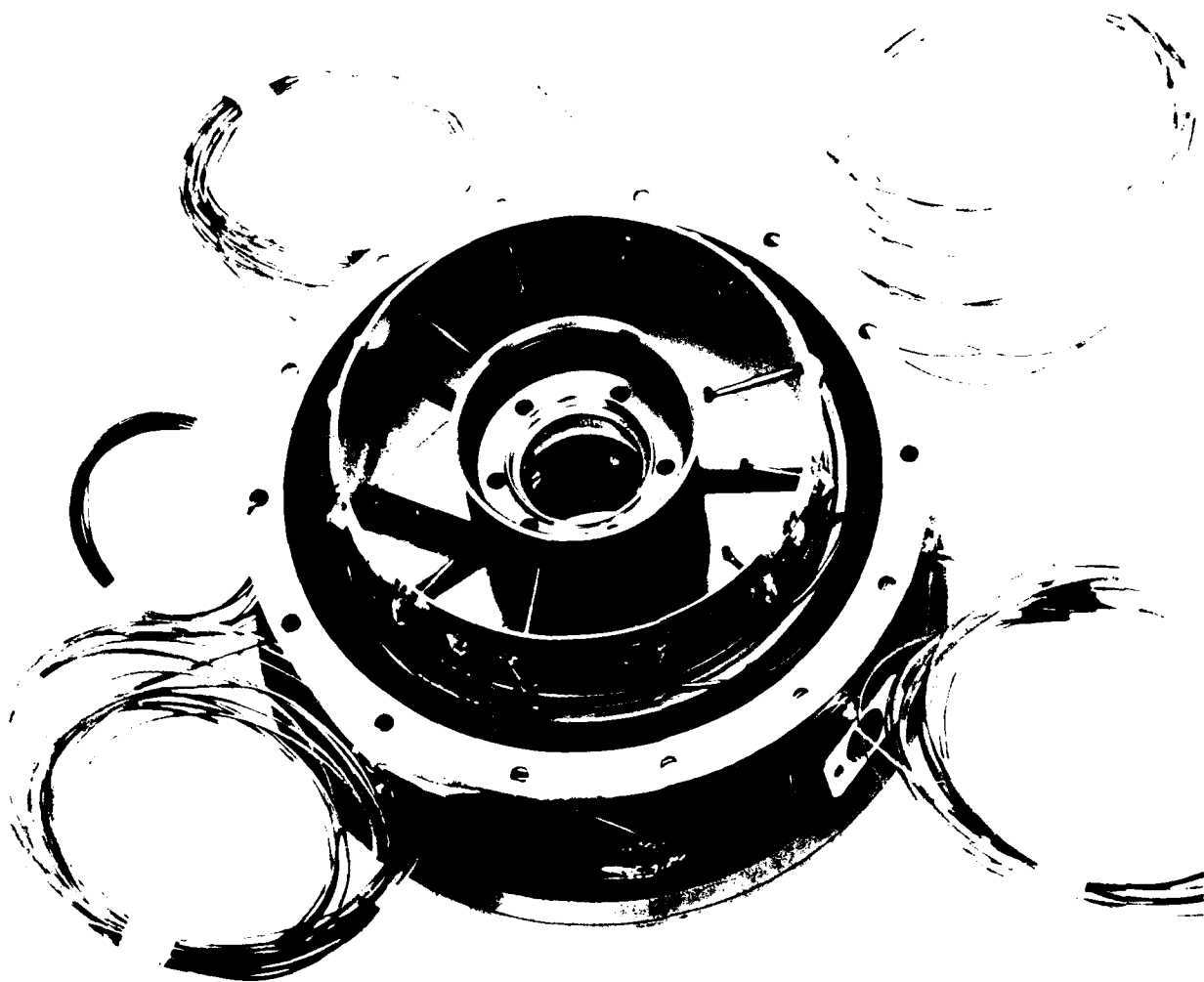


Figure 177. Exhaust duct (looking aft)  
P/N 3606195

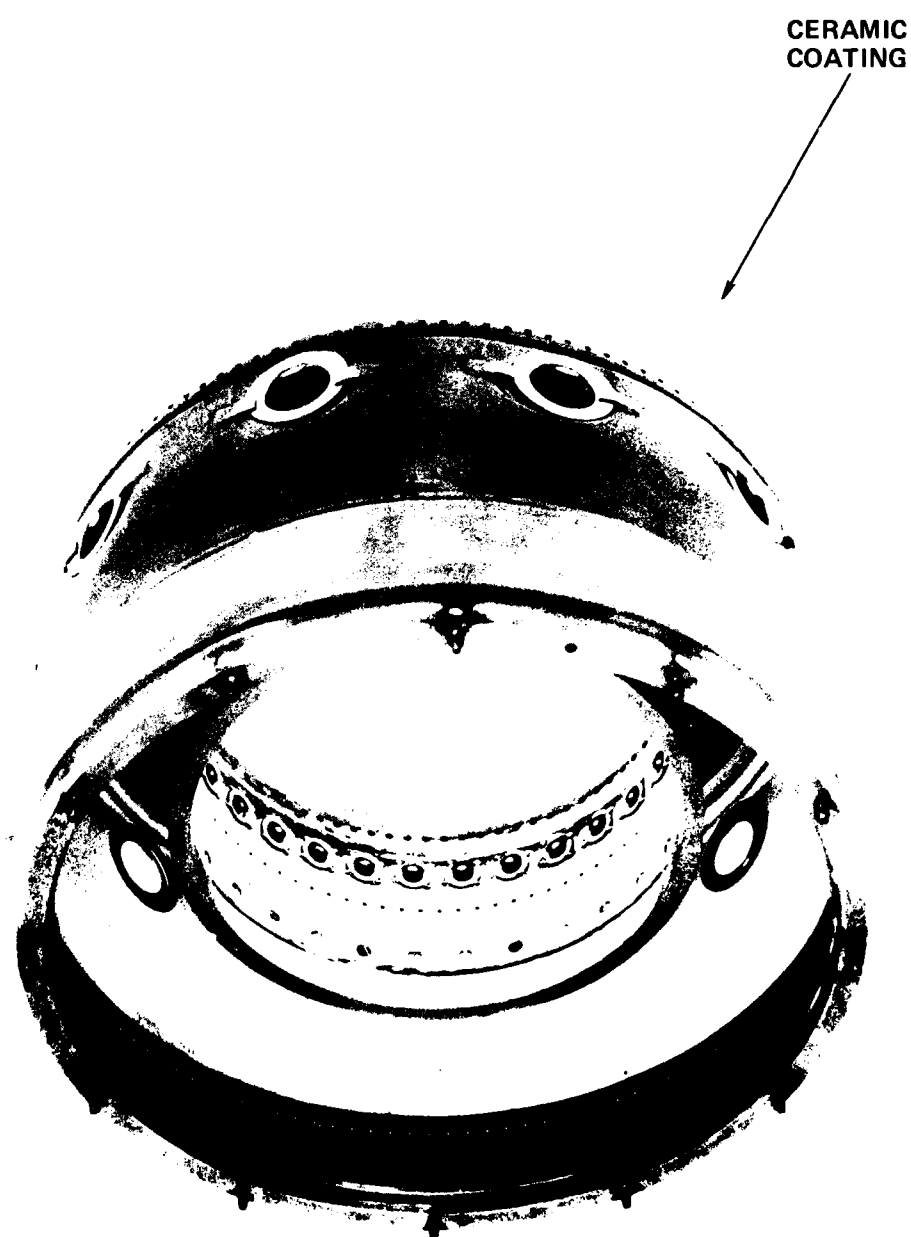
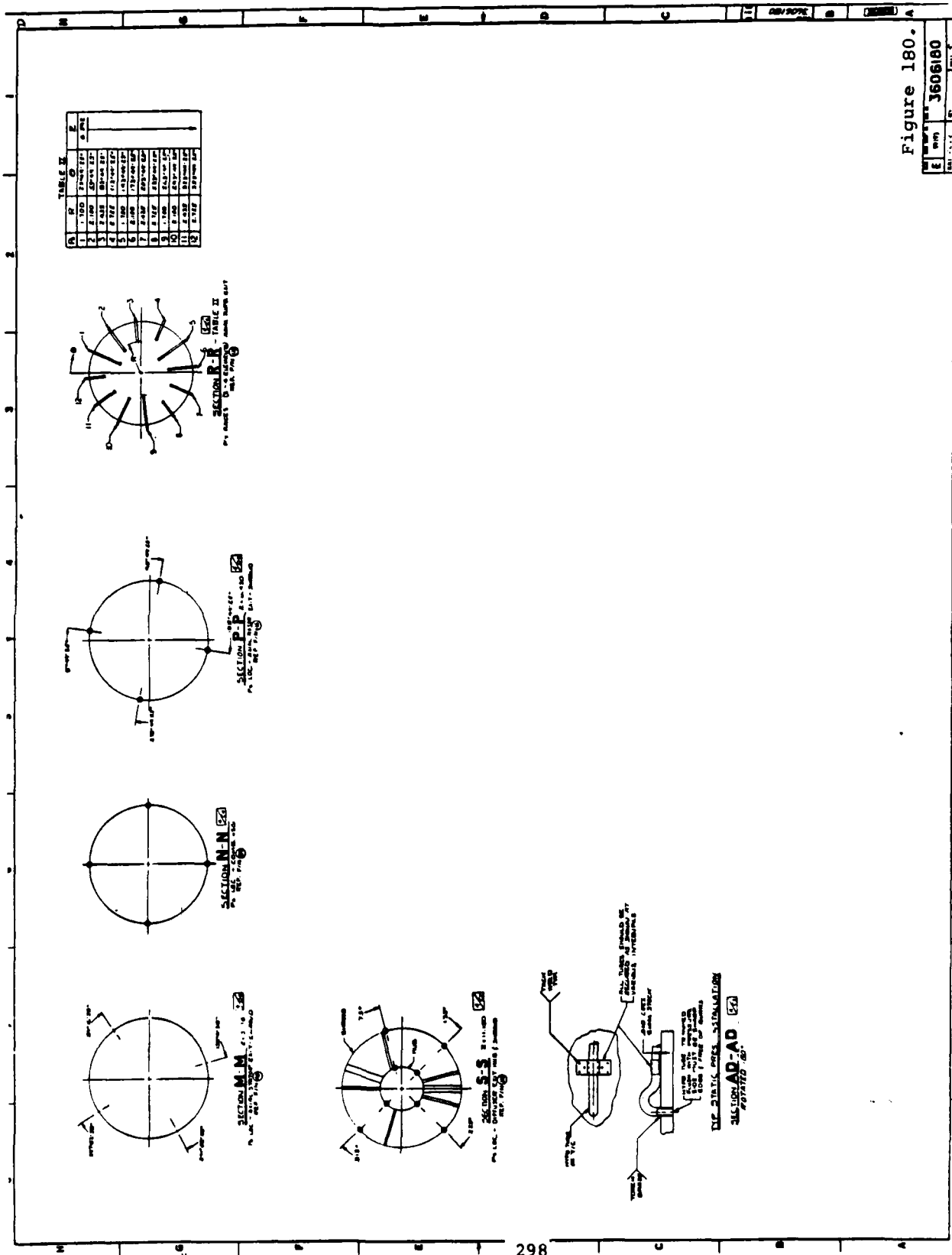


Figure 178. GTP305-2 combustor liner  
(P/N 3605621-2)





- o A monopole speed pickup was incorporated in the adapter gearbox to determine gearbox input/ICA output shaft speed
- o Existing facility instrumentation was used to determine water brake torque and speed
- o Oil flow and pressure sensors were located in the facility oil supply lines to the ICA

#### 5.4 Build and Installation Procedure

Following instrumentation the ICA was assembled in accordance with build instruction and calculation procedures contained in Appendix A. Shim calculations were performed to; adjust radial rotor backface and frontface clearances, set proper spring loads, adjust axial turbine radial tip clearance, and set proper structural gaps as defined. Figures 181 through 187 depict the rotating group and various ICA intermediate assembly stages.

ICA installation in the test facility was accomplished with General Electric personnel present to assure proper gearbox/waterbrake/ICA alignment. Once satisfactory alignments were obtained the ICA was connected and the unit was made ready for testing. Figures 188 through 190 show the ICA, gearbox, waterbrake and exhaust ducting fully instrumented and ready for test.

#### 5.5 Test Procedure

After ICA installation in the test facility, the development test procedure, included in Appendix A, was utilized for all testing. Major test procedure elements are:

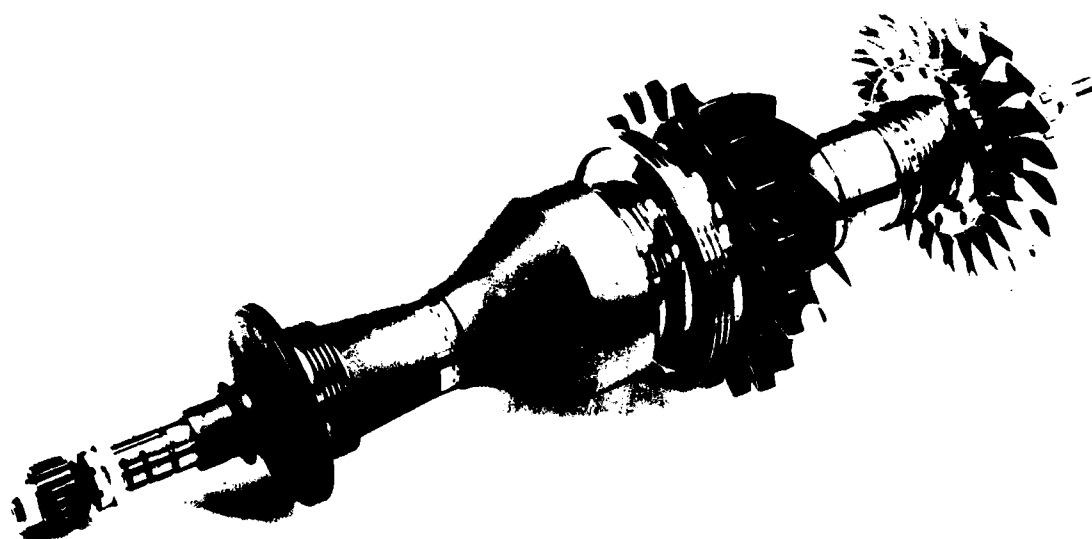


Figure 181. GTP305-2, ICA rotating group  
assembly P/N 3606189



Figure 182. ICA partial assembly P/N 3606180



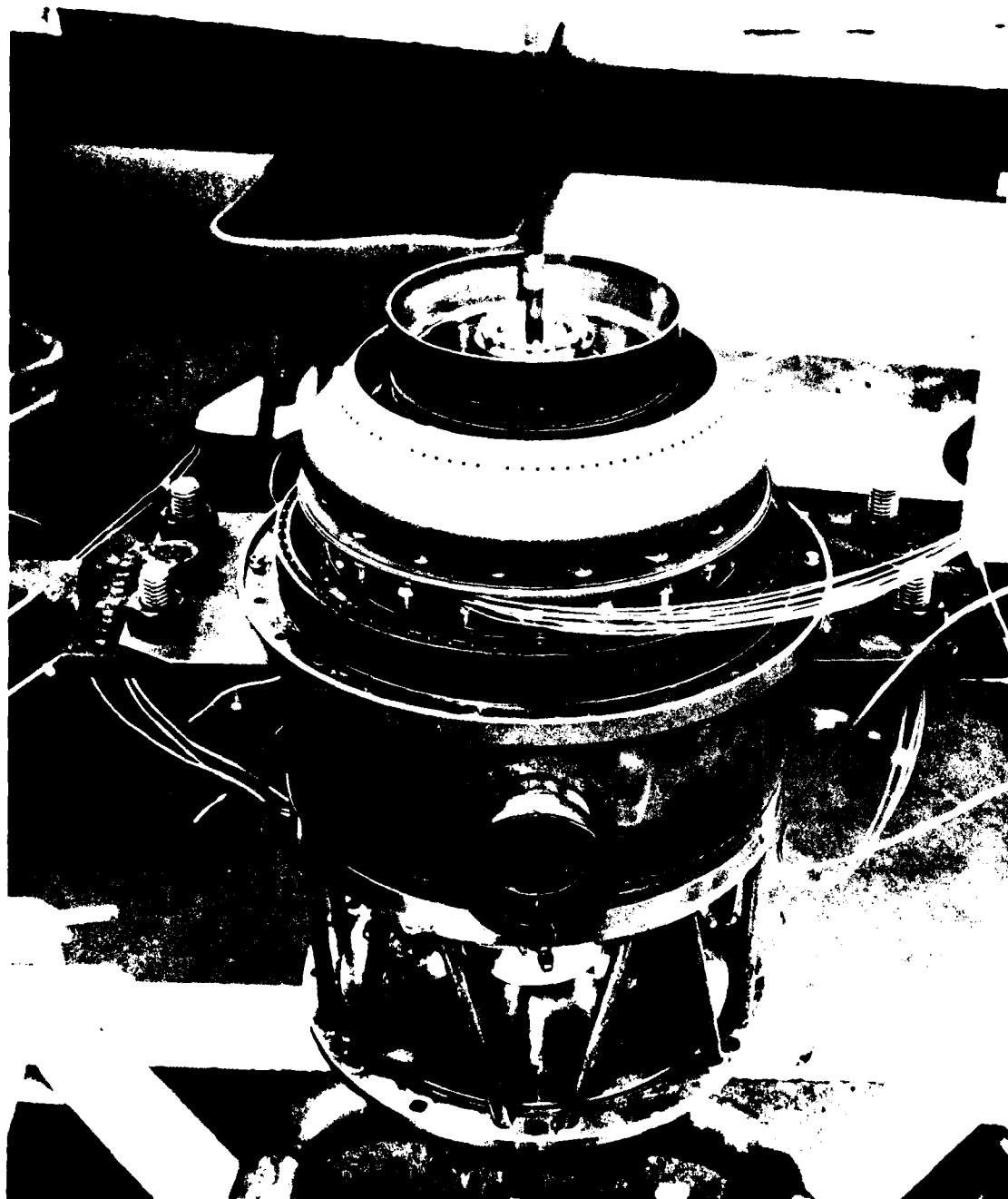


Figure 183. ICA partial assembly  
P/N 3606180

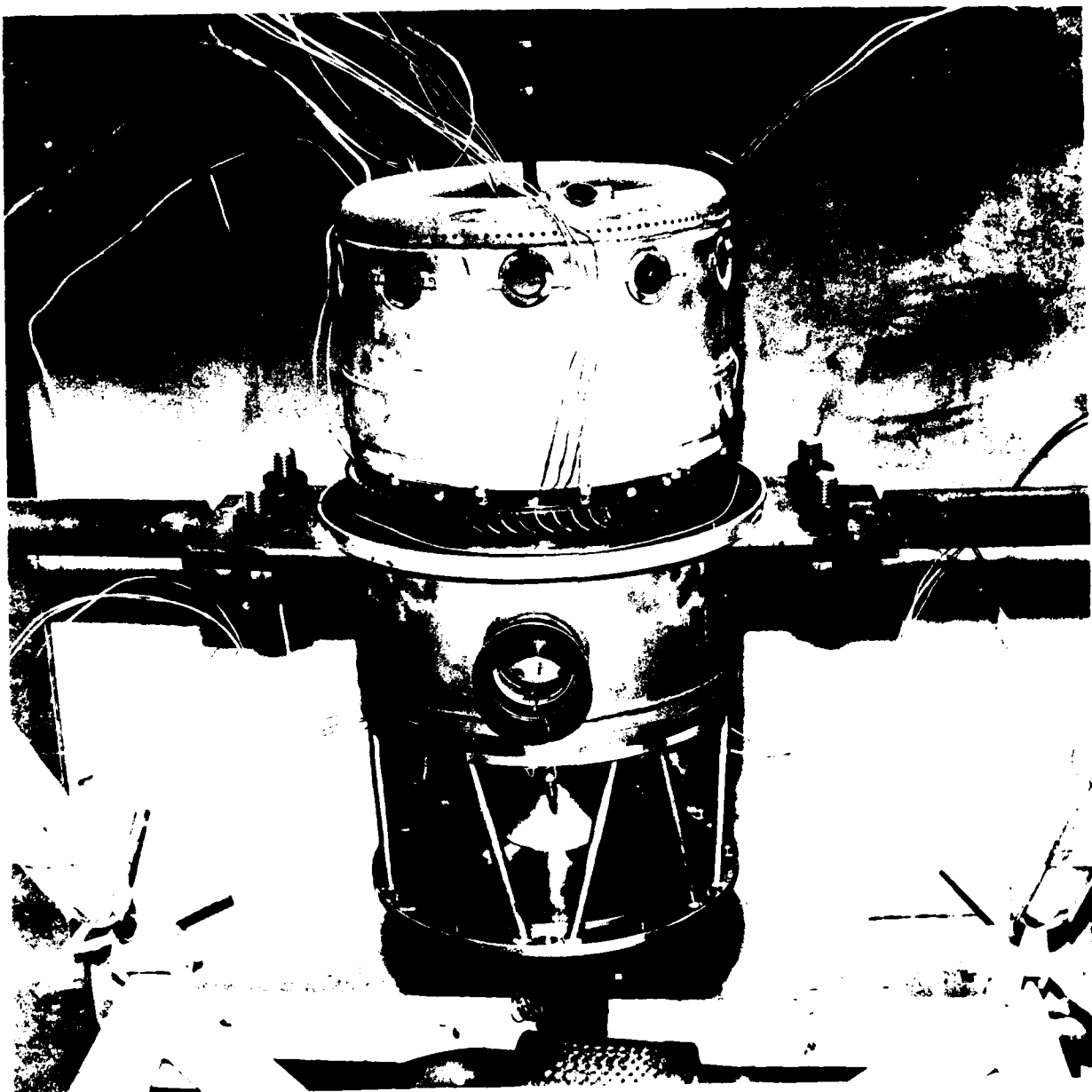


Figure 184. ICA partial assembly

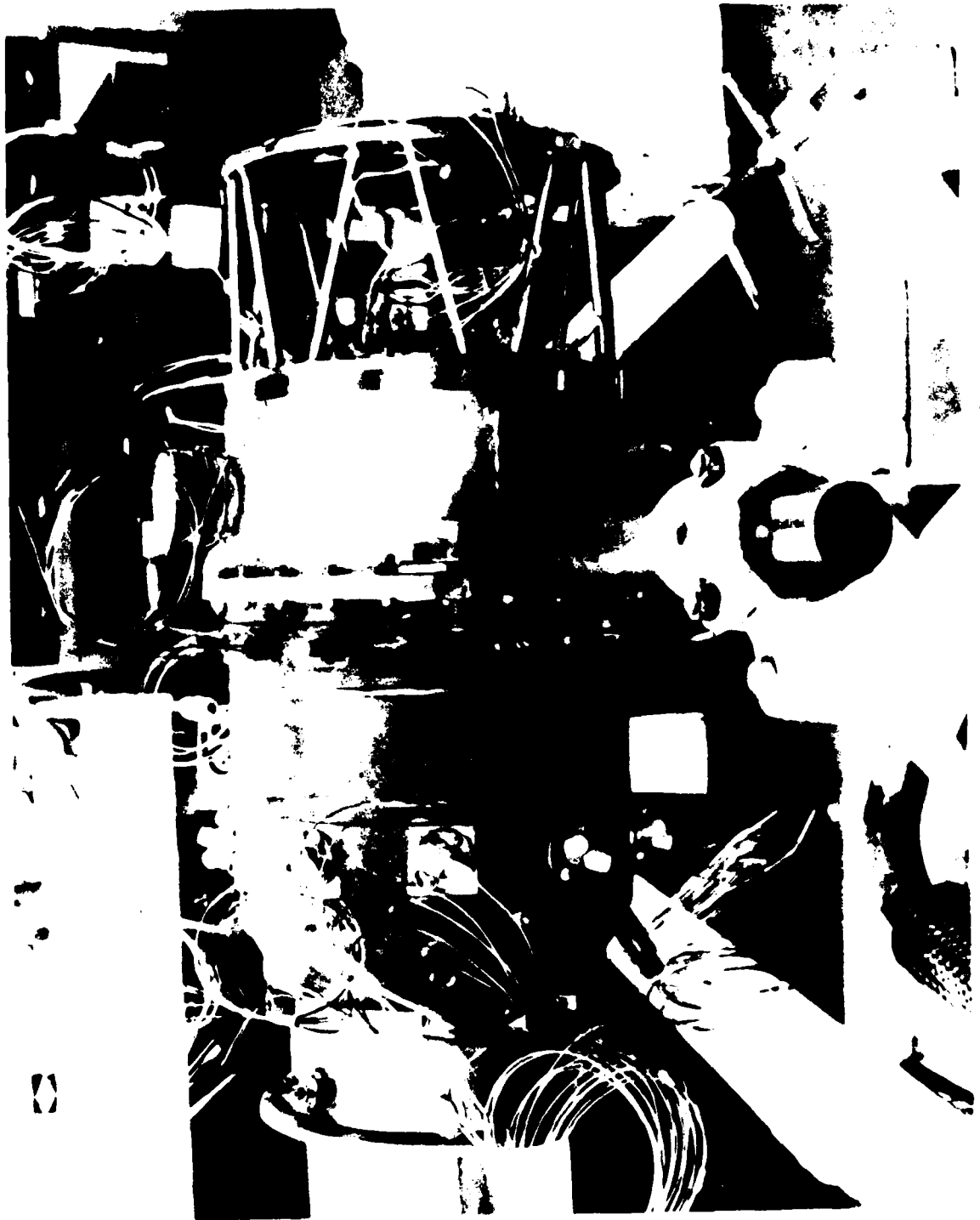


Figure 185. ICA test rig

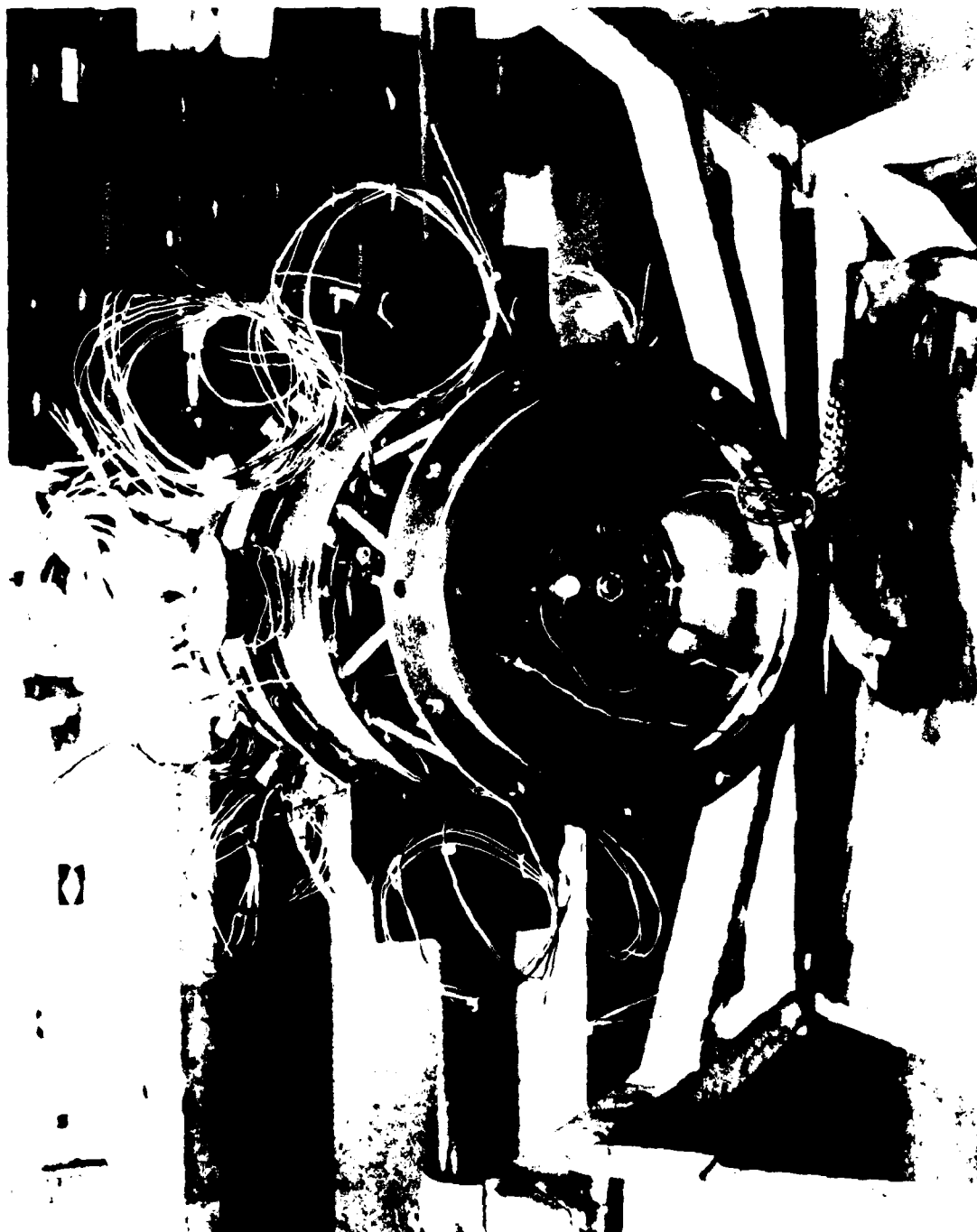


Figure 186. ICA test rig (looking aft)

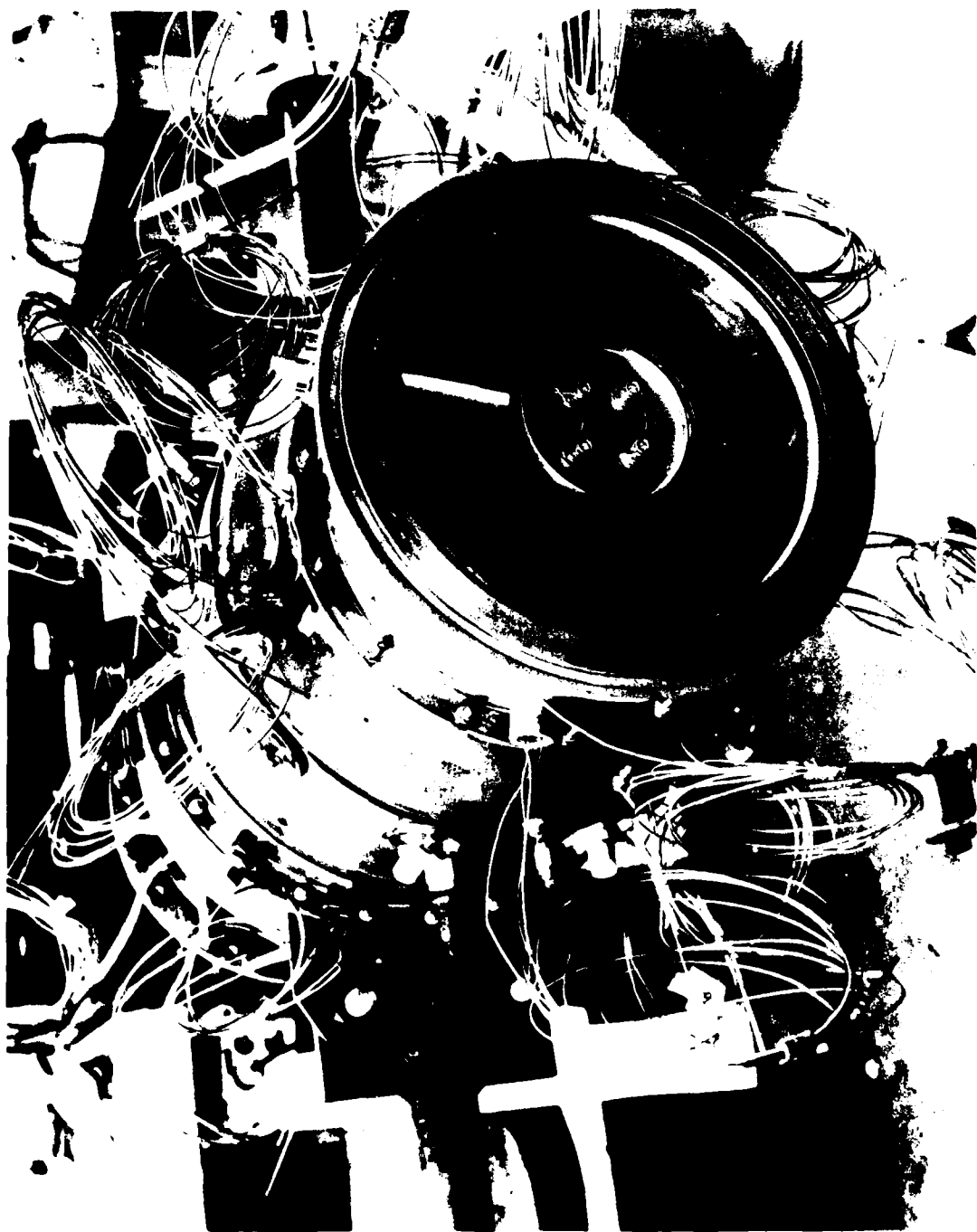


Figure 187. ICA test rig (looking forward)

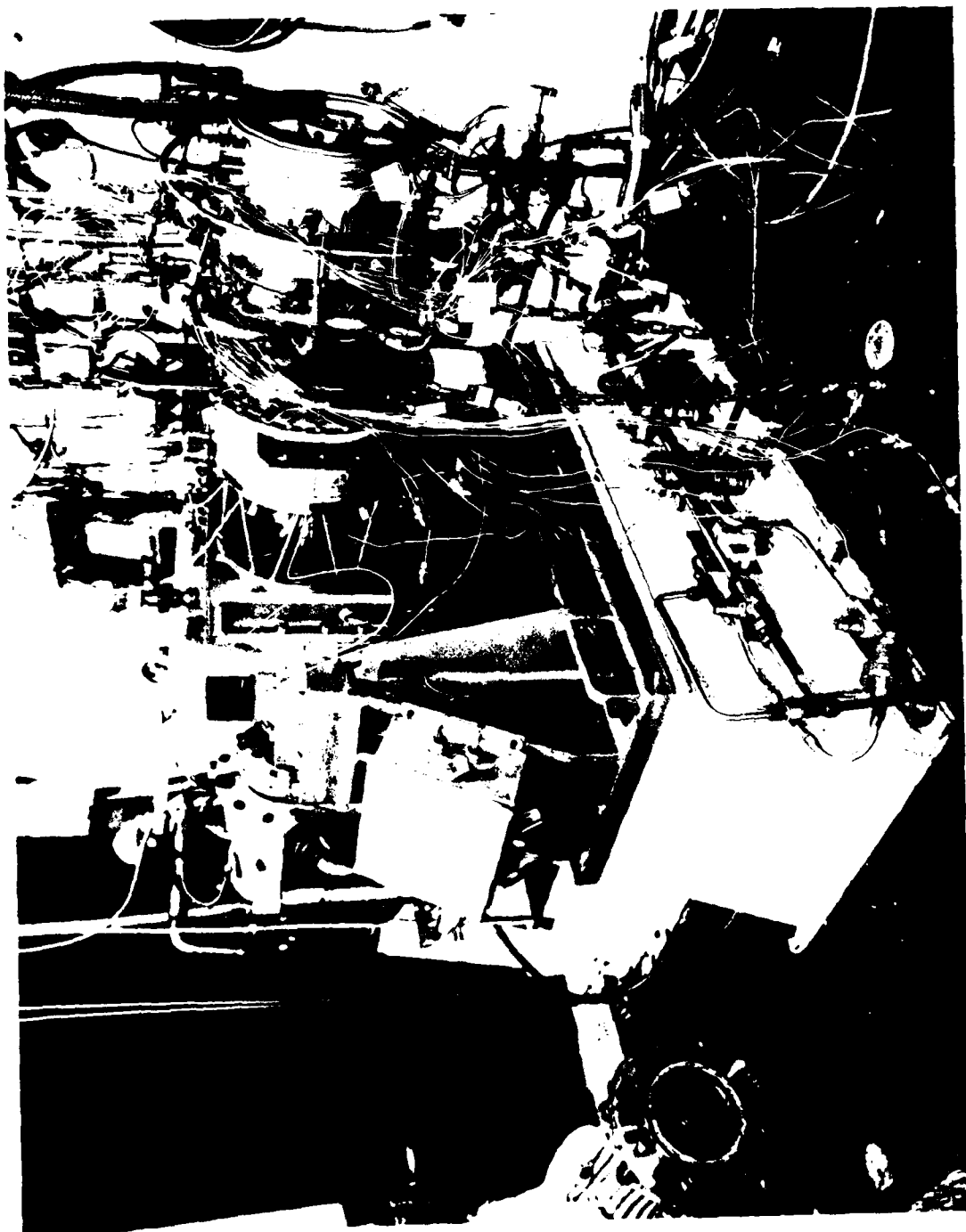


Figure 188. ICA installation prior to instrumentation hookup



Figure 189. ICA installation-instrumentation hookup

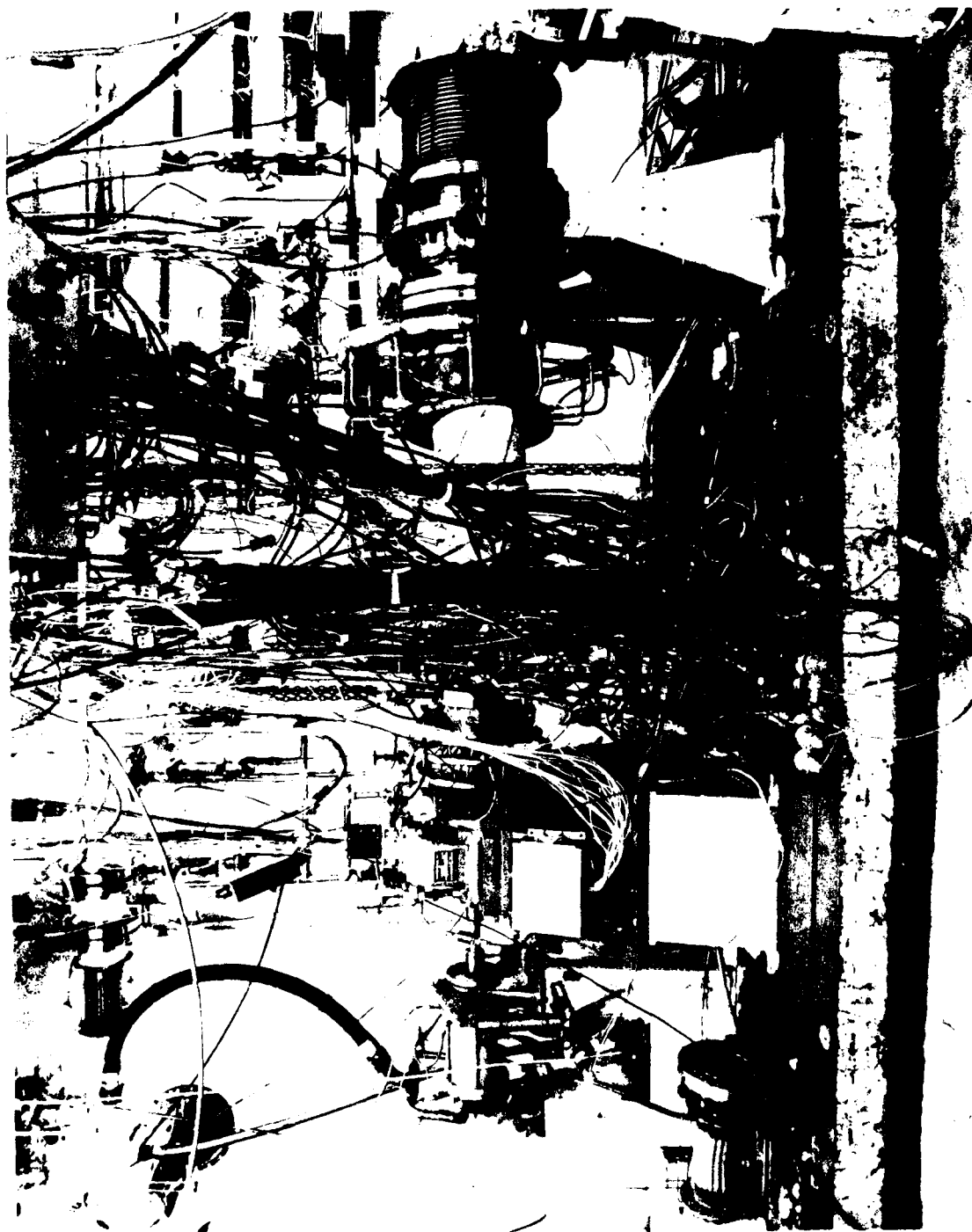


Figure 190. ICA installation showing waterbrake, gearbox,  
ICA and exhaust ducting



- o Motoring test to 100-percent design speed to verify mechanical integrity
- o Fired mechanical checkout to 100-percent speed
- o Performance demonstration with thermindex paint

Initially, the rig was motored at approximately 5000 rpm using inlet air pressure to drive the turbine. During motoring, proper oil flow to the bearings was verified and proper operation of all instrumentation, used to monitor the mechanical condition, was substantiated. The rig was accelerated slowly to 100-percent speed by increasing inlet pressure and temperature. During this acceleration, vibration data was recorded by a direct readout recorder to define rig dynamic characteristics over the full operating range. Bearing temperatures and speed were also recorded. At 60-, 80-, 100-percent speed, the output of installed instrumentation was recorded by the digital data acquisition system to verify proper instrumentation and data acquisition system operation. In addition, this motoring provided initial familiarization with the airflow and dynamometer controls for the ICA.

When mechanical integrity and proper instrumentation operation were demonstrated, the fired mechanical checkout and controls familiarization was performed. The inlet airflow and dynamometer load were set to provide airflow conditions and turbine speed equivalent to the engine ignition point. Lightoff fuel flow was then introduced and ignition achieved. Proper operation of all condition monitoring equipment was verified, at 40-percent speed. The rig was then accelerated to approximately 50,000 rpm for controls familiarization. This was done at low speed to provide a margin of safety until rig responses to control inputs were defined. Control familiarization was accomplished by operating the rig at a specific condition and then changing to a new condition to determine the proper control operations required to change to the new condition.

During this testing, the digital data acquisition system was used to record data at each operating point to allow verification of proper rig and instrumentation operation. Once controls operation was defined and mechanical integrity under fired conditions demonstrated, the rig was accelerated to 70-, 80-, 90-, 100-percent speed and design point (100-percent power) conditions were established to assure mechanical integrity over the full operating range.

Upon completion of the initial fired run, the performance demonstration and the thermindex paint tests were accomplished. Thermindex paint was applied to the combustor, combustor baffle assembly, radial turbine backshroud, and interstage duct/axial turbine stator.

Table 33 shows the seven data points selected for perform testing. However due to problems associated with mechanical vibration, a substitute data matrix was utilized. Data for this matrix, shown in Table 34, was obtained. Each performance point was determined by utilizing the data acquisition system "Quik-Look" program. This program performs a series of calculations based on raw data obtained during each 30 second data scan. Turbine speed, inlet air pressure and temperature, turbine discharge temperature, rotor inlet temperature, and flow were adjusted based on "Quik-Look" to determine the data point conditions. The "Quik-Look" printouts and design point "Bos Log" (all parameters sampled) are included in Appendix C.

The ICA was disassembled subsequent to testing and those items thermidex painted were isothermed and photographed. Details of the thermidex paint results are discussed in Section 4.

Table 35 includes ICA build and test history. As will be noted, Items 4 and 5 of this table make specific reference to Table 36 and Figure 191.

TABLE 33. INTEGRATED COMPONENTS ASSEMBLY PERFORMANCE DEMONSTRATION TEST POINTS.

Parameters to be Set by Operator for Each Test Point					Calculated Operating Parameters For Each Test Point				
Point No.	Rotor RPM (±200)	Inlet Temp. (±10°F)	Inlet Press. (±1 psi)	Turbine Discharge Temp. (±10°F)	Radial Rotor Inlet Temp. (°F)	Inlet Airflow (lb/sec)	Fuel Flow (lb/hr)	Turbine HP	Reference Net HP
1	75,684	771	109.6	865	1500	2.23	85.5	526	13
2	75,684	774	111.8	927	1600	2.23	97.7	563	48
3	75,684	776	113.8	990	1700	2.22	109.9	598	82
4	75,684	780	115.6	1055	1800	2.21	122.0	631	114
5	75,684	783	117.0	1122	1900	2.19	133.8	660	144
6	75,684	786	118.3	1191	2000	2.17	145.4	688	173
7	75,684	788	118.8	1225	2050	2.16	151.0	700	186

NOTE: Values of parameters obtained from GTP305-2 engine cycle analysis computer program for 130°F, sea level day conditions.

TABLE 34. TEST MATRIX

$P/P)_{T-DE}$	$\% N/\sqrt{\theta}$ 90*	100**	100***
5.50	1	5	9
6.50	2	6	10
7.529	3	7	11
8.5	4	8	12

\*Run at  $T_{in} = 2050^{\circ}\text{F}$ , speed  $\approx 68116.5$  rpm

\*\*Run at reduced temperature and speed,  $T_{in} \approx 1690^{\circ}\text{F}$ ,  
 $N \approx 70,000$  rpm

\*\*\*Run at full temperature and speed (design point)

Design Point Condition

$N = 75,684$   
 $T_{in} = 2050^{\circ}\text{F}$   
 $P/P)_{T-DE} = 7.529$   
 $T_{in}$

No. 11  $2050^{\circ}\text{F}$   
 No. 10  $1900^{\circ}\text{F}$   
 No. 9  $1800^{\circ}\text{F}$

TABLE 35.

Build Number	Hardware Reworked or Replaced	Test Results	Disassembly	Full/Partial Disassembly								
1	None	<p>Cold Air Data Points</p> <table><tr><td>Turbine corrected SPD</td><td>PRTD-E</td></tr><tr><td>0.90</td><td>7.0 8.0 9.0</td></tr><tr><td>1.00</td><td>7.0 8.0 9.0</td></tr><tr><td>1.10</td><td>7.0 8.0 9.0</td></tr></table> <p>Vibration levels were high on the ICA aft bearing, at 74,000 rpm 0.93 mils, 75 gs, cold run</p> <p>Hot run at 40 percent power for approximately 20 min. Shutdown because of a sudden vibration increase on the AFT bearing</p> <p>Vibration levels were unacceptable on the ICA forward bearing, at 50,000 rpm, 0.77 mils, 30 gs,</p>	Turbine corrected SPD	PRTD-E	0.90	7.0 8.0 9.0	1.00	7.0 8.0 9.0	1.10	7.0 8.0 9.0	Axial turbine/oil seal housing rub	Full
Turbine corrected SPD	PRTD-E											
0.90	7.0 8.0 9.0											
1.00	7.0 8.0 9.0											
1.10	7.0 8.0 9.0											
2	<p>Replaced</p> <p>(1) Tie rod</p> <p>(2) Axial turbine</p> <p>(3) Installed new bearings</p> <p>(4) Build 1 damaged hardware reworked</p>	<p>ICA forward bearing exhibiting high vibration levels, at 74,000 rpm, 0.7 mils, 51 gs, acceptable limits 0.5 mils, 40 gs'</p> <p>Hot run at 40-percent power, 15 min</p> <p>Hot run at 60-percent power, 45 min</p>	<p>Axial turbine rub caused rotor hub temperature increase over 2200°F. Heat load increased the tie-bolt temperature to 1800°F, causing tie rod necking</p> <p>Improper shim gap cause of rub</p> <p>Anti-rotation pin undersized</p> <p>Thrust bearing outer race rotation and forced misalignment</p>	Partial								
3	<p>Replace anti-rotation pin on the thrust bearing outer race</p> <p>All bearings were replaced</p>		<p>AIRsearch/WPAFB agreement: improve balance prior to performing 100-percent hot run</p> <p>No axial turbine/oil seal housing rub during hot run</p>	Full								

TABLE 35. (Contd)

Build Number	Hardware Reworked or Replaced	Test Results	Disassembly	Full/Partial Disassembly
4	Balance improved. Refer to Table 5-8.  Rotating Unit Check Balance PLANE C        D Spec    0.04    0.13 Build No. 1    0.029    0.073 Build No. 2    0.028    0.063 Build No. 4    0.008    0.078  Installed new bearings Axial displacement probe installed	Vibration levels substantially reduced. At 74,000 rpm ICA forward vibration was 0.23 mil, 22 gs'  Temperature alarm on front bearing set at 300°F was energized. Front bearing g loads increased on subsequent runs  At 61,000 rpm ICA forward bearing vibration increased to 0.5 mil, 40 gs'  Hot run at 40 percent power, 15 min	Rear bearing outer race rotated  Forward roller bearing rotated. Discoloration of inner race and bearing cage. Bearing cage improperly staked during manufacture (Figure 5-40)  Forward bearing housing damaged, minor surface damage occurred during bearing outer race rotation	Full
5	New bearings installed Machined forward bearing housing	Initial runs showed vibration levels comparable to Build No. 4, early runs  Water brake instability caused overspeed to 78,000 rpm  Subsequent vibration levels increased to unacceptable levels at 62,000 rpm, 1.0 mils, 60 gs' Prior to overspeed ICA forward vibration level was 0.4 mils, 24 gs' at 62,000 rpm	Forward and rear roller bearings had discolored cages. Cages were improperly staked (Figure 5-40)  Inspection of quill shaft indicated concentricities of splines and OD surfaces per S/P  Rotating unit check balanced for repeatability  Prior to Build Run Plane    Spec    oz-in    oz-in C    0.04    0.008    0.006 D    0.13    0.078    0.072  Quill shaft was out of balance and corrected  Check Balance    After Spec    oz-in    oz-in 0.00016    0.0013    0.00015  Evidence of reverse thrust on ball bearing. (Axial displacement probe measurement indicated axial shift aft of the rotating group)  Mild radial turbine rub, axial and radial plane. This is believed to have been a product of the overspeed	Partial

TABLE 35. (Contd)

Build Number	Hardware Reworked or Replaced	Test Results	Disassembly	Full/Partial Disassembly																		
6	<p>Forward bearing carrier modified</p> <p>Decreased oil mount clearance from 0.0054 to 0.041</p> <p>Oil supply to the mount was increased. Increased orifice from 0.048 to 0.075 in</p> <p>Installed two Bently probes at 90° to examine quill shaft excursion at ICA engagement</p>	<p>Vibration levels at design speed, ICA forward bearing, 0.20 mils, 15 gs', ICA AFT bearing, 0.36 mils, 30 gs'</p> <p>GTP305-2 ICA TEST MATRIX</p> <table><thead><tr><th>P/P)</th><th>T-DE</th><th>% N/θ</th></tr></thead><tbody><tr><td></td><td>90*</td><td>100** 100***</td></tr><tr><td>5.50</td><td>1</td><td>5 9</td></tr><tr><td>6.50</td><td>2</td><td>6 10</td></tr><tr><td>7.529</td><td>3</td><td>7 11</td></tr><tr><td>8.5</td><td>4</td><td>8</td></tr></tbody></table> <p>*Run at T<sub>in</sub> = 2050°F, N=68116.5 rpm.</p> <p>**Run at reduced temperature 100% corrected speed, T<sub>in</sub> 1690°F, N = 70,000 rpm</p> <p>***Run at design speed</p> <p>N = 75,685 rpm</p> <p>T<sub>in</sub> = 2050°F - No. 11</p> <p>T<sub>in</sub> = 1900°F - No. 10</p> <p>T<sub>in</sub> = 1800°F - No. 9</p> <p>Testing completed.</p> <p>Emission data recorded.</p>	P/P)	T-DE	% N/θ		90*	100** 100***	5.50	1	5 9	6.50	2	6 10	7.529	3	7 11	8.5	4	8	<p>No Evidence of vibration problems. Lower ICA forward bearing vibration levels attributed to bearing carrier modifications</p> <p>Radial turbine wheel exhibiting ICF mode. Saddle cracks in three areas.</p>	Full
P/P)	T-DE	% N/θ																				
	90*	100** 100***																				
5.50	1	5 9																				
6.50	2	6 10																				
7.529	3	7 11																				
8.5	4	8																				

TABLE 36. BALANCE INSPECTION DATA

Part No. Name	Plane of Balance	Blueprint Specification (oz in)	Balanced To (oz in)
3606183 Thrust Piston	S P	0.0025 0.0015	0.0007 0.0004
3606181 Dummy Compressor	N M	0.009 0.0049	0.0060 0.0014
3605636 Coupling Half	M	0.0022	0.0016
3605248 Turbine Rotor	M N	0.0117 0.0088	0.0096 0.0027
3605604 Coupling Half	M N	0.0006 0.0006	0.0006 0.0006
3605600 Axial Turbine	M N	0.0040 0.0040	0.0020 0.0020
976510 Coupling Half	M N	0.0009 0.0009	0.0004 0.0003
Rotating Group	C (Forward) D (Aft)	0.04 0.13	Build 4 0.008 Build 2 0.029 0.078 0.073





Figure 191 Model GTP305-2 forward roller bearing  
information

## SECTION VI

### INTEGRATED COMPONENTS ASSEMBLY TEST RESULTS

Data obtained during ICA testing was evaluated to determine aerodynamic and mechanical performance of the Model GTP305-2 turbine-end components. The following sections discuss ICA testing results.

#### 6.1 Turbine Aerodynamic Performance

Aerodynamic performance of the turbine stage was determined using ICA data along with comparisons and relationship determined earlier in cold-air testing of the turbine stage and combustion system testing. The data reduction model was based on cold-air data reduction methodology in which correlations and comparison were valid.

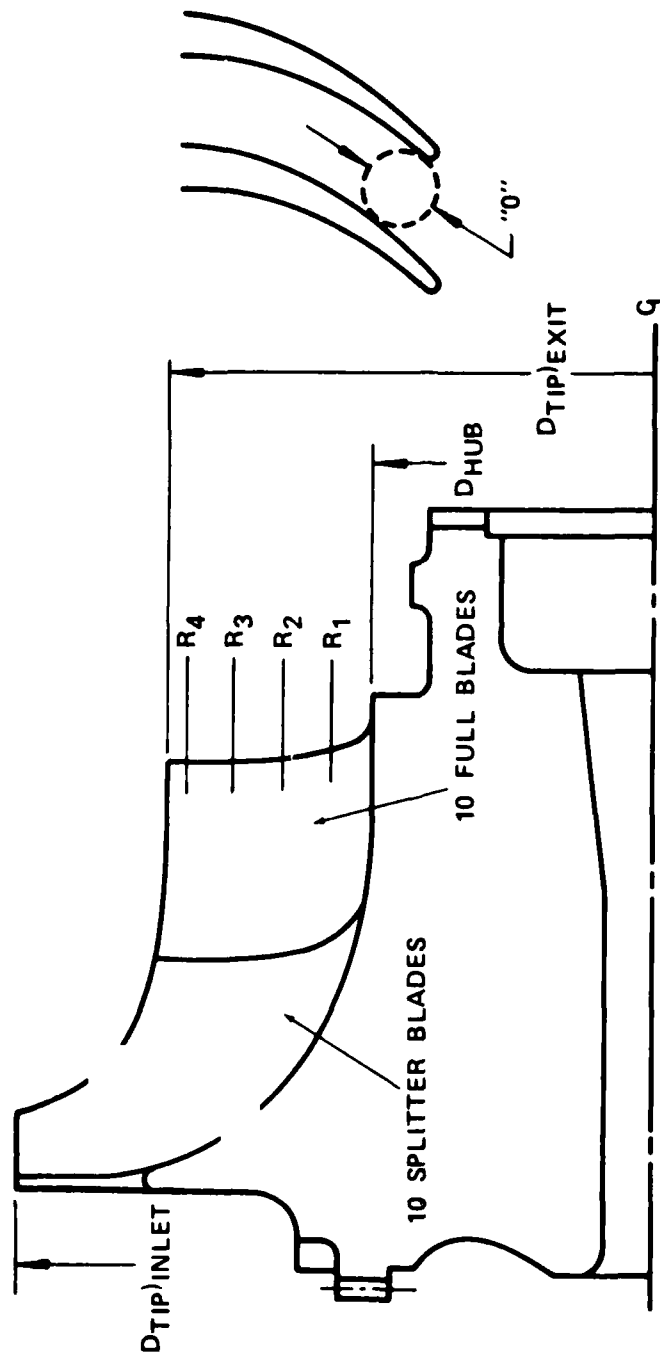
Fundamental hardware differences (see Sections 4 and 5) exist between cold-air hardware and ICA hardware due to temperature and speed effects. However, aerodynamically the two rigs are identical.

##### 6.1.1 Performance Analysis

Prior to test, all aerodynamic hardware was inspected for compliance with design intent. The cast AF2-1DA radial turbine rotor was inspected at four discrete rotor exducer throat areas as a function of rotor exit blade radius (see Table 37). The cast rotor is 1.28 percent closed compared to design intent. Similar inspections for the cast radial nozzle, axial turbine stator and axial turbine rotor are shown in Tables 38 through 40, respectively. The four major aerodynamic items are discussed below:

- o Radial turbine nozzle 5.33 percent closed

TABLE 37. RIG RADIAL ROTOR DIMENSIONAL INSPECTION



BLADE NO.	"0" AT $R_1=1.40$	"0" AT $R_2=1.60$	"0" AT $R_3=1.80$	"0" AT $R_4=2.00$
1	0.432	0.479	0.527	0.564
2	0.432	0.474	0.519	0.562
3	0.431	0.468	0.525	0.568
4	0.428	0.473	0.525	0.571
5	0.431	0.480	0.526	0.574
6	0.429	0.474	0.527	0.570
7	0.432	0.474	0.520	0.561
8	0.428	0.473	0.519	0.562
9	0.427	0.470	0.526	0.566
10	0.431	0.479	0.531	0.570
AVE	0.430	0.474	0.525	0.562
DESIGN	0.412	0.468	0.5215	0.570

DIAMETER DIMENSIONS

DTIP-EXIT 4.33

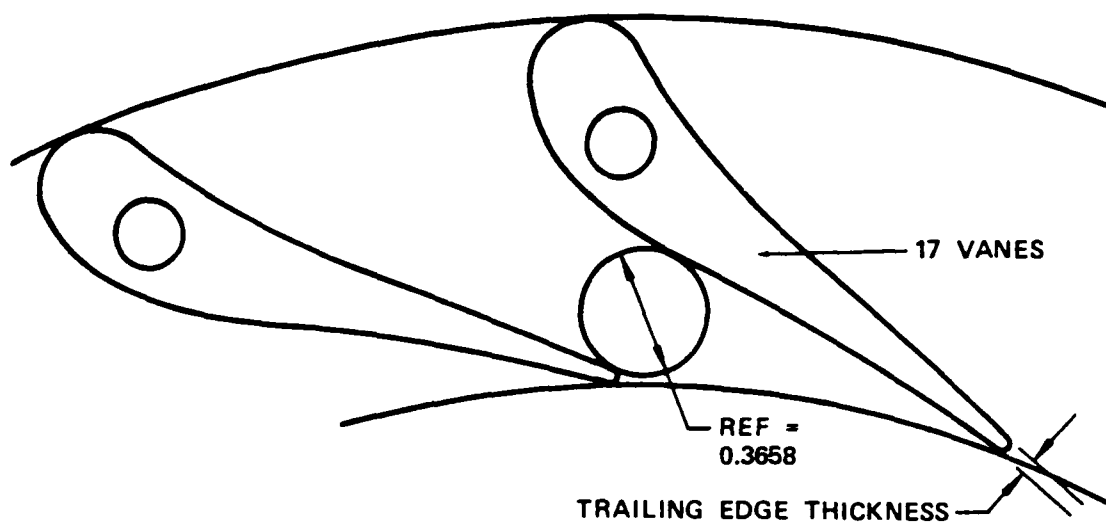
DHUB 2.520

$A_{MEASURED} = 4.478 \text{ IN}^2$

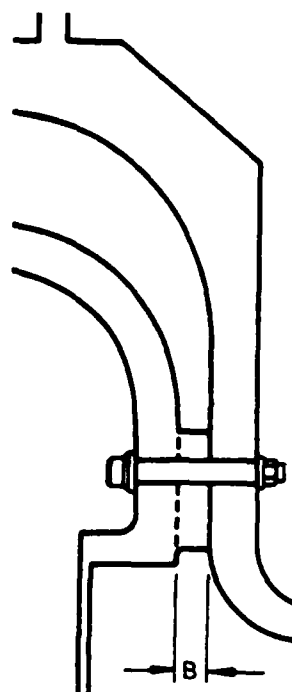
$A_{DESIGN} = 4.536 \text{ IN}^2$

$\frac{\Delta A}{A_D} = -1.28 \text{ PERCENT CLOSED}$

TABLE 38. RIG RADIAL NOZZLE DIMENSIONAL INSPECTION



VANE	THROAT DIAM	EXIT B WIDTH
1	0.350	0.307
2	0.350	0.306
3	0.349	0.304
4	0.351	0.304
5	0.350	0.303
6	0.350	0.305
7	0.349	0.306
8	0.350	0.305
9	0.351	0.304
10	0.351	0.302
11	0.350	0.303
12	0.351	0.305
13	0.350	0.306
14	0.349	0.305
15	0.350	0.306
16	0.349	0.305
17	0.350	0.306
AVE	0.3504	0.3049
DESIGN	0.3658	0.305



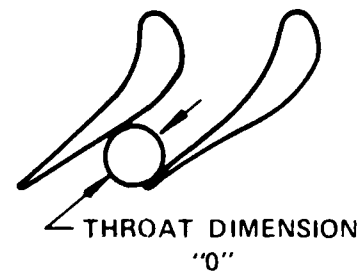
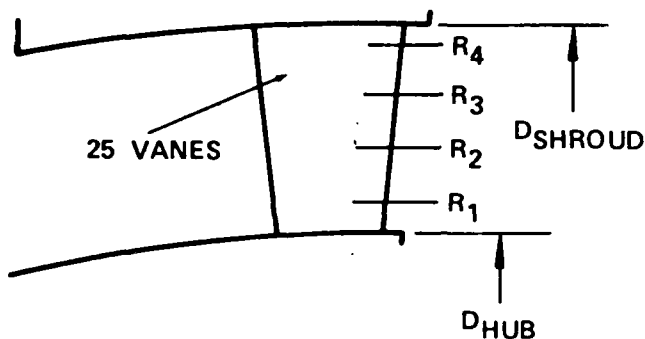
$$A_{\text{DESIGN}} = 1.8938 \text{ IN.}^2$$

$$A_{\text{MEASURED}} = 1.7930 \text{ IN.}^2$$

$$\frac{\Delta A}{A_D} = -5.32 \text{ PERCENT CLOSED}$$

ESTIMATE FILLET RADII 0.040 IN.

TABLE 39. RIG AXIAL NOZZLE DIMENSIONAL INSPECTION



$$A_{DESIGN} = 5.831 \text{ IN.}^2$$

$$A_{MEASURED} = 5.695 \text{ IN.}^2$$

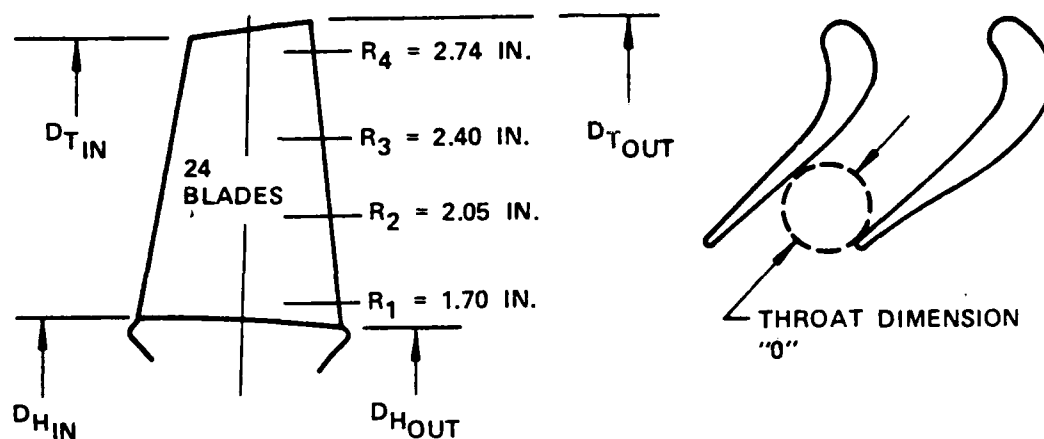
$$\frac{\Delta A}{A_D} = -2.33 \text{ PERCENT CLOSED}$$

$$D_{HUB} = 3.3195$$

$$D_{SHROUD} = 5.5732$$

VANE NO.	"0" AT $R_1=1.75$	"0" AT $R_2=2.10$	"0" AT $R_3=2.45$	"0" AT $R_4=2.66$
1	0.166	0.177	0.216	0.270
2	0.163	0.169	0.208	0.256
3	0.167	0.177	0.213	0.269
4	0.170	0.184	0.219	0.269
5	0.169	0.182	0.219	0.271
6	0.166	0.180	0.220	0.268
7	0.172	0.182	0.221	0.270
8	0.162	0.172	0.215	0.265
9	0.170	0.174	0.214	0.263
10	0.171	0.177	0.216	0.268
11	0.168	0.175	0.216	0.271
12	0.170	0.183	0.222	0.275
13	0.168	0.174	0.210	0.270
AVE	0.1678	0.17738	0.2160	0.26807
DESIGN	0.1679	0.1774	0.2161	0.2680

TABLE 40. RIG AXIAL ROTOR DIMENSIONAL INSPECTION



BLADE NO.	"0" AT $R_1=1.700$	"0" AT $R_2=2.05$	"0" AT $R_3=2.40$	"0" AT $R_4=2.74$
1	0.218	0.231	0.220	0.219
2	0.215	0.231	0.223	0.220
3	0.214	0.227	0.226	0.222
4	0.217	0.233	0.226	0.226
5	0.218	0.236	0.232	0.222
6	0.224	0.228	0.226	0.221
7	0.217	0.230	0.231	0.224
8	0.219	0.231	0.230	0.226
9	0.222	0.231	0.228	0.226
10	0.224	0.230	0.231	0.223
11	0.218	0.230	0.226	0.222
12	0.221	0.228	0.227	0.226
13	0.221	0.229	0.227	0.224
14	0.218	0.231	0.229	0.224
15	0.221	0.230	0.225	0.222
16	0.217	0.228	0.227	0.228
17	0.222	0.228	0.224	0.224
18	0.218	0.229	0.227	0.227
19	0.218	0.231	0.230	0.226
20	0.223	0.229	0.227	0.222
21	0.225	0.230	0.228	0.226
22	0.222	0.237	0.230	0.223
23	0.217	0.231	0.225	0.226
24	0.221	0.231	0.227	0.227
DESIGN	0.3232	0.2390	0.2480	0.2555

$$D_{HIN} = 3.310 \text{ AVE}$$

$$D_{TIN} = 5.620$$

$$D_{HOUT} = 3.120$$

$$D_{TOUT} = 5.650$$

$$A_{DESIGN} = 7.0704 \text{ IN.}^2$$

$$A_{MEASURED} = 6.9778 \text{ IN.}^2$$

$$\frac{\Delta A}{A_D} = -1.31 \text{ PERCENT CLOSED}$$

- o Radial turbine rotor 1.28 percent closed
- o Axial turbine stator 2.33 percent closed
- o Axial turbine rotor 1.31 percent closed

Although nominal design intent was not achieved on any single piece of hardware, all items were considered with blueprint tolerances and consistency within normal production tolerances.

Instrumentation commonality for the ICA, cold-air and combustion test rigs was maintained where feasible, primarily at the combustor inlet and turbine exit. Total combustor pressure drop was correlated using dome discharge static pressure measurements. Twelve total pressure probes located at the axial turbine rotor exit plane were used to establish overall two-stage total-to-total pressure ratio at the axial turbine exit. Radial turbine stage total-to-total pressure ratio was established from a correlation between rotor exit total pressure and interstage duct exit static pressure. This correlation, determined during cold air test No. 2A, is presented in Figure 192. Two-stage overall total-to-static pressure ratio was established with diffuser exit hub and shroud static pressure taps. Average cold rig turbine exit temperature was measured in an adiabatic mixing duct. Since this method was not feasible for ICA testing, an array of fifteen thermocouples at five immersion depths and three circumferential locations were utilized to measure the average turbine exit temperature. The ICA radial turbine nozzle was instrumented with static pressure taps at the throat and trailing edge. A nozzle flow calibration test was conducted prior to ICA testing. This calibration relates nozzle inlet corrected flow to nozzle total-to-static pressure ratio. Results are shown in Figure 193. Maximum attainable nozzle inlet corrected flow ( $W\sqrt{\theta/\delta}$ ) was 0.608 lbs/sec. Results of the measured nozzle throat area shown in Table 38 indicate a nozzle flow coefficient of 0.987, which is consistent with the cold rig nozzle coefficient of 0.99.

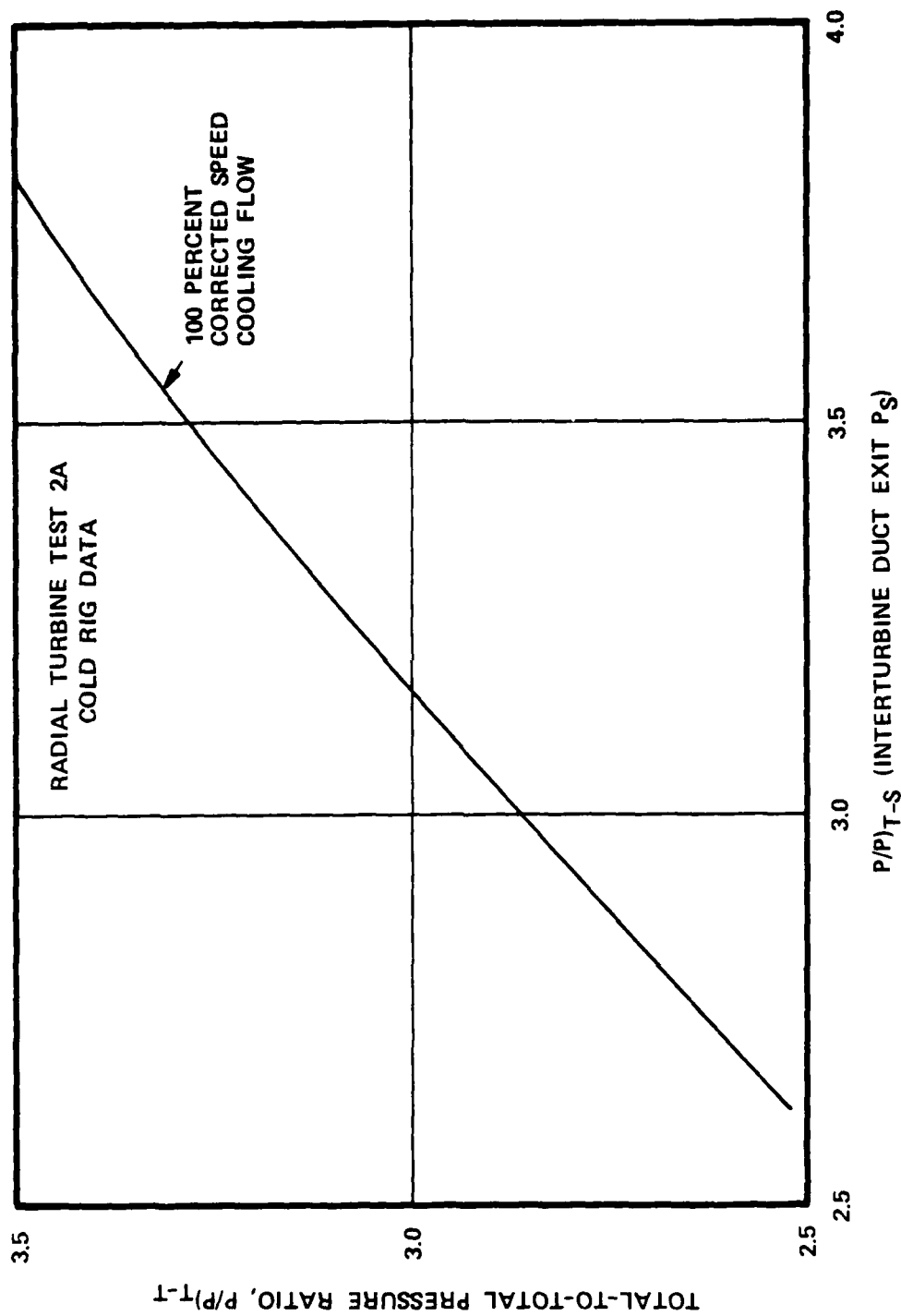


Figure 192. GTP305-2 radial turbine pressure ratio correlation



CAST RADIAL NOZZLE  
P/N 3606180

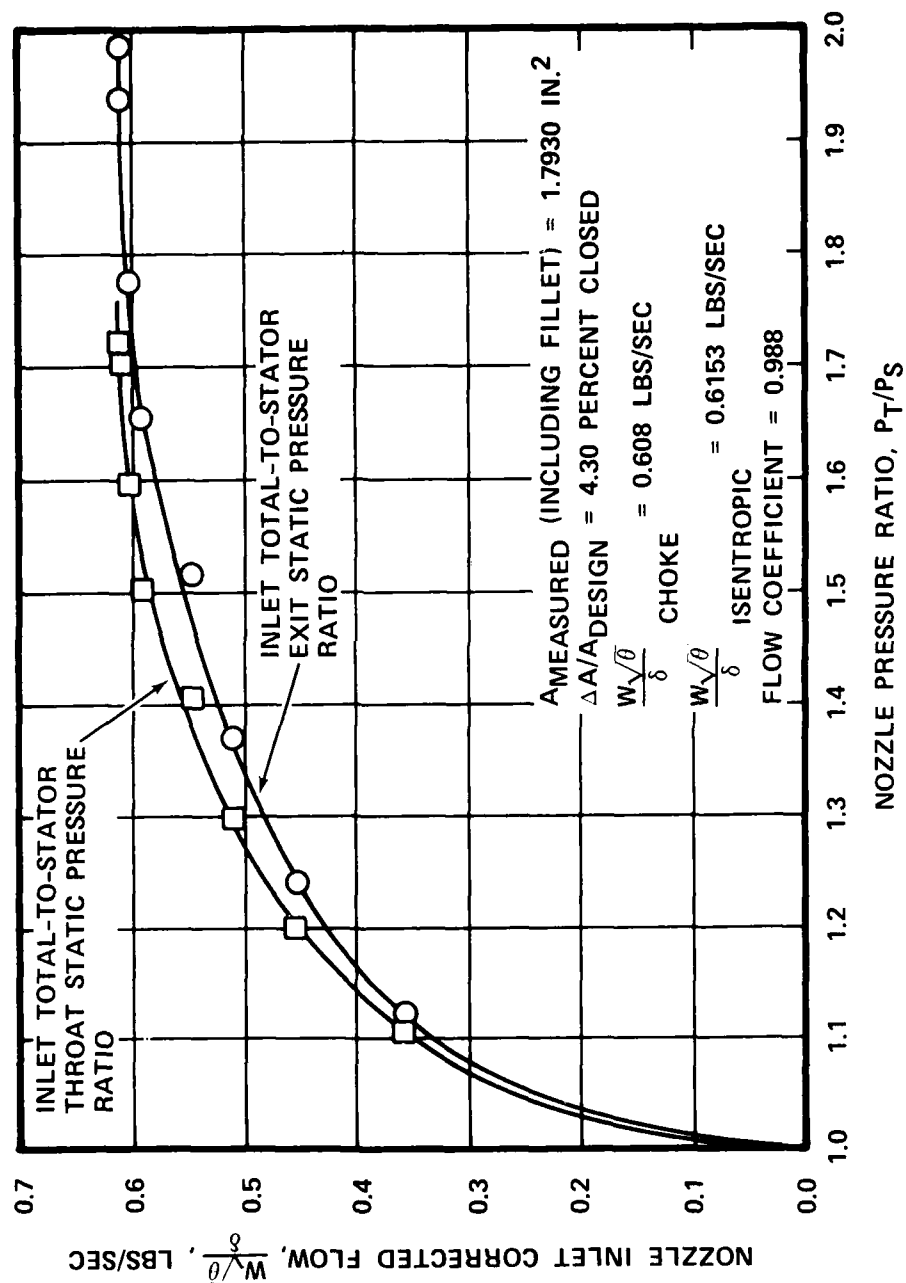


Figure 193. GTP305-2 cast radial nozzle flow calibration

Total flow entering the ICA was measured with a three inch orifice section. Bore cooling was then measured independently down stream of the main orifice with a 0.3125 inch orifice section. Radial nozzle internal cooling flow was based on a correlation of nozzle internal to trailing edge discharge static pressures. Measured static pressure was then related to cold flow calibrations for internal cooling flow magnitude.

An iterative aero-thermodynamic analysis of the ICA test data was conducted at design point temperature, pressure ratio and speed. The analysis objective was to compare overall turbine-end performance with cycle goals, and to compare turbine component performance with cold rig data. Design point analysis was based on a model defining thermodynamic conditions at selected stations throughout the turbine flow path. ICA test data cold-air test results and correlations were used to determine thermodynamic conditions. A best match model was defined as one in which calculated turbine discharge temperature equalled measured turbine discharge temperature, and calculated fuel-air ratio equalled the fuel-air ratio determined from emissions data. The raw data used in analyzing design point performance is presented in Appendix C. The measured parameters, in addition to those determined from correlations, are summarized in Table 41. Station designations identifying flow path location are presented in Figure 194. The assumptions used during data reduction are listed below:

- o Measured total inlet flow - valid
- o Measured fuel flow - valid
- o Measured discharge temperature - valid
- o Fuel-air ratio determined from emission analysis - valid

TABLE 41. DESIGN POINT PARAMETERS MEASURED OR DERIVED FROM RIG CORRELATIONS (DATA SCAN 12:12:22.55).

Station		Parameter	Value	Units
1	Rig inlet total flow	Mass flow	2.1411	lbm/sec
1A	Bore cooling flow	Mass flow	0.03202	lbm/sec
2	Combustor inlet			
	Total pressure	Pressure	111.106	psia
	Total temperature	Temp	765.81	°F
2A	Fuel flow meter	Fuel flow	0.04074	lbm/sec
Rig combustor pressure loss		$\Delta P_T/P_T$	0.041	--
3 - 4	Maximum radial turbine nozzle corrected flow	$W\sqrt{\theta/\delta}$	0.608	lbm/sec
3 - 5	Radial turbine total-to-interturbine exit static pressure ratio	$P/P)_{T-S}$	3.4628	--
	Total-to-total pressure ratio	$P/P)_{T-T}$	3.253	--
<sup>1</sup>	Total-to-total efficiency	$\eta_{T-T}$	0.865	--
5 - 6	Interturbine duct loss	$\Delta P/P$	0.017	--
Axial turbine total-to-total pressure ratio		$P/P)_{T-T}$	2.1949	--
<sup>2</sup>	Axial turbine total-to-total efficiency	$\eta_{T-T}$	0.885	--
3 - 7	Overall total-to-total pressure ratio	$P/P_{T-T})_{OA}$	7.2634	--
8	Turbine discharge total temperature	Temp	1635.34	°F

<sup>1</sup> Radial turbine clearance:  $C_b = 0.053$  inch,  $C_A = 0.054$  inch,  $C_R = 0.013$  inch

<sup>2</sup> Axial turbine rotor clearance:  $C_r = 0.013$  inch

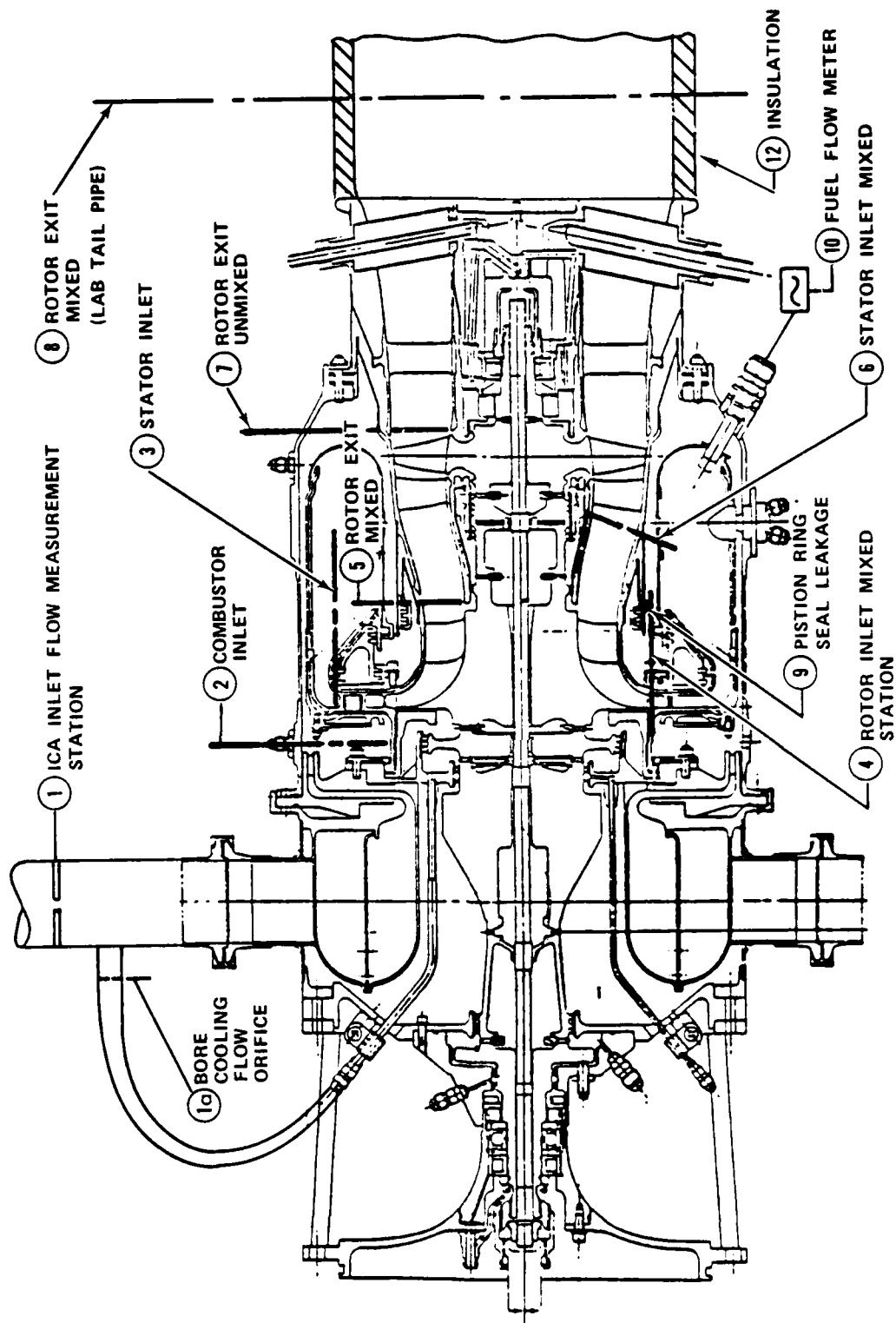


Figure 194. Stations for data reduction model

- o Average discharge total pressure - valid
- o Radial and axial turbine stage total-to-total efficiency is based on measured cold rig values corrected by measured build clearances

Several data matching iterations were required to satisfy the best match model criteria stated above.

The first iteration assumed the mainstream orifice flow (minus cooling flows) was valid and was available at the radial nozzle inlet (Station No. 3). However results indicated nozzle inlet corrected flow ( $W\sqrt{\theta/\delta}$ ) was 3.9 percent higher than the maximum allowable flow from the nozzle flow calibration and the calculated discharge temperature was approximately 7.0 degrees lower than measured. The second iteration assumed that the difference between maximum possible flow and measured flow, was lost overboard. Results of this attempt indicated the calculated fuel air ratio was excessively high. Therefore, measured inlet flow must be considered valid in order to match measured fuel-air ratio. Since this flow is higher than the measured choking nozzle flow, a certain percentage of mainstream orifice flow must be bypassing the radial nozzle. Post-test inspection of the piston ring seal (Station No. 9) indicated a measured gap which could allow mainstream orifice flow to bypass the radial nozzle and re-enter the turbine flow path at the radial turbine rotor exit (Station No. 5). An iteration on the allowable nozzle inlet flow function was required to model this possibility. Specifically, as combustor inlet flow is reduced, combustor temperature increases. Results indicated a leakage flow of 0.1011 lbs/sec was required to satisfy the required radial nozzle flow function. When this leakage flow was mixed in the interstage duct, calculated discharge temperature was approximately equal to measured discharge temperature, and an acceptable correlation between calculated and

measured fuel-air ratio was obtained. Table 42 presents the calculated results for this model. Calculated overall cooled two-stage efficiency at design point, based on this match model, is 0.893 for total-to-total ( $\eta_{T-T}$ ) and 0.875 for total-to-diffuser exit static ( $\eta_{T-DE}$ ).

ICA performance is compared with cold air data in Figure 195. Quoted ICA cooled turbine efficiencies are based on the same calculation method employed in analyzing the cold rig test data. The procedure and equations were presented in Section 4. Therefore, calculated efficiencies for the present case are defined as cycle efficiencies and account for the additional flow available for work in the axial turbine.

A comparison between the cold rig total pressure survey trace and measured ICA total pressure probes can be accomplished since the axial rotor exit total pressure probes were located at the same relative position as the cold rig. Figure 196, shows this comparison and is further evidence that ICA hot turbine-end performance is similar to cold air performance. ICA measured discharge temperature distribution can also be related to measured axial rotor exit cold rig temperature distribution. However, since measurements for the two cases were obtained at different axial locations, the intent is not to show radial gradient correlation but to indicate that significant mixing of the temperature profile has occurred from the rotor exit to the lab tailpipe. Figure 197 shows that significant axial rotor exit radial temperature gradients exist from the cold air rig. These gradients are a result of tip clearance, loss regions, and non-uniform radial work extraction. Figure 197 also shows that these temperature gradients can be reduced to provide a more uniform temperature distribution due to downstream mixing in the exhaust diffuser and lab tailpipe. Since an adiabatic mixing duct similar to that utilized in the cold air test program was not feasible for the ICA test rig, the mixing which occurred in the ICA exhaust diffuser and lab tailpipe resulted in a fairly uniform

TABLE 42. COMPUTER MATCH OF DESIGN POINT ICA DATA SCAN.

Station	Parameter	Value	Units
1 Rig inlet total flow	Mass flow	2.1411	lbm/sec
1A Bore cooling flow	Mass flow	0.03202	lbm/sec
2 Combustor inlet			
Total pressure	Pressure	111.106	psia
Total temperature	Temp	765.81	°F
Inlet airflow	Mass flow	1.9500	lbm/sec
*Stator cooling flow	Mass flow	0.0580	lbm/sec
Leakage airflow	Mass flow	0.1011	lbm/sec
2A Fuel flow meter	Fuel flow	0.04074	lbm/sec
3 Radial turbine stator inlet			
*Combustor pressure loss	$\Delta P_T/P_T$	0.041	--
Total pressure	Pressure	106.525	psia
Total temperature	Temp	2065.81	°F
Airflow plus fuel flow	Gas flow	1.99074	lbm/sec
4 Rotor inlet mixed conditions			
Total temperature	Temp	2044.92	°F
Mass flow	Gas flow	2.0487	lbm/sec
5 Radial turbine exit unmixed			
*Total-to-total pressure ratio	Pressure ratio	3.253	--
Total pressure	Pressure	32.746	psia
Total temperature	Temp	1518.09	°F
Mass flow	Gas flow	2.0487	lbm/sec
6 Axial turbine inlet mixed conditions			
*Interturbine duct loss	$\Delta P/P$	0.017	--
Total pressure	Pressure	32.189	psia
Total temperature	Temp	1479.89	°F
Mass flow	Gas flow	2.1597	lbm/sec

\*Derived from rig correlations

TABLE 42. (Contd) COMPUTER MATCH OF DESIGN POINT ICA DATA SCAN.

Station	Parameter	Value	Units
7 Axial turbine exit unmixed conditions			
Total-to-total pressure ratio	Pressure Ratio	2.195	--
Total pressure	Pressure	14.665	psia
Total temperature	Temp	1179.75	°F
Mass flow	Gas flow	2.1597	lbm/sec
8 Axial rotor exit mixed conditions (lab tailpipe)			
Total temperature calculated)	Temp	1635.1	°F
Total temperature (measured)	Temp	1635.34	°F
Total mass flow used in model	Gas flow	2.1818	lbm/sec
Total mass flow measured	Gas flow	2.1818	lbm/sec
Fuel/air ratio measured	f/a	0.190	--
Fuel/air ratio from emissions	f/a	0.189	--



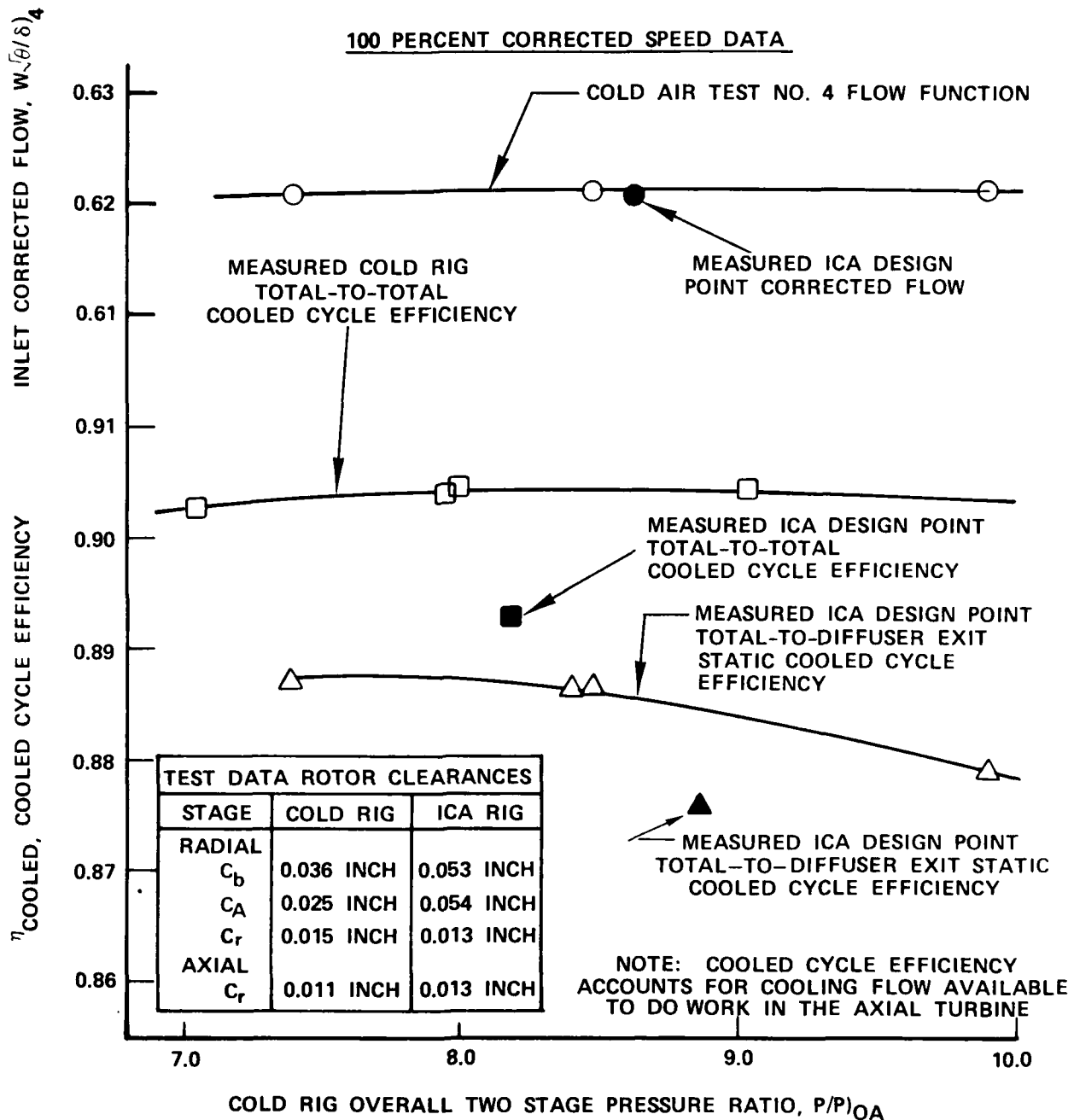


Figure 195. GTP305-2 turbine comparison of cold rig and ICA rig performance

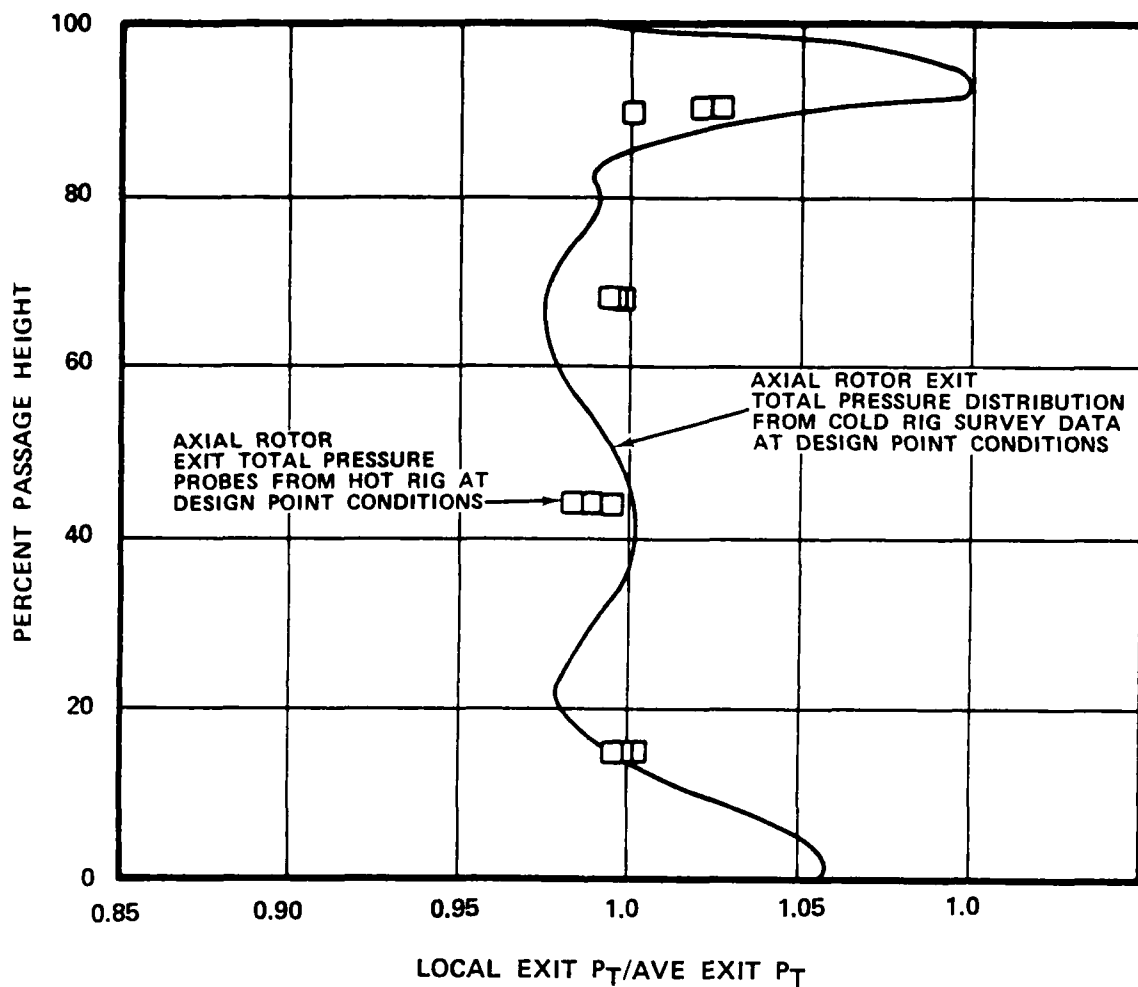


Figure 196. Comparison of hot rig and cold rig axial rotor exit total pressure distributions at design point conditions

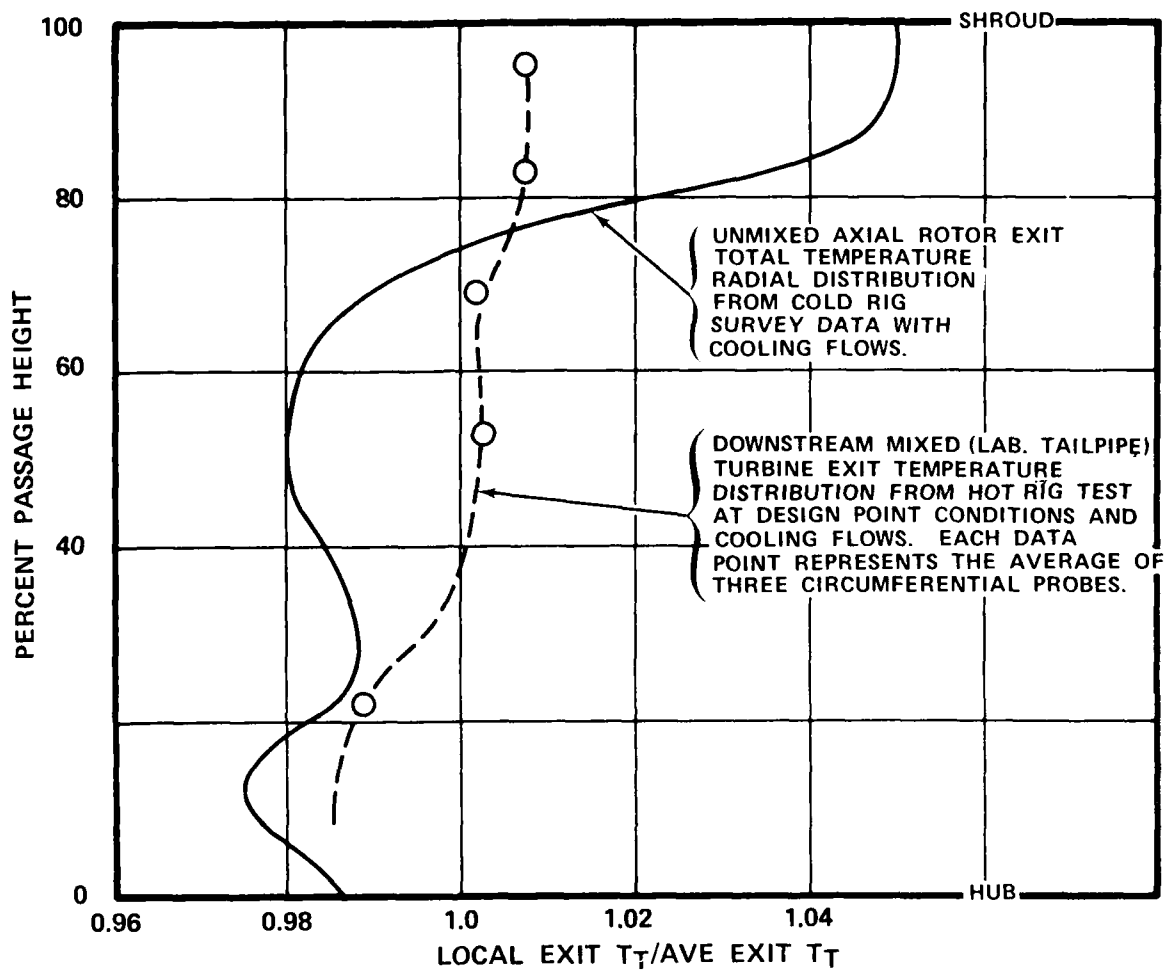


Figure 197. Comparison of hot rig and cold rig turbine exit temperature distributions at design point conditions

exit temperature and increases the confidence in the averaged exit temperature.

The ICA design point performance can also be evaluated from the measured torque obtained from a load cell attached to the water brake dynamometer. The water brake is a Kahn 3000 horsepower unit and consists of a series of perforated rotating flat plates immersed in a water chamber. The power absorbed is a function of drilled plate number and water level. The number of plates remained the same throughout the ICA testing. The water level was varied according to power output. The outer case of the water brake floats and the stationary plates attached to it react to the churning action of the rotating plates. The outer case is connected to a Balium SR4 load cell by a 12-inch lever arm. A load cell calibration curve of torque versus RC signal is then input to the data acquisition system. Measured torque was determined in this manner and is 228 ft-lbs for the design point. However, this value results from a myriad of losses between the ICA rig and the water brake. Known losses which can be estimated are listed below.

- o Gearbox
- o ICA bearing
- o Water brake bearing
- o Disk friction from dummy compression mass

In addition, component heat transfer to surrounding areas could result in an appreciable calculated loss error.

Initial calculations for parasitic losses resulted in a corrected torque value which is 7.6 percent lower than that obtained from T measurements. The load cell was therefore recalibrated using a dead weight method. Figure 198 shows this calibration and indicates the measured torque value should be increased by 2.6 percent (from 228 to 234 ft-lb). This reduces the difference

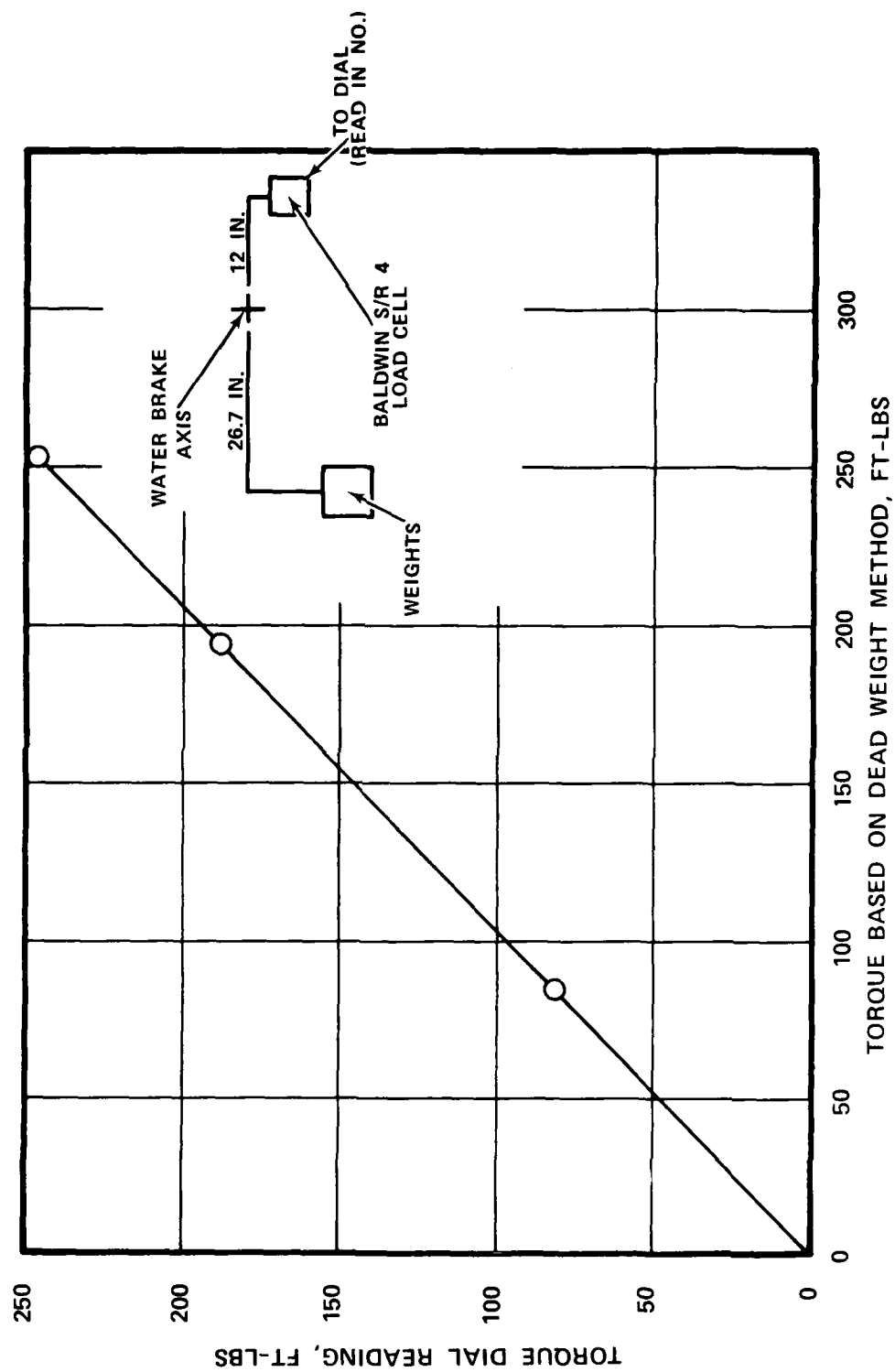


Figure 198. KAHN 3000 hp water brake dynamometer dead weight calibration

between methods to 5.0 percent which is still considered unacceptable. Measured water brake load cell torque is therefore not considered a reliable ICA rig true torque indicator due to magnitude and parasitic loss uncertainties.

In summary, the ICA design point best match model indicates:

- o Turbine rotor inlet temperature, rotational speed and pressure ratio design goals were achieved (Table 42)
- o Radial and axial turbine performance essentially duplicated cold air test performance, after differences in running clearance were accounted for
- o Approximately 4.7 percent piston ring seal leakage flow existed during ICA rig testing. This leakage re-entered the turbine interstage duct flow path and was available for work in the axial turbine
- o Design point torque determined from measured temperature, flow and pressure data is 5.0 percent higher than water brake load cell torque. The discrepancy is attributed to the magnitude and uncertainties associated with the parasitic losses between the ICA rig and the water brake load cell

#### 6.1.2 GTP305-2 Engine Performance Potential

ICA, cold turbine rig and combustor rig test results were used to re-evaluate the Model GTP305-2 engine performance capability. The updated engine cycle design point match was based on the following assumptions:

- o Design radial and axial turbine clearance ( $C_B = 0.030$ ,  $C_R = 0.015$ ,  $C_A = 0.015$ ,  $C_{r)axial} = 0.015$  inch)

- o Turbine component throat geometry is equivalent to the ICA hardware (i.e., radial turbine rotor inlet flow function is 0.621 lbs/sec)
- o Design cooling flows ( $W_{BF} = 1.5$  percent,  $W_{bore} = 1.0$  percent)
- o Cold air turbine test rig cooled overall efficiency ( $\eta_{T-DE} = 0.884$ )
- o Combustor rig pressure drop ( $\Delta P/P = 0.041$ )

All other conditions used in the original design point cycle were retained. The new design point cycle is presented in Table 43 for a sea level, 130 degree day.

Table 44 presents a comparison of original cycle match conditions and the new cycle match conditions. Turbine inlet temperature is based on 2050°F at the radial rotor inlet after stator cooling and mainstream flow mixing. Cycle efficiency is an overall inlet total-to-diffuser exit static value and accounts for the additional flow available for work in the power turbine, from the radial turbine rotor backface and interstage duct cooling flows.

## 6.2 Combustion System Performance

Combustor wall temperatures, pressure loss, combustion efficiency and exhaust emissions were evaluated at design point conditions during ICA testing. Table 45 summarizes specific combustion system performance goals and lists ICA performance levels. The combustor total pressure loss of 4.10 percent was determined from inlet total pressures and dome discharge static pressure. Dome static pressure is in close approximation of combustor discharge total pressure, due to relatively low velocities

TABLE 43. GTP305-2 DESIGN POINT CYCLE DATA.

		LHV		H/C		ALTITUDE		F/S	
		11-400-0		.18786		0.0		0.000	
COMPRESSIONS									
DRIVING TURBINE		ENERGY CONSUMPTION		WATER		SHAFT HP		TUPRINE	
		HP		C/000				MP	
		C/000		C/000				PIQUETED EFFICIENCY	



TABLE 44. COMPARISON BETWEEN ORIGINAL GTP305-2  
ENGINE CYCLE AND NEW CYCLE BASED  
ON ICA TEST RESULTS.

Sea Level, 130°F Ambient

Parameter	Original Design Point Engine Cycle	New Design Point Engine Cycle from ICA Test Results
$T_{in}$ , °F	2050.00	2050.00
Specific work, $\Delta H$ , Btu/lbm	235.00	246.14
Rotor inlet corrected flow, $W\sqrt{\theta/\delta}$ , lbs/sec	0.6150	0.621
Total-to-diffuser exit static pressure ratio, $P/P_{T-DE}$	7.529	7.671
Total-to-diffuser exit static efficiency, $\eta_{T-DE}$ *	0.850	0.884
N, rpm	75685.0	75685.0
shp, net	186.0	225.3
SFC, lbs/hr/shp	0.813	0.690
Specific power, hp/lb/sec	86.10	101.33
Combustor total pressure loss, $\Delta P/P$	0.050	0.041
Leakage flow, percent	0.020	0.020
Cooling flow, percent (bypasses radial turbine, but available to axial turbine which is accounted for in cycle efficiency)	0.025	0.025

\*Accounts for cooling flow available to do work in power turbine.

TABLE 45. GTP305-2 ICA TEST RESULTS  
AT DESIGN POINT CONDITIONS.

Parameter	Design Goal	ICA Test
Combustor Total Pressure Drop, Percent	5.0	4.10
Combustor Efficiency, Percent	>99.8	99.91
Maximum Liner Skin Temperature, °F	1500	1700
Carbon Deposits	None	None
Emissions, lb/1000 hp-hr		
HCH	No Requirement	0.49
CO	No Requirement	1.16
NO <sub>x</sub>	No Requirement	11.35

in the combustor dome area. Combustion efficiency and fuel-air ratio determined from emissions were 99.91 percent and 0.019 respectively. Gaseous emission samples were obtained from a manifold of three stationary, three-element, equal area probes located in the exhaust duct, and turbine cooling air which bypasses the combustor. HCH, CO and NO<sub>x</sub> emissions were 0.45, 1.16 and 11.35 lb/1000 hp-hr respectively. Post test inspection of combustor liner Thermindex Paint (Figure 199) shows outer wall temperatures near the primary zone were a maximum of 1500°F. One 1650°F area located on the combustor dome and ten distinct areas of 1700°F located on the combustor inner liner downstream of the primary orifices, are not shown. These results compare favorably to Tests 8 and 11 results presented in Section 4. The ceramic coating was in good condition (Figure 200), except for minor internal flaking and cracking near the fuel nozzles. There were no carbon deposits.

### 6.3 Mechanical Test Results

Post-test inspection of the ICA hardware indicated no significant problems and correlations made from the Thermindex paint indicated design integrity was achieved. The following sections describe mechanical inspection and Thermindex paint results.

#### 6.3.1 Radial Turbine Rotor

Post test inspection of the radial turbine rotor indicated two areas of distress as shown in Figures 201 through 203. Both types of distress (burned blade tips and saddle cracks) are not uncommon in first run developmental programs and are generally associated with engine transient operating during acceleration and deceleration modes. As indicated in Section 5.5 ICA Test Rig, flow, temperature and speed relationships were deliberately set at specified conditions, unlike a smooth acceleration mode for a production type APU. Since blade tip burning usually

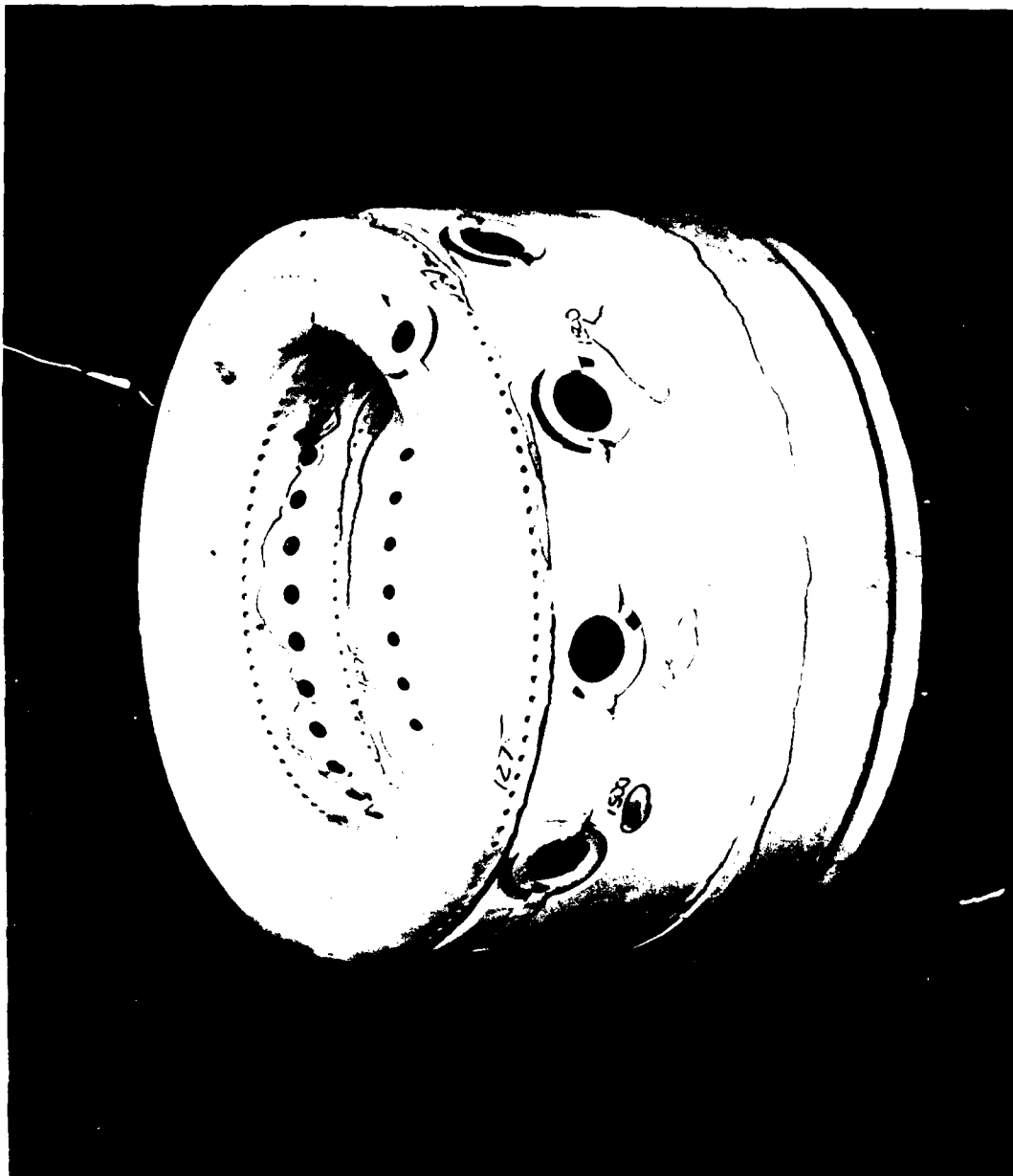


Figure 199. Model GTP305-2 combustor auxiliary power unit  
advanced technology components

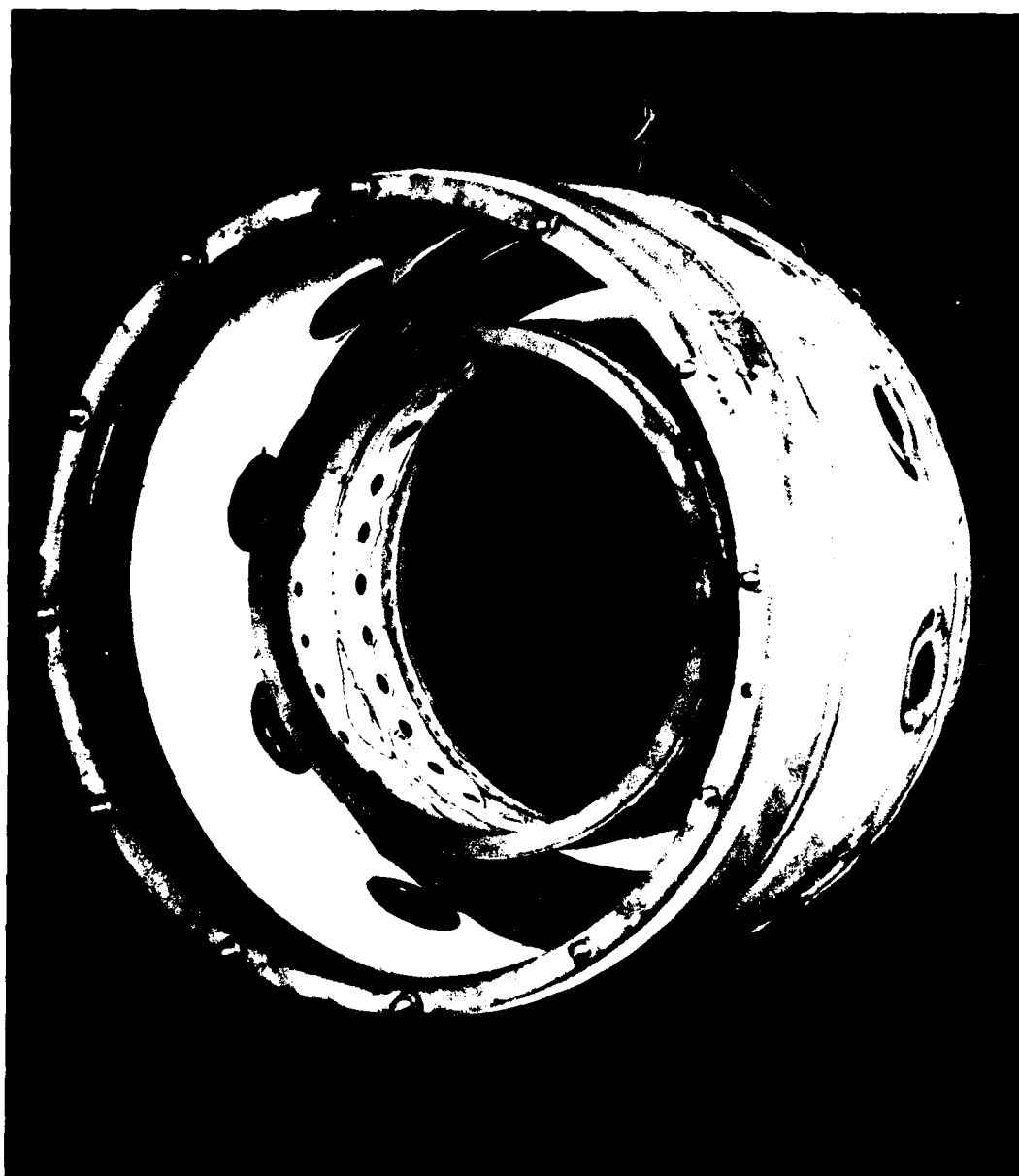


Figure 200. Model GTP305-2 combustor auxiliary power unit  
advanced technology components

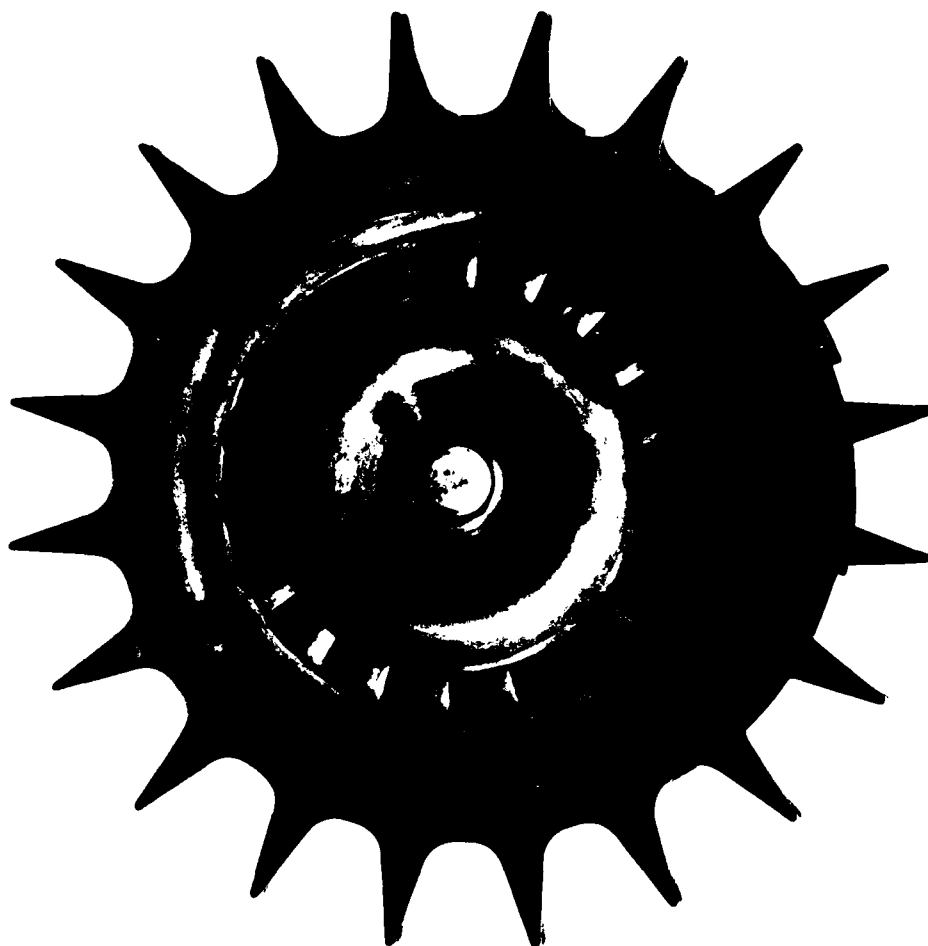


Figure 201. Model GTP305-2 Auxiliary Power Unit advanced technology components ICA radial turbine after test



Figure 202. Radial turbine (radial crack) Model GTP305-2  
Auxiliary Power Unit advanced technology  
components



Figure 203. Radial turbine (2 tangential cracks) Model 01P305-2  
Auxiliary Power Unit advanced technology components



occurs as a result of high lightoff temperatures during start and not in steady-state operations, the potential for rotor distress is more prevalent in a first run developmental start than during a well defined and controlled production mode start. Although smooth lightoffs were eventually achieved during ICA testing, initial high temperature spikes were incurred during early test rig operation. Experience has shown that utilization of production oriented fuel control monitoring systems to achieve longer but cooler start transient, normally remedies this situation and is, therefore, not considered a design problem.

Similarly, saddle cracks are normally the result of excessive temperature during start/lightoff or by quenching of the rotor. The later being a result of rapid temperature reduction while maintaining a higher air mass flow rate. As was indicated in Table 34, Section 5.5, overspeed conditions were encountered due to loss of torque control at design speed. When this happens, fuel is automatically shut off and airflow is manually decreased. Although this is a short period of time, it is analogous to quenching during fabrication heat-treatment. As stated in Section 5.2, rapid quench rates during the rotor initial heat treat cycle produced saddle cracks. Subsequent heat treat train were conducted using slower quench rates. Saddle cracks were not observed following these modifications. As stated above, production oriented control methodology corrects these first run developmental problems and, thus, rotor saddle cracking problems are resolved during the normal course of engine development.

Blade tip burning usually occurs as a result of high light-off temperatures during start and not in steady state operation. Although smooth lightoffs were achieved during ICA operation, high temperature spikes were experienced. Fuel control scheduling adjustments using current full authority digital monitoring systems would be utilized in a production mode to achieve a longer but cooler engine start. Experience has shown that this is the normal remedy.

Saddle cracks are normally the result of excessive temperatures during engine start or by quenching of the rotor. The latter is a result of rapid temperature reduction while maintaining a higher flow rate. Both conditions were experienced during test. In addition, as stated in Section 5, saddle cracking was evident during fabrication of the rotor due to quenching in the heat treat cycle. As stated above control modes correct these problems which seem to impede most new engine development programs.

#### 6.3.2 Radial Nozzle

Thermocouples and Thermindex paint were used to determine radial nozzle operating temperatures. Those located on the aft nozzle sidewall near the vane leading edge, provided the most significant comparison data. An average metal temperature of 1550°F was recorded by thermocouples located at this position, with the ICA operating at an average nozzle inlet of 2065°F and a flow rate of 2.02 lbm/sec. Using the nozzle overall design cooling effectiveness of 0.300 (see Section 3), the estimated temperature would be 1540°F.

As shown in Figures 204 and 205 the combustor ramp Thermindex paint results indicate temperatures ranging from 1750 to 1825°F. Predicted values of peak metal temperatures of 1950°F were analytically determined. Thus, from a limited thermal model picture the effectiveness of the nozzle cooling appears to be functioning and lends credance and validity to the life estimates previously stated.

#### 6.3.3 Axial Turbine Nozzle

Figure 206, shows Thermindex paint results which indicate temperature levels of 1400 to 1500°F in the hub region of with axial turbine nozzle vane temperatures between 1450 to 1500°F.



Figure 1.1. Turbine nozzle Thermindex paint results  
from TP300-2 Auxiliary Power Unit advanced  
assembly components



Figure 10. Radial turbine nozzle combustor test results Model 100000. Maximal test results. Unit: Advanced Technology Corporation.

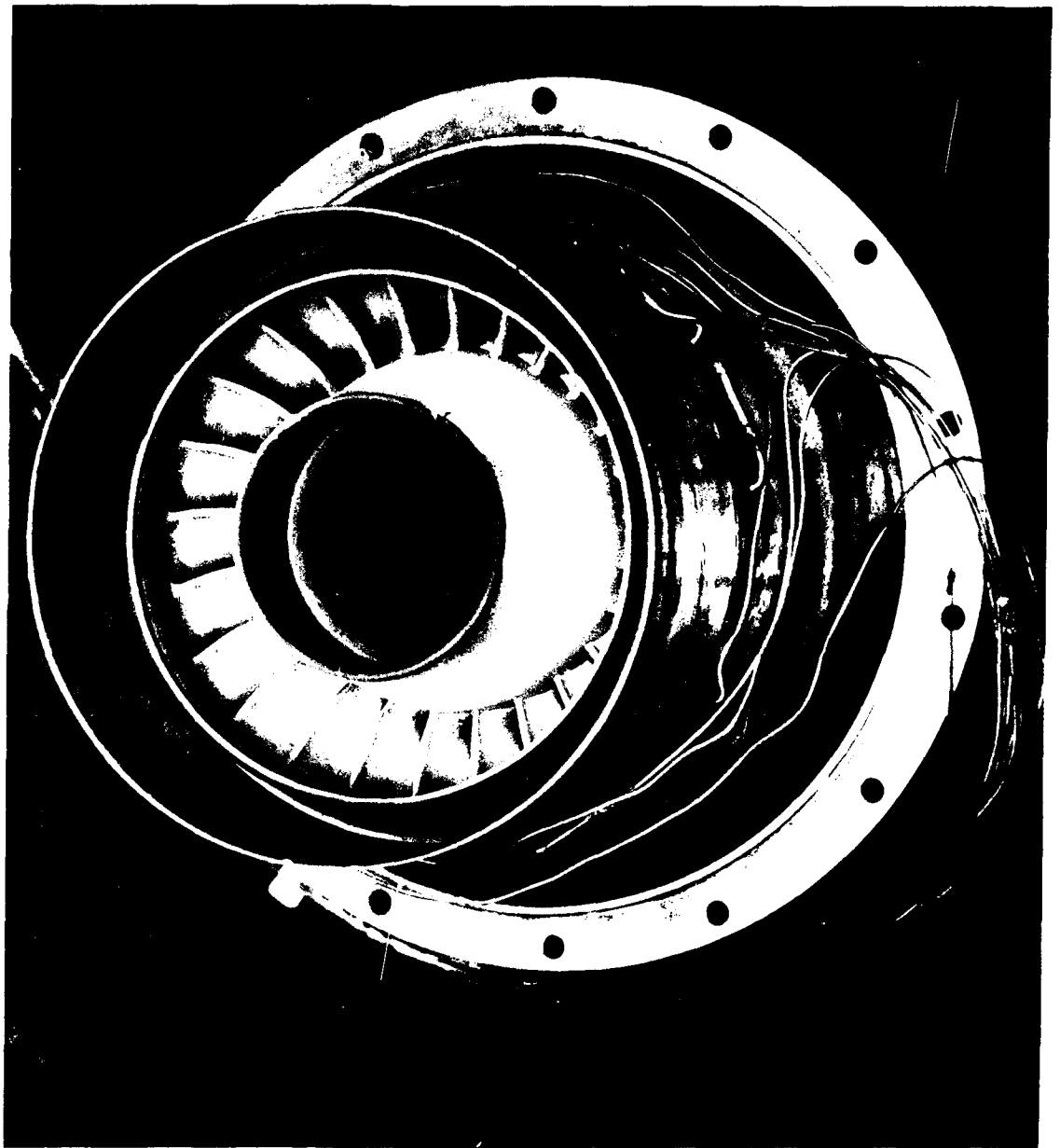


Figure 206. Axial turbine nozzle Thermindex paint results  
Model GTP305-2 Auxiliary Power Unit advanced  
technology components

These recorded metal temperatures approximate the ranges analytically predicted during design. No evidence of distress was noted during disassembly.

#### 6.3.4 Axial Turbine Rotor

The axial turbine rotor, shown in Figures 207 and 208, does not show any evidence of distress in the hub region or the blading.



Figure 207. Axial turbine (forward side) Model GTP305-2  
Auxiliary Power Unit advanced technology  
components

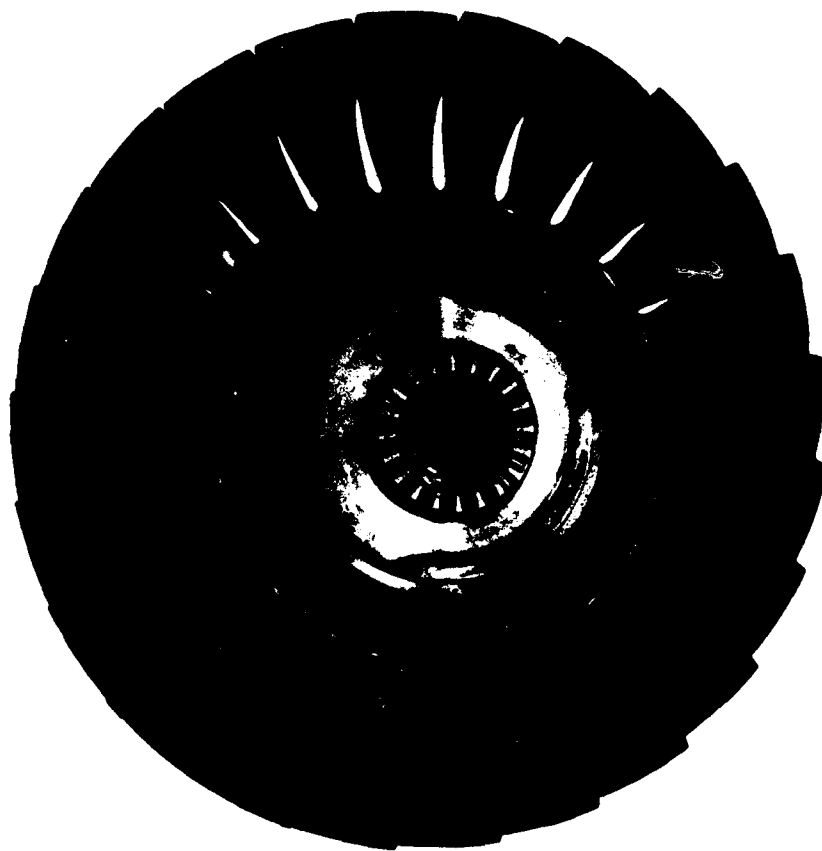


Figure 208. Axial turbine (aft side) Model GTP305-2  
Auxiliary Power Unit advanced technology  
components



## SECTION VII

### CONCLUSIONS

The components designed and tested under the Advanced Technology Components for the Model GTP305-2 Aircraft Auxiliary Power Unit included the combustion system, radial turbine stage, inter-turbine duct, axial turbine stage, and exhaust diffuser. These components were individually rig tested and then collectively rig tested in the Integrated Components Assembly (ICA) test rig at design operating conditions of temperature pressure and speed.

The combustion system for the Model GTP305-2 consisted of a reverse flow annular combustor with an AIR-ASSIST/AIR BLAST fuel injection system. Primary combustion system goals were to achieve an average combustor discharge temperature of 2067°F turbine rotor inlet temperature with cooling flow), a temperature spread factor of 0.15 and a combustor liner pressure drop of 5.0 percent.

At design point conditions, the combustor demonstrated a temperature spread factor of 0.163 and a combustor liner pressure drop of 4.1 percent. Thermal paint test results indicated liner temperatures of 1700°F at 10 discrete locations. Primary zone outer wall temperatures were 1500°F or lower. Based on AiResearch experience with a wide range of combustors, the temperature results obtained for the GTP305-2 combustor correlated with other combustors indicate a component life exceeding the contract goal of 2500 hours. Although the combustor did not demonstrate the 0.15 pattern factor goal, significant improvement was shown compared to the cycle requirement of 0.216.

The cast AF2-IDA radial turbine rotor and integrally cast radial turbine nozzle designs, together with the interturbine duct, axial stage and exhaust diffuser, were fabricated and rig tested to verify aerodynamic design. The cold-air rig test pro-

gram included single-stage radial turbine and overall two-stage tests with and without cooling flows. The radial stage test results showed the design point efficiency and interturbine duct total pressure loss were achieved. However, the significant result established from the cooled radial stage test is that no cooling flow pumping penalty is incurred with rotor backface cooling flow. Therefore, the radial turbine aerodynamic performance determined without cooling flow is applicable for cycle matching by assuming the backface cooling flow bypasses the radial stage and is mixed at the rotor exit. For the two-stage turbine test, the measured overall aerodynamic inlet total-to-exhaust diffuser exit static efficiency was .876 compared to the predicted value of .871 at design clearances and Reynolds number. The measured diffuser recovery at design point conditions was 0.447 compared to the design goal of 0.40.

Overall two-stage turbine efficiency with design cooling flows was determined from a thermodynamic heat balance between the mainstream and secondary cooling flows. Since the majority of the cooling flow was available to the axial turbine, a cooled cycle turbine "efficiency" accounted for this additional work and was then consistent with current cycle methods of bypassing cooling flows and calculating overall turbine system horsepower based on radial rotor inlet mixed flow (the radial stator cooling flow is mixed at the rotor inlet). On this basis, the design point overall total-to-diffuser exit static cooled "efficiency" is 0.884 at design speed and pressure ratio compared to the predicted value of 0.866.

AF2-IDA radial-turbine rotor castings were X-ray inspected, as-cast elevated temperature tensile strength measured, and as-cast/heat-treated room temperature tensile and stress-rupture properties determined. The rotors were HIPped in four combinations with temperatures varying from 2150 to 2250°F, pressures of 15 to 29 ksi and a constant 3-hour time period. Evaluations were

performed using four HIP conditions in combination with eight heat-treatments. Four HIP/heat-treatment combinations were selected for LCF testing on the basis of acceptable microstructures and mechanical properties. Room temperature strain-control LCF tests were performed and results analyzed on a Weibull distribution. Data analysis indicated that LCF life improvement was obtained through HIP and heat-treatment. Specifically, a 3X LCF life improvement was achieved for as-cast wheels predicted to fail in less than 1000 cycles.

The combustion system, cast radial rotor, cast radial nozzle, machined axial rotor, and axial stator, and the fabricated exhaust duct assembly were built into the integrated components assembly test rig. Testing was conducted at design operating conditions of temperature pressure and speed. ICA test results, combustion system test results and turbine cold air test results were input to the cycle model. All other cycle parameters remained unchanged. The Model GTP305-2 Advanced APU is capable of 225.3 shaft horsepower, 206.8 horsepower/FT<sup>3</sup> and 2.25 horsepower/Lb. at 130°F sea level ambient day. This compares to the design goals of 186.3 shaft horsepower, 171.0 horsepower/Ft<sup>3</sup> and 1.86 horsepower/Lb at 130°F sea level ambient day. All components lives were judged, based on analytical predictions and test data, to be adequate for a minimum of 2500 hours based on a 5-hour duty cycle.

APPENDIX A  
BUILD PROCEDURE

(30 Pages)

APPENDIX A  
BUILD PROCEDURE

The following sequence of build was utilized during ICA assembly. Shim calculation sheets are attached and provide a record for establishment of clearances and structural interfaces. This information is provided as reference material only. Refer to Drawing 3606180, Sheet 1 of 2 for part and find numbers reflected in this build procedure.

I. ROTATING GROUP SUB-ASSEMBLY

1. OBTAIN FREE LENGTH OF TIEBOLT (36J5658-1), RECORD (T1), PG20
2. ASSEMBLE ROTATING GROUP PER (3606189). PROPER TIEBOLT STRETCH REQUIRED AXIAL LOAD OF 12,000 POUNDS. STRETCH TO 4340 PSIG WHEN USING STRETCH TOOL.
3. CHECK RUNOUTS AND RECORD ON SHEET PROVIDED, PG20.
4. WHEN SATISFACTORY RUNOUTS ARE OBTAINED, MEASURE AND RECORD STRETCHED TIEBOLT LENGTH (T2), PG20. DYNAMICALLY CHECK BALANCE ROTATING GROUP PER (3606189). RECORD MEASURED UNBALANCE ON SHEET PROVIDED, PG20.
5. WHEN ACCEPTABLE UNBALANCE IS OBTAINED DYKEM MARK ALL MEMBERS OF ROTATING GROUP AND DISASSEMBLE

II. A. FORWARD BEARING SUB-ASSEMBLY

1. LOCATE ITEM #10 CARRIER (3601751-2).
2. INSERT ITEM #23 ROLLER BEARING (3605612) OUTER RACE ONLY INTO CARRIER.
3. INSERT ITEM #25 SPACER (3602796-1) INTO CARRIER WITH PIN 100° C.C.W.

FROM TOP, LOOKING FORWARD.

4. PLACE ITEM #24 BALL BEARING (358509-1) INTO CARRIER, OBTAIN

DIM. (A2)

5. OBTAIN DIM. (A1) ON ITEM #36 SEAL (3600930-2).

6. PERFORM SHIM CALCULATION C1 .

STACK ASSEMBLY ON BENCH PER SHIM CALCULATION C1 , CONSISTING OF:  
3600973-1 SPRING AND SPACER ASSEMBLY, S8154-257C SHIMS, AND  
S8157N569-030 BACKUP WASHER. ADJUST QUANTITY OF S8154-257C SHIMS  
TO OBTAIN STACKED HEIGHT 0.002-0.003 IN. LESS THAN THE C1A  
CALCULATED DIMENSION WHEN LOADED TO BOTTOM OF THE 3600973-1 ASSEMBLY.

II. B. FORWARD BEARING SUB-ASSEMBLY

1. SUB-ASSEMBLY II.A. MUST BE ACCOMPLISHED PRIOR TO II.B.
2. INSERT ITEM #26 S90-8AW-29 PIN INTO ALIGNED ANTIROTATION SLOT IN BALL BEARING AND CARRIER.
3. INSTALL SEAL ROTOR (360J761-1) IN CARRIER.
4. INSTALL ASSEMBLY II.A.6. IN CARRIER. ALIGN TABS OF 3600930-2 SEAL ASSEMBLY WITH SLOTS IN CARRIER AND PRESS TO BOTTOM.
5. INSTALL ITEM #34 LOCK WASHER (360I763-1) IN CARRIER WITH TABS IN SLOTS.
6. INSTALL ITEM #35 NUT (360I762-1). DO NOT OVER-TORQUE NUT. TORQUE NUT JUST PAST FINGER TIGHT.
7. BEND TABS ON LOCK WASHER INTO I.D. OF NUT.



AD-A087 838

AIRESEARCH MF6 CO OF ARIZONA PHOENIX

F/6 10/2

ADVANCED TECHNOLOGY COMPONENTS FOR MODEL GTP305-2 AIRCRAFT AUXI--ETC(U)

FEB 80 J R KIDWELL, 6 D LARGE

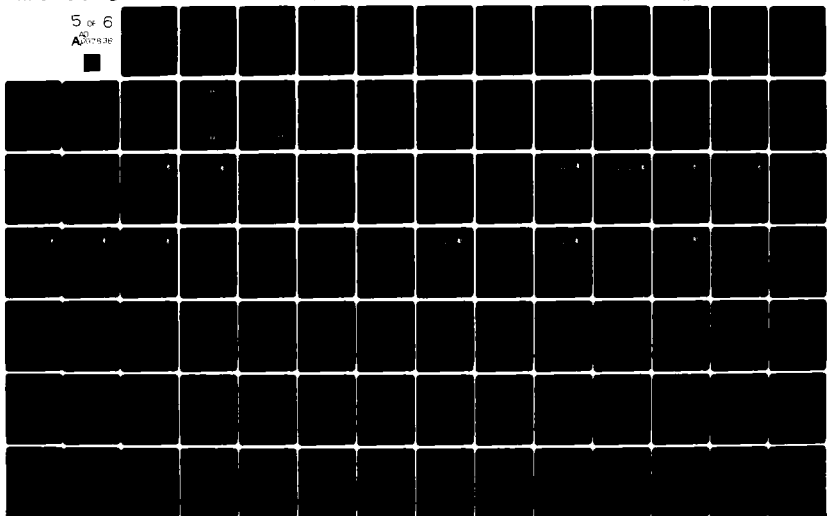
F33615-75-C-2016

UNCLASSIFIED

AFAPL-TR-79-2106

NL

5 of 6  
AD-A087 838



## II. C. FORWARD BEARING SUB-ASSEMBLY

1. SUB-ASSEMBLY II.B. MUST BE ACCOMPLISHED PRIOR TO II.C.
2. PLACE THRUST PISTON (3606183-1) IN LIQUID NITROGEN TO COOL.
3. PLACE ITEM #12 SEAL SUPPORT (3606184-1) ONTO CARRIER.
4. PLACE ASSEMBLY II.C.3. IN OVEN AT 300°F.
5. INSTALL THRUST PISTON IN CARRIER ASSEMBLY AND PRESS TO BOTTOM.
6. INSTALL OIL SLINGER (976522-1) ON THRUST PISTON AND PRESS TO BOTTOM.
7. INSTALL INNER RACE OF ITEM #23 ROLLER BEARING ONTO THRUST PISTON AND PRESS TO BOTTOM.
8. INSERT LOCK TAB (976659-1) IN THRUST PISTON. INSTALL NUT (3602786) ON THRUST PISTON, TORQUE TO 20 LB-IN.
9. RETORQUE NUT TO 450-650 LB-IN AFTER COMPONENTS ASSUME ROOM TEMPERATURE.

. III. FORWARD HOUSING SUB-ASSEMBLY

1. SUB-ASSEMBLY II MUST BE ACCOMPLISHED PRIOR TO III.
2. INSTALL ITEM #9 "0" RING AND ITEM #5 "0" RING ON ASSEMBLY II.
3. INSTALL SUB-ASSEMBLY III.2. ON ITEM #8 INLET HOUSING (3600932-1),  
SECURE WITH ITEM #7 BOLT AND LOCKWIRE.
4. INSTALL ITEM #131 TUBE ASSEMBLY (3606324-1) ON SEAL SUPPORT.
5. INSTALL ITEMS #14, 15, 92 IN ITEMS #20 AND 21, SECURE WITH  
ITEMS #18 AND 19 NUT AND BOLT. NOTE: IDENTIFY TUBE ASSY. BA, BC, AND I.
6. INSTALL ASSEMBLY III.5. AND ITEM #22 CLAMPS ON ITEM #40 SEAL SUPPORT  
(3606182-1), SECURE WITH ITEM #19.
7. INSTALL ASSEMBLY III.6. ON ASSEMBLY III.3., SECURE WITH ITEM #39  
BOLT AND LOCKWIRE.

#### IV. SIMULATED COMPRESSOR/INLET PLENUM

1. SUB-ASSEMBLY III MUST BE ACCOMPLISHED PRIOR TO IV.
2. PLACE TIE ROD (3605658-1) IN LIQUID NITROGEN TO COOL.
3. INSTALL TIE ROD IN THRUST PISTON. INSTALL G.E. COUPLING (REF. P/N 4032697) ON THRUST PISTON AND SECURE WITH LOCK RING (976505-1) AND NUT (976504-1).

NOTE: TIE BOLT EXTENSION PAST NUT TO BE  $0.130 \pm 0.005$  IN.

4. INSTALL ITEM #37 CURVIC SEAL (698468-1) IN THRUST PISTON.
5. INSTALL COUPLING HALF (976510-5) ON THRUST PISTON. NOTE: DYKEM LOCATION MARKINGS.
6. INSTALL ITEM #107 CURVIC SEAL (969528-50) IN COUPLING HALF.
7. INSTALL DUMMY WHEEL (3606181-1) ON COUPLING HALF. NOTE: DYKEM LOCATION MARKINGS.



8. INSTALL ITEM #41 INLET PLENUM (3605882-2). SECURE WITH ITEM #38 BOLT.

LOCKWIRE.

9. INSTALL ITEM #45 "O" RING ON ITEM #44 DIFFUSER (3605881-1).

10. INSTALL DIFFUSER ON ASSEMBLY IV.8.

V. LABYRINTH SEAL/BUFFER AIR/BORE COOLING AIR

1. SUB-ASSEMBLY IV MUST BE ACCOMPLISHED PRIOR TO V.
2. INSTALL ITEM #45 "O" RING AND ITEM #50 SEAL (3606185-1) ON ASSEMBLY IV.  
SECURE WITH ITEM #91 BOLT. LOCKWIRE.
3. INSTALL ITEM #46 GASKET (3606188-1) ON ITEMS #14 AND 15.
4. INSTALL ITEM #125 GASKET (3606199-1) ON ITEM #92.
5. SECURE ITEMS #14, 15, AND 92 TO SEAL WITH ITEM #49 BOLT. LOCKWIRE.
6. INSTALL WAVE WASHER (3605617-1) AND COOLING NOZZLE (3605638-1) ON  
DUMMY WHEEL. NOTE: DYKEM LOCATION MARKINGS.
7. INSTALL COUPLING HALF (3605637-1) ON DUMMY WHEEL. NOTE: DYKEM LOCATION

MARKINGS.


• VI. RADIAL TURBINE ROTOR AND RADIAL TURBINE BACK SHROUD

1. SUB-ASSEMBLY V MUST BE ACCOMPLISHED PRIOR TO VI.
2. OBTAIN DIMS. (B1)  
  
INSTALL ITEM #66 CURVIC SEAL (698335-1) AND ROTOR (3605248) ON COUPLING HALF. USING TUBE TORQUE TIEBOLT 20-40 LB-IN. MEASURE AND RECORD DIMS. (B1) REMOVE ROTOR AND CURVIC SEAL.
3. INSTALL ITEMS #59-62 SHIMS (3605651) AS REQUIRED.
4. INSTALL ITEM #65 BACK SHROUD (3606192-1). NOTE: INSTRUMENTATION LEADS TO BE ORIENTED TO ITEM #92.

VII. RADIAL TURBINE NOZZLE ASSEMBLY

1. THIS IS AN INDEPENDENT SUB-ASSEMBLY.
2. PERFORM SHIM CALCULATION C5 .
3. PLACE ITEM #72 RADIAL NOZZLE (3606193-1) ON BENCH, AFT END UP.
4. INSTALL ITEM #73 AFT SHROUD (3605627-1) ON RADIAL NOZZLE.
5. INSTALL ITEM #77 RETAINER RING (3605653-1) IN AFT SHROUD.  
INSERT ITEM #124 LOCK TEE (3605720-1).
6. INSTALL ITEMS #74, 75, AND 76 WAVE WASHER, SPACER, AND RETAINER  
(3605725-1), (3605724-1), AND (3605723-1) RESPECTIVELY ON ITEM #78  
DEFLECTOR SHROUD (3605626-1). INSTALL ITEM #79 RING SEAL (3605659-1).
7. INSTALL ASSEMBLY VII.7. IN ITEM #80 DEFLECTOR-AIR (3605625-1).  
INSERT ITEM #77 RETAINING RING (3605653-1) IN DEFLECTOR-AIR.



- 
8. INSTALL ASSEMBLY VII.8. WITH ITEM #83-86 SHIM (3605654) AS REQUIRED  
ON ASSEMBLY VII.5. SECURE WITH ITEM #87 BOLT. LOCKWIRE.

VIII. RADIAL TURBINE NOZZLE


1. SUB-ASSEMBLIES VI AND VII MUST BE ACCOMPLISHED PRIOR TO VIII.
2. PERFORM SHIM CALCULATIONS C3 AND C4 .
3. INSTALL ITEM #55-58 SHIMS (3605650), ITEM #51-54 SHIMS (3605643)  
AS REQUIRED.
4. INSTALL ITEM #67 FORWARD SHROUD (3605628-1) AND ITEM #70 SPRING  
WASHER (3605647-1) ON SUB-ASSEMBLY VII.
5. INSTALL ASSEMBLY VIII.4. ON ASSEMBLY VIII.3.
6. INSTALL ITEM #63 RETAINER (3605644-1). SECURE WITH ITEM #64 NUT.

IX. COMBUSTOR

1. SUB-ASSEMBLY VIII MUST BE ACCOMPLISHED PRIOR TO IX.
2. INSTALL ITEM #81 RING SEAL (3605656-1) IN ITEM #88 COMBUSTOR LINER (3605621-2).
3. INSTALL COMBUSTOR LINER PAYING ATTENTION TO IGNITER LOCATION AND FUEL NOZZLE ORIENTATION. PARTIAL INSTALLATION OF FUEL ATOMIZERS AND IGNITER FOR ASSEMBLY PURPOSES IS PERMISSIBLE.
4. INSTALL ITEM #69 RETAINER (3605646-1). SECURE WITH ITEM #68 NUT.

X. AXIAL NOZZLE ASSEMBLY


1. SUB-ASSEMBLY IX MUST BE ACCOMPLISHED PRIOR TO X.
2. INSTALL ITEM #37 CURVIC SEAL (698469-1), COUPLING HALF (3605604-1)  
ITEM #37 CURVIC SEAL (698469-1). NOTE: DYKEM INSTALLATION MARKING.
3. INSTALL ITEM #89 COMBUSTOR HOUSING (3605889-1), FEED INSTRUMENTATION  
FROM RADIAL NOZZLE THRU ACCESS PORTS ON HOUSING.
4. PERFORM SHIM CALCULATION C6 .
5. INSTALL ITEM #98-102 SHIM AS REQUIRED. INSTALL ITEM #82 RING SEAL  
(3605655-1). INSTALL ITEM #109 "O" RING. INSTALL ITEM #90 AXIAL  
NOZZLE ASSEMBLY, FEED INSTRUMENTATION THRU ACCESS PORTS ON HOUSING.
6. INSTALL AXIAL TURBINE ROTOR. NOTE: DYKEM INSTALLATION MARKING.

- 
7. INSTALL ITEM #93 FUEL ATOMIZER (3605635-1) ITEM #94 GASKET 3605636-1,  
SECURE WITH ITEM #43 NUT.
  8. INSTALL ITEMS #95, 96, AND 97 GASKET, SPACER, AND IGNITER (976681-1,  
3605652-1 AND 3605622-1) RESPECTIVELY.

XI. EXHAUST DUCT ASSEMBLY

1. SUB-ASSEMBLY X MUST BE ACCOMPLISHED PRIOR TO XI.
2. PERFORM SHIM CALCULATIONS C7 AND C8 .
3. PRESS ITEM #104 BELLOWS SEAL (3605613-1) INTO ITEM #103 HOUSING (3606321-1).
4. INSTALL ITEM #71 CURVIC SEAL (3605640-1) ON AXIAL ROTOR.
5. PLACE ASSEMBLY XI.3. ON AXIAL ROTOR. INSTALL SEAL ROTOR (3605639-1) ON EXTENSION ADAPTER (3605605-1) AND PLACE ON AXIAL ROTOR. NOTE: DYKEM LOCATION MARKINGS.
6. INSTALL ITEM #110 GASKET (3605632-1) ON ASSEMBLY XI.5. INSTALL ITEM #98-102 SHIMS (3605608) AS REQUIRED.

- 
7. INSTALL ITEM #116 EXHAUST DUCT (3606194-1). INSTALL ITEM #127 BRACKET (3606197-1). SECURE WITH ITEM #43 NUT.
  8. INSTALL ITEM #23 ROLLER BEARING (3605612-1). INSTALL NUT RETAINER. (3605619-1) AND TIE ROD NUT (3605618). STRETCH TIE ROD PER 3606189-1.
  9. INSTALL RETAINER (3605620-1) AND NUT (3605615-1). TORQUE NUT AS REQUIRED PER 3606189-1.
  10. INSTALL ITEM #105 GASKET (3605634-1).
  11. INSTALL ITEM #111-115 WAVE WASHER ASSEMBLY.
  12. INSTALL ITEM #121 HOUSING (3606196-1). SECURE WITH ITEM #43 NUT.
  13. INSTALL ITEM #119 GASKET (3605645-1) AND ITEM #118 OIL-IN TUBE ASSEMBLY. SECURE WITH ITEM #43 NUT. INSTALL ITEM #117 COVER (3605722-1). SECURE WITH ITEM #108 BOLT.



14. INSTALL ITEM #122 GASKET (3605633-1) AND ITEM #123 OIL-OUT TUBE ASSEMBLY,  
SECURE WITH ITEM #43 NUT. INSTALL ITEM #106 COVER (3605721-1), SECURE  
WITH ITEM #108 BOLT.

15. INSTALL ITEM #120 COVER (3605648-1). SECURE WITH ITEM #38 BOLT. LOCKWIRE.

REMAINDER OF ASSEMBLY MAY BE ACCOMPLISHED PER 3606180 SHEETS 1-5.



# INTEGRATED COMPONENTS ASSEMBLY ROTATING GROUP

- (1) 0.0005 IN.
- (2) 0.0004 IN.
- (3) — IN.
- (4) 0.001 IN.
- (5) 0.0008 IN.
- (6) 0.0015 IN.

- (7) — IN.
- (8) — IN.
- (9) 0.0002 IN.
- (10) 0.0005 IN.
- (11) 0.0009 IN.
- (12) 0.0005 IN.

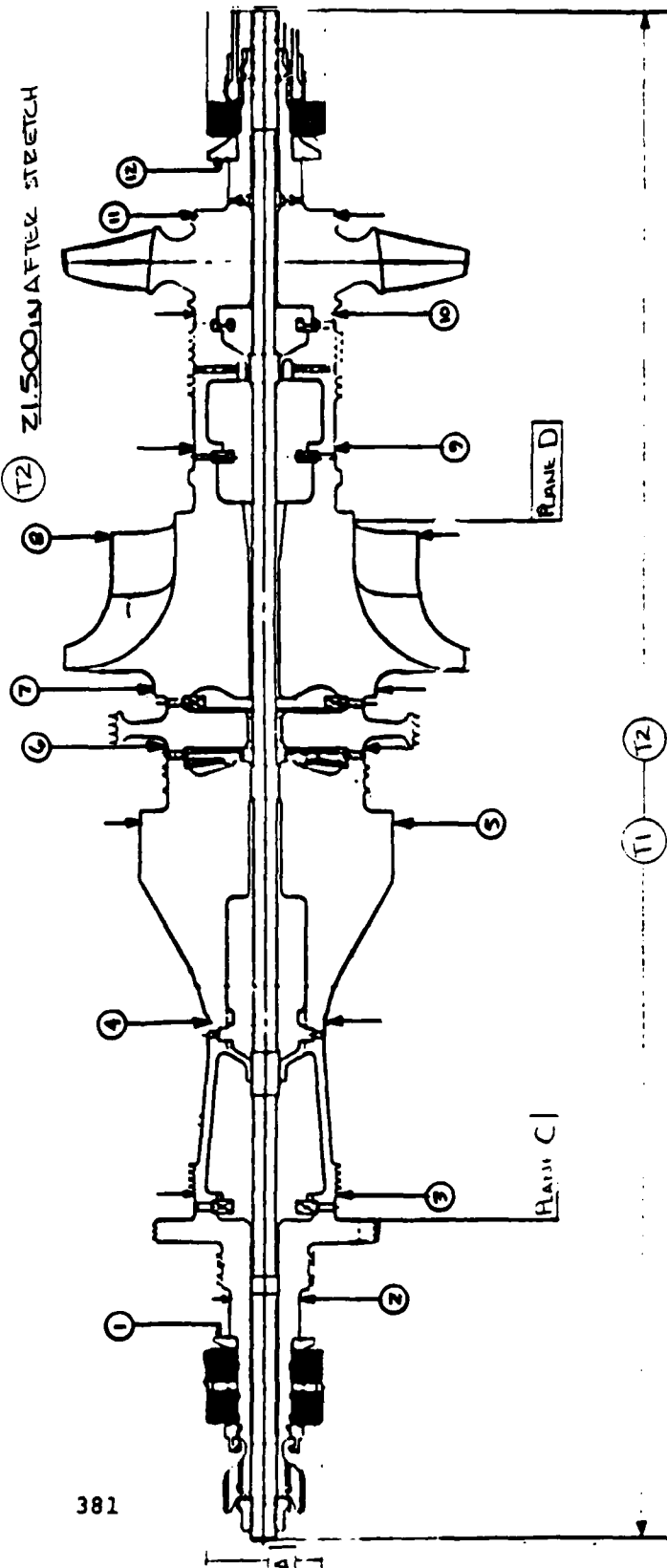
PLANE C | 0.0060 IN

PLANE D | 0.0720 IN

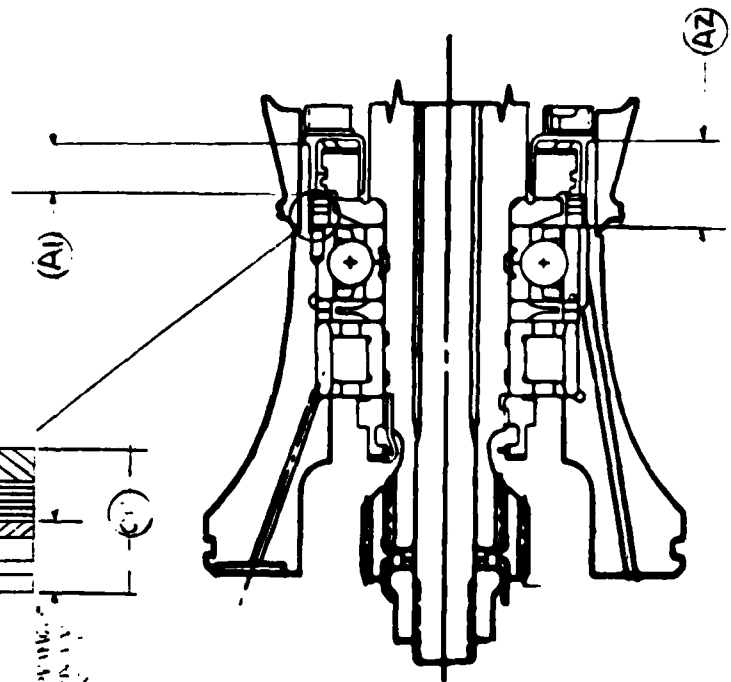
T1 | 21.415 IN BEFORE STRETCH

T2 | 21.500 IN AFTER STRETCH

381



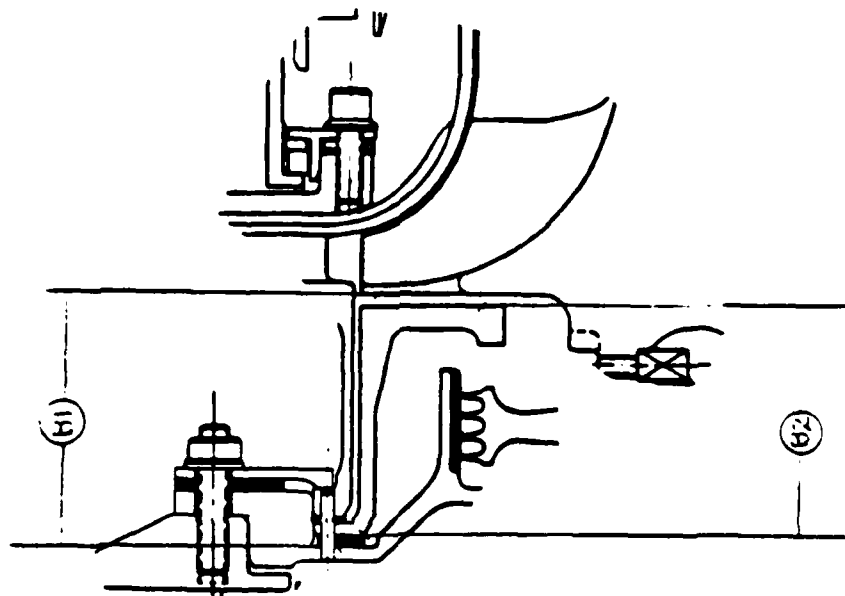
FORWARD BEARING WAVE WASHER - SHIM CALCULATION C1



(R2)	<u>0.526</u>	(F1A)	<u>0.194</u>
(A1)	<u>-0.332</u>		<u>-0.1265</u>
			SPRING SPACER ASSY

ACTUAL SLM THICKNESS: 0.0655 (CI) *JK*

# RADIAL TURBINE ROTOR BACKFACE CLEARANCE - SHIM CALCULATION C2



ADD:

(19) 1.403

RTBC 0.050

C2A = 1.453

ADD:

(21) 1.465

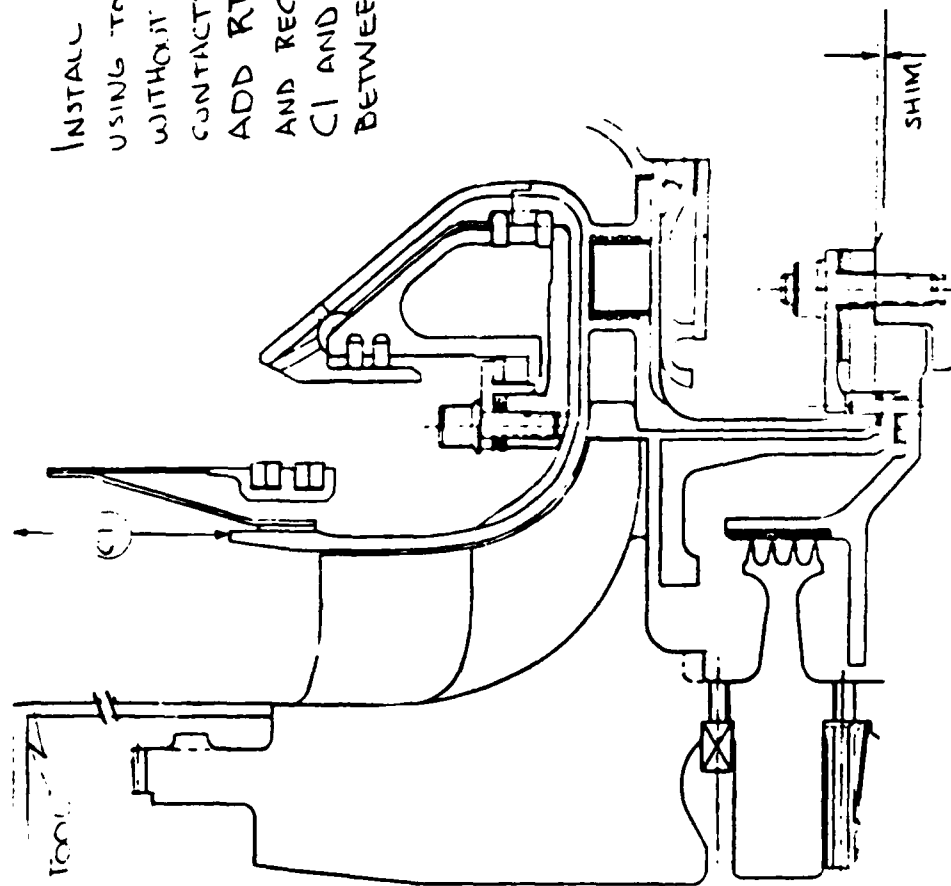
C2A = 1.453

C2B = 0.012  $\pm 0.002$

ACTUAL SHIM THICKNESS

0.010 (C2) *APK*

# RADIAL TURBINE ROTOR AXIAL FACE CLEARANCE - SHIM CALCULATION C3



INSTALL ROTOR AND STRETCH TIEBOLT USING TOOL. INSTALL RADIAL NOZZLE WITHOUT SHIMS IN PLACE SO THAT NOZZLE CONTACTS ROTOR. OBTAIN DIMENSION C1 ADD RTAFC IN. INSTALL SHIMS AND RECHECK DIMENSION C1. RECORD C1 AND FINAL C1. DIFFERENCE BETWEEN IS ACTUAL CLEARANCE

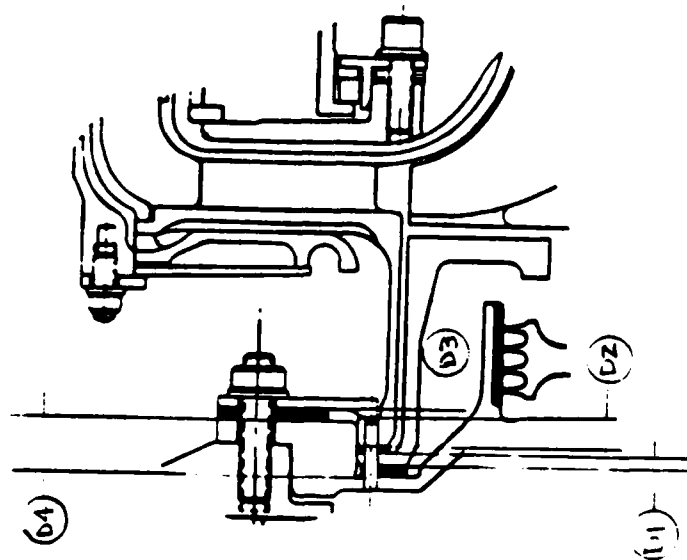
C1 BEFORE 5.729

C1 AFTER 5.785

RTAFC 0.056

ACTUAL SHIM THICKNESS  
NO SHIM REQUIRED  
C3 = 0

# RADIAL NOZZLE CLAMPING FORCE - SHIM CALCULATION C4



Add:

(C2) 0.010

(b1) 0.079

(C3) 0.0

(b2) 0.195

(b3) 0.056

C4A = 0.360

Add:

C4A 0.360

(b1) -0.354

C4B = 0.006

SUB = 0.001

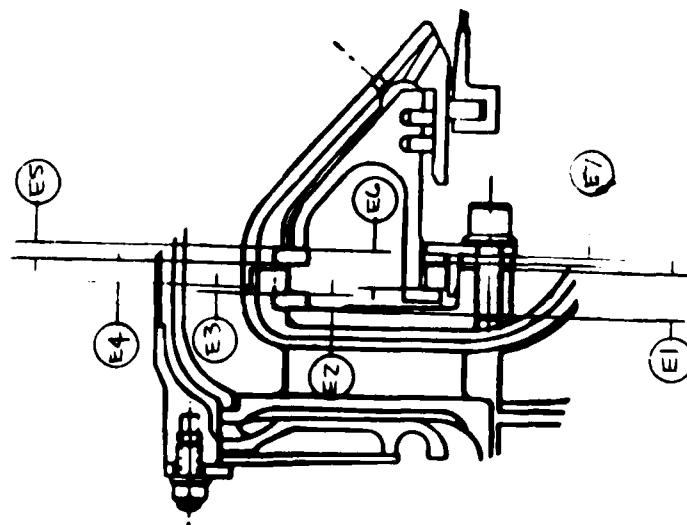
C4C = 0.005 + 0.000 in

DELETED SHIM STACK  
⇒ PINCH OF 0.006

ACTUAL SHIM THICKNESS

0 - (E4)

# RADIAL NOZZLE WAVE WASHER - SHIM CALCULATION C5



$$\textcircled{E2} \quad \underline{0.079}$$

$$\textcircled{E4} \quad \underline{0.182}$$

$$\textcircled{E5} \quad \underline{0.080}$$

$$\textcircled{E7} \quad \underline{0.066}$$

$$\text{CSA} = \underline{\underline{0.407}}$$

$$\text{Add} + \underline{0.166}$$

$$\text{CSB} \quad \underline{\underline{0.573}}$$

$$\textcircled{E1} \quad \underline{0.302}$$

$$\textcircled{E3} \quad \underline{0.001}$$

$$\textcircled{E6} \quad \underline{0.2150}$$

$$\text{CSC} = \underline{\underline{0.5250}}$$

$$\text{CSB} \quad \underline{0.573}$$

$$\text{CSC} - \underline{0.525}$$

$$\text{CSD} = \underline{\underline{0.048}} \pm 0.003 \text{ in.}$$

ACTUAL SHIM THICKNESS 0.047 *JK*

# AXIAL TURBINE ROTOR TIP CLEARANCE - SHIM CALCULATION C6

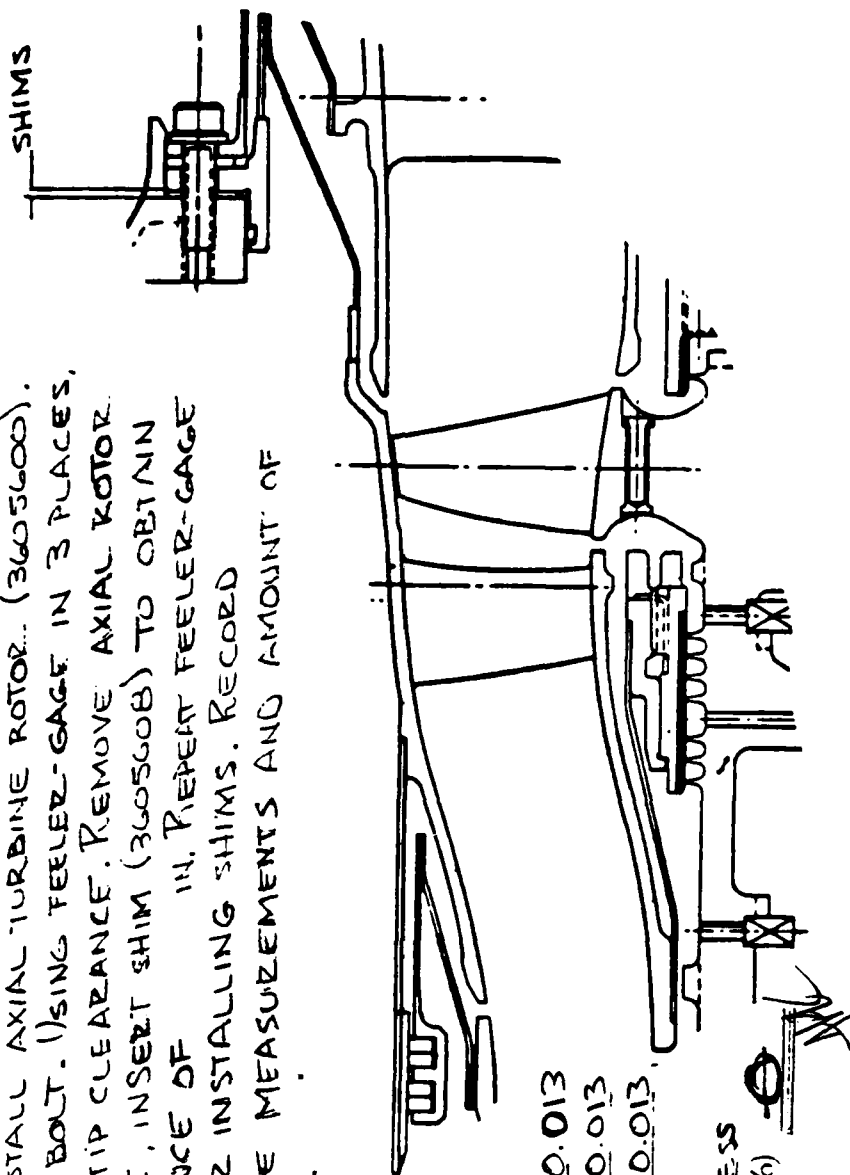
INSTALL AXIAL TURBINE NOZZLE (3605495) WITHOUT SHIMS (3605608). INSTALL AXIAL TURBINE ROTOR (3605600). STRETCH TIE BOLT. USING FEELER-GAGE IN 3 PLACES, DETERMINE TIP CLEARANCE. REMOVE AXIAL ROTOR AND NOZZLE, INSERT SHIM (3605608) TO OBTAIN TIP CLEARANCE OF .013. REPEAT FEELER-GAGE CHECK AFTER INSTALLING SHIMS. RECORD FEELER-GAGE MEASUREMENTS AND AMOUNT OF SHIMS USED.

387

NO SHIMS REQUIRED  
MACHINED ASSY.

FEELER GAGE #1 0.013  
FEELER GAGE #2 0.013  
FEELER GAGE #3 0.013

ACTUAL SHIM THICKNESS  
(C6)



27



Add

C7A 1.386

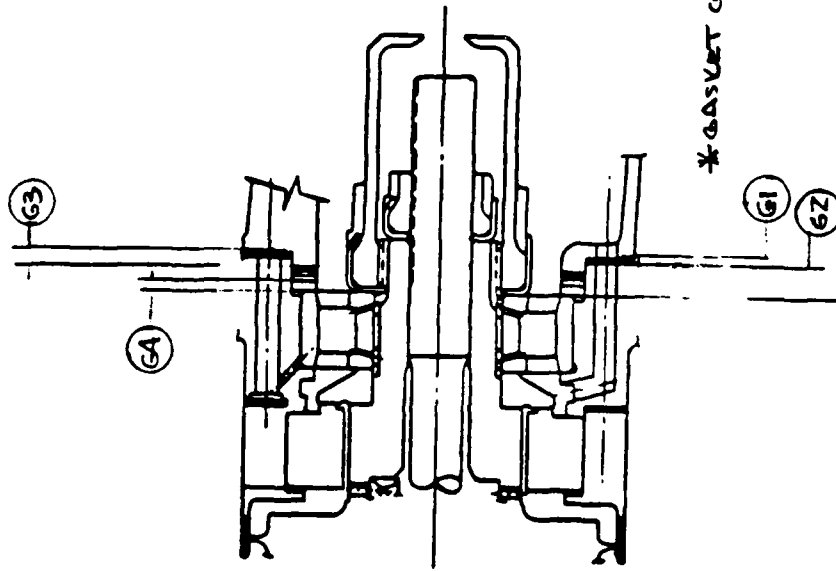
⑪ 1.305

$$C7B = \underline{0.081} \pm 0.002_{IN}$$

Actual Shim Thickness 0.080 (7) ✓



REAR BEARING WAVE WASHER - SHIM CALCULATION C8



ADD:	ADD:
(G1) 0.0314	(G3) 0.1602
(G2) 0.282	(G4) 0.0316
(G5) = 0.3134	ADD = 0.060
* SUB = 0.004	(G6) = 0.2718
(G7) = 0.3094	
	ADD:
	(G8) 0.3094
	(G9) = 0.2718
	(G10) 0.0376 ± 0.002 IN

\* GASKET COMPRESSION

ACTUAL SHIM THICKNESS (G8) 0.038 IN

390



11

APPENDIX B

DEVELOPMENT TEST PROCEDURE  
TEST AND LOG SHEETS

(57 Pages)

APPENDIX B

DEVELOPMENT TEST PROCEDURE  
TEST AND LOG SHEETS

The following pages are included as reference material. These pages include the Development Test Procedure adhered to during test of the ICA and copies of the day-to-day test log that provide a chronology of events throughout the ICA test program.



AIRRESEARCH MANUFACTURING COMPANY OF ARIZONA  
A DIVISION OF THE SASEBY CORPORATION

FOR INTERNAL USE BY  
AIRRESEARCH PERSONNEL ONLY

## DEVELOPMENT TEST PROCEDURE

DT- 6127



TEST ITEM & P/N	GTP305-2 3606180	DATE	December 11, 1978
TEST TITLE	GTP305-2 Integrated Components Assembly Testing (ICA)		
FACILITIES & SPECIAL TEST EQUIPMENT	<ol style="list-style-type: none"><li>1. C116 test cell</li><li>2. Sanborn recorders (two 8-channel)</li><li>3. Real time analyzer</li></ol>		
TEST OBJECTIVE	<p>The integrated components assembly test objective is to determine the aerodynamic and mechanical performance of the GTP305-2 turbine section components under actual operating conditions (temperature and pressure).</p>		
PREPARED BY	TASK ENGINEER	PROJECT ENGINEER	
J. W. Teets	J. W. Teets	J. R. Kidwell	



AIRSEARCH MANUFACTURING COMPANY OF ARIZONA  
A DIVISION OF THE GARRETT CORPORATION  
PHOENIX, ARIZONA



## DEVELOPMENT TEST PROCEDURE

**DT-** 6127

### 1. Test Set-Up

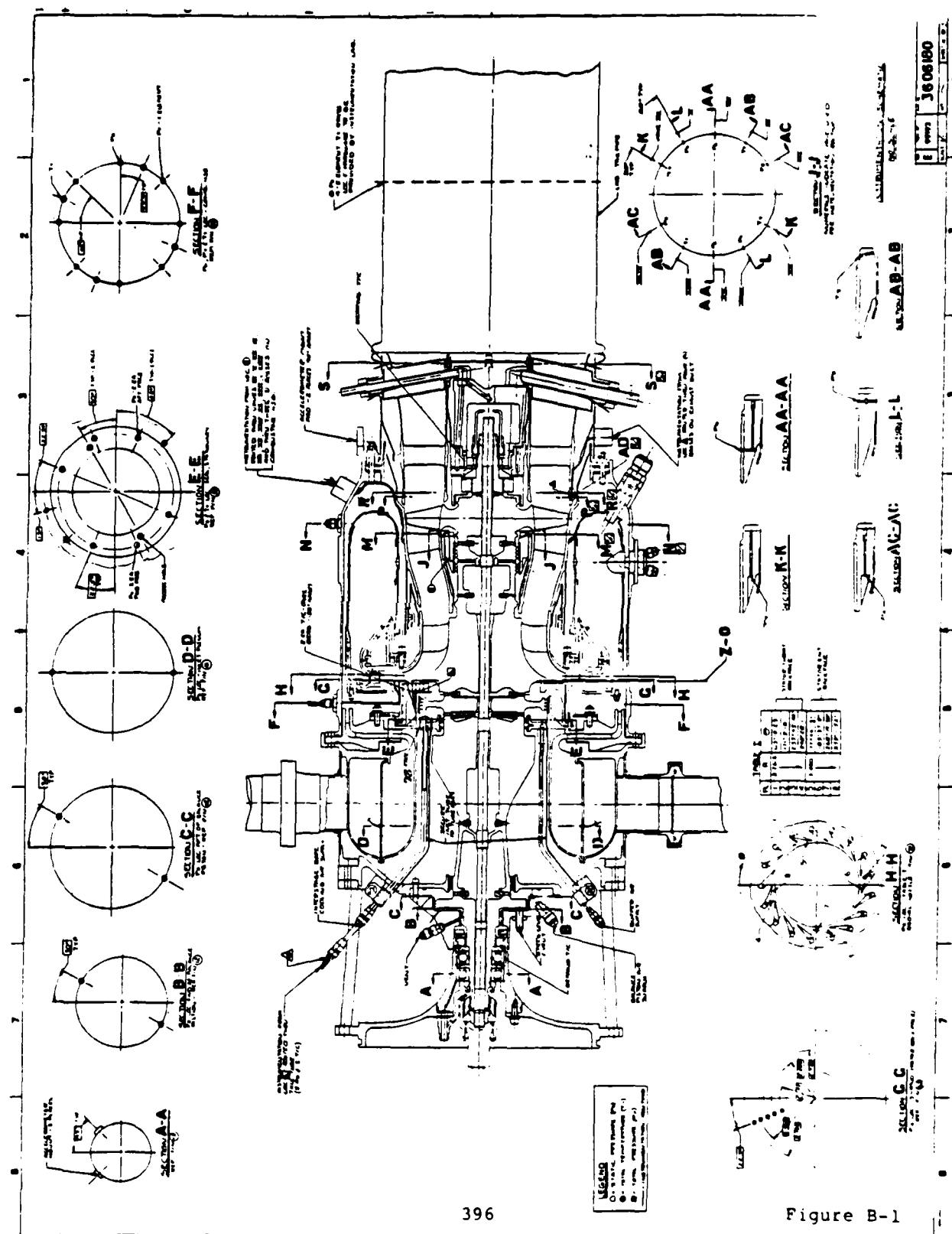
The test rig consists of actual GTP305-2 turbine section components (i.e., all engine components aft of the compressor/diffuser) mated to a forward section that simulates the compressor dynamically. This rig also provides a plenum for supplying conditioned air to the turbine. The forward structure, including bearings, is basically a GTP305-1 engine structure. Connecting this forward structure to the turbine section is a rig structure specifically designed for the GTP305-2 integrated components test rig. The length of this structure is such that the GTP305-2 engine bearing span is duplicated. The rig structure incorporates a toroidal plenum with inlet pipes at two circumferential locations for distribution of facility air to the turbine plenum. The supply plenum exit incorporates vanes to induce a 25-degree swirl to simulate combustion system inlet flow conditions. Dummy compressor rotor hardware, which duplicates engine compressor rotor mass distribution and stiffness, will be utilized to reproduce the engine rotor dynamic characteristics in the rig. A GTP305-2 engine tie-bolt is used to hold the rotating group together.

Provisions have been made in the rig to incorporate a forward thrust balance piston if calculations indicate that the thrust of the turbine components is greater than the thrust bearing capability.

Oil supply and scavenging for the forward and aft bearings will be provided by motor driven pumps which are part of the test facility.

### 2. Instrumentation

Instrumentation for the integrated components assembly testing is shown in Figures B-1 and B-2 (Drawing 3606180). Also, Tables B-1, B-2 and B-3 will be used to identify instrumentation.





1	2	3	4	5	6	7	8	9	10	11	12	13	14	15	16	17	18	19	20	21	22	23	24	25	26	27	28	29	30	31	32	33	34	35	36	37	38	39	40	41	42	43	44	45	46	47	48	49	50	51	52	53	54	55	56	57	58	59	60	61	62	63	64	65	66	67	68	69	70	71	72	73	74	75	76	77	78	79	80	81	82	83	84	85	86	87	88	89	90	91	92	93	94	95	96	97	98	99	00
---	---	---	---	---	---	---	---	---	----	----	----	----	----	----	----	----	----	----	----	----	----	----	----	----	----	----	----	----	----	----	----	----	----	----	----	----	----	----	----	----	----	----	----	----	----	----	----	----	----	----	----	----	----	----	----	----	----	----	----	----	----	----	----	----	----	----	----	----	----	----	----	----	----	----	----	----	----	----	----	----	----	----	----	----	----	----	----	----	----	----	----	----	----	----	----	----	----	----	----

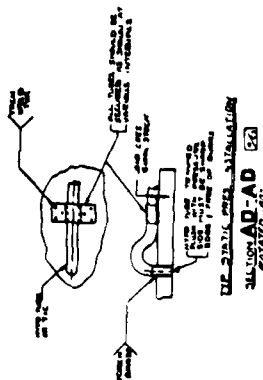
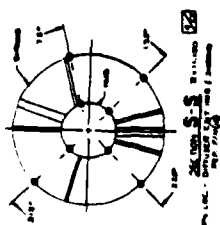
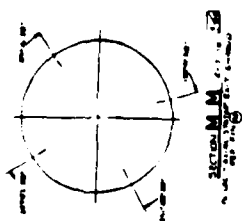
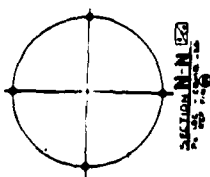
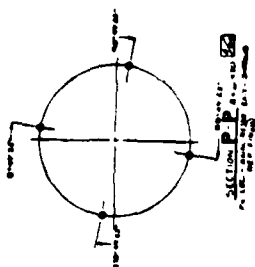
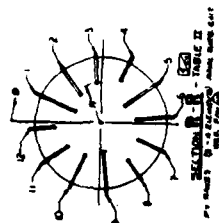


Figure B-2



AIRSEARCH MANUFACTURING COMPANY OF ARIZONA  
A DIVISION OF THE GARRETT CORPORATION

TABLE B-1. INSTRUMENTATION DATA ASSIGNMENT SHEET

Unit Type ICA Unit No. GTP305-2 Build No. 1 Test No. 1 EWO 3409-246160-09-0601

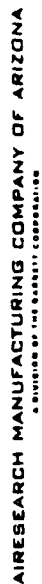
Channel	SYMBOL	NO.	PARAMETER	MASTER NO. ASSIGNED REQUIRED	RANGE UNITS	INSTRUMENTATION NUMBERS AND REMARKS	CHANNEL ADDRESS ASSIGNED
Console							
X	MØRP						
X	MØRT		Main Orifice Flow		0-150 lbs/min		
X	MØROP						
X	IBCØP		Interstage	2152-2153			
X	IBCØT		Bore	6105	0-15 lbs/sec		
X	IBCØDP		Cooling Flow	1801			
X	TURRPM		Turbin rpm		0-90,000 rpm		
X	TØRQUE		Water Brake Torque		0-300 ft-lb		
X	FUELFL		Fuel Flow				
X	FUEL T		Fuel Temp		0-150 °F		
	FUEL P		Fuel Press				
X	CINPTI-4	4	Comb. Inlet Total Press	2221-2224	15-200 psig	100 thru 103	
X	CINTTI-4	4	Comb. Inlet Total Temp	6209-6212	50-1000 °F	202 thru 205	
	CINPSI-4	4	Comb. Inlet Press	2533-2536	15-200 psig	11 thru 14	
	PSIFLI-2	2	Inlet Plenum press	3001-3002	15-200 psig	5 and 6	
X	PSSSAI-2	2	press Stationary Seal Aft	3501-3502	14-50 psig	8 and 10	
X	PSSSFI-2	2	press Stationary Seal Frwd	3503-3504	14-50 psig	7 and 9	



AIRSEARCH MANUFACTURING COMPANY OF ARIZONA  
A DIVISION OF THE GARRETT CORPORATION, OH

TABLE B-2. INSTRUMENTATION DATA ASSIGNMENT SHEET

Unit Type		ICA	Unit No.	GTP305-2	Build No.	Test No.	1	EWO	3409-246160-09-0601
Analog	Digital	Console	SYMBOL	NO.	PARAMETER	MASTER NO. ASSIGNED REQUIRED	RANGE UNITS	INSTRUMENTATION NUMBERS AND REMARKS	CHANNEL ADDRESS ASSIGNED
	X		PBPI-2	2	Press Balance Piston Frwd	3505-3506	15-50 psig	3 and 4	
	X		PBPAI-2	2	Press Balance Piston Aft	3507-3508	15-250 psig	1 and 2	
			PRBFI-5	5	Rotor Backface Press	3136-3141	14-70 psig	15 thru 19	
	X		PSNTHI-4	4	Nozzle Press Throat	2537-2540	14-70 psig	24 thru 27	
			PSNTEI-4	4	Nozzle Press Trailing Edge	2541-2545	14-70 psig	20 thru 23	
			PMSJI-6	6	Press Mid-Span Seals	3509-3514	14-17 psig	28, 30, 31, 32	
			psrdsi-4	4	Press Rotor Disch Shroud	3282-3285	14-30 psig	42 thru 45	
	X		PTRDI-12	12	Total Press Rotor Disch	3286-3297	14-30 psig	104 thru 115	
	X		PSDDSI-4	4	Press Diff Disch Shroud	3302-3305	14-30 psig	50 thru 53	
	X		PSDDHI-4	4	Press Diff Disch Hub	3306-3309	14-30 psig	46 thru 49	
			PSITPI-4	4	Press Inlet Tailpipe Shroud	3310-3313	14-30 psig	90 thru 93	
	X		TTPI-15	15	Temp Tailpipe	6401-6415	50-1500 °F	6401 thru 6415	
			PSTPI-6	6	Press Tailpipe	3314-3319	14-30 psig	95 thru 100	
	X		RBTfWD	1	Roller Brg Temp Frwd	6501	50-300 °F	320	
	X		BBTF	1	Ball Brg Temp Frwd	6502	50-300 °F	321	
	X		RBTAF	2	Roller Brg Temp Aft	6503-6504	50-300 °F	322 and 323	



Unit Type ICA Unit No. GTP305-2 Build No. 1 Test No. 1 EWO 3409-346160-09-0601

400



AIRESEARCH MANUFACTURING COMPANY OF ARIZONA  
A DIVISION OF THE BARRETT CORPORATION  
PHOENIX, ARIZONA



## DEVELOPMENT TEST PROCEDURE

DT- 6127

In addition to the instrumentation shown in Tables B-1, B-2 and B-3, the following instrumentation will be incorporated in the facility portion of the test setup.

- (a) Turbine exit temperature thermocouples will be incorporated downstream of the turbine diffuser in the insulated facility exhaust duct.
- (b) Emission probes will be incorporated in the facility exhaust duct. Four probes with three holes facing the gas flow will be used.
- (c) A monopole speed pickup will be incorporated in the adapter gearbox to determine gearbox input/integrated components assembly output shaft speed (in the unit).
- (d) Existing facility instrumentation will be used to determine water brake torque and speed.
- (e) Oil flow and pressure instrumentation will be incorporated in the facility oil supply lines to the integrated components assembly.
- (f) Vibration probe for the engine (2).
- (g) Vibration probe for the gearbox (1).
- (h) Vibration probe for the water brake (1).



AIRESEARCH MANUFACTURING COMPANY OF ARIZONA  
A DIVISION OF THE SUNDT CORPORATION  
PHOENIX, ARIZONA



## DEVELOPMENT TEST PROCEDURE

DT- 6127

### SANBORN RECORDER INFORMATION

<u>Parameter</u>	<u>Qty</u>	<u>Range</u>
Speed	1	0-100K
Tail Pipe Temperature	1	0-2000°F
Vibration Probes (Engine Front and Rear)	2	
Thrust Bearing Temperature #321	1	0-300°F
Oil Pressure	1	0-100 psig
Combustion Inlet Pressure #102	1	0-200 psig
Rotor Backface Pressure #16, #17	2	0-100 psig
Water Brake Torque	1	0-300 ft-lbf
Fuel Flow	1	0-200 lb/hr
Turbine Exit Pressure (Axial) #91	1	0-20 psig

#### 2.1 Lab Interface

The high temperature component test facility (C116) is designed to allow hot testing of engine turbine sections. The facility is provided with various energies and control systems that permit testing under a wide range of airflows, temperatures, pressures, shaft loads, and speeds.

The existing facility air supply system supplies inlet air to the hot turbine rig at temperatures from 40° to 800°F with airflows up to 1300 pounds per minute and pressures to 275 psia. However, the rig air supply system can be modified to route inlet air through an existing additional heater, which will allow inlet temperatures up to 1000°F. Airflow will then be limited to 180 ppm. The rig inlet ducting is provided with a



AI RESEARCH MANUFACTURING COMPANY OF ARIZONA  
A DIVISION OF THE GUGLIEMOTTI CORPORATION  
PHOENIX, ARIZONA



## DEVELOPMENT TEST PROCEDURE

**DT-** 6127

rupture disc for emergency shutdown in the event of an over-speed condition. The inlet system also incorporates mixing valves to mix hot and cold air for temperature control, a pressure regulating valve, airflow measuring section, and inline air filter.

The facility load absorption system consists of a gearbox and a water brake. The load applied to the test turbine is controlled by coarse and fine water flow regulating valves. Torque is measured by a load cell incorporated in the water brake support structure. This system is capable of absorbing up to 3000 hp at input speeds up to 35,000 rpm. Since the design speed of the GTP305-2 turbine is 75,684 rpm, an additional gearbox (General Electric) will be used in place of the existing facility gearbox. Gearbox installation and run-in will be in accordance with methods agreed upon by General Electric and AiResearch.

The facility is equipped with monitoring devices for critical parameters such as speed, vibration, bearing temperatures, oil pressure, water pressure, and turbine discharge temperature. These devices provide a visual readout at the control console and can provide an audio warning or unit shutdown if preset limits are exceeded.

Fuel control equipment will be used to control the fuel flow to the test turbine atomizers either as a function of speed or as a function of turbine discharge temperature. Therefore, a constant turbine speed or discharge temperature can be maintained under conditions of varying load and/or inlet conditions.

A high speed digital data acquisition system will be used to record turbine aerodynamic and mechanical performance parameters. This system is capable of recording data at a rate of 200 samples per second and can display corrected data at the test cell console within 2 minutes after a data scan is taken.



AIRRESEARCH MANUFACTURING COMPANY OF ARIZONA  
A DIVISION OF THE SABOTTE CORPORATION  
PHOENIX, ARIZONA



## DEVELOPMENT TEST PROCEDURE

DT- 6127

A quick-look scan will be used to check the preliminary turbine performance at the test cell.

The following is a list of requirements to be accomplished during the test set up and monitored during testing.

- (a) Cooling Air - Bore cooling flow will be supplied from the inlet plenum at .023 lb/sec (design point).
- (b) Buffer Air (air supply or vent)
  - 1) At the bore cooling inlet station zone C6, buffer air will be greater or equal to the bore cooling. Shop air will be used. (#9 for bias pressure)
  - 2) Thrust balance. (140 psig maximum, Figure B-3)
  - 3) Thrust balance buffer air zone E6  $\geq$  thrust balance #2. (this is a vent)
  - 4) Vent O.B. of buffer air #3 zone E6 (vent).

NOTE: Refer to Figure B-3 for the pressure values on the thrust balance.

- (c) Overtemperature Protection and Monitoring
  - 1) Tail pipe temperature set point 1350°F.
  - 2) Oil Temperature
    - o Gearbox inlet 110°F
    - o Engine bearing oil out (monitor)
  - 3) Thrust bearing temperature 300°F maximum. API meter used to monitor.
  - 4) Aft bearing temperature 300°F maximum. API meter used to monitor.



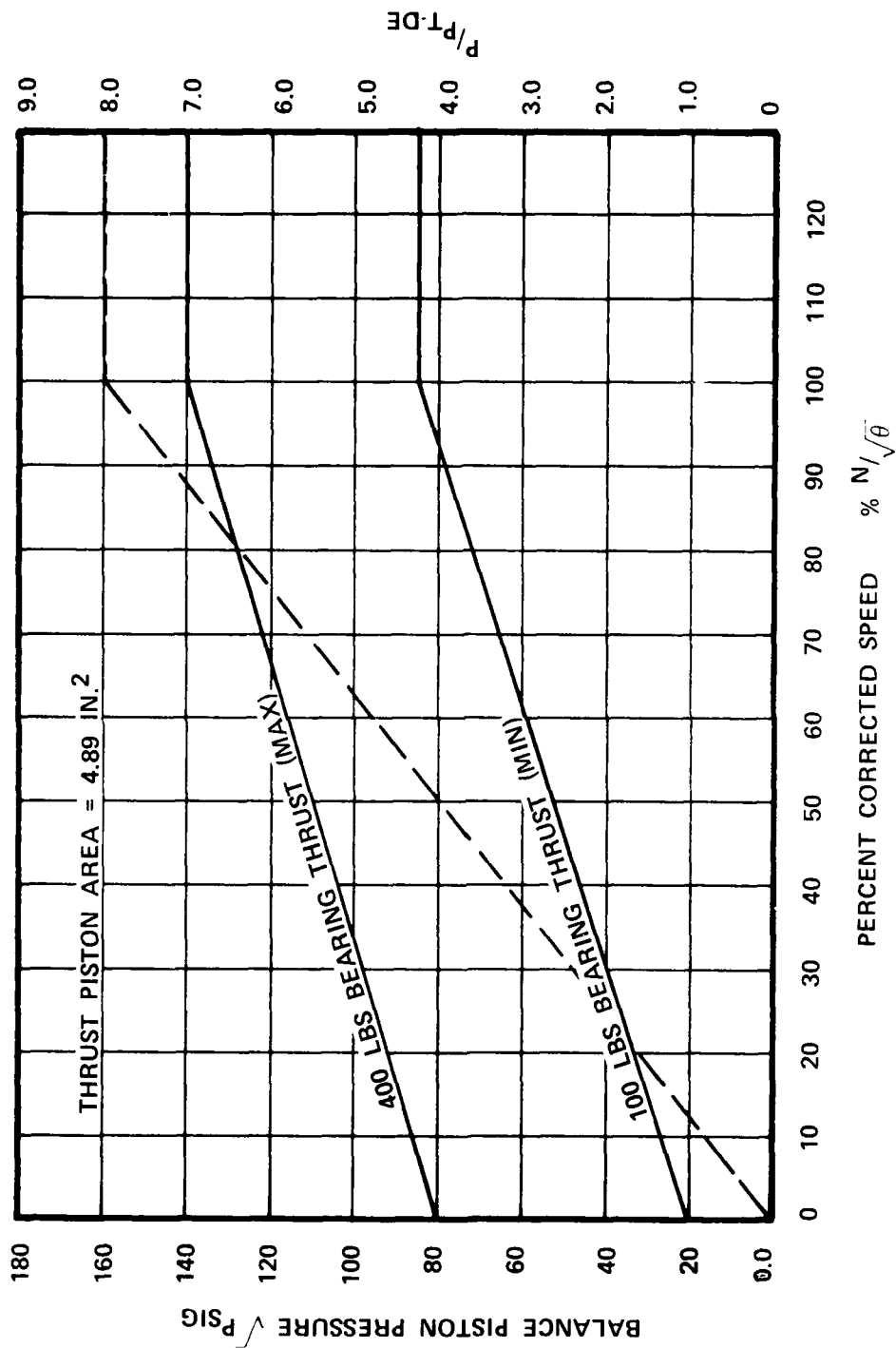


Figure B-3.



AIRESEARCH MANUFACTURING COMPANY OF ARIZONA  
A DIVISION OF THE SARGENT CORPORATION  
PHOENIX, ARIZONA



## DEVELOPMENT TEST PROCEDURE

**DT-** 6127

(d) Oil Pressure

- 1) Engine, 60 psig minimum (monitor)
- 2) Gearbox, 15 psig minimum (monitor)

(e) Vibration Probe

- 1) Engine (2)
- 2) Gearbox (1)
- 3) Water brake (1)

3. Mechanical Build

Office Memo JRK-0072-022478 defines the integrated components assembly test rig.

4. Test Procedure

The instrumented integrated components assembly will be installed in the test facility. The following tests will be performed:

- (a) Motoring test (unfired) to 100 percent design speed to verify mechanical integrity. During this procedure, cold air performance data will be at specified condition.
- (b) Fired mechanical checkout to 100 percent speed, including controls familiarization. During this hot run up, performance data will be taken at specified conditions.
- (c) Performance demonstration.
- (d) Therminindex paint test.



## DEVELOPMENT TEST PROCEDURE

DT- 6127

### 4.1 Verify Mechanical Integrity

Initially, the rig will be motored at approximately 5000 rpm using inlet air pressure to drive the turbine. While motoring, proper oil flow to the bearings will be verified and proper operation of all instrumentation used to monitor mechanical condition will be substantiated. The rig will then be accelerated slowly to 100 percent speed by increasing inlet pressure and temperature. During this acceleration, vibration data will be recorded by a direct readout recorder to define rig dynamic characteristics over the full operating range. Also, cold air performance data will be recorded at specified points. Bearing temperatures and speed will also be recorded by this recorder. While at 100 percent speed, the output of all installed instrumentation will be recorded by the digital data acquisition system to verify proper operation of the instrumentation and the data acquisition system. In addition, this motoring run will provide initial familiarization with the airflow and dynamometer controls for this rig.

### 4.2 Fired Mechanical Checkout

When mechanical integrity and proper instrumentation operation have been demonstrated, the fired mechanical checkout and controls familiarization will be performed. The inlet airflow and dynamometer load will be set to provide airflow conditions and turbine speed equivalent to the engine ignition point. Lightoff fuel flow will then be introduced and ignition achieved. Proper operation of all condition monitoring equipment will be verified. The rig will then be accelerated to approximately 50,000 rpm for controls familiarization. This will be done at low speed to provide a margin of safety until rig response to control inputs is defined. Control familiarization will be accomplished by operating the rig at a specific condition and then changing to a new condition to determine the proper controls operation required to change to a new condition. During this testing, the digital data acquisition system will be used to record data at each operating point to



AIR RESEARCH MANUFACTURING COMPANY OF ARIZONA  
A DIVISION OF THE GORDON CORPORATION  
PHOENIX, ARIZONA



## DEVELOPMENT TEST PROCEDURE

DT- 6127

allow verification of proper rig and instrumentation operation, as well as acquire low speed aerodynamic data. Once controls operation has been defined and mechanical integrity under fired conditions demonstrated, the rig will be accelerated to 100 percent speed and the design point (100 percent power) conditions established to ensure mechanical integrity over the full operating range. Combustor discharge (turbine inlet) temperature will be calculated by two methods: 1) fuel/air ratio and 2) power balance.

### A. Light-Off Procedure

- NOTES:
- 1) Set up fuel system such that both low and high flow rates can be read at the appropriate times.
  - 2) Start with discharge valve wide open.
  - 3) Rig start will be made with the initiation of fuel flow and ignition simultaneously.
  - 4) Start cooling flow into the rig after light-off stabilization.
1. Set rig airflow to 0.4 lb/sec at an inlet temperature of 238°F; refer to Table B-4.
  2. Preset fuel flow at 24 lb/hr per Table B-5, Figure B-4. Continue to flow air through the rig to clear any fuel accumulated while setting the flow.
  3. Adjust water flow through water brake to obtain torque values as shown in Figure B-5 (torque/rpm).
  4. Light off the rig with the fuel flow and ignition initiated simultaneously. Use fuel flow Table B-5 and Figure B-4. Pressure to air assist should be 5 psi above the combustor inlet pressure. Discontinue air assist after 60 percent N.

TABLE B-4. STATE POINT DATA

% N (%)	Rotor RPM	Comp Inlet Airflow (lb/sec)	Comp Exit Airflow	Comp Exit Pressure (psia)	Comp Exit Temp (°F)	Fuel Flow (lb/hr)	Radial Turbine Inlet Temp. (°F)	Turbine Exit Temp. (Axial) (°F)	Turbine HP	Net HP
100	75,684.0	2.165	2.06	119.0	786	151.0	2050	1225	702	188
	75,684.0	2.230		109.0	769	81.0	1461	842	511	0
90	68,115.6	1.790	1.71	84.0	660	63.4	1348	827	340	0
80	60,547.0	1.310	1.25	61.0	561	52.1	1338	910	204	0
70	52,978.8	.973	.93	45.4	467	43.0	1332	1004	114	-5
60	45,410.4	.715	.68	34.6	381	36.7	1389	1126	66	0
50	37,842.0	.523	.50	27.1	305	30.5	1448	1254	35	0
40	30,273.0	.405	.37	22.0	238	24.0	1427	1291	17	0



AIRESEARCH MANUFACTURING COMPANY OF ARIZONA  
A DIVISION OF THE GARRETT CORPORATION  
PHOENIX, ARIZONA

TABLE B-5. COMBUSTION SYSTEM OPERATING CONDITIONS

Atomizer Fuel Flow	Idle	80 lb/hr
	Full Power	151 lb/hr
	Ignition	20 lb/hr
Combustor Airflow	Idle	2.08 lb/sec
	Full Power	2.01 lb/sec
	Ignition	0.16 lb/sec
Combustor Inlet Temperature	Idle	770°F
	Full Power	788°F
Combustor Inlet Pressure	Idle	109.6 psia
	Full Power	118.8 psia
Average Combustor Discharge Temperature	Idle	1480°F
	Full Power	2085°F

NOTES:

1. Operating parameters are for a 130°F sea level day.
2. For test purposes, these parameters will be held within  $\pm 1$  percent of stated values.

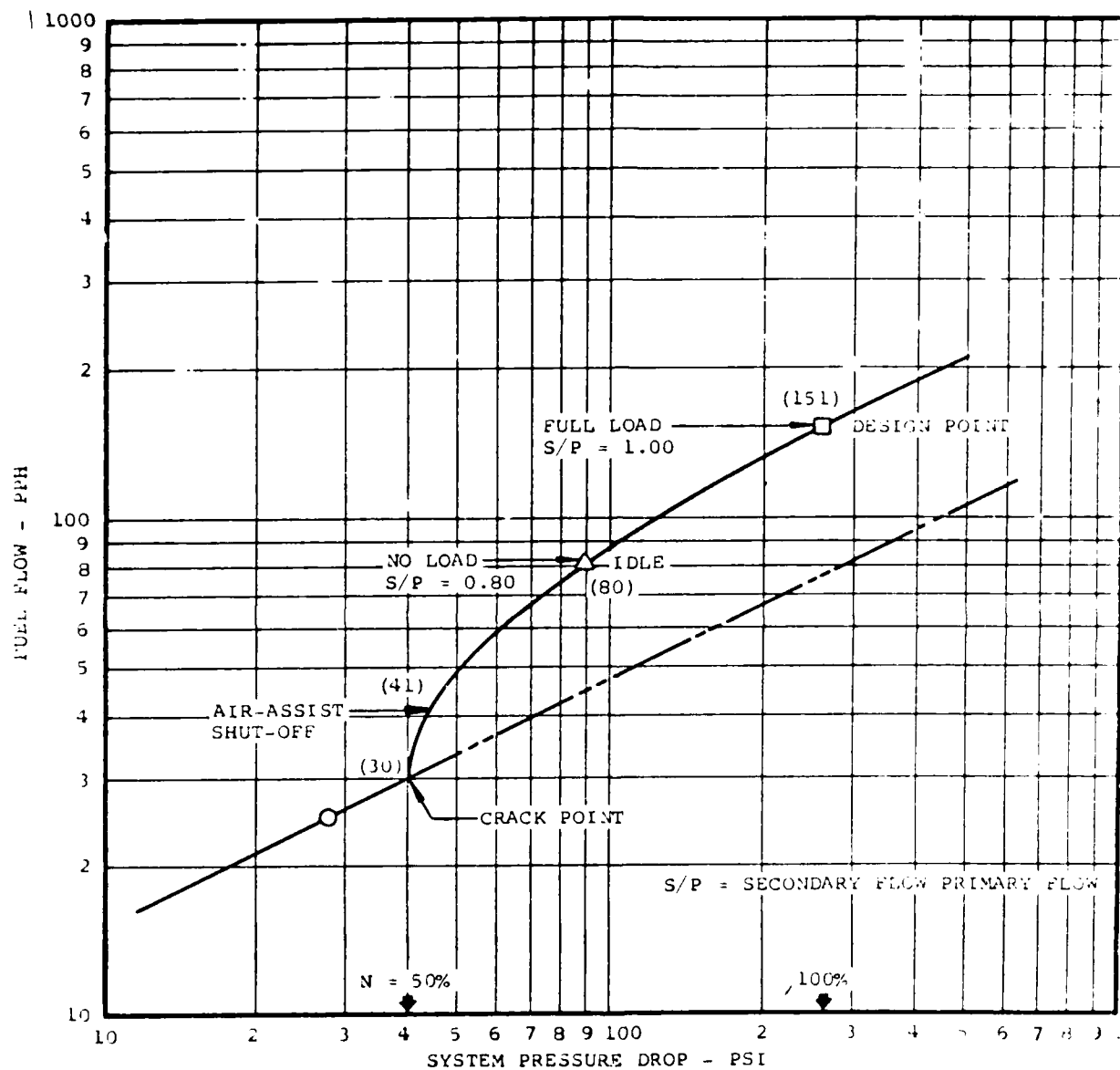


Figure B-4. GTP305-2 fuel system characteristics  
(5) air-assist/airblast, (5) pure airblast

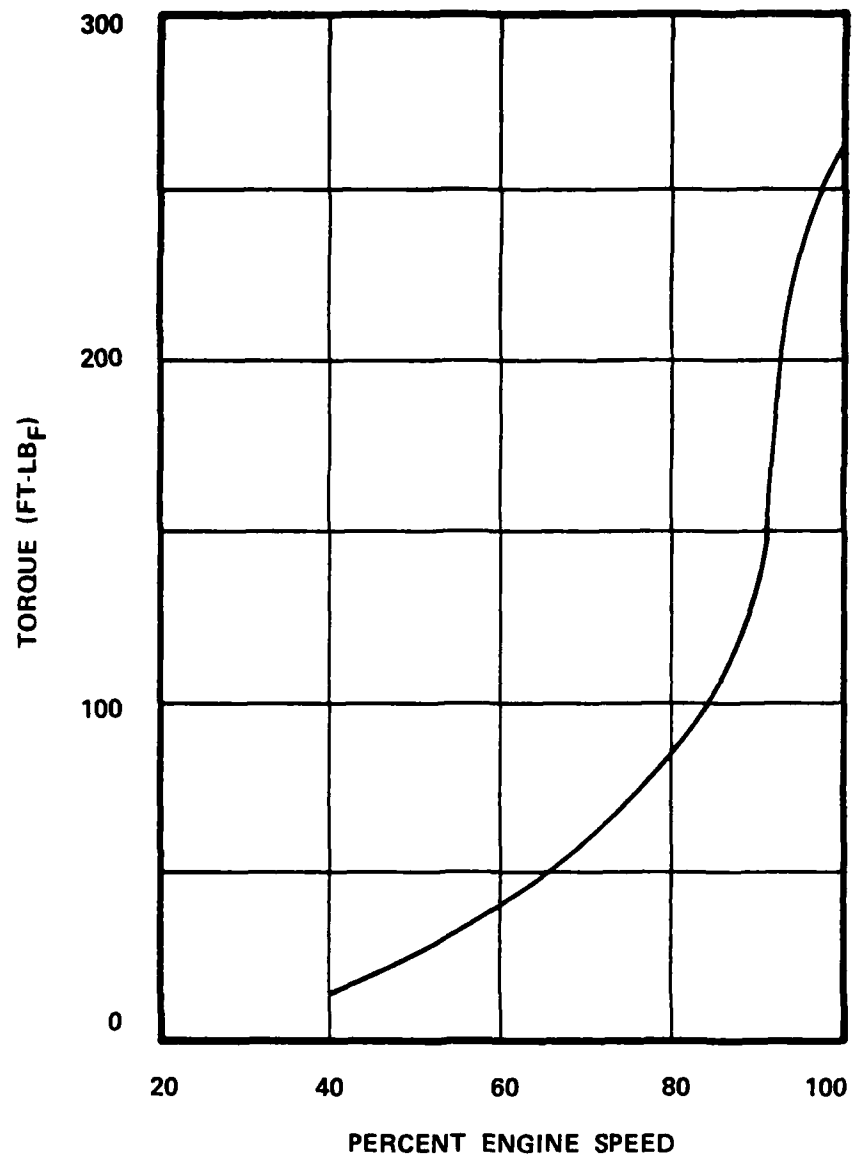


Figure B-5. Predicted waterbrake torque/percent engine speed





AIRESEARCH MANUFACTURING COMPANY OF ARIZONA  
A DIVISION OF THE GARRETT CORPORATION  
PHOENIX, ARIZONA



## DEVELOPMENT TEST PROCEDURE

**DT-** 6127

5. If light-off is not achieved after approximately 10 seconds, turn off fuel flow and ignition and repeat the above procedure with 5 lb/hr more fuel flow.

NOTE: Maintain an appropriate pressure on the thrust piston (minimum thrust, 100 lbf; maximum thrust, 400 lbf). Use Figure B-3 to obtain the pressure needed on the balance piston.

### B. Stabilize

After light-off is achieved, increase the combustor inlet temperature to 385°F keeping the turbine inlet temperature at 1360°F to 1390°F, 46,000 rpm, and 40-50 ft-lb torque.

NOTE: These data points could be varied per Table B-4 and Figure B-5.

### C. Design Point

Gradually work up to the following conditions:

1. Calculated turbine inlet temperature 2050°F.
2. Combustor inlet pressure 117.6 psia.
3. Combustor inlet temperature 787.5°F.
4. Air flow 2.06 lb/sec.
5. Torque on water brake approximately 268 ft-lb (Table B-6 and Figure B-5).

### D. Shutdown

1. Shut down by gradually decreasing air flow, pressure and fuel flow to the following conditions:

TABLE B-6. HORSEPOWER/TORQUE VALUES

% N (%)	Turbine Speed (rpm)	Shaft Speed Into the Waterbrake (rpm)	Turbine Horsepower (hp)	Accessory Horsepower (hp)	Shaft Horsepower at the Waterbrake (hp)	Torque at the Waterbrake (ft-lb)
100	75,684	13,515	702	13.5	688.5	268
90	68,115	12,163	340	10.9	329.1	142
80	60,547	10,811	204	8.6	195.4	95
70	52,978	9,460	114	6.6	107.4	60
60	45,410	8,108	66	4.9	61.1	40
50	37,842	6,757	35	3.4	31.6	25
40	30,273	5,405	17	2.2	14.8	14

NOTE:

Waterbrake Torque = 272.1 (HP Engine - HP Accessories) ; 2.94 x 10<sup>4</sup> (HP Engine - HP Accessories)  
 Engine Gear Ratio

Gear Ratio 5.6



AIR RESEARCH MANUFACTURING COMPANY OF ARIZONA  
A DIVISION OF THE ROBERTS CORPORATION  
PHOENIX, ARIZONA



## DEVELOPMENT TEST PROCEDURE

DT- 6127

- a) Turbine inlet temperature 1425°F.
  - b) Combustor inlet pressure 22 psia.
  - c) Air flow 0.4 lb/sec.
  - d) Reduce water brake torque per Figure B-6.
2. Decrease the combustor inlet temperature to 240°F then continue to decrease turbine exit temperature (tail pipe) to 1290°F.
  3. Shut down by first cutting off fuel flow, then 10 seconds later air flow.
- E. Repeat the startup/shutdown procedure if necessary to familiarize the test procedure.

### 4.3 Performance Demonstration

Upon completion of the initial fired run, the performance demonstration will be accomplished (100 percent speed). The seven performance points listed in Table B-7, which encompass 130°F, sea level day operating conditions from idle to 100 percent power in increments of 100°F turbine rotor inlet temperature, will be run. As also shown in Table B-7, each performance point will be derived by a specific turbine rotor speed, inlet air pressure and temperature, and turbine discharge temperature. After stabilization at each point, two data scans will be taken.

### 4.4 Thermindex Paint Test

Upon completion of the performance demonstration, the rig will be disassembled and inspected. Hardware condition will be noted and photographs taken. Thermindex paint will then be applied to the combustor, combustor baffle assembly, radial turbine nozzle assembly, radial turbine backshroud, and inter-stage duct/axial turbine stator. The rig will be reassembled



AIRESEARCH MANUFACTURING COMPANY OF ARIZONA  
A DIVISION OF THE GARRETT CORPORATION

TABLE B-7. INTEGRATED COMPONENTS ASSEMBLY PERFORMANCE DEMONSTRATION TEST POINTS

Parameters to be Set by Operator for Each Test Point					Calculated Operating Parameters For Each Test Point				
Point No.	Rotor RPM (×200)	Inlet Temp. (×10°F)	Inlet Press. (×1 psi)	Turbine Discharge Temp. (×10°F)	Radial Rotor Inlet Temp. (°F)	Inlet Airflow (lb/sec)	Fuel Flow (lb/hr)	Turbine HP	Reference Net HP
1	75,684	771	109.6	865	1500	2.23	85.5	526	13
2	75,684	774	111.8	927	1600	2.23	97.7	563	48
3	75,684	776	113.8	990	1700	2.22	109.9	598	82
4	75,684	780	115.6	1055	1800	2.21	122.0	631	114
5	75,684	783	117.0	1122	1900	2.19	133.8	660	144
6	75,684	786	118.3	1191	2000	2.17	145.4	688	173
7	75,684	788	118.8	1225	2050	2.16	151.0	700	186

NOTE: Values of parameters obtained from GTP305-2 engine cycle analysis computer program for  $130^{\circ}\text{F}$ , sea level day conditions.



AIRESEARCH MANUFACTURING COMPANY OF ARIZONA  
A DIVISION OF THE SARGENT CORPORATION  
PHOENIX, ARIZONA



## DEVELOPMENT TEST PROCEDURE

DT- 6127

and installed in the test cell. The rig will then be started and accelerated to 100 percent speed. The 100 percent power condition (Point 7, Table B-7) will be set up and the rig run at that condition for 10 minutes. The rig will then be shut down, removed from the test cell, and disassembled. Thermindex paint results will be analyzed and the hardware marked with isotherms and photographed.

TABLE B-8

[illegible]

# GTP305-2 FINAL DESIGN POINT CYCLE ANALYSIS

QUALIFICATION TEST LOG

E.W.O. No. 3409-246100-09-0101

Test Cell or Station No. C-116

Program GTP 305-2

Part No.

Serial No.

Development Engineer J. KIDWELL

Technician NERWOOD

Unit No. 1

Test Procedure No. INTEGRATED COMPONENTS ASSY, Rev. TEST \* 1

Date	Time	Event	Stamp
		12 DEC 78	
		CONTINUED WITH UNIT HOOKUP. INSTALLED OIL HEATER AT TANK & STARTED HEATING OIL. CONNECTED FUEL SYSTEM. CALIBRATED & INSTALLED GEAR BOX RUN-OUT PROBES WITH APPROXIMATELY 0.060" CLEARANCE BETWEEN SHAFT & PROBE. INSTALLED DISCHG. DUCT & SET UP FOR FIRST PRESS. CHECK.	
		CELL TIME 12.0 HRS.	
		TECH TIME 1 @ 12.0 HRS.	
		1 @ HRS.	
		SWINGER. TOOK 1ST PRESS. OK. SEL'S #38, #39, #41, #75, #208 + #211 ARE MISSING. SEL #75 IS A BAD PORT (REF. JUNG. B-16), SEL'S #135 THROUGH #139 OK. O.K. FIXED SEL'S #35, #49, #55, #59 + #148. TOOK 2ND PRESS OK. SEL'S #49 + #148 STILL BAD. ALSO #152 + #234 STILL PRESS LOW. FIXED PROBLEM WITH SEL #49. INST. NEW BEARS + HOSE ON SEL'S #148, #152 + #234. COULD NOT FIND ALCOHOL PUMP, SO PURGED WITH AIR. TOOK 3RD PRESS. OK. DIGITAL PROBLEMS, UNABLE TO GET PRESS. DATA PRINTED OUT.	
		2 TECHS, 8 HRS.	
		CELL 8 HRS.	
		13 DEC. 1978	
		CORRECTED MIX-UP ON STATIONARY SEAL PRESS. CONNECTIONS. ADDED PRESS. GAUGE IN WINDOW TO READ TURB. BEARING OIL IN PRESS. INSULATED TAIL PIPE & BORE COOLING AIR LINES. CHECKED & FOUND BORE COOLING AIR ORIFICE PLATE TO BE 1/2 X 0.375" WHICH WAS DESIRED SIZE. INSTALLED ORIFICE (RESTRICTOR) IN BORE COOLING AIR LINE.	
		TURNED ON AIR TO GEAR BOX & TURBINE.	

, QUALIFICATION TEST LOG			
E.W.O. No. 3409-246160-09-0601		Test Cell or Station No. C-116	
Program GTP 305-2	Part No.	Serial No. 1	
Development Engineer J. KIDWELL	Technician NORWOOD	Unit No. 1	
Test Procedure No. INTEGRATED COMPONENTS ASSY., Rev. TEST #1			
Date	Time	Event	Stamp
		13 DEC. 1978	
		FOUND WE HAD AN OIL LEAK AT REAR BEARING ASSY. REMOVED DISCHG. DUCT & FOUND PLUG HAD NOT BEEN INSTALLED IN DRILLED PASSAGE. WELDED OVER HOLE. FOUND ANOTHER OIL LEAK. SUSPECT LACK OF SCAV. POWER.	
		INSTALLED 8.071 X 3.00 IN. ORIFICE IN MAIN MEASURING SECTION.	
		SET OVERSPEED TO TRIP AT 20,000 RPM FOR OVERSPEED CHECK.	
		SWING - FABRICATED FUEL LINE TO BY-PASS FUEL CONTROL. INST. NEW UNIT FLOW METER & OIL LINES. PURGED BOTH FUEL & OIL LINES BEFORE INSTALLATION. CAPPED FUEL LINES NOT IN USE.	
		1 TECH. 6.5 HRS. CELL 6.5 HRS.	
		14 DEC. 1978	
		REPAIRED OIL LEAK IN TURB. BEAR BEARING OIL SYSTEM. CHECKED OUT WITH OIL. NO LEAKS.	
		INSTALLED DISCHG. DUCT. TURNED ON OIL SYSTEMS & PRESSURISED UNIT TO 30 PSIG. BLEW OIL OUT OF GEARBOX OUTPUT SHAFT. SHUT UNIT DOWN. INSTALLED GAUGE ON GEARBOX VENT & CONNECTED TURB. BEAR OIL SCAV. BACK TO GEARBOX. FOUND THERE WAS QUITE A BIT OF AIR LEAKING PAST TURB. BEAR BEARING.	
1130		STARTED ROTATION. ACCEL. TO 15,000 RPM. SHUT DOWN BY OVERSPEED TRIP. RESET OVERSPEED TO 50,000 RPM. SHUT DOWN AGAIN.	
1150		BY OVERSPEED. CONNECTED 2ND OVERSPEED TO 2ND SPEED PICKUP.	



## QUALIFICATION TEST LOG

E.W.O. No. 3409-246160-09-0601

Test Cell or Station No. C716

Program GTP 305-2

Part No.

Serial No. 1

Development Engineer J. KIDWELL

Technician NORIUDOD

Unit No. 1

Test Procedure No. 1 CA TEST

Rev. TEST #1

Date	Time	Event	Stamp
------	------	-------	-------

14 DEC. 1978

STARTED ROTATION - SHUT DOWN ON  
OVERSPEED. FOUND SPEED PICKUP GAIN A LITTLE1400 STARTED ROTATION - ACCELERATED TO 11,000  
RPM. TOOK TWO DATA SCANS. ACCELERATED TO  
(8) 28,000 RPM. GOT SHUT DOWN BY OVERSPEED.  
SECOND CRITICAL AT 26,000 RPM. KEAR

1408 ACCELEROMETER PEAKED AT 0.41 GILS.

SWITCHED TO #2 OVERSPEED SYSTEM. #1  
SYSTEM TRIPPING AT 28,000 RPM.1135 STARTED ROTATION. ACCELERATED TO 30,000  
RPM. RECORDED TWO SCANS. SLOWLY ACCELER-(50) ATED TO 40,000 RPM. LOST SPEED SIGNAL.  
DROPPED SPEED BACK & PICKED UP SPEED  
AGAIN. ADDED TORQUE TO 50 LB-FT. AT  
40,000 RPM. SET INLET TEMPERATURE TO 100%  
100% SPEED. RECORDED SCANS. CHANGED  
1525 UPPER LIMIT ON API 54 & UNIT SHUT DOWN(15) 1535 STARTED ROTATION. SLOWLY ACCELERATED  
1530 TO 46,000 RPM. SHUT DOWN BY OVERSPEEDSWING - REMOVED UNIT TAIL PIPE PER Eng.  
INSTRUCTIONS. OIL PRESENT IN TAIL PIPE &  
AROUND REAR BRG. COVER CLEANED OIL FROM  
STAND & CELL.TECH. 3 HRS.  
CELL 3 HRS.

15 DEC. 1978

DEV. ASSY. PERSON CHANGED GASKET UNDER  
OIL INLET TO REAR BEARING. CHECKED FOR  
OIL LEAKS O.K. REPLACED DISCHG. DUCT.PULLED SPEED PICKUP PROBES & CLEANED  
PROBES & HOLES IN THRUST PLATE. REINSTALL  
PROBES & SET THEM FOR 5 VOLT OUTPUT.1045 STARTED ROTATION & ACCELERATED TO  
30,000 RPM. 10:50 HRS. LAST DIGITAL SCAN.

11:37 RECORDED TWO SCANS.

QUALIFICATION TEST LOG

E.W.O. No. 3409-246160-09-0701 Test Cell or Station No. C-116  
 Program GTP 305-2 Part No. \_\_\_\_\_ Serial No. 1  
 Development Engineer J. KIDWELL Technician NORWOOD Unit No. 1  
 Test Procedure No. 1.C.A. TEST Rev. TEST #1

Date	Time	Event	Stamp
		15 DEC. 1978	
	1140	ACCELERATED TO 55,000 RPM. TURB. VIB. WENT TO 0.5 MILS. DECEL TO 52,000 RPM. STARTED TO RECORD TWO SCANS.	
	(3) 1145	GEARBOX REAR RUNOUT PROBE SIGNAL GETTING ERRATIC.	
	1145	SHUT DOWN TO CHECK OUT RUNOUT PROBE.	
		FOUND BAD MICRODOT CONNECTOR ON G.B. REAR RUNOUT PROBE. REPLACED CONNECTOR.	
	1300	STARTED ROTATION. ACCEL. TO 34,000 RPM. RECORDED TWO SCANS. ACCEL. TO 49,700 RPM & RECORDED TWO SCANS. ACCEL. TO 68,000 RPM & RECORDED TWO SCANS. ARMED OVERSPEED SHUTDOWN.	
	(80) 1300	RUNOUT ON REAR (TURBINE END) GEARBOX AT 1.1 MILS. ACCELERATED TO 70,000 RPM & RECORDED TWO SCANS. REDUCED SPEED TO INCREASE TORQUE. INCREASED TORQUE FROM 50 TO 120 LB.-FT. STARTED INCREASING INLET TEMP. TO GET MORE POWER. HAD REACHED 109 PSIA COMP. INLET PRESS. & 8.1 PRESS. RATIO.	
	1410	LOST REAR G.B. RUNOUT PROBE SIGNAL. STARTED SHUTTING DOWN.	
	1420	SHUT DOWN.	
		FOUND CABLE FROM AMPLIFIER BOX TO CELL PATCH PANEL SHORTED. MADE NEW CABLE & REROUTED BOTH CABLES.	
	1515	STARTED ROTATION & ACCEL. TO 60,000 RPM. RUNOUT ON G.B. REAR (TURB.) AT 1.3 MILS. & ON FRONT AT 0.9 MILS. RECORDED TWO SCANS.	
	(32) 1515	SLOWLY SHUT DOWN.	
		TECH TIME: 2 @ 8.0 HRS.	
		CELL TIME: 8.0 HRS.	
		ENERGY: 2064.4 HR.	

## QUALIFICATION TEST LOG

E.W.O. No. 3909-246160-09-0601

Test Cell or Station No. C-116

Program GTP 305-2

Part No.

Serial No. 1

Development Engineer J. KIDWELL

Technician NORWOOD

Unit No. 1

Test Procedure No. I.C.A. TEST

Rev. TEST #1

Date Time

Event

Stamp

18 DEC. 1974

PULLED TAILPIPE & REMOVED TURB. REAR BEARING OIL TRANSFER HOUSING TO BE REWORKED.

REMOVED COVER ON GEARBOX FOR GEAR INSPECTION. CHECKED & FOUND END PLAY AT TURB. TO GEARBOX QUILL SHAFT.

REPLUMBED CONTROL AIR FOR BUFFER AIR & ALSO FOR AIR ASSIST NOZZLES.

INSTALLED FLOWMETER S/N FM 379 TO MEASURE LOW FUEL FLOW. NEED TO HAVE 24 V. POWER SOURCE BEHIND SOUTH CONTROL PANEL.

CONNECTED BUFFER AIR MANIFOLD PRESS. TO LG 3884 ON NORTH PANEL.

TECH TIME 208.0 HRS.  
CELL TIME 8.0 HRS.

REWORKED REAR BEARING ASSEMBLY TO STOP OIL LEAKS. INSTALLED EMISSION PROBES & MANIFOLD ON DISCHG. DUCT. LOST TURB. REAR BEARING IS IN THE REWORK. CONNECTED TURB. REAR BRNG. SLAV. TO SEPARATE OIL SLAV. PUMP. CHECKED HOOKUP TO GEARBOX & FOUND TO BE CORRECT.

20 DEC. 1440 STARTED ROTATION. ACCELERATED TO 15,000; 33,500; 46,000; 56,000 RPM. INCREASED TORQUE LOAD & LOST TORQUE READOUT. (40) DECEL. TO 35,000 RPM & ~~WET~~ CHECKED CABLES. O.K. ACCELERATED TO 56,000 RPM. LOAD STILL FLUCTUATING.

1520 SHUT DOWN.

FOUND LOAD CELL CABLE TO BE WET. SENT LOAD CELL TO RECORDING FOR REPAIR.

CELL TIME 8.0 HRS.

TECH TIME 208.0 HRS.

ENERGY 25.2 K. AIR.

QUALIFICATION TEST LOG

E.W.O. No. 2409-246160-09-0601

Test Cell or Station No. C-116

Program GTP 305-2

Part No.

Serial No. 1

Development Engineer J. KIDWELL

Technician NORWOOD

Unit No. 1

Test Procedure No. I.C.P. TEST

Rev. TEST #1

Date Time

Event

Stamp

21 DEC. 1978

REPAIRED LOAD CELL ELECTRICAL CONNECTION. PUT TEFLON TAPE ON THREADS OF OIL SCRV. TUBE OUT OF REAR TURB. BRNG.

0950 STARTED ROTATION. ACCELERATED TO 48,300 RPM & RECORDED TWO SCANS.

(55) INCREASED LOAD TO INCREASE PRESS. RATIO. TOOK TWO SCANS AT 6.1 PRT-DE AT 100% CORRECTED SPEEDS.

1045 SHUT DOWN FOR LACK OF AIR.

REINSTALLED WATER BRAKE WATER DISCHARGE VALVE & CHECKED OUT WATER BRAKE WATER IN PRESS. GAUGE.

1125 STARTED ROTATION. SLOWLY ACCEL. TO 71,000 RPM. GEARBOX AFT. & TURB.

(65) REAR BRNG. VIBRATION HIGH. DECEL. TO 40,000 & DECREASED TORQUE. ACCEL. TO 67,000 RPM. VIBRATION WORSE ON 1230 GEARBOX. TOOK SCANS & SHUT DOWN.

CHECKED OUT & REPAIRED BEARING & LEADS. REPOSITIONED LOAD CELL.

CELL TIME 8.0 HRS.

TECH TIME 2 @ 8.0 HRS.

ENERGY 160 U. AIR.

22 DEC. 1978

1000 STARTED ROTATION. SLOWLY ACCEL. TO 90% SPEED AT 7.0:1 PRESS. RATIO.

1036 RECORDED SCANS AT 90% SPEED 7.0:1 P.R.

1054 100% 7.0:1

1100 110% 7.0:1

(100) 1117 110% SPEED 8.0:1 P.R.

1122 100% 8.0:1

1136 95.7% 8.0:1

COULD NOT LOAD WATER BRAKE ENOUGH TO SLOW SPEED DOWN TO 90%.

1140 SHUT DOWN.

## QUALIFICATION TEST LOG

E.W.O. No. 3409-246160-09-0601 Test Cell or Station No. C-116  
 Program GTP 305-2 Part No. Serial No. 1  
 Development Engineer J. KIDWELL Technician NORWOOD Unit No. 1  
 Test Procedure No. 1, C.A. TEST Rev. TEST #1

Date Time Event Stamp

1305 STARTED ROTATION. SLOWLY ACCEL. TO  
 100% SPEED AT 9.0:1 PRESS. RATIO.  
 (65) 1342 RECORDED RANS AT 100% SPEED 9.0:1 P.R.  
 1403 110% 90:1  
 1410 SHUT DOWN. TEST COMPLETE.  
 CELL TIME: 6.2 HRS.  
 TECH TIME: 2 @ 8.0 HRS.  
 ENERGY 396 U.AIR.

2 JAN. 1979

INSTALLED NEW COVER PLATE OVER  
 TURBINE REAR BEARING ASSY. PUT DRAIN  
 GLTS IN TUBE SEAL COVER TO DRAIN OIL  
 FROM REAR BEARING SUPPORT.

MOUNTED SECOND ACCELEROMETER  
 ON TURB. REAR END. NOW READS OUT  
 ON METER SIN VIB 11 ON SWITCH POSITION  
 #2. GEARBOX ACCELEROMETER READS ON  
 SWITCH POSITION #1.

1500 STARTED ROTATION. SLOWLY ACCELERATED  
 (15) TO 40,000 RPM. NEW ACCEL. READING OVER  
 1.5 MILS VIBRATION. SHUT DOWN TO CHECK  
 1515 OUT SYSTEM.

3 JAN. 1979

CHECKED OUT ACCELEROMETER - O.K.  
 CHANGED TO JET A FUEL. NO J.P. 4.  
 PURGED FUEL SYSTEM. HOOKED FUEL  
 SYSTEM TO UNIT. CHECKED OUT IGNITER  
 O.K.

1055 STARTED ROTATION. SLOWLY ACCEL. TO  
 35,000. TRIED TO DECREASE TORQUE WITH  
 LITTLE RESPONSE. BEGAN ACCELERATING &  
 TORQUE DROPPED OFF. SPEED WENT TO 55,000  
 RPM. ADDED MORE TORQUE. STARTED TO  
 ACCELERATE AGAIN & REACHED 65,000  
 RPM. TORQUE DROPPED FROM 88 TO 40 LB-FT.  
 TURBINE SPEED WENT TO 74,000 RPM.

# QUALIFICATION TEST LOG

E.W.O. No. 3409-246160-09-0601

Test Cell or Station No. C-116

Program

Part No.

Serial No. 1

Development Engineer L. KIDWELL

Technician NORMWOOD

Unit No. 1

Test Procedure No. I.C. A. TEST.

Rev. TEST #1

Date Time

Event

Stamp

3 JAN. 79 BACKED OFF ON AIR PRESS. TO DECREASE SPEED. GEARBOX RUNNOUT WENT FROM ONE TO TWO MILS. TURB FRONT VIB. DECREASED SLIGHTLY & REAR VIB. WENT FROM 0.45 MILS TO 0.6 MILS.  
1130 SHUT DOWN.

4 JAN. 1979

0930 STARTED ROTATION. ACCELERATED TO 30,000 RPM & SET TORQUE TO 14 FT. LBS. DROPPED AIR FLOW TO 0.41 #/SEC. SET AIR ASSIST PRESS. TO 5 PSIG ABOVE COMPRESSOR EXIT PRESS. SET FUEL FLOW TO 28 #/HR. RECORDED TWO SCANS.

TRIED 40 - GOOD. TPT STABILIZED AT ABOUT 1300 °F. COULD NOT LOWER FUEL FLOW BELOW 28 #/HR.

TORQUE AT 13 FT LBS., AIR FLOW AT 0.409 #/SEC NET, SPEED 25,000 RPM. TURB. SPEED STARTED DRIPPING. TURB. FRONT VIB. EXCEEDED 1.5 MILS. DURING THIS TIME THRUST PISTON PRESS. DROPPED OFF.  
1038 SHUT DOWN WITHOUT COOLING OFF.

AFTER SHUT DOWN TRIED TO ROLL UNIT OVER TO COOL DOWN. UNIT WOULD NOT ROTATE WITH 5 PSIG INLET PRESS. PULLED UNIT & DELIVERED TO DEV. ASSY.

TECH TIME: 2 @ 8.0 HRS.

CELL TIME: 8.0 HRS.

ENERGY: 24.5 U. AIR.

0.3 U. FUEL.

## QUALIFICATION TEST LOG

E.W.O. No. 3409-246160-09-0601

Test Cell or Station No. C-116

Program

Part No. 6TP305-2

Serial No.

Development Engineer JON TEETS

Technician NORWOOD

Unit No.

Test Procedure No. INTEGRATED COMPONENTS ASSY Rev. TEST #2

Date

Time

Event

Stamp

14 MARCH, 1979  
12:30. RECEIVED UNIT FROM DEV. ASSY. CHECKED  
QUILL SHAFT END PLAY. FOUND THERE  
WAS ONLY 0.030" END PLAY. CHECKED  
AND FOUND TURB. SHAFT END TO BE IN  
THE CORRECT POSITION RELATIVE TO THE  
TURB. MOUNTING FLANGE.

15 MARCH, 1979  
PULLED COVER FROM GEAR BOX. GEARS  
ARE IN THE CORRECT POSITION WITH BULL  
GEAR AGAINST THRUST BEARING. PINION  
BEARING SHAFT END SHOULD BE 0.54" BEYOND  
GEAR BOX OUTSIDE SURFACE PER PRINT.  
MEASURED DISTANCE IS 0.90". ENGINEER  
ORDERED 0.070" SHIM TO BE MADE.

INSTALLED UNIT ON STAND TO BEGIN  
INSTRUMENTATION HOOKUP. QUILL SHAFT  
END PLAY WITHOUT SHIM 0.030".

16 MARCH, 1979  
BEGAN HOOKING UP INSTRUMENTATION.  
INSTALLED 0.03 TO 0.3 GPM FLOW METER  
5/11 379 IN SYSTEM & PURGED FUEL SYSTEM.  
~~BEARING FLANGE~~

17 MARCH, 1979  
CONTINUED WITH INSTRUMENTATION HOOKUP.  
CONNECTED REF. PRESS. TO S.V. #3.  
INSTALLED 0.091" SHIM BETWEEN TURB MOUNT-  
ING FLANGE & GEAR BOX. QUILL SHAFT END  
PLAY NO 0.121".

MOVED DISCHG. VALVE ACTUATOR SO THAT  
DISCHG. VALVE CAN BE CLOSED FOR PRESS.  
CHECK.

19 MARCH, 1979  
COMPLETED INSTRUMENTATION HOOKUP.  
PUT FITTING IN BUFFER AIR TUBE TO READ  
BUFFER AIR PRESS. CONNECTED TO GAGE #47.  
REPAIRED TYRO PRESS. TAP TUBES, TOOK PRESS.  
CHECK SCAN AT 25 PSIG.

# QUALIFICATION TEST LOG

E.W.O. No. 3407-246160-09-0601

Test Cell or Station No. C-116

Program

Part No. GTP 305-2

Serial No.

Development Engineer JON TEETS

Technician NORWOOD

Unit No.

Test Procedure No. INTEGRATED COMPONENTS ASSY TESTING

TEST #2

Date

Time

Event

Stamp

19 MARCH, 1979

1530 STARTED SLOW ROLL. REAR VIB. ON UNIT UP TO 0.4 MILLS AT 4000 RPM. DROPPED SPEED & ACCELERATED AGAIN UP TO 10,000 RPM. VIB. LOOKS GOOD. SLOWLY ACCELERATED TO 25,000 RPM. RECORDED 1555 TWO SCANS. SHUT DOWN.

20 MARCH, 1979

INSTALLED GASKET IN BOTTOM AIR INLET LINE. PRESSURE CHECKED - O.K. MOVED ACTUATOR ARM TO GET DISCHG. VALVE FULL OPEN.

INSTALLED ANADIX COUNTER FOR SPEED ON NORTH PANEL.

1058 STARTED ROTATION. SLOWLY ACCELERATED TO 50,000 RPM. FRONT BEARING VIB. PICKUP SHOWING FROM 0.5 TO 0.8 MILLS FROM 35,000 RPM UP TO 50,000 RPM. ABOVE 50,000 RPM VIB. GOES ABOVE 1200 I.D. MILLS. SHUT DOWN.

BEGAN CHECKING OUT TROUBLES FOUND ON DIGITAL DATA.

CELL TIME 8.0 HRS.

TECH TIME 10.8 HRS.

ENERGY 110 V. AIR.

21 MARCH, 1979

MOVED VIBRATION PICKUP FROM AFT 10 O'CLOCK TO HORIZONTAL POSITION ON FRONT OF TURBINE. INSTALLED BAEFFELS TO BLOCK THRUST POSITION AIR FROM PICKUPS. STRAIGHTENED OUT THRUST PISTON PRESSURES.

1243 STARTED ROTATION. BOTH OVERSPEED SYSTEMS TRIPPED AT LESS THAN 25,000 RPM. RESTARTED & OVERSPEED TRIPPED AGAIN.

1258. SHUT DOWN TO CLEAN PROBES.



## QUALIFICATION TEST LOG

E.W.O. No. 3409-246160-09-0601

Test Cell or Station No. C-116

Program

Part No. GTP 305-2

Serial No.

Development Engineer JON TEETS

Technician NORWOOD

Unit No.

Test Procedure No.

I.C.A.

Rev.

TEST #2

Date	Time	Event	Stamp
21 MAR 79		REMOVED SPEED PICKUP PROBES & CLEANED PROBES & FACE OF THRUST PISTON. REINSTALLED PROBES. SET PICKUPS AT APPROX 0.025" CLEARANCE.	
	1415	STARTED ROTATION. SLOWLY ACCELERATED TO 30,000 RPM. ENGINEER CHECKING VIBRATION BY FEEL. ACCELERATED TO 40,000 RPM. VIBRATION WENT TO 1.0 MILS	
	(59)	ON BOTH HORIZONTAL & VERTICAL PICKUPS. BACKED DOWN IN SPEED TO 35,000 RPM. ENGINEER CHECKING AGAIN.	
		VERTICAL VIB. PICKUP GONE DEAD.	
	1512	SHUT DOWN TO INVESTIGATE.	
		PICKUP STILL SECURE. CABLING FROM PICKUP TO BOOM GOOD.	
		ASKED LEE SCHMIDT FOR ADVICE ABOUT VIB. PROBLEMS.	
	1543	STARTED ROTATION & ACCELERATED TO 35,000 & THEN TO 40,000 RPM WITH VIBRATION MEASERS READING VELOCITY.	
	(12)	VELOCITY INCREASED FROM 0.4 IPS. TO 0.7 IPS. WHICH WAS EXCESSIVE.	
	1555	SHUT DOWN.	

CELL TIME 8.0 HRS.  
 TECH TIME 1 @ 8.0 HRS.  
 ENERGY 126 U. AIR.

22 MARCH, 1979

REMOVED WATER COOLING SPOOL & TURB. DISCHG. DUCT. PULLED TURB. FROM GEARBOX & REMOVED QUILL SHAFT. REINSTALLED TURBINE ON GEARBOX WITHOUT DISCHG. DUCT.

1030 STARTED ROTATION. ACCELERATED TO 32,000 RPM. FRONT VIB INCREASED TO 0.6 MILS.

(10) OR 0.7 IPS. ~~VELOCITY~~ VELOCITY. SHUT DOWN.

PULLED UNIT & DELIVERED TO DEV. ASSY.

# QUALIFICATION TEST LOG

E.W.O. No. 3409-246160-09-0601

Test Cell or Station No. C-116

Program

Part No. GTP 305-2

Serial No. 1

Development Engineer JON TEETS

Technician NORWOOD

Unit No.

Test Procedure No. INTEGRATED COMPONENTS ASST, Rev. TEST #2

Date

Time

Event

Stamp

INSTALLED GEARBOX HUB #3 ON PINION SHAFT.

CHECKED QUILL SHAFT END PLAY. DISTANCE FROM GEARBOX MOUNTING FACE TO INSIDE END OF QUILL SHAFT IS ~~0.34~~ 0.34". DISTANCE FROM TURB MOUNTING FACE TO END OF TURB SHAFT IS 0.31". THIS CAUSES AN INTERFERENCE OF 0.03". INSTALLED 0.092" SHIM BETWEEN GEARBOX & TURBINE TO GIVE A QUILL SHAFT END PLAY OF 0.062". TURB. TIEBOLT PROTRUDES TOO FAR CAUSING INTERFERENCE.

INSTALLED TURB. ON STAND. HOOKED UP MINIMAL INSTRUMENTATION FOR MECH. CHECK.

INSTALLED SPEED PICKUPS SIN 257821 SET AT 9.9 VOLTS = 0.024". SIN 295581 SET AT 10.0 VOLTS = 0.025".

1455 STARTED ROTATION. ACCELERATED TO 30,000 RPM. VIB. GOOD. GEARBOX DISPLACEMENT PROBES NOT WORKING. SHUT DOWN.

CONNECTED LEADS TO DISPLACEMENT BOX IN CELL.

1510 STARTED ROTATION. G.B. DISP. READING OK. ACCELERATED TO 50,000 RPM. TURB. FRONT VIB. READING 0.8 MILS DISPLACEMENT, 0.8 IN./SEC. VELOCITY & 1.2 G'S ACCELERATION. 1520 SHUT DOWN.

DECREASED TURB. OIL PRESS. FROM 60 PSIG TO 45 PSIG.

1530 STARTED ROTATION. ACCELERATED TO 55,000 RPM. VIBRATION STILL HIGH IN FRONT BRG. 1540 0.7 MILS 1.5 IPS. & 2.0 G'S. SHUT DOWN.

1555 STARTED ROTATION WITH WATER BRAKE ROAD. ACCEL. TO 30,000 WITH TOO MUCH LOAD. DECEL. & DECREASED LOAD. ACCEL. TO 55,000 RPM. VIBRATION DOWN BUT STILL HIGH. SPEED WENT TO 58,000 RPM BECAUSE WATER 1605 BRAKE UNLOADED SOME. SHUT DOWN.

CELL TIME 8.0 HRS.

TECH TIME 2 @ 8.0 HRS.

ENERGY

430

## QUALIFICATION TEST LOG

E.W.O. No. 3409-246160-02-0601

Test Cell or Station No. C-116

Program

Part No. GTP 305-2

Serial No.

Development Engineer JON TEETS

Technician NORWOOD

Unit No.

Test Procedure No. 1CA

Rev. TEST 2

Date Time

Event

Stamp

28 MARCH, 77

HOOKED UP DIGITAL RECORDING EQUIPMENT FOR MORE MECHANICAL CHECKOUT. INSTALLED BURST SHIELD & TAIL PIPE ASSY.

DIGITAL TOOK OFF-CAL.

1450 STARTED ROTATION, SLOWLY ACCELERATED TO MAX SPEED OF 70,000 RPM. FRONT BEARING ACCELEROMETER READING 40 G'S. VIB. REAR BEARING AT 20 G'S. OVERSPEED TRIPPED & SHUT UNIT DOWN. TRIED SEVERAL TIMES TO RESTART & GOT SHUT DOWN.

CELL TIME 8.0 HRS.

TECH TIME 208.0 HRS.

ENERGY 60 U. AIR.

29 MARCH, 1977

INSTALLED CHECK VALVE IN AIR LINE INTO WATER BRAKE.

INSTALLED FLOW METER FM 378 IN LOW FLOW FUEL LINE & CHECKED OUT. INSTALLED FUEL MANIFOLDS. HAD AIR ASSIST MANIFOLD MADE INTO TWO PIECES TO INSTALL WITHOUT REMOVING TAIL PIPE. INSTALLED AIR ASSIST MANIFOLD & HOOKED UP AIR SUPPLY.

CONNECTED REMAINING INSTRUMENTATION. NOZZLE SKIN TEMP. IS NOT TERMINATED & NOT HOOKED UP.

FOUND & CORRECTED PROBLEM WITH MAIN AIR FLOW CALCULATION.

CONNECTED TWO MORE PARAMETERS TO SANDEN.

CELL TIME 7.2 HRS.

TECH TIME 167.2 HRS.

30 MARCH, 1977

CONNECTED FUEL LINE TO UNIT. INSTALLED TOP OF BURST SHIELD. INSTALLED PPR. & IN TAIL PIPE FOR PART OF OVERTEMP SHUTDOWN SYSTEM.

# QUALIFICATION TEST LOG

E.W.O. No. 3427-246160-07-0601

Test Cell or Station No. C-116

## Program

Part No. GTP 305-2

Serial No.

Development Engineer Jon Teets

Technician NORWOOD

Unit No. 1

Test Procedure No. 1.C.A.

Rev. TEST #2

Date Time

## Event

Stamp

30 MARCH 1979

0925 STARTED ROTATION. SET UP 30,000 RPM &  
22 14 LB.-FT TORQUE. RECORDED TWO SCANS.

2947 SHUT DOWN ON OVERFEED. SPEED PICKUP;  
PEPPERS NEED TO BE CLEANED

CLEANED PICKUPS & PISTON FILE WITH FREON  
& REINSTALLED PROPS.

1045 STARTED ROTATION. LOST <sup>2</sup>/SPEED PICKUP.

SWITCHED TO N<sup>o</sup> 2 SYSTEM. ACCELERATED TO 30,000 RPM TO CHECK TORQUE. DROPPED SPEED TO LIGHT-OFF CONDITIONS & STARTED TO SET FUEL FLOW. OVERSPEED SHUT DOWN TWICE.

1122 D. 200.

HAZ INSTRUMENTATION TECH. PUT SCOPE ON  
SPEED PICKUP SIGNAL.

11" STARTED ROTATION. SIGNAL LOOKS GOOD.

ACCELERATED TO 30, CORRESPONDING BACK DOWN  
T. TO 200 RPM. OVERSPEED TRIPPED OUT.

HELD OVERPOLD RESET & ATTEMPTED LIGHT OFF. FOR LIGHT SHUT OFF FULL SPEED

SIGNAL VERY HASHY AT TIMES. THE REST OF THE TIME SIGNAL IS GOOD.

114" SHOT DOWN TO CLEAN PROBES

FOUND PROBE #1 HAD BEEN RUBBED &  
PROBE #2 LOOKED BAD. INSTALLED TWO NEW  
PROBES & SET THEM AT APPROX 0.030".

14. STARTED ROTATION. H. ACCELERATED TO 3000 RPM TO CHECK TORQUE SETTING.

DROPPED SPEED TO 10,000 RPM FOR LIGHT-OFF  
NO GOOD. FUEL FLOW 3.5 LBS/HR. ACCELER-

AGED TO 30,000 RPM WITH TAIL PIPE TEMP.  
AT APPROX 1500°F. RAN FOR 1 1/2 MIN. C

SHUT DOWN FUEL FLOW. CONTINUED RPM  
TO COOL DOWNTAIL PIPE.

1530 SHUT DOWN.

CELL TIME 2.0 HRS

TECH TIME @ 5.6 HRS.

ENERGY 32.44 M.R.  
20.44 FUEL.

QUALIFICATION TEST LOG

E.W.O. No. 3424-246160-07-0601

Test Cell or Station No. C-116

Program

Part No. GTP 315-2

Serial No. 1

Development Engineer JON TEETS

Technician NORWOOD

Unit No.

Test Procedure No. 1. G.A.

Rev. TEST #2

Date Time Event Stamp

APRIL

REMOVED TAIL PIPE. CHECKED CLEARANCE BETWEEN REAR FALG OF WHEEL & REAR BEARING HOUSING. NO APPARENT CHANGE. ALSO CHECKED WHEEL TIP CLEARANCE. NO CHANGE HERE EITHER. REINSTALLED TAIL PIPE.

1215 STARTED ROTATION. SLOWLY ACCELERATED TO 45000 RPM. ADJUSTED TORQUE TO 70 LB-FT. SHUT DOWN DUE TO LACK OF AIR.

1221 STARTED ROTATION. ACCELERATED TO 45000 RPM. CHECKED TORQUE VALUE & RECORDED TWO RUNS. DECELERATED TO LIGHT-OFF CONDITIONS. TRIED TO GET LIGHT-OFF ONCE. MAIN FUEL VALVE OUTSIDE CLOSED. SHUT DOWN FUEL FLOW. TURNED ON FUEL VALVE. TRIED SEVERAL TIMES TO GET LIGHT-OFF. NONE. SHUT DOWN TO CHECK.

1400 IGNITER.

REPLACED IGNITER & RECHARGED FUEL SYSTEM.

1411 STARTED ROTATION.

1440 STARTED ROTATION.

1442 W/O VIBROTH & GAGE. SLOWLY ACCEL. TO 45000 RPM. VIB. ON FRONT BENE EXCEEDED 8 G'S. BACKED SPEED DOWN TO 42500 RPM.

1447 FRONT VIB. @ 8 G'S. KNEW AT THAT SPEED FOR 10 MIN. RECORDED DATA. COOLED UNIT 1540 LBS & SHUT DOWN.

CELL TIME 8.0 HRS.

TECH TIME 1 @ 8.0 HRS

1 @ 3.5 HRS.

ENERGY 51 U. AIR

.4 U. FUEL

2 APRIL, 1979

PULLED UNIT FROM STAND. CHECKED QUILL SHAFT END PLAY. FOUND 0.03" INTERFERANCE BETWEEN TURB. TIE BOLT END & QUILL SHAFT END WITHOUT SHIM. THIS IS SAME AS WHEN UNIT WAS INSTALLED.

QUALIFICATION TEST LOG			
E.W.O. No. 2409-246/60-09-D601		Test Cell or Station No. C-116	
Program		Part No. GTP305-2	Serial No. 1
Development Engineer JON TEETS		Technician NORWOOD	Unit No.
Test Procedure No. INTEGRATED COMPONENTS ASSY TEST, Rev. TEST # 3			
Date	Time	Event	Stamp
2 MAY, 1977		RECEIVED TURBINE FROM DEV. ASSY. HAD TWO BENTLY SPEED PICKUP PROBES & ONE AXIAL MOVEMENT BENTLY PROBE CHECKED FOR CLEARANCE VS VOLTAGE. SET ALL THREE PROBES FOR APPROX. 0.030" CLEARANCE. CHECKED QUILL SHAFT END PLAY. TURB. SHAFT IS BEHIND MOUNTING FLANGE 0.360". GEARBOX SHAFT BEYOND FLANGE - 0.332". QUILL SHAFT FLOAT WITHOUT SHIM 0.025". SHIM THICKNESS 0.090". TOTAL QUILL SHAFT END PLAY 0.118".  MOUNTED UNIT ON STAND WITH INDEX MARKS ON QUILL SHAFT & TURB. LINED UP.  CELL TIME 6.5 HRS. TECH TIME 158.0 HRS.  2 MAY 77, SWING SHIFT:  CONTINUED TEST SET-UP.  CELL TIME - 8.0 HRS. TECH TIME - 2 X 8.0 HRS.  3 MAY, 1977 INSTALLED DISCHG. SECTIONS & COMPLETED IN FLAMMENTATION HOOK-UP. INSTALLED VOLUME BOOSTER REGULATOR FOR AIR ASSIST NOZZ. TOOK TWO PRESS. CHECKS SCANS. FOUND 2 REPAIRED TWO LEAKS. CHECKED OIL SLAV. FLOW - O.K. HOOKED UP AXIAL DISPLACEMENT PROBE & CHECKED OUT. CELL TIME 8.0 HRS. TECH TIME 2 X 8.0 HRS. 3 MAY 77 SWING SHIFT: CONT. SET-UP. CELL TIME - 4.0 HRS, TECH TIME - 2 X 4.0 HRS.	

## QUALIFICATION TEST LOG

E.W.O. No. 3401-246160-09-1601

Test Cell or Station No. C-116

Program

Part No. GTP 305

Serial No. 1

Development Engineer JON TEETS

Technician NORWOOD

Unit No.

Test Procedure No. I.C.A. TEST

Rev. TEST # 3

Date	Time	Event	Stamp
------	------	-------	-------

4 MAY, 1979

(5) 0945 STARTED ROTATION. NOT GETTING GEARBOX RUNOUT. SHUT DOWN TO GET 0950 VIBRATING.

CONNECTED CABLES TO POWER SUPPLY BOX  
1015 STARTED ROTATION. CANT GET HOT AIR SUPPLY VALVE OPEN. RAN UNIT UP TO 50,000 ON COLD AIR. TOOK RECORDINGS AT 30,000, 40,000, & 50,000 RPM WITH COLD AIR ONLY. SHUT DOWN TO GET 1040, VALVE FIXED.

REPAIRED HOT LINE SUPPLY VALVE.  
1300 STARTED ROTATION. SLOWLY KEPT ACCELERATING & RECORDING DATA AT 10,000 RPM INCREMENTS. REACHED 73,500 RPM. TURB. BEARING ALARMS. SOUNDING. DID NOT RECORD DATA AT THIS POINT. ~~STOP~~ I DROPPED SPEED & TRIED LIGHT OFF. HAD TO INCREASE FLOW TO ABOUT 15% TO GET LIGHT OFF. SET UP 10% POINT & RAN ABOUT 15 MIN. 1405 SHUT DOWN.

TECH TIME: 3.0 HRS.  
CELL TIME 8.0 HRS.  
ENERGY: 135 U. AIR.

7 MAY, 1979

INCREASED TURB OIL PRESS TO 58 PSIG FROM 42 PSIG. BLEW OUT WATER BRAKE WATER PRESS. NINE. DIGITAL WORKED ON TORQUE READOUT.

(5) 1100 STARTED ROTATION. SLOWLY ACCELERATED TO 55,000 RPM. FRONT BEARING TEMP. WENT FROM 200°F TO 300°F WITH SPEED GOING FROM 50,000 TO 55,000 RPM. BACKED DOWN IN SPEED & STARTED COOLING 1155 UNIT OFF. SHUT DOWN.

SET OIL PRESS BACK DOWN TO 42 PSIG.

## QUALIFICATION TEST LOG

E.W.O. No. 3409-246160-09-0601

Test Cell or Station No. C-116

Program

Part No. GTP 305-2

Serial No. 1

Development Engineer JAY TETS

Technician NORWOOD

Unit No. 1

Test Procedure No. LCA

Rev. TEST # 3

Date	Time	Event	Stamp
------	------	-------	-------

1		7 MAY, 1979	
1305		STARTED ROTATION. SLOWLY ACCELERATED TO 60,000 RPM AT INLET TEMP OF 300°F	
(40)		OIL PRESS @ 41 PSI. FORWARD BEARING @ 275°F. REAR BEARING @ 275°F. RUNNING AT 35-40 G. 1700 RPM REAR ACCEL @ 45 G'S. BACKED UNIT DOWN & STARTED COOLING UNIT.	
		PULLED UNIT TO DELIVER TO DEV. ASSY.	

CELL TIME 8.0 HRS.

TECH TIME 5.0 HRS.

ENERGY 120 U. HR.

9 MAY 1979

INSTALLED GEARBOX SPLINE S/N 4 IN PLACE OF SPLINE S/N 3.

10 MAY 79, SWING SHIFT:

MOUNTED UNIT @ GEARBOX, SET-UP IN WORK.

CELL TIME: 8.0 HRS.

TECH TIME: 8.0 HRS X 2

11 MAY, 1979

COMPLETED INSTRUMENTATION HOOKUP. CHECKED OUT SPEED & AXIAL DISPLACEMENT PROBES. ALL O.K. CHECKED FRONT & REAR OIL SCAV FLOW. BOTH GOOD. INSTALLED NEW OIL FILTERS IN UNIT OIL LINE. CHECKED OUT ALL AUX. AIR SUPPLY SYSTEMS. HAD TWO F'S REPAIRED & HOOKED UP. MADE PRESS CHECK ON UNIT. FOUND TWO PRESS LINES NOT CONNECTED. NUMBER BURNED OFF. CONNECTED TO S.V. AT RANDOM. MADE SLOW ROLL & RECORDED SCAM.



QUALIFICATION TEST LOG

E.W.O. No. 3907-246160-09-0601

Test Cell or Station No. C 716

Program

Part No. GTP305-2

Serial No. 1

Development Engineer JAN TEETS

Technician NORMAN

Unit No. 1

Test Procedure No. J.C.A. TESTING

Rev. TEST #3

Date

Time

Event

Stamp

14 MAY, 1975

CHECKED OUT ACCELEROMETERS. ALL OK.  
ON PORTABLE VIB. TABLE.

TRIED SLOW ROLL TO 14,000 RPM. BALL  
BEARING IN FRONT OF TURB. WARMS UP  
FROM 90°F TO 130°F. VARIED THRUST  
PISTON PRESS FROM 0 TO 22 PSIG. BEARING  
TEMP. DOES NOT VARY MORE THAN 3°F.

BEFORE UNIT WAS INSTALLED ON STAND  
THE QUILL SHAFT END PLAY WAS CHECKED.  
TURB. END SHAFT IS BEHIND MTG FLANGE 0.330"  
~~SEE~~ QUILL SHAFT EXTENDS BEYOND FLANGE 0.322"  
QUILL SHAFT END PLAY W/O SHIM = 0.008"  
SHIM THICKNESS = 0.090"

QUILL SHAFT END PLAY W/ SHIM = 0.098"

1.00 STARTED SLOW ROLL. SLOWLY ACCELERATED  
TO 40,000 RECORDED TWO SCANS. ACCELERATED  
TO 40,000 RPM & RECORDED TWO SCANS.

ACCEL TO 20,000 RPM. BALL BEARING TEMP.  
ALARM SOUNDED. BACKED DOWN IN SPEED &  
SLOWLY ACCEL TO 30,000 RPM. RECORDED  
TWO SCANS WITH TEMP. ALARM SET 5°F  
1600 HIGHER WITHOUT SOUNDING. SHUT DOWN.

CELL TIME 5.0 HRS.

TECH TIME 3.0 HRS.

15 MAY, 1979

INCREASED UNIT OIL PRESS. TO 60 PSIG  
0925 STARTED ROTATION. VARIED BALANCE PISTON  
AIR PRESS TO CHECK EFFECT OF THRUST LOAD  
ON FORWARD THRUST BEARING TEMP. BY

1.00 VARYING BALANCE PISTON AIR PRESS. THE  
BEARING TEMP. CAN BE DECREASED.

TRIED TO INJECT AIR INTO WATER PRAE  
WATER LINE. CHECK VALVE STUCK CLOSED.  
1020 SHUT DOWN.

INSTALLED NEW CHECK VALVE.

# QUALIFICATION TEST LOG

E.W.O. No. 3409-246160-09-0601		Test Cell or Station No. C-116	
Program	Part No. GTP 305-2	Serial No. 1	
Development Engineer JON TEETS	Technician NORWOOD	Unit No. 1	
Test Procedure No. I.C.A. TESTING		Rev. TEST #3	
Date	Time	Event	Stamp
		15 MAY, 1979	
	1030	STARTED ROTATION. VARIED TORQUE LOAD TO TRY TO STABILIZE TORQUE. SLOWLY ACCELERATED TO 70,000 RPM. (2) STARTED RECORDING VIB. INFORMATION. LOST TORQUE. SPEED ACCELERATED TO 76,000 RPM. TURBINE AIR WAS SHUT 1120 DOWN BY OVERSPEED SWITCH. TRIED TO ROTATE GEARBOX OUTPUT SHAFT BY HAND AT NOON. COULD NOT. 1112:30 TRIED TO ROTATE UNIT AGAIN & WAS ABLE TO ROTATE OUTPUT SHAFT. AXIAL DISPLACEMENT PROBE NOW READING 15.7 VOLTS. BEFORE OVERSPEED SHUT DOWN PROBE HAD BEEN READING 9.1 VOLTS. COULD NOT MOVE THRUST BAIL. PISTON BACK TO 9.1 VOLTS WITH THRUST AIR.	
	1510	STARTED ROTATION. SLOWLY ACCELERATED TO 40,000 & RECORDED TWO SCANS. 190000. TO 50,000 & BACKED SPEED DOWN TO REDUCE TORQUE LOAD. STARTED TO ACCELERATE & HAD TO HOLD FOR DIGITAL. SHUT DOWN 1545 BE CAUSE OF AIR. TRIED TO BREAK TURBINE FREE BEFORE IT WOULD START ROTATING.	
	1653	STARTED ROTATING AFTER BREAKING FREE BY HAND. SLOWLY ACCELERATED TO 70,220 RPM. TAKING DATA AT 60,000 RPM. TRIED TO GET DATA AT 70,000 RPM. WATER BRAKE TORQUE VERY UNSTABLE. DROPPED LOW ENOUGH TO CAUSE GEARBOX RUNOUT TO 1605 BE EXCESSIVE. SHUT DOWN.	
		CELL TIME 8.0 HRS.	
		TECH TIME 1.5 HRS.	
		ENERGY 17510 UNITS OF AIR.	

# QUALIFICATION TEST LOG

E.W.O. No. 3429-246160-09-0601

Test Cell or Station No. C-116

## Program

Part No. GTP 305-2

Serial No. ... /

Development Engineer JOHN TEETS

Technician WATERWOOD

Unit No. 1

Test Procedure No. 1. C. A. TESTING, Rev. TEST #3

Rev. TEST #3

Date	Time
------	------

## Event

## Stamp

16 MAY 1979

REMOVED DISCHARGE DUCT. NO OIL  
IN UNIT. NO APPARENT WHEEL RUB.  
NO APPARENT WHEEL MOVEMENT. CHECKED  
TIGHTNESS OF REAR BEARING COVER NUTS. O.K.  
WHEEL TO SHROUD CLEARANCE 0.005" MIN.  
TO 0.007" MAX. ~~BEH~~ MEASURED FROM  
TURB. DISCHARGE FLANGE TO BACK SIDE  
OF TURBINE WHEEL IN THE M.I.B. DISTANCE  
IS 7.185" AT ONE SPOT.

17 MAY 1974

TOOK OFF-CHL. SET UP X-Y PLOTTER  
TO READ SPEED VS ACCELERATION.

1330. STARTED ROTATION. TRIED DIFFERENT  
CONDITIONS OF WATER FLOW & PRESSURE.  
(60) TO GET MORE STABLE CONDITIONS. REACHED  
65000 RPM WHEN WATER BRAKE UNLOADED,  
1430 SHUT DOWN.

ADDED THIRD WATER LINE TO THE  
WATER BREAK.

1505. STARTED ROTATION. VARIED WATER  
40 SMALL WATER FLOW PRESS. ALSO VARIED  
AND FLOW INTO THE WHITE. WATER FLOW  
1510. - FLOW UNSTABLE. SHUT DOWN.

18 May, 1977

OPENED WATER DISCHG. VALVE ON WATER  
BARGE FULL OPEN.

0945 STARTED ROTATION. SLOWLY ACCELERATED TO 60,000 RPM. TORQUE 1,100 FT LBS. CIT = 603°F, TIT = 2,330°F. SPEED STABLE, LOAD SINGLE. STARTED TO ACCEL. TO 65,000 RPM. REACHED 113 PSIG COMP. INLET TOTAL. TRIED TO INCREASE SPEED BY INCREASING INLET TEMP. TURB. FRONT VIB. WENT TO 100 G's.  
1025 SHUT DOWN TO CHECK PICKUP.  
PICKUP O.K.

# QUALIFICATION TEST LOG

E.W.O. No. _____		Test Cell or Station No. _____
Program _____	Part No. _____	Serial No. _____
Development Engineer _____	Technician _____	Unit No. _____

Test Procedure No. _____	Rev. _____
--------------------------	------------

Date	Time	Event	Stamp
------	------	-------	-------

18 MAY, 1974

1040 STARTED ROTATIONAL SET TORQUE TO ABOUT 1/2 VALUE AS FIRST RUN. WATER BRAKE TORQUE UNSTABLE. RESET TORQUE TO 4/5 AT 1250 RPM. WATER BRAKE TORQUE UNSTABLE. VIBRATION ALSO FOLLOWING HIGH VIB. ON SHUT DOWN. STARTED COOLING DOWN TO PULL QUILL SHAFT.

1125 SHUT DOWN.

PULLED UNIT FROM STAND, REMOVED QUILL SHAFT BETWEEN TURBINE & GEARBOX. REINSTALLED UNIT ON GEARBOX. DID NOT CONNECT DISCHARGE DUCT TO TURBINE FLANGE

1430 STARTED SLOW ROLL & SLOWLY ACCELERATED TO 61,200 RPM. VIBRATION STEADILY INCREASED TO 40 G'S AT 61,200 RPM. SHUT DOWN.

PULLED UNIT & DELIVERED TO DEV. ASSY. CHECKED ~~QUILL~~ TURBINE SHAFT & FOUND TO BE 0.360" BEHIND MOUNTING FLANGE.

## QUALIFICATION TEST LOG

E.W.O. No. 3409-246160-09-0601

Test Cell or Station No. C-116

Program

Part No. GTP 325-2

Serial No. 1

Development Engineer JON TEETS

Technician NDEWOOD

Unit No. 1

Test Procedure No. INTEGRATED COMPONENTS ASSY. TEST, Rev. TEST #4

Date	Time	Event	Stamp
------	------	-------	-------

19 JUNE, 1979

RECEIVED UNIT FROM DEV. ASSY. INSTALLED TWO SPEED PICKUP PROBES, TWO AXIAL DISPLACEMENT PROBES, & SET UP TWO SHAFT RUNOUT PROBES. CHECKED QUILL SHAFT END PLAY. DISTANCE FROM END OF QUILL SHAFT TO MOUNTING FLANGE: 2.325". DISTANCE FROM TURBINE SHAFT END TO MOUNTING FLANGE 2.355".  $0.355" + 0.290" - 0.325" = .120"$ . QUILL SHAFT END PLAY 0.120". INSTALLED UNIT ON STAND. MOUNTED QUILL SHAFT RUNOUT PROBE MOUNTING BRACKET. FOUND ONE QUILL SHAFT RUNOUT PROBE DRIVER BOX TO BE BAD. HAD IT REPAIRED. WILL NEED RECAL. ON DRIVER BOX AFTER TEST. HOOKED UP OIL SYSTEM & CHECKED OIL SCAV. FLOW. FLOW GOOD BOTH FRONT & BACK. BEGAN WORKING ON INSTRUMENTATION.

TECH TIME 2 @ 8.0 HRS.

CELL TIME 8.0 HRS.

SWING 19 JUNE, 1979

CONTINUED SET-UP, PREP. FOR PRESS. CHECK.

TECH TIME 2 @ 8.0 HRS.

CELL TIME 8.0 HRS.

20 JUNE, 1979

REALIZED TURBINE & QUILL SHAFT ALIGNMENT MARKS HAD NOT BEEN ALIGNED WHEN TURBINE WAS MOUNTED ON STAND. MOVED UNIT BACK FROM STAND WITH FLEX SECTION BOLTS FAR ENOUGH TO ALIGN MARKS. & THEN REMOUNTED UNIT. FINISHED INSTRUMENTATION HOOKUP. PREL. CHECKED UNIT. MASTER NOS 3302, 3421, 3140, 3514, 3305, 3307, 6240, 6232, 6506, 6505, & 6212 WERE MISSING.

RAN UNIT UP TO 40,000 RPM TO CHECK OUT SYSTEMS. TURB. VIB. INOPERATIVE. REPLACED



# QUALIFICATION TEST LOG

E.W.O. No. <u>3409-246160-09-0601</u>		Test Cell or Station No. <u>C-116</u>	
Program _____		Part No. <u>GTP 305-2</u>	Serial No. <u>1</u>
Development Engineer <u>JOHN TEETS</u>		Technician <u>NORWOOD</u>	Unit No. <u>1</u>
Test Procedure No. <u>I.C.A. TEST</u>		Rev. <u>TEST #4</u>	
Date	Time	Event	Stamp
<u>21 JUNE, 1979</u>			
		DECREASED THRUST PISTON PRESS. TO 42 PSIG.	
		RECORDED TWO SCANS AT 46,000 RPM.	
		INCREASED OIL PRESS. TO 50 PSIG.	
		RECORDED TWO SCANS AT 46,000 RPM.	
		INCREASED SPEED TO 50,000 RPM.	
		RECORDED TWO SCANS AT 50,490 RPM.	
		INCREASED THRUST PISTON PRESS. TO 50 PSIG.	
		RECORDED TWO SCANS AT 50,460 RPM.	
		INCREASED SPEED TO 55,000 RPM.	
		RECORDED TWO SCANS AT 55,120 RPM.	
		INCREASED THRUST PISTON PRESS. TO 50 PSIG.	
		RECORDED TWO SCANS AT 55,000 RPM.	
		INCREASED SPEED TO 60,000 RPM.	
		RECORDED TWO SCANS AT 60,570 RPM.	
		SHUT DOWN. LEFT OIL PRESS.	
		TO KEEP COOL UNIT.	
		TECH TIME 2.80 HRS.	
		CELL TIME 6.0 HRS.	
		ANALYST 1.60 L. AIR.	
<u>22 JUNE, 1979</u>			
		SHALL ROTATION SLOWLY ACCELERATED TO	
		46,000 RPM.	
		RECORDED TORQUE FROM 12.5 FT LBS. TO	
		11.7 FT LBS. AT 46,000 RPM.	
		RECORDED TWO SCANS AT 46,000 RPM.	
		ACCELERATED TO 50,000 RPM.	
		RECORDED TWO SCANS AT 50,000 RPM.	
		ACCELERATED TO 55,000 RPM.	
		RECORDED TWO SCANS AT 55,130 RPM.	
		ACCELERATED TO 65,000 RPM.	
		RECORDED TWO SCANS AT 65,130 RPM.	
		INCREASED OIL PRESS. FROM 50 TO 55 PSIG.	
		RECORDED TWO SCANS AT 65,130 RPM.	
		REDUCED OIL PRESS. TO 41.5 PSIG.	
		RECORDED TWO SCANS AT 65,130 RPM.	
		INCREASED OIL PRESS. TO 44 PSIG.	
		RECORDED TWO SCANS AT 65,526 RPM.	





## QUALIFICATION TEST LOG

E.W.O. No. 442 4-162-07-0601 Test Cell or Station No. C-116  
 Program \_\_\_\_\_ Part No. GTP 305-1 Serial No. \_\_\_\_\_  
 Development Engineer JAN TEETS Technician NORWOOD Unit No. 1  
 Test Procedure No. I.C.A. TEST Rev. TEST #1

Date \_\_\_\_\_ Time \_\_\_\_\_ Event \_\_\_\_\_ Stamp \_\_\_\_\_

GEARBOX ACCEL. ON SWITCH POSITION (1"),  
 & 7 O'CLOCK ACCEL. ON SWITCH POSITION #2.  
 PURGED FUEL SYSTEM & CONNECTED  
 FUEL LINE.

TEST TIME: 1245 HRS.

1220 HRS.

CELL TIME: 2 HRS.

ENGST. 1224 HRS.

25 JUNE 1972

SET UP FOR COOLING AIR ON REAR  
 ACCELEROMETERS. CHECKED COOLING WATER  
 SUPPLY VALVE O.K.

CONNECTED SECOND SANBORN RECORDER.  
 MOVING PICTURE PHOTOGRAPHER SETTING UP  
 EQUIPMENT.

STARTED ROTATION FOR LIGHT-OFF.  
 1.5. TROUBLE GETTING L/D. INCREASED  
 AIR ASSIST PRESS TO 10 PSIG OVER INLET  
 VALVE.

1445 GET LIGHT-OFF. FUEL PRESS. FLUCTUATING  
 CAUSING UNIT TO BLOW OUT NUMBER 245 TIMES.  
 WAS ABLE TO GET RELIGHT.

1453 LOST DIGITAL. RECORDED TWO SCANS AT  
 45,000 RPM.

1458 GOT CR. BACK. ACCELERATED TO  
 55,000 RPM. RECORDED TWO SCANS.

1541 ACCELERATED TO 68,400 RPM. RECORDED  
 TWO SCANS.

SET SPEED AT 90% CORRECTED L/D AIR  
 AT 5050 F. PRESS. RATIO 6.38611. RECORDED  
 SCANS. TRIED TO INCREASE PRESS. RATIO  
 TO 7.56711. COULD NOT GET ENOUGH TORQUE  
 1.2011 WATER BRAKE. TOOK POINT AT  
 90% CORRECTED SPEED (68,110 RPM), L/D AIR  
 AT 2050 F. PRESS. RATIO AT 7.371.

STARTED SLOW DECELERATION. STOPPED  
 AT 45,000 RPM TO RAISE BACK PRESS. ON

## QUALIFICATION TEST LOG

E.W.O. No. 34.22 246160-19-0601		Test Cell or Station No. C-116	
Program	Part No. GTP 305-2	Serial No. 1	
Development Engineer JON TEETS		Technician NORWOOD	Unit No. 1
Test Procedure No. 1. C. R. TEST		Rev. TEST #4	
Date	Time	Event	Stamp
25 JUNE, 1977			
(1620)		WATER BRAKE WATER. NOTICED SMOKE(?) COMING FROM TURBINE AREA. HEARD THUMP NOISE & HAD FLUID SPRAYING FROM FRONT OF UNIT & GEARBOX. SPEED DROPPED FROM 44,000 TO 29,000 RPM. SHUT DOWN OIL SPRAYING OUT OF GEARBOX. LOST ONE SCAN PUMP.	
		CELL TIME	2.0 HRS
		TECH TIME	1.8 HRS
			2.8 HRS
26 JUNE, 1977			
FOUND ONE SCAN PUMP CIRCUIT BREAKER TRIPPED. SECOND SCAN PUMP FOUND TO BE ROTATING IN THE WRONG DIRECTION. THAL FILLING GEARBOX FULL OF OIL. CORRECTED ROTATION OF PUMP. DISASSEMBLED PUMP & INSPECTED FOR EXCESSIVE WEAR. PUMP O.K. CHECKED CURRENT DRAW OF SHUT DOWN PUMP: 2.2 AMP MOTOR RATING 2.3 " PULLING 3.6 " CIRCUIT BREAKER			
CONCLUSION WAS THAT BECAUSE OF EXCESSIVE AMB. TEMP. CIRCUIT BREAKER TRIPPED SHUTTING DOWN PUMP.			
MAINTENANCE PEOPLE WARNED DOWN CELL.			
27 JUNE, 1977			
REPLACED ALL OIL SOAKED INSULATION. REINSTALLED BENTLEY PROBE WIRE & BOXES & CONNECTED LEADS. INSTALLED FRESH SWITCHES IN GEARBOX & TURBINE BEAK. BEAKING SCAN LINES. CONNECTED THEM IN SERIES WITH A P I #18-3 SO THAT SP. PRESS. IN OIL SCAN LINES WILL OPEN THE SWITCH & CAUSE TURBINE SHUT DOWN.			

QUALIFICATION TEST LOG

E.W.O. No. 3409-24612-09-0601

Test Cell or Station No. C-116

Program

Part No. GTP 305-2

Serial No. 1

Development Engineer J.C. TEETS

Technician NORMAN

Unit No.

Test Procedure No. I. C. A. TEST

Rev. TEST #4

Date	Time	Event	Stamp
		REPLACED ONE TURBINE DISCHARGE TEMP. & FIXED PRESS. LEAK. NOTED FORWARD ROLLER BEARING SANBORN RECORDER TO TURBINE REAR ROLLER BEARING.	
		GET SECOND SANBORN RECORDER INSTALLED & BOTH RECORDERS CALIBRATED. CHECKED CALIB. ON GEARBOX RUNOUT SCOPE.	
11:10	(45)	STARTED ROTATION & ACCELERATED TO 40,000 RPM TO SET TORQUE. (LAD) TO BURN OFF OIL ON PIPES. SHUT DOWN.	
11:15		REPLACED INLET OIL FILTERS AT UNIT. TESTED OIL PRESS. CHECKED FOR IGNITION SPARKS. SOUNDS O.K.	
11:25		STARTED ROTATION. SLOWLY ACCELERATED TO 50,000 RPM. REAR BEARING I.B. WENT TO 100 GS. BACKED DOWN TO 55,000 RPM. NOTICED THAT WATERBANE LUBE PRESSURE WAS DOWN. SHUT UNIT DOWN.	
11:30		HAD TO RESET CIRCUIT BREAKER TWICE TO GET PUMP TO RUN.	
		CHECKED OUT VIB. PICKUPS SYSTEMS ON NAME OF TURB. LOOKS O.K.	
		INSTALLED ACCEL. SIN 2074 IN PLACE OF 105 PICKUP SIN 1482 & SIN 2015 IN PLACE OF PICKUP SIN 1935.	
11:40		STARTED ROTATION & ACCELERATED TO 60,000 RPM. VIBRATION STILL THE SAME. DROPPED TO 27,000 RPM. INSTALLED CLAMP AROUND DISCHG. PUCT THAT HAD BEEN REMOVED TO INSULATE PUCT.	
11:45		ACCEL. TO 64,000 RPM. REAR VIBRATION PEAKED OUT AT 75 GS AT 61,000 RPM & DROPPED TO 7 GS AT 64,000 RPM. SLOWLY SHUT DOWN.	

# QUALIFICATION TEST LOG

E.W.O. No. 3429-246120-29-221

Test Cell or Station No. -116

Program \_\_\_\_\_

Part No. GTP325-2

Serial No. 1

Development Engineer JOHN TESTS

Technician NORWOOD

Unit No. 1

Test Procedure No. I. C. A. TEST

Rev. TEST #4

Date	Time	Event	Stamp
		<u>29 JUNE 1979</u>	
<u>0935</u>		<u>STARTED ROTATION, ACCELERATED TO 45,000 RPM TO CHECK TORQUE SETTING.</u>	
		<u>0940 RECORDED TWO SCANS.</u>	
		<u>7.1 2.2 2 SLOWLY ACCELERATED TO 45,000 RPM. RECORDED TWO SCANS DURING</u>	
		<u>WENT OFF 5' AT 45,000 RPM.</u>	
		<u>1005 RECORDED TWO SCANS AT 70% SPEED.</u>	
		<u>1020 3.0 2.2</u>	
		<u>1030 4.0 2.2 FUEL 132</u>	
		<u>1040 5.0 2.2 136</u>	
		<u>1050 7.5 2.2 144</u>	
		<u>1100 7.5 2.2 148</u>	
<u>1110</u>		<u>8.5 2.2 153</u>	
		<u>8.5 2.2 153</u>	
		<u>DECREASED SPEED &amp; CLOSED WATER VALVE TO WATER PUMP.</u>	
		<u>1120 RECORDED TWO SCANS PIR 5.2 90% 156</u>	
<u>1130</u>		<u>5.2 90% 156</u>	
		<u>WENT TO GET 100% SPEED AT 5.5 PRESS. RATIO. OPENING WATER PUMP</u>	
		<u>WATER VALVE. BRAKE UNLOADED &amp;</u>	
<u>1135</u>		<u>1135 TURB HIT OVERSPEEDS SHUT DOWN.</u>	
		<u>REPLACED MAIN ORIFICE AP TRANSFER.</u>	
		<u>TOOK NEW OFF-CAL.</u>	
		<u>REPLACED OVERSPEED RAPTURE DISCS &amp;</u>	
		<u>DISCS.</u>	
		<u>CHECKED OUT FRONT VIBRATION PICKUP. O.K.</u>	
		<u>CHECKED OUT FUEL FLOW. DIGITAL READING</u>	
		<u>DIFFERENT FLOW THAN PANEL METER. MADE</u>	
		<u>CORRECTION IN DIGITAL.</u>	
		<u>TECH TIME 2 &amp; 2.0 HRS.</u>	
		<u>CELL TIME 4.0 HRS.</u>	
		<u>ENERGY 180.4 K.E.</u>	
		<u>2.54 FUEL.</u>	

## QUALIFICATION TEST LOG

E.W.O. No. <u>2422-246160-09-0601</u>		Test Cell or Station No. <u>C-116</u>	
Program	Part No. <u>GTP 335-2</u>	Serial No. <u>1</u>	
Development Engineer <u>VON TEETS</u>		Technician <u>NEWOOD</u>	Unit No. <u>1</u>
Test Procedure No. <u>J. C. H. TEST</u>		Rev. <u>TEST #4</u>	
Date	Time	Event	Stamp
2 JULY, 1977			
RESET OVERSPEED TRIP TO 75,000 RPM. RANGE 2, PERIOD 1282.			
TOOK OFF-CHAL.			
STARTED ROTATION			
1000 CAT 1/D 5 STARTED ACCEL. ONE O/S #1.			
SYSTEM 17 TRIPPED SHUTTING UNIT DOWN.			
1250 CAT 2 AGAIN & AGAIN TRIPPED O/S.			
SHUT DOWN TO CLEAN SPEED PICKUP PROBLEMS.			
CLEANED & RESET PROBLEMS.			
2000 CAT 3 SPLD UP TO 35,000 RPM. O/S #2			
1500 TRIPPED OUT AGAIN.			
FOUND BAL. DISCONNECTED SYSTEM. RECONNECTED.			
CHECKED OUT "SECOND" SYSTEM - O.K.			
1000 STARTED ROTATION. TRIED TO GET			
A GOOD OFF. NO LUCK. CHECKED FOR POWER			
1500 TO FALL SOLENOID - NO POWER. SHUT DOWN			
TO TROUBLE SHOOT.			
REPAIRS OVERSPEED SHUTDOWN CONTROL.			
1500 RELOD OVERSPEED SHUT DOWN SYSTEMS. O.K.			
2000 TRIED 40 - O.K.			
O/S SYSTEM #1 SHUTS DOWN AIR SUPPLY IN			
THE "DAISEY CHAIN". SYSTEM #2 SHUTS DOWN			
GWAY FUEL.			
3 JULY, 1977			
STARTED ROTATION.			
0500 CAT 1/D 5 ACCELERATED TO 25,000 RPM. STARTED			
HAVING PROBLEMS WITH WATER BRAKE. TORQUE			
VARYING. HAVING PROBLEMS WITH G.E.T.			
0800 PROBLEMS SOLVED.			
ACCELERATED TO 45,000 RPM. RECORDED			
ONE TWO SCANS.			
ACCELERATED TO 55,000 RPM. RECORDED			
ONE TWO SCANS.			
ACCELERATED TO 65,000 RPM. RECORDED			
ONE TWO SCANS.			
ACCELERATED TO 75,000 RPM. RECORDED			
ONE TWO SCANS.			

# QUALIFICATION TEST LOG

E.W.O. No. 3#09-245160-09-0601 Test Cell or Station No. C-116  
 Program \_\_\_\_\_ Part No. GTP 305-2 Serial No. 1  
 Development Engineer JOHN TESTS Technician NORWOOD Unit No. 1  
 Test Procedure No. 1.C.A. TEST. Rev. TEST #4

Date \_\_\_\_\_ Time \_\_\_\_\_ Event \_\_\_\_\_ Stamp \_\_\_\_\_

3 JULY, 1979

~~100~~  
 INCREASED PR. TO 6.4:1. RECORDED TWO SCANS  
 101 INCREASED PR. TO 6.9:1 RECORDED TWO SCANS  
 FULL WATER BRAKE VALVE WIDE OPEN. WILL  
 HAVE TO GO TO LARGE VALVE FOR MORE  
 TORQUE.  
 INCREASED TORQUE TO 22 FT LBS TO  
 11.5:1 PRESS. RATIO.  
 140 RECORDED TWO SCANS @ 7.55:1 P.R.  
 141 RECORDED TWO SCANS @ 7.45:1 P.R.  
 TRIED TO DROP TORQUE TO GO TO 100%  
 DESIGN. CLOSING WATER BRAKE VALVE.  
 SPEED STARTED ACCELERATING TOO FAST.  
 142 SHUT IT DOWN.  
 143 NO. ACCELERATED TO 6200 RPM SET  
 TORQUE TO 119 FT LBS.  
 144 SET UP TO 100% SPEED AT DESIGN.  
 200 RECORDED 6 SETS OF SCANS AT DESIGN.  
 SHUT DOWN IN SPEED & STARTED  
 142 COOLING UNIT DOWN. RECORDED TWO SCANS  
 AT 4400 RPM ON WAY DOWN WITH TORQUE  
 SETTING AT DESIGN. CUT FUEL & CONTINUED  
 140 COOLING WITH COLD AIR. SHUT DOWN.

TECH TIME: 138.0 HRS.  
 206.0 HRS.  
 ENEROX: 285 U. AIR.  
 4.52 U. FUEL  
 CELL TIME 6.5 HRS.

APPENDIX C

"QUICK-LOOK" TABULATIONS DESIGN POINT DATA BOS LOG

(12 Pages)

# APPENDIX C

## "QUIK-LOOK" TABULATIONS DESIGN POINT DATA BOS LOG

The following pages are the "Quik-Look" tabulations corresponding to the data matrix listed below. In addition the BOS Log of the design point data (Data Point 11) used in establishing turbine performance.

TEST MATRIX

$P/P)_{T-DE}$	$\% N/\sqrt{\theta}$ 90*	100**	100***
5.50	1	5	9
6.50	2	6	10
7.529	3	7	11
8.5	4	8	12

\*Run at  $T_{in} = 2050^{\circ}F$ , speed  $\approx 68116.5$  rpm

\*Run at reduced temperature and speed,  $T_{in} \approx 1690^{\circ}F$ ,  
 $N \approx 70,000$  rpm

\*\*\*Run at full temperature and speed (design point).

### Design Point Condition

$N = 75,684$

$R_{in} = 2050^{\circ}F$

$P/P)_{T-DE} = T_{in}$

No. 11  $2050^{\circ}F$

No. 10  $1900^{\circ}F$

No. 9  $1800^{\circ}F$



C110 GTP305-2 01 04/04  
INTEGRATED COMPOUNDED ASSY TESTING (ICA)

06/25/79

OFFSET 10:25:49.02	1A 1A	RECORD 15:49:109.42		TEST C
WMOR = 1.74825	*	EFFIT = 0.486527	*	PSDUSA = -0.280438
WNET = 1.77203	*	MURP = 93.0629	*	PSDDHA = -0.060138
WMCORR = 0.635391	*	INCODE = 0.	*	INTPS1 = 12.4628
WIBOR = 0.	*	FM143 = 1044.57	*	INTPS2 = 12.5558
LBH412 = 133.187	*	TUROIL = 440.946	*	CINIT1 = 710.429
SOHET1 = 2.20287	*	CPS410 = 1755.35	*	CINIT2 = 718.105
LBH413 = 0.	*	CPS411 = 0.	*	ENGCRF = 168.364
PBAR = 14.0656	*	DENOM = 1134.88	*	TEOR = 311.974
MORUP = 1.59081	*	RbTFWD = 119.392	*	PAIR = 87.7319
MORT1 = 799.651	*	RbTF = 324.933	*	CURSPD = 31134.8
PRBF1 = 29.1081	*	RbTAF = 232.590	*	PCTSPD = 0.904670
PRBF3 = 26.8401	*	PSNTH1 = 38.9229	*	TIM412 = 2057.37
PSSSF1 = 0.207543	*	PSNTH2 = 40.1168	*	TIM413 = 714.267
PSSSF2 = 0.234070	*	PSNTH3 = 30.2355	*	TIM4B = 1893.92
PSSSA1 = 26.3627	*	PSNTH4 = 42.9152	*	CINITA = 714.267
PSSSA2 = 26.4620	*	CINPT1 = 0.101436	*	CINPTA = 78.2638
PBPA1 = 58.6189	*	CINPT2 = 77.9965	*	TTPA3 = 1216.18
PBPA2 = 58.6321	*	CINPT3 = 78.4474	*	TTPA2 = 1265.66
PBPF1 = 1.02988	*	CINPT4 = 78.4070	*	TTPA1 = 1234.87
PBPF2 = 1.12271	*	PTRD1 = 0.605935	*	PRT-DE = 0.31375
DPBP1 = 57.5890	*	PTRD2 = 0.478724	*	PRT-T = 0.03941
DPBP2 = 57.5094	*	PTRD3 = 0.342111	*	TURQU = 188.891
	*	PTRD4 = 0.357290	*	

OFFSET 10:25:49.02	1A 1B	RECORD 15:49:139.42		TEST C
WMOR = 1.75264	*	EFFIT = 0.475551	*	PSDUSA = -0.279604
WNET = 1.72635	*	MURP = 93.0510	*	PSDDHA = -0.061403
WMCORR = 0.635174	*	INCODE = 0.	*	INTPS1 = 12.4430
WIBOR = 0.	*	FM143 = 1043.57	*	INTPS2 = 12.5424
LBH412 = 131.080	*	TUROIL = 439.732	*	CINIT1 = 714.257
SOHET = 2.19389	*	CPS410 = 1731.50	*	CINIT2 = 719.932
LBH413 = 0.	*	CPS411 = 0.	*	ENGCRF = 168.047
PBAR = 14.0666	*	DENOM = 1131.89	*	TEOR = 312.190
MORUP = 1.60106	*	RbTFWD = 119.566	*	PAIR = 87.6437
MORT1 = 801.051	*	RbTF = 326.113	*	CURSPD = 31210.6
PRBF1 = 29.0616	*	RbTAF = 232.950	*	PCTSPD = 0.907074
PRBF3 = 26.7871	*	PSNTH1 = 38.8964	*	TIM412 = 2036.90
PSSSF1 = 0.194281	*	PSNTH2 = 40.0630	*	TIM413 = 716.095
PSSSF2 = 0.234070	*	PSNTH3 = 30.1957	*	CINPT = 1881.60
PSSSA1 = 26.3229	*	PSNTH4 = 42.8485	*	CINITA = 716.095
PSSSA2 = 26.4290	*	CINPT1 = 0.101436	*	CINPTA = 78.1689
PBPA1 = 58.4995	*	CINPT2 = 77.8771	*	TTPA3 = 1208.96
PBPA2 = 58.5127	*	CINPT3 = 78.3280	*	TTPA2 = 1250.14
PBPF1 = 1.04313	*	CINPT4 = 78.3015	*	TTPA1 = 1228.13
PBPF2 = 1.12271	*	PTRD1 = 0.605935	*	PRT-DE = 0.30565
DPBP1 = 57.4564	*	PTRD2 = 0.473064	*	PRT-T = 0.03391
DPBP2 = 57.3900	*	PTRD3 = 0.337051	*	TURQU = 188.705
	*	PTRD4 = 0.354780	*	

DATA POINT 2

C116 GTH305-2 01 04/04  
INTEGRATED COMPONENTS ASSY TESTING (ICA)

06/25/79

OFFSET 10:25:49.02	1A	1B	RECORD 16:06:09.42		TEST C
WMOR = 2.16944	*		EFFIT = 0.501060	*	PSDUSA = -0.437080
WNET = 2.13089	*		MORP = 115.119	*	PSDDHA = -0.062907
WMCORR = 0.635730	*		IBCOND = 0.	*	INTPS1 = 16.8390
WIBUR = 0.	*		FM143 = 1041.50	*	INTPS2 = 16.7000
LBH412 = 137.590	*		TURDIL = 439.165	*	CINTT1 = 720.454
SQTHET = 2.11503	*		CPS410 = 1817.97	*	CINTT2 = 720.192
LBH413 = 0.	*		CPS411 = 0.	*	ENGCRF = 152.434
PBAK = 14.0030	*		DENUM = 1448.02	*	TGOR = 301.261
MURDP = 2.01015	*		RBTFWO = 118.392	*	PIIN = 104.471
MORT1 = 189.332	*		BbTF = 298.398	*	CURSPD = 32282.2
PRRF1 = 37.4242	*		RBTAF = 210.567	*	PCTSPD = 0.938217
PRRF3 = 33.9492	*		PSNTH1 = 48.9367	*	TIN412 = 1400.64
PSSSF1 = 0.107753	*		PSNTH2 = 51.5090	*	TIN413 = 723.323
PSSSF2 = 0.220007	*		PSNTH3 = 39.4269	*	TINPB = 1717.01
PSSSA1 = 33.4050	*		PSNTH4 = 53.6180	*	CINTTA = 723.323
PSSSA2 = 33.6309	*		CINPT1 = 0.008174	*	CINPTA = 95.9062
PBPA1 = 57.8496	*		CINPT2 = 95.5570	*	TIPA3 = 1079.52
PBPA2 = 57.7700	*		CINPT3 = 96.0742	*	TIPA2 = 1055.67
PBPF1 = 1.02980	*		CINPT4 = 96.0075	*	TIPA1 = 1039.37
PBPF2 = 1.16250	*		PTRD1 = 1.20480	*	PRT-DE = 7.56843
DPBP1 = 56.8197	*		PTRD2 = 0.620397	*	PRT-T = 7.10212
DPBP2 = 56.6075	*		PTRD3 = 0.410410	*	TURQUE = 242.099
			PTRD4 = 0.349701	*	TURNPM = 68277.8

OFFSET 10:25:49.02	1A	1B	RECORD 16:06:39.42		TEST C
WMOR = 2.16874	*		EFFIT = 0.504313	*	PSDUSA = -0.435190
WNET = 2.13021	*		MORP = 115.470	*	PSDDHA = -0.081041
WMCORR = 0.634370	*		IBCOND = 0.	*	INTPS1 = 16.9192
WIBUR = 0.	*		FM143 = 1041.80	*	INTPS2 = 16.8062
LBH412 = 137.023	*		TURDIL = 439.165	*	CINTT1 = 721.549
SQTHET = 2.11579	*		CPS410 = 1817.31	*	CINTT2 = 727.444
LBH413 = 0.	*		CPS411 = 0.	*	ENGCRF = 152.434
PBAK = 14.0030	*		DENUM = 1451.03	*	TGOR = 300.307
MURDP = 2.01487	*		RBTFWO = 118.280	*	PIIN = 104.098
MORT1 = 791.660	*		BbTF = 298.910	*	CURSPD = 32327.1
PRRF1 = 37.6364	*		RBTAF = 216.240	*	PCTSPD = 0.939522
PRRF3 = 34.0951	*		PSNTH1 = 49.1350	*	TIN412 = 1802.30
PSSSF1 = 0.181017	*		PSNTH2 = 51.7352	*	TIN413 = 724.497
PSSSF2 = 0.220007	*		PSNTH3 = 39.6120	*	TINPB = 1717.83
PSSSA1 = 33.6044	*		PSNTH4 = 53.8441	*	CINTTA = 724.497
PSSSA2 = 33.7503	*		CINPT1 = 0.101430	*	CINPTA = 96.1450
PBPA1 = 57.9557	*		CINPT2 = 95.8020	*	TIPA3 = 1078.21
PBPA2 = 57.9822	*		CINPT3 = 96.2997	*	TIPA2 = 1055.79
PBPF1 = 1.04313	*		CINPT4 = 96.2732	*	TIPA1 = 1038.57
PBPF2 = 1.17576	*		PTRD1 = 1.21239	*	PRT-DE = 7.58399
DPBP1 = 55.9126	*		PTRD2 = 0.622927	*	PRT-T = 7.11539
DPBP2 = 56.8065	*		PTRD3 = 0.410410	*	TURQUE = 242.178
			PTRD4 = 0.357290	*	TURNPM = 68397.2

DATA POINT 3

07/03/79

OFFSPT 07:52:50.15  
WMOR = 1.83744  
WNFT = 1.78328  
WMCORR = 0.650198  
WIROR = 0.026598  
LBH412 = 100.141  
SOTNFT = 2.05201  
LBH413 = 0.  
PBAR = 14.0996  
MORNDP = 1.81016  
MORT1 = 818.249  
PRRF1 = 28.4572  
PRRF3 = 24.5905  
PSSAF1 = 0.207787  
PSSSF2 = 0.194499  
PSSSA1 = 23.7135  
PSSSA2 = 23.7667  
PBPA1 = 61.8888  
PBPA2 = 61.8888  
PBPF1 = 2.86530  
PBPF2 = 2.33380  
DPRP1 = 59.0235  
DPRP2 = 59.5550

RECORD 10106122.43  
EFFTT = 0.431221  
MORP = 91.5316  
IBCOND = 2.85132  
FM143 = 1112.67  
TUROIL = 410.314  
CPS410 = 1295.71  
CPS411 = 0.033577  
DENOM = 952.986  
RBTFFWD = 102.691  
BMTF = 314.955  
RBTAF = 206.395  
PSNTH1 = 37.8515  
PSNTH2 = 39.3796  
PSNTH3 = 30.2245  
PSNTH4 = 40.8944  
CINPT1 = 0.101486  
CINPT2 = 74.0071  
CINPT3 = 74.3525  
CINPT4 = 74.4057  
PTRD1 = 0.482259  
PTRD2 = 0.383389  
PTRD3 = 0.375783  
PTRD4 = 0.702815

TEST U  
PSDDSA = -0.261801  
PSDDHA = -0.188916  
INTPS1 = 10.9707  
INTPS2 = 10.8644  
CINTT1 = 718.053  
CINTT2 = 723.219  
BNGCRF = 155.161  
TBOR = 288.518  
PTIN = 83.9370  
CORSPD = 34094.9  
PCTSPD = 0.990902  
TIN412 = 1724.42  
TIN413 = 720.636  
TINPR = 1530.13  
CINTTA = 720.636  
CINPTA = 74.2551  
TTPA3 = 1000.49  
TTPA2 = 987.809  
TTPA1 = 995.723  
PRT-DE = 6.04985  
PRT-T = 5.75476  
TORQUE = 155.494  
TURRPM = 69963.1

OFFSPT 07:52:50.15  
WMOR = 1.83470  
WNFT = 1.78058  
WMCORR = 0.649584  
WIROR = 0.026603  
LBH412 = 100.250  
SOTNFT = 2.05359  
LBH413 = 0.054473  
PBAR = 14.1016  
MORNDP = 1.80515  
MORT1 = 818.612  
PRRF1 = 28.4479  
PRRF3 = 24.5772  
PSSAF1 = 0.207787  
PSSSF2 = 0.194499  
PSSSA1 = 23.7135  
PSSSA2 = 23.7667  
PBPA1 = 61.9818  
PBPA2 = 62.0084  
PBPF1 = 2.86531  
PBPF2 = 2.33380  
DPRP1 = 59.1165  
DPRP2 = 59.6764

RECORD 10106152.43  
EFFTT = 0.433097  
MORP = 91.5316  
IBCOND = 2.85502  
FM143 = 1113.46  
TUROIL = 409.230  
CPS410 = 1300.68  
CPS411 = 0.067154  
DENOM = 958.398  
RBTFFWD = 102.892  
BMTF = 320.037  
RBTAF = 205.122  
PSNTH1 = 37.8250  
PSNTH2 = 39.3663  
PSNTH3 = 30.2245  
PSNTH4 = 40.8811  
CINPT1 = 0.088199  
CINPT2 = 74.0602  
CINPT3 = 74.3924  
CINPT4 = 74.3658  
PTRD1 = 0.482259  
PTRD2 = 0.383389  
PTRD3 = 0.380854  
PTRD4 = 0.707886

TEST U  
PSDDSA = -0.261168  
PSDDHA = -0.188916  
INTPS1 = 10.9574  
INTPS2 = 10.8644  
CINTT1 = 719.045  
CINTT2 = 724.471  
BNGCRF = 156.299  
TBOR = 289.497  
PTIN = 83.9557  
CORSPD = 34093.0  
PCTSPD = 0.990845  
TIN412 = 1727.79  
TIN413 = 722.361  
TINPR = 1535.70  
CINTTA = 721.758  
CINPTA = 74.2728  
TTPA3 = 1002.34  
TTPA2 = 989.478  
TTPA1 = 997.434  
PRT-DE = 6.05019  
PRT-T = 5.75426  
TORQUE = 156.265  
TURRPM = 70013.1

DATA POINT 5

OFFSET 07:52:50.15  
WMOR # 1.95444  
WNFT # 1.89714  
WMCORR # 0.648393  
WIROR # 0.027985  
LBH412 # 103.074  
SQTHFT # 2.04398  
LBH413 # 0.054412  
PBAR # 14.0996  
MOROP # 1.93385  
MORT1 # 825.458  
PRRF1 # 30.9553  
PRRF3 # 26.8361  
PSSSF1 # 0.221074  
PSSSF2 # 0.207787  
PSSSA1 # 26.0123  
PSSSA2 # 26.0654  
PMPA1 # 64.1743  
PMPA2 # 64.1344  
PBPFI # 2.77279  
PBPFI2 # 2.29394  
DPRP1 # 61.4070  
DPRP2 # 61.8405

RECORD 10:15:52.43  
EFFTT # 0.442771  
MORP # 98.4177  
IBCODP # 3.00086  
FM143 # 1119.81  
TUROIL # 412.843  
CPS410 # 1334.79  
CPS411 # 0.033577  
DENOM # 1056.70  
RBTFFD # 105.399  
BBTF # 376.944  
RBTAF # 203.835  
PSNTH1 # 40.9210  
PSNTH2 # 42.6749  
PSNTH3 # 32.9484  
PSNTH4 # 44.2429  
CINPT1 # 0.068199  
CINPT2 # 79.5347  
CINPT3 # 79.9068  
CINPT4 # 79.8802  
PTRD1 # 0.383389  
PTRD2 # 0.307335  
PTRD3 # 0.297194  
PTRD4 # 0.510145

TEST D  
PSDDSA # -0.322010  
PSDDHA # -0.118213  
INTPS1 # 12.2331  
INTPS2 # 12.1268  
CINTT1 # 732.814  
CINTT2 # 737.973  
BNGCRF # 159.981  
TBOR # 294.747  
PTIN # 89.1798  
CORSPD # 34198.2  
PCTSPD # 0.993903  
TIN412 # 1707.37  
TIN413 # 739.957  
TINPR # 1522.47  
CINTTA # 735.393  
CINPTA # 79.7739  
TTPA3 # 962.354  
TTPA2 # 958.089  
TTPA1 # 965.467  
PRT-DE # 6.42993  
PRT-T # 6.16134  
TORQUE # 172.570  
TURRPM # 69900.6

OFFSET 07:52:50.15  
WMOR # 1.95088  
WNFT # 1.89355  
WMCORR # 0.647397  
WIROR # 0.028070  
LBH412 # 102.891  
SQTHFT # 2.04430  
LBH413 # 0.054409  
PBAR # 14.1006  
MOROP # 1.92788  
MORT1 # 826.273  
PRRF1 # 30.9818  
PRRF3 # 26.8361  
PSSSF1 # 0.234362  
PSSSF2 # 0.207787  
PSSSA1 # 25.9857  
PSSSA2 # 26.0389  
PMPA1 # 64.1477  
PMPA2 # 64.1211  
PBPFI # 2.75900  
PBPFI2 # 2.29394  
DPRP1 # 61.3887  
DPRP2 # 61.8272

RECORD 10:16:22.43  
EFFTT # 0.442285  
MORP # 98.3852  
IBCODP # 3.02177  
FM143 # 1119.91  
TUROIL # 413.204  
CPS410 # 1336.94  
CPS411 # 0.067154  
DENOM # 1062.37  
RBTFFD # 105.600  
BBTF # 322.204  
RBTAF # 205.215  
PSNTH1 # 40.9210  
PSNTH2 # 42.6749  
PSNTH3 # 32.9483  
PSNTH4 # 44.3492  
CINPT1 # 0.068199  
CINPT2 # 79.4816  
CINPT3 # 79.8935  
CINPT4 # 79.9068  
PTRD1 # 0.380854  
PTRD2 # 0.304600  
PTRD3 # 0.294660  
PTRD4 # 0.510145

TEST D  
PSDDSA # -0.320109  
PSDDHA # -0.141383  
INTPS1 # 12.2198  
INTPS2 # 12.1268  
CINTT1 # 733.387  
CINTT2 # 738.702  
BNGCRF # 156.061  
TBOR # 294.883  
PTIN # 89.1681  
CORSPD # 34223.5  
PCTSPD # 0.994639  
TIN412 # 1708.04  
TIN413 # 736.609  
TINPR # 1527.41  
CINTTA # 736.045  
CINPTA # 79.7606  
TTPA3 # 962.622  
TTPA2 # 958.522  
TTPA1 # 966.354  
PRT-DE # 6.42692  
PRT-T # 6.16091  
TORQUE # 173.341  
TURRPM # 69963.1

DATA POINT 6

C116 GTP305-2 01 04/04  
INTEGRATED COMPONENTS ASSY TESTING (ICA)

07/03/79

OFFSPT 07:52:50.15	RECORD 10139152.52	TEST D
WMOR = 2.29531	EFFTT = 0.407011	PSDDSA = -0.412008
WNFT = 2.22829	MORP = 118.166	PSDDHA = -0.097018
WMCORR = 0.648801	IBCODP = 3.53276	INTPS1 = 16.2193
WIKOR = 0.032584	FM143 = 1128.54	INTPS2 = 16.1396
LBH412 = 117.583	TUROIL = 415.553	CINTT1 = 758.532
SQTHFT = 2.04258	CPS410 = 1524.58	CINTT2 = 764.199
LBH413 = 0.	CPS411 = 0.	BNGCRF = 146.023
PBAH = 14.0986	DENOM = 1362.39	TBOR = 284.472
MORDP = 2.29049	RBTFFWD = 106.432	PTIN = 104.596
MORT1 = 838.119	BBTF = 258.072	CURSPD = 34270.6
PRRF1 = 38.4229	RBTAF = 203.371	PCTSPD = 0.996008
PRRF3 = 33.4932	PSNTH1 = 50.0495	TIN412 = 1704.40
PSSSF1 = 0.234362	PSNTH2 = 52.4014	TIN413 = 761.366
PSSSF2 = 0.194499	PSNTH3 = 40.9874	TINPR = 1529.16
PSSSA1 = 32.4169	PSNTH4 = 54.5939	CINTTA = 761.366
PSSSA2 = 32.4701	CINPT1 = 0.101486	CINPTA = 96.0025
PBPA1 = 57.4241	CINPT2 = 95.6658	TPA3 = 905.242
PBPA2 = 57.5703	CINPT3 = 96.1973	TPA2 = 928.178
PBPF1 = 2.83873	CINPT4 = 96.1442	TPA1 = 917.744
PBPF2 = 2.46668	PIRD1 = 0.892950	PRT-DE = 7.55529
DPAP1 = 54.5854	PIRD2 = 0.482259	PRT-T = 7.14681
DPBP2 = 55.1036	PIRD3 = 0.304800	TORQUE = 222.176
	PIRD4 = 0.467048	TURRPM = 70000.6

OFFSPT 07:52:50.15	RECORD 10140122.52	TEST D
WMOR = 2.29142	EFFTT = 0.407524	PSDDSA = -0.412008
WNFT = 2.22435	MORP = 118.166	PSDDHA = -0.097018
WMCORR = 0.647778	IBCODP = 3.55756	INTPS1 = 16.2060
WIKOR = 0.032692	FM143 = 1129.14	INTPS2 = 16.1396
LBH412 = 117.381	TUROIL = 415.372	CINTT1 = 759.520
SQTHFT = 2.04297	CPS410 = 1526.40	CINTT2 = 764.979
LBH413 = 0.	CPS411 = 0.033577	BNGCRF = 145.466
PBAH = 14.0976	DENOM = 1364.51	TBOR = 284.119
MORDP = 2.28413	RBTFFWD = 106.698	PTIN = 104.603
MORT1 = 838.998	BBTF = 260.190	CURSPD = 34285.5
PRRF1 = 38.4229	RBTAF = 203.371	PCTSPD = 0.996441
PRRF3 = 33.4932	PSNTH1 = 50.0495	TIN412 = 1705.22
PSSSF1 = 0.234362	PSNTH2 = 52.4014	TIN413 = 762.250
PSSSF2 = 0.194499	PSNTH3 = 41.0273	TINPR = 1532.32
PSSSA1 = 32.3903	PSNTH4 = 54.5806	CINTTA = 762.250
PSSSA2 = 32.4568	CINPT1 = 0.101486	CINPTA = 96.0113
PBPA1 = 58.8326	CINPT2 = 95.6393	TPA3 = 905.263
PBPA2 = 58.5403	CINPT3 = 96.1708	TPA2 = 928.137
PBPF1 = 2.82544	CINPT4 = 96.2239	TPA1 = 917.971
PBPF2 = 2.46668	PIRD1 = 0.882810	PRT-DE = 7.55638
DPAP1 = 56.0072	PIRD2 = 0.479724	PRT-T = 7.14904
DPBP2 = 56.0736	PIRD3 = 0.304800	TORQUE = 222.708
	PIRD4 = 0.469884	TURRPM = 70044.4

DATA POINT 7

C116 GTP305-2 01 04/04  
INTEGRATED COMPONENTS ASSY TESTING (ICA)

07/03/79

OFFSET 07:52:50.15  
WMOR = 2.54809  
WNFT = 2.47395  
WNCORR = 0.647338  
WIBOR = 0.035923  
LBH412 = 129.582  
SOTHFT = 2.04449  
LBH413 = 0.  
PBAR = 14.0976  
MOROP = 2.54578  
MORT1 = 844.531  
PRRF1 = 44.2429  
PRRF3 = 38.6486  
PSSSF1 = 0.260938  
PSSSF2 = 0.274225  
PSSSA1 = 37.4263  
PSSSA2 = 37.4928  
PBPA1 = 57.9474  
PBPA2 = 57.7430  
PBPF1 = 2.83873  
PBPF2 = 2.82544  
DPRP1 = 55.1036  
DPRP2 = 54.9176

RECORD 10:51:52.53  
EFFTT = 0.510534  
MORP = 133.270  
IBCOPD = 3.89088  
FM143 = 1134.89  
TUROIIL = 416.637  
CPS410 = 1690.18  
CPS411 = 0.033577  
DENOM = 1606.38  
RBTFFWD = 107.033  
BBTF = 253.300  
RBTAFF = 204.565  
PSNTH1 = 57.1318  
PSNTH2 = 59.8824  
PSNTH3 = 47.2060  
PSNTH4 = 62.7259  
CINPT1 = 0.114774  
CINPT2 = 108.143  
CINPT3 = 108.688  
CINPT4 = 108.728  
PTRD1 = 1.39491  
PTRD2 = 0.614085  
PTRD3 = 0.398600  
PTRD4 = 0.449302

TEST D  
PSDDSA = -0.531793  
PSDDHA = -0.107159  
INTPS1 = 19.5014  
INTPS2 = 19.4349  
CINTT1 = 770.955  
CINTT2 = 775.577  
BNGCRF = 152.460  
TBOR = 262.029  
PTIN = 116.486  
CORSPD = 34290.7  
PCT&PD = 0.996590  
TIN412 = 1708.44  
TIN413 = 773.266  
TINPB = 1544.14  
CINTTA = 773.266  
CINPTA = 108.519  
TTPA3 = 885.930  
TTPA2 = 912.629  
TTPA1 = 894.805  
PRT-DE = 8.45443  
PRT-T = 7.86441  
TORQUE = 261.568  
TURMPM = 70106.9

OFFSET 07:52:50.15  
WMOR = 2.54542  
WNFT = 2.47124  
WNCORR = 0.647115  
WIBOR = 0.035996  
LBH412 = 129.459  
SOTHFT = 2.04458  
LBH413 = 0.054226  
PBAR = 14.0966  
MOROP = 2.54212  
MORT1 = 845.151  
PRRF1 = 44.2296  
PRRF3 = 38.7019  
PSSSF1 = 0.260938  
PSSSF2 = 0.274225  
PSSSA1 = 37.4396  
PSSSA2 = 37.5061  
PBPA1 = 56.8926  
PBPA2 = 57.1850  
PBPF1 = 2.82544  
PBPF2 = 2.81215  
DPRP1 = 54.0672  
DPRP2 = 54.3728

RECORD 10:52:22.53  
EFFTT = 0.511400  
MORP = 133.238  
IBCOPD = 3.90754  
FM143 = 1134.69  
TUROIIL = 416.817  
CPS410 = 1686.54  
CPS411 = 0.067154  
DENOM = 1601.51  
RBTFFWD = 106.779  
BBTF = 255.974  
RBTAFF = 204.565  
PSNTH1 = 57.1451  
PSNTH2 = 59.9089  
PSNTH3 = 47.1794  
PSNTH4 = 62.7525  
CINPT1 = 0.114774  
CINPT2 = 108.063  
CINPT3 = 108.635  
CINPT4 = 108.621  
PTRD1 = 1.39237  
PTRD2 = 0.616621  
PTRD3 = 0.398600  
PTRD4 = 0.449302

TEST D  
PSDDSA = -0.531793  
PSDDHA = -0.108426  
INTPS1 = 19.5147  
INTPS2 = 19.4482  
CINTT1 = 771.007  
CINTT2 = 775.681  
BNGCRF = 152.222  
TBOR = 262.056  
PTIN = 116.409  
CORSPD = 34185.1  
PCT&PD = 0.993523  
TIN412 = 1708.64  
TIN413 = 773.773  
TINPB = 1542.48  
CINTTA = 773.344  
CINPTA = 108.440  
TTPA3 = 886.157  
TTPA2 = 912.402  
TTPA1 = 894.414  
PRT-DE = 8.44987  
PRT-T = 7.85976  
TORQUE = 261.568  
TURMPM = 69894.4

DATA POINT 8

C116 GTP105-2 01 04/04  
INTEGRATED COMPONENTS ASSY TESTING (ICA)

07/03/79

OFFSET 07:52:50.15  
WMOR = 1.81693  
WNFT = 1.76314  
WMCORR = 0.646665  
WIROR = 0.026532  
LBH412 = 102.624  
SQTHET = 2.07904  
LBH411 = 0.  
PBAR = 14.0896  
MORDP = 1.77548  
MORT1 = 832.792  
PRRF1 = 29.4139  
PRRF2 = 24.8164  
PSSSF1 = 0.221074  
PSSSF2 = 0.221074  
PSSSA1 = 24.1653  
PSSSA2 = 24.2317  
PAPA1 = 58.0084  
PAPA2 = 57.9025  
PBPF1 = 4.31365  
PBPF2 = 4.11434  
DPPA1 = 53.6951  
DPPA2 = 53.7882

RECORD 11:46:22.55  
EFFIT = 0.470430  
MORP = 92.3112  
IBCDOP = 2.88774  
FM143 = 1184.49  
TUROIL = 410.585  
CPS410 = 1336.45  
CPS411 = 0.033577  
DENOM = 944.787  
RBTFFWD = 108.345  
BBTF = 326.676  
RBTAF = 222.540  
PSNTH1 = 38.8747  
PSNTH2 = 40.3762  
PSNTH3 = 31.8854  
PSNTH4 = 41.8374  
CINPT1 = 0.088199  
CINPT2 = 74.8575  
CINPT3 = 74.9903  
CINPT4 = 74.8973  
PTRD1 = 0.436626  
PTRD2 = 0.740442  
PTRD3 = 0.718076  
PTRD4 = 1.10590

TEST D  
PSDDSA = -0.205395  
PSDDHA = -0.224408  
INTPS1 = 10.8511  
INTPS2 = 10.7050  
CINTT1 = 746.409  
CINTT2 = 751.406  
BNGCRF = 161.327  
TBOR = 267.341  
PTIN = 84.5544  
CURSPD = 36366.0  
PCTSPD = 1.05691  
TIN412 = 1782.43  
TIN413 = 748.908  
TINPR = 1554.49  
CINTTA = 748.908  
CINPTA = 74.9151  
TTPA3 = 1023.78  
TTPA2 = 1020.58  
TTPA1 = 1018.63  
PRT-DE = 6.09415  
PRT-T = 5.69776  
TORQUE = 142.647  
TURNPM = 75607.9

OFFSET 07:52:50.15  
WMOR = 1.82433  
WNFT = 1.77062  
WMCORR = 0.648258  
WIROR = 0.026345  
LBH412 = 99.7791  
SQTHET = 2.06492  
LBH411 = 0.  
PBAR = 14.0906  
MORDP = 1.79918  
MORT1 = 832.843  
PRRF1 = 29.3475  
PRRF2 = 24.7101  
PSSSF1 = 0.221074  
PSSSF2 = 0.221074  
PSSSA1 = 24.0856  
PSSSA2 = 24.1387  
PAPA1 = 57.8161  
PAPA2 = 57.7410  
PBPF1 = 4.37694  
PBPF2 = 4.08776  
DPPA1 = 53.5091  
DPPA2 = 53.6553

RECORD 11:46:152.55  
EFFIT = 0.442092  
MORP = 91.7915  
IBCDOP = 2.85983  
FM143 = 1187.49  
TUROIL = 411.127  
CPS410 = 1298.52  
CPS411 = 0.033577  
DENOM = 932.599  
RBTFFWD = 108.238  
BBTF = 329.834  
RBTAF = 223.538  
PSNTH1 = 38.7684  
PSNTH2 = 40.3363  
PSNTH3 = 31.8987  
PSNTH4 = 41.8112  
CINPT1 = 0.101486  
CINPT2 = 74.1931  
CINPT3 = 74.5651  
CINPT4 = 74.5917  
PTRD1 = 0.414346  
PTRD2 = 0.753514  
PTRD3 = 0.745913  
PTRD4 = 1.13125

TEST D  
PSDDSA = -0.202226  
PSDDHA = -0.228211  
INTPS1 = 10.8113  
INTPS2 = 10.6518  
CINTT1 = 746.149  
CINTT2 = 750.990  
BNGCRF = 161.301  
TBOR = 268.609  
PTIN = 84.1135  
CURSPD = 36448.9  
PCTSPD = 1.05931  
TIN412 = 1752.00  
TIN413 = 748.569  
TINPR = 1538.31  
CINTTA = 748.569  
CINPTA = 74.4500  
TTPA3 = 1016.69  
TTPA2 = 1013.74  
TTPA1 = 1011.60  
PRT-DE = 6.08208  
PRT-T = 5.66332  
TORQUE = 141.450  
TURNPM = 75264.1

DATA POINT 9

07/03/79

OFFSFT 07:52:50.15  
WMOR = 1.83781  
WNFT = 1.78323  
WMCORR = 0.646198  
WIROR = 0.027010  
LBH412 = 114.526  
SQTHFT = 2.12489  
LBH413 = 0.  
PBAR = 14.0886  
MOROP = 1.77316  
MORT1 = 834.706  
PRRF1 = 30.5566  
PRRF3 = 26.1983  
PSSSF1 = 0.221074  
PSSSF2 = 0.207787  
PSSSA1 = 25.5074  
PSSSA2 = 25.5738  
PBPA1 = 58.0487  
PBPA7 = 57.9557  
PBPF1 = 4.34023  
PBPF7 = 4.16749  
DPAV1 = 53.7084  
DPBP2 = 53.7882

RECORD 11:51:52.95  
EFFTT = 0.482158  
MORP = 95.0396  
IBCUDP = 2.92183  
FM143 = 1190.36  
TUROIIL = 412.030  
CPS410 = 1491.12  
CPS411 = 0.033577  
DENOM = 1044.06  
RBTFFWD = 108.613  
RBTFF = 323.479  
RBTAF = 223.379  
PSNTH1 = 40.5090  
PSNTH2 = 41.9042  
PSNTH3 = 33.0946  
PSNTH4 = 43.5785  
CINPT1 = 0.088199  
CINPT2 = 77.7143  
CINPT3 = 78.1129  
CINPT4 = 78.1395  
PTRD1 = 0.558312  
PTRD2 = 0.517751  
PTRD3 = 0.489864  
PTRD4 = 0.814361

TEST D  
PSDDSA = -0.264971  
PSDDHA = -0.214268  
INTPS1 = 11.7547  
INTPS2 = 11.6218  
CINIT1 = 749.897  
CINIT2 = 754.736  
BNGCRF = 158.640  
TBOR = 265.183  
PTIN = 87.4736  
CURSPD = 35584.9  
PCTSPD = 1.03420  
TIN412 = 1882.33  
TIN413 = 752.316  
TINPB = 1676.85  
CINTTA = 752.316  
CINPTA = 77.9889  
TTPA3 = 1093.95  
TTPA2 = 1085.88  
TTPA1 = 1091.35  
PRT-DE = 6.31626  
PRT-T = 5.95721  
TORQUE = 157.622  
TURNPM = 75614.2

OFFSFT 07:52:50.15  
WMOR = 1.84317  
WNFT = 1.78828  
WMCORR = 0.646895  
WIROR = 0.027247  
LBH412 = 114.551  
SQTHFT = 2.12374  
LBH413 = 0.  
PBAR = 14.0886  
MOROP = 1.78194  
MORT1 = 834.964  
PRRF1 = 30.4902  
PRRF3 = 26.1053  
PSSSF1 = 0.221074  
PSSSF2 = 0.207787  
PSSSA1 = 25.5605  
PSSSA2 = 25.6004  
PBPA1 = 58.1151  
PBPA7 = 58.0354  
PBPF1 = 4.35352  
PBPF7 = 4.16749  
DPAV1 = 53.7616  
DPBP2 = 53.8679

RECORD 11:52:22.55  
EFFTT = 0.479814  
MORP = 95.1695  
IBCUDP = 2.97162  
FM143 = 1190.66  
TUROIIL = 412.482  
CPS410 = 1492.95  
CPS411 = 0.033577  
DENOM = 1047.98  
RBTFFWD = 108.653  
RBTFF = 323.315  
RBTAF = 226.709  
PSNTH1 = 40.4160  
PSNTH2 = 41.7581  
PSNTH3 = 32.9484  
PSNTH4 = 43.3792  
CINPT1 = 0.088199  
CINPT2 = 77.8339  
CINPT3 = 78.2192  
CINPT4 = 78.2724  
PTRD1 = 0.563383  
PTRD2 = 0.527891  
PTRD3 = 0.502540  
PTRD4 = 0.832107

TEST D  
PSDLSA = -0.260534  
PSDDHA = -0.213000  
INTPS1 = 11.6750  
INTPS2 = 11.5421  
CINIT1 = 750.105  
CINIT2 = 754.840  
BNGCRF = 160.586  
TBOR = 265.183  
PTIN = 87.5872  
CURSPD = 35671.9  
PCTSPD = 1.03673  
TIN412 = 1879.80  
TIN413 = 752.472  
TINPB = 1676.75  
CINTTA = 752.472  
CINPTA = 78.1085  
TTPA3 = 1093.66  
TTPA2 = 1085.63  
TTPA1 = 1090.71  
PRT-DE = 6.32316  
PRT-T = 5.96032  
TORQUE = 157.914  
TURNPM = 75758.0

DATA POINT 10



C116 GTP105-2 01 04/04  
INTEGRATED COMPONENTS ASSY TESTING (ICA)

07/03/79

OFFSET 07152:50.15  
WMOR = 2.14109  
WNFT = 2.07695  
WMCORR = 0.646195  
WIROR = 0.032023  
LBH412 = 154.591  
SQTHFT = 2.20166  
LBH413 = 0.054083  
PBAR = 14.0876  
MORDP = 2.02171  
MORT1 = 839.670  
PRRF1 = 34.9810  
PRRF3 = 34.3170  
PSSSF1 = 0.234162  
PSSSF2 = 0.260938  
PSSSA1 = 33.3603  
PSSSA2 = 33.4400  
PBPA1 = 57.8759  
PBPA2 = 57.8228  
PBPF1 = 4.37694  
PBPF2 = 4.52625  
DPRV1 = 53.5490  
DPRV2 = 53.2965

RECORD 12:12:22.55  
EFFTT = 0.514202  
MORP = 116.282  
IBCDDP = 3.47113  
FM143 = 1193.84  
TURQIL = 416.004  
CPS410 = 2018.91  
CPS411 = 0.033577  
DENOM = 1512.75  
RBTFFWD = 109.121  
BBTF = 258.233  
RBTAFF = 223.578  
PSNTH1 = 50.8999  
PSNTH2 = 52.7203  
PSNTH3 = 41.9175  
PSNTH4 = 54.9527  
CINPT1 = 0.101486  
CINPT2 = 96.6757  
CINPT3 = 97.2205  
CINPT4 = 97.7869  
PTRD1 = 0.963934  
PTRD2 = 0.576058  
PTRD3 = 0.340854  
PTRD4 = 0.545637

TEST D  
PSDDSA = -0.413275  
PSDDHA = -0.087511  
INTPS1 = 16.7907  
INTPS2 = 16.7508  
CINTT1 = 762.952  
CINTT2 = 767.941  
BNGCRF = 151.295  
TBOR = 255.974  
PTIN = 105.591  
CORSPD = 34361.2  
PCTSPD = 0.998639  
TIN412 = 2054.61  
TIN411 = 765.956  
TINPB = 1912.77  
CINTTA = 765.447  
CINPTA = 97.0610  
TTPA3 = 1150.77  
TTPA2 = 1191.74  
TTPA1 = 1184.41  
PRT-DE = 7.83097  
PRT-T = 7.18102  
TORQUE = 228.267  
TURRPM = 75651.7

OFFSET 07152:50.15  
WMOR = 2.14258  
WNFT = 2.07834  
WMCORR = 0.646609  
WIROR = 0.032100  
LBH412 = 154.293  
SQTHFT = 2.20042  
LBH413 = 0.  
PBAR = 14.0886  
MORDP = 2.02595  
MORT1 = 839.929  
PRRF1 = 38.9677  
PRRF3 = 34.3170  
PSSSF1 = 0.234362  
PSSSF2 = 0.274225  
PSSSA1 = 33.2275  
PSSSA2 = 33.2939  
PBPA1 = 57.9025  
PBPA2 = 57.8228  
PBPF1 = 4.37694  
PBPF2 = 4.53954  
DPRV1 = 53.5756  
DPRV2 = 53.2832

RECORD 12:12:52.55  
EFFTT = 0.507119  
MORP = 116.217  
IBCDDP = 3.49078  
FM143 = 1195.03  
TURQIL = 414.830  
CPS410 = 2014.11  
CPS411 = 0.  
DENOM = 1519.06  
RBTFFWD = 109.242  
BBTF = 258.395  
RBTAFF = 224.564  
PSNTH1 = 50.8999  
PSNTH2 = 52.7203  
PSNTH3 = 41.9175  
PSNTH4 = 54.9394  
CINPT1 = 0.101486  
CINPT2 = 96.6225  
CINPT3 = 97.1939  
CINPT4 = 97.1939  
PTRD1 = 0.963934  
PTRD2 = 0.578594  
PTRD3 = 0.340854  
PTRD4 = 0.548172

TEST D  
PSDDSA = -0.413276  
PSDDHA = -0.087511  
INTPS1 = 16.8040  
INTPS2 = 16.7243  
CINTT1 = 763.264  
CINTT2 = 768.045  
BNGCRF = 151.507  
TBOR = 256.216  
PTIN = 105.537  
CORSPD = 34391.9  
PCTSPD = 0.999531  
TIN412 = 2051.78  
TIN413 = 765.654  
TINPB = 1918.83  
CINTTA = 765.654  
CINPTA = 97.0035  
TTPA3 = 1153.28  
TTPA2 = 1195.23  
TTPA1 = 1187.92  
PRT-DE = 7.62654  
PRT-T = 7.17626  
TORQUE = 229.145  
TURNPM = 75676.7

DATA POINT 11

AD-A087 838

AIRESEARCH MF6 CO OF ARIZONA PHOENIX F/G 10/2  
ADVANCED TECHNOLOGY COMPONENTS FOR MODEL GTP305-2 AIRCRAFT AUXI--ETC(U)  
FEB 80 J R KIDWELL, G D LARGE F33615-75-C-2016

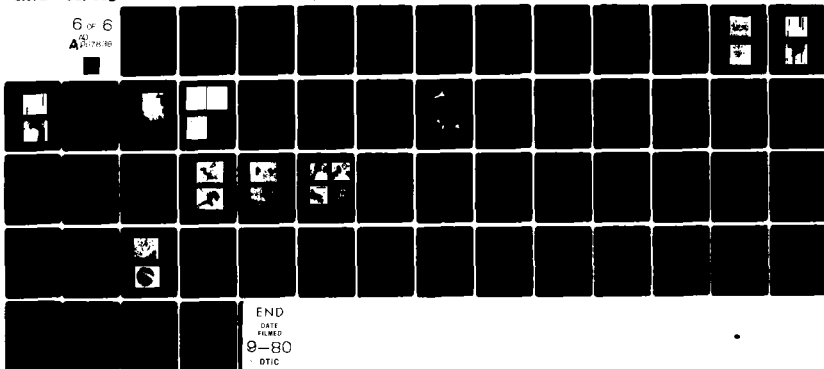
UNCLASSIFIED

AFAPL-TR-79-2106

NL

6 of 6

AD  
A087838



END

DATE

FILED

9-80

DTIC

\*PULLING TEST D ACQUIRED 03-JUL-79. OFFSET TIME: 07152150.15 RECUR TIME: 12112122.55 TIME & DATE REDUCED: 12136 03-JUL-79

C116 GTP105-2 01 04/04  
INTEGRATED COMPONENTS ASSY TESTING (ICA)

07/03/79

LOC. NO.	RAW COUNTS	ENG. VALUE	UNITS	NAME	MASTER NO.	LOC. NO.	RAW COUNTS	ENG. VALUE	UNITS	NAME	MASTER NO.
-20	13161	13161.0000	GAIN	2.5	0	53	9838	1187.7051	DEGF	TTP	6407
-19	13129	13129.0000	GAIN	10	0	54	9808	1192.9016	DEGF	TTP	6408
-18	13127	13127.0000	GAIN	40	0	55	10032	1209.9006	DEGF	TTP	6409
-17	13122	13122.0000	GAIN	160	0	56	9793	1183.0300	DEGF	TTP	6410
-16	13122	13122.0000	GAIN	640	0	57	9698	1173.1655	DEGF	TTP	6411
-15	13120	13120.0000	GAIN	2560	0	58	9539	1156.5670	DEGF	TTP	6412
-14	13119	13119.0000	GAIN	10240	0	59	9455	1147.9636	DEGF	TTP	6413
-13	47	47.0000	MUX	2.5	0	60	9485	1151.0726	DEGF	TTP	6414
-12	38	38.0000	MUX	5	0	61	9234	1125.0778	DEGF	TTP	6415
-11	21	21.0000	MUX	10	0	62	-3073	109.1213	DEGF	RTFWD	6501
-10	16	16.0000	MUX	20	0	63	8144	258.2334	DEGF	RTF	6502
-9	11	11.0000	MUX	40	0	64	6666	238.4139	DEGF	RTAF	6503
-8	12	12.0000	MUX	80	0	65	5554	223.5784	DEGF	RTAF	6504
-7	11	11.0000	MUX	160	0	66	6726	886.9839	DEGF	BORCA	6611
-6	11	11.0000	MUX	320	0	67	5811	875.1129	DEGF	BORCA	6612
-5	9	9.0000	MUX	640	0	71	49	131.2948	DEGF	BNGCRF	6505
-4	10	10.0000	MUX	1280	0	72	3988	255.9743	DEGF	TWOR	6506
-3	11	11.0000	MUX	2560	0	73	-23	149.8447	DEGF	150REV	6604
-2	11	11.0000	MUX	5120	0	74	-8732	31.7631	DEGF	32REFB	6601
-1	11	11.0000	MUX	10240	0	75	6703	1565.7009	DEGF	NOZST	6220
1	4078	14.0876	PSIA	PHAR	548	76	6598	1542.9843	DEGF	NOZST	6221
4	12083	75651.6875	RPM	TURBPM	9700	77	5232	1252.9005	DEGF	NOZST	6222
7	8303	228.2670	FT-LBS	TURBUL	4	78	6035	1422.1694	DEGF	NOZST	6230
8	17189	2018.9122	CPS	FUPLFL	410	79	6236	1464.6434	DEGF	NOZST	6231
9	4	0.0336	CPS	FUPLFL	411	80	-32708	-32708.0000	DEGF	NOZST	6232
10	12032	1193.8358	CPS	MZOUTL	401	81	-5073	-2823.3538	DEGF	NOZST	6240
11	4612	416.0043	CPS	TURBUL	402	82	6597	1542.7383	DEGF	NOZST	6241
12	-3732	2.0217	PSID	MORDP	1420	83	5732	137.9329	DEGF	NOZVPT	6245
13	5805	3.4711	PSID	TBCODP	1401	84	3913	979.7339	DEGF	NOZFLX	6246
14	3395	297.2709	PSIG	FUPLPR	1430	86	824	160.9038	DEGF	GRPUIN	6519
15	3539	17.9578	PSIG	GRUILL	1431	87	808	160.4921	DEGF	GRPUIN	6520
16	-3448	44.8461	PSIG	TUOILL	1432	89	1116	164.7665	DEGF	GRPU2	6514
17	12184	0.3966	GPM	FUGPHL	412	90	-1944	124.1893	DEGF	GRGO	6516
18	4	0.0001	GPM	FUGPHL	413	91	-1985	123.6434	DEGF	GRGO	6516
19	3076	5.6737	VOC	AXN1AP	414	92	-2611	115.2962	DEGF	GRGOUT	6517
26	-8750	31.7910	DEGF	32REFA	6602	93	-2611	115.2161	DEGF	GRGOUT	6518
27	12936	839.6704	DEGF	MORT	6511	94	-5282	79.3855	DEGF	MZOUTL	6530
28	13010	843.4966	DEGF	MORT	6512	95	-459	144.3129	DEGF	MZOUTL	6531
40	-2847	111.4889	DEGF	FUELT	1000	96	-3548	102.7885	DEGF	UOILLN	6532
41	11930	787.5676	DEGF	TBCUT	6105	97	-747	140.9961	DEGF	UOILLN	6533
42	11456	767.9318	DEGF	CINTT	6209	98	2654	185.1087	DEGF	TOILLOT	6534
43	11552	767.9318	DEGF	CINTT	6210	99	1017	163.4569	DEGF	GR801	6513
44	11529	746.5381	DEGF	CINTT	6211	100	6091	144.0989	DEGF	MZSMT	6247
45	-4214	-88.3218	DEGF	CINTT	6212	121	-3375	0.2875	PSIG	VIZEMO	1003
47	9855	1190.7187	DEGF	TTP	6401	122	195	2.5331	PSIG	2.455	1004
48	9855	1190.8080	DEGF	TTP	6402	123	1943	12.1777	PSIG	12.770	1005
49	9855	1190.6393	DEGF	TTP	6403	124	1843	24.5639	PSIG	24.557	1006
50	9727	1174.1760	DEGF	TTP	6404	125	3652	49.1327	PSIG	49.115	1007
51	9587	1161.6483	DEGF	TTP	6405	126	7391	98.2835	PSIG	98.230	1008
57	9813	1161.1077	DEGF	TTP	6406	127	11096	147.5140	PSIG	147.34	1009

DATA POINT 11

\*PULLOG\* TEST D ACQUIRED 03-JUL-79. OFFSET TIME: 07:52:50.15 RECORD TIME: 12:12:22.55 TIME & DATE REDUCED: 12:16 03-JUL-79

CL16 GTV105-2 01 04/04  
INTEGRATED COMPONENTS ASBY TESTING (ICA)

07/03/79

LOC. NO.	RAN COUNTS	ENG. VALUE	UNITS	NAME	MASTER NO.	LOC. NO.	RAN COUNTS	ENG. VALUE	UNITS	NAME	MASTER NO.
128	7976	106.0567	PSIG	PSIPL	3001	189	-3506	0.0031	PSIG	VJZERO	1043
129	8125	108.0366	PSIG	PSIPL	3002	190	969	2.4546	PSIG	VJZERO	1044
130	2	0.1015	PSIG	CINPT	2221	191	9046	12.7704	PSIG	2.455	1045
131	7270	46.4747	PSIG	CINPT	2222	192	9702	26.5939	PSIG	26.557	1046
132	7311	47.2205	PSIG	CINPT	2223	193	19414	49.2151	PSIG	49.115	1047
133	7316	97.2869	PSIG	CINPT	2224	194	951	2.4140	PSIG	PHSS	3509
134	7207	96.9016	PSIG	CINPT	2225	195	981	2.4850	PSIG	PHSS	3510
135	7295	97.0078	PSIG	CINPT	2226	196	1012	2.5636	PSIG	PHSS	3511
136	7291	97.0345	PSIG	CINPT	2227	197	873	2.2112	PSIG	PHSS	3512
137	7277	96.7687	PSIG	CINPT	2228	198	954	2.4166	PSIG	PHSS	3513
138	2808	31.3603	PSIG	PHSSA	3501	199	-3	-0.0096	PSIG	PHSS	3514
139	2811	31.4400	PSIG	PHSSA	3502	200	-350	-0.8994	PSIG	PHSS	3515
140	12	0.2346	PSIG	PHSSA	3503	201	-418	-1.0616	PSIG	PHSS	3516
141	14	0.2606	PSIG	PHSSA	3504	202	-162	-0.4126	PSIG	PHSS	3517
142	4398	57.8759	PSIG	PHSSA	3505	203	-374	-0.9501	PSIG	PHSS	3518
143	3366	57.8228	PSIG	PHSSA	3506	204	381	0.9639	PSIG	PHSS	3519
144	370	4.3269	PSIG	PHSSA	3507	205	228	0.5761	PSIG	PHSS	3520
145	335	4.3263	PSIG	PHSSA	3508	206	151	0.3809	PSIG	PHSS	3521
146	7928	38.9810	PSIG	PHSSA	3509	207	216	0.5456	PSIG	PHSS	3522
147	2604	35.7386	PSIG	PHSSA	3510	208	222	0.5604	PSIG	PHSS	3523
148	2577	34.3170	PSIG	PHSSA	3511	209	211	0.5330	PSIG	PHSS	3524
149	2626	34.9681	PSIG	PHSSA	3512	210	194	0.4899	PSIG	PHSS	3525
150	1	0.0882	PSIG	PHSSA	3513	211	250	0.6318	PSIG	PHSS	3526
151	1829	50.8999	PSIG	PHSSA	3514	212	342	0.8651	PSIG	PHSS	3527
152	3682	52.7203	PSIG	PHSSA	3515	213	342	0.8651	PSIG	PHSS	3528
153	3169	41.9175	PSIG	PHSSA	3516	214	120	0.3023	PSIG	PHSS	3529
154	4130	54.9527	PSIG	PHSSA	3517	215	230	0.5811	PSIG	PHSS	3530
155	3297	43.6641	PSIG	PHSSA	3518	216	-339	-0.8614	PSIG	PHSS	3531
156	2997	39.8978	PSIG	PHSSA	3519	217	-143	-0.3645	PSIG	PHSS	3532
157	3643	52.7336	PSIG	PHSSA	3520	218	-165	-0.4302	PSIG	PHSS	3533
158	3257	43.3526	PSIG	PHSSA	3521	219	-2	-0.0070	PSIG	PHSS	3534
159	7202	95.7721	PSIG	PHSSA	3522	220	-31	-0.0606	PSIG	PHSS	3535
160	6951	97.4370	PSIG	PHSSA	3523	221	-2	-0.0070	PSIG	PHSS	3536
161	1238	16.7907	PSIG	PHSSA	3524	222	-51	-0.1312	PSIG	PHSS	3537
162	1255	16.7506	PSIG	PHSSA	3525	223	-51	-0.1312	PSIG	PHSS	3538
163	1246	16.4047	PSIG	PHSSA	3526	224	-113	-0.2484	PSIG	PHSS	3539
164	1240	16.5515	PSIG	PHSSA	3527	225	-102	-0.2605	PSIG	PHSS	3540
165	-507	0.4542	PSIG	PHSSA	3528	226	-103	-0.2631	PSIG	PHSS	3541
170	75	2.7803	PSIG	PHSSA	3529	227	-142	-0.3619	PSIG	PHSS	3542
171	391	13.0246	PSIG	PHSSA	3530	228	-107	-0.2732	PSIG	PHSS	3543
172	751	24.7177	PSIG	PHSSA	3531	229	-65	-0.1667	PSIG	PHSS	3544
173	1505	45.2085	PSIG	PHSSA	3532	230	-57	-0.1665	PSIG	PHSS	3545
174	3015	98.2553	PSIG	PHSSA	3533	231	-60	-0.1541	PSIG	PHSS	3546
175	4531	147.4968	PSIG	PHSSA	3534	232	-62	-0.1591	PSIG	PHSS	3547
176	3570	114.2824	PSIG	PHSSA	3535	233	-63	-0.1617	PSIG	PHSS	3548
177	3506	113.5539	PSIG	PHSSA	3536						

DATA POINT 11

APPENDIX D

MODEL GTP305-2 AUXILIARY POWER UNIT  
AF2-1DA ALLOY FORGING

(44 Pages)

## APPENDIX D

### MODEL GTP305-2 AUXILIARY POWER UNIT AF2-1DA ALLOY FORGING

#### INTRODUCTION

The original AiResearch Model GTP305-1 Auxiliary Power Unit (APU) radial turbine rotor design, required a forging of AF2-1DA alloy. A cast AF2-1DA alloy rotor was designed and tooled as a means of cost reduction for the AiResearch Model GTP305-2 APU. Casting and heat treatment processes were developed under the Air Force Materials Laboratory (AFML) engine demonstration program.

Air Force Model GTP305-2 APU applications require specific low-cycle-fatigue (LCF) life of the rotating components to satisfy projected service-life requirements. However, cast AF2-1DA alloy radial turbine wheels were projected to have marginal LCF properties in the as-cast and heat treated condition. Therefore, hot isostatic pressing (HIP) was proposed to improve fatigue life by closing casting microshrinkage and eliminating crack initiation sites (Air Force Contract F33615-75-C-2016, General Electric Company). Demonstration of this phenomenon was previously accomplished during Air Force and AiResearch programs on cast INCO 713LC radial turbine wheel, used in a commercial APU, that is currently in production.

A program was proposed to AFML to investigate HIP and subsequent heat treatment, as a means of improving the Model GTP305-2 APU radial turbine wheel LCF life. This effort was funded as an add-on to an existing Air Force Propulsion Laboratory contract for unit design and rig testing (Contract Number F33615-75-C-2016). The AFML program consisted of two tasks:

- o Task I - Characterization of Baseline Material

o Task II - Application and Evaluation of HIP and Revised Heat Treatment

Under Task I, the determination of mechanical properties and microstructures of the baseline Model GTP305-2 cast AF2-1DA radial turbine wheel was accomplished. Previously developed baseline heat treatment was used on these turbine wheel castings. Room temperature LCF baseline material properties and elevated temperature tensile and stress-rupture strengths were determined using test bars removed from cast turbine wheel hub sections.

In Task II, evaluation of HIP/heat treat process combinations was performed to assess AF2-1DA LCF property response. Four different HIP cycles and four heat treatments were used in eight combinations. Material property data screening (room temperature tensile and elevated temperature stress-rupture) was conducted to select four final candidate HIP/heat treat combinations for room temperature strain controlled LCF evaluation.

The ultimate objective was to establish a manufacturing process for HIP and subsequent heat treatment utilizing Air Force manufacturing technology funding.

## SECTION II

### SUMMARY

Forty AF2-1DA alloy radial turbine wheels were cast and X-ray inspected. Thirty-eight wheels were free of obvious defects and selected for evaluation. As-cast elevated temperature tensile strength was measured and as-cast/heat treated tensile and stress-rupture properties were determined. Eight wheels were HIPped in four combinations with temperatures varying from 2150 to 2250°F, pressures of 15 or 29 ksi, and a constant three-hour time period. Four solution heat treatment temperatures were selected based on a previous investigation to cast a modified AF2-1DA alloy composition (AFML Contract Number F33615-71-C-1573). Evaluations were performed using four HIP conditions and eight HIP/heat treatment combinations of four wheels each. Samples were examined metallographically and tensile and stress-rupture properties were determined. Four HIP/heat treatment combinations were selected for LCF testing on the basis of acceptable microstructures and mechanical properties. Room temperature strain-control LCF tests were performed and results analyzed on a Weibull distribution. Data analysis indicated that LCF life improvement was obtained through HIP and heat treatment. Specifically, a 3X LCF life improvement was achieved for as-cast wheels predicted to fail in less than 1000 cycles.



SECTION III  
TECHNICAL DISCUSSION

3.1 Task I - Characterization of Baseline Material

The AF2-1DA alloy radial turbine wheel castings evaluated were procured from AiResearch Casting Company (ACC), Torrance, CA. A typical Model GTP305-2 radial turbine wheel casting is shown in Figure 164 (Page 274). Wheel serial numbers, master heat numbers (from Cannon-Muskegon Corp.) and cast AF2-1DA alloy chemistry are presented in Table D-1.

Forty cast AF2-1DA turbine wheels were X-ray inspected for hub defects. Thirty-eight were defect free while two showed possible inclusions near the center (S/N 62 and S/N 94). These two castings were not used for evaluation.

One wheel (S/N 40) was sectioned to examine the internal and surface grain structure Figure 165 (Page 275). Internal and external grain structures were compared with previous Model GTP305-2 castings and were comparable. Elevated temperature tensile tests were performed on the material from wheel S/N 40, to determine material strengths at typical HIP temperatures. Results of the four bars (0.179 inch diameter by 1.0 inch gauge), tested at 2200°F, are presented in Table D-2. Average measured ultimate strength was 4500 psi and measured elongations varied from 4.3 to 18.5 percent. No explanation was evident for the ductility spread based on location of the test specimens or the grain size of the etched test bar gauge sections. The ductility spread is considered to be due to a coarse grain that behaved as a properly oriented single crystal.

TABLE D-1. SERIAL NUMBER, MASTER HEAT NUMBER AND  
CAST AF2-1DA ALLOY CHEMISTRY

Wheel S/N	Master Heat No.	Wheel S/N	Master Heat No.	Wheel S/N	Master Heat No.
40	VF43	60	VE947	81	VE955
41	↓	61	↓	82	↓
45		63		83	
48		64		88	
51		66		89	
62		67		90	
68		69		91	
73		70		92	
79		71		93	
80		72		94	
85		74		95	
86		75		96	
87		76			
		77			
		78			

Specification Chemistry		Cannon-Muskegon Corp.		
Range		Master Heat No. Chemistry		
Element	Weight Percent	VF43	VE947	VE955
Carbon	0.12-0.16	0.13	0.13	0.12
Cobalt	9.5-10.5	9.8	9.8	9.8
Chromium	11.0-12.0	11.7	11.7	11.4
Molybdenum	2.7-3.3	3.1	3.0	3.0
Tantalum	1.4-2.0	2.0	2.0	1.92
Titanium	2.5-2.9	2.9	2.8	2.8
Aluminum	4.4-4.8	4.7	4.7	4.7
Tungsten	4.5-5.5	4.8	4.9	4.7
Hafnium	0.9-1.3	1.2	1.1	1.1
Boron	0.010-0.018	0.011	0.014	0.016
Zirconium	0.03-0.07	0.038	0.035	0.037
Iron	0.25 max	<0.20	<0.20	<0.20
Silicon	0.25 max	<0.20	<0.20	<0.20
Manganese	0.25 max	<0.20	<0.20	<0.15
Sulfur	0.015 max	<0.01	<0.01	<0.01
Phosphorus	0.015 max	<0.01	<0.01	<0.01
Nickel	Bal	Bal	Bal	Bal

TABLE D-2. 2200°F TENSILE PROPERTIES OF AS-CAST  
AF2-1DA ALLOY MEASURED ON TEST BARS  
MACHINED FROM A TURBINE WHEEL

Specimen Number	0.2% YS (psi)	UTS (psi)	EL (%)	RA (%)
40-3	3400	4400	4.3	7.8
40-7	2800	4000	6.9	12.7
40-5	3600	4600	18.0	24.6
40-8	3500	4900	18.5	29.5

YS = Yield Strength  
 UTS = Ultimate Tensile Strength  
 EL = Elongation  
 RA = Reduction of Area

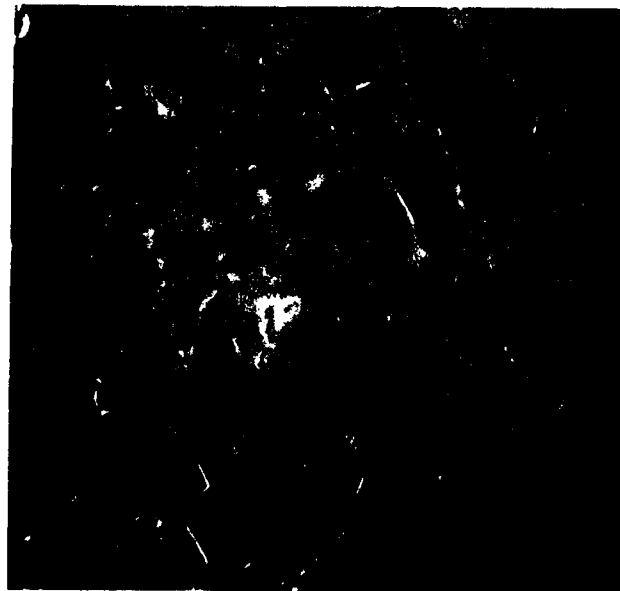
### 3.1.1 Heat Treated AF2-1DA

Five cast wheels (S/Ns 72, 75, 81, 83, and 87) were selected to establish the heat-treated (un-HIPped) baseline properties. Heat treatment cycles, as developed in the basic GTP305-2 APU program were as follows:

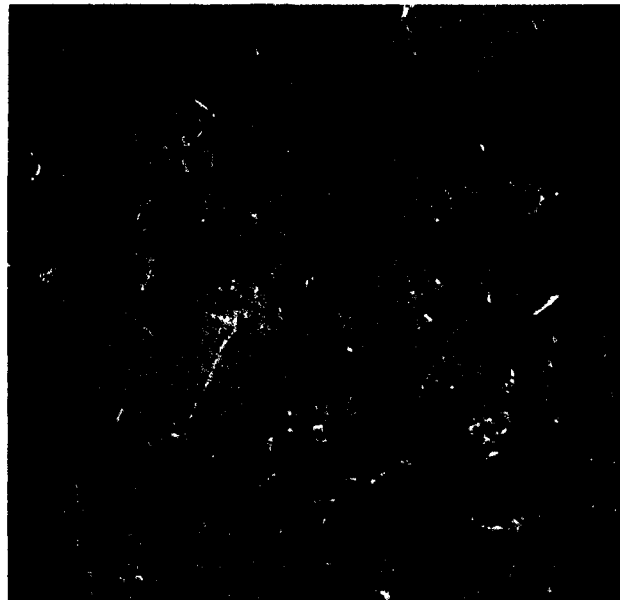
- o Solution: 2175  $\begin{smallmatrix} +20 \\ -0 \end{smallmatrix}$ °F/2 hours/gas cool
- o Intermediate Age: 1950  $\pm 25$ °F/2 hours/gas cool
- o Age: 1400  $\pm 25$ °F/16 hours/air cool

Solution treatments were performed in a vacuum furnace capable of heat treating up to sixteen wheels and obtaining a designated cooling rate of 45 to 50°F per minute (observed by gas cooling) from the solution and intermediate age temperatures. Cooling rates from the 2175°F solution, and 1950°F intermediate age temperature, were determined using a thermocouple inserted in the hub section of a scrap turbine wheel casting. This procedure provided an accurate measurement of the hub section cooling rate. After heat treatment, the five castings were fluorescent penetrant inspected with no evidence of surface cracks.

Scanning Electron Microscope (SEM) evaluation of the as-cast and heat-treated baseline material was performed. Figures D-1 and D-2 show SEM micrographs at 100 and 500X magnifications, respectively. The as-cast microstructure exhibits typical primary MC carbides, gamma/gamma prime eutectic cooling gamma prime and the absence of grain boundary precipitates. Microstructural changes observed after heat treatment, were the appearance of grain boundary precipitates and a reduction of gamma prime size, as shown in Figure D-3. Small amounts of undissolved cooling gamma prime are also evident.



AS CAST (100X)

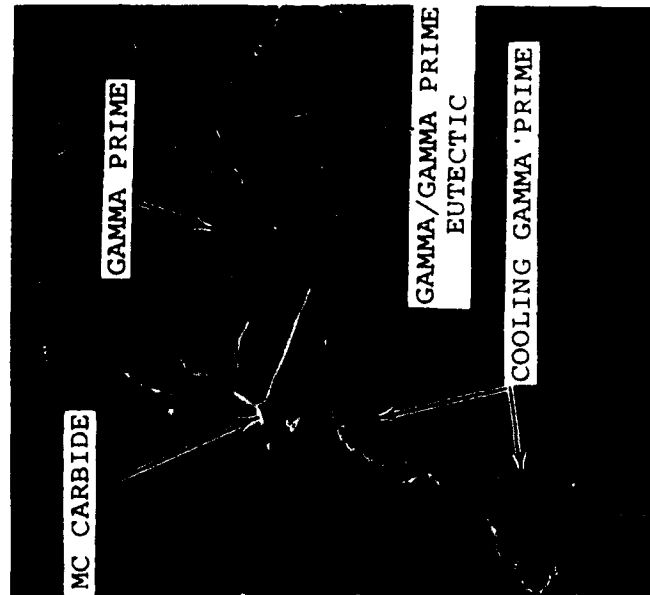


HEAT TREATED (100X)

Figure D-1. SEM micrographs of as-cast and heat-treated microstructure of the hub region of the GTP305-2 turbine casting



AS CAST (500X)

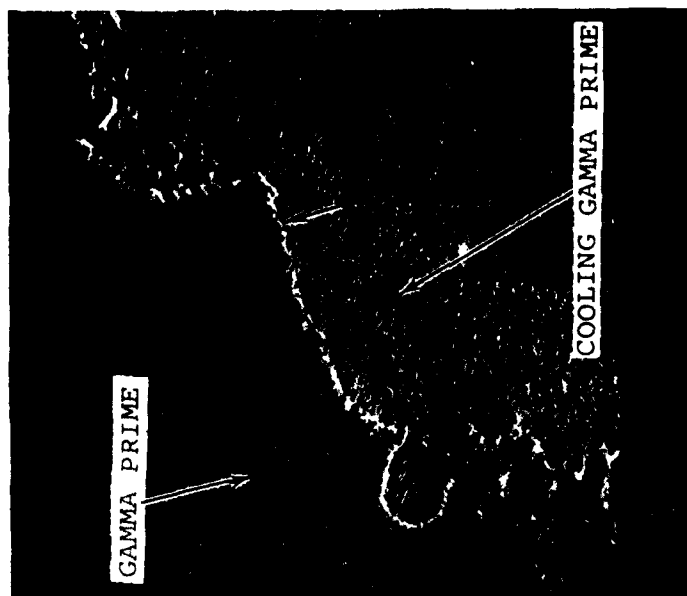


HEAT TREATED (500X)

Figure D-2. SEM micrographs of as-cast and heat-treated microstructure of the hub region of the GTP305-2 turbine casting



AS CAST (1000X)



HEAT TREATED (1000X)

Figure D-3. SEM micrographs of as-cast and heat-treated microstructure showing grain boundary areas (arrows)

### 3.1.2 Mechanical Property Determinations

Location of mechanical property test specimens removed from the castings is shown in Figure D-4. Tensile and stress-rupture testing were performed at Joliet Metallurgical Laboratories, Inc., Joliet, Illinois, and low-cycle-fatigue (LCF) testing at Mar-Test Inc., Cincinnati, Ohio.

Results of tensile tests performed on 0.250-inch diameter by 1.0-inch gauge test bars at room temperature and 1400°F, are presented in Table D-3. Room-temperature ultimate strength of specimen number 75-3 and room-temperature elongation measurements on all specimens were slightly below specification minimums. Tensile properties obtained at 1400°F were above specification minimums. Examination of room-temperature tensile test bar fracture surfaces was performed using a Scanning Electron Microscope (SEM) in an attempt to explain elongation measurements of less than 5 percent. SEM examination of fracture surfaces revealed evidence of microporosity on all room-temperature tensile test bars (Specimens No. 72-3, 75-3, and 83-5). The degree of microporosity observed appeared to be typical for as-cast superalloy turbine wheels. SEM micrographs of the microporosity observed on the test bar fracture surfaces are shown in Figure D-5. No evidence of any anomaly was found to explain elongation measurements of less than 5 percent.

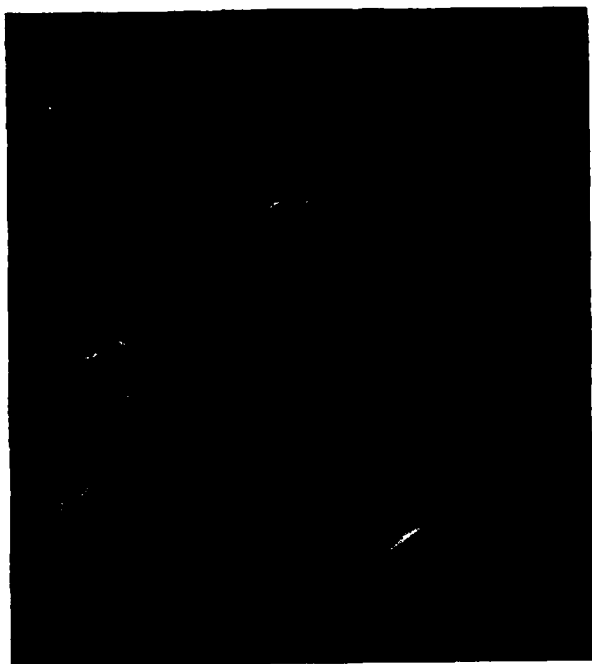
Stress-rupture testing was performed using 0.250-inch diameter by 1.0-inch gauge test bars at 1400, 1600, and 1800°F, utilizing stresses that were selected to give an average rupture life of 100 hours. Results are presented in Table D-4. As shown, rupture times and ductilities were above specification minimums when rupture times versus stresses are plotted on a Larson-Miller parameter basis (see Figure D-6).





1 and 2, LOW-CYCLE-FATIGUE  
4 and 6, CREEP-RUPTURE  
3 and 5, TENSILE  
7 and 8, TENSILE (AS-CAST CONDITION)

Figure D-4 Location of test specimens for mechanical property testing



SPEC. NO. 72-3



SPEC. NO. 75-3

Figure D-5. SEM micrographs (500%) showing microporosity (arrows) on fracture surfaces of room temperature tensile tested bars from baseline as-cast and heat-treated GTP305-2 turbine wheel castings



SPEC. NO. 83-5

TABLE D-4. ELEVATED TEMPERATURE STRESS RUPTURE  
PROPERTIES OF HEAT-TREATED\* (UN-HIPped)  
CAST AF2-1DA ALLOY TURBINE WHEELS

Specimen Number	Temperature (°F)	Stress (ksi)	Hours to Rupture	EL (%)	RA (%)
72-6	1400	90	152.4	4.0	10.6
81-4	1400	90	102.7	4.3	8.0
75-4	1600	55	158.8	7.9	11.2
83-6	1600	55	161.4	6.2	8.9
81-6	1800	27	89.0	7.8	16.2
87-4	1800	27	97.1	8.3	16.7
Property Specifica- tion Minimums	1400 1800	95 30	23.0 23.0	3.0 4.0	

\*2175°F for 2 hours with Argon Quench; plus 1950°F for 2 hours with Argon Quench; plus 1400°F for 16 hours with air cooling.

EL = Elongation  
RA = Reduction of Area

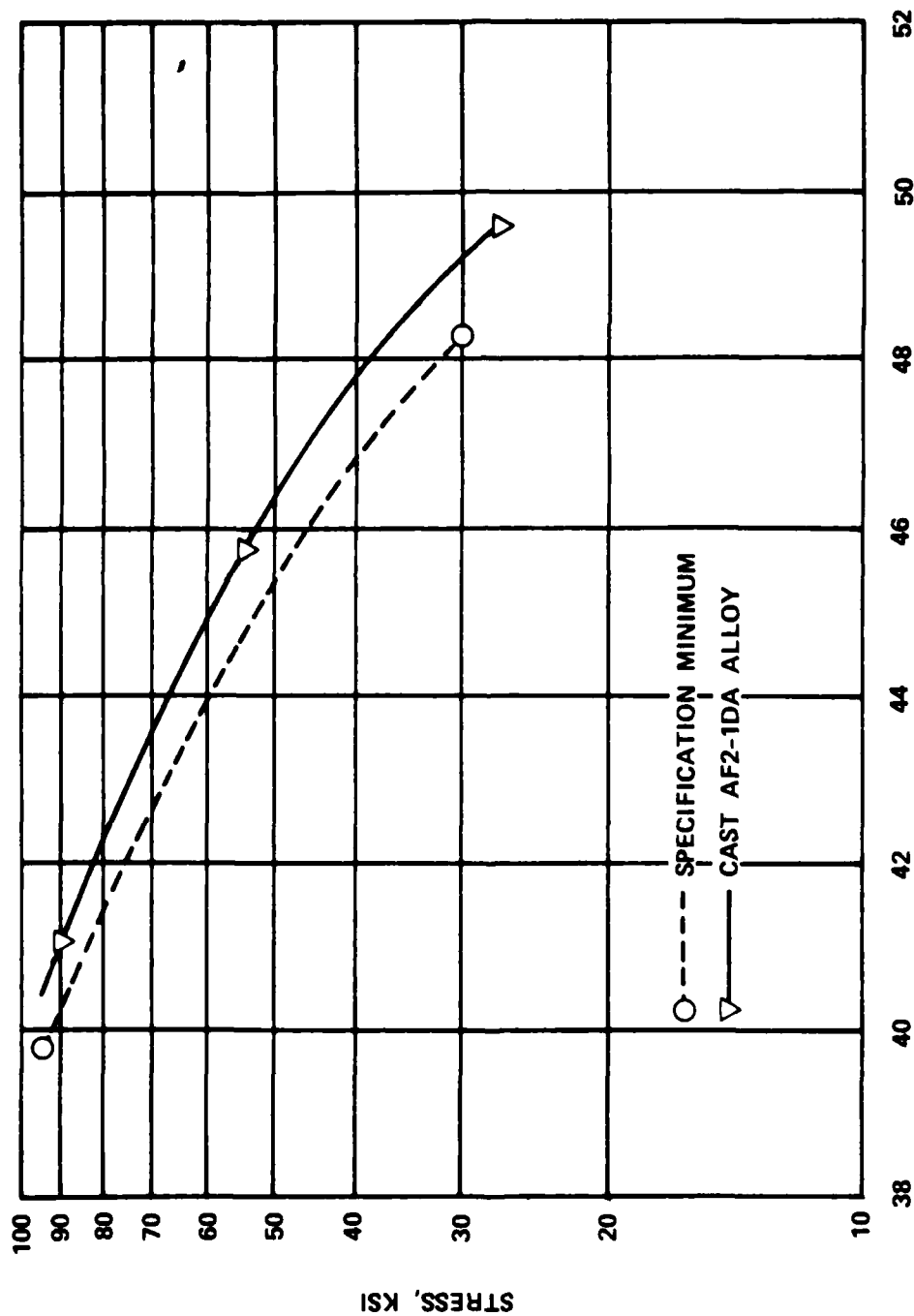


Figure D-6. Average stress-rupture test results of heat-treated (un-hipped) cast AF2-1DA alloy turbine wheels compared to specification minimums

Axial strain controlled LCF testing was conducted at room temperature using the specimen configuration shown in Figure D-7. This data, as shown in Table D-5, was used as the data base with which the HIPped AF2-1DA material was compared (Task II). Baseline LCF properties were measured using an A-ratio of infinity ( $\infty$ ).

SEM examination of the LCF test bar fracture surfaces revealed that origins were associated with primary MC carbides and initiated on the bar external surface. Some microporosity was observed near the origins.

### 3.2 Task II - Application and Evaluation of HIP and Revised Heat Treatment

Parameters for HIP of various alloys have been developed by AFML (GE refined) and various other companies. A large production cast radial turbine wheel for superalloy INCO 713LC is now being HIPped using AiResearch developed parameters.

#### 3.2.1 HIP and Heat Treatment

Thirty two cast AF2-1DA turbine wheels were selected and prepared (riser portion of wheel removed) for HIP. Four HIP runs were made using eight turbine wheels per run. Three runs were made at Industrial Materials Technology (IMT), Woburn, Mass., with the parameters shown below. These parameters were selected to cover the range currently in use for cast superalloys.

- o 2200  $\pm$ 25°F for 3 hours at 15,000 psi, argon
- o 2225  $\pm$ 25°F for 3 hours at 15,000 psi, argon
- o 2250  $\pm$ 25°F for 3 hours at 15,000 psi, argon



SAMPLE 72-4



SAMPLE 81-5

Figure D-7. Microstructure of as cast AF2-1DA showing typical shrinkage porosity  
Mag: 400X Etch: Electrolytic oxalic acid

TABLE D-5. ROOM TEMPERATURE LOW-CYCLE FATIGUE (LCF)  
 PROPERTIES OF HEAT-TREATED\* (UN-HIPPED)  
 CAST AF2-1DA ALLOY TURBINE WHEELS

Specimen Number	Total Strain Range (%)	Measured Modulus (E times 10 <sup>6</sup> psi)	Cycles to Failure
72-1	0.77	26.1	3,957
87-2	0.69	29.0	14,894
75-1	0.66	30.9	7,974
75-2	0.65	31.3	17,722
83-1	0.62	32.9	13,182
83-2	0.60	33.3	8,932
81-1	0.60	33.1	10,111
87-1	0.60	33.8	13,221

Test Parameters: Axial Strain Control, A Ratio =  $\infty$   
 20 CPM Frequency and 200 KSI  
 Pseudo-Stress

\*2175°F for 2 hours with Argon Quench; Plus  
 1950°F for 2 hours with Argon Quench; Plus  
 1400°F for 16 hours with air cooling.

The fourth run was made at Battelle Memorial Institute (BMI), Columbus, Ohio, at conditions of  $2150 \pm 25^{\circ}\text{F}$  for 3 hours at 29,000 psi, argon. These HIPped turbine wheels were heat-treated using the HIP/heat treatment combinations as shown in Table D-6.

### 3.2.2 Mechanical Property Determinations

After heat treatment, the turbine wheels were processed to obtain material for mechanical property (tensile, stress-rupture, and LCF) testing and metallographic examination. Tensile test results performed on 0.250-inch diameter by 1-inch gauge section bars are shown in Tables D-7 and D-8 for room temperature and  $1400^{\circ}\text{F}$  respectively. Tensile test results showed a trend toward slightly reduced ultimate strength and increased ductility, when compared with the as-cast baseline. Stress-rupture test results performed on 0.250-inch diameter by 1-inch gauge section bars are presented in Tables D-9, D-10 and D-11 for 1400, 1600, and  $1800^{\circ}\text{F}$  respectively. Although most test results exceeded AiResearch specification minimums, the  $1400^{\circ}\text{F}$  stress-rupture properties were poor on material HIPped at  $2150^{\circ}\text{F}$  and solution treated at  $2175^{\circ}\text{F}$ .

The general trends of HIP/heat treat processing parameters on stress-rupture life were:

- o Equivalent to higher average rupture life at 1400, 1600 and  $1800^{\circ}\text{F}$  utilizing a higher solution heat treatment with a given HIP condition
- o Equivalent to slightly lower average rupture life at 1400, 1600 and  $1800^{\circ}\text{F}$  (with the exception noted above) after HIP/heat treat processing compared to the un-HIPped heat treated baseline



TABLE D-6. HIP/HEAT TREATMENT COMBINATIONS

<u>Combination</u>	<u>No. of Wheels</u>
HIP A + HT1	4
HIP A + HT3	4
HIP B + HT1	4
HIP B + HT3	4
HIP C + HT1	4
HIP C + HT2	4
HIP D + HT1	4
HIP D + HT4	4

HIP Parameters

A = 2150°F/29 KSI/3 hours

B = 2200°F/15 KSI/3 hours

C = 2250°F/15 KSI/3 hours

D = 2250°F/15 KSI/3 hours

Heat Treatment

HT1 = 2175°F (2 hours), plus 1950°F (2 hours), plus 1400°F (16 hours)

HT2 = 2210°F (2 hours), plus 1950°F (2 hours), plus 1400°F (16 hours)

HT3 = 2250°F (2 hours), plus 1950°F (2 hours), plus 1400°F (16 hours)

HT4 = 2250°F (2 hours), plus 1950°F (2 hours), plus 1400°F (16 hours)

TABLE D-7. ROOM TEMPERATURE TENSILE PROPERTIES OF HIPped  
AND HEAT-TREATED\* CAST AF2-1DA TURBINE WHEELS

Specimen Number	HIP Parameter (°F/ksi/hrs)	Solution Temp(°F)	0.2% YS (ksi)	UTS (ksi)	EL (%)	RA (%)
51-3	2150/29/3	2175	121.6	135.2	7.3	12.1
77-3	↓	↓	122.0	131.6	6.9	6.9
88-3	↓	↓	125.8	144.9	6.6	10.4
45-3	↓	2225	119.6	128.2	6.3	14.2
64-3	↓	↓	130.0	133.1	3.4	6.4
91-3	↓	↓	124.4	133.0	3.9	11.5
41-3	2220/15/3	2175	127.6	144.3	4.9	9.4
60-3	↓	↓	119.4	138.0	7.2	9.6
95-3	↓	↓	123.3	130.4	4.4	8.9
69-3	↓	2225	119.7	128.3	5.6	8.5
78-3	↓	↓	126.8	142.9	5.9	8.9
82-3	↓	↓	128.0	143.2	5.7	9.9
48-3	2225/15/3	2175	121.4	123.9	3.9	13.7
63-3	↓	↓	124.6	131.7	4.6	15.0
93-3	↓	↓	124.8	135.0	5.3	10.8
68-3	↓	2210	120.6	131.3	6.6	13.5
76-3	↓	↓	119.5	132.2	7.5	9.1
80-3	↓	↓	127.8	139.0	5.6	11.9
66-3	2250/15/3	2175	129.3	130.3	6.1	13.0
86-3	↓	↓	119.0	127.5	6.6	16.9
92-3	↓	↓	127.7	135.8	4.8	12.0
61-3	↓	2250	123.9	139.6	3.9	11.9
67-3	↓	↓	121.3	134.4	8.9	13.0
89-3	↓	↓	117.2	122.8	7.5	17.4
Property Specification Minimum			115.0	130.0	5.0	-

\*At indicated solution temperature for 2 hours with Argon quench; plus 1950°F for 2 hours with Argon quench; plus 1400°F for 16 hours with air cooling.

HIP = Hot Isostatic Pressing

YS = Yield Strength

UTS = Ultimate Tensile Strength

EL = Elongation

RA = Reduction Area

TABLE D-8. 1400°F TENSILE PROPERTIES OF HIPped AND  
HEAT-TREATED\* CAST AF2-1DA TURBINE WHEELS

Specimen Number	HIP Parameter (°F/ksi/hrs)	Solution Temp(°F)	0.2% YS (ksi)	UTS (ksi)	EL (%)	RA (%)
51-5	2150/29/3	2175	106.7	133.4	7.0	13.0
77-5	↓	↓	111.4	140.0	7.1	10.5
96-5	↓	↓	114.0	142.0	4.9	11.8
64-5	↓	2225	117.8	128.1	4.9	9.1
73-5	↓	↓	120.3	146.9	5.6	11.1
91-5	↓	↓	114.9	149.4	7.8	8.3
41-5	2200/15/3	2175	109.0	144.5	8.1	10.9
71-5	↓	↓	111.7	130.3	5.6	11.1
95-5	↓	↓	105.9	126.7	5.6	13.8
78-5	↓	2225	118.8	143.6	5.9	10.8
82-5	↓	↓	110.8	149.1	5.7	10.3
90-5	↓	↓	104.8	133.6	8.9	13.7
63-5	2225/15/3	2175	112.6	138.8	6.5	15.5
79-5	↓	↓	108.0	139.1	6.0	10.3
93-5	↓	↓	105.4	140.6	9.0	13.3
76-5	↓	2210	105.9	142.7	7.9	11.5
80-5	↓	↓	109.9	136.0	6.4	13.8
85-5	↓	↓	111.8	137.7	7.3	9.3
70-5	2250/15/3	2175	114.6	146.0	6.9	16.4
86-5	↓	↓	106.1	139.7	7.7	11.6
92-5	↓	↓	105.6	131.2	5.9	11.2
61-5	↓	2250	112.1	145.7	8.9	12.8
74-5	↓	↓	109.7	134.7	6.4	11.8
89-5	↓	↓	107.1	111.9	2.7	5.1
Property Specification Minimum			105.0	130.0	5.0	-

\*At indicated solution temperature for 2 hours with Argon quench; plus 1950°F for 2 hours with Argon quench; plus 1400°F for 16 hours with air cooling.

HIP = Hot Isostatic Pressing

YS = Yield Strength

UTS = Ultimate Tensile Strength

EL = Elongation

RA = Reduction Area

TABLE D-9. 1400°F CREEP-RUPTURE PROPERTIES OF HIPped AND HEAT-TREATED* CAST AF2-1DA TURBINE WHEELS							
Specimen Number	HIP Parameter (°F/ksi/hrs)	Solution Temp(°F)	Temp (°F)	Stress (ksi)	Rupture Time (Hours)	EL (%)	RA (%)
51-4	2150/29/3	2175	1400	95	9.6	3.6	15.9
96-6	↓	2175	↓	↓	20.9	3.4	9.2
45-4	↓	2225	↓	↓	69.1	3.5	10.0
91-6	↓	2225	↓	↓	75.1	4.8	12.7
41-4	2200/15/3	2175	↓	↓	91.5	4.6	12.2
95-6	↓	2175	↓	↓	12.6	4.0	13.8
69-4	↓	2225	↓	↓	76.3	3.6	8.4
82-6	↓	2225	↓	↓	24.3	4.2	13.8
48-4	2225/15/3	2175	↓	↓	44.2	4.2	10.1
93-6	↓	2175	↓	↓	53.5	5.6	9.5
68-4	↓	2210	↓	↓	28.6	3.8	13.0
80-6	↓	2210	↓	↓	133.1	6.3	11.3
66-4	2250/15/3	2175	↓	↓	64.0	5.0	10.1
92-6	↓	2175	↓	↓	23.3	6.1	13.3
61-4	↓	2250	↓	↓	71.9	5.2	6.9
67-4	↓	2250	↓	↓	54.0	5.5	12.3
Specification Minimum					23.0	3.0	-

\*At indicated solution temperature for 2 hours with Argon quench; plus 1950°F for 2 hours with Argon quench; plus 1400°F for 16 hours with air cooling.

HIP = Hot Isostatic Pressing

EL = Elongation

RA = Reduction Area

TABLE D-10. 1600°F CREEP-RUPTURE PROPERTIES OF HIPPED AND HEAT-TREATED* CAST AF2-1DA TURBINE WHEELS							
Specimen Number	HIP Parameter (°F/ksi/hrs)	Solution Temperature (°F)	Temperature (°F)	Stress (ksi)	Rupture Time (Hours)	EL (%)	RA (%)
51-6	2150/29/3	2175	1600	60	68.8	12.0	17.9
77-4		2175			53.5	9.9	10.9
64-4	2200/15/3	2225			87.3	7.1	8.6
73-6		2225			89.9	8.5	8.9
41-6	2225/15/3	2175			41.5	10.5	24.3
60-4		2175			60.0	10.2	15.1
69-6	2225/15/3	2225			58.7	11.2	16.7
90-4		2225			68.5	8.0	9.5
63-4	2225/15/3	2175			50.4	9.9	14.1
79-6		2175			51.8	7.3	18.2
76-4	2250/15/3	2210			82.8	6.9	8.9
85-4		2210			84.1	6.0	7.5
70-6		2175			57.7	8.5	16.6
84-4		2175			39.5	8.8	15.1
67-6		2250			61.3	6.0	11.4
89-4		2250			2.0	1.9	1.9

\*At indicated solution temperature for 2 hours with argon quench; plus 1950°F for 2 hours with argon quench; plus 1400°F for 16 hours with air cooling.

HIP = Hot Isostatic Pressing

EL = Elongation

RA = Reduction Area

TABLE D-11. 1800°F CREEP-RUPTURE PROPERTIES OF HIPPED AND HEAT-TREATED* CAST AF2-1DA TURBINE WHEELS							
Specimen Number	Solution HIP Parameter (°F/ksi/hrs)	Temperature (°F)	Temperature (°F)	Stress (ksi)	Rupture Time (Hours)	EL (%)	RA (%)
77-6	2150/29/3	2175	1800	30	46.8	13.9	17.3
88-4		2175			48.7	13.2	28.0
64-6	2200/15/3	2225			66.4	7.5	15.3
91-4		2225			40.7	10.1	21.6
71-6	2225/15/3	2175			55.2	9.8	14.3
95-4		2175			37.5	11.8	25.7
78-4	2225/15/3	2225			46.8	11.5	24.0
90-6		2225			55.5	13.4	23.7
63-6	2225/15/3	2175			57.1	7.0	8.5
93-4		2175			38.0	9.0	23.3
76-6	2250/15/3	2210			40.1	8.8	12.0
85-6		2210			42.3	8.5	17.5
86-6	2250/15/3	2175			38.0	7.2	10.5
92-4		2175			41.1	11.0	20.9
89-6		2250			51.2	11.7	21.9
89-6					37.5	11.1	18.8
Specification Minimum					23.0	4.0	-

\*At indicated solution temperature for 2 hours with argon quench; plus 1950°F for 2 hours with argon quench; plus 1400°F for 16 hours with air cooling.

HIP = Hot Isostatic Pressing

EL = Elongation

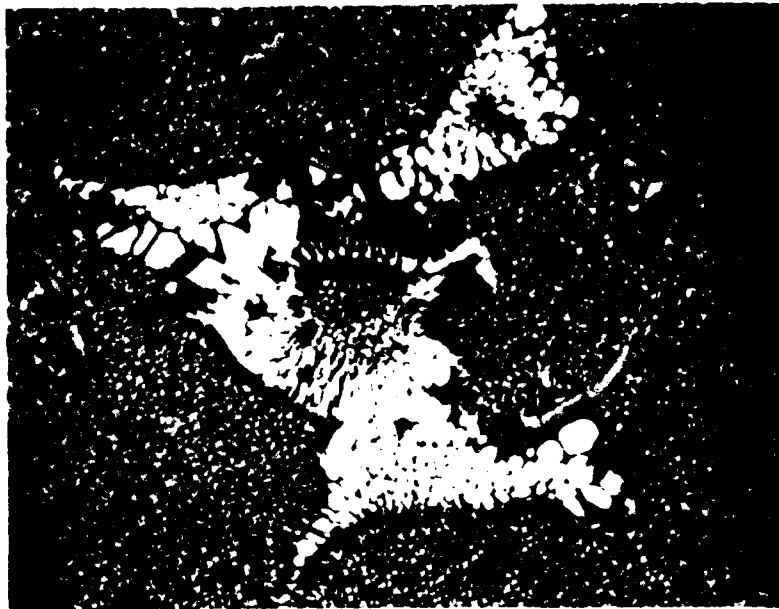
RA = Reduction Area

### 3.2.3 Metallographic Study

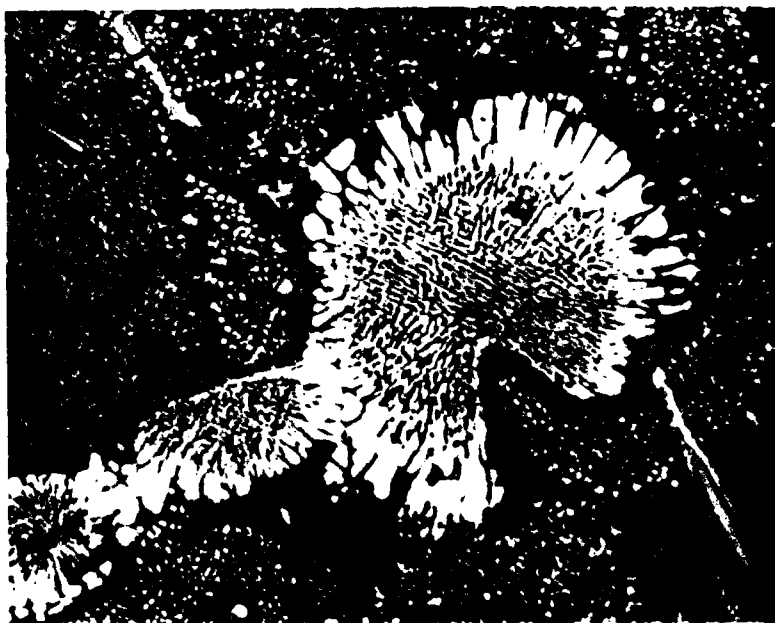
Microstructural studies were performed on each HIP/heat treatment combination and results compared with the as-cast and heat treated baseline material. Figure D-7, previously included, shows the as-cast material with typical shrinkage voids in cast AF2-1DA. Material HIPped at 2150 and 2200°F is shown in Figure D-8. No evidence of voids was detected indicating closure by HIP. Figure D-9 shows material HIPped at 2225 (void free) and 2250°F, (voids due to incipient melting) during HIP. HIP temperatures of 2225, 2200 and 2150°F, resulted in closed porosity, while 2250°F caused voids and partial solutioning of the gamma/gamma prime eutectic phase in the microstructure.

The effects of solution heat treating temperature on void formation due to incipient melting is shown in Figure D-10. As can be seen, no voids are evident in the 2175 and 2210°F solution heat treated microstructures. The 2225 and 2250°F solution heat treated microstructures exhibit void formation caused by incipient melting. Effects of solution temperature on cooling gamma prime and gamma/gamma prime eutectic phases after HIP compared with as-cast and heat treated baseline material were:

- o More undissolved cooling gamma prime and no change in eutectic gamma prime at 2175°F for 2 hours
- o 95-percent solutioning of cooling gamma prime and no change in gamma/gamma prime eutectic at 2210°F for 2 hours
- o Complete solutioning of cooling gamma prime and slight solutioning of gamma/gamma prime eutectic at 2225°F for 2 hours



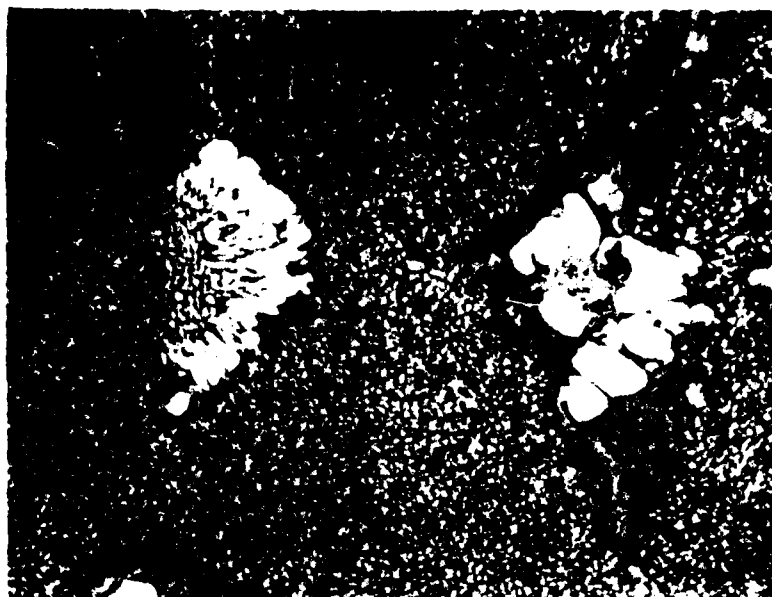
HIP TEMPERATURE: 2150°F



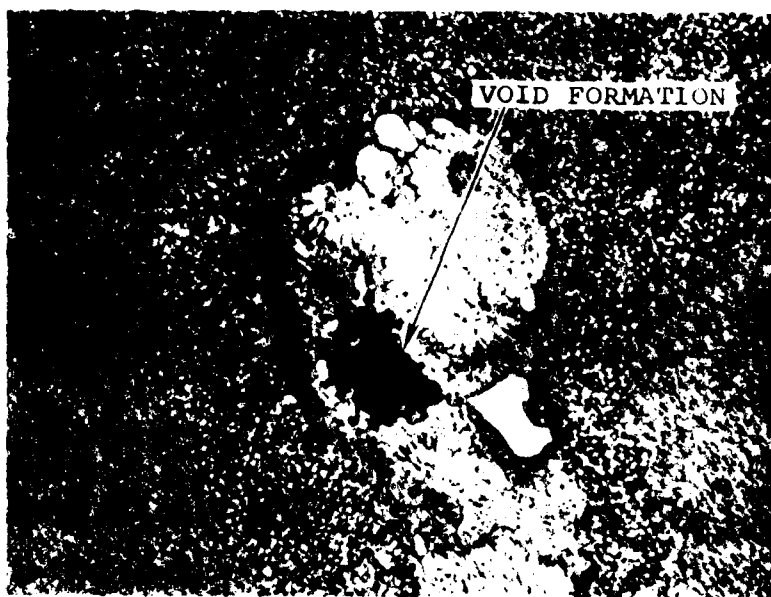
HIP TEMPERATURE: 2200°F

Figure D-8. Microstructure of HIP<sub>ped</sub> AF2-1DA alloy  
 Mag: 400X Etch: electrolytic oxalic acid



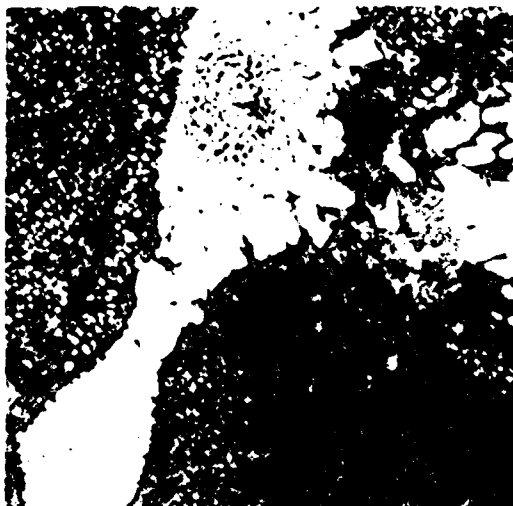


HIP TEMPERATURE: 2225°F

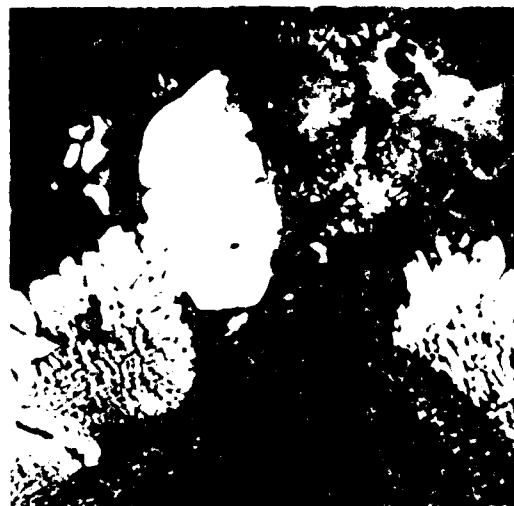


HIP TEMPERATURE: 2250°F

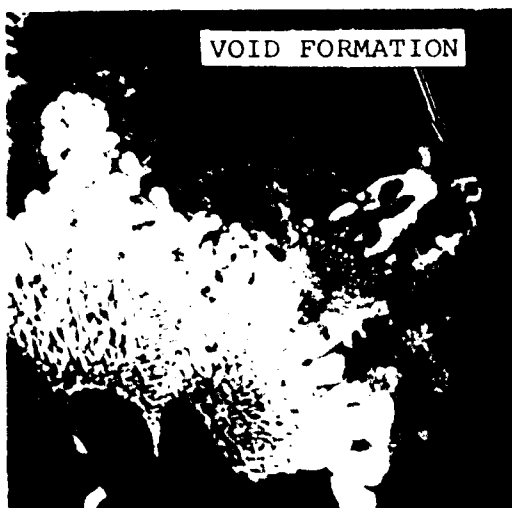
Figure D-9. Microstructure of HIP<sub>ped</sub> AF2-1DA alloy  
 note void formation from incipient melting  
 after 2250°F hip  
 Mag: 400X Etch: electrolytic oxalic acid



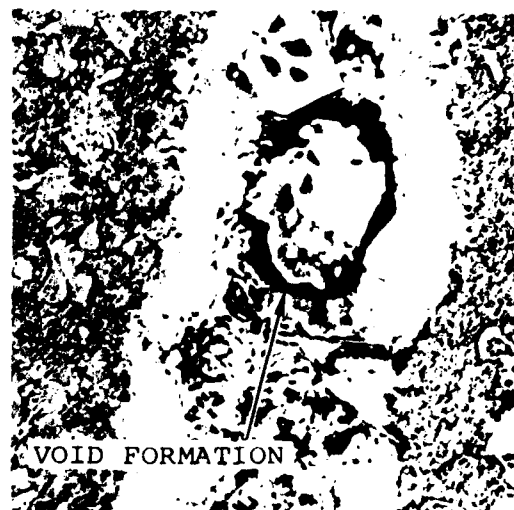
SOLUTION: 2175°F



SOLUTION: 2210°F



SOLUTION: 2225°F



SOLUTION: 2250°F

Figure D-10. Microstructure of HIP<sub>ped</sub> AF2-1DA showing effects of solution heat treatment temperature on void formation  
Mag: 400X Etch: electrolytic oxalic acid

- o Complete solutioning of cooling gamma prime and gamma/gamma prime eutectic at 2250°F for 2 hours

### 3.2.4 LCF Evaluation

Tensile and stress-rupture test results and observed micro-structure changes (void closure and subsequent formation during heat treatment), were used to select four of eight HIP/heat treatment combinations for LCF evaluation. Material processed at 2250°F was eliminated from LCF evaluation due to the incipient melting voids. Material HIPped at 2150°F and solution treated at 2175°F showed poor 1400°F stress-rupture properties and was also eliminated. The remaining five HIP/heat treatment combinations were reduced to four by selecting combinations that would help establish usable manufacturing process ranges for HIP and solution heat treatment. The four combinations are shown below:

<u>Combination</u>	<u>HIP</u>	<u>Solution Heat Treatment*</u>
1	2200°F/15 ksi/3 hours	2175°F
2	2200°F/15 ksi/3 hours	2225°F
3	2225°F/15 ksi/3 hours	2175°F
4	2225°F/15 ksi/3 hours	2210°F

\*Total heat treatment is solution temperature for 2 hours/rapid argon gas quench plus 1950°F for 2 hours/rapid argon gas quench plus 1400°F for 16 hours/air cool.

Strain control LCF tests were conducted with eight bars (Figure D-11) machined from each of the four selected HIP/heat treatment combinations. Test conditions duplicated baseline, as-cast and heat treated material; room temperature,  $A = \infty$ , 20 cpm and 200 ksi pseudo-stress (product of strain times Youngs Modulus). Test results are presented in Tables D-12 and D-13.

Improved LCF life data, compared with the cast plus heat treated baseline material is indicated for each HIP/heat treatment combination. Figures D-12 through D-15 reflect Weibull

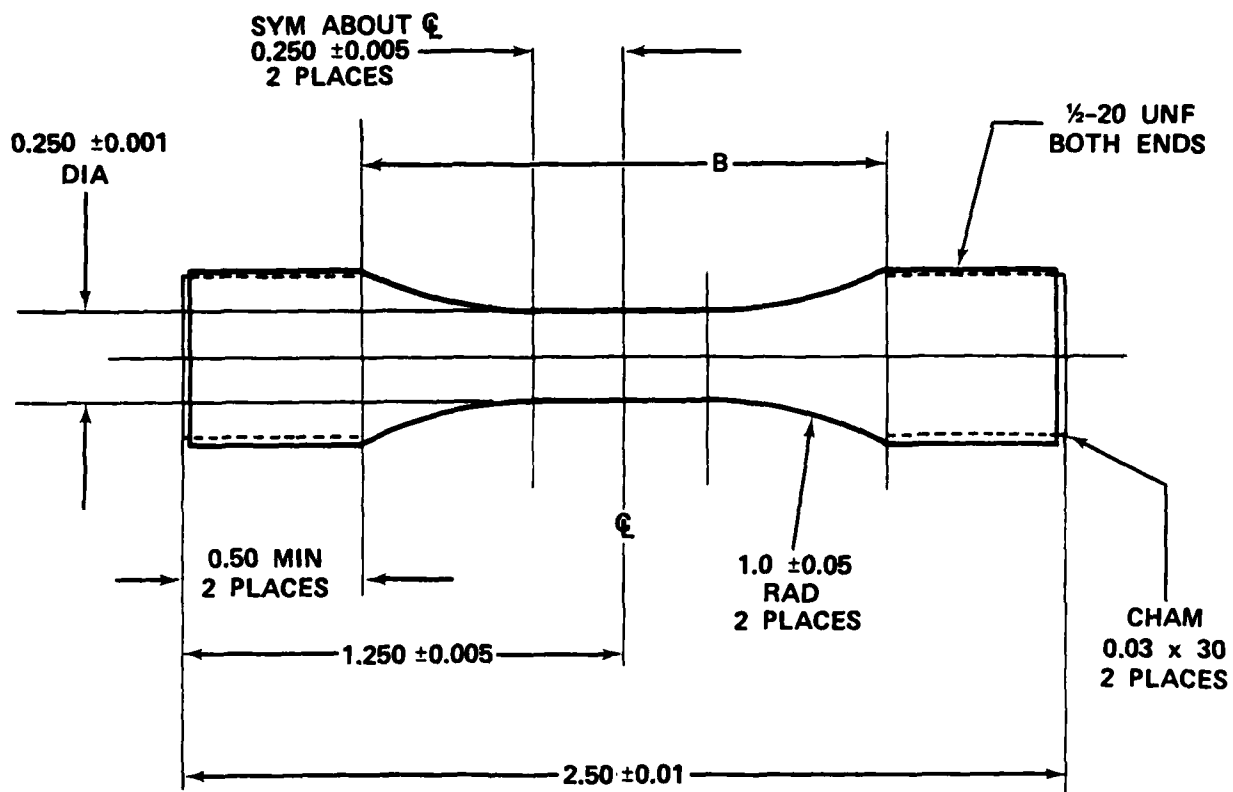


Figure D-11. Uniform section LCF test specimen

TABLE D-12. ROOM TEMPERATURE LOW-CYCLE-FATIGUE (LCF) PROPERTIES OF HIPPED AND HEAT-TREATED\* CAST AF2-1DA ALLOY TURBINE WHEELS.

Specimen Number	HIP Parameter (°F/ksi/ hrs)	Solution Temperature (°F)	Total Strain Range (%)	Measured Modulus (E times 10 <sup>6</sup> psi)	Cycles to Failure	Remarks
71-1	2200/15/3	2175	0.86	23.2	9,080	
71-2			0.79	25.4	9,128	
60-1			0.64	31.1	10,901	
95-1			0.62	32.2	25,566	
41-2			0.60	34.1	15,998	
95-2			0.55	36.2	22,144	
60-2			0.54	36.7	21,011	
41-1			0.52	38.2	23,414	
90-1		2225	0.69	29.5	14,392	
82-2			0.69	32.8	1,892	226 ksi pseudo-stress
82-1			0.66	30.3	11,455	
69-1			0.66	31.0	8,539	
69-2			0.61	32.7	13,180	
78-1			0.59	34.5	16,427	
78-2			0.57	34.9	15,651	
90-2			0.47	42.6	20,603	

Test Parameters: Axial strain control, A Ratio =  $\infty$ , 20 Hz frequency and 200 ksi pseudo-stress

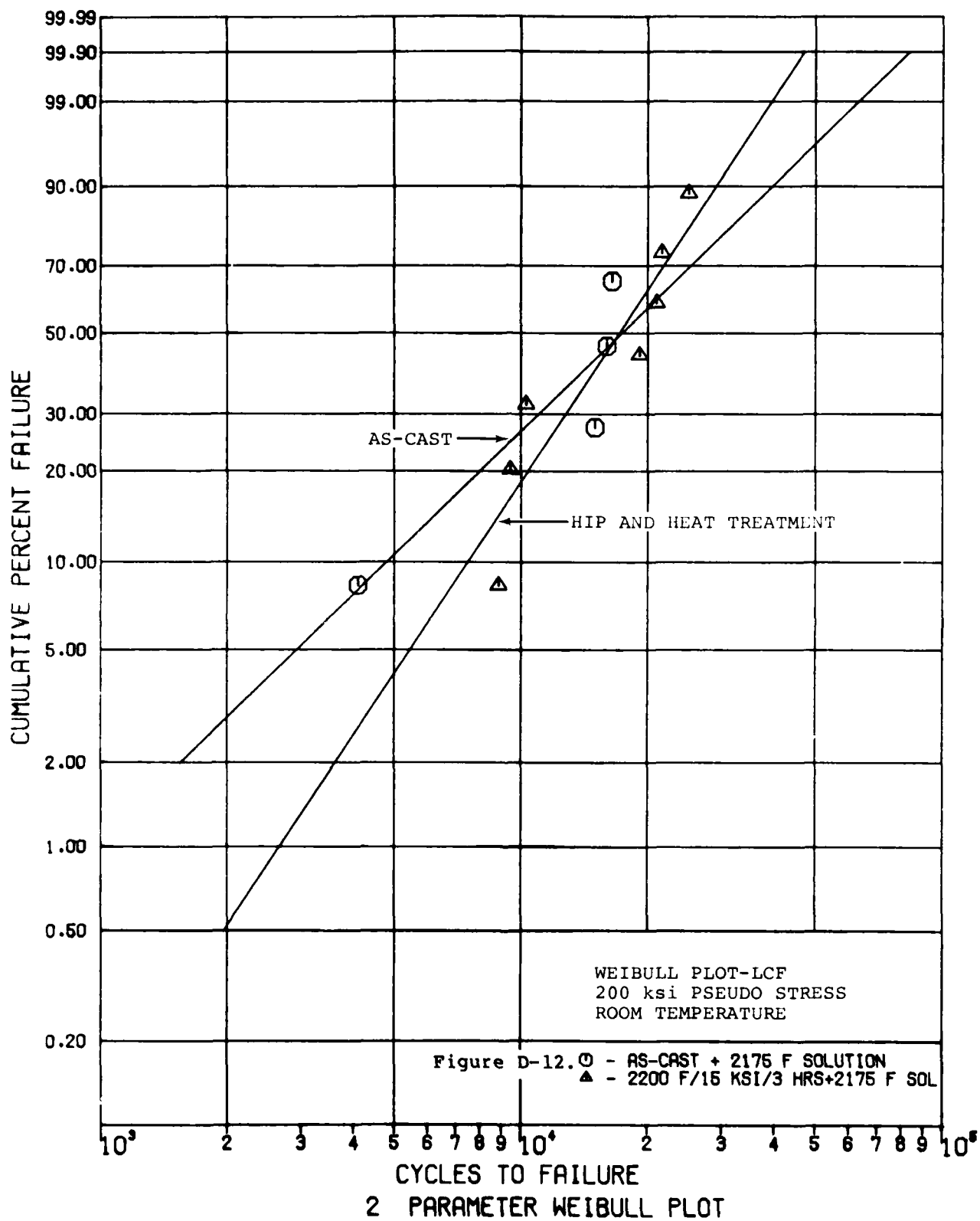
\*At indicated solution temperature for 2 hours with argon quench; plus 1950°F for 2 hours with argon quench; plus 1400°F for 16 hours with air cooling.

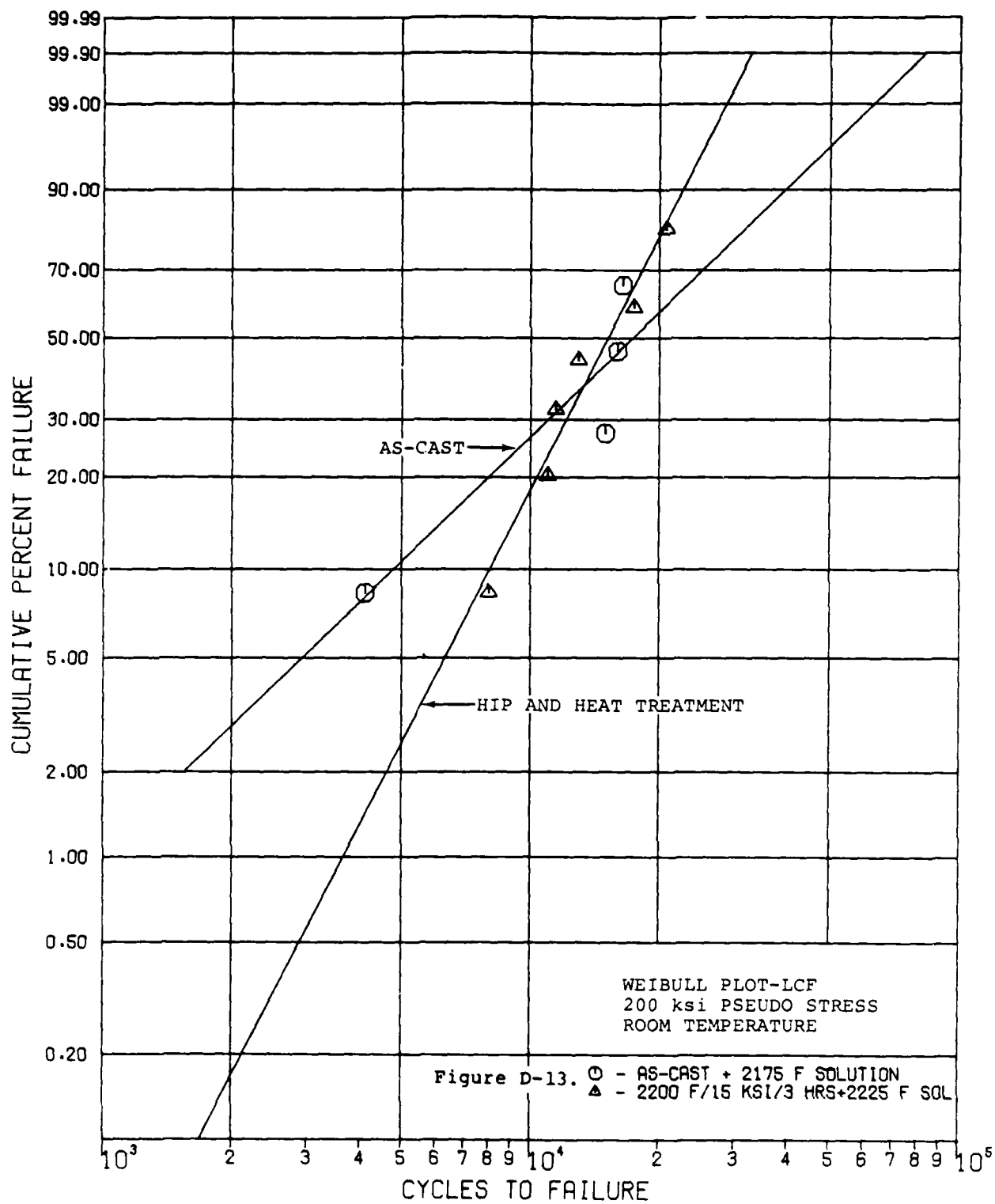
TABLE D-13. ROOM TEMPERATURE LOW-CYCLE-FATIGUE PROPERTIES OF HIPPED AND HEAT-TREATED\* CAST AF2-1DA ALLOY TURBINE WHEELS.

Specimen Number	HIP Parameter (°F/ksi/ hrs)	Solution Temperature (°F)	Total Strain Range (%)	Measured Modulus (E times 10 <sup>6</sup> psi)	Cycles to Failure	Remarks
79-1	2225/15/3	2175	0.65	31.0	10,840	188 ksi pseudo-stress
63-1			0.63	31.7	13,538	
48-2			0.60	33.5	9,108	
63-2			0.55	34.1	13,781	
93-2			0.54	36.9	22,047	
48-1			0.53	37.5	24,318	
93-1			0.52	38.3	15,970	
79-2			-	-	-	
80-2		2210	0.85	23.4	6,168	
80-1			0.76	26.7	8,177	
85-2			0.71	28.1	9,218	Specimen buckled equipment malfunction
76-1			0.70	28.5	16,146	
85-1			0.67	30.0	16,986	
76-2			0.57	35.0	13,312	
68-2			0.52	38.5	21,560	
68-1			0.47	42.7	7,567	

Test Parameters: Axial strain control, A ratio = ∞, 20 Hz frequency and 200 ksi pseudo-stress

\*At indicated solution temperature for 2 hours with argon quench; plus 1950°F for 2 hours with argon quench; plus 1400°F for 16 hours with air cooling.

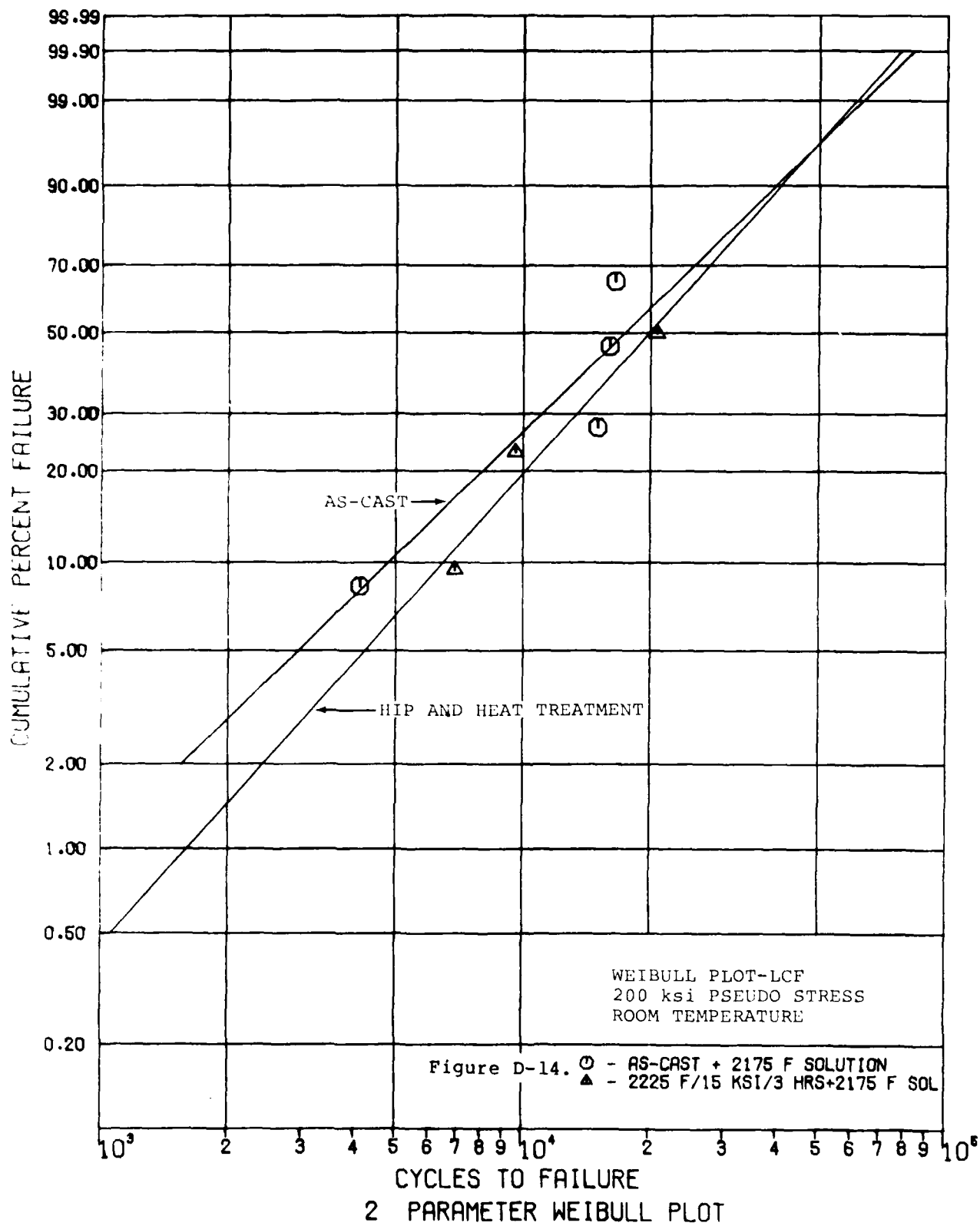


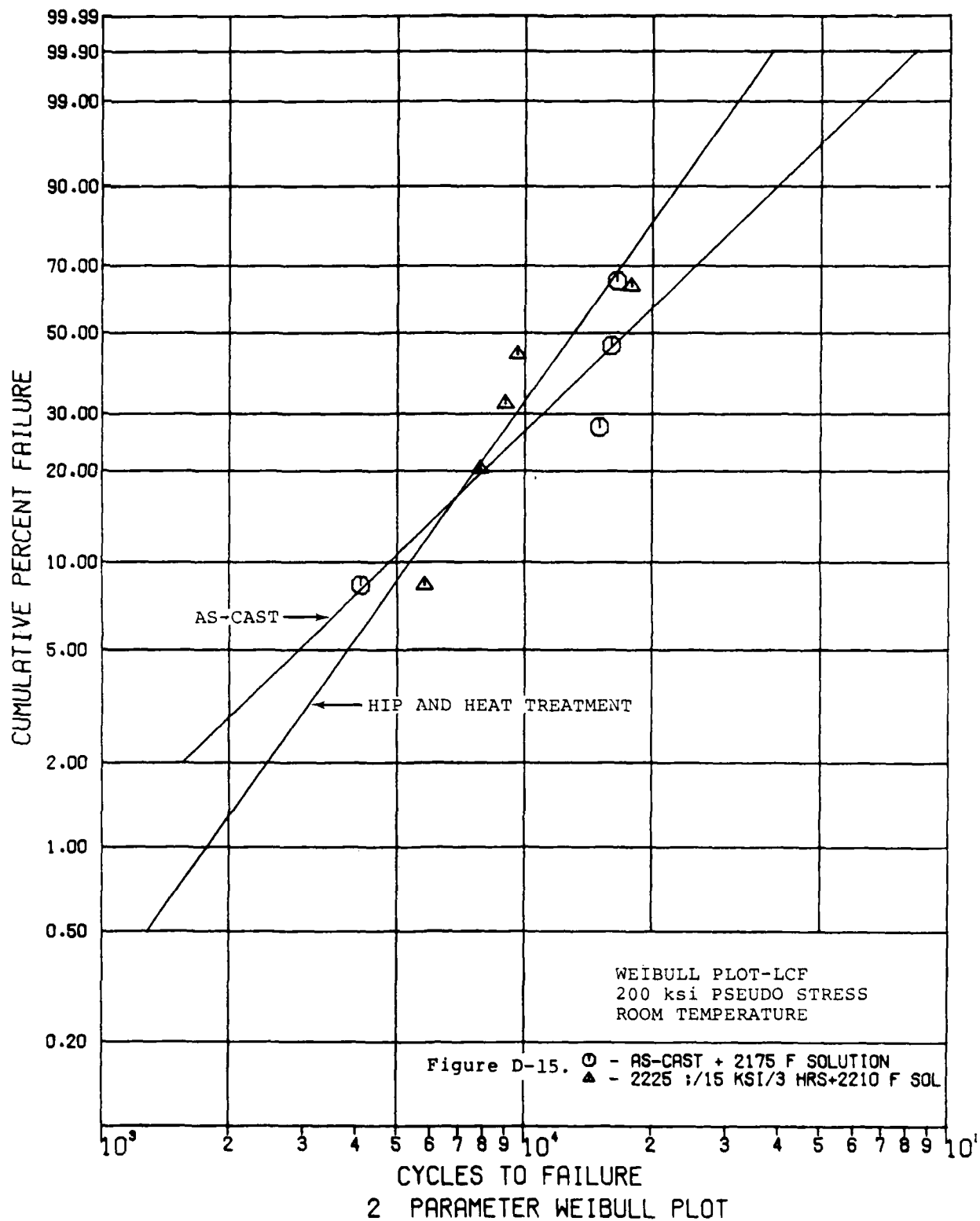


WEIBULL PLOT-LCF  
200 ksi PSEUDO STRESS  
ROOM TEMPERATURE

Figure D-13.  $\circ$  - AS-CAST + 2175 F SOLUTION  
 $\Delta$  - 2200 F/15 KSI/3 HRS+2225 F SOL





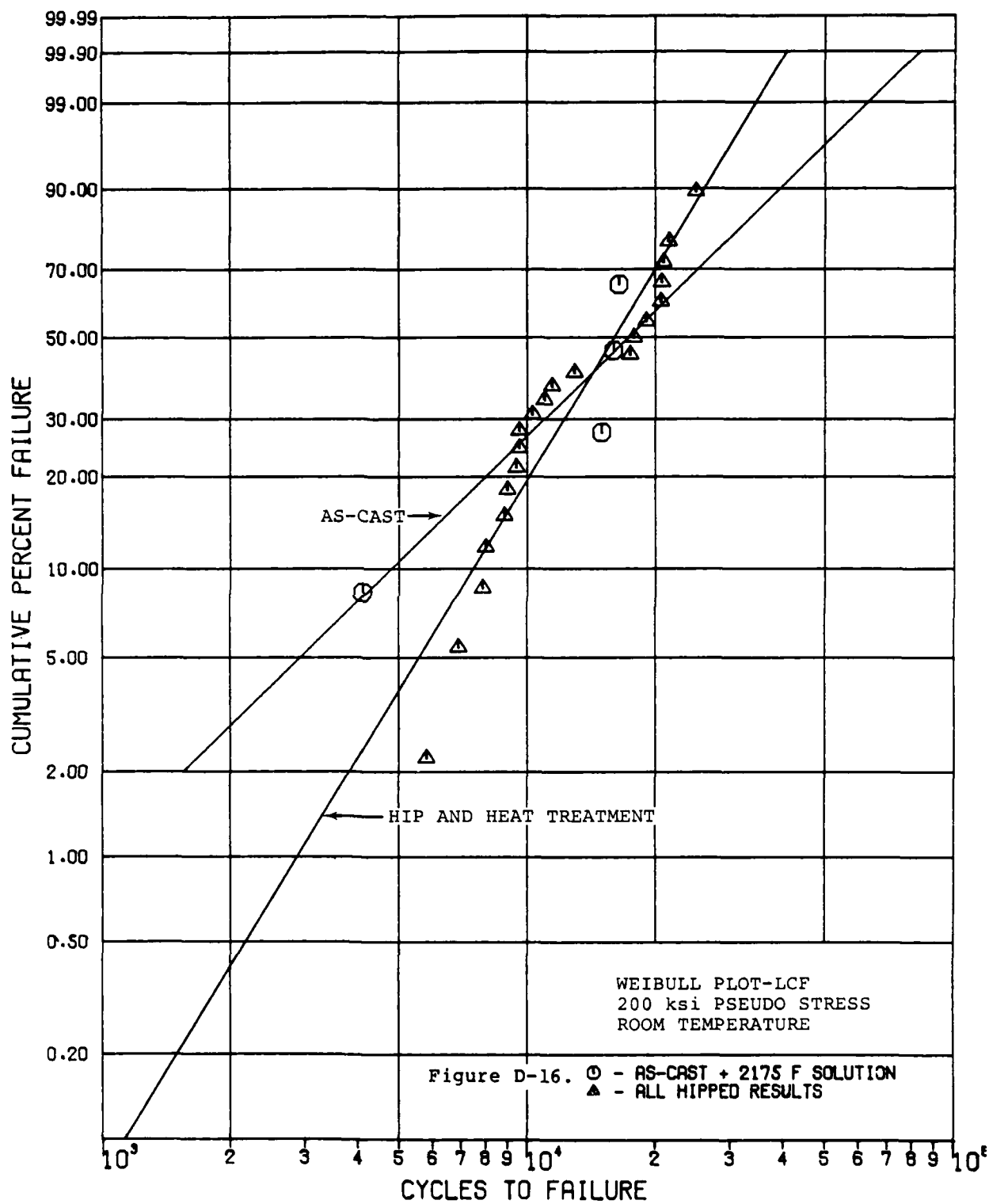


plots for individual HIP and heat treatment combinations. Figure D-16 shows inclusive HIP data compared with the cast and heat treated baseline. The lower cumulative percent failure range component early failures and is of greatest concern in LCF design considerations. The cumulative HIP curve (Figure D-16) shows that at one-percent cumulative failure life, HIP improves life by a factor of three, when compared with the as-cast baseline.

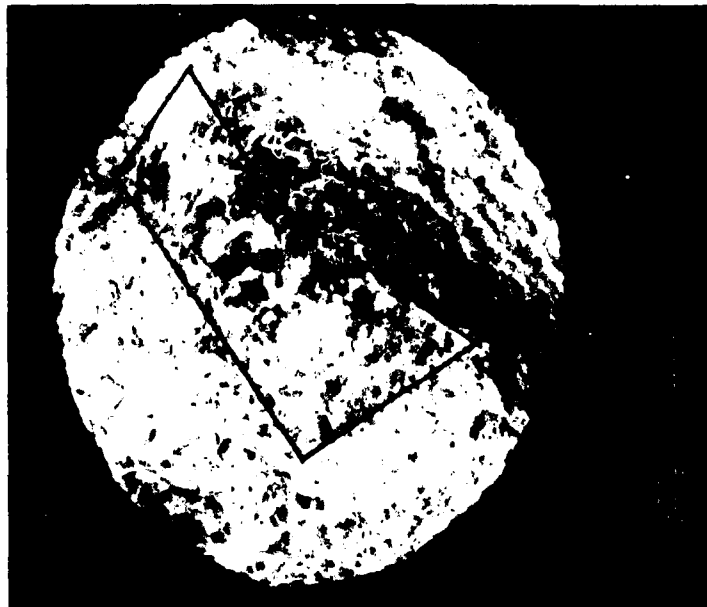
SEM examination of LCF test bar fracture surfaces revealed that origins were again associated with MC carbides and initiated on the external surface. Specimen number 82-2 was the only exception. The fracture surface of this specimen exhibited an internal origin associated with an inclusion type defect as shown in Figure D-17. Energy dispersive X-ray analysis revealed that the defect contained areas of high hafnium, tantalum and titanium. The defect source was not pursued because it was not considered part of this program. Two 2225°F solution heat-treatment specimens, exhibited small voids caused by incipient melting.

### 3.2.5 Process Selection

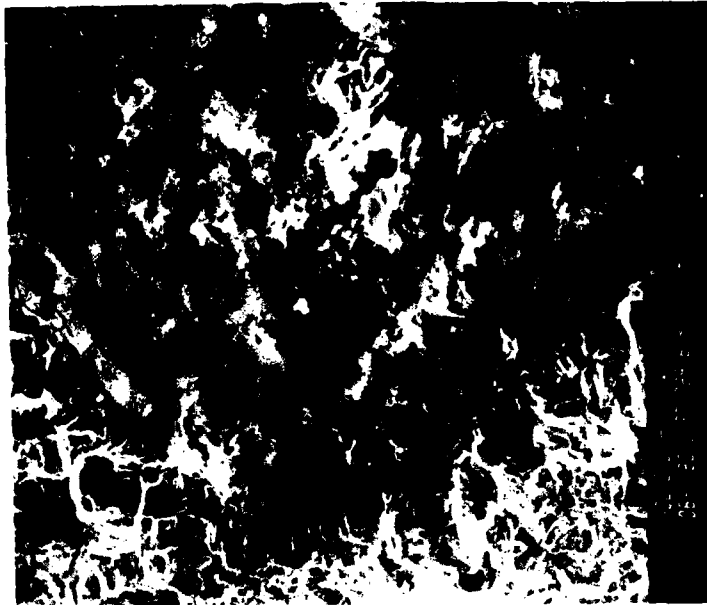
Tensile, stress-rupture and LCF testing of various HIP and heat treatment combinations that resulted in increased fatigue life, were used to define the manufacturing process parameters. Acceptable HIP parameter limits identified were 2200 to 2225°F for 3 hours at 15 ksi argon. However, this range must be extended since HIP vendors typically require a  $\pm 25^\circ\text{F}$  nominal temperature variance. The requirement to open the range on the lower end to 2175°F, exists because HIP at 2250°F produced voids. It is assumed the 2175°F/15 ksi parameters will effect closure since the HIP cycle at 2150°F for 3 hours at 29 ksi argon resulted in complete closure. Pressure is well above the 2200°F yield strength of 2,800 to 3,600 psi (see Table D-1 previously included).



2 PARAMETER WEIBULL PLOT



20 x MAG.



60 x MAG.

Figure D-17. SEM micrographs showing specimen numbered 82-2 LCF test bar fracture surface, exhibiting inclusion type defect (enclosed area). (A) area of high Hf, (B) area of high Hf, Ta and Ti and (C) area of fracture origin. This was the only inclusion found on LCF test bar fracture surfaces

Acceptable solution heat treatment temperature range limits, (after HIP) selected from the mechanical property results, are 2175 to 2210°F (2225°F produced voids). These limits need not be extended since this temperature control spread is sufficient for most vacuum furnace operations. Adherence to this critical temperature range is paramount to proper heat treatment.

Recommended HIP/heat treatment manufacturing process parameters are listed below:

- o HIP 2200  $\pm 25^{\circ}\text{F}$ /3 hours/15 ksi argon
- o Heat treatment
  - Solution 2190  $\begin{smallmatrix} +20^{\circ}\text{F} \\ -15^{\circ}\text{F} \end{smallmatrix}$  (2 hours) argon gas quench 40 to 50°F per minute
- o Intermediate Age 1950  $\pm 25^{\circ}\text{F}$  (2 hours) argon gas quench 40 to 50°F per minute
  - Age 1400  $\pm 25^{\circ}\text{F}$  (16 hours) air cool

Tensile and stress-rupture test results from HIP/heat treatment combinations within acceptable processing ranges, were selected from a large data population and averages analyzed. Table D-14 shows room temperature and 1400°F tensile test results compared with as-cast and heat treated baseline and AiResearch specification minimum values. HIP material properties exceed minimum values, exhibit improved ductility, and are comparable with as-cast baseline material.

Stress-rupture results shown in Figure D-18 compare as-cast, heat treated, HIP and specification minimum limits on a Larson-Miller plot. Rupture properties after HIP are above minimum values, and comparable to as-cast.

TABLE D-14. TENSILE TEST RESULTS OF HIP/HEAT TREATMENT COMBINATIONS\* WITHIN ACCEPTABLE PROCESSING RANGES (ALL VALUES ARE AVERAGE)

<u>Room Temperature</u>	<u>0.2% YS (ksi)</u>	<u>UTS (ksi)</u>	<u>EL (%)</u>	<u>RA (%)</u>
Cast + Heat Treated	123.4	134.7	4.2	10.7
HIP + Heat Treated	123.2	134.0	5.6	11.3
Specification Minimum	115.0	130.0	5.0	--
<u>1400°F</u>				
Cast + Heat Treated	112.6	137.1	6.0	14.9
HIP + Heat Treated	109.0	137.4	6.9	12.2
Specification Minimum	105.0	130.0	5.0	--

*Hip/Solution Temperature	HIP = Hot Isotatic Pressing
2200°F/2175°F	YS = Yield Strength
2225°F/2175°F	UTS = Ultimate Tensile Strength
2225°F/2210°F	RA = Reduction of Area
	EL = Elongation

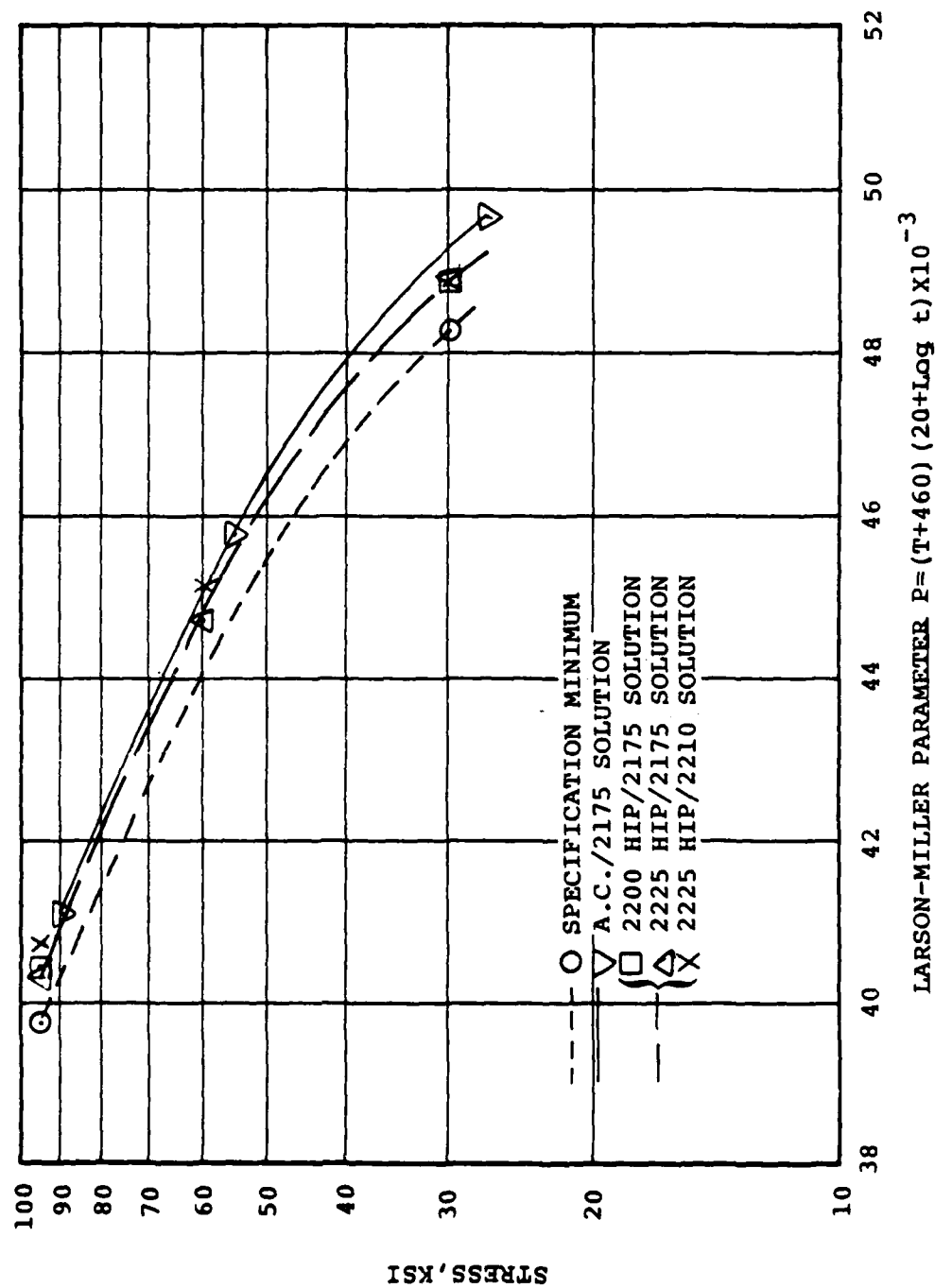


Figure D-18. As-cast and HIP stress-rupture test results AF2-1DA alloy compared with AiResearch specifications



## SECTION IV

### CONCLUSIONS AND RECOMMENDATIONS

#### 4.1 Conclusions

- o Uniaxial LCF testing indicates life improvement by a factor of 3, for cast AF2-1DA alloy (Mod 2A) turbine wheels, using HIP
- o Tensile and stress-rupture properties of HIPped castings exceed AiResearch specification minimum for cast AF2-1DA alloy and are equivalent to as-cast properties

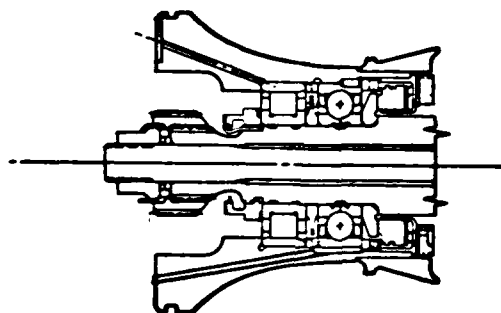
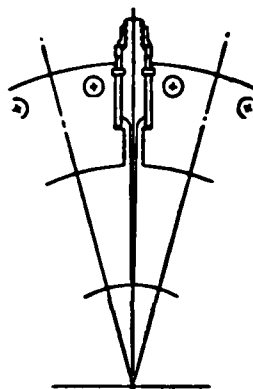
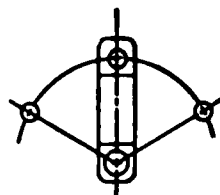
#### 4.2 Recommendation

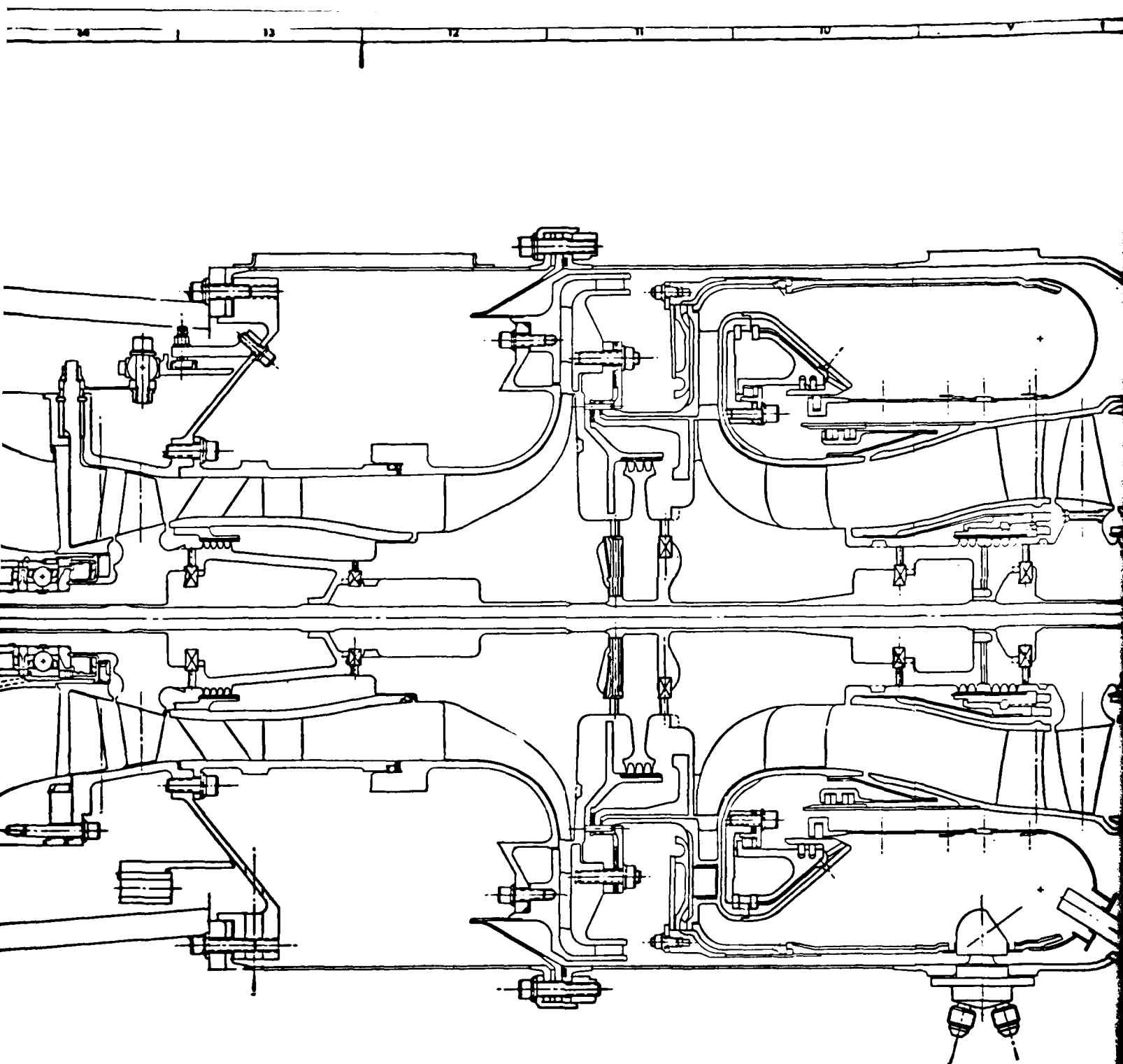
- o Cast AF2-1DA alloy (Mod 2A) turbine wheels should be HIPped prior to heat treatment to improve LCF properties

APPENDIX E

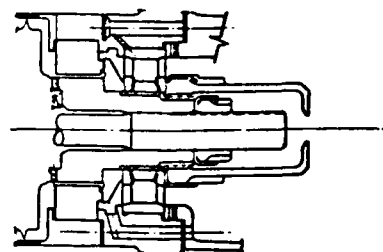
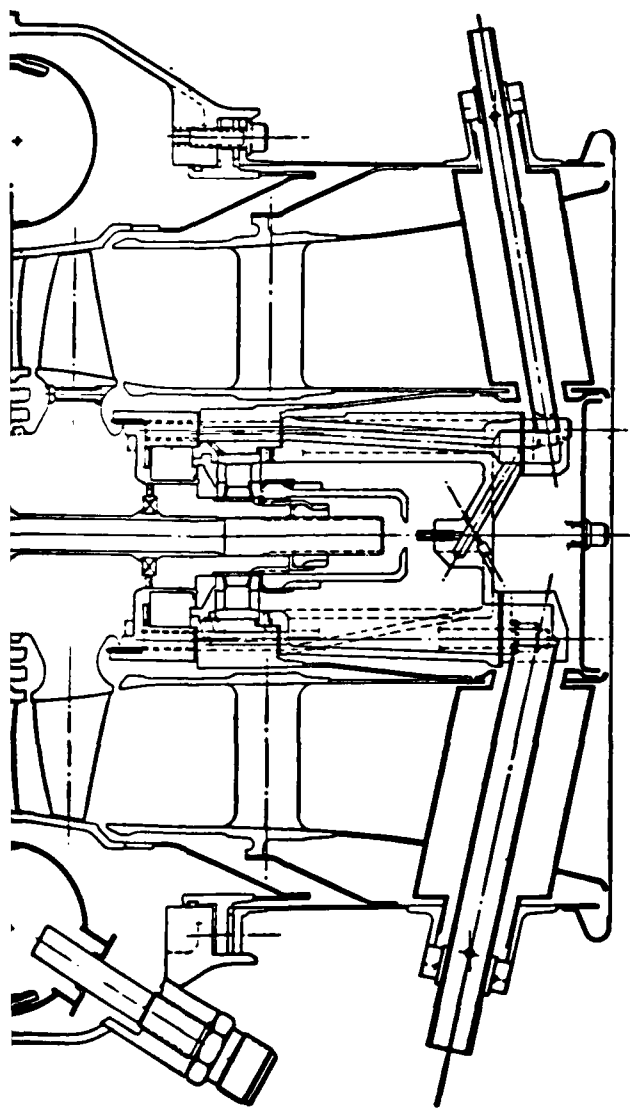
Layout Drawing No. L3621610  
Assembly Drawing No. 3605630  
Assembly Drawing No. 3605727

гэсгю



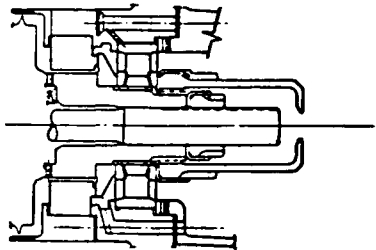


L 3621610



L 3621610

REVISIONS			
NO.	DESCRIPTION	DATE	BY
1			
2			



REVISIONS			
NO.	DESCRIPTION	DATE	BY
1			
2			

L 3621610	
CONCEPTUAL LAYOUT OF ADVANCED APU	
J 00100	L 3621610
SCALE 2/1	WT

L 3621610

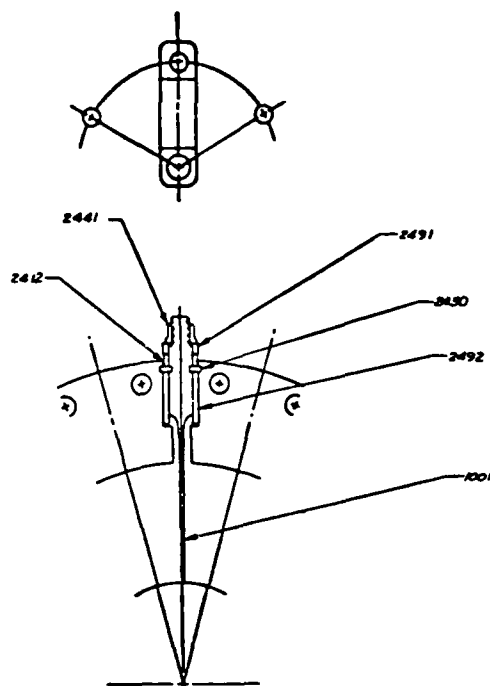
20

19

18

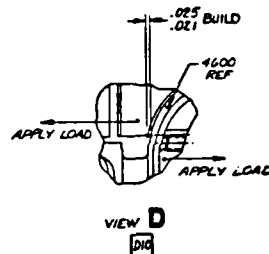
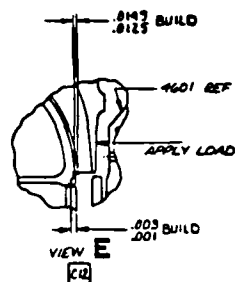
16

15



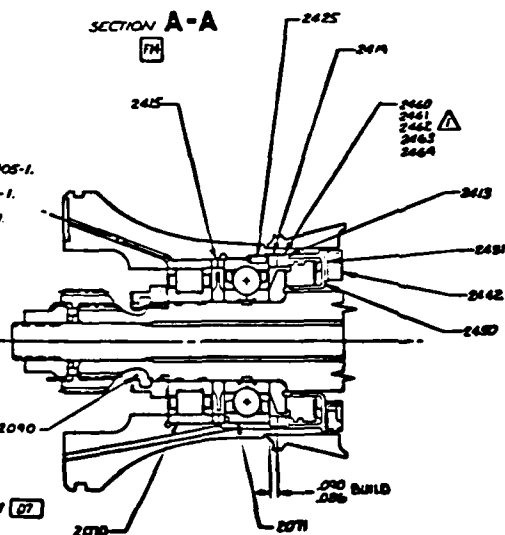
SECTION A-A

F74



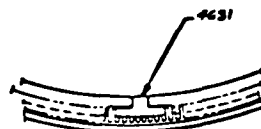
VIEW D

D10



VIEW B

B4



SECTION C-C

B4

17. DIAMETRAL STACK DEPICTED ON 3606905-1.

18. AXIAL STACK DEPICTED ON 3606906-1.

19. TORQUE VALUES PER AIRSEARCH AF5439.

20. LOCKWIRE PER MS33590.

21. SHIM AS REQD TO OBTAIN .166 BUILD DIM [E10] SHIM RANGE (.020-.079).

22. SHIM AS REQD TO OBTAIN .016 BUILD DIM [D10] SHIM RANGE (.0235-.0435).

23. SHIM AS REQD TO OBTAIN .023 BUILD DIM [E7] SHIM RANGE (.020-.042).

24. SHIM AS REQD TO OBTAIN .001 PINCH BUILD [D12] SHIM RANGE (.020-.087).

25. SHIM AS REQD TO OBTAIN .090 BUILD DIM [C9] SHIM RANGE (.020-.1018).

26. SHIM AS REQD TO OBTAIN .0165 BUILD DIM [C8] SHIM RANGE (.0218-.1248).

27. SHIM AS REQD TO OBTAIN .060 BUILD DIM [D7] SHIM RANGE (.020-.0472).

28. SHIM AS REQD TO OBTAIN .002 BUILD DIM [E7] SHIM RANGE (.020-.084).

29. SHIM AS REQD TO OBTAIN .015 BUILD DIM [E7] SHIM RANGE (.019-.078).

30. 25 LB LOAD TO BE APPLIED IN DIRECTION NOTED WHEN PERFORMING SHIMMING FOR BUILD DIM.

31. SHIM AS REQD TO OBTAIN .001 PINCH BUILD.

32. SHIM AS REQD TO OBTAIN .012 BUILD DIM [F4]

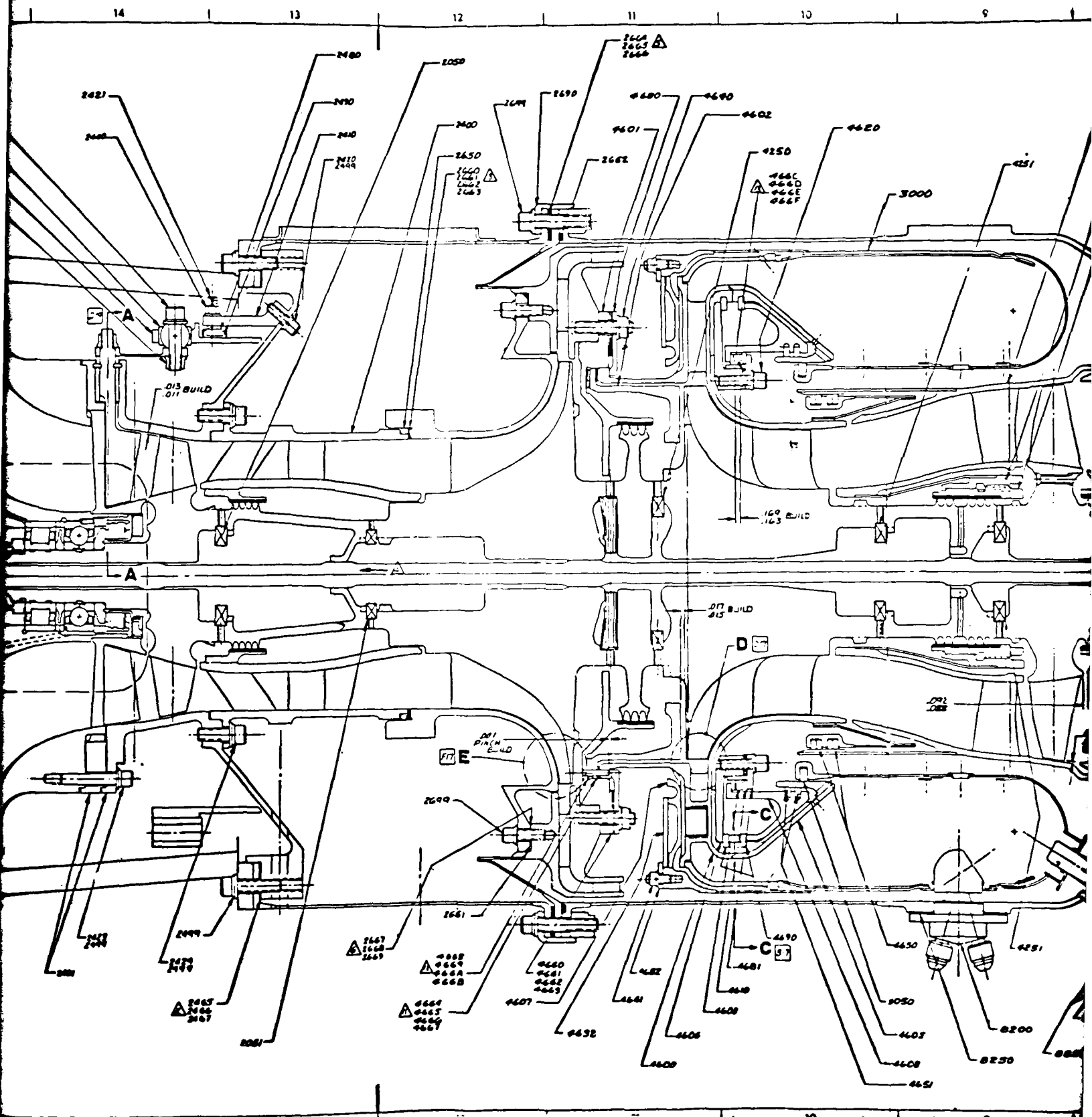
33. SHIM AS REQD TO OBTAIN .088 BUILD DIM [B8] SHIM RANGE (.022-.0512).

20

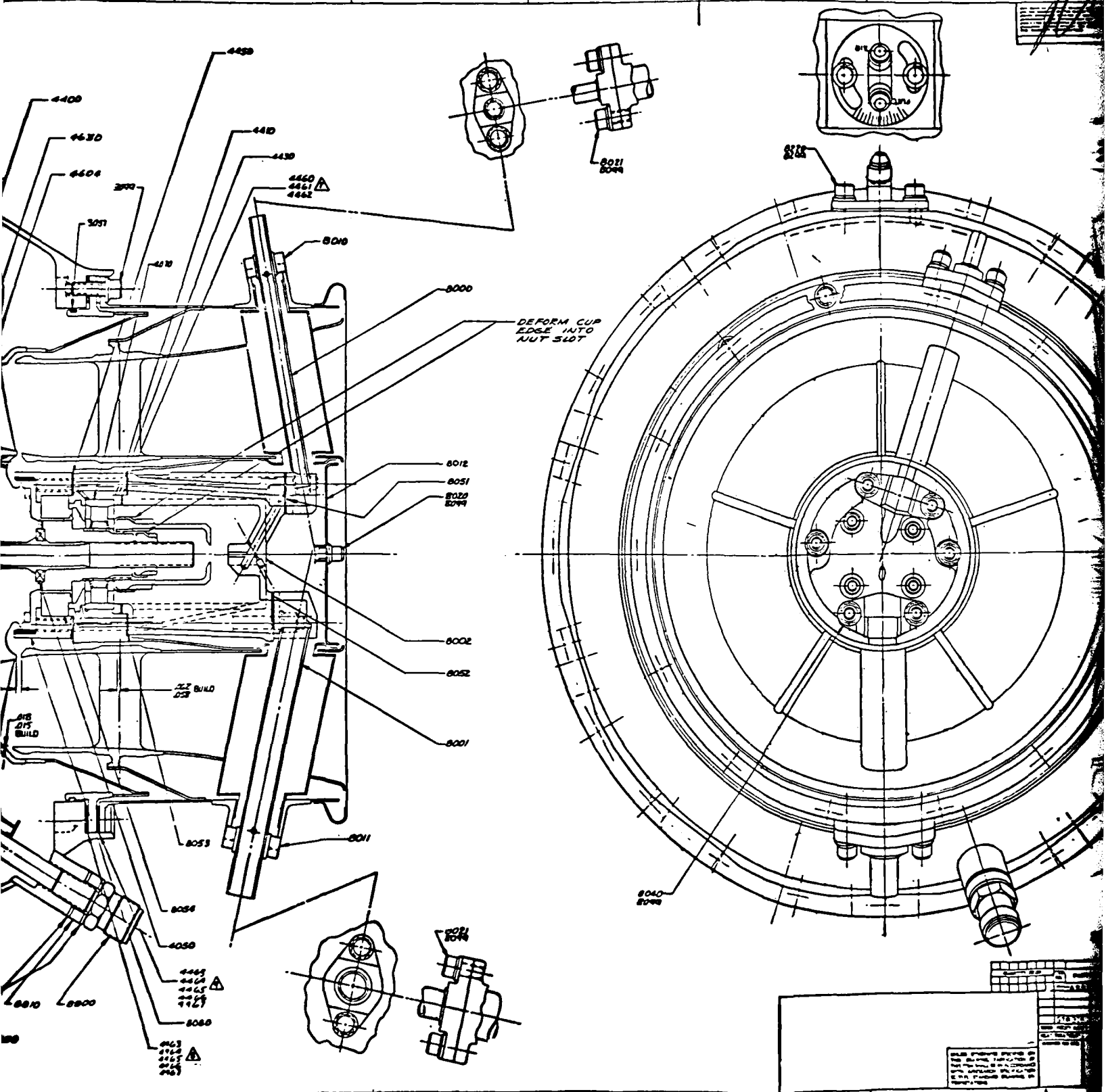
10

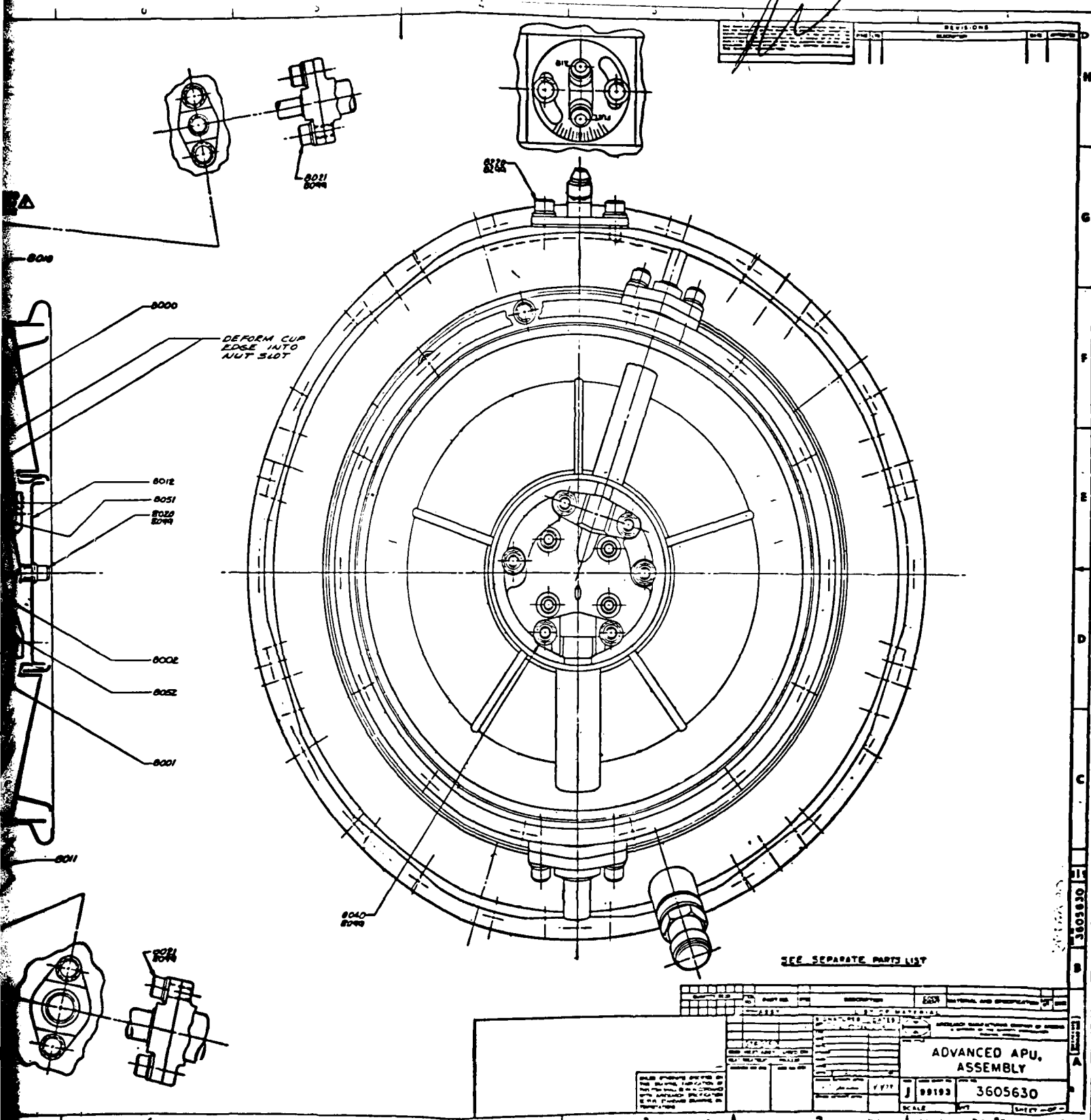
..

..









REV	DATE	DESCRIPTION	BY	CHECKED	APPROVED
1					
2					
3					
4					
5					
6					
7					
8					
9					
10					
11					
12					
13					
14					
15					
16					
17					
18					
19					
20					
21					
22					
23					
24					
25					
26					
27					
28					
29					
30					
31					
32					
33					
34					
35					
36					
37					
38					
39					
40					
41					
42					
43					
44					
45					
46					
47					
48					
49					
50					
51					
52					
53					
54					
55					
56					
57					
58					
59					
60					
61					
62					
63					
64					
65					
66					
67					
68					
69					
70					
71					
72					
73					
74					
75					
76					
77					
78					
79					
80					
81					
82					
83					
84					
85					
86					
87					
88					
89					
90					
91					
92					
93					
94					
95					
96					
97					
98					
99					
100					

ADVANCED APU,  
ASSEMBLY

3605630



A

**1**

1



A

1

1